ICRP ref: 4889-2039-6370

Annals of the ICRP

ICRP PUBLICATION 1XX

Dose coefficients for intakes of radionuclides by members of the public: Part 1

Editor-in-Chief
C.H. CLEMENT

Associate Editor
H. YU

Authors on behalf of ICRP
F. Paquet, M.R. Bailey, R.W. Leggett, T. Smith, E. Blanchardon, A. Giussani, J.W. Marsh, G. Ratia, C. Samuels, D. Gregoratto, V. Berkovski, D. Jokisch

PUBLISHED FOR

The International Commission on Radiological Protection

by

SAGE

Please cite this issue as 'ICRP, 202X. Dose coefficients for intakes of radionuclides by members of the public: Part 1. ICRP Publication 1XX, Ann. ICRP XX(X)'

CONTENTS

171

ICRP Publication 1XX

172 DOSE COEFFICIENTS FOR INTAKES OF RADIONUCLIDES 173 BY MEMBERS OF THE PUBLIC: PART 1

174 ICRP Publication XXX

175 Approved by the Commission in 20YY

176

177 **Abstract**– This report is the first in a series of documents giving age-dependent dose
178 coefficients for members of the public for environmental intakes of radionuclides by inhalation
179 and ingestion. This series replaces the Publication 56 series of documents, update some data
180 from Publication 119, and comes in addition to the series on occupational intakes of
181 radionuclides by workers (OIR series). The revised dose coefficients have been calculated
182 using the Publication 100 Human Alimentary Tract Model (HATM) and the Publication 130
183 revision of the Human Respiratory Tract Model (HRTM). Revisions have also been made to
184 many of the models that describe the systemic biokinetics of radionuclides absorbed to blood,
185 making them more physiologically realistic representations of uptake and retention in organs
186 and tissues and of excretion. Changes have been implemented that were introduced in
187 Publication 103 to: the radiation weighting factors used in the calculation of equivalent doses
188 to tissues; the tissue weighting factors used in the calculation of effective dose; and the separate
189 calculation of equivalent doses to males and females with sex-averaging in the calculation of
190 effective dose. Reference anatomical computational phantoms such as those in Publication 110
191 and Publication 143 (i.e. models of the human body based on medical imaging data), have
192 replaced many of the composite mathematical models used for previous calculations of organ
193 doses. Dose calculations were also improved by using updated radionuclide data in Publication
194 107 and specific absorbed fraction data in Publication 133 and Publication 1XX.

196 *Keywords:* Environmental exposure; Internal dose assessment; Biokinetic and dosimetric
197 models

198
199
200

MAIN POINTS

- **This report is the first in a series of documents giving age-dependent dose coefficients for members of the public for environmental intakes of radionuclides by inhalation and ingestion. This series replaces the Publication 56 series of documents and update some data from Publication 119.**

- **The data provided are age-dependent dose coefficients for members of the public for environmental intakes of radionuclides by inhalation and ingestion. As in the Publication 56 series, dose coefficients are presented in this series of reports for intakes by 3-mo-old infants, 1-, 5-, 10-, and 15-y-old children, and adults.**

- **The data provided in the printed reports are restricted to tables of committed effective dose per intake (Sv Bq^{-1}) for inhalation and ingestion. Data are provided for all absorption types and for the most common isotope(s) of each element. The electronic data that accompanies this series of reports contains a comprehensive set of committed effective and equivalent dose coefficients.**

- **This first report provides the data above for some of the elements already described in OIR Parts 2–3 (ICRP Publications 134, 137) i.e.: Hydrogen (H), Carbon (C), Phosphorus (P), Sulphur (S), Calcium (Ca), Iron (Fe), Cobalt (Co), Nickel (Ni), Zinc (Zn), Selenium (Se), Strontium (Sr), Yttrium (Y), Zirconium (Zr), Niobium (Nb), Molybdenum (Mo), Technetium (Tc), Ruthenium (Ru), Silver (Ag), Antimony (Sb), Tellurium (Te), Iodine (I), Caesium (Cs), Barium (Ba), Iridium (Ir), Lead (Pb), Bismuth (Bi), Polonium (Po), Radon (Rn), and Radium (Ra).**

1. INTRODUCTION

1.1. Scope of this series of reports

(1) Environmental intakes of radionuclides by members of the public may occur as the result of planned or accidental discharge from a range of industrial, medical, educational and research facilities. Dose coefficients have been calculated for radioisotopes of the elements which are expected to be released into the environment as a result of human activities such as uranium mining and milling, conversion, enrichment and fabrication, power station operations, fuel reprocessing, waste storage and disposal, and considered to be of significance for environmental radiation protection purposes. In addition, naturally occurring radionuclides are present in the environment and their concentrations may be modified by human activities. Consequently, the range of radionuclides to be addressed includes those of natural origin, fission products, actinides, and activation products.

(2) The chemical forms considered in this report series are those found in workplaces and already described in the Occupational Intakes of Radionuclides (OIR) series (ICRP, 2015, 2016a, 2017, 2019, 2022). Since most of the radionuclides released in the environment may be gradually internalised in the food chain, an additional organic chemical form is taken into consideration for ingestion by humans.

(3) To provide dose coefficients for members of the public, it is necessary to take into account the effect of age on the biokinetics of radionuclides and on anatomical and physiological data. The biokinetic data used for the adults in this series of reports are taken from the OIR series (ICRP, 2015, 2016a, 2017, 2019, 2022). Additional data for infants and children are presented in this series for the calculation of a comprehensive set of dose coefficients.

(4) An adequate assessment of environmental internal exposure resulting from intakes of radionuclides is essential for the design, planning and authorisation of a facility or activity, and for the retrospective demonstration of compliance with regulatory requirements.

(5) The protection quantities defined by ICRP, equivalent dose and effective dose, are fundamental to the application of ICRP recommendations. The concept of effective dose provides a single quantity that may be used to characterise both internal and external individual exposures in a manner that is independent of the individual's body-related parameters, such as sex, age (for adults), anatomy, physiology and race. In order to achieve wide applicability, the protection quantities effective dose and equivalent dose are defined using computational models with broad averaging of physiological parameter values. Specifically, *Publication 89* (ICRP, 2002a) defines the key parameters of the Reference Individuals (the mass, geometry and composition of human organs and tissues), while this series of reports provides relevant parameters for the Reference Members of the Public of each reference age, including an associated set of ICRP reference biokinetic models.

(6) Effective dose is not an individual-specific dose quantity, but rather the dose to a Reference Person under specified exposure conditions. In the general case, the Reference Person can be either a Reference Worker or a Reference Individual of a specified age.

(7) After intake of radionuclides, doses received by organs and tissues are protracted over time and so equivalent and effective doses are accumulated over time. The resulting quantities are referred to as committed doses. Internal exposure of members of the public should be assessed in terms of the protection quantity committed effective dose.

(8) This series of reports provides a comprehensive set of dose coefficients (i.e. committed effective dose and committed equivalent doses to organs or tissues per intake). These data may

be used for both prospective assessments and retrospective assessments. Prospective assessments provide estimates of intakes and resulting doses using information on projected exposures to radionuclides obtained at the design and planning stage of a facility or practice. These assessments generally make use of default assumptions about exposure conditions and default values for parameters describing material-specific properties, such as the particle size distribution of an inhaled aerosol or the absorption characteristics of a material after inhalation or ingestion. Retrospective assessments use the results of individual monitoring and environmental monitoring to assess doses in order to demonstrate compliance with regulatory requirements. These assessments may, in some circumstances, make use of specific information relating to the exposure, as discussed in Section 6 of *Publication 130* (ICRP, 2015).

(9) This series of reports contains detailed information on the ICRP reference models used for the derivation of dose coefficients. The information provided in this first report of the series includes overviews of the ICRP reference Human Respiratory Tract Model (HRTM) as revised in *Publication 130* (ICRP, 2015), and an overview of the ICRP reference Human Alimentary Tract Model (HATM) (ICRP, 2006). Descriptions of the structures and parameter values of the reference systemic biokinetic models are also presented in this series of reports.

(10) The material presented in this series of reports is not intended for applications beyond the scope of environmental radiation protection. An example of such an application is the assessment of a case of substantial radionuclide intake, where organ doses can approach or exceed the thresholds for tissue reactions, and where medical treatment may require an individual-specific reconstruction of the magnitude of absorbed doses and associated parameters characterising the exposure. In such a case, the individual-related estimates of absorbed doses in organs or tissues should be made. Such individual-related assessments are beyond the scope of this series of reports.

(11) In some exceptional circumstances, when public exposure has occurred and absorbed doses in organs or tissues are below the thresholds for tissue reactions, the data presented in the OIR series of reports (ICRP, 2015, 2016a, 2017, 2019, 2022) could be used for planning of bioassay monitoring programmes (usually based on the use of whole body and/or thyroid monitors) and interpretation of bioassay monitoring data obtained for adult members of the public.

(12) The *Publication 56* series: *Publications 56, 67, 69, 71, 72, 88* and *95* (ICRP, 1990, 1993, 1995a, 1995b, 1995c, 2001, 2004) (Table 1.1) gave dose coefficients for members of the public, for intakes of radionuclides by inhalation and ingestion, referencing the Recommendations issued in *Publication 60* (ICRP, 1991) and the anatomical and physiological data in *Publication 23* (ICRP, 1975). It applied the *Publication 66* HRTM (ICRP, 1994b) for inhaled radionuclides, the basic anatomical and physiological data for the skeleton in *Publication 70* (ICRP, 1995d) and systemic biokinetic models for selected isotopes of 31 elements given in *Publications 56, 67, 69* and *71* (ICRP, 1990, 1993, 1995a, 1995b). The biokinetic models for the gastrointestinal tract and systemic biokinetic models for other elements were taken from *Publication 30* and modified by addition of explicit excretion pathways to improve dose estimates for the urinary bladder and colon walls. A compilation of dose coefficients for intakes of radionuclides by workers and members of the public was then produced in *Publication* 119 (ICRP 2012).

313 Table 1.1. Summary of previous reports on dose coefficients for members of the public from intakes of radionuclides.

ICRP Publication No. (year)	Application	Contents
56 (1989)	Inhalation* and ingestion	Age-dependent biokinetic models with effective dose coefficients and tissue equivalent dose coefficients for selected radioisotopes of H, C, Sr, Zr, Nb, Ru, I, Cs, Ce, Pu, Am, and Np. Predates *Publication 60* (ICRP, 1991) hence used tissue weighting factors from *Publication 26* (ICRP, 1977). Predates *Publication 66* (ICRP, 1994b), hence used lung model from *Publication 30* (ICRP, 1979). The dose coefficients given in *Publication 56* were superseded by those in *Publications 67* and *71*.
67 (1993)	Ingestion*	Age-dependent biokinetic models with effective dose coefficients and tissue equivalent dose coefficients for ingestion of selected radioisotopes of S, Co, Ni, Zn, Mo, Tc, Ag, Te, Ba, Pb, Po, and Ra. Updated biokinetic models are given for Sr, Pu, Am, and Np. Updated dose coefficients are given for H, C, Sr, Zr, Nb, Ru, I, Cs, Ce, Pu, Am, and Np using tissue weighting factors from *Publication 60* (ICRP, 1991).
69 (1995)	Ingestion*	Age-dependent biokinetic models with effective dose coefficients and tissue equivalent dose coefficients for ingestion of selected radioisotopes for Fe, Sb, Se, Th, and U.
71 (1995)	Inhalation*	Effective dose coefficients and tissue equivalent dose coefficients for inhalation of the radioisotopes of elements covered in *Publications 56*, *67*, and *69*, plus isotopes of Ca and Cm for which age-dependent biokinetic models are also given. HRTM applied.
72 (1996)	Inhalation and ingestion*	Effective dose coefficients for radioisotopes of the 31 elements covered in *Publications 56*, *67*, *69*, and *71*, plus radioisotopes of the further 60 elements covered in *Publications 30* and *68*. Intakes by both ingestion and inhalation. HRTM applied.
CD1 (1999)	Inhalation and ingestion*†	A database of effective and tissue equivalent dose coefficients for 10 aerosol particle sizes and 10 times after intake. All radionuclides covered in *Publications 68* and *72*. Consistent with the dose coefficients in *Publications 68* and *72*. Extensive help files also provided.
88 (2001)	Inhalation and ingestion†	Fetal dose coefficients for intakes before and during pregnancy of the 31 elements covered in *Publications 56*, *67*, *69*, and *71*, including doses to the embryo and fetus and to the child from activity retained at birth.

ICRP Publication No. (year)	Application	Contents
CD2 (2002)	Inhalation and ingestion†	A database of effective and tissue equivalent fetal dose coefficients for 10 aerosol particle sizes and five times after birth. All radionuclides covered in *Publication 88*. Consistent with the dose coefficients in *Publication 88*. Extensive help files also provided.
95 (2004)	Inhalation and ingestion†	Infant dose coefficients from intakes in maternal milk, for intakes by the mother, before and during pregnancy, and during the period of breastfeeding, of the 31 elements covered in *Publication 88*, plus isotopes of Na, Mg, P and K. For the four elements not included in *Publication 88*, doses to the embryo and fetus following maternal intakes before and during pregnancy are also given.
CD3 (2005)	Inhalation and ingestion†	A database of effective and tissue equivalent dose coefficients from intakes in maternal milk, for acute and chronic intakes by the mother, before and during pregnancy, and during the period of breastfeeding (more scenarios than in *Publication 95*), for ingestion and inhalation of vapours and 10 aerosol particle sizes. All radionuclides covered in *Publication 95*. Consistent with the dose coefficients in *Publication 95*, and also for additional intergration times. Extensive help files also provided.
119 (2012)	Inhalation and ingestion*†	Compilation of dose coefficients for intakes of radionuclides by workers and members of the public, and conversion coefficients for use in occupational radiological protection against external radiation from *Publications 68*, *72*, and *74* (ICRP, 1994a, 1995c, 1996).

* Age-dependent dose coefficients for members of the public (3 mo, 1, 5, 10, and 15 y, and adult).
† Dose coefficients also given for workers.

(13) This series of reports provides revised age-dependent dose coefficients for members of the public for intakes of radionuclides by inhalation and ingestion, replacing the Publication 56 series. As in the *Publication 56* series, dose coefficients are presented in this series of reports for intakes by 3-mo-old infants, 1-, 5-, 10-, and 15-y-old children, and adults. In most cases the adult is taken to be aged 20 y. Exceptions are made for the alkaline earth elements, lead, thorium, uranium, neptunium, plutonium, americium and curium (ICRP, 1993, 1995a). For these elements, the transfer rates for the adult apply to age 25 y, because some of the transfer rates in the biokinetic models are equated with bone formation rates, which are expected to remain elevated up to about age 25 y. In the calculations of the activity in source regions of the body, following intakes at these ages, continuous changes with age in the transfer rates governing its distribution and retention are obtained by linear interpolation according to age. This also applies to the transfer of activity from the small intestine to body fluids. For application to other ages and protracted intakes, it is considered here, as in the *Publication 56* series (e.g. ICRP, 1990) that tissue doses can be estimated by applying the age-specific dose coefficients to the age ranges given below:

3 mo: from 0 to 12 mo of age
1 y: from 1 y to 2 y
5 y: more than 2 y to 7 y
10 y: more than 7 y to 12 y
15 y: more than 12 y to 17 y
Adult: more than 17 y

(14) As in the *Publication 56* series, a single Reference Person is used to represent each age-group. Generally, biokinetic parameter values for males have been adopted because of the availability of biokinetic data. Where there are known differences between sexes in the biokinetics of an element, this is noted in the relevant section of the biokinetic data in OIR: Parts 2–5 (ICRP, 2016a, 2017, 2019, 2022) or in this volume. Energy absorption is considered in models representing the Reference Male and Reference Female at each age.

(15) These dose coefficients are provided for intake by inhalation and ingestion in a range of physico-chemical forms for each radionuclide, and in the case of inhalation, in a range of aerosol particle size distributions.

(16) While the generic definition of protection quantities remains unchanged in the most recent recommendations of (Publication 103, ICRP, 2007), there have been changes that affect calculated values of dose per radiation exposure, including changes to radiation and tissue weighting factors, updated and expanded sets of specific absorbed fractions (Publication 133, ICRP, 2016, Publication 1XX, 202X) supported in large part by adoption of reference computational phantoms (Publication 110, ICRP, 2009, Publication 143, 2020), and the development of the new generation of reference biokinetic models.

(17) The full data set of the report series is provided as an electronic annex. The printed documents contain a selected set of data and materials. Data are presented in a standard format for each element and its radioisotopes. Tabulated dose coefficients may be used to determine committed effective dose from a known intake of a radionuclide. A full description of the information provided for each element and radioisotope is given in Section 4.

(18) The revised dose coefficients have been calculated using the *Publication 100* (ICRP, 2006) HATM and the revision of the *Publication 66* (ICRP, 1994b) HRTM described in *Publication 130* (ICRP, 2015). The revisions made to the HRTM are described in Annex A of *Publication 130*. In addition, information is provided in OIR: Parts 2–5 (ICRP, 2016a, 2017, 2019, 2022) and in this volume on absorption to blood following inhalation and ingestion of different chemical forms of elements and their radioisotopes. In selected cases, it is judged that

the data are sufficient to make material-specific recommendations. Revisions have been made to many models for the systemic biokinetics of radionuclides, making them more physiologically realistic representations of uptake and retention in organs and tissues and of excretion.

(19) Biokinetic models, reference physiological data, computational phantoms and radiation transport calculation codes are used for the calculation of dose coefficients (ICRP, 2007). ICRP publishes dose coefficients for the inhalation or ingestion of individual radionuclides by members of the public, giving both equivalent doses to organs and tissues, and effective dose (ICRP, 1991, 2007). The steps in the calculation (Fig. 1.1) can be summarised as follows:

- By use of the reference biokinetic models, the distribution and retention of radionuclides in body organs and tissues of the Reference Member of the Public are determined as a function of time after intake by inhalation or ingestion. For radiation protection purposes, it is assumed that all biokinetic parameters of the Reference Individual representing each age group are invariant on sex, anatomy, physiology, race and other individual-related factors, but based on reference male parameter values where sex-specific models are available. In this series of reports, the time-dependent activity is calculated in each source region over a period following the intake, which is taken to be 50 y for adults and from intake to age 70 y for children;
- Age and sex-dependent specific absorbed fractions are used to compute S-coefficients (ICRP, 2016b and forthcoming). The specific absorbed fractions are based on whole-body voxel phantoms (ICRP, 2009, 2020), skeletal models, and stylised models of alimentary and respiratory tract geometries.
- The radiation weighting factors are applied to determine sex-specific committed equivalent dose coefficients to an organ or tissue;
- The sex-specific committed equivalent dose coefficients are sex-averaged; and
- The tissue weighting factors are then applied to determine the sex-averaged committed effective dose coefficient, produced for different reference age-groups.

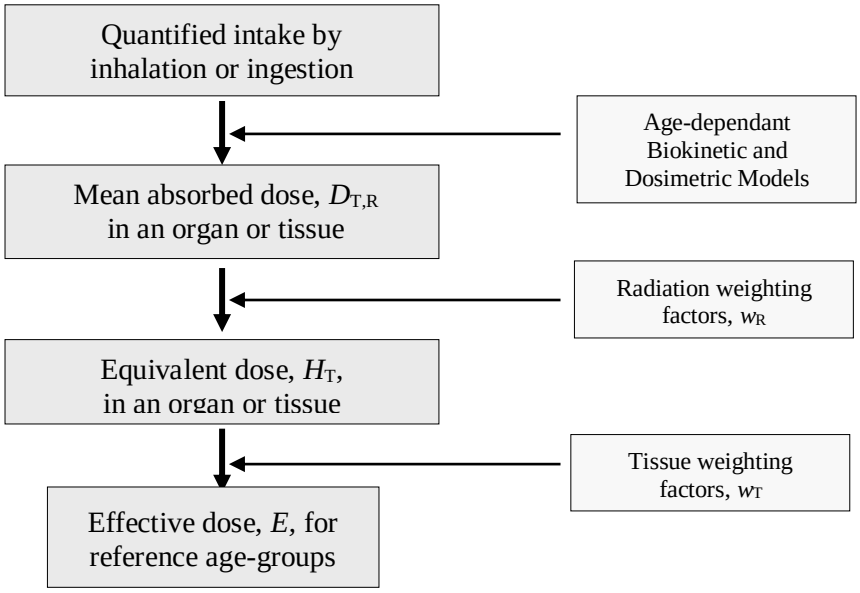

Fig. 1.1. Calculation of absorbed dose and the protection quantities, equivalent and effective dose – for intakes of radionuclides.

(20) The details of the computational procedure used in this report series are described in Section 2.7.

1.2. Changes in Publication 103 that affect the calculation of equivalent and effective dose

(21) In the 2007 Recommendations issued in *Publication 103* (ICRP, 2007), the concept and use of equivalent and effective dose remain unchanged, but a number of revisions were made to the methods used in their calculation. Changes were introduced in the radiation and tissue weighting factors, from the values previously recommended in *Publication 60* (ICRP, 1991). Since radiation weighting factors (w_R) for photons, electron and α particles are unchanged, the only difference of potential importance to internally deposited radionuclides is for neutrons (Table 1.2). The changes made do not reflect the availability of additional data but rather a reconsideration of the appropriate treatment of radiation weighting for protection purposes. The abandonment of a step function for neutron w_R as a function of energy is a reflection of the fact that in practice, only a continuous function has been used. The major change in the continuous function is a lower w_R value at low energies which more properly reflects the low linear energy transfer contribution from secondary photons. In addition, there are good theoretical reasons for assuming that w_R values at high energies will converge with that for protons.

Table 1.2. ICRP radiation weighting factors (ICRP, 2007)

Radiation Type	Radiation weighting factor, w_R
Photons	1
Electrons and muons	1
Protons and charged pions	2
α particles, fission fragments, heavy ions	20
Neutrons	Revised continuous function of neutron energy

(22) The values of tissue weighting factors (w_T) recommended in *Publication 103* (ICRP, 2007) are shown in Table 1.3. Changes from values given in *Publication 60* (ICRP, 1991) reflect improved knowledge of radiation risks. The main sources of data on cancer risks are the follow-up studies of the Japanese atomic bomb survivors, used to derive risk coefficients averaged over seven Western and Asian populations with different background cancer rates (ICRP, 2007). The new w_T values are based on cancer incidence rather than mortality data, adjusted for lethality, loss of quality of life and years of life lost. Weighting for hereditary effects is now based on estimates of disease in the first two generations rather than at theoretical equilibrium. The main changes in w_T values in the 2007 Recommendations are a decrease (from 0.2 to 0.08) for gonads and an increase (from 0.05 to 0.12) for breast and for remainder, which now includes more organs and tissues. The remainder dose is now calculated as the arithmetic mean of the doses to the thirteen organs and tissues for each sex (Table 1.3). The so-called splitting rule in the treatment of the remainder in Publication 60 (ICRP, 1991) is no longer used and hence the effective dose is additive. Tissue weighting factors continue to represent averages across the sexes and across all ages.

Table 1.3. *Publication 103* (ICRP, 2007) tissue weighting factors

Tissue	w_T	$\sum w_T$
Bone-marrow, breast, colon, lung, stomach, remainder tissues (13 for each sex*)	0.12	0.72
Gonads	0.08	0.08
Urinary bladder, oesophagus, liver, thyroid	0.04	0.16
Bone surface, brain, salivary glands, skin	0.01	0.04

*Remainder tissues: adrenals, ET regions of the respiratory tract, gall bladder, heart, kidneys, lymphatic nodes, muscle, oral mucosa, pancreas, prostate (male), small intestine, spleen, thymus, uterus/cervix (female).

(23) A further important change introduced in the 2007 Recommendations is that doses from external and internal sources are calculated using reference computational phantoms of the human body (ICRP, 2009, 2020). In the past, the Commission did not specify a particular phantom, and various mathematical phantoms such as hermaphrodite Medical Internal Radiation Dose (MIRD)-type phantoms (Snyder et al., 1969), the sex-specific models of Kramer et al. (1982), or the age-specific phantoms of Cristy and Eckerman (1987) have been used. Voxel models, constructed from medical imaging data of real people, give a more realistic description of the human body than afforded in mathematical (or stylised) phantoms. Thus, the ICRP decided to use voxel models to define the reference phantoms to be used in the calculations of dose distribution in the body for both internal and external exposures. These models (or computational phantoms), described in *Publication 110* (ICRP, 2009) and in *Publication 143* (ICRP, 2020) , are representative of the Reference Members of the Public. They are designed specifically for the calculation of the radiological protection quantities corresponding to the effective dose concept of the 2007 Recommendations. These computational phantoms have been supplemented with additional models when necessary and used to compute new specific absorbed fractions in *Publication 133* (ICRP, 2016) and *Publication 1XX* (ICRP, 202X). The updated specific absorbed fractions include energy-dependent values for electrons and alpha particles representing a significant improvement to radiation protection dosimetry compared to non-energy dependent values in *Publication 30* (ICRP, 1982). For each age group, equivalent doses to organs and tissues, H_T, are calculated separately for the Reference Male and Female and then averaged in the calculation of effective dose, E:

$$E = \sum_T w_T \left[\frac{H_T^M + H_T^F}{2}\right] \quad (1.1)$$

where:

$$H_T^M = \sum_T w_R D_{R,T} \quad \text{(male)}$$

$$H_T^F = \sum_T w_R D_{R,T} \quad \text{(female)}$$

(24) It is made clear in *Publication 103* (ICRP, 2007) that effective dose is intended for use as a protection quantity on the basis of reference values and relates to reference persons

rather than specific individuals. The main uses of effective dose are in prospective dose assessment for planning and optimisation in radiological protection, and retrospective demonstration of compliance for regulatory purposes. Sex-averaging in the calculation of equivalent and effective doses, implicit in the past use of hermaphrodite mathematical phantoms, is now explicit in the averaging of equivalent doses to male and female phantoms. Sex- and age-averaging in the derivation of tissue weighting factors can be seen to obscure differences in estimates of absolute radiation detriment between men and women and between adults and children. However, practical protection would not be improved by calculating effective dose separately for males and females and to do so might give a misleading impression of the precision of these quantities.

1.3. Biokinetic models implemented in this series of reports

(25) Biokinetic models for individual elements and their radioisotopes are used to calculate the total number of transformations occurring within specific tissues, organs or body regions (source regions) during a given period of time (usually 50 y for adults, or to age 70 y for children) by determining the time-integrated activity in each source region. Dosimetric models are used to calculate the deposition of energy in all important organs/tissues (targets) for transformations occurring in each source region, taking account of the energies and yields of all emissions (Section 2.7). Committed absorbed dose in target regions (in grays) can then be calculated, knowing the number of decays occurring in source regions and energy deposition in target regions.

(26) Biokinetic models of the alimentary and respiratory tracts are used to define the movement of radionuclides within these systems, resulting in absorption to blood and/or loss from the body. The behaviour of radionuclides absorbed to blood is described by element-specific systemic models that range in complexity. The models used in this series of reports are described in Section 2.

1.4. Dosimetry implemented in this series of reports

(27) Dose calculations involve the use of nuclear decay data, anthropomorphic phantoms that describe the human anatomy and codes that simulate radiation transport and energy deposition in the body. The data provided in this report series are calculated using revised decay data (*Publication 107*, ICRP, 2008), the ICRP reference computational phantoms of the adult and children based on medical imaging data (ICRP, 2009, 2020), separate models for the skeletal (Hough et al., 2011; O'Reilly et al., 2016; Pafundi et al., 2010), alimentary (ICRP, 2006), and respiratory tract anatomies (ICRP, 1994b), and well-established Monte Carlo codes (Kawrakow et al., 2006; Niita et al., 2010; Pelowitz, 2008). Radiation transport in the anatomical phantoms and models provides age, radiation, and sex-dependent tables of specific absorbed fractions (ICRP, 2016b and forthcoming; Schwarz et al., 2021a, 2021b).

(28) For all dose calculations, radionuclides are assumed to be uniformly distributed throughout source regions, although these can be whole organs (e.g. liver) or a thin layer within a tissue (e.g. mucosa layers in the alimentary tract). Similarly, target cells are assumed to be uniformly distributed throughout target regions that vary in size from whole organs to layers of cells. Doses from 'cross-fire' radiation between source and target regions are important for penetrating photon radiation. For 'non-penetrating' α and β particle radiations, energy will in most cases be largely deposited in the tissue in which the radionuclide is deposited. Photon and electron transport are followed for most source and target combinations. Additionally, special

considerations are taken into account for α and β emissions in a number of important cases. These include:

- Doses to target cells in the walls of the respiratory tract airways from radionuclides in the airways (ICRP, 1994b);
- Doses to target cells in the alimentary tract from radionuclides in the lumen (ICRP, 2006); and
- Doses to cells adjacent to inner bone surfaces (50-μm layer; see below) and all red marrow from radionuclides on bone surfaces and within bone mineral.

1.4.1. Nuclear decay data, Publication 107

(29) A fundamental requirement for dose calculations is reliable information on half-life, modes of decay, and the energies and yields of the various radiations emitted by radionuclides and their progeny (Eckerman et al., 1994; Endo et al., 2003, 2005). The calculations in this report use the nuclear decay data provided in Publication 107 (ICRP, 2008). This publication replaces *Publication 38* (ICRP, 1983) and consists of an explanatory text, with an accompanying CD-ROM providing data on the radiation emissions of 1252 radioisotopes of 97 elements. Radioisotopes of elements of atomic number less than 101 were included in *Publication 107* if their half-lives exceed 1 min, or if they are the progeny of a selected radionuclide and if the basic nuclear structure data enabled a meaningful analysis of their emissions. CD-ROM use has enabled the complete listing of emitted radiations, and more details of Auger cascades and spontaneous fission data. The data given include: energies and intensities of emitted radiations; β, neutron, and Auger and Coster-Kronig (CK) electrons spectra; spontaneous fission radiations and α recoil; half-lives, branching decay and chains; and no cut-off on the number of emissions.

(30) In this series of reports, dose coefficients are presented for almost all radionuclides included in *Publication 107* (ICRP, 2008) that have half-lives equal to or greater than 10 min, and for other selected radionuclides. For radionuclides with decay chains, all parent radionuclides with half-lives equal to or greater than 10 min are included, but no constraint is placed on the half-lives of progeny radionuclides.

1.4.2. Adult reference computational phantoms, Publication 110

(31) As outlined above, the 2007 Recommendations (ICRP, 2007) adopted the use of realistic anatomical models to replace the stylised computational phantoms of human anatomy previously used in the calculation of dose coefficients for both external and internal radiation protection (Cristy, 1980; Cristy and Eckerman, 1987). These were indeed limited in their ability to capture anatomic realism. The new reference phantoms are voxel models based on segmented tomographic data of real individuals obtained from computed tomography (CT) or magnetic resonance imaging.

(32) *Publication 110* (ICRP, 2009) describes the development and intended use of the computational phantoms of the Reference Adult Male and the Reference Adult Female. They were constructed after modifying the voxel models of two individuals whose body height and mass closely matched reference values (Zankl et al., 2002, 2003, 2007). The report describes the methods used for this process and the anatomical and computational characteristics of the resulting phantoms.

(33) *Publication 143* (ICRP, 2020) describes the development and intended use of the age-dependent paediatric reference computational phantoms. CT images for the newborn were based on prospective images of cadavers (Lee et al., 2007; Nipper et al., 2002). For other

reference ages, the CT images came from retrospective review and image retrieval from radiology archives (Lee et al., 2010).

(34) The reference computational phantoms are used, together with codes that simulate radiation transport and energy deposition, for the assessment of the specific absorbed fraction of energy per unit mass, Φ, in an organ or tissue due to emissions in a source organ or region from which equivalent doses and the effective dose are calculated successively.

1.4.3. Advances in skeletal dosimetry

(35) In *Publication 130* (ICRP, 2015), the skeletal dosimetry models of *Publication 30* (ICRP, 1979) were substantially updated for all radiations emitted from internally deposited radionuclides – α particles, electrons, β particles, photons, and neutrons (e.g. from spontaneous fission). Improvements over the *Publication 30* models include a more refined treatment of the dependence of the absorbed fraction on particle energy, marrow cellularity, and bone-specific spongiosa micro-architecture. Two reference sets of skeletal images were established for radiation transport simulation. The first included 1-mm ex-vivo CT images of some 38 skeletal sites harvested from a 40-y old male cadaver (Hough et al., 2011). These images were used to establish fractional volumes of cortical bone, trabecular spongiosa, and medullary cavities by skeletal site, and to serve as the macroscopic geometric model for particle transport. The second included 30-µm microCT images of cored samples of trabecular spongiosa to establish fractional volumes of trabecular bone and marrow tissues, and to serve as the microscopic geometric model for particle transport. Both image sets were then combined during paired-image radiation transport (PIRT) of internally emitted electrons (Shah et al., 2005). Source tissues were: bone marrow (active and inactive), mineral bone surfaces (trabecular and cortical), and mineral bone volumes (trabecular and cortical). Target regions considered were: active marrow (surrogate tissue for the hematopoietic stem and progenitor cells), and a revised 50-µm model of the skeletal endosteum (surrogate tissue for the osteoprogenitor cells) (see 'Endosteum' in the Glossary). Absorbed fractions for internally deposited α particles and neutron-generated recoil protons were established based on path length-based transport algorithms given in Jokisch et al. (2011; 2011). Values of absorbed fractions to active marrow and endosteum for internally-emitted photons and neutrons were obtained by first tallying energy-dependent particle fluences within the spongiosa and medullary cavity regions of the *Publication 110* Reference Adult Male and Reference Adult Female voxel phantoms (ICRP, 2009) and then applying fluence-to-absorbed dose response functions (DRFs). Further details on the derivations of these photon and neutron skeletal DRFs are given in Johnson et al. (2011) and Bahadori et al. (Bahadori et al., 2011), respectively, as well as in Annexes D and E of *Publication 116* (ICRP, 2010a).

1.5. Pregnancy and breast-feeding

(36) ICRP has provided information in *Publications 88* and *95* (ICRP, 2001, 2004) on doses to the embryo, fetus and newborn child following intake of radionuclides by female members of the public and workers either before or during pregnancy or during lactation. Comparisons of fetal dose coefficients given in *Publication 88* with corresponding adult dose coefficients showed that doses received by a woman from intakes before or during pregnancy will in most cases be substantially greater than doses to her fetus. However, doses to the offspring can exceed doses to the mother for a number of radionuclides. In particular, the requirements of skeletal development during fetal growth, particularly in late pregnancy, can lead to significant uptake of radioisotopes of phosphorus and of calcium and, to a lesser extent,

other alkaline earth elements. Thus, offspring to adult dose ratios were up to factors of approximately 10–20 for isotopes of P and Ca and 2–6 for isotopes of Sr (ICRP, 2004; Stather et al., 2003). Uptake of radioisotopes of iodine by the fetal thyroid can also lead to greater doses to the fetus than to the mother following intakes late in pregnancy (dose ratios of up to approximately 3) (Berkovski et al., 2003). Other radionuclides for which doses to the fetus can exceed doses to the mother include tritium as tritiated water, ^{14}C and ^{35}S. Offspring to adult dose ratios are greatest following ingestion or inhalation of soluble (Type F) forms. Values of offspring to adult dose ratios may change as a result of future calculations following from *Publication 103* (ICRP, 2007) and associated changes. Offspring protection may also be of concern when the dose ratio is <1, since an effective dose of 1 mSv to the embryo, fetus or newborn child might be reached at otherwise acceptable levels of occupational dose (Phipps et al., 2001).

(37) In general, doses to the infant from radionuclides ingested in breast milk are estimated to be small in comparison with doses to the Reference Adult (ICRP, 2004). On the basis of the models developed in *Publication 95* (ICRP, 2004), it is only in the cases of tritiated water, ^{45}Ca, ^{75}Se and ^{131}I that infant doses may exceed adult doses, by factors of between 1 and 3. Infant doses are highest when maternal intakes by ingestion occur shortly after birth, because maximum transfer occurs under these conditions. Ratios of infant to adult doses are generally lower for intakes by inhalation than for ingestion. Comparisons with *Publication 88* (ICRP, 2001) doses to the offspring due to in-utero exposures show that in most cases, these are more important than doses that may result from breast feeding; exceptions include ^{60}Co, ^{131}I and ^{210}Po. ICRP intends to provide a revision of these dose coefficients in a later report in this series.

1.6. Structure of the report

(38) This series of reports provides revised dose coefficients for EIR by inhalation and ingestion, replacing the *Publication 56* series, which gave doses to members of the public from intake of radionuclides: *Publications 56*, *67*, *69*, *71*, *72*, *88* and *95* (ICRP, 1990, 1993, 1995a, 1995b, 1995c, 2001, 2004).

(39) Section 2 of this report gives an overview of the biokinetic and dosimetric models used to calculate dose coefficients and bioassay functions. It describes the main features of the *Publication 130* (ICRP, 2015) revision of the HRTM and the *Publication 100* HATM (ICRP, 2006). Section 2 also provides an introduction to the models used in this report series to describe the systemic biokinetics of elements and their radioisotopes. Dosimetric models and the ICRP computational methodology are also explained.

(40) Section 3 describes general aspects of internal dose assessment, including sources of uncertainties.

(41) Section 4 provides a brief outline of the types of information included in subsequent parts of this series of reports: biokinetic data and dose coefficients for individual elements and their radioisotopes. Each element section provides dose coefficients: committed effective dose per Bq intake (Sv Bq^{-1}) for inhalation and ingestion of all relevant radioisotopes. Data are provided in the printed reports of the series and in electronic annexes.

(42) The data provided in the printed reports are restricted to tables of committed effective dose per intake (Sv Bq^{-1}). For intakes by inhalation, data are provided for all absorption types of the most common isotope(s), and for an activity median aerodynamic diameter (AMAD) of 1 μm. In cases for which sufficient information is available (principally for actinides and for gas and vapour forms), lung absorption is specified for different chemical forms, and dose

coefficients are calculated accordingly. Dose coefficients for intake by ingestion are also given, for different chemical forms when sufficient information is available.

(43) The electronic data that accompanies this series of reports and that are available on the ICRP website contain a comprehensive set of committed effective and equivalent dose coefficients, for most of the isotopes presented in *Publication 107* (ICRP, 2008), and for a range of physico-chemical forms and aerosol AMADs and activity median thermodynamic diameters (AMTDs).

(44) The electronic data are made of a set of data files with dose coefficients and other radionuclide-specific data which may be accessed by the user directly or by using the accompanying Data Viewer. The Data Viewer permits rapid navigation of the dataset and visualisation of the data in tabulated and graphical formats.

2. BIOKINETIC AND DOSIMETRIC MODELS

2.1. Introduction

(45) This Section gives an overview of the biokinetic and dosimetric models used to calculate dose coefficients and bioassay functions, as they apply to the general population. It describes the main features of the Human Respiratory Tract Model (HRTM, ICRP, 1994b), as updated in *Publication 130* (ICRP, 2015), and of the Human Alimentary Tract Model (HATM, ICRP, 2006). It provides an introduction to the models used in this series of reports to describe the systemic biokinetics of elements and their radioisotopes. Dosimetric models and methodology are also explained.

(46) Radionuclide exposures in the environment can lead to intakes by a number of routes: inhalation, ingestion, entry through intact skin and wounds. Fig. 2.1 summarises the routes of intake, internal transfers, and routes of excretion.

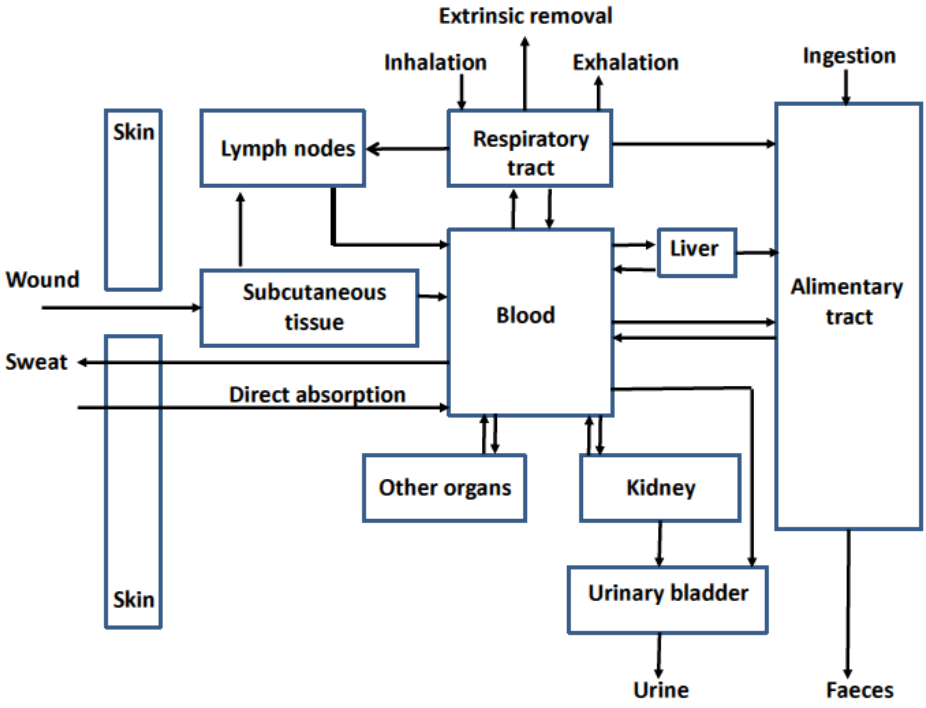

Fig. 2.1. Summary of the main routes of intake, transfer and excretion of radionuclides in the body.

(47) Following inhalation, inhaled particles containing radionuclides deposit in the various regions of the respiratory tract, with deposition in each being mainly dependent on particle size (ICRP, 1994b, 2002b). Removal from the respiratory tract occurs mainly by dissolution and absorption to blood, and the competing process of transport of particles to the throat followed by their entry into the alimentary tract. The proportions absorbed to blood or cleared by particle transport depend on the speciation and the solubility of the material, and on the radioactive half-life of the radionuclide. The HRTM is also applied here to gases and vapours and to inhalation of radon and its radioactive progeny.

(48) For ingestion of radionuclides, the *Publication 30* (ICRP, 1979) model of the gastrointestinal tract has been replaced by the Human Alimentary Tract Model (HATM)

described in *Publication 100* (ICRP, 2006), which is applied in this series of reports. The model is also used for radionuclides in particles cleared to the throat from the respiratory tract after inhalation. In the HATM, fractional absorption of radionuclides is specified by the alimentary tract transfer factor, f_A, instead of the f_1 value as given for the gastrointestinal model described in *Publication 30* (ICRP, 1979). The f_A value describes total absorption from all regions of the alimentary tract, although the default assumption is that all absorption takes place in the small intestine.

(49) Intact skin is an effective barrier against entry of most substances into the body, and few radionuclides cross it to any significant extent (see Section 3.4.1 of *Publication 130* (ICRP, 2015)). Exceptions of practical importance include forms of tritium, carbon and iodine. There is no general model for absorption of radionuclides through the skin because of the wide range of possible exposure scenarios. Both the radiation dose to the area of skin contaminated and the dose to the whole body as a result of absorption should be considered. ICRP (1991, 2007) recommends that local skin doses should be calculated to sensitive cells, assumed to be at a depth of 70 μm, or averaged over the layer of tissue 50 to 100 μm below the skin surface and averaged over the most exposed 1 cm^2 of skin tissue. This applies to activity either distributed over the skin surface or aggregated in particles. No dosimetric models are recommended by ICRP for calculating doses from radionuclides deposited on the skin and no dose coefficients are given.

(50) ICRP has generally not given advice on assessing doses from intakes of radionuclides transferred from wound sites to blood and other organs and tissues. Internal exposure resulting from wounds almost always arises because of accidents in the workplace, rather than as a result of routine operations that are subject to the normal environmental controls. Uptake from wounds can vary greatly depending on the circumstances of a particular incident, and in practice, the assessment of internal contamination is treated on a case-by-case basis. As a result, provision of generic dose coefficients or bioassay functions would be of limited value. Information on the transfer of radionuclides from wound sites has, however, been reviewed by a Scientific Committee of the U.S. National Council on Radiation Protection and Measurements (NCRP), and these data have been used to develop a model to describe the transfer of material from wounds after intakes in different physico-chemical forms (NCRP, 2006). Section 3.4 of *Publication 130* (ICRP, 2015) summarises the main features of the NCRP model. Dose coefficients for injection as the route of intake are given in the electronic annexe to the OIR series of reports, which may assist in assessment of doses after wound contamination. These coefficients are not given in this series of report, since contamination by wound is not a common way of exposure for the members of the public.

(51) For each route of intake, a portion of the radionuclide entering the body is absorbed to blood and distributed systemically. The systemic distribution of radionuclides in the body can be diffuse and relatively homogeneous, as for the examples of tritiated water and radioisotopes of potassium and caesium, or may be localised in certain organs or tissues, as for the examples of radioisotopes of iodine (thyroid), alkaline earth elements (bone), and plutonium (bone and liver). Systemic biokinetic models are used to describe the distribution and excretion of radionuclides absorbed to blood. The systemic models for the elements have been reviewed and revised as necessary to take account of more recent information and provide models that are appropriate for both dosimetry and bioassay interpretation.

(52) Removal of deposited material from the body occurs principally by urinary and faecal excretion although radionuclides may also be lost by exhalation or through the skin (e.g. tritiated water). Urinary excretion is the removal in urine of radionuclides from blood following filtration by the kidneys. Faecal excretion has two components: systemic (endogenous) faecal excretion, which represents removal of systemic material via the alimentary tract due to biliary

secretion from the liver and secretions at other sites along the alimentary tract; and direct (exogenous) faecal excretion, of the material passing unabsorbed through the alimentary tract after ingestion or clearance to the throat from the respiratory system after inhalation. The reference models outlined in this section are assigned reference parameter values, and used to calculate body or organ content at specified times after acute or chronic intake. Together with dosimetric data, they are used to calculate reference dose coefficients.

2.2. Human Respiratory Tract Model (HRTM)

(53) The HRTM is described in full in *Publication 66* (ICRP, 1994b). It was applied to calculate inhalation dose coefficients for workers and members of the public in *Publications 68*, *71*, *72*, *88* and *95* (ICRP, 1994a, 1995b, 1995c, 2001, 2004), and bioassay functions in *Publication 78* (ICRP, 1997). Further guidance on its use was given in ICRP *Supporting Guidance 3* (ICRP, 2002b).

(54) The HRTM was updated in *Publication 130* (ICRP, 2015) to take account of data accumulated since its publication, although the basic features of the model remain unchanged. The revised HRTM (ICRP, 2015) is used in this series of reports, as described below. Simple changes from the original HRTM are noted in this section. The major changes made relate to the clearance of deposited material by both particle transport and absorption to blood. These changes involved review and analysis of relevant recent information, and judgements in implementing the changes in the HRTM: they are described in Annex A of *Publication 130* (ICRP, 2015).

(55) A summary of the main features of the revised HRTM is given here, in particular those relating to age dependence. The HRTM applies explicitly to all members of the population, giving parameter values for 3-mo-old infants, 1-, 5-, 10- and 15-y-old children, and adults. The principal age-specific aspects are unchanged from those described in *Publication 71* (ICRP, 1995b). In this report, as in *Publications 71* and *72* (ICRP, 1995b, 1995c), only one Reference Individual is used to represent each age group. For those ages at which *Publication 66* provides separate parameter values for males and females (10 y and above), the male values are used here for the Reference Individual representing the age group. Nevertheless, tissue doses are calculated for males and females separately, before being combined to calculate the effective doses to Reference Individuals. If inhalation doses specific to females should be required, then data given in *Publication 66* enable them to be calculated. However, for a given exposure, differences in doses between males and females of the same age are small, because for females both intake and body mass are smaller than for males by approximately 20% (ICRP, 1995b).

(56) As in the original version of the HRTM, the respiratory tract is treated as two tissues: the extrathoracic (ET) and the thoracic (TH) airways. The sub-division of these tissues into regions was based mainly on differences in sensitivity to radiation. The TH regions are bronchial, (BB: trachea, airway generation 0, and bronchi, airway generations 1–8), bronchiolar (bb: airway generations 9–15), alveolar–interstitial (AI: the gas exchange region, airway generations ≥16); and the TH lymph nodes, LN_{TH}. The ET regions are the anterior nasal passage, ET_1; the posterior nasal passages, pharynx and larynx, ET_2; and the ET lymph nodes LN_{ET} (Fig. 2.2). For consistency with the HATM, the oral passage is now not included in region ET_2 as it was in *Publication 66*. This does not affect results obtained with the model, because deposition in ET from air entering the mouth was taken to occur only in the larynx.

(57) Values of dimensions of the airways, and scaling factors for subjects of different ages, are specified in *Publication 66* (ICRP, 1994b). In order to apply the model to different age groups, dimensions of conducting and respiratory airways are scaled by body height and

Functional Residual Capacity, respectively. It is assumed that the branching structure of the airways (BB and bb) is complete at birth, and that the number of alveoli increases linearly with time, from 40% of the adult total at 3 mo, to 80% at 1 y. The mass of the AI is scaled on the basis of body mass. These dimensions are used with the deposition model to calculate regional deposition, and are also used to derive masses of target tissues (see below).

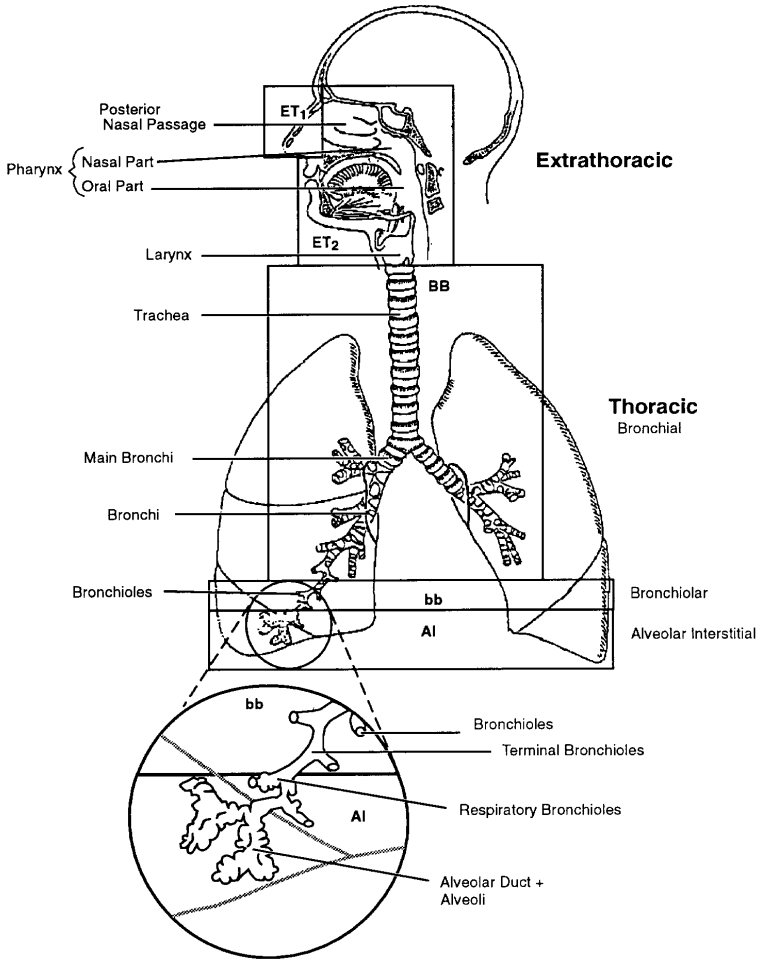

Fig. 2.2. Respiratory tract regions defined in the HRTM. Note that the oral part of the pharynx is no longer part of ET_2. ET_1: extrathoracic region including the anterior nasal passage; ET_2 extrathoracic region including posterior nasal passage, pharynx and larynx; BB: bronchial region; bb: bronchiolar region; AI: alveolar–interstitial region. Taken from ICRP (1994b).

2.2.1. Physiology

(58) This section is essentially unchanged from the corresponding section of *Publication 71* (ICRP, 1995b). The HRTM enables inhalation dose coefficients to be calculated, and also intake per exposure (time-integrated activity concentration in air), and hence doses per exposure, which are frequently required for environmental dose assessments. Two factors relate intake to exposure: inhalability and ventilation.

(59) Inhalability is the ratio of the particle concentration in the air entering the respiratory tract to that in the ambient air (taken to be 1 for particles with an aerodynamic diameter smaller than approximately 1 μm). The inertia of larger particles increases the concentration in the air entering the nose or mouth when facing into a wind, and reduces it otherwise, the average net

effect being to reduce it to approximately half that in the ambient air for particles with aerodynamic diameters greater than approximately 30 μm. For convenience, inhalability is taken into account in the calculation of regional deposition fractions, rather than being treated separately. Inhalability is assumed to be independent of age and sex.

Table 2.1. Ventilation parameters for Reference Individuals*. Taken from Table 4 of *Publication 71*, (ICRP, 1995b)†.

Exercise level		Age					
		3 mo	1 y	5 y	10 y (Male)	15 y (Male)	Adult (Male)
Sleep	f_R (min^{-1})	38	34	23	17	14	12
	B (m^3 h^{-1})	0.09	0.15	0.24	0.31	0.42	0.45
Sitting	f_R (min^{-1})	–	36	25	19	15	12
	B (m^3 h^{-1})	–	0.22	0.32	0.38	0.48	0.54
Light exercise	f_R (min^{-1})	48	46	39	32	23	20
	B (m^3 h^{-1})	0.19	0.35	0.57	1.12	1.38	1.5
Heavy exercise	f_R (min^{-1})	–	–	–	44	36	26
	B (m^3 h^{-1})	–	–	–	2.22	2.92	3.0

*Reference values, given to sufficient precision for calculational purposes, which may be greater than would be chosen to reflect the certainty with which the average value of each parameter is known.
†Table 4 of *Publication 71* (ICRP, 1995b) was based on Table B15 of *Publication 66*, (ICRP, 1994b). f_R = frequency, B = ventilation rate.

(60) Ventilation, the breathing frequency and tidal volume, is the main factor in the model that depends on age and level of exercise. This is also the aspect for which there are comprehensive data relating to women and children as well as men. Reference values of the primary quantities, breathing frequency, f_R, (breaths per min) and ventilation rate, B, (m^3 h^{-1}), are given in Table 2.1 for each age group and for four levels of exercise: sleep, sitting, light exercise, and heavy exercise. For 3-mo-old infants, and for 1- and 5-y-old children, the values of f_R and B are the same for males and females. For the other age groups, where there are differences, male values are given (see Para. (55)). However, the values for 10-y-old males and females only differ for heavy exercise.

(61) The HRTM enables deposition fractions to be calculated separately for nose breathing and mouth breathing. Account can therefore be taken of the oro-nasal breathing that takes place in most individuals at heavy exercise, and in habitual mouth-breathers at all levels of exercise. It is assumed [see Para. 158 and Table 11 of *Publication 66*, (ICRP, 1994b)] that the fraction of total ventilatory airflow passing through the nose in normal nasal augmenters (nose-breathers) is 100% at sleep, sitting and light exercise, and 50% at heavy exercise. These fractions are taken to be independent of age and sex.

(62) The results of habit surveys are summarised in Annexe B (Respiratory Physiology) of *Publication 66* (ICRP, 1994b). Table 2.2 gives the distribution of time spent in various activities, taken from Table 4 of *Publication 71* (ICRP, 1995b). For 3-mo-, 1-, 5- and 10-y-old children, the time budgets in Table 2.2 are the same for males and females; and for the other age groups, male values are given (see Para. (55)). These results have been used to provide reference values, for calculating dose coefficients for environmental exposure, of the number of hours per day spent at each of the four levels of exercise, which are given in Table 2.3. For

10-y-old children, the values in Table 2.3 (and hence the deposition fractions derived from them in Table 2.4) are the same for males and females, because the time budget for 10-y-old children (Table 2.2) does not include heavy exercise, the only level at which there are differences in ventilation parameter values between males and females.

(63) These parameter values can be used to determine intake per exposure, and are also used with the deposition model to determine regional deposition.

Table 2.2. Daily time budget (h) for environmental exposure of Reference Individuals. Taken from Table 5 of *Publication 71*, (ICRP, 1995b)*.

Location			Age					
			3 mo	1 y	5 y	10 y	15 y (Male)	Adult (Male)
Indoors	At home:	Asleep	17	14	12	10	10	8.5
		Awake	7†	5‡	6‡	8‡	7§	7‡
	Elsewhere (*eg*. at work)			4‡	3‡	3‡	4§	6.5‡
Outdoors				1‡	3‡	3‡	3¶	2**

* Table 5 of *Publication 71* (ICRP, 1995b), was based on Table B16 of *Publication 66* (ICRP, 1994b), but only for the six Reference Individuals for which dose coefficients are given in *Publication* 71 and this series of reports.
† Light exercise
‡ One-third sitting + two-thirds light exercise
§ One-half sitting + one-half light exercise
¶ Two-thirds light exercise + one-third heavy exercise
** One-half sitting + three-eighths light exercise + one-eighth heavy exercise

Table 2.3. Daily time budget* and ventilation parameters† at each exercise level for environmental exposure of members of the public (Reference Individuals)‡ at various ages. Taken from Table 6 of *Publication 71*, (ICRP, 1995b).

Exercise level	3 mo			1 y			5 y		
	h	$m^3\ h^{-1}$	m^3	h	$m^3\ h^{-1}$	m^3	h	$m^3\ h^{-1}$	m^3
1. Sleep	17.0	0.09	1.53	14.0	0.15	2.10	12.0	0.24	2.88
2. Sitting				3.33	0.22	0.73	4.0	0.32	1.28
3. Light exercise	7.0	0.19	1.33	6.67	0.35	2.33	8.0	0.57	4.56
4. Heavy exercise									
Total			2.86			5.16			8.72

Exercise level	10 y			15 y(Male)			Adult (Male)		
	h	$m^3\ h^{-1}$	m^3	h	$m^3\ h^{-1}$	m^3	h	$m^3\ h^{-1}$	m^3
1. Sleep	10.0	0.31	3.10	10.0	0.42	4.20	8.0	0.45	3.60
2. Sitting	4.67	0.38	1.77	5.5	0.48	2.64	6.0	0.54	3.24
3. Light exercise	9.33	1.12	10.45	7.5	1.38	10.35	9.75	1.5	14.63
4. Heavy exercise				1.0	2.92	2.92	0.25	3.0	0.75
Total			15.3			20.1			22.2

* The number of hours per day spent at each exercise level given above are reference values (see below). Generally, they are based on the distributions of time given in Table 2.2, and rounded to the nearest 0.01 h. For the adult male however, the time asleep has been rounded down from 8.5 h to 8 h for consistency with the Reference Worker (Table 6 of *ICRP Publication 66*). The time spent sitting has been correspondingly increased by 0.5 h.
† The ventilation rates ($m^3\ h^{-1}$) are reference values taken from Table 2.1.
‡ The daily volumes inhaled (m^3) at each exercise level are derived from the reference values of time spent at each activity, and of ventilation rate. See Para. (62).
§ Reference values, given to sufficient precision for calculational purposes, which may be greater than would be chosen to reflect the certainty with which the average value of each parameter is known.

2.2.2. Deposition

2.2.2.1. Aerosols of (solid or liquid) particulate materials

(64) Deposition refers to the initial processes that determine how much of the material in the inhaled air remains behind after exhalation. The deposition model described in *Publication 66* (ICRP, 1994b) evaluates fractional deposition of an aerosol in each region, for all aerosol sizes of practical interest (0.6 nm – 100 μm). For radionuclides inhaled in particulate form (aerosols), it is assumed that entry and regional deposition in the respiratory tract of a given subject are governed only by the size distribution of the aerosol particles. Deposition fractions of gases and vapours are determined by their chemical form: see below.

(65) Deposition in the extrathoracic (ET) airways was determined empirically. Deposition measurements in men were related to characteristic parameters of particle size and airflow. The resulting deposition efficiencies were scaled by anatomical dimensions to predict deposition in women and children. In *Publication 66* (ICRP, 1994b) it was assumed that particles deposited in the nasal passage during inhalation are partitioned equally between ET_1 and the posterior nasal passage, which is part of ET_2. (However, because of the way the deposition efficiencies were calculated for polydisperse aerosols during inhalation and exhalation, for most aerosol sizes of interest in radiation protection the deposition fractions given in *Publications 66* (ICRP, 1994b) and *71* (ICRP, 1995b) are somewhat higher for ET_2 than for ET_1.)

(66) For the thoracic (TH) airways, a theoretical model of gas transport and particle deposition was used to calculate particle deposition in each of the BB, bb, and AI regions, and to quantify the effects of the subject's lung size and breathing rate. To model particle deposition, the regions were treated as a series of filters, during both inhalation and exhalation. The efficiency of each was evaluated by considering aerodynamic (gravitational settling, inertial impaction) and thermodynamic (diffusion) processes acting competitively. Regional deposition fractions were calculated for aerosols having lognormal particle size distributions, with geometric standard deviations taken to be a function of the median particle diameter, increasing from a value of 1.0 at 0.6 nm to a value of 2.5 above approximately 1 μm *(Publication 66*, Para. 170, ICRP, 1994b).

(67) Deposition fractions for each individual subject and exercise level are given (to two significant figures) in *Publication 66*, Annexe F, Tables F3 (sleep); F4 (sitting); F5 (light exercise); F6 (heavy exercise) (ICRP, 1994b) and in Annex A of ICRP (2002b).

(68) As described in Annex A of *Publication 130*, (ICRP, 2015), recent human experimental studies showed that the distribution of the deposit in the ET airways is more accurately characterised by mean deposition fractions of 65% to ET_1 and 35% to ET_2. In this report, the deposition values of ICRP Publication 66 (ICRP, 1994b) are adopted for the TH airways, whereas the deposition in the ET airways is redistributed according to the new experimental results. For particles inhaled through the nose, this is done by partitioning the total deposit in the ET airways, [sum of ET_1 and ET_2, as calculated using the original HRTM (ICRP, 1994b)], summing to give the total deposit in the ET airways, and then re-partitioning 65% to ET_1 and 35% to ET_2 (ANNEX A). For particles inhaled through the mouth (for example during heavy exercise, when the HRTM assumes that 50% of the air is inhaled through the mouth by habitual nose-breathers) there is no deposition in ET_1 and the fraction deposited in ET_2 remains as calculated using the original HRTM

(69) No changes are made here to the *Publication 66* implementation of the deposition model for aerosols, except for the re-distribution of the deposit in the ET airways between regions ET_1 and ET_2 (see above). To calculate dose coefficients for inhalation of radionuclides by members of the public, the subjects are taken to be normal nose-breathers whose time is spent according

to the distributions given in Table 2.3. For environmental exposure to most radionuclides, the default Activity Median Aerodynamic Diameter (AMAD) is taken to be 1 μm [*Publication 66*, Para. 181 (ICRP, 1994b); Dorrian and Bailey (1996); Dorrian (1997); Section B9.2 of ICRP (2002b)], in agreement with the fact that an AMAD of a few microns is characteristic of aerosols produced by dispersion mechanisms. The short-lived progeny of radon, on the contrary, are formed as airborne free ions, which react rapidly with trace gases and vapours to form particles approximately 1-nm diameter ('unattached progeny'). These in turn may attach to existing atmospheric aerosol particles ('attached progeny'). Appropriate size distributions are recommended in the radon inhalation section in OIR: Part 3 (ICRP, 2017).

(70) Values of fractional deposition in each region of the respiratory tract of the Reference Individual are given in Table 2.4 for aerosols of 1 μm AMAD. Values for aerosols of other sizes are given in ANNEX A. Generally, these deposition fractions do not vary markedly with age. The relatively high deposition in the BB region of the 15-y-old when compared to the other age-groups arises from the 1 h per day of heavy exercise, which is more than at other ages, and which involves oro-nasal breathing. Since deposition in the mouth is smaller than in the nose, there is greater penetration to, and hence deposition in, the BB region.

Table 2.4. Regional deposition of inhaled aerosols with an activity median aerodynamic diameter of 1 μm for the Reference Individuals* (% of inhaled activity). Based on Table A.1 in Annex A.

Age	3 mo	1 y	5 y	10 y	15 y (Male)	Adult (Male)
Region	Deposition (%)†,‡					
ET_1	31.31	31.44	25.81	26.40	20.49	21.94
ET_2	16.85	16.92	13.90	14.22	11.55	11.92
BB	1.04	1.04	1.04	1.17	1.69	1.29
Bb	2.05	1.71	1.85	1.70	2.00	1.95
AI	8.56	9.64	9.86	9.51	10.65	11.48
Total	59.81	60.75	52.46	53.00	46.38	48.58

ET1: extrathoracic region including the anterior nasal passage; ET2 extrathoracic region including posterior nasal passage, pharynx and larynx; BB: bronchial region; bb: bronchiolar region; AI: alveolar–interstitial region. Based on ICRP (1994b).

* The Reference Individual was assigned the deposition and clearance parameter values of healthy, non-smoking, normal nose-breathers. The distributions of time spent at each of the four reference exercise levels are as given in Table 2.3. The deposition fractions are volume-weighted average values for deposition at the four exercise levels (ANNEX A).

† Reference values, given to sufficient precision for calculation purposes, which may be greater than would be chosen to reflect the certainty with which the average value of each parameter is known.

‡ The particles are assumed to have density 3.00 g cm^{-3}, and shape factor 1.5. The particle aerodynamic diameters are assumed to be log-normally distributed with geometric standard deviation, σg of approximately 2.50 [the value of σg is not a reference value, but is derived from the corresponding AMTD (ICRP, 1994b)].

2.2.2.2. Gases and vapours

(71) For radionuclides inhaled as aerosols, the HRTM assumes that total and regional deposits in the respiratory tract are determined only by the size distribution of the inhaled particles. The situation is different for gases and vapours, for which deposition in the respiratory tract depends entirely on the chemical form. In this context, deposition refers to how much of the material in the inhaled air remains in the body after exhalation. Almost all inhaled gas

molecules contact airway surfaces, but usually return to the air unless they dissolve in, or react with, the surface lining. The fraction of an inhaled gas or vapour that is deposited in each region thus depends on its solubility and reactivity.

(72) As for particulate forms of radionuclides, default parameter values are provided for use in the absence of more specific information. The general defaults for gases and vapours are 100% total deposition in the respiratory tract (regional deposition: 20% ET_2, 10% BB, 20% bb and 50% AI) with Type F absorption (Section 2.2.4). This classification is somewhat different from that recommended in *Publication 66*, but simpler to apply. In particular, it is assumed by default that there is no deposition in ET_1. The SR-0, -1, -2, classification described in *Publication 66* and applied in *Publication 71* was not found to be helpful and is not used here.

(73) This series of reports covers gaseous and vapour forms of compounds of a number of elements, including hydrogen, carbon, sulphur and iodine. In each case, parameter values are given for total deposition, regional deposition and absorption.

2.2.3. Clearance: particle transport

(74) The model describes several routes of clearance from the respiratory tract (Fig. 2.3). Some material deposited in ET_1 is removed by extrinsic means such as nose-blowing. In other regions, clearance is competitive between the movement of particles towards the alimentary tract and lymph nodes (particle transport), and the absorption into blood of material from the particles in the respiratory tract. Removal rates due to particle transport and absorption to blood are taken to be independent of each other. It is further assumed that all clearance rates are independent of age and sex.

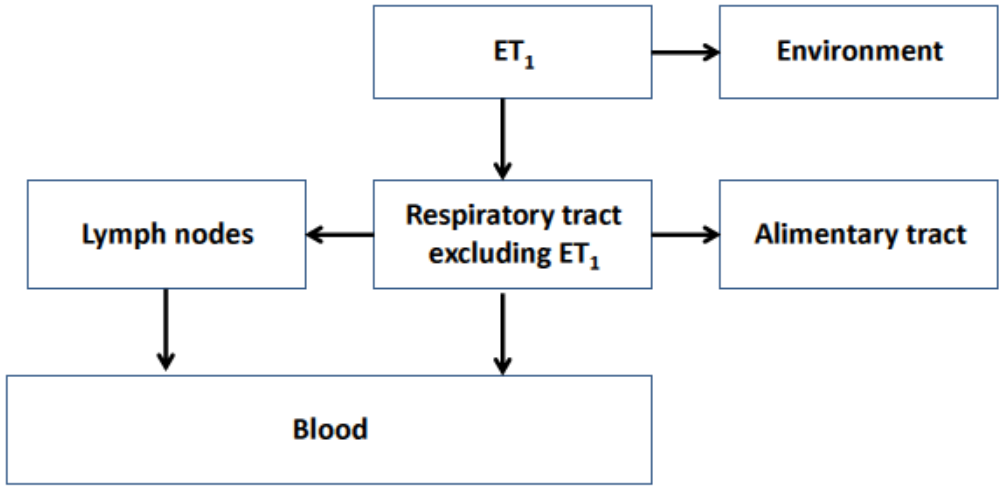

Fig. 2.3. Routes of clearance from the respiratory tract. ET_1: anterior nasal passage. Taken from ICRP (2015).

(75) As in the original HRTM, it is assumed that particle transport rates are the same for all materials. A generic compartment model is therefore provided to describe particle transport of all materials. The revised particle transport model adopted in *Publication 130* (ICRP, 2015), and applied in this series of reports, is shown in Fig. 2.4. (Annex A of *Publication 130* gives details of the the revisions made.) Reference values of rate constants were derived, as far as possible, from human studies, since particle transport rates are known to vary greatly among mammalian species.

(76) The clearance rates for most of the material deposited in the conducting airways (regions ET_1, ET_2, BB and bb) are based on the results of human volunteer experiments. During breathing through the nose, approximately 65% of the deposit in the ET airways is deposited in the anterior nasal passage, ET_1, and is cleared with a half-time of approximately 8 h (rate of 2.1 d^{-1}): approximately one-third by nose blowing, and two-thirds by transfer to ET_2. This is implemented with particle transport rates of 0.6 d^{-1} from compartment ET_1 to the Environment and 1.5 d^{-1} from ET_1 to compartment ET'_2 (Fig. 2.4). Most particles deposited in ET_2, or transferred to it from other regions (ET_1 and BB), are cleared rapidly by mucociliary action to the throat and swallowed with a time scale of approximately 10 min. This is represented by clearance from the compartment ET'_2 to the oesophagus at a rate of 100 d^{-1}.

(77) Throughout the bronchial tree (BB and bb regions), mucus velocities generally increase towards the trachea, so that residence times range from a few days in the smallest, most distal, bronchioles to less than 1 h in the trachea and main bronchi. This is represented by clearance rates of 0.2 d^{-1} (half-time approximately 3.5 d) from compartment bb′ to compartment BB′, and 10 d^{-1} (half-time approximately 2 hours) from BB′ to ET'_2.

(78) Experiments in several animal species have shown that a very small fraction of particles deposited in the conducting airways is retained (sequestered) in the airway wall. To take account of this, it is assumed that 0.2% of material deposited in regions ET_2, BB and bb is retained in the airway wall (compartments ET_{seq}, BB_{seq}, and bb_{seq} respectively). Material is cleared from these compartments to regional lymph nodes at a rate of 0.001 d^{-1} (half-time approximately 700 d).

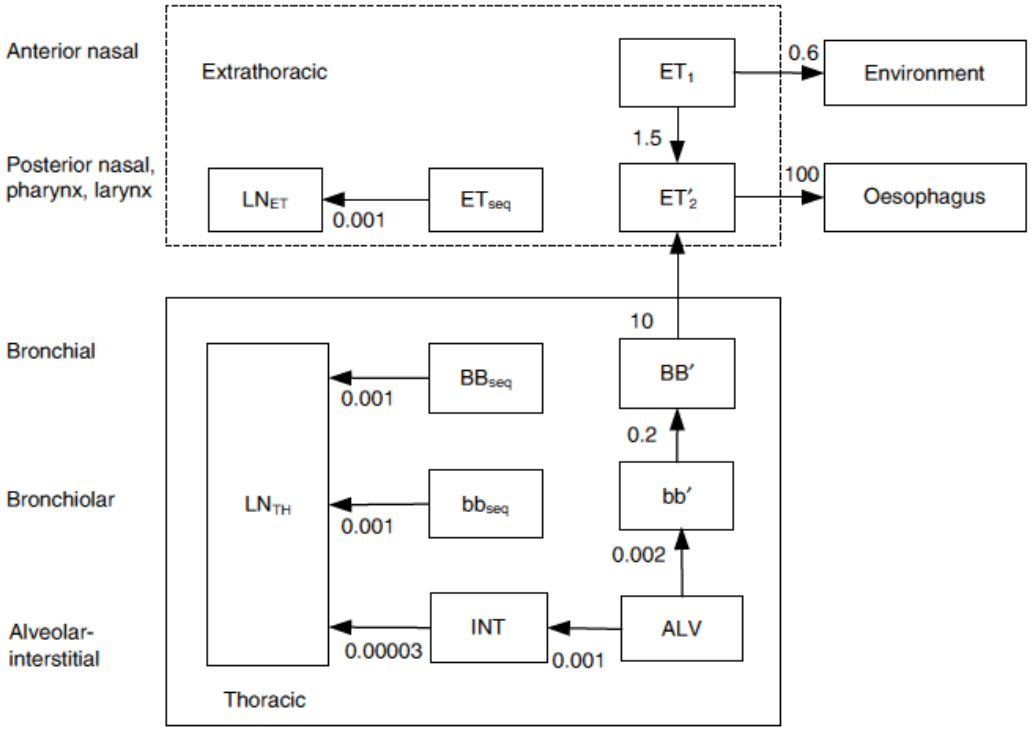

Fig. 2.4. Compartment model representing time-dependent particle transport from each respiratory tract region in the revised Human Respiratory Tract Model. Taken from ICRP (2015). *Rates shown alongside arrows are reference values in units of d^{-1}. It is assumed that 0.2% of material deposited in the posterior nasal passage, pharynx, and larynx (ET_2), bronchi (BB), and bronchioles (bb) is retained in the airway wall (ET_{seq}, BB_{seq}, and bb_{seq}, respectively).* ET_1: retention of material deposited in the anterior nose (region ET_1, which is not subdivided); ET_{seq}: long-term retention ($t_{½}$ approximately 700 d) in airway tissue of a small fraction of

particles deposited in the nasal passages; LN_{ET}: lymphatics and lymph nodes that drain the ET regions; LN_{TH}: lymphatics and lymph nodes that drain the TH regions; ET'_2 short-term retention ($t_{½}$ approximately 10 min) of the material deposited in the posterior nasal passage, larynx and pharynx (ET_2 region) except for the small fraction (taken to be 0.002) retained in ET_{seq}; BB′: retention ($t_{½}$ approximately 100 min) of particles in the BB, with particle transport to ET'_2; bb′: retention ($t_{½}$ approximately 3.5 d) of the particles in the bb, with particle transport to BB′; BB_{seq}: long-term retention ($t_{½}$ approximately 700 d) in airway walls of a small fraction of the particles deposited in the bronchial region; bb_{seq}: long-term retention ($t_{½}$ approximately 700 d) in airway walls of a small fraction of the particles deposited in the bronchiolar region; ALV: retention ($t_{½}$ approximately 250 d) of particles deposited in the alveoli. A fraction (0.67) of the deposit is removed by particle transport to the ciliated airways (bb′), while the remainder penetrates to the interstitium (INT); INT: very long-term retention ($t_{½}$ approximately 60 y) of the particles deposited in the alveoli that penetrate to the interstitium: the particles are removed slowly to the lymph nodes.

(79) Human lung clearance has been quantified in several experimental studies for up to approximately 1 y after inhalation, by which time approximately 50% of the deposit in the AI region remained. Measurements of activity in the chest after occupational exposure, and of activity in the lungs at autopsy, show that some material can be retained in the lungs for decades (ICRP, 1994b). This is represented in the revised model by deposition in the alveolar compartment (ALV), which clears at an overall rate of 0.003 d^{-1} (half-time of approximately 250 d): to the bronchial tree (compartment bb′) at a rate of 0.002 d^{-1} and to the interstitial compartment (INT) at a rate of 0.001 d^{-1}. Compartment INT clears very slowly to the regional lymph nodes (rate of 0.00003 d^{-1}). Thus, approximately 33% of the deposit in the AI region is sequestered in the interstitium.

(80) Fig. 2.4 as it stands would describe the retention and clearance of an insoluble material. However, as noted above, there is in general simultaneous absorption to blood.

2.2.4. Clearance: absorption to blood

(81) Absorption to blood depends on the physical and chemical form of the deposited material. In both the original and revised HRTM, it is assumed (by default) to occur at the same rate in all regions (including the lymph nodes), except ET_1 for which it is assumed that no absorption takes place. It is recognised that absorption is likely to be faster in the AI region where the air-blood barrier is thinner than in the conducting airways (ET, BB and bb regions), but there is insufficient information available to provide a general systematic basis for taking this into account, such as a scaling factor for different rates in different regions.

(82) In the HRTM, absorption is treated as a two-stage process: dissociation of the particles into material that can be absorbed into blood (dissolution); and absorption into blood of soluble material and of material dissociated from particles (uptake). The clearance rates associated with both stages can be time-dependent.

(83) *Dissolution:* both the original and revised HRTM use the same simple compartment model to represent time-dependent dissolution. It is assumed that a fraction (f_r) dissolves relatively rapidly, at a rate s_r, and the remaining fraction ($1 - f_r$) dissolves more slowly, at a rate s_s [Fig. 2.5(a)].

(84) A limitation of this system is that it can only represent an overall dissolution rate that decreases with time. To overcome this, *Publication 66* also describes a more flexible system, shown in Fig. 2.5(b). In this, the material deposited in the respiratory tract is assigned to compartments labelled ‘Particles in initial state’ in which it dissolves at a constant rate s_p.

Material is simultaneously transferred (at a constant rate s_{pt}) to a corresponding compartment labelled 'Particles in transformed state' in which it has a different dissolution rate, s_t. With this system, the initial dissolution rate is approximately s_p and the final dissolution rate is approximately s_t. Thus, with a suitable choice of parameters, including $s_t > s_p$, an increasing dissolution rate can be represented. The ratio of s_p to s_{pt} approximates to the fraction that dissolves rapidly.

(85) It may be noted that any time-dependent dissolution behaviour that can be represented using the model shown in Fig. 2.5(a) can also be represented by the model shown in Fig. 2.5(b) with a suitable choice of parameter values. Thus, if the dissolution rate decreases with time, as is usually the case, either system could be used, and would give the same results, with the following values:

$$s_p = s_s + f_r\,(s_r - s_s) \qquad (2.1)$$
$$s_{pt} = (1 - f_r)\,(s_r - s_s)$$
$$s_t = s_s$$

However, the reverse is not true, as noted above.

(86) The system shown in Fig. 2.5(b) was applied by default in earlier publications (ICRP, 1994a, 1995b, 1997). The additional flexibility it provides is, however, rarely required in practice. The simpler approach, shown in Fig. 2.5(a), is therefore adopted now as the default, with the more flexible approach retained as an alternative. Examples of materials that show dissolution rates that increase with time, which have been represented by 'particles in initial state' and 'particles in transformed state', including plutonium-238 dioxide, are given in the element sections in OIR: Parts 3 and 4 (ICRP, 2017, 2019).

(87) *Uptake:* uptake to blood of dissolved material is usually assumed to be instantaneous. For some elements, however, part of the dissolved material is absorbed rapidly into blood, but a significant fraction is absorbed more slowly because of binding to respiratory tract components. To represent time-dependent uptake, it is assumed that a fraction (f_b) of the dissolved material is retained in the 'bound' state, from which it goes into blood at a rate s_b, while the remaining fraction ($1 - f_b$) enters blood instantaneously (Fig. 2.5). In the model, material in the 'bound' state is not cleared by particle transport processes, but only by uptake to blood. Thus, only one 'bound' compartment is required for each region, except for ET_1, from which no absorption takes place.

(88) The system shown in Fig. 2.5 applies to each of the compartments in the particle transport model shown in Fig. 2.4. It is assumed that no absorption takes place from ET_1, but if the model in Fig. 2.5(a) is used, the ET_1 deposit still has to be partitioned between fast and slow compartments because material is cleared from ET_1 to ET_2, from which absorption does take place.

(89) For all elements, default values of parameters are recommended, according to whether the absorption is considered to be fast (Type F), moderate (M) or slow (S). For gases or vapours, instantaneous uptake to blood may be recommended: Type V (very fast).

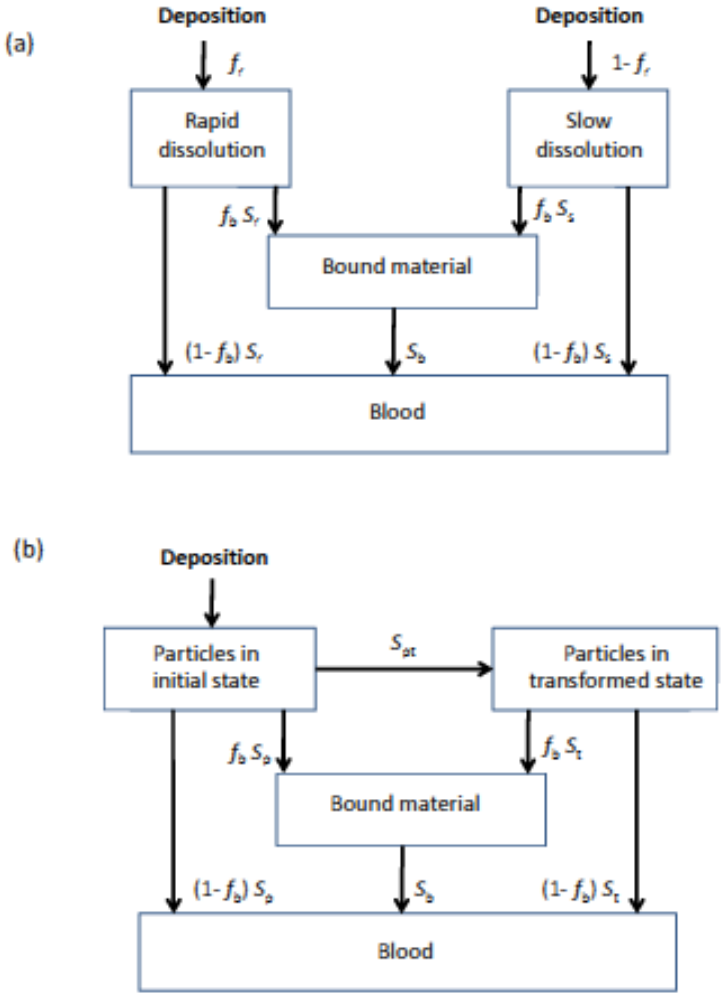

Fig. 2.5. Alternative compartment models representing time-dependent absorption to blood (dissolution and uptake). *In the model shown in Fig. 2.5(a), a fraction f_r of the deposit is initially assigned to the compartment labelled 'Rapid dissolution', and the rest of the deposit ($1 - f_r$) is initially assigned to the compartment labelled 'Slow dissolution'. In the model shown in Fig. 2.5(b), all the deposit is initially assigned to the compartment labelled 'Particles in initial state', and material in the compartment labelled 'Particles in transformed state' is subject to particle transport at the same rate as material in the compartment labelled 'Particles in initial state'. Material in the compartment labelled 'Bound material' is not subject to particle transport and is cleared only by uptake into blood.*
f_r: fraction of the deposit that dissolves rapidly, at a rate s_r; ($1 - f_r$): fraction of deposit that dissolves more slowly, at a rate s_s; f_b: fraction of the dissolved material that is retained in the bound state and from which it goes to blood at a rate s_b; s_r: rate of rapid dissolution; s_s: rate of slow dissolution; s_b: transfer rate from the bound state to the blood; s_{pt}: transfer rate of material from the compartment 'Particles in initial state' to the compartment 'Particles in transformed state'; s_p: dissolution rate of material from compartment 'Particles in initial state'; s_t: dissolution rate of material from the compartment 'Particles in transformed state'.

(90) The original default reference values for Types F, M and S given in *Publication 66* (ICRP, 1994b) were not based on reviews of experimental data but on comparison with particle transport rates. For example, the value of 100 d^{-1} for the rapid dissolution rate, s_r, was chosen to equal the particle clearance rate from the nose (ET_2) to the throat.

(91) In developing OIR: Parts 2 – 5 (ICRP, 2016a, 2017, 2019, 2022), detailed reviews were conducted of the absorption characteristics of inhaled materials relevant to radiological protection. They are summarised in the inhalation sections of each element.

(92) Where information was available, specific parameter values were derived from experimental data from both in-vivo and in-vitro studies. These provided a database to give guidance on selecting values that are representative of materials that are generally considered to clear at 'fast', 'moderate' or 'slow' rates. Values selected on that basis for default Type F, M and S have been adopted in the revised HRTM used in this series of documents (see below).

(93) Material-specific rates of absorption have been adopted in the element sections of the OIR for a limited number of selected particulate materials, i.e. those for which:

- There are *in-vivo* data from which specific parameter values can be derived;
- Results from different studies are consistent;
- It was considered that occupational exposure to the material is likely; and
- The specific parameter values are sufficiently different from default Type F, M or S parameter values to justify providing additional specific dose coefficients.

(94) Relatively more use is made of material-specific parameter values for gases and vapours than for particulate materials, because of the dependence of deposition in the respiratory tract on chemical form.

(95) Other materials were assigned to default types using suitable experimental data if available, as reviewed in the element sections. *Publication 66* (ICRP, 1994b) did not give criteria for assigning materials to absorption types on the basis of experimental results. Criteria were developed in *Publication 71* (ICRP, 1995b) and their application was discussed further in *Supporting Guidance 3* (ICRP, 2002b). Type M is assumed for all particulate forms of most elements in the absence of information on which assignment to an absorption type could be made. A material is assigned to Type F if the amount absorbed into blood by 30 d after an acute intake is greater than the amount that would be absorbed over the same period from a hypothetical material with a constant rate of absorption of 0.069 d^{-1} (corresponding to a half time of 10 d) under identical conditions. Similarly, a material is assigned to Type S if the amount absorbed into blood by 180 d after an acute intake is less than the amount that would be absorbed over the same period from a hypothetical material with a constant rate of absorption to blood of 0.001 d^{-1} (corresponding to a half-time of approximately 700 d) under identical conditions. Particulate forms of each element were assigned to the HRTM default absorption Types using these criteria. However, to make use of the limited information available for many materials, some flexibility was applied (ICRP, 2015).

(96) For soluble (Type F) forms of each element, estimates were made of the overall rate of absorption from the respiratory tract to blood, where information was available. It is assumed that this can be represented by the rapid dissolution rate, s_r, which is a characteristic of the element. Because of the wide variation between elements in the estimated value of s_r, element-specific values were adopted in the OIR series and in this series of documents for those elements for which an estimate of the value could be made (Table 2.5).

1166 Table 2.5. Element-specific absorption parameter values used in the OIR: Parts 2–5 and in this
1167 series of reports.

Element	OIR Part	Rapid dissolution rate, s_r (d^{-1})	Bound fraction, f_b	Uptake rate, s_b (d^{-1})	Absorption from the alimentary tract*, f_A	
					Soluble	Relatively insoluble
Hydrogen	2	100	0	–	1	0.1
Beryllium	5	30	0	–	0.005	
Carbon	2	100	0	–	1	
Fluorine	5	30	0	–	1	
Sodium	5	30	0	–	1	
Magnesium	5	30	0	–	0.5	0.2
Aluminium	5	30	0	–	0.003	1×10^{-4}
Silicon	5	30	0	–	0.5	0.01
Phosphorus	2	1	0	–	0.8	
Sulphur	2	30	0	–	1	0.1
Chlorine	5	30	0	–	1	
Potassium	5	30	0	–	1	
Calcium	2	70	0	–	0.4	
Scandium	5	30	0	–	0.001	
Titanium	5	30	0	–	0.001	
Vanadium	5	30	0	–	0.2	0.01
Chromium	5	30	0	–	0.01	
Manganese	5	30	0	–	0.05	
Iron	2	100	0	–	0.1	
Cobalt	2	1	0.03	0.002	0.1	0.05
Nickel	5	3	0	–	0.05	0.01
Copper	5	30	0	–	0.5	
Zinc	2	30	0	–	0.5	
Gallium	5	30	0	–	0.001	
Germanium	5	30	0	–	1	
Arsenic	5	30	0	–	1	0.3
Selenium	5	30	0	–	0.8	
Bromine	5	30	0	–	1	
Rubidium	5	30	0	–	1	
Strontium	2	30	0	–	0.25	0.01
Yttrium	2	1			1×10^{-4}	
Zirconium	2	30	0	–	0.002	
Niobium	2	30	0	–	0.01	
Molybdenum	2	30	0	–	0.9	0.05
Technetium	2	100	0	–	0.9	
Ruthenium	3	30	0.5	0.1	0.05	
Rhodium	5	30	0	–	0.05	
Palladium	5	30	0	–	0.005	
Silver	5	1	0	–	0.05	

Element	OIR Part	Rapid dissolution rate, s_r (d^{-1})	Bound fraction, f_b	Uptake rate, s_b (d^{-1})	Absorption from the alimentary tract*, f_A	
					Soluble	Relatively insoluble
Cadmium	5	30	0	–	0.05	
Indium	5	30	0	–	0.005	
Tin	5	30	0	–	0.02	
Antimony	3	30	0	–	0.05	
Tellurium	3	50	0	–	0.3	
Iodine	3	100	0	–	1	
Caesium	3	100	0	–	1	0.1
Barium	3	20	0	–	0.2	1×10^{-4}
Cerium‡	4	1	0.07	0.02	5×10^{-4}	
Hafnium	5	30	0	–	0.002	
Tantalum	5	30	0	–	0.001	
Tungsten	5	30	0	–	0.5	0.01
Rhenium	5	30	0	–	0.9	
Osmium	5	30	0	–	0.01	
Iridium	3	30	0	–	0.01	
Platinum	5	30	0	–	0.01	0.001
Gold	5	30	0	–	0.1	
Mercury	5	30	0.24	2.1	0.1	
Thallium	5	30	0	–	1	
Lead	3	100	0.5	1.7	0.2	
Bismuth	3	1	0	–	0.05	
Polonium	3	3	0	–	0.1	
Astatine	5	30	0	–	1	
Radon	3		0	–	1	
Francium	5	30	0	–	1	
Radium	3	10	0	–	0.2	
Actinium	4	0.4	0.002	0	5×10^{-4}	
Thorium	3	50	0	–	5×10^{-4}	
Protactinium	4	50	0	–	5×10^{-4}	
Uranium	3	10	0	–	0.02	0.002
Neptunium	4	30	0	–	5×10^{-4}	
Plutonium§	4	0.4	0.002	0	5×10^{-4}	1×10^{-5}
Americium	4	0.4	0.002	0	5×10^{-4}	
Curium	4	0.4	0.002	0	5×10^{-4}	
Berkelium	4	0.4	0.002	0	5×10^{-4}	
Californium	4	0.4	0.002	0	5×10^{-4}	
Einsteinium	4	0.4	0.002	0	5×10^{-4}	
Fermium	4	0.4	0.002	0	5×10^{-4}	

*Adult values for ingested materials. Applies to all forms unless more than one value is given. In those cases described in this table as 'Soluble' and 'Relatively insoluble'; other values apply to some elements ingested in diet: see element section for details.

‡Parameter values applied to the rest of the lanthanide series: lanthanum (Atomic number Z=57) to lutetium (Z=71).

[§]Plutonium respiratory tract parameter values are applied to the higher actinides series: americium (Z=95) to fermium (Z=100), and to actinium by analogy with americium.

(97) Evidence for retention in the bound state, rather than by transformation into particulate material, may be in one or more forms: e.g. systemic uptake rather than faecal clearance of the retained material; slower clearance than for insoluble particles deposited in the same region of the respiratory tract; or autoradiography showing diffuse rather than focal retention of activity.

(98) The bound state was included in the model mainly to take account of slow clearance of soluble materials from the alveolar region. By default, it would be assumed that the same bound state parameter values apply in all regions. In some cases (e.g. a long-term bound state for a long-lived α-emitter), this could lead, unintentionally, to high calculated doses to the BB and bb regions. Because of the high weighting (apportionment factors) that these tissues are given, this could in turn lead to high calculated equivalent doses to the lungs. Hence, in the OIR and in this series of documents, it is assumed that for those elements for which a bound state is adopted ($f_b > 0$), it is applied in the conducting airways (ET_2, BB and bb regions) only if there is experimental evidence to support that.

(99) For some elements, for which there is little or no experimental data on absorption from the respiratory tract, element-specific absorption parameter values (s_r, f_b and s_b) have been based on chemical analogy, notable for some of the lanthanides and actinides (Table 2.5).

(100) As noted above, the specific parameter values derived from experimental data (from both in-vivo and in-vitro studies) provided a database to give guidance on selecting values that are representative of materials that are generally considered to clear at 'fast', 'moderate' or 'slow' rates. This was not a representative survey from which central values could be derived by objective statistical means. Rather, it provided a basis for informing judgements, as described in Annex A of *Publication 130* (ICRP, 2015). Updated default values for the revised HRTM and applied in this series of documents are given in Table 2.6.

Table 2.6. Default absorption parameter values for Type F, M, and S materials[*,†] in the revised Human Respiratory Tract Model.

Type		F(fast)	M (moderate)	S (slow)
Fraction dissolved rapidly	f_r	1	0.2	0.01
Dissolution rates:				
Rapid (d^{-1})	s_r	30[‡]	3[§]	3[§]
Slow (d^{-1})	s_s	–	0.005	10^{-4}

*Reference values, given with sufficient precision for calculation purposes, which may be greater than would be chosen to reflect the certainty with which the average value of each parameter is known.

[†]The bound state is also used for default types of some elements (Table 2.5).

[‡]Element-specific rapid dissolution rates are adopted for Type F forms of many elements (Table 2.5).

[§]The element-specific value for Type F is also used for Types M and S if it is less than 3 d^{-1}.

(101) The default absorption rates, expressed as approximate half-times, and the corresponding amounts of material deposited in each region that reach blood (from the respiratory tract) can be summarised as follows.

- Type V: 100% absorbed instantaneously. Regional deposition does not need to be assessed for such materials, because in dose calculations, they can be treated as if they were injected directly into blood.
- Type F: For the general default value of 30 d^{-1} for s_r, 100% absorbed with a half-time of approximately 30 min. There is rapid absorption of almost all material deposited in bb and AI, approximately 80% of material deposited in BB, approximately 25% of material deposited in ET_2, and approximately 20% of material deposited in ET_1. The

other material deposited in BB and ET_2 is cleared to the alimentary tract by particle transport.

- Type M: For the general default value of 3 d^{-1} for s_r, 20% absorbed with a half-time of approximately 6 h and 80% with a half-time of approximately 140 d. There is rapid absorption of approximately 20%, 5%, 0.5% and 0.4% of material deposited in bb, BB, ET_2 and ET_1, respectively. Approximately 80% of the deposit in AI eventually reaches blood.
- Type S: For the general default value of 3 d^{-1} for s_r, 1% absorbed with a half-time of approximately 6 h and 99% with a half-time of approximately 7000 d. There is rapid absorption of approximately 1%, 0.25%, 0.03% and 0.02% of material deposited in bb, BB, ET_2 and ET_1, respectively. Approximately 30% of the deposit in AI eventually reaches blood.

(102) For absorption Types F, M, and S, some of the material deposited in ET_1 is removed by extrinsic means. Most of the material deposited in the respiratory tract that is not absorbed is cleared to the alimentary tract by particle transport. The small amounts transferred to lymph nodes continue to be absorbed into blood at the same rate as in the respiratory tract.

(103) For material cleared from the respiratory tract to the alimentary tract, the default assumption made is that fractional absorption in the alimentary tract is the product of f_r and f_A, where f_A is fractional absorption in the alimentary tract for relatively soluble forms of the element (Section 2.3.3) and for the Reference Individual. This approach was based on the consideration that f_r represents the soluble fraction of the material, which is available for absorption in the alimentary tract, and f_A represents alimentary tract absorption of the soluble fraction. In taking this approach, it was recognised that it is important not to overestimate absorption in the alimentary tract greatly, because this could lead to overestimation of predicted urinary excretion, and hence corresponding under-estimation of intakes from urine bioassay measurements.

2.2.5. Progeny radionuclides formed in the respiratory tract

(104) The following applies specifically to progeny formed in the respiratory tract after inhalation of the parent radionuclide. Progeny radionuclides formed before inhalation and inhaled with the parent are generally treated as separate intakes, and so each progeny radionuclide inhaled is assumed to adopt the biokinetics appropriate to the element of which it is an isotope. Many issues relating to the behaviour of progeny in the respiratory tract arise in connection with the natural decay series, which are therefore shown in ANNEX A, Figs. B.1 (uranium-238 series), B.2 (uranium-235 series) and B.3 (thorium-232 series).

(105) *Publication 66* (Para. 272, ICRP, 1994b) noted that it would be expected that:

- the rate at which a particle dissociates is determined by the particle matrix and therefore the dissolution parameter values of the inhaled material would be applied to progeny formed within particles in the respiratory tract (‘shared kinetics’);
- progeny radionuclides formed as noble gases, including radon, would be exceptions because they would diffuse from the particles; and
- the behaviour of dissociated material would depend on its elemental form, and so, for example, bound fraction parameter values for a progeny radionuclide would not be those of the parent (‘independent kinetics’).

(106) Nevertheless, in previous applications of the HRTM [e.g. *Publications 71* and *72* (ICRP, 1995b, 1995c)], with the exception of noble gases, the absorption parameter values of the parent were applied to all members of the decay chain formed in the respiratory tract (shared

kinetics). After detailed consideration of the issues involved (Annex A of Publication 130, ICRP, 2015), the same approach is taken in the OIR and in this series of documents.

(107) Nevertheless, where experimental results are available which allow direct comparisons between the absorption behaviour of a parent radionuclide, and that of its radioactive progeny, they are summarised in the inhalation section of the parent element (e.g. uranium, thorium).

(108) For calculation purposes, the assumption that noble gases, including radon, that are formed as progeny within the respiratory tract escape from the body at a rate of 100 d^{-1} is applied in this series of documents.

(109) For material cleared from the respiratory tract to the alimentary tract, fractional absorption in the alimentary tract is assumed to be $f_r^* f_A$ (see above). In the case of progeny formed in the respiratory tract, f_r is taken to be that of the parent deposited in the respiratory tract (reflecting the particle matrix), but the value of f_A is taken to be that of the progeny radionuclide entering the alimentary tract.

(110) Following absorption to blood, progeny formed in the respiratory tract are assumed to behave according to the systemic model applied to the element as a progeny of the parent radionuclide.

2.2.6. Respiratory tract dosimetry

(111) The HRTM dosimetric model is described in Chapter 8 of *Publication 66* (ICRP, 1994b). For dosimetric purposes, the respiratory tract is treated as two tissues: the TH and ET airways. These are sub-divided into regions, primarily based on considerations of differences in sensitivity to radiation. The TH regions are BB, bb, AI, and LN_{TH}. The ET regions are ET_1, ET_2, and LN_{ET} (Fig. 2.2).

(112) The dose to each respiratory tract region is calculated as the average dose to the target region which contains the target cells at risk. In the AI region and lymph nodes (LN_{TH} and LN_{ET}), the cells at risk are thought to be distributed throughout the region, and the average dose to the whole lung and the lymph nodes, respectively, is calculated. For the regions making up the conducting airways (ET_1, ET_2, BB and bb), the target cells are considered to lie in a layer of tissue at a certain range of depths from the airway surface and the average dose to this layer is calculated. The target cells identified in ET_1, ET_2, BB and bb, assumed to be independent of age and sex, are given in Table 2.7. The masses of tissue containing target cells in each region, for each age and sex, for use in dose calculations, are given in Table 2.8.

(113) In each of these regions, there are also several possible source regions. For example, in the bb region, particles retained in the airway wall (bb_{seq}) are taken to be in a macrophage layer at a depth of 20–25 μm (i.e. below the target cells); activity ‘bound’ to the epithelium is uniformly distributed in it; and account is also taken of irradiation from activity present in the AI region. In the original HRTM, there were two phases of mucociliary clearance: activity in the fast phase of clearance was taken to be in a mucus layer above the cilia; and activity in the slow phase of clearance was taken to be in the mucus between the cilia. In the revised HRTM, there is only one phase of clearance, and activity is distributed throughout the mucus as specified below.

(114) For each source/target combination, *Publication 66* (ICRP, 1994b) provides absorbed fractions for nonpenetrating radiations: α, β, and electrons; in each case, as a function of energy. Since these absorbed fractions are not represented in the voxel phantoms because of inadequate spatial resolution, the values given in *Publication 66* (ICRP, 1994b) are used in the OIR and in this series of reports. They were derived using a single cylindrical geometry to represent each region of the conducting airways (ET_1, ET_2, BB, bb): the representative bronchus for BB having

a diameter of 5 mm and the representative bronchiole for bb having a diameter of 1 mm. The absorbed fractions for the single phase BB and bb source regions were derived as the thickness-weighted sum of the slow and fast clearing source regions, as tabulated in *Publication 66* (ICRP, 1994b). Absorbed fractions were considered to be age-independent. The age-dependence of the target mass created age-dependence in the specific absorbed fraction.

(115) To take account of differences in sensitivity between tissues, the equivalent dose, H_i, to each region, *i*, is multiplied by a detriment apportionment factor, the Assigned fraction, A_i, representing the region's estimated sensitivity relative to that of the whole organ. The recommended values of A_i are also given in Table 2.7. In *Publication 103* (ICRP, 2007), the ET and TH lymph nodes were included in the tissue 'lymphatic nodes', which is itself included in the list of remainder tissues and organs (Table 1.3), and so are no longer included in the ET and TH airways, respectively, as they were in the original HRTM. The fractions, A_i, of w_T that they were assigned in *Publication 66* are reassigned to other regions in Table 2.7. The weighted sum of the equivalent dose, H_i, to each region, is the equivalent dose to the ET or TH airways, respectively:

(116) The tissue weighting factor, w_T of 0.12 specified for lung in *Publication 103* (ICRP, 2007) is applied to the equivalent dose to the TH region, H_{TH}. The ET airways are included in the list of remainder tissues and organs (Table 1.3).

$$H_{ET} = H_{ET_1} A_{ET_1} + H_{ET_2} A_{ET_2} \qquad (2.2)$$

$$H_{TH} = H_{BB} A_{BB} + H_{bb} A_{bb} + H_{AI} A_{AI}$$

Where: $H_{BB} = \frac{H_{BB_{sec}} + H_{BB_{bas}}}{2}$

Table 2.7. Target regions of the respiratory tract (independent of age and sex).

Tissue	Region	Target cells	Mucus thickness* (μm)	Epithelial thickness* (μm)	Depth of target cells* (μm)	Assigned fraction* A_i of w_T
ET	ET_1	Basal	–	50	40–50	0.001
	ET_2	Basal	15	50	40–50	0.999
TH	BB	Secretory (BB_{sec})	5	55	10–40	1/3
		Basal (BB_{bas})	5	55	35–50	
	bb	Secretory	2	15	4–12	1/3
	AI		–	–	‡	1/3

ET, extrathoracic; TH, thoracic; ET_1, anterior nasal passage; ET_2, posterior nasal passage, pharynx and larynx; BB: bronchial; bb: bronchiolar; AI: alveolar–interstitial.

*Reference values, given to sufficient precision for calculation purposes, which may be greater than would be chosen to reflect the certainty with which the average value of each parameter is known. For the BB, bb and AI regions, each value of A_i is exactly one-third.

‡Average dose to region calculated.

Table 2.8. Masses of target regions in the respiratory tract in several Reference Individuals*

Region	Mass (kg)						
Age	3 mo	1 y	5 y	10 y	15 y (Male)	Adult (Male)	Adult (Female)
ET_1	2.792×10^{-6}	4.133×10^{-6}	8.284×10^{-6}	1.263×10^{-5}	1.852×10^{-5}	2.000×10^{-5}	1.729×10^{-5}
ET_2	6.28×10^{-5}	9.30×10^{-5}	1.864×10^{-4}	2.843×10^{-4}	4.166×10^{-4}	4.500×10^{-4}	3.890×10^{-4}
BB_{sec}‡	2.531×10^{-4}	3.105×10^{-4}	4.695×10^{-4}	6.220×10^{-4}	8.169×10^{-4}	8.648×10^{-4}	7.771×10^{-4}
BB_{bas}‡	1.266×10^{-4}	1.553×10^{-4}	2.348×10^{-4}	3.110×10^{-4}	4.085×10^{-4}	4.324×10^{-4}	3.885×10^{-4}
bb	5.014×10^{-4}	5.967×10^{-4}	9.469×10^{-4}	1.305×10^{-3}	1.768×10^{-3}	1.949×10^{-3}	1.874×10^{-3}
AI§	9.04×10^{-2}	1.51×10^{-1}	3.01×10^{-1}	4.97×10^{-1}	8.59×10^{-1}	1.100	9.041×10^{-1}

ET_1, anterior nasal passage; ET_2, posterior nasal passage, pharynx and larynx; BB_{sec} secretory cells in the bronchial region; BB_{bas}; basal cells in the bronchial region; bb: bronchiolar; AI: alveolar–interstitial.
*Reference values, given to sufficient precision for calculation purposes, which may be greater than would be chosen to reflect the certainty with which the average value of each parameter is known.
†Adult Male and Adult Female values were taken from Table 3.3 of *Publication 130* (ICRP, 2015). Values for other subjects are taken from Table 10 of *Publication 71* (ICRP, 1995b). These values are given to two significant figures in Table 5 of *ICRP Publication 66* (ICRP, 1994b).
‡Masses for BB_{sec} and BB_{bas} are the masses of bronchial epithelium through which the secretory cells and basal cells, respectively, are distributed and are based on reference values of airway dimensions.
§The mass of AI includes blood but excludes lymph nodes.

2.3. Human Alimentary Tract Model (HATM)

(117) The HATM described in *Publication 100* (ICRP, 2006) has been used in this report series in replacement of the *Publication 30* (ICRP, 1979) model of the gastrointestinal tract.. This replacement was motivated by a number of developments, including the availability of improved information on the gut transit of materials, and developments in our understanding of the location of sensitive cells. The model structure is shown in Fig. 2.6, and parameter values are shown in Table 2.10. As for the HRTM, an important feature of the HATM is the specific calculation of doses to target regions containing sensitive cells for cancer induction, and the consideration of specific absorption and/or retention values, where information is available. The HATM and the HRTM are compatible and inter-connected, as shown in Fig. 2.6.

2.3.1. Structure

(118) The HATM depicts the entry of a radionuclide into the oral cavity by ingestion or into the oesophagus after particle transport from the respiratory tract. It describes the sequential transfer through all alimentary tract regions, including the oral cavity, oesophagus, stomach, small intestine, and segments of the colon, followed by emptying in faeces. Doses are calculated for all these regions. The colon is partitioned, for the purposes of dose calculations, into right colon, left colon and rectosigmoid (the sigmoid colon and rectum) based on the availability of transit time data. The rectum is included with the sigmoid colon, as the rectosigmoid, because of difficulties in determining transit times separately and because the rectum does not have a specific w_T value. Total colon doses are combined as a mass-weighted mean to include the right colon, left colon and rectosigmoid:

$$H_{\text{colon}} = \frac{H_{\text{RC}} m_{\text{RC}} + H_{\text{LC}} m_{\text{LC}} + H_{\text{RS}} m_{\text{RS}}}{m_{\text{RC}} + m_{\text{LC}} + m_{\text{RS}}} \qquad (2.2b)$$

(119) where m_{RC}, m_{LC} and m_{RS} are the corresponding masses of three sections of the colon (Table 2.9).

Table 2.9. Typical values for masses of walls in the colon region (g) (from ICRP *Publication 100*)

Section	New-born	1 y	5 y	10 y	15 y		Adult	
					male	female	male	female
Right colon	7	20	49	85	122	122	150	145
Left colon	7	20	49	85	122	122	150	145
Rectosigmoid	3	10	22	40	56	56	70	70

2.3.2. Model parameters

(120) The HATM presents different transit times for solid foods, liquids, and total diet, in the mouth, oesophagus and stomach. First-order kinetics is assumed. This is a considerable simplification of the complex processes involved in transfer of material through the lumen of the alimentary tract, but is expected to provide a reasonably accurate representation of the mean residence time of a radionuclide in each segment of the tract.

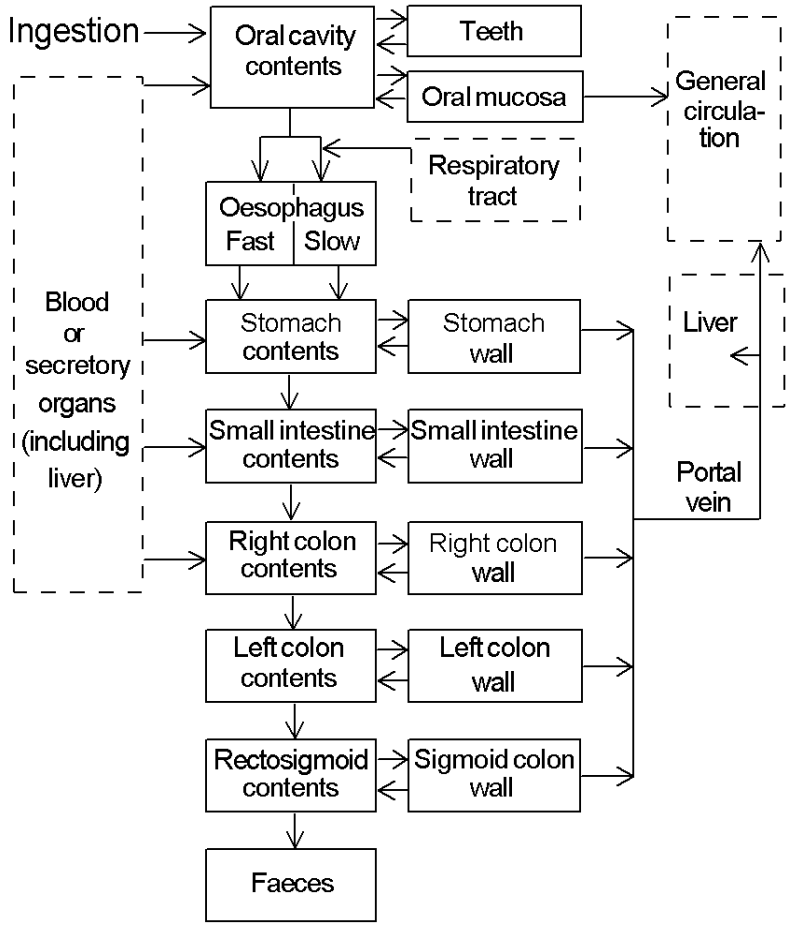

Fig. 2.6. Structure of the Human Alimentary Tract Model. The dashed boxes are included to show connections between the HATM and the HRTM and systemic biokinetic models. Taken from ICRP (2006).

Table 2.10. Age-specific HATM transfer coefficients (per d) for total diet[*,†]

From	To	Transfer coefficient[‡] (d^{-1})			
		Age 3 months	Age 1 year	Age 5–15 years	Adult male
O-cavity	Oesophag-c-Fast	38,880	6480	6480	6480
O-cavity	Oesophag-c-Slow	4320	720	720	720
Oesophag-c-Fast	St-cont	21,600	12,343	12,343	12,343
Oesophag-c-Slow	St-cont	2880	2160	2160	2160
St- cont	SI-cont	19.2	20.57	20.57	20.57
SI-cont	RC-cont	6	6	6	6
RC-cont	LC-cont	3	2.4	2.182	2
LC-cont	RSig-cont	3	2.4	2.182	2
RSig-cont	Faeces	2	2	2	2

[*]Abbreviations: O-cavity = oral cavity content, Oesophag-c = oesophagus content, St = stomach, cont = content, SI = small intestine, RC = right colon, LC = left colon, RSig = rectosigmoid.

[†]Other transfer coefficients not given here are assumed to be zero unless specified in the relevant element section. In most cases, uptake to blood from the alimentary tract is taken to occur from the SI contents, without retention in SI wall. The corresponding transfer coefficient is $\frac{f_A \times \lambda_{SI,RC}}{1-f_A}$, where $\lambda_{SI,RC}$ is the transfer coefficient from SI contents to RC contents.

[‡]The degree of precision of the values given is for computational purposes and does not reflect the certainty with which the central values are known.

2.3.2.1. Modifying factors

(121) The default regional transit times given in the HATM are central estimates based on collected data for a given sex, age group, and type of material (e.g. solids, liquids, caloric liquids, or non-caloric liquids). As extensively illustrated in *Publication 100* (ICRP, 2006), transit of material through each of the major segments of the tract shows considerable inter- and intra-subject variability even under normal conditions. Extremely large deviations from the norm may result from constipation, diarrhoea, unusual diet, pharmaceuticals, and a variety of diseases that affect the nervous system or increase energy requirements, for example.

2.3.2.2. Sex-specific values

(122) The HATM provides sex-specific parameter values for adults for dimensions and transit times of contents through the regions. Although the dimensions of the stomach and intestines are generally smaller in females than males, the estimated central transit times through these regions are approximately one-third greater in females than in males. However, taking into account the large variability in transit times through any region of the alimentary tract both in males and females, the Reference adult Individual is assigned the reference transit times for the adult male.

2.3.2.3. Material entering from the respiratory tract or in saliva

(123) Mucus and associated materials cleared from the respiratory tract enter the oesophagus via the oropharynx. For ingested food and liquids, the HATM specifies two components of oesophageal transit, representing relatively fast transfer of 90% of the swallowed material

(mean transit time of 4 s (age 3 months) to 7 s (age 1 year and older) for total diet) and relatively slow transit of the residual 10% (30 s (age 3 months) to 40 s (age 1 year and older) for total diet). It is assumed that the slower oesophageal transit time applies to all material cleared from the respiratory tract.

2.3.3. Absorption from the alimentary tract

(124) Radionuclides may enter the alimentary tract: directly as a result of ingestion; indirectly after inhalation and mucociliary escalation of particles from the respiratory tract to the oropharynx and oesophagus; or in secretions such as saliva, bile, or gastric juice. Alternatively, they may be produced in the alimentary tract by decay of a parent radionuclide. The absorption of radionuclides to blood is specified in the HATM as a fraction of the amount entering the alimentary tract, with total absorption denoted as f_A (ICRP, 2006). The model structure allows for the use of data on absorption in any region, where information is available. In most cases, no information will be available on the regional absorption of radionuclides, and the default assumption is that all absorption takes place in the small intestine, i.e. $f_A = f_{SI}$. As a default, it is also assumed that there is no recycling from the wall to the contents of the alimentary tract.

(125) Some f_A values recommended in this report are the same as the f_1 values given previously for use with the *Publications 30, 56, 67 and 69* models (ICRP, 1979, 1980, 1981, 1988, 1990, 1993, 1995a) as there is not sufficient new information to warrant a revision in the value. Specific data of absorption from other regions are considered in the small number of cases for which they were available, although in some cases (e.g. relatively long-lived isotopes of iodine), doses to alimentary tract regions and other tissues are insensitive to assumptions regarding the site of absorption (ICRP, 2006).

(126) The extent of absorption of radionuclides will depend on the element and its chemical forms. Changes in chemical forms are likely to occur during digestive processes, beginning in the mouth, but principally occurring in the stomach and the small intestine. These changes in chemical form or speciation will determine the availability of the radionuclide for absorption and hence the extent of uptake through the intestinal epithelium to bloodstream (ICRP, 2006).

2.3.3.1. Effect of chemical forms

(127) The values of f_1 and f_A recommended in *Publication 30* (ICRP, 1979, 1980, 1981, 1988) and in the OIR report series apply primarily to the intakes of chemical forms of the elements expected to be encountered in a workplace. These values are not necessarily appropriate for environmental exposures. For example, occupational exposures may involve ingestion of inorganic forms of radionuclides not normally present in the environment. Environmental exposures mainly involve ingestion of radionuclides incorporated into food materials, bound to organic constituents of food, and/or inorganic forms present in food and/or water. It has been shown that incorporation of radionuclides into food, which contains complexing agents such as citrates, phytates, and other organic acids, may lead in general to greater absorption than ingestion of inorganic forms of an element, although for some elements (e.g. molybdenum) the reverse is true. This factor should be considered when extrapolating the result of animal studies performed with inorganic forms of elements to humans ingesting radionuclides in mixed diets containing a variety of potential complexing agents. The absorption of radionuclides from drinking water may be increased when ingested after a period without food.

(128) Environmental exposures have been reviewed in the *Publication 56 series* (ICRP, 1990, 1993, 1995a) and in *Publication 100* (ICRP, 2006). For elements with absorption fraction

greater than 0.5 in *ICRP Publication 30* and for which there was no specific information on absorption from food, *Publication 67* (ICRP, 1993) applied an absorption fraction of 1. Specific values proposed in the present report are based on the content of the above mentioned ICRP Publications as well as on any more recent information on the fractional absorption of organic forms of ingested radionuclides available from the scientific literature.

2.3.3.2. Effects of age on absorption parameters

(129) There is evidence from animal experiments and some supporting human data that absorption of many elements is substantially greater in newborn mammals than in adults. Data on the effect of age and other factors on the intestinal absorption of radionuclides have been reviewed in the *Publication 56 series* in order to specify values of absorption fraction for use in the calculation of age-related dose coefficients for members of the public (Table 2.11). Dose coefficients were given for radioisotopes of 31 elements, considered to be of potential importance in terms of public exposures, and for a number of age groups including 3-month-old infants and 1-year-old children. Absorption is greatest immediately after birth and decreases progressively over the suckling period. Thus, it was considered likely that adult values of absorption will apply in many cases to intakes by weaned infants later in the first year of life. Nevertheless, the approach adopted had been to specify infant values of absorption for the 3-month-old infant that were taken to apply as averages over the first year of life. This was recognised as a conservative assumption, particularly when applied to the consumption of solid foods in the latter part of the first year. The most appropriate use of the 3-month-old infant's values of absorption is in the calculation of dose coefficients for radionuclide ingestion in mothers' milk (ICRP, 2004) and concurrent intakes in other forms during the first 6 months of life. In the *Publication 56 series*, where no age-specific human or animal data were available, for elements with a fractional absorption in the adult of 0.001 or less, a value 10 times the value for the adult was assumed for the first year of life; for absorption fraction values between 0.01 and 0.5 in the adult, an increase by a factor of 2 was assumed; for absorption values greater than 0.5 in the adult, complete absorption was assumed in the first year of life. The same approach is applied in this series.

Table 2.11. Fractional absorption values for adults and infants as used in *ICRP publication 56* series, (from ICRP, 2006)

Element	Adult	3-month-old infant
H, C, Cs, S, Mo, I	1	1
Se	0.8	1
Zn, Tc, Po	0.5	1
Te, Sr*, Ca*	0.3	0.6
Ba*, Ra*, Pb*	0.2	0.6
Co*, Fe*	0.1	0.6
Sb	0.1	0.2
Ru, Ni, Ag	0.05	0.1
U	0.02	0.04
Zr, Nb	0.01	0.02
Ce, Th, Np, Pu, Am	0.0005	0.005

* Intermediate values for 1-, 5-, 10-, and 15-year-old children: 0.4 for Sr, Ca, and Pb; 0.3 for Co, Ra and Ba; and 0.2 for Fe.

2.3.3.3. Absorption fraction for progeny radionuclides produced in the alimentary tract

(130) The default absorption fraction f_A for a radionuclide *X* produced in the alimentary tract by decay of an ingested parent radionuclide *Y* is the reference f_A for *X* as a parent. If *X* has multiple reference values corresponding to different chemical or physical forms, then the default f_A is the highest reference value provided for *X*.

2.3.3.4. Ingestion of inhaled materials

(131) For inhaled particles reaching the alimentary tract after clearance from the respiratory tract, it is appropriate to take account of solubility in the lungs in specifying f_A values. For some elements exhibiting a range in solubility according to their physicochemical form, there is evidence that the reduced solubility of Type M or S materials is also associated with reduced intestinal absorption. For a radionuclide that is transferred from the respiratory tract to the alimentary tract, the default f_A value is determined as the product of the fraction of inhaled material with rapid dissolution (f_r) for the absorption type and the f_A value for soluble forms of the element.

(132) The default absorption fraction f_A for a progeny radionuclide produced in the respiratory or alimentary tract by decay of a parent radionuclide inhaled is the product of f_r for the assigned absorption type and the reference f_A for for the progeny radionuclide when ingested as a parent radionuclide. If the progeny radionuclide has multiple reference values of f_A when ingested as a parent, corresponding to different chemical or physical forms, then the default value of f_A for the progeny radionuclide produced in the respiratory or alimentary tract is the product of f_r for the absorption type of the parent and the highest reference value provided.

2.3.3.5. Reabsorption of material

(133) Some of the biokinetic models used in this report series to predict the systemic behaviour of radionuclides depict secretion from systemic compartments into the contents of the alimentary tract. Activity transferred from systemic compartments into the small intestine or higher segments of the alimentary tract is assumed to be subject to reabsorption to blood. In such cases, the default absorption fraction f_A for the secreted activity is the reference f_A for ingestion of the radionuclide. If multiple reference values of f_A are given for different forms of the ingested radionuclide *X*, the default f_A for the secreted activity is the highest reference value provided for *X*.

2.3.4. Retention in the alimentary tract regions

(134) The model structure allows, where information is available, for the use of data on retention of radionuclides in different compartments. Human and animal data suggesting or showing retention of ingested radionuclides on teeth or in mucosal tissues of the walls of alimentary tract regions, principally the small intestine, can be used to refine calculation of doses to the alimentary tract. High levels of retention of radionuclides in the small intestine of neonates have been shown to be associated with high levels of absorption in a number of mammalian species (Fritsch et al., 1988; Nuclear Energy Agency (NEA), 1988; Sullivan, Hardy, et al., 1984; Sullivan, Miller, et al., 1984; Sullivan, Ruemmler, et al., 1984). An example given in *Publication 100* (ICRP, 2006) for cadmium shows that retention of ^{115}Cd on teeth increases the estimated dose to the oral mucosa by almost two orders of magnitude compared to that calculated using the *Publication 30* model (ICRP, 1979, 1980). Similarly, retention of ^{59}Fe in the wall of the small intestine may increase the equivalent dose to the wall by

approximately a factor of two, compared to that calculated with the *Publication 30* model (ICRP, 1979, 1980). However, in both examples, these increases in organ doses do not lead to significant changes in the committed effective doses, which are dominated by contributions from other tissues (ICRP, 2006). Information on retention in alimentary tract tissues is given, where available, in individual element sections of this and the OIR report series.

2.3.5. Alimentary tract dosimetry

(135) The HATM allows explicit calculations of dose to target regions for cancer induction within each alimentary tract region, considering doses from radionuclides in the contents of the regions, and considering mucosal retention of radionuclides when appropriate.

(136) The oesophagus and oral cavity will receive very low doses from ingested radionuclides because of short transit times in these regions (ICRP, 2006). However, they were included because a specific w_T is assigned to the oesophagus (ICRP, 2007), and because retention in the mouth, on teeth for example, can result in a substantial increase in dose to the oral mucosa (which was added to the organs and tissues constituting the remainder in *Publication 103*).

(137) In general, the alimentary tract regions of greater importance in terms of doses and cancer risk are the stomach and particularly the colon. While the small intestine may receive greater doses than the stomach, it is not sensitive to radiation-induced cancer and is not assigned a specific w_T value (ICRP, 2007). Small intestine is therefore included with the organs and tissues constituting the remainder (ICRP, 2007).

(138) An important refinement in the HATM is the methodology used to calculate doses in the various regions from non-penetrating α and electron radiations. In *Publication 30* (ICRP, 1979), it was assumed that the dose to the wall of any gastrointestinal region from β- and α-emitters in the contents was 100% and 1%, respectively, of the dose at the surface of the contents. By contrast, the HATM takes account of the location of the target cells in the mucosal layer of the wall of each gastrointestinal region and the depth of penetration of β and α particles into the wall. The targets relating to cancer induction are taken in each case to be the epithelial stem cells, located in the basal layers of the stratified epithelia of the oral cavity and oesophagus and within the crypts that replenish the single cell layer epithelium of the stomach and small and large intestines.

(139) This new methodology generally results in substantially lower estimates of doses to the colon from α- and β-emitting radionuclides in the colon contents than obtained using the *Publication 30* model (ICRP, 1979). This is because of the loss of the α particles and electrons energies in the colon contents and in the mucosal tissue overlying the target stem cells (at a depth of 280–300 μm at all ages). This reduces energy deposition in the target region for electrons and results in zero contribution to dose in the target region from α particles emitted within the contents. In the absence of retention of radionuclides in the alimentary tract wall, doses from ingested α-emitters to all regions of the alimentary tract will be solely due to their absorption to blood and subsequent irradiation from systemic activity in soft tissues or to the emission of other types of radiation (e.g. electrons or photons).

(140) The consequences of this decrease in local colon dose on the total committed effective dose will vary according to the radionuclide. Examples given in *Publication 100* (ICRP, 2006) for ^{55}Fe, ^{90}Sr and ^{239}Pu show that this decrease of local dose to the colon has little or no impact on the effective dose since the dominating contributions are from equivalent doses to organs and tissues from activity absorbed to blood. In general, the effect on effective dose is small for radionuclides with large f_A values or long-lived radionuclides with long-term retention in the body. However, for the example of ^{106}Ru (f_A = 0.05), there is a decrease in committed effective

dose by approximately a factor two, due to the major contribution to effective dose from equivalent doses to colon (decreased by a factor five) and other alimentary tract regions for this radionuclide.

(141) Calculations of doses in *Publication 100* (ICRP, 2006) were based on preliminary values of absorbed fractions of electrons and α particles to stem cell layers of each section of the alimentary tract. In this report, new calculations have been performed for both particle types and for both content and wall sources using improved absorption fraction values. Among others, new models of segment folding have been implemented for regions within the small intestine. Additional details are given in *Publication 133* and *Publication 143* (ICRP, 2016b, 2020).

2.4. Biokinetic models for systemic radionuclides

2.4.1. Parent radionuclides

(142) A model that describes the time-dependent distribution and excretion of a radionuclide in the body after it reaches the systemic circulation is referred to here as a systemic biokinetic model. In contrast to ICRP's biokinetic models describing the behaviour of radionuclides in the respiratory and alimentary tracts, ICRP's systemic biokinetic models usually have been element-specific models with regard to model structure as well as parameter values. A generic model structure that depicts all potentially important systemic repositories and paths of transfer of all elements of interest in radiation protection would be too complex to be of much practical use. However, generic model structures have been used occasionally in previous ICRP documents to describe the systemic biokinetics of small groups of elements, typically chemical families, known or expected to have qualitatively similar behaviour in the body. For example, *Publication 20* (ICRP, 1973) introduced a generic model formulation for the alkaline earth elements calcium, strontium, barium, and radium, but provided element-specific values for most model parameters. In Parts 1–3 of *Publication 30* (ICRP, 1979, 1980, 1981), a model developed for plutonium, including parameter values as well as model structure, was applied to most actinide elements. The biokinetic models for several of these actinide elements were modified in Part 4 of *Publication 30* (ICRP, 1988), where the model structure for plutonium was used as a generic structure; a common set of parameter values was applied to plutonium, americium and curium; and element-specific values were applied to selected parameters in the models for other elements. The use of generic systemic model structures was increased in ICRP's reports on doses to members of the public from intake of radionuclides (ICRP, 1993, 1995a, 1995b, 2001, 2004) and was further expanded in the OIR series of documents (ICRP, 2015, 2016a, 2017, 2019, 2022) because it facilitates the development, description and application of systemic biokinetic models.

(143) The systemic biokinetic models used in this series of reports generally follow a physiologically descriptive modelling scheme applied on a more limited scale in the series of ICRP reports on doses to members of the public from intake of radionuclides [referred to here as the '*Publication 56* series' (ICRP, 1990, 1993, 1995a, 1995b, 1995c, 2001, 2004)]. That is, the model structures include one or more compartments representing blood, depict feedback of activity from extravascular repositories to blood (i.e. they are recycling models), and as far as practical, depict the main physiological processes thought to determine the systemic biokinetics of individual elements.

(144) The systemic biokinetic models for some elements, such as iodine and iron, are developed within model structures specifically designed to describe the unique behaviour of these elements in the body. The models for most elements, however, have been constructed within one of the two generic model structures applied in the *Publication 56* series to bone-

seeking radionuclides (Figs. B.2 and B.3), or variations of those structures. This was done not only for bone-seeking elements but also for a number of elements that show relatively low deposition in bone (e.g. cobalt and ruthenium) because the main repositories and paths of movement of those elements in the body are included in one or the other of these two structures. In some cases, the model structure as applied in the *Publication 56* series has been modified slightly to accommodate specific characteristics of an element or simplified in view of the limited information on certain aspects of the biokinetics of an element.

(145) The systemic biokinetic models used in this report include explicit routes of biological removal of systemic activity in urine and faeces. Additional excretion pathways, such as sweat, are also depicted in the models for some elements.

(146) The biokinetic model adopted for the urinary bladder is described in *Publications 67* and *68* (ICRP, 1993, 1994a). To represent the kinetics of the bladder in terms of first-order processes, the rate of elimination from the bladder is taken to be 40 d^{-1}, 32 d^{-1} and 12 d^{-1} for the 3 months infant, the 1 y child and the older age groups respectively.

(147) In many of the systemic models used in the present series, activity is assumed to be removed in faeces after transfer from systemic compartments into specified segments of the alimentary tract representing element-specific endogenous secretion pathways. The rates of transfer of secreted material through different segments of the alimentary tract are element-independent rates specified in the HATM. Activity transferred from systemic compartments into the contents of the small intestine or higher segments of the tract is assumed to be re-absorbed in part, into blood. Activity assigned to the contents of the right colon or lower sections of the tract is assumed not to be subject to re-absorption.

2.4.2. Radioactive progeny

(148) A dose coefficient for a radionuclide that gives rise to a chain of radionuclides through radioactive decay (called a ‘parent’ radionuclide) includes doses from radioactive progeny produced in vivo following intake of the parent. The dose coefficient may depend strongly on assumptions concerning the biokinetics of the progeny.

(149) In *Publications 30* and *68* (ICRP, 1979, 1994a), the general assumption was made that chain members produced in systemic compartments following intake of a parent radionuclide adopt the biokinetics of the parent. This is referred to as the assumption of ‘shared kinetics’. The alternative assumption of ‘independent kinetics’ of chain members was made in *Publication 68* when the parent was an isotope of lead, radium, thorium or uranium, and also for iodine progeny of tellurium and for noble gas isotopes arising in various chains. The implementation of independent kinetics of progeny was based on a general pattern of behaviour of systemically produced progeny radionuclides suggested by a review of experimental studies and follow-up of occupationally exposed workers (Leggett et al., 1984). That is, the data suggested that most radioactive progeny produced in soft tissue or bone surface tended to migrate from the parent and begin to follow their characteristic biological behaviour, while radionuclides produced in bone volume tended to remain with the parent radionuclide in bone over the period of observation.

(150) The assumption of independent kinetics is generally applied in this report series to progeny radionuclides produced in systemic compartments other than bone volume compartments, or absorbed to blood after production in the respiratory or alimentary tract. The basic assumption is that a progeny radionuclide follows its characteristic behaviour from its time of production in, or absorption into, the systemic pool. The implementation of this assumption is not always straightforward due to structural differences in the systemic models for many parent and progeny combinations. For example, a radionuclide may be born in an

explicitly designated tissue in the parent's model that is not an explicitly designated tissue in the progeny radionuclide's characteristic model. When this happens, the rate of removal of the progeny radionuclide from the tissue and the destination of the removed activity must be defined before the model can be solved.

(151) Even if the progeny radionuclide is produced in a tissue that is an explicitly designated source organ in the progeny radionuclide's characteristic model, implementation of the default treatment of independent kinetics may become somewhat arbitrary if the progeny radionuclide's model divides the tissue into compartments that are not identifiable with compartments in the parent's model. For example, this may occur if the division of the tissue into compartments is based on physiological or anatomical considerations for the parent and on a kinetic basis for the progeny, or vice versa. Such issues of compartment identifiability are addressed on a case-by-case basis.

(152) Each of the element sections in this report series describes the implementation of the assumption of independent kinetics for dosimetrically significant progeny of radioisotopes of the element. The method of implementation depends on: the availability of specific information on the behaviour of chain members produced *in vivo*, the sensitivity of dose estimates to uncertainties in the behaviour of chain members, the lengths of radionuclide chains for that element, and the complexity and consistency of the characteristic systemic models for chain members. In a number of cases, a simplified description of the systemic kinetics is used for radionuclides after their production *in vivo*. This is particularly true for short-lived progeny radionuclides, which are assumed in some cases to decay at their site of production, or for noble gases, for which the detailed mechanistic models applied in this report series as parent radionuclides are replaced by much simpler models for application to their behaviour following production *in vivo*. These simpler descriptions are judged adequate for practical purposes in view of the uncertainties in its short-term behaviour following production *in vivo*. In all cases, the systemic model applied to an element *X* as a progeny of a parent element *Y* is the same for all chains headed by *Y* as the parent. For example, the systemic model applied to ^{224}Ra produced in a systemic pool following intake of ^{228}Th is also applied to ^{223}Ra produced in a systemic pool following intake of ^{227}Th.

2.5. Summary of rules for treatment of radioactive progeny

(153) As in the OIR series of reports (ICRP, 2015, 2016a, 2017, 2019, 2022), the following assumptions are made in this series of reports concerning the fate of progeny radionuclides produced in the body by radioactive decay.

(154) For all radionuclides with the exception of noble gases:

- The parameter values describing absorption of the inhaled parent from the respiratory tract to blood are applied to all members of the decay chain formed in the respiratory tract.
- The systemic biokinetics of a progeny radionuclide produced by decay in a systemic compartment, or absorbed to blood following production by decay in the respiratory tract or alimentary tract, is defined in the element section for the parent, given in OIR: Parts 2–5 (ICRP, 2016a, 2017, 2019, 2022) or in this series of reports. As a rule with some exceptions, the systemic biokinetics of the progeny is assumed to be independent of the systemic biokinetics of the parent. For decay chains whose members are all isotopes of the same element, the progeny are assigned the same kinetics as the parent throughout the body.

- The default absorption fraction f_A for a progeny radionuclide produced by decay in the contents of the alimentary tract (in the small intestine or a higher compartment) following ingestion of a parent radionuclide, or produced in a systemic compartment and subsequently transferred into the alimentary tract content, is the reference value of f_A for the progeny radionuclide when ingested as a parent. If the radionuclide has multiple reference values corresponding to different chemical or physical forms, then the default value of f_A is the highest reference value provided.
- The default absorption fraction, f_A, for a progeny radionuclide produced in the respiratory tract following inhalation of a parent, or produced in the alimentary tract following transfer of activity from the respiratory tract to the alimentary tract, is the product of the fraction of inhaled material with rapid dissolution (f_r) for the assigned absorption type and the reference value of f_A for the progeny radionuclide when ingested as a parent radionuclide. If the progeny radionuclide has multiple reference values of f_A when ingested as a parent, corresponding to different chemical or physical forms, then the default value of f_A is the product of f_r for the absorption type and the highest reference value provided.

(155) Noble gases produced in compartments of the respiratory tract and in the alimentary tract models by radioactive decay are assumed to escape from these compartments directly to the environment at a rate of 100 d^{-1} without transfer to the blood compartment and without transfer between compartments of respiratory tract and alimentary tract models. It is assumed that progeny of such noble gases formed within the body follow the rules of independent kinetics stated in Para. (152).

2.6. Medical intervention

(156) If medical treatment to prevent uptake or enhance excretion is administered, then the data provided in the models summarised in this report series cannot be used directly to assess committed effective doses from monitoring information (Bhattacharyya et al., 1992; IAEA, 1996; NCRP, 1980). In such circumstances, a programme of special monitoring (Section 5.5 of Publication 130, ICRP, 2015) should be undertaken to follow the retention of the particular contaminant in the person, and these data should be used to make a specific assessment of committed dose.

2.7. Methodology for dose calculations – The ICRP dosimetry system

(157) The ICRP dosimetry system is presented below as applied to assessment of organ equivalent dose and effective dose following intakes of radionuclides. The system involves numerical solution of reference biokinetic models, yielding the time-dependent number of nuclear transformations in various source tissues. These solutions are then coupled with reference data on nuclear decay information, target tissue masses, and fractions of emitted energy released from source tissue regions that are deposited in target tissue regions as defined in the reference phantoms in *Publication 110* and *Publication 143* (ICRP, 2009, 2020). Presented below is the computational formalism of these dosimetry calculations consistent with the protection quantities defined in *Publication 103* (ICRP, 2007). More detailed data are presented in ICRP Publication 133 (ICRP, 2016b).

2.7.1. Computational solutions to the ICRP reference biokinetic models

(158) The HRTM (ICRP, 1994b, 2015), the HATM (ICRP, 2006), and the systemic biokinetic models of this report describe the dynamic behaviour of radionuclides within the body. Given the routes of intake, the models predict the subsequent uptake to the systemic circulation, the distribution among tissues of the body, and the routes of elimination from the body. Superimposed on these dynamics are in-situ radioactive decay and the ingrowth of radioactive progeny. Consequently, the uptake, distribution and elimination of all progeny are predicted, in addition to those of the parent radionuclide.

(159) The compartment models of the respiratory and alimentary tract coupled with those of the systemic biokinetics define a system of first-order differential equations. The solution to the set of equations is the time-dependent distribution of the radionuclide and its radioactive progeny, if any, in mathematical compartments (pools) that are associated with anatomical regions in the body.

(160) If $N_{i,j}(t)$ represents the number of atoms of radionuclide i in compartment j at time t, the rate of change of these atoms is given in Eq. (2.3):

$$\frac{dN_{i,j}(t)}{dt} = \sum_{\substack{k=1 \\ k\neq j}}^{M} N_{i,k}\lambda_{i,k,j} - N_{i,j}\left[\sum_{\substack{k=1 \\ k\neq j}}^{M} \lambda_{i,j,k} + \lambda_i^P\right] + \sum_{h=1}^{i-1} N_{h,j}\lambda_h^P\beta_{h,i} \qquad (2.3)$$

where:

M is the number of compartments describing the kinetics;

$N_{i,k}$ is the number of atoms of chain member i in donor compartment k and varies with time;

$\lambda_{i,j,k}$ is the fractional transfer rate of chain member i from compartment j (donor compartment) to compartment k (receiving compartment) in the biokinetic model which may vary with age;

λ_i^p is the physical decay constant of chain member i;

$N_{h,j}$ is the number of atoms of precursor nuclide h in compartment j and varies with time;

λ_h^P is the physical decay constant of precursor chain member h; and

$\beta_{h,i}$ is the fraction of the decays of chain member h forming member i.

(161) Given the initial conditions specified for the compartments, $N_{i,j}(0)$, Eq. (2.3) defines the dynamic behaviour of the radionuclide and its progeny within the human body. The first term on the right-hand side of Eq. (2.3) represents the rate of flow of chain member i into compartment j from all donor compartments. The second term represents the rate of removal of member i from compartment j both by transfer to receiving compartments and by physical decay. The third term addresses the ingrowth of member i within compartment j due to the presence of its precursors h in the compartment. The number of atoms of the precursor multiplied by its physical decay is the activity of the precursor, $A_{h,j}$. Note that the members of the decay chain are assumed to be of order such that the precursors of member i have indexes less than i. An ordered listing of the chain members can be obtained using the DECDATA software distributed with *Publication 107* (ICRP, 2008).

(162) If all terms in Eq. (2.3) are multiplied by the physical decay constant of the chain member being considered the rate of change of the activity of chain member i in compartment j is obtained as shown in Eq. (2.4).

$$\frac{dA_{i,j}(t)}{dt} = \sum_{\substack{k=1 \\ k\neq j}}^{M} A_{i,k}\lambda_{i,k,j} - A_{i,j}\left[\sum_{\substack{k=1 \\ k\neq j}}^{M} \lambda_{i,j,k} + \lambda_i^P\right] + \sum_{k=1}^{i-1} A_{h,j}\beta_{h,i}\lambda_i^P \qquad (2.4)$$

(163) The system of N × M ordinary first-order differential equations is generally solved using suitable numerical methods, under the assumption that $A_{i,j}(0) = 0$ for all compartments with the exception of compartments of intake where nonzero initial conditions are only applied to the parent nuclide (i.e. i=1).

(164) To calculate the numerical values of the dose coefficients, it is necessary to associate the biokinetic compartments of Eq. (2.4) with anatomical source regions indexed by r_S. A source region may or may not be a living tissue (for example, stomach content may be a source organ but is not a living tissue) and may consist of more than one kinetic compartment. The time-dependent activity in source region r_S is the sum of the time-dependent activity in each biokinetic compartment j comprising the source region:

$$A_i(r_S, t) = \sum_{j}^{Q} A_{i,j}(t) \qquad (2.5)$$

(165) where Q represents the total number of compartments comprising the source region being considered.

(166) For intakes in reference adults, dosimetric quantities are invariant with time and it is convenient to integrate the activity in Eq. (2.5) over the 50-year commitment period to obtain the total number of nuclear transformations as in the OIR series (ICRP 2015). For intakes in reference children the dosimetric quantities vary as reference child ages. The integration must then wait until after the time-varying activity is multiplied by a time-varying dose per transformation (*S*-coefficient.)

(167) Dividing the activity in Eq. (2.5) by the total initial activity taken into the body, $\sum_j A_{1,j}(0)$, gives the rate of nuclear transformations per activity intake, $a_i(r_S, t)$:

$$a_i(r_S, t) = \frac{A_i(r_S, t)}{A_{exhaled,0} + \sum_j A_{1,j}(0)} \qquad (2.6)$$

(168) where the denominator includes the prompt exhaled activity $A_{exhaled,0}$, (pertinent for inhalations, as only a fraction of the intake activity is deposited in the compartments of the HRTM) and the summation of parent activity (i=1) in all compartments at t = 0. Note that in *Publication 130*, the denominator was erroneously described as excluding this exhaled activity. This error was corrected in *Publication 133*.

2.7.2. Computation of the ICRP reference dose coefficients for organ equivalent dose

(169) The equivalent dose rate coefficient in target region r_T of the Reference Male, $\dot{h}^M(r_T, t)$and the Reference Adult Female, $\dot{h}^F(r_T, t)$, are given by:

$$\dot{h}^M(r_T, t) = \sum_i \sum_{r_S} a_i(r_S, t)\, S_w^M(r_T \leftarrow r_S, t)_i \qquad (2.7)$$

$$\dot{h}^F(r_T, t) = \sum_i \sum_{r_S} a_i(r_S, t)\, S_w^F(r_T \leftarrow r_S, t)_i \qquad (2.8)$$

The *S*-coefficients, $S_{\mathrm{w}}^{\mathrm{M}}(r_{\mathrm{T}} \leftarrow r_{\mathrm{S}}, t)_{\mathrm{i}}$ and $S_{\mathrm{w}}^{\mathrm{F}}(r_{\mathrm{T}} \leftarrow r_{\mathrm{S}}, t)_{\mathrm{i}}$ give the radiation-weighted equivalent dose in target region r_{T} due to a nuclear transformation of chain member i in source region r_{S} [Sv $(\mathrm{Bq})^{-1}$] for the male and female reference individuals, respectively. Note that the outer summation extends over the parent nuclide and its progeny.

(170) The committed equivalent dose coefficients in each target region are given by integrating the time-dependent equivalent dose rate coefficients over the commitment period as shown in Eqs. (2.9) and (2.10). For intakes in the reference adult, the commitment period, τ, is 50 years. For children the commitment period is found by subtracting the age at intake, t_o, from 70 years.

$$h_{\mathrm{T}}^{\mathrm{M}}(\tau) = \int_{t_o}^{t_o+\tau} \dot{h}^{\mathrm{M}}(r_{\mathrm{T}}, t)\, dt \qquad (2.9)$$

$$h_{\mathrm{T}}^{\mathrm{F}}(\tau) = \int_{t_o}^{t_o+\tau} \dot{h}^{\mathrm{F}}(r_{\mathrm{T}}, t)\, dt \qquad (2.10)$$

(171) A number of tissues listed in Table 1.3 used to compute the effective dose are considered to be represented by a single target region r_{T}. In cases where more than one tissue region defines the target tissue, fractional weighting of the equivalent dose must be made. The committed equivalent dose coefficients for tissue T in the reference adult male, $h^{\mathrm{M}}(\tau)$, and adult female, $h^{\mathrm{F}}(\tau)$, are thus given as:

$$h_{\mathrm{T}}^{\mathrm{M}}(\tau) = \sum_{r_{\mathrm{T}}} f(r_{\mathrm{T}}, T)\, h^{\mathrm{M}}(r_{\mathrm{T}}, \tau) \qquad (2.11)$$

$$h_{\mathrm{T}}^{\mathrm{F}}(\tau) = \sum_{r_{\mathrm{T}}} f(r_{\mathrm{T}}, T)\, h^{\mathrm{F}}(r_{\mathrm{T}}, \tau) \qquad (2.12)$$

where the target region fractional weights $f(r_{\mathrm{T}},T)$, are the proportions of the equivalent dose in tissue T associated with target region r_{T}. With the exception of the tissues addressed in Table 2.12, the tissues of Table 1.3 are represented by a single target region and thus for these tissues $f(r_{\mathrm{T}},T) = 1$. In Table 2.12, values of $f(r_{\mathrm{T}},T)$ for the ET and Thoracic (TH or Lung) regions are taken to be equivalent to their risk apportionment factors as assigned in the revised HRTM ("Assigned fractions" in Table 2.7). These, at least, are assumed to be the same for children, in the absence of information (ICRP, 1995b) (Table 2.7). For the colon, values of $f(r_{\mathrm{T}},T)$ $f(r_{\mathrm{T}}, \mathrm{T})$are taken to be the fractional masses of the stem cell layers within the alimentary tract walls [see Table 7.8 of *Publication 100* (ICRP, 2006)]. For the lymphatic nodes, values of $f(r_{\mathrm{T}},T)$ are taken to be the fractional masses of lymphatic nodes (not lymphatic tissues) within the ET, TH and non-respiratory regions consistent with data given previously in *Publication 66* (ICRP, 1994b).

Table 2.12. Target region fractional weights, $f(r_{\mathrm{T}},T)$

Tissue, T	r_{T}	$f(r_{\mathrm{T}},T)$
ET	ET_1	0.001
	ET_2	0.999
TH	BB*	1/3
	bb	1/3
	AI	1/3
Colon	Right colon	0.4

	Left colon	0.4
	Rectosigmoid	0.2
Lymphatic nodes	LN_{ET}	0.08
	LN_{TH}	0.08
	Lymph (systemic)	0.84

ET, extrathoracic; TH, thoracic; ET_1, anterior nasal passage; ET_2, posterior nasal passage, pharynx, and larynx; BB, bronchial; bb, bronchiolar; AI, alveolar–interstitial; LN_{ET}, ET lymph nodes; LN_{TH}, TH lymph nodes.
*The basal and secretory cells are two target regions weighted equally.

2.7.3. Computation of the ICRP reference dose coefficients for the effective dose

(172) As defined in *Publication 103* (ICRP, 2007), the committed effective dose coefficient, $e(\tau)$, is then:

$$e(\tau) = \sum_T w_T \left[\frac{h_T^M(\tau) + h_T^F(\tau)}{2}\right] \qquad (2.13)$$

where w_T is the tissue weighting factor for tissue T of Table 1.3 and $h_T^M(\tau)$, and $h_T^F(\tau)$, are the corresponding committed equivalent dose coefficients for these same tissues in the Reference Male and Reference Female, respectively.

2.7.4. Implementation of specific absorbed fractions within the ICRP dosimetry system

(173) The time-dependent radiation-weighted S coefficient [Sv (Bq-s)$^{-1}$] for a radionuclide is calculated as:

$$S_w(r_T \leftarrow r_S, t) = \sum_R w_R \sum_i E_{R,i}\ Y_{R,i}\ \Phi(r_T \leftarrow r_S, E_{R,i}, t) \qquad (2.14)$$

where:

- $E_{R,i}$ is the energy of the i^{th} radiation of type R emitted in nuclear transformations of the radionuclide;
- $Y_{R,i}$ is the yield of the i^{th} radiation of type R per nuclear transformation;
- w_R is the radiation weighting factor for radiation type R (Table 1.2); and
- $\Phi(r_T \leftarrow r_S, E_{R,i}, t)$is the specific absorbed fraction, defined as the fraction of energy $E_{R,i}$ of radiation type R emitted within the source tissue r_S that is absorbed per mass in the target tissue r_T at time t after intake.

(174) The energies and yields of the emitted radiations, $E_{R,i}$ and $Y_{R,i}$, are taken from *Publication 107* (ICRP, 2008). For β emissions, the spectral data are used in the calculation of S_w rather than mean values [i.e. the inner summation in Eq. (2.14) is replaced by the integral over the spectrum].

(175) For both sexes, the values of the specific absorbed fractions for all the radiations emitted in nuclear transformations as tabulated in *Publication 107* (ICRP, 2008) have been published in *Publications 133* and *XXX* (ICRP, 2016b, 20XX). Specific absorbed fractions at the tabulated energies are found by piecewise cubic Hermite spline (PCHIP) interpolation (Fritsch and Carlson 1980).

(176) For intakes in children, the S-coefficient varies with respect to time. Interpolation is also performed to obtain S-coefficients at non-reference ages. At ages between 1 and 20 years

old, the same PCHIP interpolation technique described above is applied using *S*-coefficients at each of the reference ages as input into the interpolation algorithm.

(177) *Publication 89* describes the complexities associated with growth rates in different tissues in the first year of life. Accordingly, during the first year of life a weighted linear interpolation is used as given in Eq. (2.15) where x is a fractional factor determined using Eq. (2.16).

$$S_w(t) = x[S_w(1y) - S_w(0y)] + S_w(0y) \qquad (2.15)$$

$$x = \begin{cases} t^{[0.3+0.7(1-t)^{10}]}, & 0 \le t < \dfrac{100\ d}{365\ d} \\ t^{[0.16+0.84(1-t)^{5}]}, & \dfrac{100\ d}{365\ d} \le t < 1y \end{cases} \qquad (2.16)$$

(178) In Eq. (2.16), t is given as the fraction of 1 year (365 days). Justification for this interpolation is provided in *Publication XXX*.

(179) As described in *Publication XXX* the specific absorbed fractions for photons, electrons and neutrons for many source and target geometries are based on Monte Carlo radiation transport calculations (Zankl et al., 2012; Schwarz et al., 2021a,b) performed using the reference phantoms for the ICRP reference adult male and female described in *Publication 110* (ICRP, 2009) and the paediatric reference phantoms described in *Publication 143* (ICRP, 2020). These phantoms are constructed from tomographic images of real individuals.

(180) For α particles, the specific absorbed fractions are the inverse of the mass of the target region if $r_S = r_T$ and 0 if $r_S \neq r_T$. Exceptions occur for source and target regions within the respiratory and alimentary tracts, in the skeleton, urinary bladder and gall bladder. In these cases, only a fraction of the alpha energy emitted within the source region is deposited in the target region, and that fraction may be energy dependent. Separate models were used to compute specific absorbed fractions in these regions.

(181) In the alimentary and respiratory tracts, absorbed fractions for photons are derived using the reference phantoms (ICRP, 2009, 2020). The absorbed fraction data for electrons and alpha particles in the alimentary tract of *Publication 100* (ICRP, 2006) have been updated with supplementary calculations included in *Publication 133* (ICRP, 2016b) and *Publication XXX* (ICRP, 20XX). The absorbed fractions for electrons and alpha particles in the respiratory tract given in *Publication 66* (ICRP, 1994b) are presented in *Publication 133* (ICRP, 2016b) and *Publication XXX* (ICRP, 20XX).

(182) The biokinetic models consider that uptake occurs in the following skeletal source regions:

- trabecular bone surfaces and volumes;
- cortical bone surfaces and volumes;

(183) Surfaces of bone include:

- Haversian canal within the cortical bone cortex surrounding all regions of trabecular spongiosa;
- Haversian canal within the cortical bone of the long-bone shafts; and
- surfaces separating medullary marrow cavities and cortical bone shafts of the long bones;
- trabecular bone marrow, corresponding to the marrow within regions of trabecular spongiosa – both active and inactive marrow; and

- cortical bone marrow, corresponding to the marrow within the medullary marrow shafts of the long bones, as well as the fluids within the Haversian canals of cortical bone. In the adult, the marrow of the long bone shafts is inactive marrow.

(184) The skeletal target regions are:

- the 50-µm endosteal region (referred to as bone surface in Table 1.3); and
- active (red) marrow.

The target tissue, bone surface, of Table 1.3 is the soft tissues within 50 µm of the surfaces of mineral bone and is thought to be the region within which the osteoprogenitor cells associated with bone cancer reside. This target tissue is independent of the marrow cellularity (the fraction of bone marrow volume that is haematopoietically active). The systemic biokinetic models may identify the 'active marrow' or the 'trabecular marrow' as source regions and specific absorbed fractions are given for both source regions in *Publications 133 and 143* (ICRP, 2016b, 2020) .

2.7.5. Contribution of radioactive progeny to dose

(185) As in earlier ICRP publications, the dose coefficients in this report series account for ingrowth of radioactive progeny following the intake of the parent radionuclide. The coefficients are for the intake of the parent nuclide: i.e. upon intake, the progeny are absent. Inhalation of radon is an exception where the radioactive progeny are assumed to be present at intake.

(186) Generally, the systemic biokinetic model includes a compartment denoted as 'Other' which contains the systemic activity not explicitly assigned to compartments of identified organs and tissues. 'Other' is the complement of the explicitly designated compartments; that is, this compartment consists of all systemic tissues other than those associated with explicitly identified compartments in the systemic biokinetic model. When independent kinetics are assumed for progeny radionuclides, each member of the decay chain may have different sets of compartments, and as a result, the anatomic identity of the 'Other' compartment varies among the chain members. Two alternative computational procedures to address this situation were discussed in Annexe C.3 of *Publication 71* (ICRP, 1995b).

3. GENERAL ASPECTS OF INTERNAL DOSE ASSESSMENT

3.1. Introduction

(187) The effective dose calculated for protection purposes is determined from the equivalent doses to organs and tissues of the human body, which are in turn calculated from the mean absorbed doses to those organs and tissues (Section 1.2). Effective dose provides a value which takes account of the given exposure conditions, but not of the characteristics of a specific individual. In particular, the tissue weighting factors that are used to determine effective dose are selected, rounded values representing averages over many individuals of different ages and both sexes. The equivalent doses to each organ or tissue of the Reference Male and the Reference Female are averaged, and these averaged doses are each multiplied with the corresponding tissue weighting factor to determine the sex-averaged effective dose for the Reference Person (ICRP, 2007). It follows that effective dose does not provide an individual-specific dose, but rather that for a Reference Person under given exposure conditions (ICRP, 2007).

(188) There may be some circumstances in which parameter values may be changed from the reference values in the calculation of effective dose. It is therefore important to distinguish between those reference parameter values that might be changed in the calculation of effective dose under particular circumstances of exposure, and those values that cannot be changed under the definition of effective dose. As effective dose applies to a Reference Person, individual-specific parameter values should not be changed whereas material-specific parameter values may be changed. Examples of individual-specific parameters include those describing the dosimetric phantom, respiratory tract model breathing and particle transport parameters, HATM parameters other than the alimentary tract transfer factor, f_A, and all systemic model parameters. Examples of material-specific parameters include lung-to-blood absorption parameters, aerosol parameters such as the AMAD of the inhaled aerosol, and f_A.

(189) In the majority of cases, assessed doses are low in comparison with dose limits, and for such cases, it is likely that dose assessments will make use of the recommended default values for material-specific parameters, and the tabulated dose coefficients that accompany this series of reports. However, in some circumstances, such as where assessed doses are likely to be close to or exceed dose limits, material-specific parameter values other than the recommended defaults may be used. Further information and guidance is given in Section 6 of *Publication 130* (ICRP, 2015).

(190) In unusual cases where doses to specified individuals may exceed dose limits substantially and radiation risks need to be assessed, specific estimates of organ or tissue doses are necessary to determine organ-specific risks. In such cases, absorbed dose in organs should be calculated and used with the most appropriate biological effectiveness and risk factor data (ICRP, 2007). This retrospective individual dose assessment should only be performed by professionals with recognised expertise, skills and practical experience. It is beyond the scope of this publication to give advice on how to perform individualised retrospective dose and risk assessments.

3.2. Uncertainties in internal dose assessment

(191) *Publication 103* (ICRP, 2007) makes the following statement with respect to the assessment of uncertainties:

In order to assess radiation doses, models are necessary to simulate the geometry of the external exposure, the biokinetics of incorporated radionuclides, and the human body. The reference models and necessary reference parameter values are established and selected from a range of experimental investigations and human studies through judgements. For regulatory purposes, these models and parameter values are fixed by convention and are not subject to uncertainty.

(192) It follows that there is no requirement to assess or record the uncertainty associated with an individual dose assessment performed to demonstrate compliance with regulatory requirements. Nevertheless, there are circumstances in which the assessment of uncertainties associated with internal dose assessments may be useful. For example, the assessment of uncertainties associated with a specified monitoring procedure might provide important information for optimising the design of a monitoring programme. Where uncertainties in assessed effective dose are evaluated, uncertainties in material-specific model parameter values should be considered, but individual-specific model parameter values should be taken to be fixed at their reference values.

3.3. Uncertainties in biokinetic models

(193) Biokinetic models are used in radiation protection to predict the time-dependent distribution and retention of a radionuclide in the body and the rate of excretion of the radionuclide in urine and faeces. These models are used in this report series to derive dose coefficients following intakes of radionuclides by inhalation or ingestion.

(194) The following categorisation of the main types of information used to develop biokinetic models and assess model reliability is taken from a paper by Leggett (2001). Investigations of the reliability of many of the biokinetic models that have been used in ICRP reports can be found in the following papers and reports published by Apostoaei et al., (1998); Leggett et al., (2001; 1998, 2007, 2008); Harrison et al., (2001, 2002); Bolch et al., (2001, 2003); Skrable et al., (2002); Likhtarev et al. (2003); Apostoaei and Miller (2004); Sánchez (2007); Pawel et al., (2007); NCRP (2009), Li et al. (2014).

3.3.1. Uncertainties associated with the formulation (structure) of a biokinetic model

(195) The confidence that can be placed in predictions of a biokinetic model for an element or compound depends not only on uncertainties associated with parameter values of the model but also on uncertainties associated with the model structure. Such uncertainties may arise because the structure provides an oversimplified representation of the known processes, because unknown processes have been omitted from the model, or because part or all of the model formulation is based on mathematical convenience rather than consideration of processes. Some combination of these limitations in model structure is associated with virtually all biokinetic models for radionuclides. These limitations hamper the assignment of meaningful uncertainty statements to the parameter values of a model because they cast doubt on the interpretation of the parameter values.

3.3.1.1. Types of information used to construct biokinetic models for elements

(196) Regardless of the model formulation or modelling approach, a biokinetic model for an element or compound, particularly a systemic model, is usually based largely on some combination of the following sources of information:

- H1: direct information on humans, i.e. quantitative measurements of the element in human subjects;
- H2: observations of the behaviour of chemically similar elements in human subjects;
- A1: observations of the behaviour of the element in non-human species; and
- A2: observations of the behaviour of one or more chemically similar elements in non-human species.

H2, A1 and A2 data serve as surrogates for H1, (direct information on humans) which is the preferred type of information on which to base a biokinetic model.

(197) H1, H2, A1 and A2 data are sometimes supplemented with various other types of information or constraints, such as quantitative physiological information (e.g. rates of bone restructuring); considerations of mass balance; predictions of theoretical models based on fundamental physical, chemical, and mathematical principles (e.g. a theoretical model of deposition of inhaled particles in the different segments of the lung); experimental data derived with anatomically realistic physical models (e.g. hollow casts of portions of the respiratory tract used to measure deposition of inhaled particles); and in-vitro data (e.g. dissolution of compounds in simulated lung fluid). Among these supplemental sources of information, mass balance and quantitative physiological data (data type P) have particularly wide use.

3.3.2. Sources of uncertainty in applications of human data

(198) It is desirable to base a biokinetic model for an element or compound on observations of the time-dependent distribution and excretion of that element in human subjects (H1 data). Some degree of this type of direct information is available for most essential elements, as well as for some important non-essential elements, such as caesium, lead, radium, uranium, americium and plutonium. Depending on the degree of biological realism in the model formulation, it may be possible to supplement element-specific information for human subjects with quantitative physiological information for humans on the important processes controlling the biokinetics of the element of interest. For example, in *Publications 67*, *69*, and *71* (ICRP, 1993, 1995a, 1995b), long-term removal of certain radionuclides from bone volume is identified with bone turnover.

(199) Although it is the preferred type of information for purposes of model construction, H1 data often have one or more of the following limitations: small study groups, coupled with potentially large inter-subject variability in the biokinetics of an element; short observation periods, coupled with potentially large intra-subject variability; use of unhealthy subjects whose diseases may alter the biokinetics of the element; paucity of observations for women and children; collection of small, potentially non-representative samples of tissue; inaccuracies in measurement techniques; uncertainty in the pattern or level of intake of the element; atypical study conditions; and inconsistency in reported values. In some cases, inconsistency in reported values may provide some of the best evidence of the uncertain nature of the data.

(200) An important tool in the development of biokinetic models for radionuclides has been the use of reference organ contents of stable elements, as estimated from autopsy measurements on subjects chronically exposed at environmental levels or at elevated levels encountered in occupational exposures (ICRP, 1975). Such data are commonly used to adjust parameter values of biokinetic models or introduce new model components to achieve balance between reported values of intake, total-body content, and excretion of stable elements. Balance considerations can provide useful constraints on model parameters, provided that the data have been collected under carefully controlled conditions. However, balance considerations have often been based

on data from disparate sources of information and unreliable measurement techniques, and in some cases, may have led to erroneous models or parameter values.

(201) A confidence statement based on H1 data would reflect a variety of factors, such as the reliability of the measurement technique(s), the number and state of health of the subjects, representativeness of the subjects and biological samples, consistency in data from different studies, knowledge concerning the level and pattern of intake, and the relevance of the information to the situation being modelled. For example, confidence in a parameter value based on H1 data would be reduced if the data were determined in a study on any of the following study populations: several seriously ill subjects with known intakes; several healthy subjects with poorly characterised intakes; or one healthy subject with known intake.

3.3.3. Uncertainty in interspecies extrapolation of biokinetic data

(202) Interspecies extrapolation of biokinetic data is based on the concept of a general biological regularity across the different species with regard to cellular structure, organ structure, and biochemistry. Mammalian species, with cellular structure, organ structure, biochemistry, and body temperature regulation particularly close to those of man are expected to provide better analogies to man than do non-mammalian species with regard to biokinetics of contaminants.

(203) Despite the broad structural, functional, and biochemical similarities among mammalian species, interspecies extrapolation of biokinetic data has proven to be an uncertain process. Similarities across species are often more of a qualitative than quantitative nature, in that two species that handle an internally deposited radionuclide in the same qualitative manner may exhibit dissimilar kinetics with regard to that substance. Moreover, there are important structural, functional and biochemical differences among the mammalian species, including differences in specialised organs, hepatic bile formation and composition, level of biliary secretion, urine volume and acidity, the amount of fat in the body, the magnitude of absorption or secretion in various regions of the digestive tract, types of bacteria in the digestive tract, and microstructure and patterns of remodelling of bones.

(204) In general, the choice of an animal model will depend strongly on the processes and subsystems of the body thought to be most important in the biokinetics of the radionuclide in humans, because a given species may resemble humans with regard to certain processes and subsystems, but not others. For example, data on monkeys or baboons may be given relatively high weight for purposes of modelling the distribution of a radionuclide in the skeleton due to the close similarities in the skeletons of non-human primates and humans. Data on dogs may be given relatively high weight for purposes of modelling the rate of loss of a radionuclide from the liver due to broad quantitative similarities between dogs and humans with regard to hepatic handling of many radionuclides.

(205) A physiologically based model provides the proper setting in which to extrapolate data from laboratory animals to man, in that it helps to focus interspecies comparisons on specific physiological processes and specific subsystems of the body for which extrapolation may be valid, even if whole-body extrapolations are invalid. Depending on the process being modelled, it may be preferable in some cases to limit attention to data for a single species or small number of species, and in other cases, to appeal to average or scaled data for a collection of species.

(206) The degree of confidence that can be placed in a model value based on animal data depends on the quality and completeness of the data and the expected strength of the animal analogy for the given situation. Thus, one must consider potential experimental and statistical problems in the data as well as the logical basis for extrapolation of those particular data to humans. Relatively high confidence might be placed in a model value based on animal data: if

fairly extensive interspecies comparisons have been made and include observations on the species expected to be most human-like; if these comparisons suggest a strong basis for interspecies extrapolation, either because the data are species-invariant or because the physiological processes governing the biokinetics of the element in different species have been reasonably well established; if the model structure allows meaningful extrapolation to man, usually on the basis of physiological processes; and if such processes have been well quantified in humans (i.e. the central value for humans has been reasonably well established). A fairly wide uncertainty interval is indicated if data are available only for species that frequently exhibit qualitative differences from man (e.g. if data were available only for rats) or if no meaningful basis for extrapolation to man has been established with regard to the quantity of interest. Whatever the quality of the animal data, the uncertainty interval should reflect the fact that some confidence in the predictive strength of the data is lost when the data are extrapolated across species.

3.3.4. Uncertainty in inter-element extrapolation of biokinetic data

(207) Biokinetic models for elements are often constructed partly or wholly from data for chemically similar elements, on the basis of empirical evidence that chemical analogues often exhibit close physiological similarities. For example, the alkaline earth elements, calcium, strontium, barium and radium, exhibit many physiological as well as chemical similarities (ICRP, 1993), and the alkali metals rubidium and caesium closely follow the movement of their chemical analogue, potassium.

(208) There are, however, counterexamples to the premise that chemical analogues are also physiological analogues. For example, the alkali metals potassium and sodium share close physical and chemical similarities but exhibit diametrically opposite behaviours in the body, with potassium being primarily an intracellular element and sodium being primarily an extracellular element.

(209) Moreover, some of the chemically similar elements that behave in a qualitatively similar fashion in the body may exhibit quite different kinetics. For example, caesium appears to follow the behaviour of potassium in the body in a qualitative sense, but is distributed somewhat differently from potassium at early times after intake and exhibits a substantially longer whole-body retention time.

(210) The level of confidence that can be placed in a model value based on human data for a chemically similar element depends on the quality and completeness of the data for the analogue, as well as the expected strength of the analogy for the given situation. Whatever the quality of the data for the chemical analogue, the confidence interval should reflect the fact that some confidence in the predictive strength of the data is lost when the data are extrapolated across elements.

(211) The strength of the chemical analogy for a given element depends largely on the extent to which the chemically similar elements have been found to be physiologically similar. That is, the analogy would be considered strong for a pair of elements if a relatively large set of experimental data indicates that these elements have essentially the same qualitative behaviour in the body and that their quantitative behaviour is either similar or differs in a predictable fashion. In view of counterexamples to the premise that chemically similar elements are necessarily physiologically similar, the chemical analogy does not provide high confidence if the elements in question have not been compared in animals or man.

(212) If a chemical analogue has been shown to be a good physiological analogue, then application of human data on the chemical analogue (H2 data) may be preferable to application of animal data on the element of interest (A1 data). For example, for purposes of constructing

or evaluating a biokinetic model for americium in humans, use of quantitative human data on the physiological analogue curium seems preferable to use of the best quantitative animal data on americium. Similar statements can be made for radium and barium, rubidium and potassium, or other pairs of close physiological analogues. On the other hand, if two chemically similar elements show only broad physiological similarities, the animal analogy may be preferred to the chemical analogy, particularly if element-specific data are available for a variety of animal species (as is the case, for example, for uranium and calcium). In general, lower confidence would be placed in animal data for a chemical analogue than in animal data for the element of interest.

3.3.5. Uncertainty in central estimates stemming from variability in the population

(213) 'Uncertainty' refers here to lack of knowledge of a central value for a population, and 'variability' refers to quantitative differences between different members of a population. Although uncertainty and variability are distinct concepts, the variability in biokinetic characteristics within a population is often an important factor contributing to the uncertainty in a central estimate of a biokinetic quantity. This is because such variability complicates the problem of identifying the central tendency of these characteristics in the population due to the small number of observations generally available and the fact that usually, subjects of biokinetic studies are not randomly selected.

(214) Variability in the biokinetics of radionuclides, pharmaceuticals, or chemicals in human populations appears to result from many different physiological factors or modulating host factors of an environmental nature, including age, sex, pregnancy, lactation, exercise, disease, stress, smoking and diet. Large inter-individual biokinetic variations sometimes persist in the absence of appreciable environmental differences and suggest that these variations may be genetically controlled. In real-world situations, genetic and environmental factors may interact dynamically, producing sizable variations in the behaviour of substances taken into the human body.

3.4. Uncertainties in dosimetric models

(215) Dosimetric models are used to estimate the mean absorbed dose resulting from radiations emitted by nuclear transformations of radionuclides present in the body. The absorbed dose is computed for target regions (organs, tissues, or regions of tissues) considered to be radiosensitive. Radiation weighting factors and tissue weighting factors are applied to the mean absorbed dose to determine the equivalent and effective dose. The weighting factors are assigned reference values, and as such, are not regarded as uncertain quantities. Thus, the uncertainties associated with an estimated equivalent dose to an organ, for example, are considered to be those associated with the underlying mean absorbed dose.

(216) The physical and anatomical parameters contributing to uncertainties in the mean absorbed dose for internal emitters are:

- Energy and intensity of the nuclear and atomic radiations emitted by the radionuclide and by any radioactive progeny;
- Interaction coefficients of the emitted radiations in tissues;
- Elemental composition of the tissues of the body;
- Volume, shape, and density of the organs of the body; and

- Parameters describing the spatial relationship of the source regions (regions containing the radionuclide) and the target regions (radiosensitive organs and tissues for which dose values are desired).

(217) Limitations are present in the computational model representing the anatomy and in the numerical procedures used to calculate the energy absorbed in the target regions. The magnitudes of these uncertainties vary with radiation type, the energy of the radiation, and the specific source-target pair. The adoption of computational phantoms based upon medical imaging data (often referred to as voxel phantoms) has reduced the uncertainties associated with cross-irradiation of tissues by photon and neutron radiations to some extent by providing more realistic spatial relationships of some source and target regions (ICRP, 2009, 2020). However, the absorbed dose is frequently dominated by the contributions from non-penetrating radiations. For source and target regions that cannot be resolved in the medical image data, e.g. source and target regions in the respiratory and alimentary tracts and in the skeleton, uncertainties are associated with the computational models used to represent these regions.

(218) The anatomical models are static and thus do not address uncertainties in the spatial position of the organs due to breathing and posture other than reclining.

(219) The parameters of the dosimetric model contributing to uncertainties in the absorbed dose are those physical parameters associated with the nuclear transformation processes that determine the energy and intensity of the emitted radiation, and parameters which govern the transport radiations in the body. Attenuation and absorption coefficients for photons involve relatively small uncertainties, typically less than 10%, but somewhat higher uncertainties are ascribed to soft tissue stopping power values for α particles and electrons. Improvements in the basic nuclear data have reduced the uncertainties in the physical half-lives of radionuclides and the branching fractions of decay modes. The simplified procedures used in the dosimetric calculations to address the delayed β and gamma radiations of spontaneous fission can contribute to substantial uncertainties in the mean absorbed dose in some tissues.

(220) The dosimetric calculations must associate an anatomical region (source region) with each biokinetic compartment. Many biokinetic models partition the systemic activity among a few identified organs/tissues and include a compartment referred to as ‘Other tissue’ which represents the residual activity (See Section 2.7). The dosimetric procedure distributes the activity in the ‘Other tissue’ compartment uniformly among all tissues not explicitly identified in the model. Substantial uncertainty may be associated with the mean absorbed dose for tissues that are members of ‘Other tissue’. ‘Other tissue’ frequently includes tissues assigned an explicit tissue weighting factor. For example, breast tissue is rarely explicitly identified as a source region in biokinetic models, and thus, its mean absorbed dose is often based on its inclusion in ‘Other tissue’.

(221) A number of numerical methods are capable of solving the set of potentially large numbers (hundreds) of coupled differential ‘stiff’ equations that describe the kinetics, although frequently the demands of numerical accuracy have to be balanced with computational time. Compartment-model issues contributing to uncertainties in the mean absorbed dose include the assumed biokinetics of members of a decay chain (independent or shared kinetics), and the representation of ‘Other’ tissues when their anatomical identity varies among the decay chain members [Section 2.7.5 and Annex C of *Publication 71* (ICRP, 1995b)].

4. DATA PROVIDED FOR ELEMENTS AND RADIOISOTOPES

(222) This Section describes the information provided in subsequent parts of this series of reports. The data provided are reference values for the purposes of radiation protection. The biokinetic parameter values of the Reference Members of the Public and data provided here are invariant with sex, race, health status and other individual-specific characteristics.

(223) Each element section in the EIR series includes reviews of data on inhalation, ingestion and systemic biokinetics and the structure and parameter values of the reference systemic biokinetic model. (For inhalation, reviews of data in OIR Parts 2 – 5 are adopted.) Dosimetric data provided include dose coefficients (committed effective dose and committed equivalent dose to named organs or tissues, Sv Bq^{-1}) for inhalation and ingestion of all relevant radioisotopes. Dosimetric data are calculated using the revised HRTM (ICRP, 2015), the HATM (ICRP, 2006) and the reference systemic biokinetic models defined in this series of reports for the Reference Individuals.

(224) Committed effective dose and committed equivalent dose to named organs and tissues per intake [or 'dose per intake coefficient' $e(\tau)$, Sv Bq^{-1}] are provided for assessments of the effective dose to each Reference Member of the Public. These coefficients should be used for the assessments based on the activity of the intake; the activity intake can be assessed prospectively (i.e. at the design or planning stage) or retrospectively (i.e. based on monitoring data).

4.1. Data provided in the printed reports and electronic annexes

(225) The data provided in the printed reports are restricted to tables of committed effective dose per intake (Sv Bq^{-1}) for inhalation and ingestion. Data are provided for all absorption types and for the most common isotope(s) of each element. In cases for which sufficient information is available (principally for actinide elements), lung absorption is specified for certain chemical forms, and dose coefficients are calculated accordingly. Dose coefficients are also calculated for specific gas and vapour forms of some elements, because deposition in the respiratory tract depends on chemical form. The sizes of particles inhaled by the Reference Individuals are assumed to be log-normally distributed with an AMAD of 1 μm and geometric standard deviation σ_g of approximately 2.5 (Paragraph 170, ICRP, 1994b). They are assumed to have a density of 3.00 g cm^{-3}, and a shape factor of 1.5 (Paragraph 181, ICRP, 1994b). An exception is made for the short-lived progeny of radon, described in the inhalation section in OIR: Part 3 (ICRP, 2017).

(226) The electronic annex that accompanies this series of reports contains a comprehensive set of committed effective and equivalent dose coefficients per intake. Data are presented for almost all radionuclides included in *Publication 107* that have half-lives equal to or greater than 10 min, and for other selected radionuclides. Data are provided for a range of physico-chemical forms and for aerosols with median sizes ranging from an AMTD of 0.001 μm to an AMAD of 20 μm. Data for intake by ingestion (for specified values of f_A) are also provided.

4.2. Quality assurance of data presented

(227) The Commission attaches particular importance to quality assurance. The Task Group of Committee 2 on Internal Dose Coefficients arranged for the quantities given in this series of reports to be calculated independently at different laboratories, using different computer codes. Any discrepancies in these calculations are investigated and resolved before publication.

5. HYDROGEN (Z = 1)

(228) Tritium may be released into the environment in three main chemical forms: tritium gas, tritiated water, and organic compounds of tritium (organically-bound tritium, OBT). In the environment, tritium gas is gradually converted to tritiated water. In this section, dosimetric data are given for tritium ^{3}H.

5.1. Routes of Intake

5.1.1. Inhalation

(229) Extensive information on absorption of tritium from the respiratory tract is available from occupational exposures, and from human volunteer studies with inhaled tritium gas and tritiated water. Information is also available from experimental studies of tritiated organic compounds and particulate forms (mainly metal tritides and luminous compounds), in rats and *in vitro*. For details see Section 2 of *Publication 134* (ICRP, 2016a).

(230) Absorption parameter values and types, and associated f_A values for gas and vapour forms of hydrogen (tritium) are given in Table 5.1 and for particulate forms in Table 5.2 (both taken from Section 2 of *Publication 134*). Exposures to gas or vapour forms of tritium are more common than exposures to particulate forms, and it is therefore recommended in this series of documents that gas/vapour form is assumed in the absence of information.

Table 5.1. Deposition and absorption for gas and vapour forms of hydrogen (tritium)[*,†]

Chemical form/origin	Percentage deposited[‡]						Absorption[*]	
	Total	ET_1	ET_2	BB	bb	AI	Type	f_A
Tritiated water (HTO)	100[§]	0	20	10	20	50	V	[**]
Tritium gas (HT)	0.01[§]	0	0.002	0.001	0.002	0.005	V	[**]
Tritiated methane ($CH_{4-x}T_x$)	0.3[§]	0	0.06	0.03	0.06	0.15	V	[**]
Unspecified[†]	100[¶]	0	20	10	20	50	F	1.0[††]

ET_1, anterior nasal passage; ET_2, posterior nasal passage, pharynx and larynx; BB, bronchial; bb, bronchiolar; AI, alveolar-interstitial.

[*]It is assumed that for tritium the bound state can be neglected, i.e. $f_b = 0.0$. For intake of these forms of tritium the systemic model for HTO is applied to absorbed activity.

[†]For tritium in unspecified gas or vapour form (including unspecified organic vapours), the default option for gases and vapours is recommended: 100% total deposition in the respiratory tract; default distribution between regions[¶] and Type F absorption.

[‡]Percentage deposited refers to how much of the material in the inhaled air remains in the body after exhalation. Almost all inhaled gas molecules contact airway surfaces, but usually return to the air unless they dissolve in, or react with, the surface lining. In the case of tritium gas and methane, a small fraction is absorbed into body fluids and of that, a fraction is metabolised and the rest subsequently exhaled.

[§]Since instantaneous absorption to blood is assumed, calculations can be performed assuming direct injection into blood, and the regional deposition does not need to be considered. However, for completeness, the default distribution is assumed[¶].

[¶]Default distribution between regions (20% ET_2, 10% BB, 20% bb and 50% AI).

[**]Not applicable for absorption Type V, because all activity deposited in the respiratory tract is instantaneously absorbed.

[††]The value of $f_A = 1$ is applicable to all age-groups.

Table 5.2. Absorption parameter values for inhaled particulate forms of tritium and for ingested tritium.

Inhaled particulate materials[*]		Absorption parameter values[†] f_r	s_r (d^{-1})	s_s (d^{-1})
Specific parameter values[‡]				
Biogenic organic compounds		1	100	–
Default parameter values[§,¶]				
Absorption Type	Assigned forms			
F	$LaNi_{4.25}Al_{0.75}$ tritide	1	100	–
M[**]	Glass fragments; luminous paint; titanium tritide; zirconium tritide	0.2	3	0.005
S	Carbon tritide; hafnium tritide	0.01	3	1×10^{-4}

Ingested materials[††]						
Assigned forms[*]	Age-dependent absorption from the alimentary tract, f_A					
	3 months	1 year	5 years	10 years	15 years	Adult
Biogenic organic compounds[‡]	1	1	1	1	1	1
Tritiated water and other soluble forms (as assigned to Type F for inhalation)	1	1	1	1	1	1
Relatively insoluble forms (Types M and S)	0.2	0.1	0.1	0.1	0.1	0.1

[*]The systemic model for HTO is applied to intake of all forms of tritium other than biogenic tritiated organic compounds, for which the systemic model for OBT is applied.

[†]It is assumed that for tritium the bound state can be neglected, i.e. $f_b = 0.0$. The value of s_r for Type F forms of hydrogen (100 d^{-1}) is element-specific. The values for Types M and S (3 d^{-1}) are the general default values.

[‡]See Section 2 of *Publication 134* (ICRP, 2016a) for summary of information on which parameter values are based, and on ranges of parameter values observed for individual materials. For biogenic organic compounds, Type F default parameter values are used for absorption from the respiratory and alimentary tracts, but a specific systemic model, OBT, for absorbed tritium.

[§]Materials (e.g. "Glass fragments") are generally listed here where there is sufficient information to assign to a default absorption Type, but not to give specific parameter values (see Section 2 of *Publication 134*).

[¶]For inhaled material deposited in the respiratory tract and subsequently cleared by particle transport to the alimentary tract, the default f_A values for inhaled materials are applied: i.e. the product of f_r for the absorption Type and the f_A value for ingested soluble forms of tritium applicable to the age-group of interest (1.0).

[**]Default Type M is recommended for use in the absence of specific information on which the exposure material can be assigned to an Absorption Type, e.g. if the form is unknown, or if the form is known but there is no information available on the absorption of that form from the respiratory tract.

[††] Activity transferred from systemic compartments into segments of the alimentary tract is assumed to be subject to reabsorption to blood. The default absorption fraction f_A for the secreted activity is the highest f_A value for ingestion of the radionuclide applicable to the age-group of interest (1.0).

5.1.2. Ingestion

5.1.2.1. Tritiated water

(231) Tritiated water is rapidly and completely absorbed to blood after ingestion with no difference between ages.

5.1.2.2. Organically-bound Tritium

(232) The major part of tritium intake by members of the public will occur by ingestion of food into which tritium has been incorporated through both plant and animal components. Such organically bound tritium (OBT) will be present in many different chemical compounds

including proteins, carbohydrates, fats and nucleic acids. In the human alimentary tract, foodstuffs containing OBT will undergo digestion to yield small molecules which are readily absorbed. A small proportion of the tritium will probably be present in indigestible fibres and will be non-absorbable. However, it is assumed that non-absorbable OBT represents a very small proportion of the total dietary OBT.

(233) In *Publication 134 (OIR Part 2)*, an f_A of 1 was adopted for both tritiated water and organic compounds, although it was recognized that absorption may be substantially less than complete in the case of some organic compounds. In this report, an f_A of 1 is adopted for tritium in food and for all soluble forms. An f_A of 0.1 is adopted for relatively insoluble forms of tritium for adults. For 3-month-old infants, this values is increased to $f_A = 0.2$.

5.1.3. Systemic Distribution, Retention and Excretion

5.1.3.1. Background

(234) Two different systemic models are used in this report to develop dose coefficients for two forms of tritium commonly encountered in the environment. These are referred to as the HTO (tritiated water) and the OBT (organically bound tritium) models. OBT refers to carbon-bound tritium formed in plants and animals through natural biological processes.

(235) Studies of the fate of inhaled or ingested HTO in humans and laboratory animals indicate that HTO is rapidly absorbed to blood and mixed with total-body water. A few percent of the absorbed amount is converted to OBT. The retention time for OBT appears to depend on the metabolic activity of the tissue in which it deposits. The retention time of the unconverted HTO presumably is determined by the rate of water turnover, which varies with age and may be estimated on the basis of the mass of total-body water and total energy expenditure at a given age. The average retention time of OBT appears from animal studies to be substantially longer than that of unconverted HTO. Two phases of relatively long-term retention of tritium in the body observed in persons exposed to tritium in the workplace (OIR Part 2, *Publication 134*) are assumed to represent two phases of OBT retention.

(236) Inaba et al. (1984) studied the tissue distribution and urinary excretion of tritium administered as tritiated water via a stomach tube to rats of various ages. Younger animals generally showed a shorter residence time of tritium in the body than did mature animals. Incorporation of tritium in tissues was assessed both in the aqueous fraction and organic components of the studied tissues, which included brain, liver, muscle, testis, and blood. Over the first several days the activity concentration in tissue water decreased rapidly while that in the organic portion decreased more slowly.

(237) Ingested food containing OBT undergoes digestion in the gastrointestinal tract, yielding small molecules that are for the most part readily absorbed to blood. Studies in animals administered various forms of OBT indicate relatively high concentrations of activity in fat, muscle, and brain (Pietrzak-Flis et al., 1978). The authors of *Publication 56* (ICRP, 1990) interpreted reported data for laboratory animals as indicating that 9-45% of ingested OBT is incorporated into organic constituents of tissues and, on average, about 9 times more OBT is present in body tissues after intakes of OBT than after intakes of HTO.

5.1.3.2. HTO Model

(238) The model for systemic HTO applied in *Publication 134* (OIR Part 2) to workers is applied here to adult members of the public. The model is extended to pre-adult ages by adjustment of a set of parameter values representing turnover of body water and a second set of parameter values representing turnover of a substantial portion of the body's carbon content.

The turnover rate of body water is assumed to be the same as the turnover rate of tritium retained in the body as tritiated water. The turnover rate of carbon is assumed to be the same as the rate of turnover of tritium retained in the body as OBT.

(239) The structure of the HTO model is shown in Fig. 5.1. Parameter values are listed in Table 5.3.

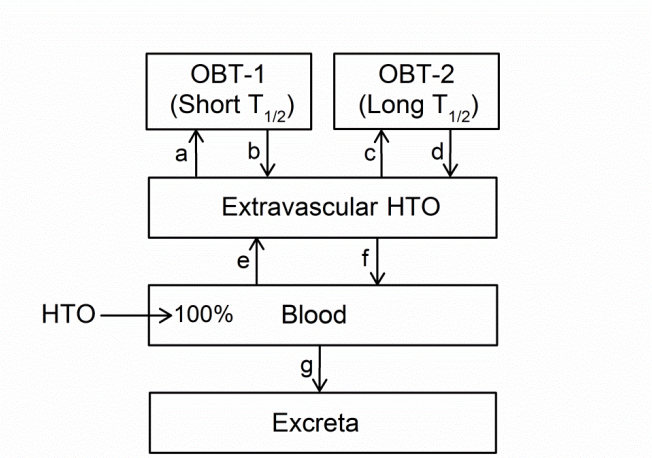

Fig. 5.1. Structure of the HTO systemic model. Transfer from blood to excreta (or excretion pathways) is divided as follows: 55% to urinary bladder contents; 4% to right colon contents; 12% exhaled with no retention in lungs; 29% removed through the skin (sweat plus insensible loss) with no retention in skin.

(240) The model includes compartments representing blood, extravascular body water that exchanges rapidly with blood, and two components of retention of tritium converted in vivo to OBT. Excretion is from the blood compartment only. The following partition of excreted tritium (not shown in Fig. 5.1) is applied to all age groups on the basis of reference data for water balance in adult humans (ICRP, 2002a): urine (via the urinary bladder contents), 55%; faeces (via the right colon contents), 4%; exhalation, 12%; and loss through skin (sweat plus insensible loss), 29%. For the worker or adult member of the public, the transfer coefficient from Blood to Excreta yields an initial removal half-time from the body of about 10 d, and the transfer coefficients from compartments OBT-1 and OBT-2 back to Extravascular HTO correspond to half-times of about 40 d and 1 y, respectively.

Table 5.3. Transfer coefficients for the HTO model

Path*	Transfer coefficient (d^{-1})					
	Infant	1 y	5 y	10 y	15 y	Adult
Blood to Extravascular HTO	4.00E+02	4.00E+02	4.00E+02	4.00E+02	4.00E+02	4.00E+02
Extravascular HTO to OBT-1	1.32E-03	1.26E-03	1.26E-03	9.00E-04	6.60E-04	6.00E-04
Extravascular HTO to OBT-2	1.76E-04	1.68E-04	1.68E-04	1.20E-04	8.80E-05	8.00E-05
Blood to urinary bladder contents	3.85E-01	3.85E-01	3.85E-01	3.85E-01	3.85E-01	3.85E-01
Blood to RC-contents	2.80E-02	2.80E-02	2.80E-02	2.80E-02	2.80E-02	2.80E-02
Blood to Excreta	2.87E-01	2.87E-01	2.87E-01	2.87E-01	2.87E-01	2.87E-01
Extravascular HTO to Blood	9.68E+01	9.24E+01	9.24E+01	6.60E+01	4.84E+01	4.40E+01
OBT-1 to Extravascular HTO	6.93E-02	4.33E-02	4.33E-02	3.47E-02	2.08E-02	1.73E-02
OBT-2 to Extravascular HTO	7.60E-03	4.75E-03	4.75E-03	3.80E-03	2.28E-03	1.90E-03

*RC = right colon

(241) Derivation of age-specific parameter values for HTO entering the systemic circulation follows the same general assumptions applied in *Publication 56* (ICRP, 1990) to model HTO kinetics. The turnover rate of tritium in the compartment in Fig. 5.1 labeled 'Extravascular HTO' is estimated from reference values for energy expenditure and the mass of total-body water, based on the physiological premise that 1 ml of water is required for each kcal of energy expended (ICRP, 1975). The turnover rate of tritium in the compartments labeled 'OBT-1' and 'OBT-2' are based on derived relative age-specific rates of carbon turnover.

(242) The age- and sex-specific values for energy expenditure applied here are taken from Table 2.29 of *Publication 89* (ICRP, 2002a). The mass of total-body water is assumed to be 74% of total-body mass in the infant; 60% at ages 1, 5, and 10 y; 59% in the 15-y-old and adult male; 56% in the 15-y-old female; and 50% in the adult female (Altman and Katz, 1961). Age- and sex-specific total-body masses are taken from *Publication 89* (ICRP, 2002a). Age-specific water turnover rates are derived separately for males and females and then sex-averaged (and rounded) for each age to estimate a sex-independent turnover rate. For example, the rate of turnover of body water for a male or female at age 10 y is estimated as (1 kcal ml^{-1} × 1900 kcal d^{-1})/ (32,000 g × 0.6 × 1 g/ml) = 0.099 d^{-1}, where 1900 kcal d^{-1}, 32,000 g, and 0.6 are reference values for energy expenditure, total-body mass, and body water as a fraction of total-body mass, respectively, at age 10 y. The derived water turnover rates for the infant and ages 1, 5, 10, and 15 years, normalized to a value of 1 for the adult to derive scaling factors for extension of adult transfer coefficients to younger ages, are 2.2, 2.1, 2.1, 1.5, and 1.1, respectively. (Normalized rather than absolute turnover rates for HTO are used here because this potentially biased method of derivation of HTO turnover rates overestimates the observed average retention time of HTO in adults by roughly 10%.) These scaling factors are applied to outflow rates from the compartment 'Extravascular HTO' (transfer coefficients *a*, *c*, and *f* in Fig. 5.1) in the model for the adult. For example, based on a scaling factor for age 10 y of 1.5 and adult value of 44 d^{-1} for transfer coefficient *f*, the value assigned to transfer coefficient *f* for age 10 y is 1.5 × 44 d^{-1} = 66 d^{-1}.

(243) The reader is referred to the section on carbon biokinetics for a discussion of the method of derivation of relative turnover rates of carbon at different ages. The following multiplicative factors given in the section on carbon are used to scale transfer coefficients *b* and *d* in Fig. 5.1 (outflow rates from OBT compartments) from adult values to values for ages 100 d, 1 y, 5 y, 10 y, and 15 y, respectively: 4.0, 2.5, 2.5, 2.0, and 1.2. For example, based on a scaling factor for age 10 y of 2.0 and an adult value of 0.01733 d^{-1} for transfer coefficient *b* (Fig. 5.1), the value assigned to transfer coefficient *b* for age 10 y is 2.0 × 0.01733 d^{-1} = 0.03466 d^{-1}.

(244) The outflow rate from Blood is assumed to be independent of age. That is, adult values for transfer coefficients *e* and *g* (Fig. 5.1) are assigned to all ages.

5.1.3.3. OBT model

(245) ICRP *Publication 56* recommended a default model for OBT in which it is assumed that 50% of OBT entering the systemic circulation enters into bonds with carbon and is cleared with the same half-time as carbon. The remaining 50% is assumed to be rapidly metabolized to HTO.

(246) Similar assumptions are made here regarding the initial behaviour of OBT following its uptake to blood. Specifically, it is assumed as indicated in Fig. 5.2 that 50% of organically bound tritium is converted to tritiated water upon entering blood and 50% moves immediately to the compartment representing intermediate-term retention of organically bound tritium (OBT-1 in Fig. 5.2). Subsequently the fate of deposited tritium is described by the age-specific

model for tritiated water describe above. That is, the transfer coefficients summarized in Table 5.3 apply to OBT as well as HTO subsequent to assignment of 50% of the absorbed OBT to compartment OBT-1 and the remaining 50% to Blood.

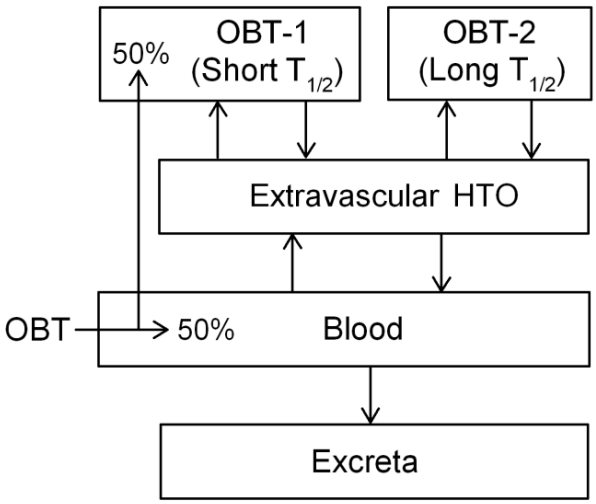

Fig. 5.2. Structure of the model for tritium initially entering blood as OBT. This differs from the model for HTO only in that 50% of tritium entering Blood is assumed to transfer immediately to OBT-1.

5.2. Dosimetric data for tritium

Table 5.4. Committed effective dose coefficients (Sv Bq^{-1}) for the inhalation or ingestion of ^{3}H compounds

	Effective dose coefficients (Sv Bq^{-1})					
Inhaled gases or vapours	3 mo	1 y	5 y	10 y	15 y	Adult
Tritiated water (HTO)	1.1E-10	7.2E-11	3.6E-11	2.7E-11	2.1E-11	2.0E-11
Tritium gas (HT)	1.1E-14	7.2E-15	3.6E-15	2.7E-15	2.1E-15	2.0E-15
Tritiated methane ($CH_{4-x}T_x$)	3.3E-13	2.2E-13	1.1E-13	8.2E-14	6.2E-14	5.9E-14
Unspecified gas or vapour form (including unspecified organic vapours)	1.1E-10	7.2E-11	3.6E-11	2.7E-11	2.1E-11	2.0E-11
Inhaled particulate materials (1 µm AMAD aerosols)						
Type F, Biogenic organic compounds (OBT)	9.6E-11	8.0E-11	3.6E-11	2.7E-11	2.1E-11	2.2E-11
Type F, $LaNi_{4.25}Al_{0.75}$ tritide	5.5E-11	3.7E-11	1.6E-11	1.2E-11	8.3E-12	8.2E-12
Type M, Glass fragments, luminous paint, titanium tritide, zirconium tritide; all unspecified compounds	2.6E-10	2.2E-10	1.2E-10	7.1E-11	5.0E-11	4.6E-11
Type S, Carbon tritide, hafnium tritide	1.4E-09	1.4E-09	9.0E-10	6.1E-10	5.4E-10	5.6E-10
Ingested materials						
Adult f_A = 1.0, Tritium in food and other soluble forms (as assigned to Type F for inhalation)	1.1E-10	7.2E-11	3.6E-11	2.7E-11	2.0E-11	1.9E-11
Adult f_A = 0.1, Relatively insoluble forms (Types M and S)	2.2E-11	7.2E-12	3.6E-12	2.7E-12	2.1E-12	2.0E-12
Adult f_A = 1.0, Biogenic organic compounds (OBT)	1.9E-10	1.5E-10	7.8E-11	5.8E-11	5.1E-11	5.1E-11

6. CARBON (Z = 6)

6.1. Routes of Intake

6.1.1. Inhalation

(247) Some information on absorption from the respiratory tract is available for inhaled gases of carbon in man and in experimental animals. Some information is also available on the behaviour of ^{14}C-labelled compounds and particles, mainly in rats, and on forms of carbon labelled with other radionuclides. For details see Section 3 of *Publication 134* (ICRP, 2016a). Absorption parameter values and types, and associated f_A values for gas and vapour forms of carbon are given in Table 6.1 and for particulate forms in Table 6.2 (both taken from Section 3 of *Publication 134*). Exposures to both gas/vapour forms and particulate forms of carbon are common, and it is therefore recommended in this series of documents that in the absence of information 50% particulate; 50% gas/vapour should be assumed.

Table 6.1. Deposition and absorption for gas and vapour forms of carbon*

	Percentage deposited†						Absorption		Systemic
Chemical form/origin	Total	ET_1	ET_2	BB	bb	AI	Type	f_A	model‡
Carbon monoxide (CO)	40§	0	8	4	8	20	V	**	CO
Carbon dioxide (CO_2)	100§	0	20	10	20	50	V	**	CO_2
Methane (CH_4)	0.3§	0	0.06	0.03	0.06	0.15	V	**	Methane
Unspecified	100¶	0	20	10	20	50	F	1.0††	C

ET_1, anterior nasal passage; ET_2, posterior nasal passage, pharynx and larynx; BB, bronchial; bb, bronchiolar; AI, alveolar-interstitial.

*For carbon in unspecified gas or vapour form (including unspecified organic vapours), the default option for gases and vapours is recommended: 100% total deposition in the respiratory tract; default distribution between regions¶ and Type F absorption. It is assumed that for carbon the bound state can be neglected i.e. $f_b = 0$.

†*Percentage deposited* refers to how much of the material in the inhaled air remains in the body after exhalation. Almost all inhaled gas molecules contact airway surfaces, but usually return to the air unless they dissolve in, or react with, the surface lining. In the case of methane, a small fraction is absorbed into body fluids and of that, a fraction is metabolised and the rest subsequently exhaled.

‡CO = Systemic model for carbon monoxide; CO_2 = Systemic model for carbon dioxide/bicarbonate; C = Generic systemic model for other ^{14}C compounds (Section 3.2.3.2. of Publication 134, ICRP, 2016a).

§Since instantaneous absorption to blood is assumed, calculations can be performed assuming direct injection into blood, and the regional deposition does not need to be considered. However, for completeness, the default distribution is assumed¶.

¶Default distribution between regions (20% ET_2, 10% BB, 20% bb and 50% AI).

**Not applicable for absorption Type V, because all activity deposited in the respiratory tract is instantaneously absorbed.

††The value of $f_A = 1$ is applicable to all age-groups.

Table 6.2. Absorption parameter values for inhaled particulate forms of carbon and for ingested carbon

Inhaled particulate materials*		Absorption parameter values† f_r	s_r (d^{-1})	s_s (d^{-1})
Specific parameter values‡				
Barium carbonate		1	100	–
Default parameter values§,¶				
Absorption Type	Assigned forms			
F	–	1	100	–
M**	–	0.2	3	0.005
S	Elemental carbon, carbon tritide	0.01	3	1×10^{-4}

Ingested materials††						
Assigned forms*	Age-dependent absorption from the alimentary tract, f_A					
	3 months	1 year	5 years	10 years	15 years	adult
Barium carbonate‡	1	1	1	1	1	1
All other forms	1	1	1	1	1	1

*Following uptake into body fluids, the generic systemic model for carbon is used (Section 3.2.3.2. of Publication 134, ICRP, 2016a), with the exception of barium carbonate, for which the carbon dioxide/bicarbonate systemic model (Section 3.2.3.2.) is applied to the absorbed carbon.

†It is assumed that for carbon the bound state can be neglected i.e. $f_b = 0$. The value of s_r for Type F forms of carbon (100 d^{-1}) is element-specific. The values for Types M and S (3 d^{-1}) are the general default values.

‡See Section 3 of *Publication 134* for summary of information on which parameter values are based, and on ranges of parameter values observed for individual materials. For barium carbonate, Type F default parameter values are used for absorption from the respiratory and alimentary tracts, but a specific systemic model, carbon dioxide/bicarbonate, for absorbed carbon.

§Materials (e.g. elemental carbon) are generally listed here where there is sufficient information to assign to a default absorption Type, but not to give specific parameter values (see Section 3 of *Publication 134*).

¶For inhaled material deposited in the respiratory tract and subsequently cleared by particle transport to the alimentary tract, the default f_A values for inhaled materials are applied: i.e. the product of f_r for the absorption Type and the f_A value for ingested soluble forms of carbon applicable to the age-group of interest (1.0).

**Default Type M is recommended for use in the absence of specific information on which the exposure material can be assigned to an absorption type, e.g. if the form is unknown, or if the form is known but there is no information available on the absorption of that form from the respiratory tract.

††Activity transferred from systemic compartments into segments of the alimentary tract is assumed to be subject to reabsorption to blood. The default absorption fraction f_A for the secreted activity is the highest value for ingestion of the radionuclide applicable to the age-group of interest (1.0).

6.1.2. Ingestion

(248) For the general public, ^{14}C in foodstuffs is the most important source of this radionuclide. The uptake of carbon from the alimentary tract is highly dependent on the form in which it is ingested and can be almost complete (for more details, see section 3 of ICRP, 2016a). *Publication 30* (ICRP, 1981) and *Publication 134* (ICRP, 2016a) recommended that, in the absence of compound-specific information, organic compounds labelled with radioactive isotopes of carbon should be assumed to be completely absorbed from the gastrointestinal tract. This recommendation is retained here for all organic compounds, including proteins, carbohydrates, fats and nucleic acids. The f_A value is taken to be 1 for all chemical forms and all ages.

6.1.3. Systemic Distribution, Retention and Excretion

6.1.3.1. Background

(249) The biokinetics of systemic carbon depends on the carbon compound taken into the body. Internally deposited ^{14}C-labelled compounds have shown residence times varying from a few hours to several months in human volunteers. The distribution of radiocarbon in the body and the fractions of ingested or inhaled activity lost by exhalation, urinary excretion, and faecal excretion also depend on the nature of the carbon compound taken into the body (*Publication* 134, ICRP, 2016a).

(250) Results of animal studies indicate that the metabolism of some ^{14}C-labelled compounds varies with age. For example, metabolic incorporation and release of ^{14}C from labelled glycine or stearic acid was more rapid in young rats than in mature rats (Medovar, 1976; Osipov, 1983). At 8-30 d following intraperitoneal injection of ^{14}C-labeled carbonate, the biological half-time of ^{14}C in bone was 12-15 d in growing rats and 30-40 d in mature rats (Schubert and Armstrong, 1949).

(251) On the other hand, some ^{14}C-labelled compounds have shown little if any variation with age in ^{14}C kinetics. For example, Leide-Svegborn et al. (1999) studied the biokinetics of ^{14}C in four adults and eight children (ages 7-14 y) undergoing ^{14}C urea breath test for Helicobacter pylori (HP) infection, and in four adult volunteers. After oral administration of ^{14}C-urea, samples of exhaled air were taken up to 180 d after administration and samples of urine were collected up to 40 d. In 16 subjects including 11 patients who were not HP positive, ~88% of the administered activity was excreted in urine over the first 3 d in both adults and children. Adults exhaled slightly more activity on average than did children over the first 20 d.

(252) In *Publication* 56 (ICRP, 1990), a generic systemic biokinetic model was applied to ^{14}C-labelled compounds for which specific biokinetic data are not available. It was assumed that inhaled or ingested ^{14}C-labelled compounds are instantly and uniformly distributed throughout all tissues of the body and removed from the body with biological half-time that increases with increasing age. The half-time for a given age was based on balance considerations. For example, the half-time for an adult was derived from the assumptions of daily carbon intake of 0.3 kg and a carbon pool of mass 16 kg in Reference Man (ICRP, 1975): $T_{1/2} = \ln 2 \times$ total body carbon / daily carbon intake = 0.693(16/0.3) ~ 40 d. Half-times of 8, 15, 19, 26, and 32 d were derived for the infant and ages 1, 5, 10, and 15 y, respectively.

6.1.3.2. Biokinetic models for systemic carbon

(253) In this publication, compound-specific biokinetic models are applied to carbon that reaches the systemic circulation as carbon monoxide, carbon dioxide, bicarbonate, or methane. A common model is applied to carbon dioxide and bicarbonate. A generic systemic model for carbon is applied to unspecified forms of carbon. For example, the generic model is used to develop dose coefficients for inhalation of particulate forms of carbon described as Type F, Type M, or Type S material.

(a) Generic model

(254) The generic model for the adult member of the public is the same as the generic model for occupational intake of carbon applied in *Publication 134* (OIR Part 2). The model is extended to pre-adults by introduction of age-specific parameter values that reflect faster turnover of body carbon in infants, children, and adolescents than in adults.

(255) The structure of the generic model and its connections to the respiratory and alimentary tract models are shown in Fig. 6.1. Age-specific transfer coefficients are listed in Table 6.3.

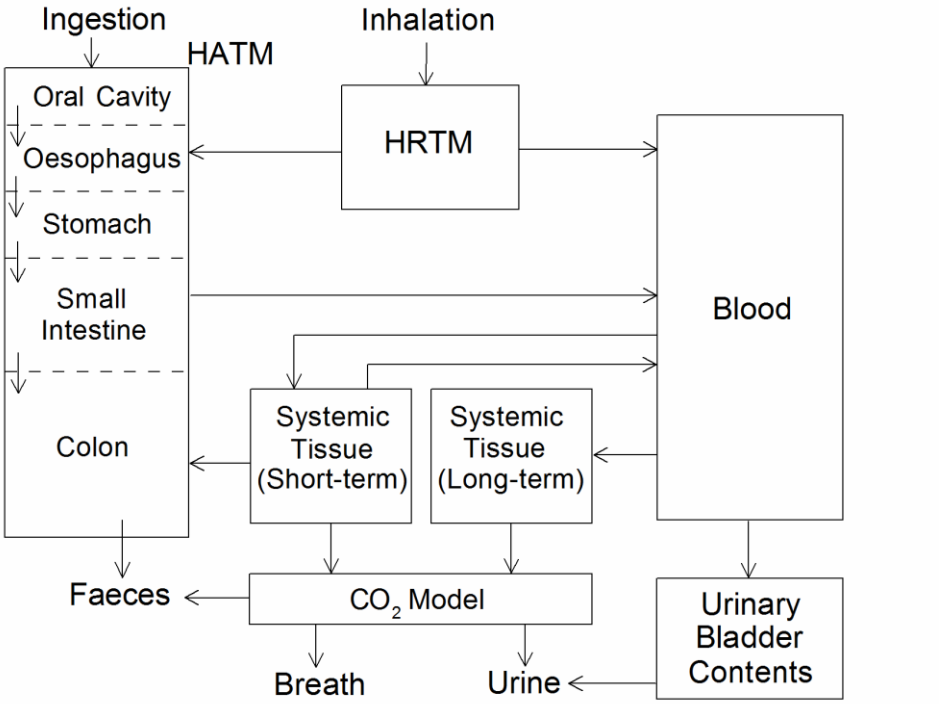

Fig. 6.1. Structure of the generic model for radiocarbon labelled substances. HRTM is the Human Respiratory Tract Model. HATM is the Human Alimentary Tract Model. Activity transferred to Colon enters Right colon contents.

Table 6.3. Transfer coefficients for the generic model for systemic carbon*

Path†	Transfer coefficient (d^{-1})					
	Infant	1 y	5 y	10 y	15 y	Adult
Blood to Short-term tissue	1.20E+00	1.20E+00	1.20E+00	1.20E+00	1.20E+00	1.20E+00
Blood to Long-term tissue	3.00E-01	3.00E-01	3.00E-01	3.00E-01	3.00E-01	3.00E-01
Blood to UB contents	1.50E+00	1.50E+00	1.50E+00	1.50E+00	1.50E+00	1.50E+00
Short-term tissue to Blood	3.70E-01	2.31E-01	2.31E-01	1.85E-01	1.11E-01	9.24E-02
Short-term tissue to CO_2 model‡	2.77E-01	1.73E-01	1.73E-01	1.39E-01	8.32E-02	6.93E-02
Short-term tissue to RC contents	6.93E-02	6.93E-02	6.93E-02	6.93E-02	6.93E-02	6.93E-02
Long-term tissue to CO_2 model‡	3.96E-02	2.48E-02	2.48E-02	1.98E-02	1.19E-02	9.90E-03

*In addition to transfer coefficients in the CO_2 model described in this section
†UB = urinary bladder, RC = right colon
‡Initially enters Blood 1 in the CO_2 model

(256) The behaviour of carbon that reaches blood is assumed to vary with age due to two factors: (1) a decrease with increasing age in the turnover rate of relatively exchangeable carbon (assumed to be the carbon contained in soft tissues and bone surface) due to a decrease in energy expenditure per unit mass of stable carbon, and (2) a decrease with increasing age in the turnover rate of carbon in bone volume due to a decreasing bone turnover rate. The distribution of carbon outflow from blood and the rate of movement of carbon from bone surface to bone volume are assumed to be independent of age.

(257) Differences with age in the rate of removal of carbon from systemic compartments other than bone volume compartments are based on age- and sex-specific reference values for energy expenditure, E_A, at age A (infant, 1 y, 5 y, 10 y, 15 y, or adult) tabulated in *Publication*

89 (ICRP, 2002a), and estimates of the stable carbon content C_A of the total body minus bone volume at age A. The mass of carbon transferred daily from soft tissues plus bone surface to blood is assumed to be proportional to energy expenditure with the proportionality constant k being independent of age. C_A is based on a formula proposed by Kyere et al. (1982), in which total-body carbon excluding that in bone mineral is estimated as $(0.77 \times F) + (3.25 \times N)$, where F is the mass of body fat and N is essentially the mass of body nitrogen excluding nitrogen in bone. Age-specific values of F and N applied here are based on Tables 2.3.1 and Table 13.2, respectively, of *Publication* 89 (ICRP, 2002a). For a given sex and pre-adult age A, the rate of removal of carbon from a soft-tissue or bone-surface compartment relative to that for an adult of the same sex is estimated as $(E_A / C_A) / (E_{adult} / C_{adult})$, and the rounded average of relative values for males and females is used to scale selected parameter values (outflow rates from certain tissues to blood) from the adult to age A. Specifically, the following multiplicative factors are used to scale transfer coefficients from soft tissues or bone surface to blood in adults to corresponding transfer coefficients for ages 100 d, 1 y, 5 y, 10 y, and 15 y, respectively: 4.0, 2.5, 2.5, 2.0, and 1.2.

(258) The rate of removal of carbon from trabecular or cortical bone volume at a given age is assumed to be the same as the rate of bone turnover for that bone type at that age. Reference age-specific trabecular and cortical bone turnover rates are taken from *Publication* 89 (ICRP, 2002a).

(b) Model for carbon monoxide

(259) The systemic model for occupational inhalation of CO applied in *Publication 134* (OIR Part 2) is assigned here to all age groups.

(c) Model for carbon dioxide and bicarbonate

(260) A common model is applied here to systemic carbon taken into the body as carbon dioxide or bicarbonate. The model structure is shown in Fig. 6.2. Age-specific parameter values are listed in Table 6.4.

(261) The model for the adult is the same as the systemic model applied in OIR Part 2 (*Publication 134*) to inhalation of carbon dioxide by a worker. The method of extension of parameter values for the adult to pre-adult ages is the same as that for the generic model for carbon described above. In fact, this model for carbon dioxide is a sub-model of the generic model described above (see box labeled 'CO_2 model' in Fig. 6.1).

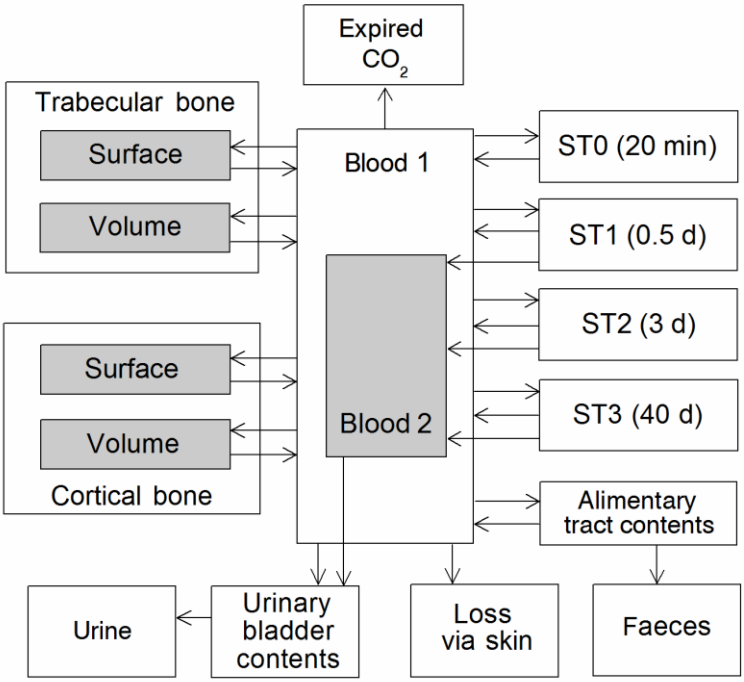

Fig. 6.2. Structure of the systemic model used in this report for carbon taken into the body as carbon dioxide or bicarbonate. Values in parentheses are removal half-times. ST0, ST1, ST2, and ST3 are soft tissue (ST) compartments.

Table 6.4. Transfer coefficients in the model for systemic carbon dioxide and bicarbonate

Path*	Transfer coefficient (d^{-1})					
	Infant	1 y	5 y	10 y	15 y	Adult
Blood 1 to environment	3.65E+01	3.65E+01	3.65E+01	3.65E+01	3.65E+01	3.65E+01
Blood 1 to ST0	6.00E+01	6.00E+01	6.00E+01	6.00E+01	6.00E+01	6.00E+01
Blood 1 to ST1	1.80E+00	1.80E+00	1.80E+00	1.80E+00	1.80E+00	1.80E+00
Blood 1 to ST2	3.00E-01	3.00E-01	3.00E-01	3.00E-01	3.00E-01	3.00E-01
Blood 1 to ST3	4.40E-01	4.40E-01	4.40E-01	4.40E-01	4.40E-01	4.40E-01
Blood 1 to Trabecular surface	9.00E-02	9.00E-02	9.00E-02	9.00E-02	9.00E-02	9.00E-02
Blood 1 to Cortical surface	6.00E-02	6.00E-02	6.00E-02	6.00E-02	6.00E-02	6.00E-02
Blood 1 to Trabecular volume	6.00E-03	6.00E-03	6.00E-03	6.00E-03	6.00E-03	6.00E-03
Blood 1 to Cortical volume	4.00E-03	4.00E-03	4.00E-03	4.00E-03	4.00E-03	4.00E-03
Blood 1 UB contents	6.50E-01	6.50E-01	6.50E-01	6.50E-01	6.50E-01	6.50E-01
Blood 1 to RC contents	1.50E-01	1.50E-01	1.50E-01	1.50E-01	1.50E-01	1.50E-01
ST0 to Blood 1	2.00E+02	1.25E+02	1.25E+02	9.98E+01	5.99E+01	4.99E+01
ST1 to Blood 1	5.32E+00	3.33E+00	3.33E+00	2.66E+00	1.60E+00	1.33E+00
ST2 to Blood 1	8.87E-01	5.55E-01	5.55E-01	4.44E-01	2.66E-01	2.22E-01
ST3to Blood 1	6.66E-02	4.16E-02	4.16E-02	3.33E-02	2.00E-02	1.66E-02
ST1 to Blood 2	2.22E-01	1.39E-01	1.39E-01	1.11E-01	6.65E-02	5.55E-02
ST2 to Blood 2	3.70E-02	2.31E-02	2.31E-02	1.85E-02	1.11E-02	9.24E-03
ST3 to Blood 2	2.77E-03	1.73E-03	1.73E-03	1.39E-03	8.32E-04	6.93E-04
Trabecular surface to Blood 1	6.93E-02	4.33E-02	4.33E-02	3.47E-02	2.08E-02	1.73E-02
Cortical surface to Blood 1	6.93E-02	4.33E-02	4.33E-02	3.47E-02	2.08E-02	1.73E-02
Trabecular volume to Blood 1	8.22E-03	2.88E-03	1.81E-03	1.32E-03	9.59E-04	4.93E-04

Cortical volume to Blood 1	8.22E-03	2.88E-03	1.53E-03	9.04E-04	5.21E-04	8.21E-05
Blood 2 to UB contents	1.00E+03	1.00E+03	1.00E+03	1.00E+03	1.00E+03	1.00E+03

[*]UB = urinary bladder, RC = right colon

(d) Model for methane

(262) The age-specific biokinetic model for systemic carbon inhaled as methane extends the model for occupational intake of methane applied in *Publication 134* (OIR Part 2) to pre-adult ages. The generic model structure for carbon (Fig. 6.1 and Fig. 6.2) is modified by the addition of a blood compartment that receives methane absorbed from the respiratory tract. For all age groups it is assumed that carbon leaves this blood compartment with a half-time of 10 min, with 70% removed in expired air and 30% depositing in the short-term soft-tissue compartment shown in Fig. 6.1. Outflow rates from all blood compartments are assumed to be independent of age. Other transfer coefficients in the model are taken from the age-specific generic model for systemic carbon defined in Table 6.3. Transfer coefficients for the generic model for systemic carbon[*]Table 6.3 and Table 6.4.

6.2. Dosimetric data for carbon

Table 6.5. Committed effective dose coefficients (Sv Bq^{-1}) for the inhalation or ingestion of ^{14}C compounds.

	Effective dose coefficients (Sv Bq^{-1})					
Inhaled gases or vapours	3 mo	1 y	5 y	10 y	15 y	Adult
Carbon monoxide (CO)	1.9E-11	1.2E-11	5.8E-12	3.5E-12	2.1E-12	1.8E-12
Carbon dioxide (CO_2)	4.6E-11	4.6E-11	2.1E-11	1.4E-11	1.5E-11	1.3E-11
Methane (CH_4)	4.6E-13	3.1E-13	1.6E-13	9.8E-14	5.9E-14	5.1E-14
Unspecified	5.4E-10	5.0E-10	2.6E-10	1.9E-10	1.7E-10	1.7E-10
Inhaled particulate materials (1 µm AMAD aerosols)						
Type F, Barium carbonate (CO_2 model)	4.2E-11	3.8E-11	1.6E-11	1.0E-11	8.9E-12	8.0E-12
Type F	2.8E-10	2.6E-10	1.2E-10	8.4E-11	6.7E-11	7.0E-11
Type M, All unspecified forms	4.0E-09	3.5E-09	2.0E-09	1.3E-09	1.0E-09	9.7E-10
Type S, Elemental carbon, carbon tritide	2.5E-08	2.4E-08	1.8E-08	1.3E-08	1.3E-08	1.3E-08
Ingested materials						
Adult f_A = 1.0, All chemical forms	5.1E-10	4.7E-10	2.5E-10	1.8E-10	1.6E-10	1.6E-10
Adult f_A = 1.0, Bicarbonate	4.8E-11	4.8E-11	2.3E-11	1.5E-11	1.5E-11	1.3E-11

7. PHOSPHORUS (Z = 15)

7.1. Routes of Intake

7.1.1. Inhalation

(263) Information on absorption from the respiratory tract is available from a few experimental studies on the behaviour of inhaled phosphorus. However, most of it relates to phosphates for which the cation, rather than the phosphorus itself, was radiolabelled. For details see Section 4 of *Publication 134* (ICRP, 2016a). Absorption parameter values and types, and associated f_A values for particulate forms of phosphorus are given in Table 7.1 (taken from Section 4 of *Publication 134*).

Table 7.1. Absorption parameter values for inhaled and ingested phosphorus

		Absorption parameter values*		
Inhaled particulate materials		f_r	s_r (d^{-1})	s_s (d^{-1})
Default parameter values†,‡				
Absorption Type	Assigned forms			
F	Sodium phosphate	1	1	–
M§	Yttrium, stannic and zinc phosphates	0.2	1	0.005
S	–	0.01	1	1×10^{-4}

Ingested materials¶	Age-dependent absorption from the alimentary tract, f_A					
Assigned forms	3 months	1 year	5 years	10 years	15 years	adult
All forms	1	0.9	0.9	0.9	0.9	0.8

*It is assumed that for phosphorus the bound state can be neglected i.e. $f_b = 0$. The values of s_r for Type F, M and S forms of phosphorus (1 d^{-1}) are element-specific.

†Materials (e.g. sodium phosphate) are listed here where there is sufficient information to assign to a default absorption type, but not to give specific parameter values (see Section 4 of Publication 134, ICRP, 2016a).

‡For inhaled material deposited in the respiratory tract and subsequently cleared by particle transport to the alimentary tract, the default f_A values for inhaled materials are applied: i.e. the product of f_r for the absorption Type and the f_A value for ingested soluble forms of phosphorus applicable to the age-group of interest (*e.g.* 0.8 for adults).

§Default Type M is recommended for use in the absence of specific information on which the exposure material can be assigned to an absorption type, e.g. if the form is unknown, or if the form is known but there is no information available on the absorption of that form from the respiratory tract.

¶Activity transferred from systemic compartments into segments of the alimentary tract is assumed to be subject to reabsorption to blood. The default absorption fraction f_A for the secreted activity is the highest f_A value for ingestion of the radionuclide applicable to the age-group of interest (*e.g.* 0.8 for adults).

7.1.2. Ingestion

7.1.2.1. Adults

(264) Dietary phosphorus in the form of inorganic phosphate and phosphorus-containing biomolecules such as nucleic acids and phospholipids is well absorbed from the small intestine. High calcium diets may precipitate calcium phosphate and reduce the availability of phosphate; however, vitamin D, sodium phytate and fat counteract this tendency (For details see

Publication 100, ICRP, 2006, and Section 4 of Publication 134, 2016a). In *Publication 30* (ICRP, 1979) and in the *OIR Series* (ICRP, 2016a) the recommended absorption fraction was 0.8 for all compounds of the element. This value is used here; that is, $f_A = 0.8$ for all compounds.

7.1.2.2. Children

(265) The Food and Nutrition Board of the US Institute of Medicine reports somewhat higher absorption values in infants and children than in adults (Institute of Medicine, 1997). A value of $f_A = 0.9$ is used here for 1-, 5-, 10- and 15-y-old children. For 3-month-old infants, an f_A of 1 is adopted here.

7.1.3. Systemic Distribution, Retention and Excretion

7.1.3.1. Age-specific data

(266) The behavior of phosphorus in bone closely resembles that of calcium. Rapid uptake of both elements occurs on all bone surfaces. Calcium and phosphorus diffuse throughout bone volume within a few hours to days after uptake to blood. Both elements can penetrate into the interior of bone crystal. The exchangeable and non-exchangeable fractions of the total bone mineral are approximately the same for phosphorus and calcium (Neuman and Neuman, 1958; Parfitt and Kleerekoper, 1980).

(267) Uptake of calcium or phosphorus is much greater in forming or growing bone than in mature bone. Phosphorus and calcium show high concentration in forming osteons (Parfitt and Kleerekoper, 1980). In rats injected intraperitoneally with ^{32}P, skeletal uptake decreased with increasing age at injection, from about 90% of the injected amount at age 15 d to about 17% at age 170 d (Bonner, 1948).

(268) Stather (1974) compared the distribution and retention of ^{32}P and the alkaline earths ^{45}Ca, ^{85}Sr, and ^{133}Ba in the mouse skeleton. At 24 h after intraperitoneal injection into 8-week-old mice the distribution of the four radionuclides was virtually the same throughout the skeleton, but skeletal content as a percentage of injected activity differed from one radionuclide to another: ^{32}P, 21.6%; ^{45}Ca, 61.5%; ^{85}Sr, 37.3%; and ^{133}Ba, 48.8%. The skeletal burden represented about 37% of total-body ^{32}P compared with about 90% of total-body ^{85}Sr.

(269) Bauer and Carlsson (1955) compared the uptake of ^{32}P and ^{45}Ca by bone (tibial shaft) and incisors in adult rats over the first 5 d after simultaneous subcutaneous injection of these radionuclides. The percentage of the administered ^{45}Ca found in bone was consistently about 2.3 times the percentage of administered ^{32}P in the same bone samples at corresponding times after administration. The ratio of uptake of ^{45}Ca and ^{32}P was about the same for incisors as for bone.

7.1.3.2. Systemic model

(270) The structure of the age-specific biokinetic model for systemic phosphorus and the transfer coefficients for the adult member of the public are the same as in the model for phosphorus for the worker, adopted in *Publication 134* (ICRP, 2016a). The model structure is shown in Fig. 7.1. Transfer coefficients for all six ages at intake are listed in Table 7.2.

(271) The extension of transfer coefficients for phosphorus from mature adults to pre-adult ages is based on the age-specific data summarized above together with analogy with the age-specific model for calcium applied in this report and in *Publication 71* (ICRP, 1995b).

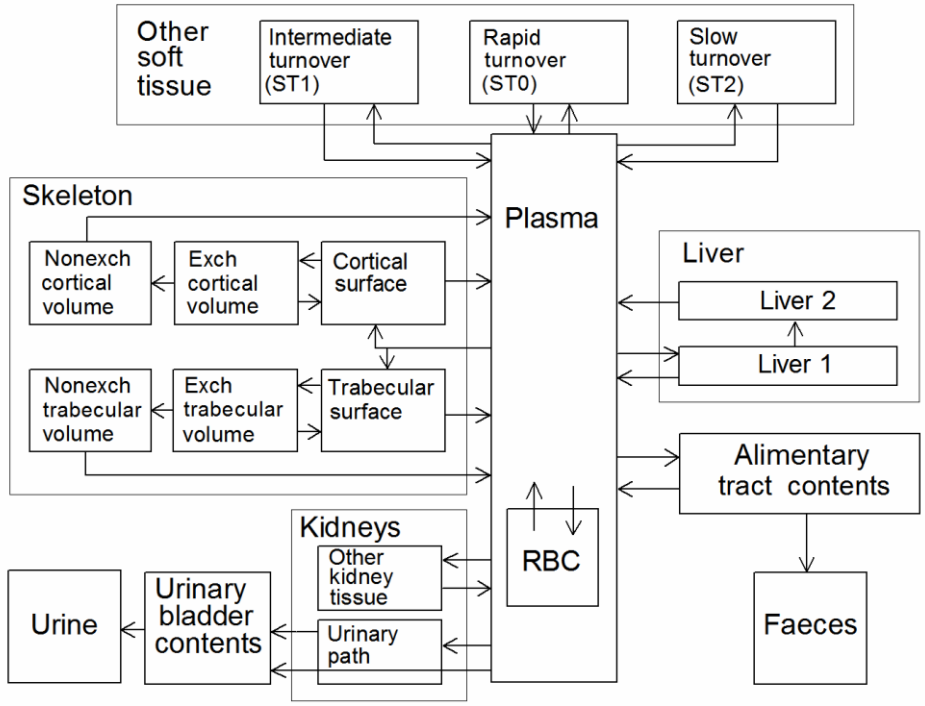

Fig. 7.1. Structure of the model for systemic phosphorus. Activity transferred from Plasma to Alimentary tract contents enters Right colon contents. Activity transferred from Alimentary tract contents to Plasma represents activity absorbed from Small intestine contents to Plasma. Abbreviations: exch = exchangeable, nonexch = non-exchangeable, RBC = red blood cells.

(272) Deposition fractions for phosphorus on trabecular and cortical bone surfaces at a given age are assumed to be 0.8 times corresponding values for calcium. Transfer coefficients describing the translocation of calcium in the skeleton and removal from skeletal compartments to blood are applied without change to phosphorus. Based on these assumptions the percentage of administered radiocalcium in bone will be roughly 2.3 times the percentage of administered radiophosphorus beyond a few days post administration due to faster excretion and hence lower recycling of phosphorus than calcium.

2791 Table 7.2. Age-specific transfer coefficients for phosphorus

Path[a]	Transfer coefficient (d^{-1})					
	Infant	1 y	5 y	10 y	15 y	Adult
Plasma to UB-contents	2.20E+00	3.52E+00	3.74E+00	3.04E+00	2.24E+00	4.40E+00
Plasma to RC-contents	1.00E-01	1.60E-01	1.70E-01	1.38E-01	1.02E-01	2.00E-01
Plasma to Trab. surface	4.80E+00	2.88E+00	2.84E+00	4.52E+00	6.61E+00	4.44E+00
Plasma to Cort. surface	1.92E+01	1.15E+01	9.96E+00	1.34E+01	1.71E+01	3.56E+00
Plasma to ST0	5.09E+00	8.14E+00	8.65E+00	7.02E+00	5.19E+00	1.02E+01
Plasma to ST1	5.09E+00	8.14E+00	8.65E+00	7.02E+00	5.19E+00	1.02E+01
Plasma to ST2	5.00E-02	8.00E-02	8.50E-02	6.90E-02	5.10E-02	1.00E-01
Plasma to RBC	1.20E+00	1.92E+00	2.04E+00	1.66E+00	1.22E+00	2.40E+00
Plasma to Urinary path	2.00E-01	3.20E-01	3.40E-01	2.76E-01	2.04E-01	4.00E-01
Plasma to Other kidney tissue	7.00E-02	1.12E-01	1.19E-01	9.66E-02	7.14E-02	1.40E-01
Plasma to Liver 1	2.00E+00	3.20E+00	3.40E+00	2.76E+00	2.04E+00	4.00E+00
RBC to Plasma	6.93E-01	6.93E-01	6.93E-01	6.93E-01	6.93E-01	6.93E-01
ST0 to Plasma	3.47E-01	3.47E-01	3.47E-01	3.47E-01	3.47E-01	3.47E-01
ST1 to Plasma	3.47E-02	3.47E-02	3.47E-02	3.47E-02	3.47E-02	3.47E-02
ST2 to Plasma	3.80E-04	3.80E-04	3.80E-04	3.80E-04	3.80E-04	3.80E-04
Urinary path to UB-contents	6.93E-01	6.93E-01	6.93E-01	6.93E-01	6.93E-01	6.93E-01
Other kidney tissue to Plasma	3.47E-02	3.47E-02	3.47E-02	3.47E-02	3.47E-02	3.47E-02
Liver 1 to Liver 2	3.47E-01	3.47E-01	3.47E-01	3.47E-01	3.47E-01	3.47E-01
Liver 1 to Plasma	1.04E+00	1.04E+00	1.04E+00	1.04E+00	1.04E+00	1.04E+00
Liver 2 to Plasma	3.47E-02	3.47E-02	3.47E-02	3.47E-02	3.47E-02	3.47E-02
Cort. surface to Plasma	5.78E-01	5.78E-01	5.78E-01	5.78E-01	5.78E-01	5.78E-01
Cort. surface to Exch. Cort. volume	1.16E-01	1.16E-01	1.16E-01	1.16E-01	1.16E-01	1.16E-01
Trab. surface to Plasma	5.78E-01	5.78E-01	5.78E-01	5.78E-01	5.78E-01	5.780E-01
Trab. surface to Exch. Trab. volume	1.16E-01	1.16E-01	1.16E-01	1.16E-01	1.16E-01	1.160E-01
Exch. Cort. volume to Cort. surface	2.77E-03	2.77E-03	2.77E-03	2.77E-03	2.77E-03	2.77E-03
Exch. to Nonexch. Cort. volume	4.16E-03	4.16E-03	4.16E-03	4.16E-03	4.16E-03	4.16E-03
Exch. Trab. volume to Trab. surface	2.77E-03	2.77E-03	2.77E-03	2.77E-03	2.77E-03	2.77E-03
Exch. to Nonexch. Trab. volume	4.16E-03	4.16E-03	4.16E-03	4.16E-03	4.16E-03	4.16E-03
Nonexch. Cort. volume to Plasma	8.22E-03	2.88E-03	1.53E-03	9.04E-04	5.21E-04	8.21E-05
Nonexch. Trab. volume to Plasma	8.22E-03	2.88E-03	1.81E-03	1.32E-03	9.59E-04	4.93E-04

2792
2793 Abbreviations: UB = urinary bladder, RBC = red blood cells, Trab = trabecular, Cort = cortical, Exch =
2794 exchangeable, Non-exch = non-exchangeable, RC = Right colon

7.2. Dosimetric data for phosphorus

Table 7.3. Committed effective dose coefficients (Sv Bq^{-1}) for the inhalation or ingestion of ^{32}P compounds.

	Effective dose coefficients (Sv Bq^{-1})					
Inhaled particulate materials (1 µm AMAD aerosols)	3 mo	1 y	5 y	10 y	15 y	Adult
Type F, Sodium phosphate	1.3E-08	7.3E-09	3.1E-09	1.9E-09	1.4E-09	9.2E-10
Type M, Yttrium, stannic and zinc phosphates; all unspecified forms	1.1E-08	8.4E-09	4.5E-09	3.0E-09	2.3E-09	2.1E-09
Type S	1.1E-08	9.2E-09	5.1E-09	3.5E-09	2.6E-09	2.5E-09
Ingested materials						
Adult f_A = 0.8, All forms	2.4E-08	1.3E-08	6.2E-09	3.5E-09	2.9E-09	1.7E-09

8. SULPHUR (Z = 16)

8.1. Routes of Intake

8.1.1. Inhalation

(273) Some information on absorption from the respiratory tract is available for inhaled gases of sulphur in man and in experimental animals. Most of the information available on inhaled particulate forms of sulphur relates to sulphates. For details see Section 5 of *Publication 134* (ICRP, 2016a).

(274) Absorption parameter values and types, and associated f_A values for gas and vapour forms of sulphur are given in Table 8.1 and for particulate forms in Table 8.2,(taken from Section 5 of of *Publication 134*).

(275) Exposures to both gas/vapour forms and particulate forms of sulphur are common, and it is therefore recommended in this series of documents that in the absence of site-specific information 50% particulate; 50% gas/vapour should be assumed.

Table 8.1. Deposition and absorption for gas and vapour forms of sulphur*

	Percentage deposited†						Absorption		
Chemical form/origin	Total	ET_1	ET_2	BB	bb	AI	Type	f_A¶	Systemic model‡
Sulphur dioxide	100§	0	20	10	20	50	F	1.0	Inorganic
Carbon disulphide	100§	0	20	10	20	50	F	1.0	Inorganic
Hydrogen sulphide	100§	0	20	10	20	50	F	1.0	Inorganic
Carbonyl sulphide	100§	0	20	10	20	50	F	1.0	Inorganic
Other organic	100§	0	20	10	20	50	F	1.0	Organic
Unspecified*	100§	0	20	10	20	50	F	1.0	Inorganic

ET_1, anterior nasal passage; ET_2, posterior nasal passage, pharynx and larynx; BB, bronchial; bb, bronchiolar; AI, alveolar-interstitial.

*For sulphur in unspecified gas or vapour form, the default option for gases and vapours is recommended: 100% total deposition in the respiratory tract; default distribution between regions§ and Type F absorption. It is assumed that for sulphur the bound state can be neglected i.e. $f_b = 0$.

†*Percentage deposited* refers to how much of the material in the inhaled air remains in the body after exhalation. Almost all inhaled gas molecules contact airway surfaces, but usually return to the air unless they dissolve in, or react with, the surface lining. For the forms of sulphur considered here, it is assumed that most, if not all, of the inhaled sulphur is absorbed into body fluids.

‡Systemic models for inorganic sulphur and organic sulphur, Section 8.13.

§Default distribution between regions (20% ET_2, 10% BB, 20% bb and 50% AI).

¶The value of $f_A = 1$ is applicable to all age-groups.

Table 8.2. Absorption parameter values for inhaled particulate forms of sulphur and for ingested sulphur

Inhaled particulate materials*		Absorption parameter values† f_r	s_r (d^{-1})	s_s (d^{-1})
Default parameter values‡,§				
Absorption Type	Assigned forms			
F	Caesium, nickel, strontium, thorium sulphates¶	1	30	-
M**	Barium sulphate	0.2	3	0.005
S	—	0.01	3	0.0001

Ingested materials††	Age-dependent absorption from the alimentary tract, f_A					
Assigned forms	3 months	1 year	5 years	10 years	15 years	adult
Organic sulphur in food and all soluble forms	1	1	1	1	1	1
Most forms of inorganic sulphur	1	1	1	1	1	1
Specific inorganic sulphur: Elemental sulphur and thiosulphate	0.2	0.1	0.1	0.1	0.1	0.1

*Following uptake into body fluids, the systemic model for inorganic sulphur is used, (see Section 8.1.3.1)

†It is assumed that for sulphur the bound state can be neglected i.e. $f_b = 0$. The values of s_r for Type F, M and S forms of sulphur (30, 3 and 3 d^{-1}, respectively) are the general default values.

‡Materials (e.g. caesium sulphate) are generally listed here where there is sufficient information to assign to a default absorption type, but not to give specific parameter values (see Section 5 of Publication 134, ICRP, 2016a).

§For inhaled material deposited in the respiratory tract and subsequently cleared by particle transport to the alimentary tract, the default f_A values for inhaled materials are applied: i.e. the product of f_r for the absorption type and the f_A value for ingested soluble forms of sulphur applicable to the age-group of interest (1.0).

¶In the case of thorium sulphate the thorium is assigned to Type M and the sulphur to Type F.

**Default Type M is recommended for use in the absence of specific information on which the exposure material can be assigned to an absorption type, e.g. if the form is unknown, or if the form is known but there is no information available on the absorption of that form from the respiratory tract.

††Activity transferred from systemic compartments into segments of the alimentary tract is assumed to be subject to reabsorption to blood. The default absorption fraction f_A for the secreted activity is the highest f_A value for ingestion of the radionuclide applicable to the age-group of interest (1.0).

8.1.2. Ingestion

8.1.2.1. Adults

(276) Elemental sulphur and thiosulphate were found to be little absorbed after oral administration. Some other inorganic forms of sulphur were shown to be completely absorbed. Volwiler et al. (1955) reported that the fractional absorption of sulphur in adult men was greater than 0.6 for organic compounds. Minski and Vennart (1971) measured absorption in rats and obtained a mean value for the absorption fraction of ^{35}S 1-methionine of 0.92 ± 0.18 (± 1 SD). Because there appears to be almost complete absorption of ^{35}S ingested as amino acids or other organic compounds, almost complete absorption of ^{35}S incorporated in foodstuffs is expected to occur. ICRP *Publication 30* (ICRP, 1980) recommended absorption fractions of 0.8 for inorganic forms of sulphur and 0.1 for elemental sulphur. In *Publication 134* (ICRP, 2016a), the recommended f_A values were 1 for unspecified inorganic and organic compounds,

and 0.1 for elemental sulphur and thiosulphate. For sulphur present in the diet, an absorption fraction of 1 was adopted by *Publication 67* (ICRP, 1993). The same value of $f_A = 1$ is adopted here. For ingestion of elemental sulphur and thiosulphate a lower $f_A = 0.1$ is adopted.

8.1.2.2. Children

(277) There are few data available on the absorption of sulphur in infants and children. Shohl and Sato (1923) showed that an 8-month-old baby lost about 3% of its dietary sulphur intake in faeces, which indicates absorption of at least 97%. This value is consistent with available data for adults. However, Wright et al. (1960) reported sulphur balance studies which indicated that 68-90% of dietary sulphur was absorbed by pre-adolescent girls, apparently depending on dietary nitrogen levels. An f_A value of 1 is adopted here for infants and children for sulphur ingested in food and in soluble forms. An f_A value of 0.2 is adopted for ingestion of elemental sulphur and thiosulphate by 3 month old infants.

8.1.3. Systemic Distribution, Retention and Excretion

(278) By 15 min post intraperitoneal administration of ^{35}S as sodium sulfate to 7-day-old rats, radiographs revealed the highest activity concentration in cartilage at the epiphyseal-diaphyseal junction of long bones and lower concentrations throughout the epiphysis (Dziewiatkowski, 1952). The pattern of deposition did not change over the first 24 h, and the concentration in cartilage continued to increase during that time. The activity in articular cartilage appeared to decrease by roughly one-third from 1 to 4 days after injection.

(279) Dziewiatkowski (1954) administered ^{35}S-labeled sodium sulfate to 10-, 30-, and 300-day-old rats by intraperitoneal injection and determined activity in fluids and tissues at 12, 24, 48, and 96 h. Over the first 24 hours about 51% and 64% of the administered activity was excreted by 30- and 300-day-old rats, respectively. At 1 d the concentration of ^{35}S in ends of femurs of 10-day-old rats was about 10 times that in 30-day-old rats and 25 times that in 300-day-old rats. Measurements of activity in femurs and humeri indicated that activity had been incorporated mainly into chondroitin sulfate of growing cartilage.

(280) McElligott and Collins (1960) studied the *in vitro* uptake of ^{35}S-labeled sulphate in samples of human articular and costal cartilage from human subjects. The samples were collected at 44 necropsies on subjects ranging in age from 5 d to 83 y and by biopsy from subjects of age 23-68 y. Samples generally were collected during the first day or two after death. A total of 54 costal cartilages and 32 articular cartilages were examined. Uptake of activity by costal cartilage was high in infants a few days old, somewhat lower in older children, and much lower in adult and elderly subjects, apparently due to increased cellularity and more active individual cells in young cartilage. In articular cartilage, however, uptake was substantially greater in adults than in two pre-adult subjects.

8.1.3.1. Systemic model for inorganic sulphur

(281) The systemic model for inorganic sulphur applied in Publication 134 (OIR Part 2, ICRP, 2016a) to workers is applied here to adult members of the public. The structure of the model for sulphur entering the systemic circulation in inorganic form is shown in Fig. 8.1. Parameter values are given in Table 8.3.

(282) The systemic behaviour of sulphur is assumed to be independent of age except for a higher uptake by cartilage in pre-adults than in adults, considering the importance of cartilage as a repository for inorganic sulphur and the relatively large mass of cartilage in pre-adults compared to total-body mass. The age-specific transfer coefficient of sulphur from blood to

cartilage is scaled from the adult value based on relative reference masses of cartilage as a fraction of total body mass at different ages (ICRP, 2002a). This yields rounded scaling factors of 3.0, 2.4, 2.1, 1.7, and 1.3 for infants and ages 1, 5, 10, and 15 y, respectively. The value 1.3 for age 15 y is an average of different values derived for males and females. The scaling factor for the infant is rounded upward from the derived value of ~2.5 in view of the relatively high cellularity and sulphur concentration of cartilage early in life (ICRP, 1995d).

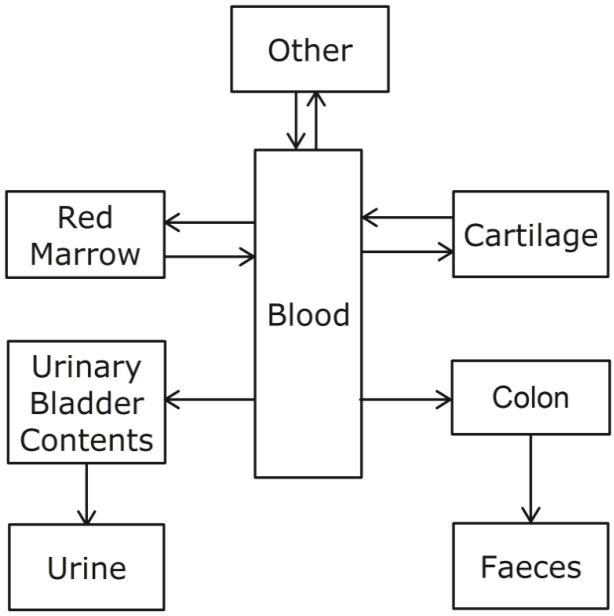

Fig. 8.1. Structure of the systemic model for inorganic sulphur. Activity transferred from Blood to Colon enters the Right colon contents.

Table 8.3. Transfer coefficients for the systemic model for inorganic sulphur

Path[a]	Transfer coefficient (d^{-1})					
	Infant	1 y	5 y	10 y	15 y	Adult
Blood to Red marrow	7.50E-02	7.50E-02	7.50E-02	7.50E-02	7.50E-02	7.50E-02
Blood to Cartilage	7.50E-01	6.00E-01	5.25E-01	4.25E-01	3.25E-01	2.50E-01
Blood to Other	1.75E-01	1.75E-01	1.75E-01	1.75E-01	1.75E-01	1.75E-01
Blood to Urinary bladder contents	1.80E+00	1.80E+00	1.80E+00	1.80E+00	1.80E+00	1.80E+00
Blood to Right colon contents	2.00E-01	2.00E-01	2.00E-01	2.00E-01	2.00E-01	2.00E-01
Red marrow to Blood	3.00E-01	3.00E-01	3.00E-01	3.00E-01	3.00E-01	3.00E-01
Cartilage to Blood	1.00E-01	1.00E-01	1.00E-01	1.00E-01	1.00E-01	1.00E-01
Other to Blood	3.50E+00	3.50E+00	3.50E+00	3.50E+00	3.50E+00	3.50E+00

8.1.3.2. Systemic model for organic sulphur

(283) The systemic model for organic sulphur applied in *Publication 134* (OIR Part 2) to workers is applied here to adult members of the public. Parameters for the adult are applied to all age groups.

(284) The model structure is shown in Fig. 8.2. Parameter values are listed in Table 8.4.

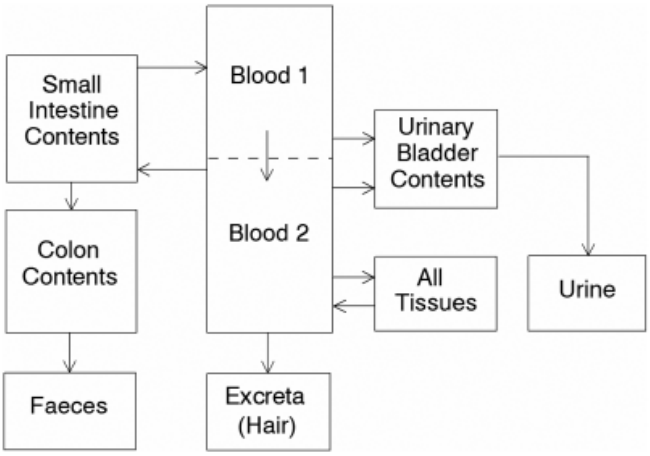

Fig. 8.2. Structure of the systemic model for organic sulphur.

Table 8.4. Transfer coefficients for the systemic model for organic sulphur

Path*	Transfer coefficient (d^{-1})					
	Infant	1 y	5 y	10 y	15 y	Adult
Blood 1 to Blood 2	8.30E+00	8.30E+00	8.30E+00	8.30E+00	8.30E+00	8.30E+00
Blood 1 to UB contents	4.00E+00	4.00E+00	4.00E+00	4.00E+00	4.00E+00	4.00E+00
Blood 2 to UB contents	1.10E-03	1.10E-03	1.10E-03	1.10E-03	1.10E-03	1.10E-03
Blood 2 to Excreta	9.00E-04	9.00E-04	9.00E-04	9.00E-04	9.00E-04	9.00E-04
Blood 2 to SI contents	2.00E-04	2.00E-04	2.00E-04	2.00E-04	2.00E-04	2.00E-04
Blood 2 to All tissues	1.70E-02	1.70E-02	1.70E-02	1.70E-02	1.70E-02	1.70E-02
All tissues to Blood 2	4.20E-03	4.20E-03	4.20E-03	4.20E-03	4.20E-03	4.20E-03

*UB = Urinary bladder, SI = Small intestine

8.2. Dosimetric data for sulphur

Table 8.5. Committed effective dose coefficients (Sv Bq^{-1}) for the inhalation or ingestion of ^{35}S compounds.

	Effective dose coefficients (Sv Bq^{-1})					
Inhaled gases or vapours	3 mo	1 y	5 y	10 y	15 y	Adult
Sulphur dioxide, carbon disulphide, hydrogen sulphide, carbonyl sulphide and other unspecified inorganic gases and vapours	2.9E-10	2.1E-10	1.1E-10	7.0E-11	4.9E-11	5.5E-11
Other organic	9.6E-09	7.1E-09	3.7E-09	2.2E-09	1.3E-09	1.2E-09
Inhaled particulate materials (1 µm AMAD aerosols)						
Type F, Caesium, nickel, strontium and thorium sulphates	1.2E-10	8.6E-11	3.6E-11	2.2E-11	1.4E-11	1.6E-11
Type M, Barium sulphates; all unspecified forms	2.3E-09	1.9E-09	1.1E-09	7.0E-10	5.6E-10	5.2E-10
Type S	3.6E-09	3.1E-09	1.8E-09	1.2E-09	9.1E-10	8.5E-10
Ingested materials						
Adult f_A = 1.0, Sulphur in food and all soluble forms	1.9E-10	1.3E-10	5.8E-11	3.3E-11	2.0E-11	2.7E-11
Adult f_A = 0.1, Elemental sulphur and thiosulphate	4.1E-11	1.5E-11	7.5E-12	4.6E-12	2.9E-12	3.1E-12

9. CALCIUM (Z = 20)

9.1. Routes of Intake

9.1.1. Inhalation

(285) No information was found on the behaviour of inhaled calcium in man. Information on absorption from the respiratory tract is available from experimental studies of calcium chloride. For details see Section 6 of *Publication 134* (ICRP, 2016a). Absorption parameter values and types, and associated f_A values for particulate forms of calcium are given in Table 9.1(taken from Section 6 of *Publication 134)*.

Table 9.1. Absorption parameter values for inhaled and ingested calcium

Inhaled particulate materials		Absorption parameter values* f_r	s_r (d^{-1})	s_s (d^{-1})
Default parameter values†,‡				
Absorption Type	Assigned forms			
F	Chloride	1	70	–
M§		0.2	3	0.005
S	–	0.01	3	1×10^{-4}

Ingested materials¶	Age-dependent absorption from the alimentary tract, f_A					
Assigned forms	3 months	1 year	5 years	10 years	15 years	adult
All forms	0.6	0.5	0.5	0.5	0.5	0.4

*It is assumed that for calcium the bound state can be neglected i.e. $f_b = 0$. The value of s_r for Type F forms of calcium (70 d^{-1}) is element-specific. The values for Types M and S (3 d^{-1}) are the general default values.

†Materials (e.g. chloride) are generally listed here where there is sufficient information to assign to a default absorption Type, but not to give specific parameter values (see see Section 6 of *Publication 134* (ICRP, 2016a) .

‡For inhaled material deposited in the respiratory tract and subsequently cleared by particle transport to the alimentary tract, the default f_A values for inhaled materials are applied: i.e. the product of f_r for the absorption type and the f_A value for ingested soluble forms of calcium applicable to the age-group of interest (*e.g.* 0.4 for adults).

§Default Type M is recommended for use in the absence of specific information on which the exposure material can be assigned to an absorption type, e.g. if the form is unknown, or if the form is known but there is no information available on the absorption of that form from the respiratory tract.

¶Activity transferred from systemic compartments into segments of the alimentary tract is assumed to be subject to reabsorption to blood. The default absorption fraction f_A for the secreted activity is the highest value for ingestion of the radionuclide applicable to the age-group of interest (e.g. 0.4 for adults).

9.1.2. Ingestion

9.1.2.1. Adults

(286) Calcium is an essential element and physiological mechanisms facilitate its intestinal absorption. It has been measured in numerous volunteer studies and in most cases fractional absorption was in the range 0.2 to 0.5, with some reported higher values and a large inter-individual variation among healthy subjects. Calcium absorption is influenced by the

intraluminal concentration of ionized calcium and by morphological (positive correlation with body size) and nutritional factors. Fractional calcium absorption is increased by high intakes of vitamin D, by a high protein or carbohydrate diet, by calcium deficiency or low calcium intake and by pregnancy or lactation. On the other hand, old age, sprue diseases, caffeine intake, oral supplementation with magnesium, or ingestion of calcium binding agents such as EDTA or citrate ions decreases calcium absorption in humans. Calcium absorption occurs mainly from the small intestine. However, a few percent of calcium may also be absorbed from other sites, such as the colon. In *Publications 30* (ICRP, 1980) and *71* (ICRP, 1995b), an absorption fraction of 0.3 was recommended. An f_A value of 0.4 for all chemical forms was recommended in *Publication 134* (ICRP, 2016a). The same value $f_A = 0.4$ is adopted here for adults.

9.1.2.2. Children

(287) The developing rat has been used in a number of investigations of the ontogeny of calcium absorption after ingestion of simple salts (Ghishan et al., 1980; Halloran and DeLuca, 1980; Pansu et al., 1983; Taylor et al., 1962). In general, these studies demonstrated that during the suckling period, ionic calcium is absorbed via a passive, non-vitamin-D-dependent process (Ghishan et al., 1980; Pansu et al., 1983) that contrasts with the adult mode of absorption which involves an active vitamin-dependent process (Dostal and Toverud, 1984). Blake and Henning (1988) studied calcium absorption in 14- and 28-day-old rats and compared absorption of ^{45}Ca in milk and $^{45}CaCl_2$. They showed that for suckling rats (14 days old), transport and absorption of ^{45}Ca from milk was slower during the first 3 h after introduction into the stomach than that observed for ^{45}Ca administered as the chloride. By 6 h after intubation, absorption was similar in both cases and was 90% of the ingested activity. Overall efficiency of ^{45}Ca absorption from $^{45}CaCl_2$ was significantly less in adult rats. It was postulated that in neonates, ^{45}Ca from $CaCl_2$ traverses the intestinal wall as ionic calcium and enters the mucosa passively, perhaps via simple diffusion due to increased permeability of the brush border membranes (Dostal and Toverud, 1984). In contrast, ^{45}Ca in milk entering the small intestine remains associated with milk protein. There are a number of reports of measurements of calcium absorption in infants and children, using stable isotope techniques. Hillman et al. (1988) obtained a mean absorption fraction of 0.5 for seven infants, about 2 weeks of age, with a range of 0.4-0.6. Values of up to 0.8 have been measured for premature infants (Ehrenkranz et al., 1985; Liu et al., 1989). For six children ranging in age from 11 to 17 y, mean absorption was estimated as 0.4 with a range of 0.3-0.5 (Miller et al., 1989). *Publication 71* used values of absorption fraction of 0.6 for 3-mo-old infants and 0.4 for l-, 5-, 10- and 15-y-old children. The value $f_A = 0.6$ is retained here for 3-mo-old infants while a value $f_A = 0.5$ is adopted for l-, 5-, 10- and 15-y-old children.

9.1.3. Systemic Distribution, Retention and Excretion

9.1.3.1. Summary of biokinetic data

(288) The biokinetics of calcium has been investigated extensively in physiological and clinical studies and to some extent in radiobiological studies. Biokinetic data for systemic calcium are reviewed in Leggett (1992a), *Publication 71* (ICRP, 1995b), and *Publication 134* (ICRP, 2016a).

(289) The alkaline earth elements strontium, barium, and radium are physiological analogues of calcium but exhibit somewhat different systemic kinetics from calcium and from one another due to discrimination by biological membranes and hydroxyapatite crystals of bone (ICRP, 1993; Leggett, 1992a). Strontium is a much closer biokinetic analogue of calcium than is barium or radium.

(290) Data on the systemic behaviour of calcium in adults are reviewed in *Publication 134*. Briefly, plasma disappearance curves for these elements indicate an outflow rate of several hundred plasma volumes per day and rapid equilibration with an extravascular pool roughly three times the size of the plasma pool. Soft tissues initially accumulate most of the systemic burden, but bone becomes the primary systemic repository for calcium after a few days. Following acute input of a stable calcium isotope into blood of an adult human, soft tissues are estimated to contain nearly half of the injected amount at 1 d, one-fourth at 10 d and <1% beyond 100 d. Bone is projected to contain roughly a third of the injected amount at 1-100 d and to lose the accumulated amount with a half-time of a few years for trabecular bone and a few decades for cortical bone. Available data suggest that the urinary excretion rate is moderately higher than the faecal excretion rate.

(291) Calcium entering bone initially deposits on bone surface, from which activity is removed with an estimated half-time on the order of 1 d. Most of the calcium atoms leaving bone surface return to blood, but a portion diffuse into a bone volume pool referred to as exchangeable bone volume. Calcium atoms entering exchangeable bone volume may return to bone surface or blood over a period of weeks or months or may transfer to nonexchangeable bone volume, meaning that they become firmly fixed in bone crystals. It appears that calcium, strontium, barium, and radium are all about equally likely to transfer from bone surface to exchangeable bone volume but that the likelihood of becoming firmly fixed in bone crystal decreases in the order calcium > strontium > barium > radium. Data from human and animal studies indicate that the rate of loss of alkaline earth tracers from bone over the first few months after acute uptake to blood increases in the order calcium < strontium < barium < radium. Presumably these four elements are removed from trabecular or cortical non-exchangeable bone volume compartments at the rate of bone restructuring of that bone type, so that the rate of transfer from non-exchangeable bone volume is independent of the element.

(292) There is a sizable literature on the age-specific kinetics of calcium, strontium, barium, and radium in human subjects and laboratory animals (Anderson and Comar, 1968; Atherton et al., 1965; Bauer et al., 1957; Bronner et al., 1956; Bruenger et al., 1983, 1989; Decker et al., 1964; Domanski et al., 1980; Glad et al., 1960; Henrichs et al., 1984; Kallfelz and Wentworth, 1969; Kereiakes et al., 1968; Kulp and Schulert, 1962; Lee et al., 1965; Likhtarev et al., 1975; Lloyd, C.W. Jones, Bruenger, Atherton, et al., 1983; Macdonald et al., 1965; Osanov et al., 1971; Parks et al., 1978; Parks and Keane, 1983; Stather, 1974; Wellman et al., 1970; Woodard and Dwyer, 1972). It has been established that uptake of each of these elements is greater in growing bone than in mature bone. Changes with age in their fractional deposition in the skeleton are roughly proportional to the age-specific rate of calcium addition to bone resulting from bone growth plus bone remodeling (Figure 9.1). At times remote from exposure, skeletal burdens acquired during periods of growth tend to remain higher than those acquired by mature skeletons except for skeletal burdens acquired during or soon after infancy when there is a particularly high rate of bone turnover. Both deposition and removal of the calcium-like elements is greater in areas of bone undergoing rapid remodeling than in areas of relatively slow remodeling. Greater deposition of these elements the younger skeleton results in less systemic radium available for excretion and distribution to soft tissues.

9.1.3.2. Systemic model

(293) The age-specific model for systemic calcium is taken from *Publication 67* (ICRP, 1993). The same model with parameter values for the adult was adopted in *Publication 134* for application to workers.

(294) The structure of the model is shown in Fig. 9.1. Transfer coefficients are listed in Table 9.2.

(295) Extension of the calcium model to preadult ages is based on results of studies of the age-specific behavior of calcium and its physiological analogues strontium, barium, and radium in human subjects and laboratory animals. These studies have demonstrated that deposition of these elements in bone is higher, and removal from bone is faster, at preadult ages than in adults. The age-specific deposition fraction for bone, and the division of that deposition between trabecular and cortical bone surface, are based on the estimated rates of calcium addition to each of these bone types. For preadult ages the deposition fractions for soft tissues and excretion pathways are reduced uniformly from the values for adults to reflect the elevated competition from bone for circulating calcium. The removal half-times from bone surface and exchangeable bone volume compartments are assumed to be independent of age. The removal half-times from bone volume compartments to blood are reference age-specific bone turnover rates (ICRP, 2002a). Removal half-times from soft-tissue compartments are assumed to be independent of age.

(296) The reader is referred to Leggett (1992a), *Publication 67* (ICRP, 1993), and *Publication 71* (ICRP, 1995b) for more detailed descriptions of the basis for age-specific parameter values for calcium and physiologically related elements.

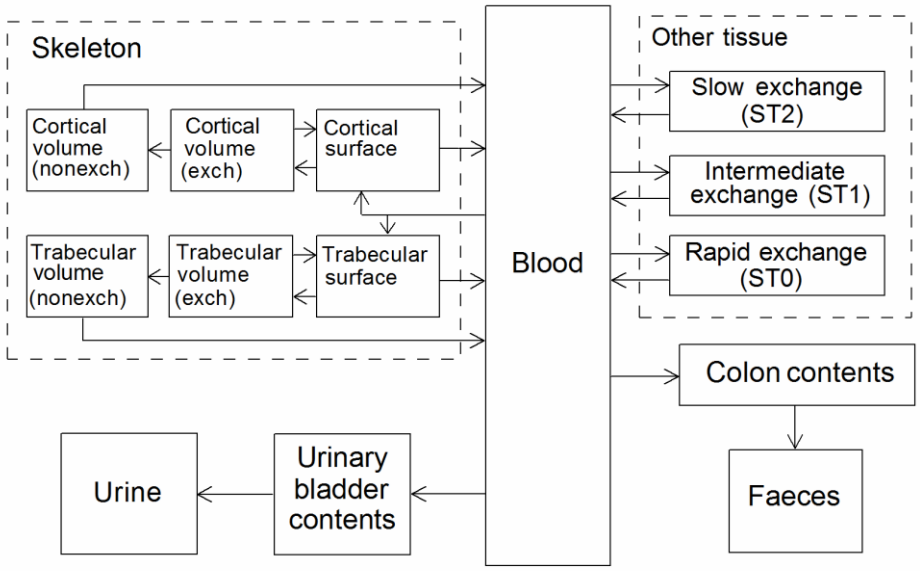

Fig. 9.1. Structure of the model for systemic calcium. exch = exchangeable, nonexch = non-exchangeable. Activity transferred to Colon enters Right colon contents.

3079 Table 9.2. Transfer coefficients for the model for systemic calcium

Path*	Transfer coefficient (d^{-1})					
	Infant	1 y	5 y	10 y	15 y	Adult
Blood to Urinary bladder contents	2.00E-01	4.40E-01	4.80E-01	3.52E-01	2.08E-01	6.00E-01
Blood to Right colon contents	1.50E-01	3.30E-01	3.60E-01	2.64E-01	1.56E-01	4.50E-01
Blood to Trab surface	2.25E+00	1.35E+00	1.33E+00	2.12E+00	3.10E+00	2.08E+00
Blood to Cort surface	9.00E+00	5.40E+00	4.67E+00	6.28E+00	8.00E+00	1.67E+00
Blood to ST0	2.90E+00	6.38E+00	6.96E+00	5.10E+00	3.02E+00	8.70E+00
Blood to ST1	5.00E-01	1.10E+00	1.20E+00	8.80E-01	5.20E-01	1.50E+00
Blood to ST2	2.50E-04	5.50E-04	6.00E-04	4.40E-04	2.60E-04	7.50E-04
Trab surf to Blood	5.78E-01	5.78E-01	5.78E-01	5.78E-01	5.78E-01	5.78E-01
Trab surf to Exch Trab vol	1.16E-01	1.16E-01	1.16E-01	1.16E-01	1.16E-01	1.16E-01
Cort surf to Blood	5.78E-01	5.78E-01	5.78E-01	5.78E-01	5.78E-01	5.78E-01
Cort surf to Exch Cort vol	1.16E-01	1.16E-01	1.16E-01	1.16E-01	1.16E-01	1.16E-01
ST0 to Blood	9.67E-01	2.13E+00	2.32E+00	1.70E+00	1.01E+00	2.90E+00
ST1 to Blood	1.73E-01	1.73E-01	1.73E-01	1.73E-01	1.73E-01	1.73E-01
ST2 to Blood	3.80E-04	3.80E-04	3.80E-04	3.80E-04	3.80E-04	3.80E-04
Exch Trab vol to Trab surf	2.77E-03	2.77E-03	2.77E-03	2.77E-03	2.77E-03	2.77E-03
Exch Trab vol to Nonexch Trab vol	4.16E-03	4.16E-03	4.16E-03	4.16E-03	4.16E-03	4.16E-03
Exch Cort vol to Cort surf	2.77E-03	2.77E-03	2.77E-03	2.77E-03	2.77E-03	2.77E-03
Exch Cort vol to Nonexch Cort vol	4.16E-03	4.16E-03	4.16E-03	4.16E-03	4.16E-03	4.16E-03
Nonexch Trab vol to Blood	8.22E-03	2.88E-03	1.81E-03	1.32E-03	9.59E-04	4.93E-04
Nonexch Cort vol to Blood	8.22E-03	2.88E-03	1.53E-03	9.04E-04	5.21E-04	8.21E-05

3080 *Trab = Trabecular, Cort = cortical, surf = surface, vol = volume, Exch = Exchangeable, Nonexch =
3081 Nonexchangeable

9.2. Dosimetric data for calcium

Table 9.3. Committed effective dose coefficients (Sv Bq^{-1}) for the inhalation or ingestion of ^{45}Ca compounds.

	Effective dose coefficients (Sv Bq^{-1})					
Inhaled particulate materials (1 µm AMAD aerosols)	3 mo	1 y	5 y	10 y	15 y	Adult
Type F, Chloride	5.0E-09	2.8E-09	9.7E-10	5.6E-10	4.8E-10	2.2E-10
Type M, All unspecified forms	5.3E-09	4.2E-09	2.3E-09	1.5E-09	1.2E-09	1.0E-09
Type S	8.0E-09	7.0E-09	4.0E-09	2.6E-09	2.1E-09	1.9E-09
Ingested materials						
Adult f_A = 0.4, All forms	7.2E-09	3.5E-09	1.4E-09	7.7E-10	7.3E-10	2.7E-10

10. IRON (Z = 26)

10.1. Routes of Intake

10.1.1. Inhalation

10.1.1.1. Absorption Types and parameter values

(297) Extensive information was found on the behaviour of iron inhaled in oxide form in both animals and in man, because it has been used as a test material to study lung clearance. Some information on absorption from the respiratory tract was also found on other forms, such as the chloride. For details, see Section 7 of of *Publication 134* (ICRP, 2016a).

(298) Absorption parameter values and types, and associated f_A values for particulate forms of iron are given in Table 10.1 (taken from Section 7 of *Publication 134*).

Table 10.1. Absorption parameter values for inhaled and ingested iron

Inhaled particulate materials		Absorption parameter values* f_r	s_r (d^{-1})	s_s (d^{-1})
Default parameter values†,‡				
Absorption Type	Assigned forms			
F	—	1	100	–
M§	Ferric chloride; ferric oxide	0.2	3	0.005
S	Corrosion products	0.01	3	1×10^{-4}

Ingested materials¶	Age-dependent absorption from the alimentary tract, f_A					
Assigned forms	3 months	1 year	5 years	10 years	15 years	adult
All forms	0.6	0.2	0.2	0.2	0.2	0.1

*It is assumed that for iron the bound state can be neglected, *i.e.*, $f_b = 0.0$. The value of s_r for Type F forms of iron (100 d^{-1}) is element-specific. The values for Types M and S (3 d^{-1}) are the general default values.

†Materials (e.g. ferric chloride) are generally listed here where there is sufficient information to assign to a default absorption Type, but not to give specific parameter values (see Section 7 of *Publication 134*, ICRP, 2016a).

‡For inhaled material deposited in the respiratory tract and subsequently cleared by particle transport to the alimentary tract, the default f_A values for inhaled materials are applied: i.e. the product of f_r for the absorption Type and the f_A value for ingested soluble forms of iron applicable to the age-group of interest (*e.g.* 0.1 for adults).

§Default Type M is recommended for use in the absence of specific information on which the exposure material can be assigned to an absorption type, e.g. if the form is unknown, or if the form is known but there is no information available on the absorption of that form from the respiratory tract.

¶Activity transferred from systemic compartments into segments of the alimentary tract is assumed to be subject to reabsorption to blood. The default absorption fraction f_A for the secreted activity is the highest value for ingestion of the radionuclide applicable to the age-group of interest (*e.g.* 0.1 for adults).

10.1.2. Ingestion

10.1.2.1. Adults

(299) Inorganic iron, usually as ferric or ferrous salts, is present in many foods as a natural constituent or after supplementation with iron, and as the major form of ambient iron present in water and air. Biologically incorporated iron, usually in haem from haemoglobin, myoglobin, and cytochromes, is derived from animal tissues and/or their constituents present in the diet.

Because of the nutritional significance of iron, its gastrointestinal absorption has been investigated extensively in man and animals (Bothwell et al., 1979; Brozovic, 1975; ICRP, 1975; Nuclear Energy Agency (NEA), 1988). In numerous normal human subjects, absorption fractions of 0.01-0.07 have been obtained when iron was ingested with a wide variety of vegetable foods, whereas values of 0.1-0.2 are typically obtained when iron is added to meat and fish. However, individual studies produced mean figures as great as 0.4 for men and 0.6 for women.

(300) Iron absorption is influenced by the amount of iron in the diet, age, gender, the body's state of iron repletion, the chemical form ingested, and substances in the diet and gastrointestinal secretions which act to alter iron absorption. Lowered iron status of the individual results in increased iron uptake, as shown by menstruating women and sufferers from anaemia. Uptake is also increased during pregnancy and lactation. These latter points, associated to hormonal differences, result in higher iron absorption in females compared to males (Brozovic, 1975; Fletcher et al., 1994; Woodhead et al., 1991). Iron absorption measured in pregnant women gave absorption fractions of about 0.1, 0.25, and 0.3 in the first, second, and third trimester. Healthy older adults appear to absorb iron similarly to younger adults (Freiman et al., 1963; Marx, 1979). Iron incorporated in food of animal origin is generally better absorbed than that from vegetables (Layrisse and Martinez-Torres, 1971; Martinez-Torres and Layrisse, 1973). Haem iron is usually better absorbed than non-haem iron in normal and iron-deficient subjects (Bjorn Rasmussen et al., 1974; Layrisse and Martínez-Torres, 1972). Ferrous iron tends to be absorbed more efficiently than ferric because of its greater solubility. In the alimentary tract, gastric hydrochloric acid, bile, and certain organic and amino acids can augment iron absorption, whereas bicarbonate from pancreatic secretions, phosphates, phytates, carbonates, tannates, oxalates, and/or EDTA can decrease iron absorption. Ingestion of human milk and organic acids (ascorbic, lactic, citric…) are enhancers of iron absorption, while dietary fibres (pectins, cellulose…), tannates in tea, polyphenols in coffee and even calcium supplements in diet are potent inhibitors.

(301) In normal iron balance, iron absorption occurs predominantly in the small intestine and is regulated such that absorption replaces loss. Iron is known to be, in some circumstances, retained in the wall of the small intestine. Available data are consistent with a half-time of intestinal retention of about 3 d for 20% of ingested iron, dependent on the iron status (ICRP, 2006).

(302) In *Publications 30* (ICRP, 1980), *69* (ICRP, 1995a) and *134* (ICRP, 2016a) an absorption fraction of 0.1 for both males and females was recommended. This value adequately represents iron absorption in many cases, e.g. in healthy adult male and postmenopausal female subjects, with iron in inorganic forms, and in vegetarian diets. For the adult dose coefficients given in this report an f_A value of 0.1 is applied to all forms of ingested iron.

10.1.2.2. Children

(303) Gorten *et al.* (1963) reported a fractional absorption of ^{59}Fe of 0.32 (range 0.068-0.74) following administration to healthy premature infants (1-2-week-old) as ascorbate in a milk meal. In infants younger than 1.5 mo, values of fractional absorption of 0.56-0.91 were obtained using ^{59}Fe citrate administered in a milk meal; in infants 1.5-3 mo of age, values obtained were 0.15-0.38 (Garby and Sjolin, 1959). Children in the first year of life had a fractional absorption of 0.48-0.7 of iron administered with breast milk (Saarinen et al., 1977), 0.03-0.3 of iron administered with infant formulas based on soya protein extract or cow's milk (Rios et al., 1975; Saarinen and Siimes, 1977), and about 0.03 from carrier-free radioiron

activity (Rios et al., 1975; Saarinen et al., 1977; Saarinen and Siimes, 1977). Saarinen et al. (1977) also compared the absorption of ^{59}Fe in 6-7-mo-old infants who had been exclusively breast-fed or had been weaned from breast to cow's milk prior to the age of 2 mo. In each case, ^{59}Fe sulphate was administered during feeding after a 3 h fast and the absorption values obtained were 0.5 ± 0.08 (SEM, n 11) for the breast-fed infants and 0.2 ± 0.05 (*n* = 16) for those fed cow's milk. Iron absorption in infants and children is inversely related to age but has not usually been measured in direct comparison with that in adults (Cristy and Leggett, 1986). In one comparative study, children 4-52-mo-old absorbed approximately 0.1 of the ^{59}Fe from a milk meal, in comparison with adult males who absorbed 0.028 from a similar meal (Schulz and Smith, 1958). The absorption of ^{59}Fe biologically incorporated in eggs was approximately 0.11 in children 1-4.5 y of age and 0.06 in children 5-15 y of age (Schulz and Smith, 1958). ^{59}Fe-labelled ferrous ascorbate administered in lemonade yielded mean absorption values of 0.08-0.16 in children 7-8 y of age, and 0.15-0.17 in children 9-10 y of age (Darby et al., 1947). The higher values obtained in the older children in this experiment could be related to increased iron requirements during growth and development. After a 12 h fast, four normal children ages 6-11 y were given ^{59}Fe with 5 mg of carrier iron, both in the form of ferrous sulphate. The percentage absorption values were 5, 8, 17, and 27% (mean 13.5%) (Erlandson et al., 1962). In adolescence enhanced absorption of iron would also be expected; the daily requirement of iron in adolescent males and females is respectively about 30 and 50% higher than in adults (Bothwell et al., 1979).

(304) Although the published values of absorption are quite variable, those for children are generally higher than those for adults, attributable in part to the relatively greater requirements of iron for growth and development. For all forms of iron absorption fraction values of 0.6 for 3-mo-old infants, and 0.2 for 1-, 5-, 10-, and 15-y-old children were recommended in *Publication* 69 (ICRP, 1995a). The same values are adopted here for f_A.

10.1.3. Systemic Distribution, Retention and Excretion

10.1.3.1. Adults

(305) *Publication 134* (ICRP, 2016a) describes the typical behavior of systemic iron in healthy adult humans, based mainly on the authoritative review and analyses by Bothwell et al. (1979) (See also Barton and Edwards, 2000; Green et al., 1968; Leggett et al., 2000; Munro and Linder, 1978; Saito et al., 1964; Trubowitz and Davis, 1982)

(306) The body's iron content may be divided into two categories: essential (functional) iron and storage iron. Essential iron is the portion of the body's iron that fulfills critical physiological functions, e.g., as components of oxygen carrying proteins and various enzymes involved in metabolic processes. The adult human body typically contains 30-40 mg of essential iron per kg of body mass. About 80-85% of this is found in haemoglobin within the red blood cells (RBC), about 10-12% is found in myoglobin within muscle and other tissues, and the remainder is distributed throughout the body tissues as haem enzymes (2-3% of body iron) and non-haem enzymes (3-4% of body iron). Storage iron is an iron reserve in the body that assures an adequate supply of iron for normal physiological processes during periods of low intake or rapid loss of iron. Storage iron is located mainly in the reticuloendothelial (RE) system and hepatic parenchyma. Essential and storage iron typically represent about 70% and 30%, respectively, of total-body iron in adult males and about 85% and 15%, respectively, in pre-menopausal adult females.

(307) The iron content in the total body of a typical adult human is about 3.5-4.5 g in males and 2.0-2.5 g in females. The following tissue distribution of iron is estimated for an adult male with a total-body content of 3.9 g: erythrocytes, 2300 mg; liver hepatocytes, 400 mg; liver RE

cells, 50 mg, RE cells of bone marrow, 320 mg; spleen (mainly RE cells), 80 mg; other RE cells, 300 mg; erythroid marrow, 80 mg; plasma transferrin, 2.9 mg; remaining plasma, 0.4 mg; and remainder of the body, 400 mg. The distribution in adult females is expected to be roughly proportional to that in males with the main exception of iron storage sites such as the liver, which typically contain only about a third as much iron in females as in males.

(308) Iron is distributed by blood plasma. Nearly all plasma iron is bound to the transport protein transferrin. The removal half-time of transferrin iron from plasma to tissues is about 90 minutes. Most of the transferrin-bound iron leaving plasma enters a circuit starting in the erythroid marrow. Another portion enters the extravascular spaces and returns to plasma mainly via the lymphatics. The rest is delivered to the parenchymal tissues, mainly the liver.

(309) The mean hepatic non-haem iron concentration is roughly 0.1 mg/g liver in women, compared with 0.3 mg/g liver in adult males. The average mass of storage iron in bone marrow is about 300 mg in adult males and 100 mg in adult females. The erythroid marrow takes up transferrin iron from plasma for incorporation into haemoglobin. Most of this iron appears in circulating red blood cells (RBC) in the next few days and remains there for the life span of the cells, which is on the order of 110-120 d in adult humans. The portion that does not appear in circulating RBC consists of defective cells or extruded components of developing cells. This portion, called the wastage iron of erythropoiesis, typically represents 20-30% of iron that enters the erythroid marrow. This portion is collected by the body's reticuloendothelial (RE) system, degraded, and returned to plasma.

(310) Iron is lost very slowly from the body. Obligatory losses occur via the gastrointestinal tract, skin, and genitourinary tract. Average daily loss of iron from the body has been estimated as 12-14 μg/kg in the adult male. Average daily loss in the pre-menopausal adult female may be about 50% higher due to loss of circulating iron via menstruation.

10.1.3.2. Pre adults

(311) The average concentration of iron in the total body at birth is about 80 mg/kg. About 60-65% is contained in the blood as circulating hemoglobin, about 30% is storage iron divided about equally between liver and other body tissues, and a few percent is contained in the erythroid cells of the marrow, in myoglobin, and in intracellular enzymes.

(312) During the first 2 mo after birth erythropoiesis nearly ceases, and the hemoglobin concentration in blood declines from about 17 g/dl to about 11 g/dl. As growth continues, the red cell mass increases so that nearly all storage iron has been used in the first few months. The iron reserve gradually builds up to about 5 mg/kg during growth. In the male there is a further increase between the ages of 15 to 30 y to about 12-15 mg/kg.

(313) The rate of excretion of iron may be substantially higher in infants and children than in adults, when expressed as daily loss per kg of body weight. Garby et al. (1964) estimated daily losses in children to be 0.03 mg/kg in infants using a radioisotopic technique. Data of Elian et al. (1966) on the rate of blood loss in faeces at ages 2-17 months indicates daily loss on the order of 25 mg via the gastrointestinal tract alone. A similar rate of loss was estimated by Hoag et al. (1961) using ^{59}Fe-labeled red blood cells.

(314) Fetal and neonatal red blood cells have a shorter life span than those in adults (Harrison, 1979; Pearson, 1967; Trubowitz and Davis, 1982). Reported measurements are variable but indicate life spans in the fetus and infant no greater than about 70-90 d. The age at which the adult value is attained does not appear to be known.

10.1.3.3. Biokinetic model for systemic iron

(315) The model for systemic iron applied in *Publication 134* (ICRP, 2017) to workers is applied here to adult members of the public. That model is designed to reproduce observations of the short-term behavior of radio-iron in healthy adult males and the typical total-body distribution of stable iron in adult males indicated earlier, based on reference values for dietary intake and gastrointestinal absorption of iron.

(316) The systemic model for the adult is extended to pre-adult ages based on the following assumptions: the rate of loss of storage iron is inversely proportional to iron stores as a fraction of total-body iron; the rate of loss of iron from the body is twice as high through age 10 y as in adults but attains the adult value by age 15 y; and the life span of red blood cells 70 d in infants, 80 d at 1 y, 90 d at 5 y, 100 d at 10 y, and 110 d at 15 y, compared with 120 d in adults, The transfer coefficients describing all other aspects of iron metabolism are assumed to be independent of age, i.e., the values for adults are assigned to all age groups.

(317) The structure of the model for iron is shown in Fig. 10.1. Parameter values are given in Table 10.2.

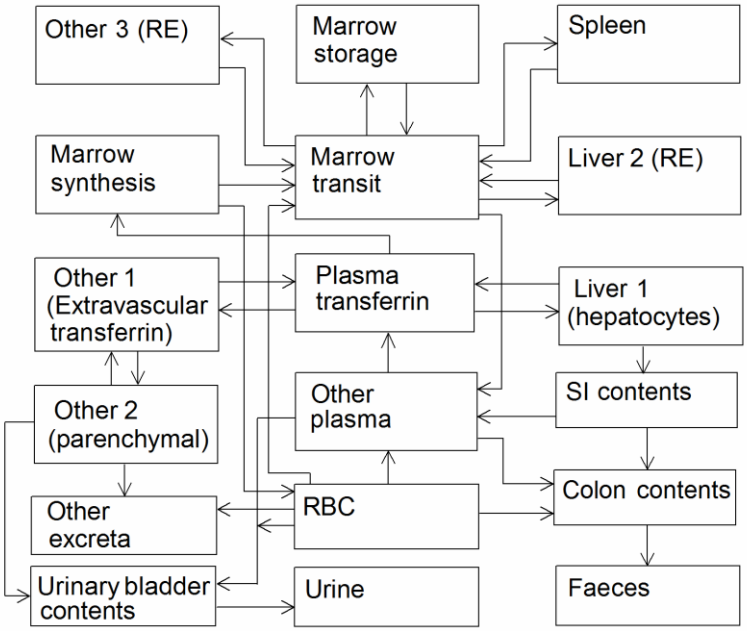

Fig. 10.1. Structure of the biokinetic model for systemic iron. RE = Reticoendothelial cells, RBC = Red blood cells, SI = Small intestine.

3278 Table 10.2. Transfer coefficients for the model for systemic iron

Path*	Transfer coefficient (d^{-1})					
	Infant	1 y	5 y	10 y	15 y	Adult
Other plasma to Plasma transferrin	7.00E+01	7.00E+01	7.00E+01	7.00E+01	7.00E+01	7.00E+01
Other plasma to UB contents	2.00E-02	2.00E-02	2.00E-02	2.00E-02	1.00E-02	1.00E-02
Other plasma to RC contents	2.00E-01	2.00E-01	2.00E-01	2.00E-01	1.00E-01	1.00E-01
Plasma transferrin to RM synthesis	9.43E+00	9.43E+00	9.43E+00	9.43E+00	9.43E+00	9.43E+00
Plasma transferrin to Liver 1	5.55E-01	5.55E-01	5.55E-01	5.55E-01	5.55E-01	5.55E-01
Plasma transferrin to EV transferrin	1.11E+00	1.11E+00	1.11E+00	1.11E+00	1.11E+00	1.11E+00
RBC to Other plasma	1.43E-03	1.25E-03	1.11E-03	1.00E-03	9.09E-04	8.33E-04
RBC to RM transit	1.21E-02	1.06E-02	9.43E-03	8.48E-03	7.95E-03	7.29E-03
RBC to RC contents	6.86E-04	6.00E-04	5.33E-04	4.80E-04	2.18E-04	2.00E-04
RBC to UB contents	5.14E-05	4.50E-05	4.00E-05	3.60E-05	1.64E-05	1.50E-05
RM synthesis to RBC	2.43E-01	2.43E-01	2.43E-01	2.43E-01	2.43E-01	2.43E-01
RM synthesis to RM transit	1.04E-01	1.04E-01	1.04E-01	1.04E-01	1.04E-01	1.04E-01
RM transit to Other plasma	1.39E+00	1.39E+00	1.39E+00	1.39E+00	1.39E+00	1.39E+00
RM transit to RM storage	6.35E-02	6.35E-02	6.35E-02	6.35E-02	6.35E-02	6.35E-02
RM transit to Liver 2	1.06E-02	1.06E-02	1.06E-02	1.06E-02	1.06E-02	1.06E-02
RM transit to Spleen	1.70E-02	1.70E-02	1.70E-02	1.70E-02	1.70E-02	1.70E-02
RM transit to Other RE	6.35E-02	6.35E-02	6.35E-02	6.35E-02	6.35E-02	6.35E-02
RM storage to RM transit	9.50E-03	7.60E-03	7.60E-03	5.70E-03	4.18E-03	3.80E-03
Liver 2 to RM transit	9.50E-03	7.60E-03	7.60E-03	5.70E-03	4.18E-03	3.80E-03
Spleen to RM transit	9.50E-03	7.60E-03	7.60E-03	5.70E-03	4.18E-03	3.80E-03
Other RE to RM transit	9.50E-03	7.60E-03	7.60E-03	5.70E-03	4.18E-03	3.80E-03
Liver 1 to Plasma transferrin	9.10E-03	7.28E-03	7.28E-03	5.46E-03	4.00E-03	3.64E-03
Liver 1 to SI contents	3.70E-04	3.70E-04	3.70E-04	3.70E-04	3.70E-04	3.70E-04
EV transferrin to Plasma transferrin	8.88E-01	8.88E-01	8.88E-01	8.88E-01	8.88E-01	8.88E-01
EV transferrin to Other parenchyma	2.22E-01	2.22E-01	2.22E-01	2.22E-01	2.22E-01	2.22E-01
Other parenchyma to EV transferrin	3.18E-03	2.54E-03	2.54E-03	1.91E-03	1.40E-03	1.27E-03
Other parenchyma to Excreta	1.14E-03	1.14E-03	1.14E-03	1.14E-03	5.70E-04	5.70E-04
Other parenchyma to UB contents	6.00E-05	6.00E-05	6.00E-05	6.00E-05	3.00E-05	3.00E-05

3279 *UB = Urinary bladder, RC = Right colon, RM = Red marrow, SI = Small intestine, EV = Extravascular, RBC =
3280 Red blood cells, RE = reticuloendothelial

10.2. Dosimetric data for iron

Table 10.3. Committed effective dose coefficients (Sv Bq^{-1}) for the inhalation or ingestion of ^{59}Fe compounds.

	Effective dose coefficients (Sv Bq^{-1})					
Inhaled particulate materials (1 µm AMAD aerosols)	3 mo	1 y	5 y	10 y	15 y	Adult
Type F	3.3E-08	2.0E-08	9.1E-09	6.6E-09	4.3E-09	4.0E-09
Type M, Ferric chloride, ferric oxide; all unspecified forms	1.4E-08	9.3E-09	5.1E-09	3.5E-09	2.6E-09	2.6E-09
Type S, Corrosion products	1.1E-08	9.1E-09	5.2E-09	3.5E-09	2.7E-09	2.8E-09
Ingested materials						
Adult f_A = 0.1, All forms	4.6E-08	1.2E-08	6.3E-09	4.6E-09	3.2E-09	1.7E-09

11. COBALT (Z = 27)

11.1. Routes of Intake

11.1.1. Inhalation

(318) There have been a number of reported studies of the lung retention of ^{60}Co following accidental inhalation, usually of an oxide. Information on absorption from the respiratory tract is available from experimental studies of cobalt in a variety of forms, including nitrate, chloride, oxides, fused aluminosilicate particles (FAP) and polystyrene (PSL). For details see Section 8 of *Publication 134* (ICRP, 2016a). Absorption parameter values and types, and associated f_A values for particulate forms of cobalt are given in Table 11.1 (taken from Section 8 of *Publication* 134).

Table 11.1. Absorption parameter values for inhaled and ingested cobalt

		Absorption parameter values*		
Inhaled particulate materials		f_r	s_r (d^{-1})	s_s (d^{-1})
Default parameter values†,‡				
Absorption Type	Assigned forms			
F	Nitrate, chloride	1	1	–
M§	–	0.2	1	0.005
S	Oxide, FAP, PSL	0.01	1	1×10^{-4}

Ingested materials¶	Age-dependent absorption from the alimentary tract, f_A					
Assigned forms	3 months	1 year	5 years	10 years	15 years	adult
Cobalt in diet and soluble forms	0.6	0.2	0.2	0.2	0.2	0.1
Oxides	0.3	0.1	0.1	0.1	0.1	0.05

*It is assumed that for cobalt the bound fraction f_b is 0.03 with an uptake rate s_b = 0.002 d^{-1} is applied to material in the AI region and LN_{TH}. It is assumed that f_b = 0.0 for material in the ET_2, BB and bb regions and LN_{ET}. The values of s_r for Type F, M and S forms of cobalt (1 d^{-1},) are element-specific.

†Materials (e.g. nitrate) are listed here where there is sufficient information to assign to a default absorption Type, but not to give specific parameter values (see Section 8 of ICRP, 2016a).

‡For inhaled material deposited in the respiratory tract and subsequently cleared by particle transport to the alimentary tract, the default f_A values for inhaled materials are applied: i.e. the product of f_r for the absorption type and the f_A value for ingested soluble forms of cobalt applicable to the age-group of interest (*e.g.* 0.1 for adults).

§Default Type M is recommended for use in the absence of specific information on which the exposure material can be assigned to an absorption type, e.g. if the form is unknown, or if the form is known but there is no information available on the absorption of that form from the respiratory tract.

¶Activity transferred from systemic compartments into segments of the alimentary tract is assumed to be subject to reabsorption to blood. The default absorption fraction f_A for the secreted activity is the highest value for ingestion of the radionuclide applicable to the age-group of interest (*e.g.* 0.1 for adults).

11.1.2. Ingestion

11.1.2.1. Adults

(319) The gastrointestinal absorption of cobalt is variable and affected by the mass and the chemical form entering the body. Cobalt and iron share a joint absorption pathway and generally similar levels of absorption (Schade et al., 1970). A few percents of trace quantities of insoluble forms like oxides are absorbed. About 10 - 30% is absorbed from large amounts of cobalt or carrier and from soluble inorganic forms like nitrate or chloride (for details, see section 8 of ICRP, 2016a). A significantly higher uptake of ingested cobalt was observed by Christensen et al. (Christensen et al., 1993) in females than in males. Increased cobalt absorption is also observed in subjects suffering from iron deficiency (Pollack et al., 1965; Valberg et al., 1969). The absorption of radioactive cobaltous chloride appears to diminish when it is administered after a meal or pre-tagged to protein (Paley and Sussman, 1963). Taylor (1959, 1962) measured cobalt absorption in rats after administration of $CoCl_2$, cobalt in cows' milk, or lactose solutions and obtained values of approximately 0.3–0.4%. Nishimura et al. (1976) administered ^{60}Co chloride and ^{58}Co vitamin B_{12} to rats and compared whole-body retention after oral and intravenous administration. Absorption was then estimated to be 3% for cobalt in its inorganic form and 70% for the vitamin-incorporated element. If fish or marine algae are maintained in sea water containing radioactive ^{60}Co before being fed to rats, fractional absorption of the element is much higher than that of inorganic cobalt. Thus Inaba et al. (1982) reported tissue retention in rats at 2 days after administration of ^{60}Co incorporated in fish as 30% of the activity administered, whereas a value of 3% was obtained after administration of $^{60}CoC1_2$. For ^{60}Co in crab meat, absorption by human volunteers was estimated to be about 5% (ICRP, 1993). The fractional absorption of ^{60}Co from cockles collected on the Irish Sea coast in the UK was investigated in a human volunteer study by Hunt (1998), and a value of approximately 0.2 was obtained. In *Publication 30* (ICRP, 1979) an absorption fraction value of 0.3 was recommended for organically complexed cobalt compounds and for all inorganic compounds of the element, excluding oxides and hydroxides. In *Publication 67* (ICRP, 1993), it was considered that the range of results reported in human studies suggested that in most cases of normal adults the fractional absorption of trace quantities of cobalt was less than 0.1 and an absorption fraction of 0.1 was therefore adopted for intakes by adult members of the public. In *Publication 134*, an f_A value of 0.1 was adopted for ingestion of all chemical forms but insoluble oxides for which an f_A value of 0.05 was recommended. The f_A value of 0.1 is adopted here for ingestion of soluble forms of cobalt and for cobalt in food. For oxides, the f_A value of 0.05 is adopted.

11.1.2.2.Children

(320) The absorption of both ^{60}Co chloride and ^{60}Co vitamin B_{12} following oral administration can be much higher in young than in adult rats (Nishimura et al., 1976). At 3 days after administration as the chloride, retention by 7-day-old rats (10%) was approximately 30 times the adult value (0.3%). Retention of the element incorporated into the vitamin B_{12} (nearly 100%) was almost double the adult value (55%). A study of cobalt balance in girls aged between 6 and 10 years (Engel et al., 1967) gave an estimated absorption of 0.57. This relatively high cobalt absorption could be associated with the stimulation of iron absorption during periods of rapid growth. As there was evidence that absorption of cobalt may be increased in childhood an absorption fraction of 0.3 was recommended in *Publication 67* for children from 1 to 15 years. An absorption fraction of 0.6 was recommended in *Publication 67* as an average for the first year of life. The same values as for iron are adopted here for cobalt in diet and for soluble cobalt: $f_A = 0.6$ for 3-month-old infants and $f_A = 0.2$ for 1- to 15-year-old children. Value $f_A = 0.3$ for 3-month-old infants and $f_A = 0.1$ for 1- to 15-year-old children are adopted for ingestion of oxides.

11.1.3. Systemic Distribution, Retention and Excretion

(321) The model for systemic cobalt applied in *Publication 134* (ICRP, 2016a) to workers is applied here to adult members of the public. That model was based mainly on data from controlled studies of retention of activity in the total body, liver, and blood, and the rate of excretion of activity in urine and faeces, in healthy human subjects administered radioisotopes of cobalt. The data for human subjects were supplemented with measurements of the time-dependent distribution of systemic activity following administration of cobalt isotopes to laboratory animals.

(322) There is little information on age related changes in the biokinetics of systemic cobalt in mammalian species. A study by Nishimura et al. (1976) on rats indicated greater retention of ^{60}Co in immature rats than in adult rats following ingestion of ^{60}Co chloride or ^{58}Co vitamin B_{12}, but this appeared to be due entirely to increased intestinal absorption of cobalt in immature animals. The investigators concluded that retention of absorbed cobalt by the animals was virtually independent of age.

(323) The systemic behaviour of cobalt is assumed here to be independent of age except that activity is assumed to be removed from trabecular or cortical bone volume to blood at the age-specific rate of turnover of that bone type.

(324) The structure of the model for cobalt is shown in Fig. 11.1. Parameter values are given in Table 11.2.

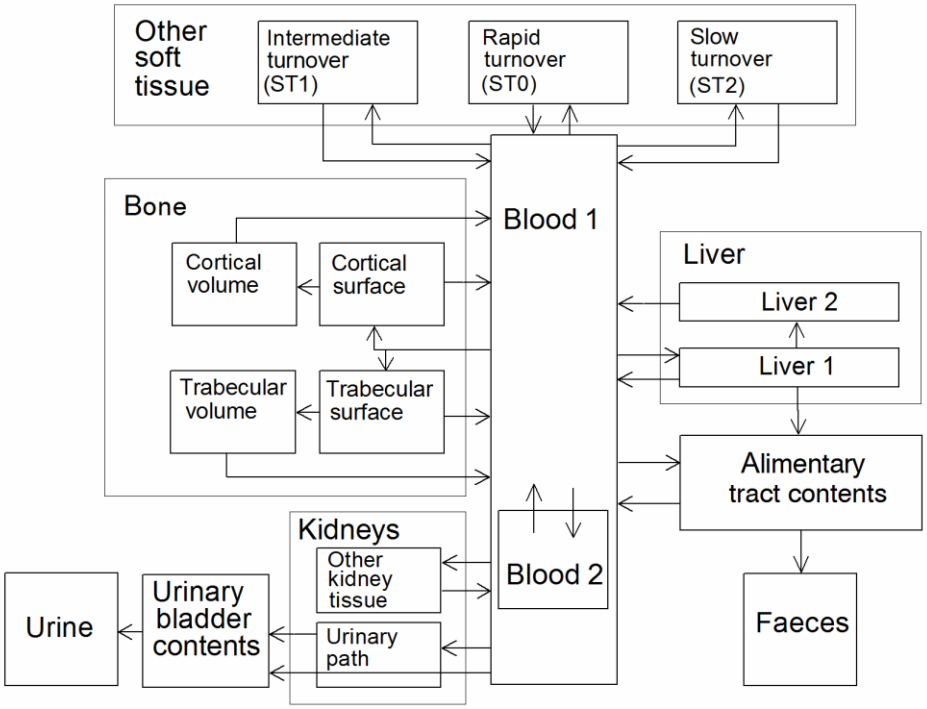

Fig. 11.1. Structure of the systemic model for cobalt. Activity transferred from Blood 1 to Alimentary tract contents enters Right colon contents. Activity transferred from Liver 1 to Alimentary tract contents enters Small intestine contents. Activity transferred from Alimentary tract contents to Blood 1 represents absorption from the small intestine to blood.

Table 11.2. Transfer coefficients for the model for systemic cobalt

Path*	Transfer coefficient (d^{-1})					
	Infant	1 y	5 y	10 y	15 y	Adult

Blood 1 to Liver 1	7.00E+01	7.00E+01	7.00E+01	7.00E+01	7.00E+01	7.00E+01
Blood 1 to Right colon contents	4.00E+00	4.00E+00	4.00E+00	4.00E+00	4.00E+00	4.00E+00
Blood 1 to ST0	1.80E+01	1.80E+01	1.80E+01	1.80E+01	1.80E+01	1.80E+01
Blood 1 to ST1	1.00E+01	1.00E+01	1.00E+01	1.00E+01	1.00E+01	1.00E+01
Blood 1 to ST2	4.00E+00	4.00E+00	4.00E+00	4.00E+00	4.00E+00	4.00E+00
Blood 1 to Cortical bone surf	6.00E+00	6.00E+00	6.00E+00	6.00E+00	6.00E+00	6.00E+00
Blood 1 to Trabecular bone surf	6.00E+00	6.00E+00	6.00E+00	6.00E+00	6.00E+00	6.00E+00
Blood 1 to Urinary path	9.00E+00	9.00E+00	9.00E+00	9.00E+00	9.00E+00	9.00E+00
Blood 1 to Other kidney tissue	1.00E+00	1.00E+00	1.00E+00	1.00E+00	1.00E+00	1.00E+00
Blood 1 to Blood 2	1.20E+01	1.20E+01	1.20E+01	1.20E+01	1.20E+01	1.20E+01
Blood 2 to Blood 1	6.93E-01	6.93E-01	6.93E-01	6.93E-01	6.93E-01	6.93E-01
Liver 1 to SI contents	9.24E-02	9.24E-02	9.24E-02	9.24E-02	9.24E-02	9.24E-02
Liver 1 to Blood 1	3.47E-01	3.47E-01	3.47E-01	3.47E-01	3.47E-01	3.47E-01
Liver 1 to Liver 2	2.31E-02	2.31E-02	2.31E-02	2.31E-02	2.31E-02	2.31E-02
Liver 2 to Blood 1	1.90E-03	1.90E-03	1.90E-03	1.90E-03	1.90E-03	1.90E-03
ST0 to Blood 1	9.90E-02	9.90E-02	9.90E-02	9.90E-02	9.90E-02	9.90E-02
ST1 to Blood 1	1.39E-02	1.39E-02	1.39E-02	1.39E-02	1.39E-02	1.39E-02
ST2 to Blood 1	9.50E-04	9.50E-04	9.50E-04	9.50E-04	9.50E-04	9.50E-04
Cortical surf to Blood 1	8.42E-02	8.42E-02	8.42E-02	8.42E-02	8.42E-02	8.42E-02
Cortical bone surf to Cortical vol	1.49E-02	1.49E-02	1.49E-02	1.49E-02	1.49E-02	1.49E-02
Trabecular bone surf to Blood 1	8.42E-02	8.42E-02	8.42E-02	8.42E-02	8.42E-02	8.42E-02
Trabecular surf to Trabecular vol	1.49E-02	1.49E-02	1.49E-02	1.49E-02	1.49E-02	1.49E-02
Cortical bone vol to Blood 1	8.22E-03	2.88E-03	1.53E-03	9.04E-04	5.21E-04	8.21E-05
Trabecular bone vol to Blood 1	8.22E-03	2.88E-03	1.81E-03	1.32E-03	9.59E-04	4.93E-04
Urinary path to UB contents	4.62E-01	4.62E-01	4.62E-01	4.62E-01	4.62E-01	4.62E-01
Other kidney tissue to Blood 1	1.90E-03	1.90E-03	1.90E-03	1.90E-03	1.90E-03	1.90E-03
Blood 1 to UB contents	6.00E+01	6.00E+01	6.00E+01	6.00E+01	6.00E+01	6.00E+01

3390 *UB = Urinary bladder, surf = surface, vol = volume, SI = Small intestine

11.2. Dosimetric data for cobalt

Table 11.3. Committed effective dose coefficients (Sv Bq^{-1}) for the inhalation or ingestion of ^{57}Co compounds.

	Effective dose coefficients (Sv Bq^{-1})					
Inhaled particulate materials (1 µm AMAD aerosols)	3 mo	1 y	5 y	10 y	15 y	Adult
Type F, Nitrate, chloride	1.4E-09	7.1E-10	4.0E-10	2.7E-10	1.9E-10	1.8E-10
Type M, All unspecified forms	2.2E-09	1.9E-09	1.0E-09	7.1E-10	5.2E-10	5.6E-10
Type S, Oxide, FAP, PSL	4.3E-09	3.9E-09	2.3E-09	1.5E-09	1.2E-09	1.3E-09
Ingested materials						
Adult f_A = 0.1, Cobalt in diet and soluble forms	2.2E-09	6.9E-10	4.1E-10	2.8E-10	2.0E-10	1.2E-10
Adult f_A = 0.05, Oxides	1.2E-09	4.4E-10	2.6E-10	1.8E-10	1.3E-10	8.8E-11

Table 11.4. Committed effective dose coefficients (Sv Bq^{-1}) for the inhalation or ingestion of ^{58}Co compounds.

	Effective dose coefficients (Sv Bq^{-1})					
Inhaled particulate materials (1 µm AMAD aerosols)	3 mo	1 y	5 y	10 y	15 y	Adult
Type F, Nitrate, chloride	3.9E-09	2.1E-09	1.2E-09	8.0E-10	5.5E-10	5.3E-10
Type M, All unspecified forms	6.3E-09	5.1E-09	3.0E-09	2.0E-09	1.5E-09	1.7E-09
Type S, Oxide, FAP, PSL	8.7E-09	7.5E-09	4.4E-09	3.0E-09	2.2E-09	2.6E-09
Ingested materials						
Adult f_A = 0.1, Cobalt in diet and soluble forms	6.1E-09	2.5E-09	1.5E-09	1.0E-09	7.1E-10	5.4E-10
Adult f_A = 0.05, Oxides	3.8E-09	1.9E-09	1.1E-09	7.9E-10	5.5E-10	4.6E-10

Table 11.5. Committed effective dose coefficients (Sv Bq^{-1}) for the inhalation or ingestion of ^{60}Co compounds.

	Effective dose coefficients (Sv Bq^{-1})					
Inhaled particulate materials (1 µm AMAD aerosols)	3 mo	1 y	5 y	10 y	15 y	Adult
Type F, Nitrate, chloride	3.0E-08	1.6E-08	9.7E-09	6.7E-09	5.3E-09	5.2E-09
Type M, All unspecified forms	3.7E-08	3.1E-08	1.9E-08	1.3E-08	1.0E-08	1.1E-08
Type S, Oxide, FAP, PSL	1.2E-07	1.2E-07	8.2E-08	5.9E-08	5.6E-08	6.3E-08
Ingested materials						
Adult f_A = 0.1, Cobalt in diet and soluble forms	4.7E-08	1.5E-08	9.8E-09	6.8E-09	5.4E-09	3.2E-09
Adult f_A = 0.05, Oxides	2.5E-08	9.1E-09	5.8E-09	4.1E-09	3.2E-09	2.1E-09

12. NICKEL (Z = 28)

12.1. Routes of Intake

12.1.1. Inhalation

(325) Inhalation of nickel radioisotopes is not generally of major concern, but because of the recognised chemical toxicity of nickel, numerous studies have been conducted on its behaviour following deposition in the respiratory tract (see e.g. Goodman et al., 2011; National Research Council (NRC) and Committee on Medical and Biological Effects of Environmental Pollutants, 1975; Sivulka, 2005). Information is available from experimental studies of nickel compounds including carbonyl, chloride, sulphate, sulphides, and oxide: mostly in rats, with a few studies in dogs or monkeys. For details see Section 15 of *Publication 151* (ICRP, 2022).

(326) Absorption parameter values and types, and associated f_A values for gas and vapour forms of nickel are given in Table 12.1 and for particulate forms in Table 12.2 (both taken from Section 15 of *Publication 151*). Exposures to gas or vapour forms of nickel are relatively unusual compared to exposures to particulate forms, and it is therefore recommended in this series of documents that particulate form should be assumed in the absence of information (ICRP, 2002b).

Table 12.1. Deposition and absorption for gas and vapour forms of nickel.

	Percentage deposited (%)*						Absorption
	Total	ET_1	ET_2	BB	bb	AI	Type
Chemical form/origin							
Nickel carbonyl	100[†]	0	20	10	20	50	F

	Age-dependent absorption from the alimentary tract, f_A					
	3 months	1 year	5 years	10 years	15 years	Adult
Chemical form/origin						
Nickel carbonyl	0.5	0.05	0.05	0.05	0.05	0.05

ET_1, anterior nasal passage; ET_2, posterior nasal passage, pharynx and larynx; BB, bronchial; bb, bronchiolar; AI, alveolar-interstitial.

**Percentage deposited* refers to how much of the material in the inhaled air remains in the body after exhalation. Almost all inhaled gas molecules contact airway surfaces, but usually return to the air unless they dissolve in, or react with, the surface lining.

[†]Default distribution between regions: 20% ET_2, 10% BB, 20% bb and 50% AI.

Table 12.2. Absorption parameter values for inhaled and ingested nickel.

Inhaled particulate materials		Absorption parameter values* f_r	s_r (d^{-1})	s_s (d^{-1})
Default parameter values†,‡				
Absorption Type	Assigned forms			
F	Chloride, sulphate, monosulphide, subsulphide	1	3	–
M§	Nickel metal	0.2	3	0.005
S	Oxide	0.01	3	1×10^{-4}

Ingested materials¶	Age-dependent absorption from the alimentary tract, f_A					
Assigned forms	3 months	1 year	5 years	10 years	15 years	Adult
Nickel in diet, soluble and unspecified forms	0.5	0.05	0.05	0.05	0.05	0.05
Nickel metal	0.1	0.01	0.01	0.01	0.01	0.01
Nickel oxide	5×10^{-3}	5×10^{-4}	5×10^{-4}	5×10^{-4}	5×10^{-4}	5×10^{-4}

*It is assumed that for nickel the bound state can be neglected, i.e. f_b = 0.0. The value of s_r for Type F forms of nickel (3 d^{-1}) is element-specific. The values for Types M and S (3 d^{-1}) are the general default values.

†Materials (e.g. chloride) are generally listed here where there is sufficient information to assign to a default absorption Type, but not to give specific parameter values (see Section 15 of *Publication 151* (ICRP, 2022)).

‡For inhaled material deposited in the respiratory tract and subsequently cleared by particle transport to the alimentary tract, the default f_A values for inhaled materials are applied: i.e. the product of f_r for the absorption ype and the f_A value for ingested soluble forms of nickel applicable to the age-group of interest (*e.g.* 0.05 for adults).

§Default Type M is recommended for use in the absence of specific information on which the exposure material can be assigned to an absorption type, e.g. if the form is unknown, or if the form is known but there is no information available on the absorption of that form from the respiratory tract.

¶Activity transferred from systemic compartments into segments of the alimentary tract is assumed to be subject to reabsorption to blood. The default absorption fraction f_A for the secreted activity is the highest value for any form of the radionuclide applicable to the age-group of interest (*e.g.* 0.05 for adults).

12.1.2. Ingestion

12.1.2.1. Adults

(327) Numerous studies have been conducted on the behaviour of ingested nickel. Information is available from studies of human volunteers, accidental and environmental exposure, experimental studies of nickel compounds including citrate, carbonate, oxalate, nitrate, chloride, sulphate, sulphides, metal and oxide in rats, calves and dogs. For details see *Publication 151* (ICRP, 2022). In *Publications 30* (ICRP, 1981) and *67* (ICRP, 1993) an absorption fraction of 0.05 was recommended for all nickel compounds ingested by adults. As indicated in Table 12.3, a value of f_A = 0.05 is adopted here for nickel in drinking water and in food. For ingestion of nickel metal and oxide, lower f_A values of 0.01 and 5×10^{-4} are respectively recommended for adults.

12.1.2.2. Children

(328) Paquet et al (1998) demonstrated an increased absorption of nickel chloride in rats with decreasing age: 1- to 7-d-old neonates absorbed 40 times more nickel than adults. 14-d-old rats absorbed 10 times more than adults and the values for 21-d-old, close to weaning age,

were not significantly different from adults. In *Publications 30* and *67*, an absorption fraction of 0.1 was recommended for infants. In this publication, for soluble forms, unspecified forms and nickel in diet, an f_A = 0.5 is adopted for 3-month-old infants. For nickel metal and oxide, f_A values of 0.1 and 5×10^{-3} respectively are adopted for ingestion by 3-month-old infants. For children of 1 year and older the same f_A values as for adults are recommended.

12.1.3. Systemic distribution, retention and excretion

(329) An updated systemic model for occupational intake of nickel is described in *Publication 151* (ICRP, 2022). Due to a paucity of information on age related changes in the systemic behavior of nickel, that model is applied here to members of the public of ages except that activity is assumed to be removed from trabecular or cortical bone volume to blood at the age-specific rate of turnover of that bone type.

(330) The structure of the model for nickel is shown in Fig. 12.1. Parameter values are given in Table 12.3.

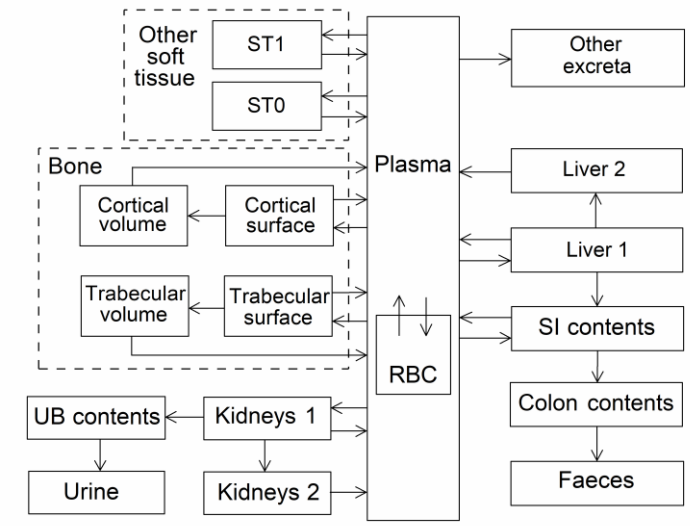

Fig. 12.1. Structure of the model for nickel. UB = urinary bladder, RBC = red blood cells, SI = small intestine. Activity transferred from Plasma to Colon contents enters Right colon contents.

Table 12.3. Transfer coefficients for the model for systemic nickel

Path*	Transfer coefficient (d^{-1})					
	Infant	1 y	5 y	10 y	15 y	Adult
Plasma to Kidneys 1	1.27E+01	1.27E+01	1.27E+01	1.27E+01	1.27E+01	1.27E+01
Plasma to SI contents	1.80E-01	1.80E-01	1.80E-01	1.80E-01	1.80E-01	1.80E-01
Plasma to Liver 1	4.50E-01	4.50E-01	4.50E-01	4.50E-01	4.50E-01	4.50E-01
Plasma to Cort bone surf	6.75E-01	6.75E-01	6.75E-01	6.75E-01	6.75E-01	6.75E-01
Plasma to Trab bone surf	6.75E-01	6.75E-01	6.75E-01	6.75E-01	6.75E-01	6.75E-01
Plasma to ST0	7.20E+00	7.20E+00	7.20E+00	7.20E+00	7.20E+00	7.20E+00
Plasma to ST1	1.20E+00	1.20E+00	1.20E+00	1.20E+00	1.20E+00	1.20E+00
Plasma to RBC	7.50E-02	7.50E-02	7.50E-02	7.50E-02	7.50E-02	7.50E-02
Plasma to Excreta	3.40E-01	3.40E-01	3.40E-01	3.40E-01	3.40E-01	3.40E-01
RBC to Plasma	2.31E-01	2.31E-01	2.31E-01	2.31E-01	2.31E-01	2.31E-01

Kidneys 1 to Plasma	3.50E+01	3.50E+01	3.50E+01	3.50E+01	3.50E+01	3.50E+01
Kidneys 1 to UB contents	1.50E+01	1.50E+01	1.50E+01	1.50E+01	1.50E+01	1.50E+01
Kidneys 1 to Kidneys 2	1.30E-03	1.30E-03	1.30E-03	1.30E-03	1.30E-03	1.30E-03
Kidneys 2 to Plasma	1.73E-03	1.73E-03	1.73E-03	1.73E-03	1.73E-03	1.73E-03
Liver 1 to Plasma	1.90E+00	1.90E+00	1.90E+00	1.90E+00	1.90E+00	1.90E+00
Liver 1 to Liver 2	2.90E-01	2.90E-01	2.90E-01	2.90E-01	2.90E-01	2.90E-01
Liver 1 to SI contents	1.46E+00	1.46E+00	1.46E+00	1.46E+00	1.46E+00	1.46E+00
Liver 2 to Plasma	1.73E-03	1.73E-03	1.73E-03	1.73E-03	1.73E-03	1.73E-03
ST0 to Plasma	1.90E+00	1.90E+00	1.90E+00	1.90E+00	1.90E+00	1.90E+00
ST1 to Plasma	1.73E-03	1.73E-03	1.73E-03	1.73E-03	1.73E-03	1.73E-03
Cort bone surf to Plasma	1.90E+00	1.90E+00	1.90E+00	1.90E+00	1.90E+00	1.90E+00
Cort bone surf to Cort bone vol	1.92E-02	1.92E-02	1.92E-02	1.92E-02	1.92E-02	1.92E-02
Trab bone surf to Plasma	1.90E+00	1.90E+00	1.90E+00	1.90E+00	1.90E+00	1.90E+00
Trab bone surf to Trab bone vol	1.92E-02	1.92E-02	1.92E-02	1.92E-02	1.92E-02	1.92E-02
Cort bone vol to Plasma	8.22E-03	2.88E-03	1.53E-03	9.04E-04	5.21E-04	8.21E-05
Trab bone vol to Plasma	8.22E-03	2.88E-03	1.81E-03	1.32E-03	9.59E-04	4.93E-04

3474 *SI = small intestine, Cort = cortical, Trab = trabecular, surf = surface, vol = volume, UB = urinary bladder

12.2. Dosimetric data for nickel

Table 12.4. Committed effective dose coefficients (Sv Bq^{-1}) for the inhalation or ingestion of ^{59}Ni compounds.

	Effective dose coefficients (Sv Bq^{-1})					
Inhaled gases or vapours	3 mo	1 y	5 y	10 y	15 y	Adult
Nickel carbonyl	1.1E-09	7.3E-10	4.4E-10	2.6E-10	1.8E-10	1.6E-10
Inhaled particulate materials (1 µm AMAD aerosols)						
Type F, Chloride, sulphate, monosulphide, subsulphide	3.9E-10	1.5E-10	8.6E-11	5.1E-11	3.6E-11	3.5E-11
Type M, Nickel metal; all unspecified forms	4.7E-10	3.7E-10	2.0E-10	1.2E-10	8.8E-11	8.1E-11
Type S, Oxide	2.8E-09	2.9E-09	2.1E-09	1.6E-09	1.6E-09	1.6E-09
Ingested materials						
Adult f_A = 0.05, Nickel in diet, soluble and unspecified forms	6.1E-10	5.5E-11	3.2E-11	2.0E-11	1.3E-11	1.1E-11
Adult f_A = 0.01, Nickel metal	1.3E-10	1.6E-11	8.6E-12	5.5E-12	3.4E-12	2.8E-12
Adult f_A = 5.0E-04, Nickel oxide	1.3E-11	6.3E-12	3.0E-12	2.1E-12	1.1E-12	6.7E-13

Table 12.5. Committed effective dose coefficients (Sv Bq^{-1}) for the inhalation or ingestion of ^{63}Ni compounds.

	Effective dose coefficients (Sv Bq^{-1})					
Inhaled gases or vapours	3 mo	1 y	5 y	10 y	15 y	Adult
Nickel carbonyl	3.0E-09	2.1E-09	1.2E-09	7.4E-10	5.0E-10	4.7E-10

Inhaled particulate materials (1 µm AMAD aerosols)						
Type F, Chloride, sulphate, monosulphide, subsulphide	1.1E-09	4.1E-10	2.4E-10	1.4E-10	9.9E-11	9.8E-11
Type M, Nickel metal; all unspecified forms	1.4E-09	1.1E-09	6.2E-10	3.9E-10	2.9E-10	2.7E-10
Type S, Oxide	3.7E-09	6.6E-09	4.7E-09	3.5E-09	3.3E-09	3.4E-09
Ingested materials						
Adult f_A = 0.05, Nickel in diet, soluble and unspecified forms	1.7E-09	1.4E-10	8.0E-11	4.8E-11	3.2E-11	3.0E-11
Adult f_A = 0.01, Nickel metal	3.4E-10	2.7E-11	1.6E-11	9.6E-12	6.4E-12	6.0E-12
Adult f_A = 5.0E-04, Nickel oxide	1.7E-11	1.4E-12	8.1E-13	4.8E-13	3.2E-13	3.0E-13

3479
3480

13. ZINC (Z = 30)

13.1. Routes of Intake

13.1.1. Inhalation

13.1.1.1. Absorption Types and parameter values

(331) Little information was found on the behaviour of inhaled zinc in man. Information on absorption from the respiratory tract is available from experimental studies of several compounds of zinc or associated with corrosion products. For details see Section 9 of *Publication 134* (ICRP, 2016a). Absorption parameter values and Types, and associated f_A values for particulate forms of zinc are given in Table 13.1 (taken from Section 9 of *Publication 134*).

Table 13.1. Absorption parameter values for inhaled and ingested zinc

		Absorption parameter values*		
Inhaled particulate materials		f_r	s_r (d^{-1})	s_s (d^{-1})
Default parameter values†,‡				
Absorption Type	Assigned forms			
F	Oxide, chromate	1	30	–
M§	Nitrate, phosphate	0.2	3	0.005
S	Corrosion products	0.01	3	1×10^{-4}

Ingested materials¶						
Assigned forms	Age-dependent absorption from the alimentary tract, f_A					
	3 months	1 year	5 years	10 years	15 years	adult
All forms	1	0.5	0.5	0.5	0.5	0.5

*It is assumed that for zinc the bound state can be neglected i.e. $f_b = 0$. The values of s_r for Type F, M and S forms of zinc (30, 3 and 3 d^{-1}, respectively) are the general default values.

†Materials (e.g. zinc oxide) are listed here where there is sufficient information to assign to a default absorption Type, but not to give specific parameter values (see Section 9 of *Publication* 134 (ICRP, 2016a)).

‡For inhaled material deposited in the respiratory tract and subsequently cleared by particle transport to the alimentary tract, the default f_A values for inhaled materials are applied: i.e. the product of f_r for the absorption type and the f_A value for ingested soluble forms of zinc applicable to the age-group of interest (*e.g.* 0.5 for adults).

§Default Type M is recommended for use in the absence of specific information on which the exposure material can be assigned to an absorption type, e.g. if the form is unknown, or if the form is known but there is no information available on the absorption of that form from the respiratory tract.

¶Activity transferred from systemic compartments into segments of the alimentary tract is assumed to be subject to reabsorption to blood. The default absorption fraction f_A for the secreted activity is the highest value for ingestion of the radionuclide applicable to the age-group of interest (*e.g.* 0.5 for adults).

13.1.2. Ingestion

13.1.2.1. Adults

(332) Zinc absorption in humans is influenced by numerous factors including fasting, meal composition, the amount of daily dietary zinc and the state of health. Volunteer studies showed gastrointestinal absorption of inorganic zinc of about 0.2, increased to 0.4 - 0.9 in fasting subjects. Tracer studies in which either stable or radioactive zinc isotopes were incorporated

in meals fed to normal adult volunteers have produced individual absorption values ranging up to about 60%, with a value of about 30% being typical (Sandstrom et al., 1989; Sandström et al., 1987; Solomons and Cousins, 1984). It has been suggested that some foods, such as milk and beef may enhance dietary zinc uptake (Evans and Johnson, 1980; Solomons et al., 1982), while bran and phytate reduce it (Sandstrom and Cederblad, 1980; Turnlund et al., 1984). Studies in which human volunteers have ingested crab meat containing ^{65}Zn gave absorption fractions of about 0.15 (ICRP, 1993), and an average value of 0.35 (range 0.25-0.45) was obtained in seven volunteers for ^{65}Zn in fish (Honstead and Brady, 1967). In *Publication 30* (ICRP, 1980), an absorption fraction of 0.5 was recommended for all forms of Zn. The same value was recommended in *Publication 67* (ICRP, 1993) for dietary intakes, although it may be an overestimate for zinc in some foods. An f_A of 0.5 was also recommended in *Publication 134* (ICRP, 2016a) for all chemical forms of zinc. The same f_A = 0.5 is adopted here for dietary forms of zinc ingested by adults.

13.1.2.2.Children

(333) Sullivan *et al.* (1984) showed an increase by a factor 4 in gastrointestinal absorption and tissue retention (67%) in 2-day-old neonatal rats compared with adult rats (16%). Ballou and Thompson (1961) showed that absorption fell abruptly after weaning in rats. Studies by Sherif et al. (1981) with rats showed a progressive decrease of gastrointestinal absorption with age from the weaning period (17-20 days) to 80 days. Ghishan et al. (1982) observed 90% absorption in suckling rats compared with 45% in adolescent rats given $^{65}ZnCl_2$ solution. Similar results have been reported for mice (ICRP, 1993). An absorption fraction of 1 was recommended in *Publication* 67 for 3-month-old infants. For children of 1 year and older the absorption fraction for the adult (0.5) was used in *Publication 67*. The same values are adopted here for f_A.

13.1.3. Systemic Distribution, Retention and Excretion

13.1.3.1.Summary of biokinetic data

(334) Biokinetic data for zinc in adult humans were reviewed in *Publication 134* (ICRP, 2016a). Briefly, 60% or more of absorbed or intravenously injected zinc isotope rapidly accumulates in the liver. High concentrations are also seen in the kidneys and pancreas at early times. The label gradually shifts largely to skeletal muscle and bone, which have low rates of accumulation but extended retention of zinc. Faecal loss is the primary route of endogenous excretion and appears to arise from pancreatic secretions together with smaller losses in liver bile, saliva, and other secretions. External measurements of ^{65}Zn in human subjects following intravenous or oral administration indicate two main components of systemic retention with half-times on the order of 1-3 wk (15-30%) and 300-450 d (70-85%). Biokinetic studies on human subjects have been too short to identify any components of long-term retention that may arise, for example, from binding of zinc to bone mineral (ICRP, 2016a). Results of autopsy studies indicate that muscle contains about 55-65% and bone about 20-30% of zinc in the adult human body.

(335) Griffin et al. (2000) investigated the biokinetics of zinc in 7 healthy girls of age 8-11 y. ^{67}Zn and ^{70}Zn were measured in blood, urine, and faeces over a 6-day period following ingestion of ^{67}Zn and intravenous injection of ^{70}Zn. The data were used to develop transfer coefficients for a first-order compartmental model containing systemic compartments representing plasma, red blood cells, tissues with relatively fast turnover, and tissues with relatively slow turnover. The systemic model was connected to an alimentary tract model

depicting the stomach, small intestine, and colon. The derived mean transfer coefficients and model predictions were compared with those of a previously derived model for adult females based on similar techniques (Lowe et al., 1997). The investigators concluded that the transfer coefficients between plasma and tissue compartments were similar for children and adults except for transfer from plasma to the fast-turnover tissue compartment, which was judged to be significantly higher in children than in adults.

(336) Haumont (1961) examined the distribution of zinc in bones of young adult dogs and immature rats and found elevated concentrations of zinc at sites undergoing calcification. Zinc was detected in the haversian systems of compact bone and in endochondral bone recently deposited in the metaphysis. Following intravenous administration of ^{65}Zn to rats of different ages, the highest activity concentrations were found in liver, kidneys, and pancreas at early times and in bone at late times (Ballou and Thompson, 1961). In rats fed ^{65}Zn by gavage at age 6, 14, 19, 26, 36, or 94 d, the mean content of the femur at 1 d was 0.48, 2.0, 1.8, 1.4, 1.6, and 1.0% of the retained amount (Ballou and Thompson, 1961). Calhoun et al. (1970) observed a significantly increased uptake of intravenously administered ^{65}Zn in healing bones of rats compared with healthy bones of control rats, apparently related to the increased bone formation rate. Bergman et al. (1972) examined the importance of zinc to cell proliferation in endochondral growth sites of bone in white rats using zinc-deficient feeding and autoradiography. The results of the study suggest that zinc is required in bone formation, especially in the synthesis of the organic matrix. Data of Sullivan et al. (1984) for ingestion of ^{65}Zn by rats indicate that the ratio of activity in liver to that in skeleton was not affected by age.

(337) Studies on weanling and 7-week-old mice were conducted to investigate whether bone serves as a reservoir of available zinc (Murray and Messer, 1981). The results indicated that availability of bone zinc depended on the rate of bone resorption. In calcium deficiency there was an increased deposition of zinc in bone, suggesting limited substitution of zinc for calcium in bone mineral.

(338) Bawden and Hammarström (1977) studied the distribution of ^{65}Zn in young rats by autoradiography following intraperitoneal injection. The liver showed a high activity concentration within a few hours. The activity concentration eventually became higher in bone and dentine than in other tissues.

(339) Liu-Sheng et al. (1991) studied the absorption and systemic kinetics of ^{65}Zn in suckling (1-20 d old), adolescent (20-70 d), young adult (70-100 d), and mature adult (>100 d) mice administered a ^{65}Zn solution by stomach tube or intraperitoneal injection. Systemic activity was found mainly in the liver, muscle, lung, kidneys, and bone (femora). The residence time of ^{65}Zn in the total body increased with age. Whole-body retention could be described by a sum of 2-3 exponential terms. Among the studied tissues, bone showed the longest component of retention.

13.1.3.2. Systemic model

(340) The model for systemic zinc applied in *Publication 134* (ICRP, 2016a) to workers is applied here to adult members of the public. The model for adults is modified as follows for application to pre-adult ages: (1) the deposition fractions for trabecular and cortical bone surface are increased by 50% over the adult value for all pre-adult ages, (2) the deposition fraction for intermediate-term soft tissue in the adult is reduced for pre-adult ages to balance the increased deposition on bone surface, and (3) activity is assumed to be removed from trabecular or cortical bone volume to blood at the age-specific rate of turnover of that bone type.

(341) The structure of the model for zinc is shown in Fig. 13.1. Parameter values are given in Table 13.2.

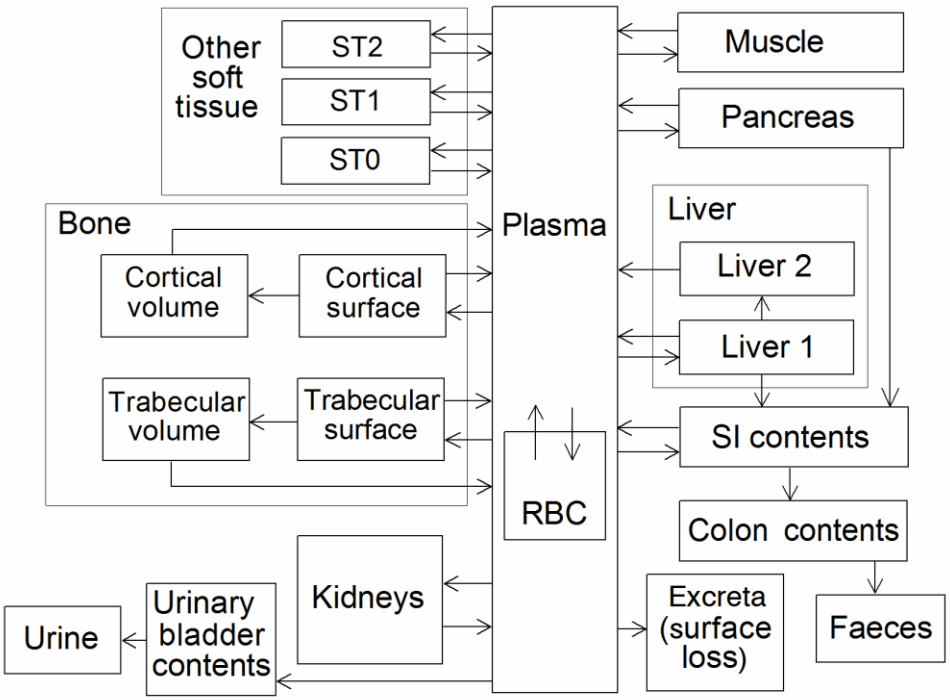

Fig. 13.1. Structure of the systemic model for zinc. RBC = red blood cells; SI = small intestine.

3610 Table 13.2. Transfer coefficients for the model for systemic zinc

Path*	Transfer coefficient (d^{-1})					
	Infant	1 y	5 y	10 y	15 y	Adult
Plasma to Liver 1	6.00E+01	6.00E+01	6.00E+01	6.00E+01	6.00E+01	6.00E+01
Plasma to Kidneys	4.00E+00	4.00E+00	4.00E+00	4.00E+00	4.00E+00	4.00E+00
Plasma to Pancreas	3.00E+00	3.00E+00	3.00E+00	3.00E+00	3.00E+00	3.00E+00
Plasma to Muscle	2.00E+00	2.00E+00	2.00E+00	2.00E+00	2.00E+00	2.00E+00
Plasma to RBC	1.50E+00	1.50E+00	1.50E+00	1.50E+00	1.50E+00	1.50E+00
Plasma to ST0	4.00E+01	4.00E+01	4.00E+01	4.00E+01	4.00E+01	4.00E+01
Plasma to ST1	2.98E+01	2.98E+01	2.98E+01	2.98E+01	2.98E+01	3.00E+01
Plasma to ST2	4.00E-01	4.00E-01	4.00E-01	4.00E-01	4.00E-01	4.00E-01
Plasma to UB contents	1.30E-01	1.30E-01	1.30E-01	1.30E-01	1.30E-01	1.30E-01
Plasma to Excreta	1.30E-01	1.30E-01	1.30E-01	1.30E-01	1.30E-01	1.30E-01
Plasma to SI contents	2.00E-01	2.00E-01	2.00E-01	2.00E-01	2.00E-01	2.00E-01
Plasma to Trab bone surf	2.25E-01	2.25E-01	2.25E-01	2.25E-01	2.25E-01	1.50E-01
Plasma to Cort bone surf	4.50E-01	4.50E-01	4.50E-01	4.50E-01	4.50E-01	3.00E-01
Liver 1 to Plasma	1.00E+01	1.00E+01	1.00E+01	1.00E+01	1.00E+01	1.00E+01
Liver 1 to SI contents	6.70E-02	6.70E-02	6.70E-02	6.70E-02	6.70E-02	6.70E-02
Liver 1 to Liver 2	1.00E+01	1.00E+01	1.00E+01	1.00E+01	1.00E+01	1.00E+01
Liver 2 to Plasma	6.00E-01	6.00E-01	6.00E-01	6.00E-01	6.00E-01	6.00E-01
Kidneys to Plasma	7.00E-01	7.00E-01	7.00E-01	7.00E-01	7.00E-01	7.00E-01
Pancreas to Plasma	1.50E+00	1.50E+00	1.50E+00	1.50E+00	1.50E+00	1.50E+00
Pancreas to SI contents	1.00E+00	1.00E+00	1.00E+00	1.00E+00	1.00E+00	1.00E+00
Muscle to Plasma	5.00E-03	5.00E-03	5.00E-03	5.00E-03	5.00E-03	5.00E-03
RBC to Plasma	1.40E-01	1.40E-01	1.40E-01	1.40E-01	1.40E-01	1.40E-01
ST0 to Plasma	1.00E+01	1.00E+01	1.00E+01	1.00E+01	1.00E+01	1.00E+01
ST1 to Plasma	3.00E+00	3.00E+00	3.00E+00	3.00E+00	3.00E+00	3.00E+00
ST2 to Plasma	1.00E-02	1.00E-02	1.00E-02	1.00E-02	1.00E-02	1.00E-02
Trab bone surf to Plasma	1.00E-02	1.00E-02	1.00E-02	1.00E-02	1.00E-02	1.00E-02
Cort bone surf to Plasma	1.00E-02	1.00E-02	1.00E-02	1.00E-02	1.00E-02	1.00E-02
Trab bone surf to Trab bone vol	5.30E-04	5.30E-04	5.30E-04	5.30E-04	5.30E-04	5.30E-04
Cort bone surf to Cort bone vol	5.30E-04	5.30E-04	5.30E-04	5.30E-04	5.30E-04	5.30E-04
Trab bone vol to Plasma	8.22E-03	2.88E-03	1.81E-03	1.32E-03	9.59E-04	4.93E-04
Cort bone vol to Plasma	8.22E-03	2.88E-03	1.53E-03	9.04E-04	5.21E-04	8.21E-05

3611 *RBC = red blood cells, UB = Urinary bladder, Trab = trabecular, Cort = cortical, surf = surface, vol = volume,
3612 SI = Small intestine

13.2. Dosimetric data for zinc

Table 13.3. Committed effective dose coefficients (Sv Bq^{-1}) for the inhalation or ingestion of ^{65}Zn compounds.

	Effective dose coefficients (Sv Bq^{-1})					
Inhaled particulate materials (1 µm AMAD aerosols)	3 mo	1 y	5 y	10 y	15 y	Adult
Type F, Oxide, chromate	2.4E-08	1.1E-08	6.1E-09	4.0E-09	2.8E-09	2.7E-09
Type M, Nitrate, phosphate; all unspecified compounds	1.1E-08	6.7E-09	4.0E-09	2.7E-09	2.0E-09	2.1E-09
Type S, Corrosion products	9.4E-09	8.5E-09	5.2E-09	3.6E-09	2.8E-09	3.2E-09
Ingested materials						
Adult f_A = 0.5, All forms	4.7E-08	1.5E-08	9.5E-09	6.2E-09	4.6E-09	4.3E-09

14.SELENIUM (Z = 34)

14.1.Routes of Intake

14.1.1. Inhalation

14.1.1.1.Absorption Types and Parameter Values

(342) No information was found on the behaviour of inhaled selenium in man. Information on absorption of selenium from the respiratory tract is available from experimental studies of forms of selenium including selenious acid (H_2SeO_3) and elemental selenium, which were conducted mainly to investigate the potential health hazard of selenium emitted during fossil fuel combustion. For details see Section 20 of *Publication* 151 (ICRP, 2022).

(343) Absorption parameter values and Types, and associated f_A values for particulate forms of selenium are given in Table 14.1 (taken from Section 20 of *Publication* 151).

Table 14.1. Absorption parameter values for inhaled and ingested selenium

		Absorption parameter values*		
Inhaled particulate materials		f_r	s_r (d^{-1})	s_s (d^{-1})
Default parameter values†,‡				
Absorption type	Assigned forms			
F	Selenium dioxide, selenious acid, elemental selenium	1	30	–
M§	—	0.2	3	0.005
S	—	0.01	3	0.0001

Ingested materials¶	Age-dependent absorption from the alimentary tract, f_A					
Assigned forms	3 months	1 year	5 years	10 years	15 years	adults
selenium in diet	1	0.8	0.8	0.8	0.8	0.8

*It is assumed that for selenium the bound state can be neglected *i.e.* $f_b = 0$. The value of s_r for Type F (30 d^{-1}) is element-specific. The values for types M and S (3 d^{-1}) are the general default values.

†Materials (*e.g.* selenium dioxide) are generally listed here where there is sufficient information to assign to a default absorption Type, but not to give specific parameter values (see Section 20 of ICRP, 2021).

‡For inhaled material deposited in the respiratory tract and subsequently cleared by particle transport to the alimentary tract, the default f_A values for inhaled materials are applied: *i.e.*, the product of f_r for the absorption type and the f_A value for ingested soluble forms of selenium applicable to the age-group of interest (*e.g.* 0.8 for adults).

§Default Type M is recommended for use in the absence of specific information on which the exposure material can be assigned to an absorption type, e.g. if the form is unknown, or if the form is known but there is no information available on the absorption of that form from the respiratory tract.

¶Activity transferred from systemic compartments into segments of the alimentary tract is assumed to be subject to reabsorption to blood. The default absorption fraction f_A for the secreted activity is the highest value for ingestion of the radionuclide applicable to the age-group of interest (*e.g.* 0.8 for adults).

14.1.2. Ingestion

14.1.2.1.Adults

(344) The behaviour of dietary selenium has been studied in balance studies, stable isotope and radiotracer human volunteer experiments. The gastrointestinal absorption of some other organic and inorganic forms of selium has also been evaluated in humans, monkeys, rats, mice and dogs. For details, see Section 20 of *Publication* 151 (ICRP, 2022). A f_A value = 0.8 is adopted here for ingestion of selenium in diet by adult members of the public.

14.1.2.2.Children

(345) Limited data are available on the absorption of selenium in young animals. Nishimura et al. (1991) reported that in 6-d-old rats given ^{75}Se as selenite, fractional absorption was much greater than in adults (> 0.6). In 14-d-old rats intermediate values were obtained. Like in *Publication* 69 (ICRP, 1995a), the same f_A value as is adopted for adults (0.8) is used here for l-, 5-, l0-, and 15-y-old children. For 3-mo-old infants an f_A of 1 is adopted.

14.1.3. Systemic Distribution, Retention and Excretion

(346) No information was found on age related changes in the systemic kinetics of selenium. An updated systemic biokinetic model for occupational intake of selenium is described in Section 20 of *Publication* 151 (ICRP, 2022). That model is applied here to intake of selenium at any age.

(347) The model structure is shown in Fig. 14.1. The transfer coefficients are listed in Table 14.2.

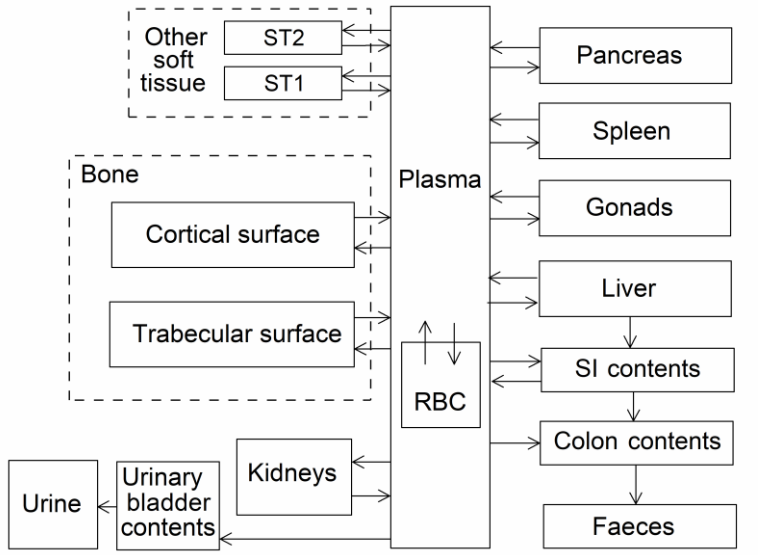

Fig. 14.1. Structure of the model for systemic selenium. Activity transferred from Plasma to Colon contents enters Right colon contents. SI = Small intestine.

Table 14.2. Transfer coefficients for the model for systemic selenium

Path[a]	Transfer coefficient (d^{-1})					
	Infant	1 y	5 y	10 y	15 y	Adult
Plasma to Liver	1.20E+00	1.20E+00	1.20E+00	1.20E+00	1.20E+00	1.20E+00
Plasma to Kidneys	6.00E-01	6.00E-01	6.00E-01	6.00E-01	6.00E-01	6.00E-01
Plasma to Pancreas	8.00E-02	8.00E-02	8.00E-02	8.00E-02	8.00E-02	8.00E-02
Plasma to Spleen	1.10E-01	1.10E-01	1.10E-01	1.10E-01	1.10E-01	1.10E-01
Plasma to Testes	4.00E-02	4.00E-02	4.00E-02	4.00E-02	4.00E-02	4.00E-02

Plasma to Ovaries	1.30E-02	1.30E-02	1.30E-02	1.30E-02	1.30E-02	1.30E-02
Plasma to ST1	5.20E+00	5.20E+00	5.20E+00	5.20E+00	5.20E+00	5.20E+00
Plasma to ST2	5.00E-01	5.00E-01	5.00E-01	5.00E-01	5.00E-01	5.00E-01
Plasma to UB contents	1.00E+00	1.00E+00	1.00E+00	1.00E+00	1.00E+00	1.00E+00
Plasma to RC contents	4.00E-01	4.00E-01	4.00E-01	4.00E-01	4.00E-01	4.00E-01
Plasma to Trab bone surf	2.00E-01	2.00E-01	2.00E-01	2.00E-01	2.00E-01	2.00E-01
Plasma to Cort bone surf	2.00E-01	2.00E-01	2.00E-01	2.00E-01	2.00E-01	2.00E-01
Plasma to RBC	5.00E-01	5.00E-01	5.00E-01	5.00E-01	5.00E-01	5.00E-01
Liver to Plasma	8.00E-02	8.00E-02	8.00E-02	8.00E-02	8.00E-02	8.00E-02
Kidneys to Plasma	8.00E-02	8.00E-02	8.00E-02	8.00E-02	8.00E-02	8.00E-02
Spleen to Plasma	8.00E-02	8.00E-02	8.00E-02	8.00E-02	8.00E-02	8.00E-02
Pancreas to Plasma	8.00E-02	8.00E-02	8.00E-02	8.00E-02	8.00E-02	8.00E-02
Testes to Plasma	8.00E-02	8.00E-02	8.00E-02	8.00E-02	8.00E-02	8.00E-02
Ovaries to Plasma	8.00E-02	8.00E-02	8.00E-02	8.00E-02	8.00E-02	8.00E-02
ST1 to Plasma	8.00E-02	8.00E-02	8.00E-02	8.00E-02	8.00E-02	8.00E-02
ST2 to Plasma	5.00E-03	5.00E-03	5.00E-03	5.00E-03	5.00E-03	5.00E-03
RBC to Plasma	3.50E-02	3.50E-02	3.50E-02	3.50E-02	3.50E-02	3.50E-02
Trab bone surf to Plasma	1.50E-02	1.50E-02	1.50E-02	1.50E-02	1.50E-02	1.50E-02
Cort bone surf to Plasma	1.50E-02	1.50E-02	1.50E-02	1.50E-02	1.50E-02	1.50E-02

[a]UB = urinary bladder, RC = right colon, Trab = trabecular, Cort = cortical, RBC = red blood cells, surf = surface

14.2. Dosimetric data for selenium

Table 14.3. Committed effective dose coefficients (Sv Bq^{-1}) for the inhalation or ingestion of ^{75}Se compounds.

	Effective dose coefficients (Sv Bq^{-1})					
Inhaled particulate materials (1 µm AMAD aerosols)	3 mo	1 y	5 y	10 y	15 y	Adult
Type F, Selenium dioxide, selenious acid, elemental selenium	8.4E-09	6.1E-09	3.3E-09	2.3E-09	1.2E-09	1.2E-09
Type M, All unspecified forms	5.2E-09	4.2E-09	2.4E-09	1.7E-09	1.1E-09	1.2E-09
Type S	5.7E-09	5.0E-09	2.9E-09	2.0E-09	1.5E-09	1.7E-09
Ingested materials						
Adult f_A = 0.8, Selenium in diet	1.6E-08	1.1E-08	6.6E-09	4.6E-09	2.7E-09	2.5E-09

Table 14.4. Committed effective dose coefficients (Sv Bq^{-1}) for the inhalation or ingestion of ^{79}Se compounds.

	Effective dose coefficients (Sv Bq^{-1})					
Inhaled particulate materials (1 µm AMAD aerosols)	3 mo	1 y	5 y	10 y	15 y	Adult
Type F, Selenium dioxide, selenious acid, elemental selenium	1.4E-08	9.9E-09	5.3E-09	3.5E-09	1.2E-09	9.2E-10
Type M, All unspecified forms	8.5E-09	6.9E-09	4.0E-09	2.6E-09	1.6E-09	1.4E-09
Type S	2.7E-08	2.7E-08	1.9E-08	1.5E-08	1.4E-08	1.4E-08
Ingested materials						
Adult f_A = 0.8, Selenium in diet	2.7E-08	1.7E-08	1.0E-08	7.0E-09	2.7E-09	1.9E-09

15. STRONTIUM (Z = 38)

15.1. Routes of Intake

15.1.1. Inhalation

(348) Some information is available on the behaviour of inhaled strontium in man following accidental intakes of several compounds. Information on absorption from the respiratory tract is available from experimental studies of strontium as chloride, sulphate, titanate, irradiated fuel fragments, or in fused aluminosilicate particles (FAP) and polystyrene (PSL). For details see Section 10 of of *Publication 134* (ICRP, 2016a).

(349) Absorption parameter values and types, and associated f_A values for particulate forms of strontium are given in Table 15.1 (taken from Section 10 of *Publication 134*).

Table 15.1. Absorption parameter values for inhaled and ingested strontium

		Absorption parameter values*		
Inhaled particulate materials		f_r	s_r (d^{-1})	s_s (d^{-1})
Default parameter values†,‡				
Absorption Type	Assigned forms			
F	Chloride, sulphate and carbonate	1	30	–
M§	Fuel fragments	0.2	3	0.005
S	FAP, PSL, Strontium titanate	0.01	3	1×10^{-4}

Ingested material¶	Age-dependent absorption from the alimentary tract, f_A					
Assigned forms	3 months	1 year	5 years	10 years	15 years	adult
Strontium in diet and in soluble forms	0.6	0.4	0.4	0.4	0.4	0.25
Insoluble forms (assigned as type S)	0.02	0.01	0.01	0.01	0.01	0.01

*It is assumed that for strontium the bound state can be neglected i.e. $f_b = 0$. The values of s_r for Type F, M and S forms of strontium (30, 3 and 3 d^{-1}, respectively) are the general default values.

†Materials (e.g. chloride) are generally listed here where there is sufficient information to assign to a default absorption Type, but not to give specific parameter values (see Section 10 of *Publication 134* (ICRP, 2016a)).

‡For inhaled material deposited in the respiratory tract and subsequently cleared by particle transport to the alimentary tract, the default f_A values for inhaled materials are applied: i.e. the product of f_r for the absorption type and the f_A value for ingested soluble forms of strontium applicable to the age-group of interest (*e.g.* 0.25 for adults).

§Default Type M is recommended for use in the absence of specific information on which the exposure material can be assigned to an absorption type, e.g. if the form is unknown, or if the form is known but there is no information available on the absorption of that form from the respiratory tract.

¶Activity transferred from systemic compartments into segments of the alimentary tract is assumed to be subject to reabsorption to blood. The default absorption fraction f_A for the secreted activity is the highest value for ingestion of the radionuclide applicable to the age-group of interest (*e.g.* 0.25 for adults).

15.1.2. Ingestion

15.1.2.1. Adults

(350) Due to the presence of strontium isotopes in fall-out material and its long-term retention in bone as a calcium analogue, the metabolism of strontium has been the subject of a number of human volunteer studies. Similar fractional absorption values, typically in the range 0.1 – 0.4 (Harrison et al., 2001) with a central value around 0.2, were obtained from studies in which inorganic forms of radiostrontium was administered orally in solution and from experiments where known quantities of radiostrontium incorporated in food were ingested. An exception was strontium titanate ($SrTiO_3$) which shows low levels of absorption of about 0.01. A number of factors have been found to increase strontium absorption, including fasting, low dietary levels of calcium, magnesium and phosphorus, milk diets and vitamin D. By contrast, sex, age at exposure in adult groups, smoking, exercise or use of oral contraceptives in young females do not seem to significantly change the intestinal absorption of strontium. Radioactive strontium has been shown to accumulate in teeth. Most of this deposit comes from gastrointestinal absorption and subsequent systemic distribution but a small part may also be adsorbed directly from the oral cavity onto the dental plaque and enamel during mastication. Unfortunately not enough information is available to derive robust parameters for Sr adsorption and retention on teeth. (For more details see Section 10 of *Publication 134*, ICRP, 2016a). In *Publication 30* (ICRP, 1979), the recommended absorption values were 0.01 for $SrTiO_3$ and 0.3 for all other compounds. In *Publication 67* (ICRP, 1993), a value of 0.3 was recommended for dietary intakes by adults. Due to the strong link between strontium and calcium absorption and the known discrimination in favour of calcium, a default f_A value of 0.25 was recommended in *Publication 134* for all chemical forms but strontium titanate. The same value of 0.25 for f_A is adopted here for adults and for strontium in food and in other soluble forms. For ingestion of strontium titanate and other type S forms, an f_A of 0.01is adopted.

15.1.2.2.Children

(351) Results obtained by Widdowson et al. (1960) suggest that absorption of strontium in 7-day-old infants fed with cows' milk is greater than 73%. Bedford et al. (1960) reported that absorption in 5-15-year-old children was the same as in adults. However, studies on beagles and rats have shown that the period of increased absorption of strontium extends beyond the time of weaning. In the beagle, retention values for strontium at 3-9 days after ingestion were 20%, 15% and 8% in 48-, 80- and 140-day-old animals, respectively (Della Rosa et al., 1965). The absorption of strontium in 35- and 75-day-old rats was estimated as 70-90% by Gran (1960) compared with 12% in 270-day-old rats. Taylor et al. (1962) obtained absorption values of 0.95±0.004 (standard error, n = 31) for 14–18-day-old rats and 0.74 ± 0.024 (standard error, n = 5) for 22-day-old animals. A value of 0.6 was recommended in *Publication 67* for infants. For ages 1-15 years a value of 0.4 was chosen in *Publication 67*, based on the consideration that there may be elevated absorption of strontium throughout the period of growth. Harrison et al. (2001) proposed confidence intervals of 0.1–0.5 for 10-year-old children, and 0.15–0.75 for 3-month-old infants. The values of f_A 0.6 for 3-month-old infants and 0.4 for ages 1-15 years are adopted here. For ingestion of strontium titanate and other type S forms by 3-month-old infants, an f_A of 0.02 is adopted.

15.1.3. Systemic Distribution, Retention and Excretion

15.1.3.1.Age-specific data

(352) Strontium is a chemical and physiological analogue of calcium but has somewhat different biokinetics from calcium due to discrimination between these elements by biological membranes and hydroxyapatite crystals of bone. For example, strontium is less effectively

absorbed from the intestines and more effectively excreted by the kidney than calcium and is lost from bone at a higher rate than calcium over the first few months after deposition in bone (Bauer et al. 1955, Spencer et al. 1960, Barnes et al. 1961, Cohn et al. 1963, Decker et al. 1964, Harrison et al. 1967).

(353) The biokinetics of strontium has been studied extensively in human subjects and laboratory animals. Differences with age in the systemic behavior of strontium in humans are reasonably well understood from studies of the uptake and retention of environmental ^{90}Sr in persons of all ages; control studies of the fate of strontium isotopes in humans and laboratory animals at different stages of life; and comparison with age-specific data for chemical and physiological analogues of strontium.

(354) A large database related to the transfer of ^{90}Sr from food and milk to the human skeleton was developed in the 1950s and 1960s (Fig. 15.1). Interpretation of the environmental data with regard to systemic biokinetics is complicated by the gradual accumulation of ^{90}Sr in the body and uncertainties in the level of uptake of ingestion ^{90}Sr to blood at any age. More easily interpreted age-specific human data are available from controlled human studies (Fig. 15.2), but such data are limited for children and generally involved unhealthy children. Age-specific data on retention of strontium in laboratory animals, particular beagles (Fig. 15.3), help to clarify the behavior of strontium at early times after intake as well as relative patterns of buildup and decline of strontium in bone at different stages of bone development. Because strontium is a close physiological analogue of calcium, data from controlled studies of calcium in humans provide supporting information for selection of age-specific parameter values for strontium.

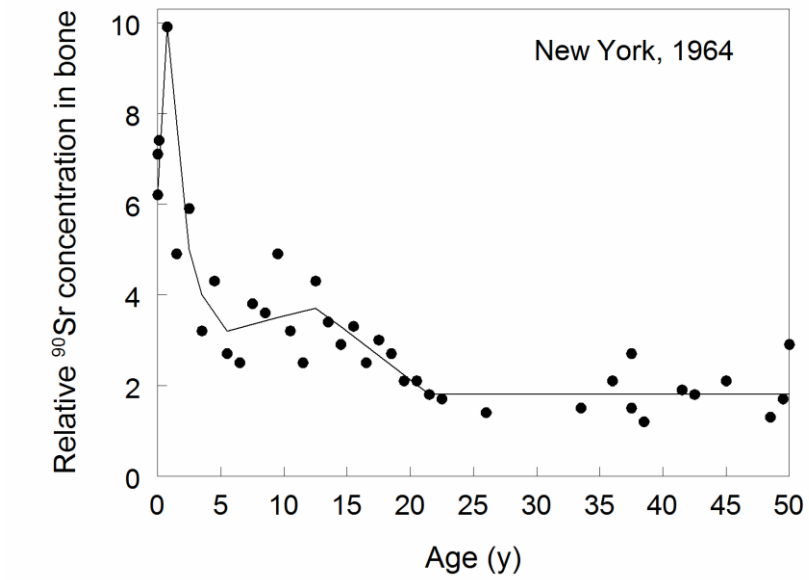

Fig. 15.1. Observed differences with age in the concentration of ^{90}Sr in bone in persons exposed to environmental ^{90}Sr from fallout (after Leggett et al., 1982).

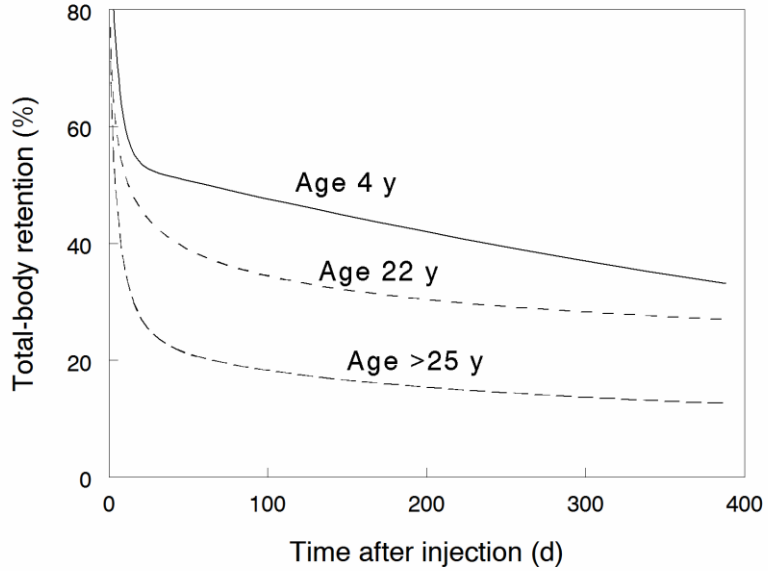

Fig. 15.2. Observed differences with age in total-body retention of strontium as a function of time after intravenous injection (after Leggett, 1992a; data collected from several sources).

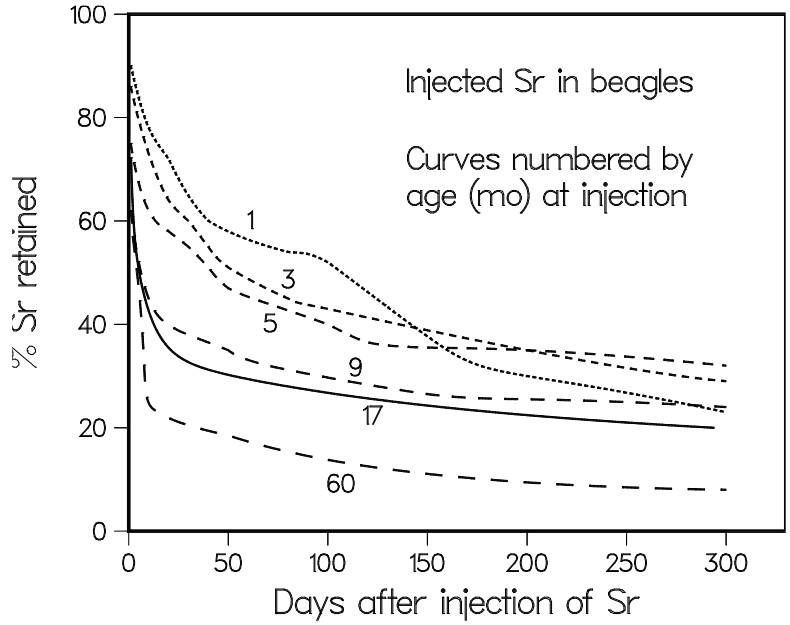

Fig. 15.3. Observed differences with age in total-body retention of strontium in dogs as a function of time after intravenous injection. Figure from (Leggett, 1992a); data collected from several studies.

15.1.4. Systemic model

(355) A number of age-specific biokinetic models for strontium have been developed (Aarkrog, 1971; Bennett, 1975; Harley, 1966; ICRP, 1990, 1993; Kulp and Schulert, 1962; Leggett, 1992a; Leggett et al., 1982; Papworth and Vennart, 1984; Rivera, 1967; Shagina et al., 2003, 2015). Although different conceptual frameworks have been used, the various models

yield broadly consistent estimates with regard to accumulation and retention of ingested strontium in bone, the dominant repository for systemic strontium.

(356) The systemic model adopted in *Publication 67* (ICRP, 1993) is applied in this report. The model structure is shown in Fig. 15.4. Transfer coefficients are listed in Table 15.2.

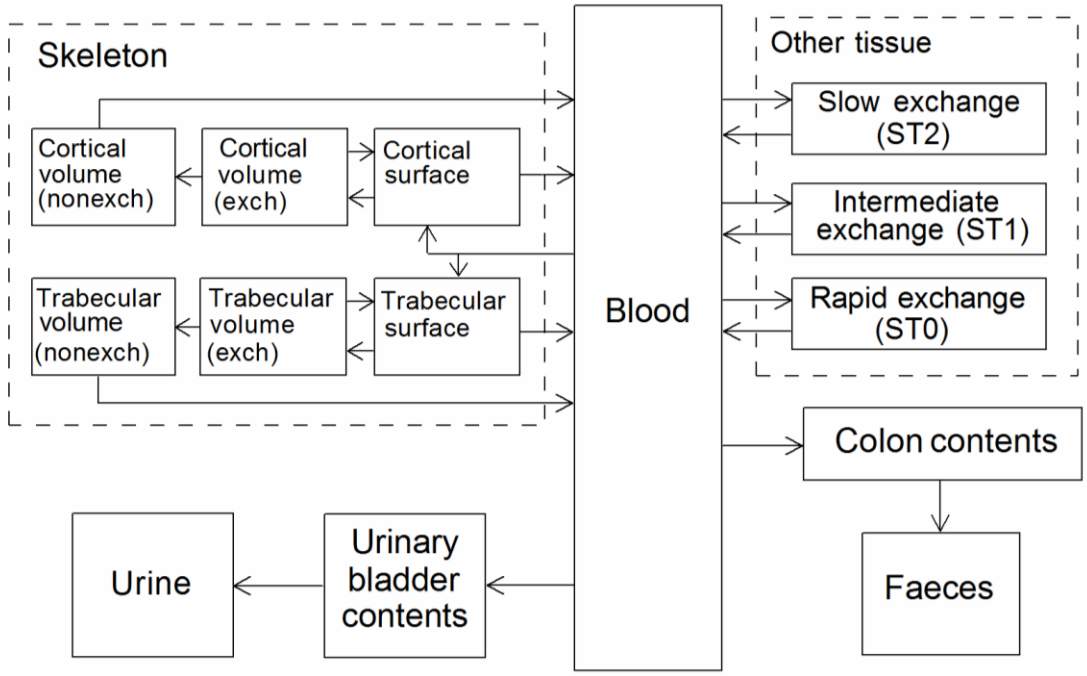

Fig. 15.4. Structure of the biokinetic model for systemic strontium. Abbreviations: exch = exchangeable, nonexch = non-exchangeable. Activity transferred from Blood to Colon contents enters Right colon contents.

3800 Table 15.2. Age-specific transfer coefficients for strontium

	Transfer coefficient (d^{-1})					
Pathway	100 d	1 y	5 y	10 y	15 y	Adult
Blood to UB contents	5.77E-01	1.27E+00	1.38E+00	1.02E+00	6.00E-01	1.73E+00
Blood to Right colon contents	1.75E-01	3.85E-01	4.20E-01	3.08E-01	1.82E-01	5.25E-01
Blood to Trabecular bone surf	2.25E+00	1.35E+00	1.33E+00	2.12E+00	3.10E+00	2.08E+00
Blood to Cortical bone surf	9.00E+00	5.40E+00	4.67E+00	6.28E+00	8.00E+00	1.67E+00
Blood to ST0	2.50E+00	5.50E+00	6.00E+00	4.40E+00	2.60E+00	7.50E+00
Blood to ST1	5.00E-01	1.10E+00	1.20E+00	8.80E-01	5.20E-01	1.50E+00
Blood to ST2	1.00E-03	2.20E-03	2.40E-03	1.80E-03	1.00E-03	3.00E-03
Trabecular bone surf to Blood	6.01E-01	6.01E-01	6.01E-01	6.01E-01	6.01E-01	5.78E-01
Trab bone surf to Exch trab bone vol	9.24E-02	9.24E-02	9.24E-02	9.24E-02	9.24E-02	1.16E-01
Cort bone surf to Blood	6.01E-01	6.01E-01	6.01E-01	6.01E-01	6.01E-01	5.78E-01
Cort bone surf to Exch cort bone vol	9.24E-02	9.24E-02	9.24E-02	9.24E-02	9.24E-02	1.16E-01
ST0 to Blood	8.33E-01	1.83E+00	2.00E+00	1.47E+00	8.67E-01	2.50E+00
ST1 to Blood	1.16E-01	1.16E-01	1.16E-01	1.16E-01	1.16E-01	1.16E-01
ST2 to Blood	3.80E-04	3.80E-04	3.80E-04	3.80E-04	3.80E-04	3.80E-04
Exch trab bone vol to trab bone surf	4.30E-03	4.30E-03	4.30E-03	4.30E-03	4.30E-03	4.30E-03
Exch to Non-exch trab bone vol	4.30E-03	4.30E-03	4.30E-03	4.30E-03	4.30E-03	4.30E-03
Exch cort bone vol to cort bone surf	4.30E-03	4.30E-03	4.30E-03	4.30E-03	4.30E-03	4.30E-03
Exch to Non-exch cort bone vol	4.30E-03	4.30E-03	4.30E-03	4.30E-03	4.30E-03	4.30E-03
Non-exch cort bone vol to Blood	8.22E-03	2.88E-03	1.53E-03	9.04E-04	5.21E-04	8.21E-05
Non-exch trab bone vol to Blood	8.22E-03	2.88E-03	1.81E-03	1.32E-03	9.59E-04	4.93E-04

3801

15.2. Dosimetric data for strontium

Table 15.3. Committed effective dose coefficients (Sv Bq^{-1}) for the inhalation or ingestion of ^{85}Sr compounds.

	Effective dose coefficients (Sv Bq^{-1})					
Inhaled particulate materials (1 µm AMAD aerosols)	3 mo	1 y	5 y	10 y	15 y	Adult
Type F, Chloride, sulphate and carbonate	4.0E-09	1.7E-09	8.2E-10	6.8E-10	6.2E-10	2.7E-10
Type M, Fuel fragments; all unspecified forms	3.6E-09	2.6E-09	1.5E-09	1.0E-09	8.0E-10	7.9E-10
Type S, FAP, PSL, Strontium titanate	4.3E-09	3.6E-09	2.1E-09	1.4E-09	1.1E-09	1.2E-09
Ingested materials						
Adult f_A = 0.01, Insoluble forms (assigned as Type S)	1.0E-09	8.2E-10	4.6E-10	3.3E-10	2.4E-10	2.1E-10
Adult f_A = 0.25, Strontium in diet and in soluble forms	6.4E-09	2.3E-09	1.3E-09	1.0E-09	9.7E-10	3.8E-10

Table 15.4. Committed effective dose coefficients (Sv Bq^{-1}) for the inhalation or ingestion of ^{89}Sr compounds.

	Effective dose coefficients (Sv Bq^{-1})					
Inhaled particulate materials (1 µm AMAD aerosols)	3 mo	1 y	5 y	10 y	15 y	Adult
Type F, Chloride, sulphate and carbonate	2.4E-08	9.3E-09	3.2E-09	2.0E-09	2.3E-09	7.0E-10
Type M, Fuel fragments; all unspecified forms	2.1E-08	1.6E-08	8.5E-09	5.6E-09	4.6E-09	4.0E-09
Type S, FAP, PSL, Strontium titanate	2.5E-08	2.1E-08	1.2E-08	8.1E-09	6.3E-09	6.1E-09
Ingested materials						
Adult f_A = 0.01, Insoluble forms (assigned as Type S)	3.1E-09	1.8E-09	1.1E-09	7.4E-10	5.1E-10	4.0E-10
Adult f_A = 0.25, Strontium in diet and in soluble forms	3.7E-08	1.1E-08	4.7E-09	3.0E-09	3.5E-09	8.9E-10

Table 15.5. Committed effective dose coefficients (Sv Bq^{-1}) for the inhalation or ingestion of ^{90}Sr compounds.

	Effective dose coefficients (Sv Bq^{-1})					
Inhaled particulate materials (1 µm AMAD aerosols)	3 mo	1 y	5 y	10 y	15 y	Adult
Type F, Chloride, sulphate and carbonate	2.4E-07	9.2E-08	4.2E-08	6.1E-08	9.5E-08	2.5E-08
Type M, Fuel fragments; all unspecified forms	1.4E-07	9.9E-08	5.6E-08	5.0E-08	5.9E-08	3.2E-08
Type S, FAP, PSL, Strontium titanate	6.0E-07	6.2E-07	4.8E-07	3.9E-07	4.0E-07	4.1E-07
Ingested materials						
Adult f_A = 0.01, Insoluble forms (assigned as Type S)	1.3E-08	3.5E-09	1.9E-09	2.4E-09	3.6E-09	1.1E-09
Adult f_A = 0.25, Strontium in diet and in soluble forms	3.7E-07	1.1E-07	5.6E-08	8.2E-08	1.3E-07	2.4E-08

16. YTTRIUM (Z = 39)

16.1. Routes of Intake

16.1.1. Inhalation

(357) Information on absorption from the respiratory tract is available from experimental studies of yttrium mainly as chloride or in fused aluminosilicate particles (FAP). For details see Section 11 of *Publication 134* (ICRP, 2016a). Absorption parameter values and types, and associated f_A values for particulate forms of yttrium are given in Table 16.1 (taken from Section 11 of *Publication 134*).

Table 16.1. Absorption parameter values for inhaled and ingested yttrium

		Absorption parameter values*		
Inhaled particulate materials		f_r	s_r (d^{-1})	s_s (d^{-1})
Default parameter values†,‡				
Absorption Type	Assigned forms			
F	Chloride	1	1	–
M§	Oxide, phosphate	0.2	1	0.005
S	FAP	0.01	1	1×10^{-4}

Ingested material¶	Age-dependent absorption from the alimentary tract, f_A					
Assigned forms	3 months	1 year	5 years	10 years	15 years	adult
All chemical forms	1×10^{-3}	5×10^{-4}	5×10^{-4}	5×10^{-4}	5×10^{-4}	1×10^{-4}

*It is assumed that for yttrium the bound state can be neglected i.e. $f_b = 0$. The values of s_r for Type F, M and S forms of yttrium (1 d^{-1}, respectively) are element-specific.

†Materials (e.g. Chloride) are listed here where there is sufficient information to assign to a default absorption type, but not to give specific parameter values (see Section 11 of *Publication 134*, ICRP, 2016a).

‡For inhaled material deposited in the respiratory tract and subsequently cleared by particle transport to the alimentary tract, the default f_A values for inhaled materials are applied: i.e. the product of fr for the absorption type and the f_A value for ingested soluble forms of yttrium applicable to the age-group of interest (*e.g.* 1×10^{-4} for adults).

§Default Type M is recommended for use in the absence of specific information on which the exposure material can be assigned to an absorption type, e.g. if the form is unknown, or if the form is known but there is no information available on the absorption of that form from the respiratory tract.

¶Activity transferred from systemic compartments into segments of the alimentary tract is assumed to be subject to reabsorption to blood. The default absorption fraction f_A for the secreted activity is the highest value for ingestion of the radionuclide applicable to the age-group of interest (*e.g.* 1×10^{-4} for adults).

16.1.2. Ingestion

16.1.2.1. Adults

(358) There is little information on absorption of ingested yttrium but it appears to be very low. In *Publications 30* and *134* (ICRP, 1987, 2016a) an absorption fraction of 1×10^{-4} was recommended. The same f_A value of 1×10^{-4} is adopted here for all chemical forms ingested by adult members of the public.

16.1.2.2. Children

(359) Consistently with the approach of *Publication 56* (ICRP, 1990), an $f_A = 10^{-3}$ is adopted here for 3 month old infants and an intermediate value of 5×10^{-4} is adopted here for 3 month old infants to 15 year old children.

16.1.3. Systemic Distribution, Retention and Excretion

16.1.3.1. Biokinetic model for systemic yttrium

(360) The model for systemic yttrium applied in *Publication 134* (ICRP, 2016a) to workers is applied here to adult members of the public. That model is based on results of a controlled study of retention and excretion of intravenously administered ^{88}Y in healthy human subjects, supplemented with results of biokinetic studies of yttrium isotopes in laboratory animals.

(361) Yttrium is considered a bone seeker and by analogy with more extensively studied bone seekers is expected to have higher deposition in growing bone than in mature bone. Studies on laboratory animals indicate, however, that changes with age in uptake by bone may be less pronounced for yttrium than for some bone seekers such as strontium or lead (MacDonald et al., 1952; Stevenson, 1975).

(362) In the age-specific model for yttrium applied in this report, fractional deposition of yttrium in bone is assumed to be 50% higher in infants than in adults (i.e., the deposition fraction in bone is assumed to be 0.6 in infants compared with 0.4 in adults) and 25% higher in persons of age 1-15 y than in adults. Bone deposits are assumed to be equally divided between trabecular and cortical bone surfaces. The skeletal behaviour of yttrium deposited on bone surfaces is described by the generic model for bone-surface-seekers (Annex B of ICRP, 2015), except that yttrium biologically removed from bone is assumed to return to blood rather than to be channeled through bone marrow.

(363) For a given pre-adult age the deposition fractions for soft tissues and excretion pathways are reduced from the adult value to account for elevated competition for circulating yttrium from bone surfaces at the pre-adult age. The deposition fraction for a soft-tissue or excretion pathway at a given pre-adult age is the value for the adult multiplied by the ratio (1-B)/(1-A) where A and B are fractional depositions in bone in the adult and the given pre-adult age, respectively.

(364) The structure of the model for systemic yttrium is shown in Fig. 16.1. Parameter values are given in Table 16.2.

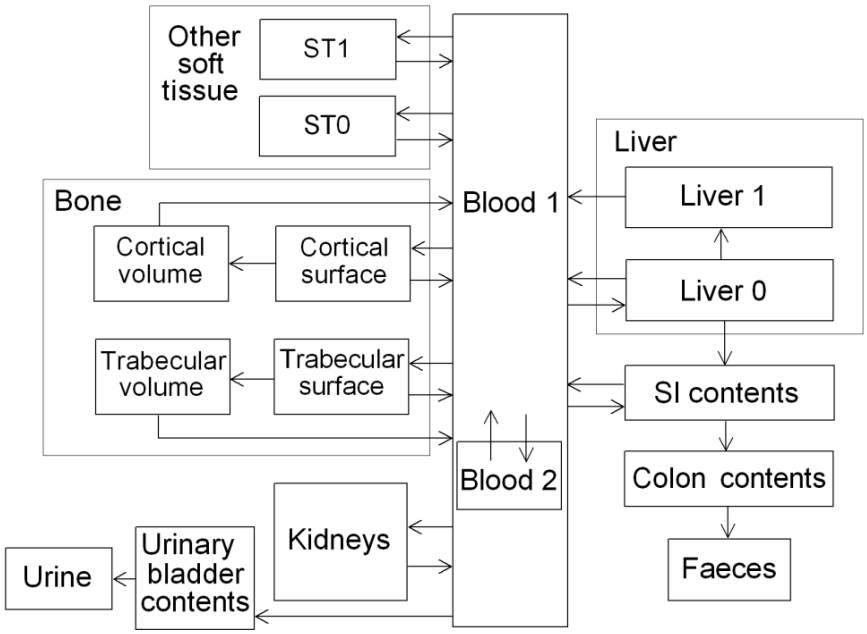

Fig. 16.1. Structure of the biokinetic model for systemic yttrium. SI = Small intestine.

3875 Table 16.2. Transfer coefficients for the model for systemic yttrium

Path[a]	Transfer coefficient (d^{-1})					
	Infant	1 y	5 y	10 y	15 y	Adult
Blood 1 to Blood 2	3.32E-01	4.15E-01	4.15E-01	4.15E-01	4.15E-01	4.98E-01
Blood 1 to Liver 0	1.11E+00	1.38E+00	1.38E+00	1.38E+00	1.38E+00	1.66E+00
Blood 1 to Kidneys	1.11E-01	1.38E-01	1.38E-01	1.38E-01	1.38E-01	1.66E-01
Blood 1 to ST0	2.43E+00	3.04E+00	3.04E+00	3.04E+00	3.04E+00	3.65E+00
Blood 1 to ST1	8.85E-01	1.11E+00	1.11E+00	1.11E+00	1.11E+00	1.33E+00
Blood 1 to UB contents	1.66E+00	2.08E+00	2.08E+00	2.08E+00	2.08E+00	2.49E+00
Blood 1 to SI contents	1.11E-01	1.38E-01	1.38E-01	1.38E-01	1.38E-01	1.66E-01
Blood 1 to Trab bone surf	4.98E+00	4.15E+00	4.15E+00	4.15E+00	4.15E+00	3.32E+00
Blood 1 to Cort bone surf	4.98E+00	4.15E+00	4.15E+00	4.15E+00	4.15E+00	3.32E+00
Blood 2 to Blood 1	4.62E-01	4.62E-01	4.62E-01	4.62E-01	4.62E-01	4.62E-01
Liver 0 to SI contents	2.31E-02	2.31E-02	2.31E-02	2.31E-02	2.31E-02	2.31E-02
Liver 0 to Liver 1	1.16E-01	1.16E-01	1.16E-01	1.16E-01	1.16E-01	1.16E-01
Liver 0 to Blood 1	9.24E-02	9.24E-02	9.24E-02	9.24E-02	9.24E-02	9.24E-02
Liver 1 to Blood 1	1.90E-03	1.90E-03	1.90E-03	1.90E-03	1.90E-03	1.90E-03
Kidneys to Blood 1	1.90E-03	1.90E-03	1.90E-03	1.90E-03	1.90E-03	1.90E-03
ST0 to Blood 1	2.31E-01	2.31E-01	2.31E-01	2.31E-01	2.31E-01	2.31E-01
ST1 to Blood 1	1.90E-03	1.90E-03	1.90E-03	1.90E-03	1.90E-03	1.90E-03
Trab bone surf to Blood 1	8.22E-03	2.88E-03	1.81E-03	1.32E-03	9.59E-04	4.93E-04
Trab bone surf to Trab bone vol	8.22E-03	2.88E-03	1.81E-03	1.32E-03	9.59E-04	2.47E-04
Trab bone vol to Blood 1	8.22E-03	2.88E-03	1.81E-03	1.32E-03	9.59E-04	4.93E-04
Cort bone surf to Blood 1	8.22E-03	2.88E-03	1.53E-03	9.04E-04	5.21E-04	8.21E-05
Cort bone surf to Cort bone vol	8.22E-03	2.88E-03	1.53E-03	9.04E-04	5.21E-04	4.11E-05
Cort bone vol to Blood 1	8.22E-03	2.88E-03	1.53E-03	9.04E-04	5.21E-04	8.21E-05

3876 [a]UB = Urinary bladder, Trab = trabecular, Cort = cortical, surf = surface, vol = volume, SI = Small intestine

16.2. Dosimetric data for yttrium

Table 16.3. Committed effective dose coefficients (Sv Bq^{-1}) for the inhalation or ingestion of ^{90}Y compounds.

	Effective dose coefficients (Sv Bq^{-1})					
Inhaled particulate materials (1 µm AMAD aerosols)	3 mo	1 y	5 y	10 y	15 y	Adult
Type F, Chloride	3.4E-09	2.4E-09	1.1E-09	7.5E-10	5.2E-10	4.1E-10
Type M, Oxide, phosphate; all unspecified forms	4.5E-09	3.4E-09	1.8E-09	1.2E-09	8.6E-10	7.9E-10
Type S, FAP	4.8E-09	3.6E-09	1.9E-09	1.3E-09	9.5E-10	8.9E-10
Ingested materials						
Adult f_A = 0.0001, All chemical forms	3.1E-09	2.4E-09	1.5E-09	1.0E-09	6.5E-10	5.6E-10

17. ZIRCONIUM (Z = 40)

17.1. Routes of Intake

17.1.1. Inhalation

(365) Some information was found on the behaviour of inhaled zirconium in man, mainly associated with irradiated fuel. Information on absorption from the respiratory tract is available from experimental studies of zirconium as oxalate, oxide, and irradiated uranium dioxide. For details see Section 12 of *Publication 134* (ICRP, 2016a). Absorption parameter values and types, and associated f_A values for particulate forms of zirconium are given in Table 17.1 (taken from Section 12 of *Publication 134*).

Table 17.1. Absorption parameter values for inhaled and ingested zirconium

		Absorption parameter values*		
Inhaled particulate materials		f_r	s_r (d^{-1})	s_s (d^{-1})
Default parameter values†,‡				
Absorption Type	Assigned forms			
F	–	1	30	–
M§	Oxalate	0.2	3	0.005
S	Carbonate, oxide, tritide	0.01	3	$1x10^{-4}$

Ingested material¶	Age-dependent absorption from the alimentary tract, f_A					
Assigned forms	3 months	1 year	5 years	10 years	15 years	adult
Zirconium in food	0.02	0.01	0.01	0.01	0.01	0.01
All other chemical forms	0.02	0.002	0.002	0.002	0.002	0.002

*It is assumed that for zirconium the bound state can be neglected i.e. $f_b = 0$. The values of s_r for Type F, M and S forms of zirconium (30, 3 and 3 d^{-1}, respectively) are the general default values.

†Materials (e.g. zirconium oxalate) are listed here where there is sufficient information to assign to a default absorption type, but not to give specific parameter values (see Section 12 of *Publication 134*, ICRP, 2016).

‡For inhaled material deposited in the respiratory tract and subsequently cleared by particle transport to the alimentary tract, the default f_A values for inhaled materials are applied: i.e. the product of f_r for the absorption type and the f_A value for ingested soluble (excluding dietary) forms of zirconium applicable to the age-group of interest(*e.g.* 0.002 for adults).

§Default Type M is recommended for use in the absence of specific information on which the exposure material can be assigned to an absorption type, e.g. if the form is unknown, or if the form is known but there is no information available on the absorption of that form from the respiratory tract.

¶Activity transferred from systemic compartments into segments of the alimentary tract is assumed to be subject to reabsorption to blood. The default absorption fraction f_A for the secreted activity is the highest value for ingestion of the radionuclide applicable to the age-group of interest (e.g. 0.01 for adults).

17.1.2. Ingestion

17.1.2.1. Adults

(366) Based on human and animal data, the gastrointestinal absorption of inorganic forms of zirconium appears to be less than one percent (for more details see Section 12 of *Publication 134*, ICRP, 2016). *Publications 30* and *134* (ICRP, 1979, 2016a) recommended an absorption

fraction of 0.002 for all chemical forms of zirconium. Because an absorption fraction of 0.01 was recommended in *Publication 30* for niobium, a chemically similar element, and because zirconium uptake might be higher for biologically incorporated forms of the element present in low concentrations in the diet, an absorption fraction of 0.01 was recommended in *Publication 56* (ICRP, 1990) for calculating dose coefficients for the ingestion of zirconium by adults in the population. The same value f_A = 0.01 is adopted here for ingestion by adults of zirconium in food. For all other chemical forms, an f_A of 0.002 is adopted.

17.1.2.2.Children

(367) Studies by Matsusaka et al. (1969) with newborn mice and by Shiraishi and Ichikawa (1972) with newborn rats both showed increased absorption and intestinal retention in the immediate postnatal period. Estimates of absorption from the results of Shiraishi and Ichikawa (1972) were 2% and 1% for 5 day and 16 day old rats, respectively, compared with less than 0.1% in adults. Retention in the gut wall attributable to pinocytotic uptake into intestinal epithelial cells accounted for about 10% of the dose administered to rats under 14 days of age but fell off rapidly, consistent with closure of the gut towards the end of the suckling period. Suppression of pinocytosis by administration of cortisone decreased both retention and absorption. These results indicate a higher absorption of zirconium in the newborn infant and an absorption fraction of 0.02 was therefore recommended for the 3 months old infant by *Publication* 56. *Publication* 56 recommended a value of 0.01 for children of 1 year and older. The same values of f_A are adopted here for dietary intakes of zirconium by children. For 3-month-old infants, a higher f_A value of 0.02 is adopted for all chemical forms.

17.1.3. Systemic Distribution, Retention and Excretion

(368) The model for systemic zirconium applied in *Publication 134* (ICRP, 2016a) to workers is applied here to adult members of the public. That model depicts the following general behavior of zirconium in mature humans or laboratory animals. About half of zirconium atoms entering blood transfer to tissues and excretion pathways within a few hours, and the remainder bind to plasma proteins and are cleared more slowly from blood. More than 95% of zirconium atoms leaving blood deposit in tissues. The remainder enter excretion pathways, primarily the urinary bladder contents. Soft tissues initially contain most of the extravascular zirconium, but bone eventually accumulates >90% of the systemic burden due to a much slower turnover than soft tissues. Zirconium atoms that reach blood have a long residence time in the body due to its low excretion rate and tenacious retention in bone.

(369) The effect of age on absorption and retention of zirconium was studied in rats (Shiraishi and Ichikawa, 1972), but the results are difficult to interpret regarding comparative systemic kinetics at different ages. Based on findings for more extensively studied bone seekers, zirconium is expected to have higher deposition in growing bone than in mature bone. Based on analogy with niobium, zirconium's neighbor in the period table, fractional deposition of zirconium in bone is assumed to be 50% higher in infants than in adults and 25% higher at ages 1-15 y than in adults. This moderate decline with increasing age in skeletal deposition of niobium is based on studies of changes with age in the systemic kinetics of niobium in swine and sheep (Mraz and Eisele, 1977b). Bone deposits of zirconium are assumed to be equally divided between trabecular and cortical bone surfaces. The skeletal behaviour of zirconium deposited on bone surfaces is described by the generic model for bone-surface-seekers (ICRP, 2015), except that zirconium removed from bone is assumed to return to blood rather than to be channeled through bone marrow.

(370) For a given pre-adult age the deposition fractions in soft tissues and excretion pathways are reduced from the adult value to account for elevated competition from bone surfaces for circulating zirconium. The deposition fraction for a soft-tissue or excretion pathway at a given pre-adult age is the value for the adult multiplied by the ratio (1-B)/(1-A) where A and B are fractional depositions in bone in the adult and the given pre-adult age, respectively.

(371) The structure of the model for zirconium is shown in Fig. 17.1. Parameter values are given in Table 17.2.

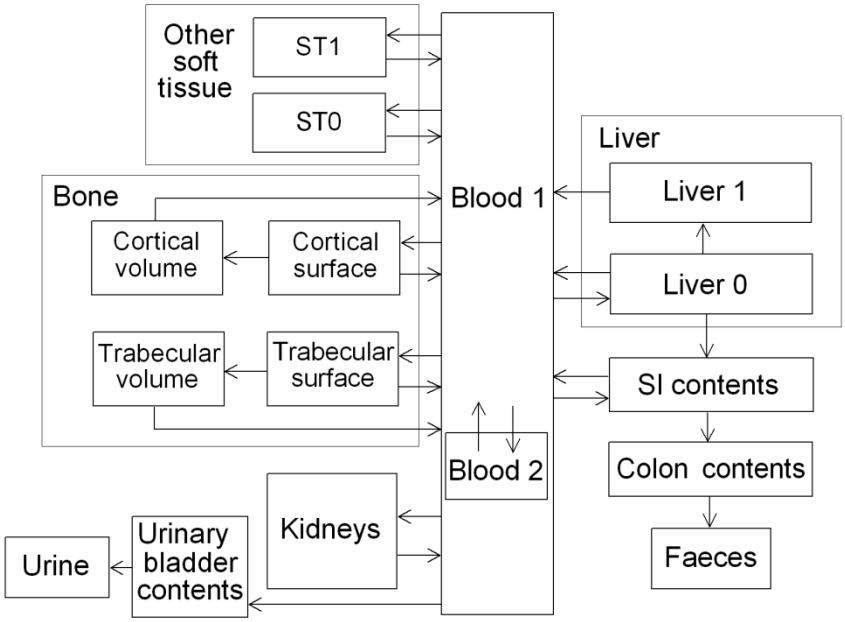

Fig. 17.1. Structure of the biokinetic model for systemic zirconium. SI = Small intestine.

3968 Table 17.2. Transfer coefficients for the model for systemic zirconium

Path[a]	Transfer coefficient (d^{-1})					
	Infant	1 y	5 y	10 y	15 y	Adult
Blood 1 to Blood 2	1.82E+00	1.91E+00	1.91E+00	1.91E+00	1.91E+00	2.00E+00
Blood 1 to Liver 0	6.84E-02	7.17E-02	7.17E-02	7.17E-02	7.17E-02	7.50E-02
Blood 1 to Kidneys	1.14E-02	1.19E-02	1.19E-02	1.19E-02	1.19E-02	1.25E-02
Blood 1 to ST0	1.82E+00	1.91E+00	1.91E+00	1.91E+00	1.91E+00	2.00E+00
Blood 1 to ST1	3.42E-02	3.58E-02	3.58E-02	3.58E-02	3.58E-02	3.75E-02
Blood 1 to UB contents	9.12E-02	9.56E-02	9.56E-02	9.56E-02	9.56E-02	1.00E-01
Blood 1 to SI contents	2.28E-02	2.39E-02	2.39E-02	2.39E-02	2.39E-02	2.50E-02
Blood 1 to Trab bone surf	5.63E-01	4.69E-01	4.69E-01	4.69E-01	4.69E-01	3.75E-01
Blood 1 to Cort bone surf	5.63E-01	4.69E-01	4.69E-01	4.69E-01	4.69E-01	3.75E-01
Blood 2 to Blood 1	4.62E-01	4.62E-01	4.62E-01	4.62E-01	4.62E-01	4.62E-01
Liver 0 to SI contents	1.16E-01	1.16E-01	1.16E-01	1.16E-01	1.16E-01	1.16E-01
Liver 0 to Liver 1	4.62E-01	4.62E-01	4.62E-01	4.62E-01	4.62E-01	4.62E-01
Liver 0 to Blood 1	1.16E-01	1.16E-01	1.16E-01	1.16E-01	1.16E-01	1.16E-01
Liver 1 to Blood 1	1.00E-02	1.00E-02	1.00E-02	1.00E-02	1.00E-02	1.00E-02
Kidneys to Blood 1	1.00E-02	1.00E-02	1.00E-02	1.00E-02	1.00E-02	1.00E-02
ST0 to Blood 1	4.62E-01	4.62E-01	4.62E-01	4.62E-01	4.62E-01	4.62E-01
ST1 to Blood 1	2.00E-02	2.00E-02	2.00E-02	2.00E-02	2.00E-02	2.00E-02
Trab bone surf to Blood 1	8.22E-03	2.88E-03	1.81E-03	1.32E-03	9.59E-04	4.93E-04
Trab bone surf to Trab bone vol	8.22E-03	2.88E-03	1.81E-03	1.32E-03	9.59E-04	2.47E-04
Trab bone vol to Blood 1	8.22E-03	2.88E-03	1.81E-03	1.32E-03	9.59E-04	4.93E-04
Cort bone surf to Blood 1	8.22E-03	2.88E-03	1.53E-03	9.04E-04	5.21E-04	8.21E-05
Cort bone surf to Cort bone vol	8.22E-03	2.88E-03	1.53E-03	9.04E-04	5.21E-04	4.11E-05
Cort bone vol to Blood 1	8.22E-03	2.88E-03	1.53E-03	9.04E-04	5.21E-04	8.21E-05

3969 [a]UB = Urinary bladder, Cort = cortical, Trab = trabecular, surf = surface, vol = volume, SI = Small intestine

17.2. Dosimetric data for zirconium

Table 17.3. Committed effective dose coefficients (Sv Bq^{-1}) for the inhalation or ingestion of ^{95}Zr compounds.

	Effective dose coefficients (Sv Bq^{-1})					
Inhaled particulate materials (1 µm AMAD aerosols)	3 mo	1 y	5 y	10 y	15 y	Adult
Type F	1.7E-08	1.4E-08	6.7E-09	3.7E-09	3.0E-09	2.7E-09
Type M, Oxalate; all unspecified forms	1.4E-08	1.2E-08	6.6E-09	4.2E-09	3.4E-09	3.4E-09
Type S, Carbonate, oxide, tritide	1.7E-08	1.5E-08	8.7E-09	5.9E-09	4.5E-09	4.8E-09
Ingested materials						
Adult f_A = 0.002, All other chemical forms	2.7E-09	1.2E-09	7.0E-10	4.9E-10	3.4E-10	3.2E-10
Adult f_A = 0.01, Zirconium in food	2.7E-09	1.7E-09	9.5E-10	6.3E-10	4.6E-10	4.2E-10

18. NIOBIUM (Z = 41)

18.1. Routes of Intake

18.1.1. Inhalation

(372) Some information was found on the behaviour of inhaled niobium in man, mainly associated with irradiated fuel. Information on absorption from the respiratory tract is available from experimental studies of niobium as oxalate, oxide, and irradiated uranium dioxide. For details see Section 13 of *Publication 134* (ICRP, 2016a). Absorption parameter values and types, and associated f_A values for particulate forms of niobium are given in Table 18.1 (taken from Section 13 of *Publication 134*).

Table 18.1. Absorption parameter values for inhaled and ingested niobium

		Absorption parameter values*		
Inhaled particulate materials		f_r	s_r (d^{-1})	s_s (d^{-1})
Default parameter values†,‡				
Absorption Type	Assigned forms			
F		1	30	–
M§	Oxalate	0.2	3	0.005
S	Carbonate, oxide	0.01	3	$1x10^{-4}$

Ingested materials¶						
Assigned forms	Age-dependent absorption from the alimentary tract, f_A					
	3 months	1 year	5 years	10 years	15 years	adult
All forms	0.02	0.01	0.01	0.01	0.01	0.01

*It is assumed that for niobium that the bound state can be neglected, i.e. f_b = 0.0. The values of s_r for Type F, M and S forms of niobium (30, 3 and 3 d^{-1}, respectively) are the general default values.

†Materials (e.g. niobium oxalate) are listed here where there is sufficient information to assign to a default absorption type, but not to give specific parameter values (see Section 13 of *Publication 134*, ICRP, 2016).

‡For inhaled material deposited in the respiratory tract and subsequently cleared by particle transport to the alimentary tract, the default f_A values for inhaled materials are applied: i.e. the product of f_r for the absorption type and the f_A value for ingested soluble forms of niobium applicable to the age-group of interest (*e.g.* 0.01 for adults).

§Default Type M is recommended for use in the absence of specific information on which the exposure material can be assigned to an absorption type, e.g. if the form is unknown, or if the form is known but there is no information available on the absorption of that form from the respiratory tract.

¶Activity transferred from systemic compartments into segments of the alimentary tract is assumed to be subject to reabsorption to blood. The default absorption fraction f_A for the secreted activity is the highest value for ingestion of the radionuclide applicable to the age-group of interest (e.g. 0.01 for adults).

18.1.2. Ingestion

18.1.2.1. Adults

(373) Data on the gastrointestinal absorption of niobium are available from a number of animal studies and indicate absorbed fractions from 4×10^{-4} to 4×10^{-2} depending on chemical forms and animal species (see section 13 of *Publication 134* for more details). *Publications 30* , *56* and *134* (ICRP, 1979, 1990, 2016a) recommended a default value of 0.01 for all chemical

forms. This value of $f_A = 0.01$ is also adopted here for the ingestion of niobium in food by adults in the population.

18.1.2.2.Children

(374) Absorption of niobium is increased in suckling animals and falls to adult values by about the time of weaning. Variable results have been obtained, however, for different species. Mraz and Eisele (1977a) measured absorption of about 5.5% and 4% in newborn and 7 day old rats respectively, compared with about 0.1% in 21 day old weaned rats. Higher values of about 40% and 35% were obtained for 1 day old pigs and sheep respectively, compared with values of less than 0.5% in weaned animals (Mraz and Eisele, 1977b). Harrison et al. (1990) have shown that in 2 day old guinea pigs absorption of ^{95}Nb administered as the citrate is about 1.5% compared with 0.8% in adults. Further results on absorption and intestinal retention of niobium in neonatal mammals were published by Naylor et al. (1989). Paquet et al. (1998) observed that when ^{95}Nb oxalate was given to 1-day-old rats, absorption was increased by a factor of 200, as compared to adult rats. In *Publication 56*, an absorption fraction of 0.02 was recommended for 3-month-old infants and a value of 0.01 was recommended for children of 1 year and older. The same f_A values are adopted here for absorption of niobium in food by children. For the 3-month-old infants, an f_A of 0.02 is adopted here.

18.1.3. Systemic Distribution, Retention and Excretion

(375) The model for systemic niobium applied in *Publication 134* (ICRP, 2016a) to workers is applied here to adult members of the public. That was based on results of biokinetic studies of laboratory animals exposed to radioisotopes of niobium. The data indicate that half or more of niobium atoms entering blood transfer to tissues and excretion pathways within a few hours, and the remainder clears much more slowly due to binding with plasma proteins. Excretion is mainly in urine. Niobium distributes somewhat uniformly throughout the body but is retained much longer in bone than in other tissues, so that bone eventually contains a large portion of the total-body content. Niobium depositing in bone appears to be retained largely on bone surfaces. Total-body retention generally has been described in terms of two retention components of roughly equal size. The short-term component typically has a biological half-time of a few days, and the long-term component has a half-time of at least a few months. Reported biokinetic studies have not been sufficiently long to characterize longer-term components of retention such as may be present in bone.

(376) Mraz and Eisele (1977b) compared the behavior of niobium in newborn and weaned swine and sheep. the skeletons of newborn and weaned swine contained 66% and 51%, respectively, of intravenously administered ^{95}Nb. The corresponding values for newborn and weaned sheep were 67% and 43%, respectively. Based on these findings, it is assumed here that the fraction of absorbed niobium that deposits in bone decreases moderately with age after infancy. The fraction of outflow from blood to bone surface is assumed to be 25% greater at ages 1-15 y than in adults and 50% greater in infants than in adults. Bone deposits of niobium are assumed to be equally divided between trabecular and cortical bone surfaces. The skeletal behaviour of niobium deposited on bone surfaces is described by the generic model for bone-surface-seekers (Annex B of *Publication 130*, ICRP, 2015), except that niobium biologically removed from bone is assumed to return to blood rather than to be channeled through bone marrow.

(377) For a given pre-adult age the adult deposition fractions for soft tissues and excretion pathways are reduced from the adult value to account for elevated competition for circulating niobium from bone surfaces. The deposition fraction for a soft-tissue or excretion pathway at a

given pre-adult age is the value for the adult multiplied by the ratio (1-B)/(1-A) where A and B are fractional depositions in bone in the adult and the given pre-adult age, respectively. The structure of the model for niobium is shown in Fig. 18.1. Parameter values are given in Table 18.2.

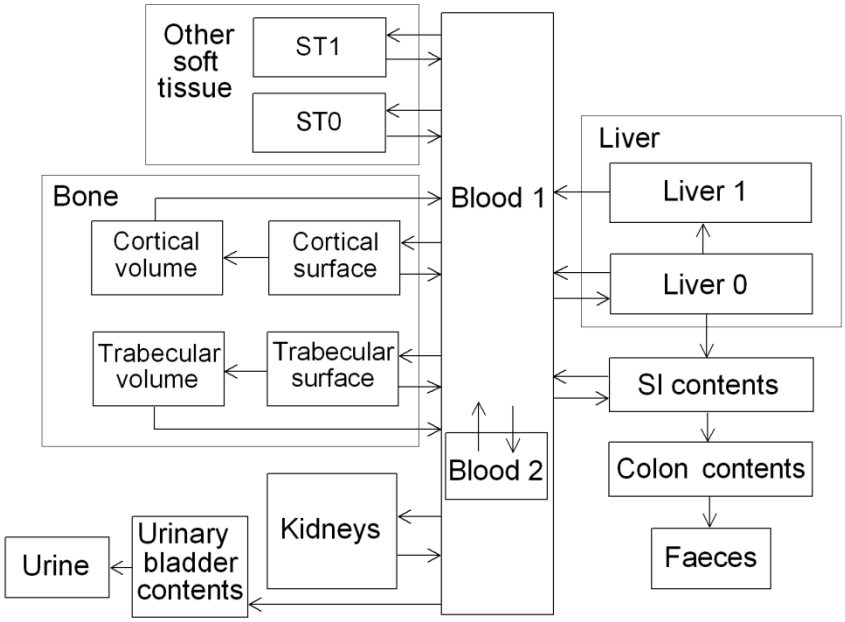

Fig. 18.1. Structure of the biokinetic model for systemic niobium. SI = Small intestine.

4058 Table 18.2. Transfer coefficients for the model for systemic niobium

Path[a]	Transfer coefficient (d^{-1})					
	Infant	1 y	5 y	10 y	15 y	Adult
Blood 1 to Blood 2	3.15E+00	3.18E+00	3.18E+00	3.18E+00	3.18E+00	3.20E+00
Blood 1 to Liver 0	2.36E-01	2.38E-01	2.38E-01	2.38E-01	2.38E-01	2.40E-01
Blood 1 to Kidneys	3.94E-02	3.97E-02	3.97E-02	3.97E-02	3.97E-02	4.00E-02
Blood 1 to ST0	3.15E+00	3.18E+00	3.18E+00	3.18E+00	3.18E+00	3.20E+00
Blood 1 to ST1	1.18E-01	1.19E-01	1.19E-01	1.19E-01	1.19E-01	1.20E-01
Blood 1 to UB contents	8.66E-01	8.73E-01	8.73E-01	8.73E-01	8.73E-01	8.80E-01
Blood 1 to SI contents	7.88E-02	7.94E-02	7.94E-02	7.94E-02	7.94E-02	8.00E-02
Blood 1 to Trab bone surf	1.80E-01	1.50E-01	1.50E-01	1.50E-01	1.50E-01	1.20E-01
Blood 1 to Cort bone surf	1.80E-01	1.50E-01	1.50E-01	1.50E-01	1.50E-01	1.20E-01
Blood 2 to Blood 1	1.39E+00	1.39E+00	1.39E+00	1.39E+00	1.39E+00	1.39E+00
Liver 0 to SI contents	5.78E-02	5.78E-02	5.78E-02	5.78E-02	5.78E-02	5.78E-02
Liver 0 to Liver 1	2.31E-01	2.31E-01	2.31E-01	2.31E-01	2.31E-01	2.31E-01
Liver 0 to Blood 1	5.78E-02	5.78E-02	5.78E-02	5.78E-02	5.78E-02	5.78E-02
Liver 1 to Blood 1	5.00E-03	5.00E-03	5.00E-03	5.00E-03	5.00E-03	5.00E-03
Kidneys to Blood 1	5.00E-03	5.00E-03	5.00E-03	5.00E-03	5.00E-03	5.00E-03
ST0 to Blood 1	1.39E+00	1.39E+00	1.39E+00	1.39E+00	1.39E+00	1.39E+00
ST1 to Blood 1	1.00E-02	1.00E-02	1.00E-02	1.00E-02	1.00E-02	1.00E-02
Trab bone surf to Blood 1	8.22E-03	2.88E-03	1.81E-03	1.32E-03	9.59E-04	4.93E-04
Trab bone surf to Trab bone vol	8.22E-03	2.88E-03	1.81E-03	1.32E-03	9.59E-04	2.47E-04
Trab bone vol to Blood 1	8.22E-03	2.88E-03	1.81E-03	1.32E-03	9.59E-04	4.93E-04
Cort bone surf to Blood 1	8.22E-03	2.88E-03	1.53E-03	9.04E-04	5.21E-04	8.21E-05
Cort bone surf to Cort bone vol	8.22E-03	2.88E-03	1.53E-03	9.04E-04	5.21E-04	4.11E-05
Cortical vol to Blood 1	8.22E-03	2.88E-03	1.53E-03	9.04E-04	5.21E-04	8.21E-05

4059 [a]UB = Urinary bladder, Cort = cortical, Trab = trabecular, surf = surface, vol = volume, SI = Small intestine

18.2. Dosimetric data for niobuim

Table 18.3. Committed effective dose coefficients (Sv Bq^{-1}) for the inhalation or ingestion of ^{95}Nb compounds.

	Effective dose coefficients (Sv Bq^{-1})					
Inhaled particulate materials (1 µm AMAD aerosols)	3 mo	1 y	5 y	10 y	15 y	Adult
Type F	2.5E-09	1.9E-09	1.0E-09	6.6E-10	4.7E-10	4.6E-10
Type M, Oxalate; all unspecified forms	4.2E-09	3.4E-09	1.9E-09	1.3E-09	9.9E-10	1.1E-09
Type S, Carbonate, oxide	5.3E-09	4.3E-09	2.5E-09	1.7E-09	1.3E-09	1.4E-09
Ingested materials						
f_A = 0.01, All forms	1.3E-09	1.1E-09	6.3E-10	4.5E-10	3.1E-10	3.0E-10

19. MOLYBDENUM (Z = 42)

19.1. Routes of Intake

19.1.1. Inhalation

(378) Little information is available on the behaviour of inhaled molybdenum in man following accidental intakes, or from experimental studies in animals. For details see Section 14 of *Publication 134* (ICRP, 2016a). Absorption parameter values and types, and associated f_A values for particulate forms of molybdenum are given in Table 19.1 (taken from Section 14 of *Publication 134*).

Table 19.1. Absorption parameter values for inhaled and ingested molybdenum

Inhaled particulate materials		Absorption parameter values* f_r	s_r (d^{-1})	s_s (d^{-1})
Default parameter values†,‡				
Absorption Type	Assigned forms			
F	Chloride and ammonium molybdate	1	30	–
M§	Oxide	0.2	3	0.005
S	–	0.01	3	0.0001

Ingested materials¶	Age-dependent absorption from the alimentary tract, f_A					
Assigned forms	3 months	1 year	5 years	10 years	15 years	adult
Molybdenum in food	1	0.6	0.6	0.6	0.6	0.6
Molybdenum in water	1	0.9	0.9	0.9	0.9	0.9
Sulfide	0.1	0.05	0.05	0.05	0.05	0.05

*It is assumed that for molybdenum the bound state can be neglected i.e. $f_b = 0$. The values of s_r for Type F, M and S forms of molybdenum (30, 3 and 3 d^{-1}, respectively) are the general default values.

†Materials (e.g. molybdenum chloride) are listed here where there is sufficient information to assign to a default absorption type, but not to give specific parameter values (see Section 14 of *Publication 134*, ICRP, 2016).

‡For inhaled material deposited in the respiratory tract and subsequently cleared by particle transport to the alimentary tract, the default f_A values for inhaled materials are applied: i.e. the product of f_r for the absorption type and the f_A value for ingested soluble forms of molybdenum applicable to the age-group of interest (*e.g.* 0.9 for adults).

§Default Type M is recommended for use in the absence of specific information on which the exposure material can be assigned to an absorption type, e.g. if the form is unknown, or if the form is known but there is no information available on the absorption of that form from the respiratory tract.

¶Activity transferred from systemic compartments into segments of the alimentary tract is assumed to be subject to reabsorption to blood. The default absorption fraction f_A for the secreted activity is the highest value for ingestion of the radionuclide applicable to the age-group of interest (*e.g.* 0.9 for adults).

19.1.2. Ingestion

(379) Molybdenum is an essential trace element naturally present in soils and waters. It is generally absorbed fairly readily from the gastrointestinal tract except for molybdenum disulphide which is only poorly absorbed. The gastrointestinal absorption of molybdenum

depends on its concentration in the diet, the amounts of copper and sulphur present, and the age (for more details, see section 14 of *Publication 134*, ICRP, 2016).

19.1.2.1. Adults

(380) The intestinal absorption of molybdenum from aqueous solutions and labelled foodstuffs was investigated with stable isotopes in a number of human volunteer studies (Cantone, Bartolo, et al., 1997; Cantone, De Bartolo, et al., 1997; Giussani, 2008; Giussani et al., 2006, 2007; Giussani, Heinrichs, et al., 1998; Giussani, Roth, et al., 1998; Sievers, Dörner, et al., 2001; Sievers, Oldigs, et al., 2001; Turnlund et al., 1999; Turnlund, Keyes and Peiffer, 1995; Turnlund, Keyes, Peiffer, et al., 1995; Werner et al., 1998). The fractional absorption of inorganic forms of molybdenum (chloride and ammonium-molybdate) from aqueous solutions was greater than 0.85 for administration of up to 40 μg Mo kg^{-1} body weight, then it decreased with increasing tracer amount, being about 0.6 at 80 μg Mo kg^{-1} body weight (Giussani et al., 2006; Turnlund, Keyes and Peiffer, 1995; Turnlund, Keyes, Peiffer, et al., 1995; Werner et al., 1998). For molybdenum intrinsically incorporated in foodstuffs (salad, beans, tomatoes) the absorbed fraction was between 0.3 and 0.6, and the absorption from a composite meal was around 0.5 (Giussani et al., 2006, 2007; Giussani, Heinrichs, et al., 1998; Turnlund et al., 1999; Werner et al., 1998).

(381) Previous balance studies in humans (Engel et al., 1967; Robinson et al., 1973; Tipton et al., 1966, 1969) had shown intestinal absorption from complete meals to be between 0.3 and 0.8, in reasonable agreement with the stable tracer studies. However, results of these balance studies are biased by the contribution of endogenous molybdenum to the faecal excretion, and by the fact that increased levels of molybdenum in the diet were partially obtained by additional administration of molybdenum in liquid solutions, for which intestinal absorption is known to be very high.

19.1.2.2. Children

(382) A study conducted with 10 infants with gestational age 30-39 weeks (Sievers, Dörner, et al., 2001) found that absorbed fraction of molybdenum from milk and baby formulas is 0.975% (0.96-0.99). Metabolic balance data were obtained for 36 pre-adolescent girls, aged 6-10 years, which showed that there is considerable variation in retention of molybdenum from various diets (Engel et al., 1967). An absorbtion fraction of 0.63 - 0.78 was derived from the data on excretion for this group of children (Coughtrey and Thorne, 1983), however these values are subject to the aforementioned biases.

(383) In *Publication 30* (ICRP, 1979), the recommended absorption fraction for adults were 0.05 for the sulphide and 0.8 for all other compounds of the element. The value of 1 was adopted in *Publication 67* (ICRP, 1993) for dietary intakes. In *Publication 134* (ICRP, 2016a), the recommended values for adults were 0.05 for sulphide and 0.9 for all other compounds. The f_A values adopted in this report for adults and children of 1 year and older are 0.05 for sulphide, 0.6 for dietary molybdenum, 0.9 for compounds other than sulphide in aqueous form. For 3-month-old infants, f_A values of 0.1 and 1 are adopted for the sulphide and for all other forms of molybdenum respectively.

19.1.3. Systemic Distribution, Retention and Excretion

(384) The model for systemic molybdenum applied in *Publication 134* (ICRP, 2016a) to workers is based largely on results of biokinetic studies on healthy volunteers administered stable isotopes of molybdenum as tracers (Cantone et al., 1995; Giussani, 2008; Giussani et al.,

2007; Giussani, Heinrichs, et al., 1998; Turnlund, Keyes and Peiffer, 1995; Turnlund, Keyes, Peiffer, et al., 1995; Werner et al., 2000). Blood, liver, and kidneys are the only explicitly depicted regions (Fig. 19.1). The model predicts that most of the systemic activity is contained in the liver from a few hours to several weeks after acute uptake of a molybdenum radioisotope to blood.

(385) Limited data for rats indicate a shorter retention time for molybdenum in young animals than in mature animals (ICRP, 1993). However, the rat may not be a suitable laboratory model for human biokinetics of molybdenum due to much different requirements for molybdenum in humans and rats.

(386) The model for systemic molybdenum applied in *Publication 134* to workers is applied here to members of the public of all ages. The age-independent parameter values are listed in Table 19.2.

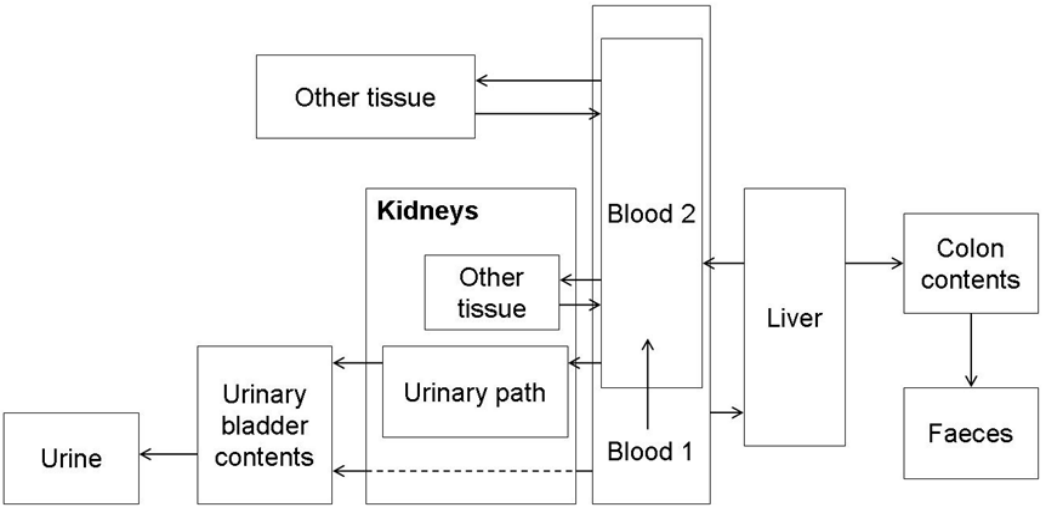

Fig. 19.1. Structure of the biokinetic model for systemic molybdenum. Activity transferred from Liver to Colon contents enters Right colon contents.

4153 Table 19.2. Transfer coefficients for the model for systemic molybdenum

Path[a]	Transfer coefficient (d^{-1})					
	Infant	1 y	5 y	10 y	15 y	Adult
Blood 1 to Blood 2	1.25E+01	1.25E+01	1.25E+01	1.25E+01	1.25E+01	1.25E+01
Blood 1 to Liver	1.42E+01	1.42E+01	1.42E+01	1.42E+01	1.42E+01	1.42E+01
Blood 1 to UB contents	6.50E+00	6.50E+00	6.50E+00	6.50E+00	6.50E+00	6.50E+00
Blood 2 to Kidneys 1	1.70E+00	1.70E+00	1.70E+00	1.70E+00	1.70E+00	1.70E+00
Blood 2 to Kidneys 2	1.15E-01	1.15E-01	1.15E-01	1.15E-01	1.15E-01	1.15E-01
Blood 2 to Other	1.73E+00	1.73E+00	1.73E+00	1.73E+00	1.73E+00	1.73E+00
Liver to RC contents	4.80E-03	4.80E-03	4.80E-03	4.80E-03	4.80E-03	4.80E-03
Liver to Blood 2	1.22E-02	1.22E-02	1.22E-02	1.22E-02	1.22E-02	1.22E-02
Kidneys 2 to Blood 2	4.74E-02	4.74E-02	4.74E-02	4.74E-02	4.74E-02	4.74E-02
Kidneys 1 to UB contents	1.40E+00	1.40E+00	1.40E+00	1.40E+00	1.40E+00	1.40E+00
Other to Blood 2	3.23E-02	3.23E-02	3.23E-02	3.23E-02	3.23E-02	3.23E-02

4154 [a]UB = Urinary bladder, RC = Right colon

19.2. Dosimetric data for molybdenum

Table 19.3. Committed effective dose coefficients (Sv Bq^{-1}) for the inhalation or ingestion of ^{99}Mo compounds.

	Effective dose coefficients (Sv Bq^{-1})					
Inhaled particulate materials (1 µm AMAD aerosols)	3 mo	1 y	5 y	10 y	15 y	Adult
Type F, Chloride and ammonium molybdate	1.7E-09	1.2E-09	5.3E-10	3.7E-10	2.1E-10	1.9E-10
Type M, Oxide; all unspecified forms	2.4E-09	1.8E-09	9.5E-10	6.6E-10	4.8E-10	4.4E-10
Type S	2.6E-09	1.9E-09	1.0E-09	7.2E-10	5.4E-10	5.0E-10
Ingested materials						
Adult f_A = 0.05, Sulphide	3.0E-09	2.0E-09	1.1E-09	7.7E-10	5.1E-10	4.4E-10
Adult f_A = 0.6, Molybdenum in food	3.0E-09	1.7E-09	9.7E-10	6.6E-10	4.3E-10	3.7E-10
Adult f_A = 0.9, Molybdenum in water	1.4E-09	1.1E-09	6.6E-10	4.7E-10	3.0E-10	2.6E-10

20. TECHNETIUM (Z = 43)

20.1. Routes of Intake

20.1.1. Inhalation

(387) Most of the experimental information available on the behaviour of technetium following deposition in the respiratory tract relates to pertechnetate, or materials labelled with ^{99m}Tc, especially diethylenetriaminepentaacetic acid (DTPA). Some information is also available from accidental human intakes. For details see Section 15 of *Publication 134* (ICRP, 2016a). Absorption parameter values and types, and associated f_A values for particulate forms of technetium are given in Table 20.1 (taken from Section 15 of *Publication 134*, ICRP, 2016a).

Table 20.1. Absorption parameter values for inhaled and ingested technetium

		Absorption parameter values*		
Inhaled particulate materials		f_r	s_r (d^{-1})	s_s (d^{-1})
Default parameter values†,‡				
Absorption Type	Assigned forms			
F	Pertechnetate, Tc-DTPA	1	100	–
M§	–	0.2	3	0.005
S	–	0.01	3	0.0001

Ingested material¶						
Assigned forms	Age-dependent absorption from the alimentary tract, f_A					
	3 months	1 year	5 years	10 years	15 years	adult
Technetium in food	1	0.5	0.5	0.5	0.5	0.5
Pertechnetate	1	0.9	0.9	0.9	0.9	0.9

*It is assumed that for technetium the bound state can be neglected, i.e. $f_b = 0.0$. The value of s_r for Type F forms of technetium (100 d^{-1}) is element specific. The values for Types M and S (3 d^{-1}) are the general default values.

†Materials (e.g. pertechnetate) are generally listed here where there is sufficient information to assign to a default absorption type, but not to give specific parameter values (see Section 15 of *Publication 134* (ICRP 2016b)).

‡For inhaled material deposited in the respiratory tract and subsequently cleared by particle transport to the alimentary tract, the default f_A values for inhaled materials are applied: i.e. the product of f_r for the absorption type and the f_A value for ingested soluble (excluding dietary) forms of technetium applicable to the age-group of interest (*e.g.* 0.9 for adults).

§Default Type M is recommended for use in the absence of specific information on which the exposure material can be assigned to an absorption type, e.g. if the form is unknown, or if the form is known but there is no information available on the absorption of that form from the respiratory tract.

¶Activity transferred from systemic compartments into segments of the alimentary tract is assumed to be subject to reabsorption to blood. The default absorption fraction f_A for the secreted activity is the highest value for ingestion of the radionuclide applicable to the age-group of interest (*e.g.* 0.9 for adults).

20.1.2. Ingestion

20.1.2.1. Adults

(388) The most stable species of technetium in aqueous solution is the pertechnetate ion (TcO_4^-). Pertechnetate appears to be the most likely form prevailing in the environment (Till et al., 1979). Technetium administered as pertechnetate is generally well absorbed by human

subjects with fractional absorption up to 0.95 (*Publication 134*, ICRP, 2016a). In *Publication 134*, an f_A value of 0.9 was recommended for all chemical forms in the workplace. Incorporation into foods appears to reduce technetium absorption. The fractional absorption of technetium from the gut is reduced to half of that following administration of pertechnetate, when soya-bean and animal tissue with incorporated technetium were fed to rats and guinea pigs (Sullivan et al., 1978). Similar results in rats and sheep fed technetium either as pertechnetate or incorporated in maize have been obtained by Gerber et al. (1989). The fractional absorption of ^{99}Tc from cockles collected on the Irish Sea coast in the UK was investigated in a human volunteer study by Hunt (1998), and a value of approximately 0.6 was obtained. A low value of around 0.1 was also obtained in a volunteer study of absorption of ^{99}Tc from lobster flesh (Harrison and Phipps, 2001; Hunt, 1998). As technetium in food was less readily absorbed than the pertechnetate, an absorption fraction of 0.5 was recommended in *Publication 67* (ICRP, 1993). The same value of $f_A = 0.5$ is adopted here for ingestion by adults of technetium in food. For ingestion of pertechnetate an $f_A = 0.9$ is adopted.

20.1.2.2.Children

(389) Technetium gavaged in the form of pertechnetate is well absorbed by both adult and neonatal rats (Sullivan, Miller, et al., 1984). In *Publication 67*, a value of 1 was applied for 3-month-old infants. For children of 1 year and older the absorption fraction for the adult (0.5) was used. The same values are adopted here for f_A of technetium in food. For ingestion of pertechnetate by 3-month-old infants, an f_A of 1 is adopted.

20.1.3. Systemic Distribution, Retention and Excretion

(390) The model for systemic technetium applied in *Publication 134* (ICRP, 2016a) to workers is applied here to adult members of the public. That model is based primarily on data from biokinetic studies of technetium administered in the commonly encountered form pertechnetate (TcO_4^-). As discussed in *Publication 134*, the initial distribution of pertechnetate resembles that of inorganic iodide. Pertechnetate and iodide are selectively concentrated in the thyroid, salivary glands, and stomach wall. In contrast to iodide, pertechnetate trapped by the thyroid is not organically bound in the thyroid but is mainly released back to blood over a period of hours. Over time the pertechnetate ion and iodide exhibit markedly different excretion patterns. Iodide is excreted primarily in urine. In adults, roughly 30% of technetium intravenously administered as pertechnetate is excreted in urine over the first day, but thereafter the urinary excretion rate decreases markedly while cumulative faecal excretion increases and may eventually exceed cumulative urinary excretion. Most of the absorbed or injected pertechnetate is lost from the body within a few days, but a small percentage is retained for weeks or longer. During extended intake, relatively high concentrations are found in bone, kidneys, liver, skin, hair, and thyroid.

(391) No useful information was found on age related changes in the systemic behavior of technetium. It is assumed here that the systemic behaviour of technetium is independent of age except that activity is assumed to be removed from trabecular or cortical bone volume to blood at the age-specific rate of turnover of that bone type.

The structure of the model for technetium is shown in Fig. 20.1. Parameter values are given in Table 20.2.

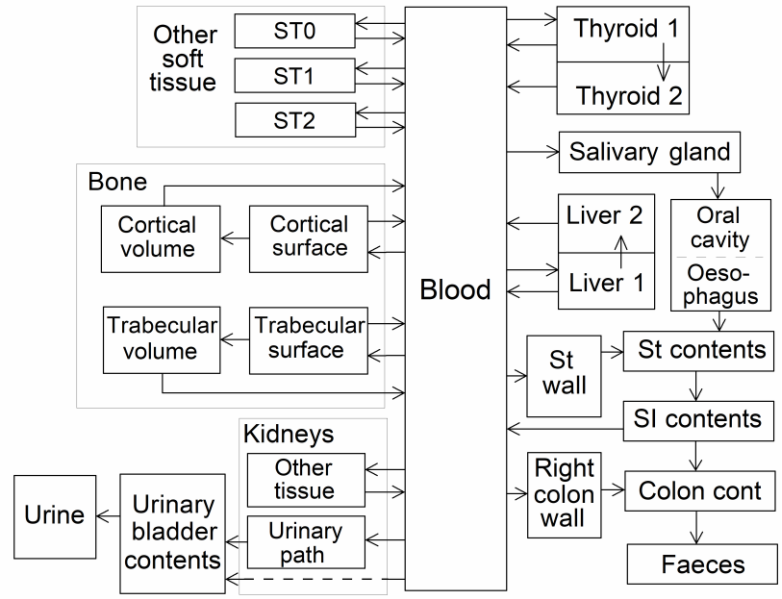

Fig. 20.1. Structure of the biokinetic model for systemic technetium. Activity transferred to Colon contents enters Right colon contents. St = Stomach, SI = Small intestine, cont = contents

Table 20.2. Transfer coefficients for the model for systemic technetium

Path[a]	Transfer coefficient (d^{-1})					
	Infant	1 y	5 y	10 y	15 y	Adult
Blood to Thyroid 1	7.00E+00	7.00E+00	7.00E+00	7.00E+00	7.00E+00	7.00E+00
Blood to ST0	7.19E+01	7.19E+01	7.19E+01	7.19E+01	7.19E+01	7.19E+01
Blood to ST1	3.00E+00	3.00E+00	3.00E+00	3.00E+00	3.00E+00	3.00E+00
Blood to ST2	1.80E-01	1.80E-01	1.80E-01	1.80E-01	1.80E-01	1.80E-01
Blood to UB contents	1.70E+00	1.70E+00	1.70E+00	1.70E+00	1.70E+00	1.70E+00
Blood to Salivary glands	2.60E+00	2.60E+00	2.60E+00	2.60E+00	2.60E+00	2.60E+00
Blood to St wall	4.30E+00	4.30E+00	4.30E+00	4.30E+00	4.30E+00	4.30E+00
Blood to Urinary path	7.00E-01	7.00E-01	7.00E-01	7.00E-01	7.00E-01	7.00E-01
Blood to Other kidney tissue	4.00E-02	4.00E-02	4.00E-02	4.00E-02	4.00E-02	4.00E-02
Blood to Liver 1	4.50E+00	4.50E+00	4.50E+00	4.50E+00	4.50E+00	4.50E+00
Blood to RC wall	3.40E+00	3.40E+00	3.40E+00	3.40E+00	3.40E+00	3.40E+00
Blood to Cort bone surf	3.50E-01	3.50E-01	3.50E-01	3.50E-01	3.50E-01	3.50E-01
Blood to Trab bone surf	3.50E-01	3.50E-01	3.50E-01	3.50E-01	3.50E-01	3.50E-01
Thyroid 1 to Blood	1.00E+02	1.00E+02	1.00E+02	1.00E+02	1.00E+02	1.00E+02
Thyroid 1 to Thyroid 2	1.00E+00	1.00E+00	1.00E+00	1.00E+00	1.00E+00	1.00E+00
Thyroid 2 to Blood	1.00E+00	1.00E+00	1.00E+00	1.00E+00	1.00E+00	1.00E+00
ST0 to Blood	5.00E+01	5.00E+01	5.00E+01	5.00E+01	5.00E+01	5.00E+01
ST1 to Blood	4.62E-01	4.62E-01	4.62E-01	4.62E-01	4.62E-01	4.62E-01
ST2 to Blood	3.47E-02	3.47E-02	3.47E-02	3.47E-02	3.47E-02	3.47E-02
Salivary glands to Oral cavity	5.00E+01	5.00E+01	5.00E+01	5.00E+01	5.00E+01	5.00E+01
St wall to St contents	5.00E+01	5.00E+01	5.00E+01	5.00E+01	5.00E+01	5.00E+01
Urinary path to UB contents	8.32E+00	8.32E+00	8.32E+00	8.32E+00	8.32E+00	8.32E+00
Other kidney tissue to Blood	3.47E-02	3.47E-02	3.47E-02	3.47E-02	3.47E-02	3.47E-02
Liver 1 to Blood	8.23E+00	8.23E+00	8.23E+00	8.23E+00	8.23E+00	8.23E+00

Liver 1 to Liver 2	8.32E-02	8.32E-02	8.32E-02	8.32E-02	8.32E-02	8.32E-02
Liver 2 to Blood	3.47E-02	3.47E-02	3.47E-02	3.47E-02	3.47E-02	3.47E-02
RC wall to RC contents	1.39E+00	1.39E+00	1.39E+00	1.39E+00	1.39E+00	1.39E+00
Cort bone surf to Blood	4.57E-01	4.57E-01	4.57E-01	4.57E-01	4.57E-01	4.57E-01
Cort bone surf to Cort bone vol	4.62E-03	4.62E-03	4.62E-03	4.62E-03	4.62E-03	4.62E-03
Trab bone surf to Blood	4.57E-01	4.57E-01	4.57E-01	4.57E-01	4.57E-01	4.57E-01
Trab bone surf to Trab bone vol	4.62E-03	4.62E-03	4.62E-03	4.62E-03	4.62E-03	4.62E-03
Cort bone vol to Blood	8.22E-03	2.88E-03	1.53E-03	9.04E-04	5.21E-04	8.21E-05
Trab vol to Blood	8.22E-03	2.88E-03	1.81E-03	1.32E-03	9.59E-04	4.93E-04

4238 [a]UB = Urinary bladder, RC = Right colon, Cort = cortical, Trab = trabecular, St = Stomach, Trab = Trabecular,
4239 Cort = Cortical, surf = surface, vol = volume

20.2. Dosimetric data for technetium

Table 20.3. Committed effective dose coefficients (Sv Bq^{-1}) for the inhalation or ingestion of ^{99}Tc compounds.

Inhaled particulate materials (1 μm AMAD aerosols)	Effective dose coefficients (Sv Bq^{-1})					
	3 mo	1 y	5 y	10 y	15 y	Adult
Type F, Pertechnetate, Tc-DTPA	1.8E-09	1.2E-09	4.5E-10	2.5E-10	1.6E-10	1.3E-10
Type M, All unspecified forms	8.1E-09	7.1E-09	4.0E-09	2.6E-09	2.0E-09	1.9E-09
Type S	5.4E-08	5.5E-08	4.1E-08	3.1E-08	3.1E-08	3.1E-08
Ingested materials						
Adult f_A = 0.5, Technetium in food	3.4E-09	1.2E-09	5.2E-10	2.9E-10	2.0E-10	1.5E-10
Adult f_A = 0.8, Pertechnetate	3.4E-09	2.0E-09	9.2E-10	5.0E-10	3.5E-10	2.7E-10

Table 20.4. Committed effective dose coefficients (Sv Bq^{-1}) for the inhalation or ingestion of ^{99m}Tc compounds.

Inhaled particulate materials (1 μm AMAD aerosols)	Effective dose coefficients (Sv Bq^{-1})					
	3 mo	1 y	5 y	10 y	15 y	Adult
Type F, Pertechnetate, Tc-DTPA	4.9E-11	3.6E-11	1.6E-11	9.9E-12	6.4E-12	5.5E-12
Type M, All unspecified forms	5.0E-11	3.7E-11	2.0E-11	1.4E-11	1.1E-11	1.0E-11
Type S	4.9E-11	3.7E-11	2.0E-11	1.4E-11	1.1E-11	1.0E-11
Ingested materials						
Adult f_A = 0.5, Technetium in food	1.1E-10	5.6E-11	3.0E-11	2.0E-11	1.4E-11	1.3E-11

Adult f_A = 0.8, Pertechnetate	1.1E-10	7.2E-11	3.8E-11	2.4E-11	1.6E-11	1.4E-11

4244

21. RUTHENIUM (Z = 44)

21.1. Routes of Intake

21.1.1. Inhalation

(392) Some information is available on the behaviour of inhaled ruthenium in man following accidental intakes as an oxide or in irradiated fuel fragments. Information on absorption from the respiratory tract is available from experimental studies of ruthenium as tetroxide, chloride, citrate, dioxide, and irradiated uranium dioxide. For details see Section 2 of *Publication 137* (ICRP, 2017). Absorption parameter values and types, and associated f_A values for gas and vapour forms of ruthenium are given in Table 21.1 and for particulate forms in Table 21.2 (taken from Section 2 of *Publication 137*). Exposures to gas and vapour forms of ruthenium are relatively unusual compared to exposures to particulate forms, and it is therefore recommended in this series of documents that particulate form is assumed in the absence of information.

Table 21.1. Deposition and absorption for gas and vapour forms of ruthenium.

	Percentage deposited (%)*						Absorption†		
Chemical form/origin	Total	ET_1	ET_2	BB	bb	AI	f_r	s_r (d^{-1})	s_s (d^{-1})
Ruthenium tetroxide	100[b]	40	40	12	7	1	0.5	1	0.001

Chemical form/origin	Age-dependent absorption from the alimentary tract, f_A					
	3 months	1 year	5 years	10 years	15 years	Adult
Ruthenium tetroxide	0.02	0.01	0.01	0.01	0.01	0.01

ET_1, anterior nasal passage; ET_2, posterior nasal passage, pharynx and larynx; BB, bronchial; bb, bronchiolar; AI, alveolar-interstitial.

**Percentage deposited* refers to how much of the material in the inhaled air remains in the body after exhalation. Almost all inhaled gas molecules contact airway surfaces, but usually return to the air unless they dissolve in, or react with, the surface lining.

†It is assumed that for ruthenium the bound fraction f_b is 0.05 with an uptake rate s_b = 0.1 d^{-1}, and that this applies throughout the respiratory tract (ET_2, BB, bb and AI regions, and associated lymph nodes LN_{ET} and LN_{TH}).

Table 21.2. Absorption parameter values for inhaled particulate forms of ruthenium and for ingested ruthenium.

		Absorption parameter values*		
Inhaled particulate materials		f_r	s_r (d^{-1})	s_s (d^{-1})
Default parameter values†,‡				
Absorption Type	Assigned forms			
F	Chloride, oxalate	1	30	–
M§	Citrate	0.2	3	0.005
S	Dioxide	0.01	3	1×10^{-4}

Ingested material¶						
Assigned forms	Age-dependent absorption from the alimentary tract, f_A					
	3 months	1 year	5 years	10 years	15 years	adult

All forms	0.1	0.05	0.05	0.05	0.05	0.05

[*]It is assumed that for ruthenium the bound fraction f_b is 0.05 with an uptake rate s_b = 0.1 d^{-1}, and that this applies throughout the respiratory tract (ET_2, BB, bb and AI regions, and associated lymph nodes LN_{ET} and LN_{TH}). The values of s_r for Type F, M and S forms of ruthenium (30, 3 and 3 d^{-1}, respectively) are the general default values.
[†]Materials (e.g. ruthenium chloride) are listed here where there is sufficient information to assign to a default absorption type, but not to give specific parameter (see Section 2 of *Publication 137*, ICRP, 2017).
[‡]For inhaled material deposited in the respiratory tract and subsequently cleared by particle transport to the alimentary tract, the default f_A values for inhaled materials are applied: i.e. the product of f_r for the absorption type and the f_A value for ingested soluble forms of ruthenium applicable to the age-group of interest (*e.g.* 0.05 for adults).
[§]Default Type M is recommended for use in the absence of specific information on which the exposure material can be assigned to an absorption type, e.g., if the form is unknown, or if the form is known but there is no information available on the absorption of that form from the respiratory tract.
[¶]Activity transferred from systemic compartments into segments of the alimentary tract is assumed to be subject to reabsorption to blood. The default absorption fraction f_A for the secreted activity is the highest value for ingestion of the radionuclide applicable to the age-group of interest (*e.g.* 0.05 for adults).

21.1.2. Ingestion

21.1.2.1. Adults

(393) Results from a number of human and animal studies show fractional absorption in the range 0.8 – 15% depending on the physical and chemical form administered and the nutritional status of the subject (for more details, see section 2 of *Publication 137*, ICRP, 2017). In *Publication 30* (ICRP, 1980), an absorption fraction of 0.05 was recommended for all chemical forms of ruthenium. This value was also recommended in *Publication 56* (ICRP, 1990) for dietary intakes as well as in *Publication 137*. The same value f_A = 0.05 is adopted here for ruthenium ingested in food by adults in the population.

21.1.2.2. Children

(394) Few data are available on the absorption of ruthenium in the young. Newborn mice absorbed about 7% of ^{106}Ru administered as the chloro-complex in dilute HCl (Matsusaka et al., 1969) but 21 days old and adult mice absorbed less than 1%. Inaba et al. (1984) found 0.8% absorption of carrier free ^{103}Ru in suckling (5 days old) rats after administration as the chloride compared with 0.5% in adults. These results suggest that for young infants a higher absorption fraction than is applied to adults is appropriate. For the 3 months infant an absorption fraction of 0.1 was recommended in *Publication 56* for isotopes of ruthenium in food. For children of 1 year and older an absorption fraction of 0.05 was recommended in *Publication 56*. Harrison et al. (2001) proposed confidence intervals of 0.005 to 0.1 for adults, 0.005–0.15 for 10-year-old children, and 0.005–0.2 for 3-month-old infants. The same values as in *Publication 56* are adopted here for children : f_A = 0.1 for 3-mo-old and f_A = 0.05 for older children.

21.1.3. Systemic Distribution, Retention and Excretion

(395) The model for systemic ruthenium applied in *Publication 137* (ICRP, 2017) to workers is applied here to adult members of the public. That model is based where feasible on biokinetic data derived in controlled studies of ruthenium kinetics in human subjects. However, most transfer coefficients are based at least in part on observations of the distribution, retention, and excretion of ruthenium isotopes in laboratory animals, particularly dogs.

(396) No useful information was found regarding age related changes in the biokinetics of systemic ruthenium. The systemic behaviour of ruthenium is assumed to be independent of age except that activity is assumed to be removed from trabecular or cortical bone volume to blood at the age-specific rate of turnover of that bone type.

(397) The structure of the model for ruthenium is shown in Fig. 21.1. Parameter values are given in Table 21.3.

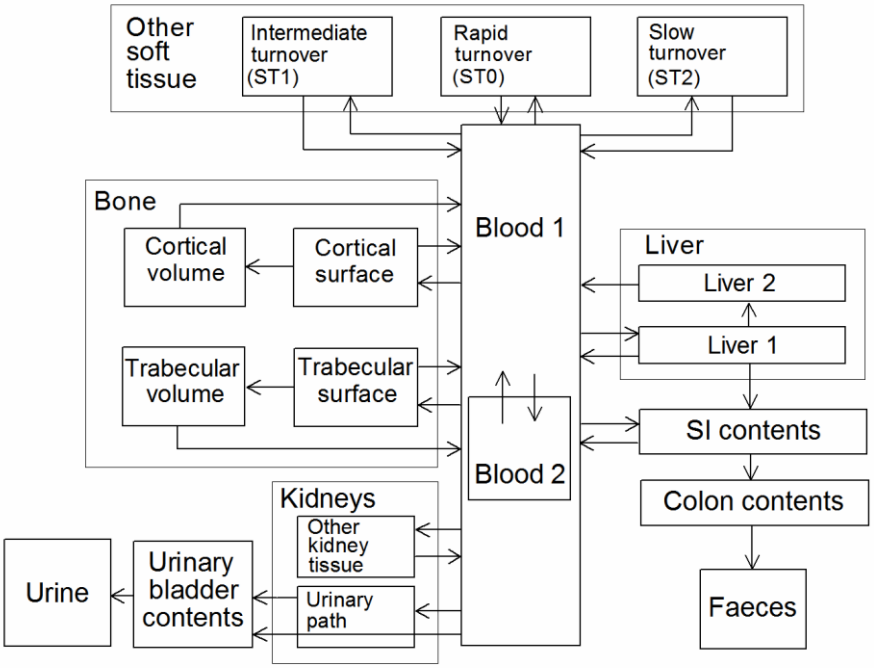

Fig. 21.1. Structure of the biokinetic model for systemic ruthenium. SI = Small intestine.

4323 Table 21.3. Transfer coefficients for the model for systemic ruthenium

Path[a]	Transfer coefficient (d^{-1})					
	Infant	1 y	5 y	10 y	15 y	Adult
Blood 1 to SI contents	3.00E+00	3.00E+00	3.00E+00	3.00E+00	3.00E+00	3.00E+00
Blood 1 to UB contents	1.70E+01	1.70E+01	1.70E+01	1.70E+01	1.70E+01	1.70E+01
Blood 1 to Liver 1	1.20E+01	1.20E+01	1.20E+01	1.20E+01	1.20E+01	1.20E+01
Blood 1 to Urinary path	7.76E+00	7.76E+00	7.76E+00	7.76E+00	7.76E+00	7.76E+00
Blood 1 to Other kidney tissue	2.40E-01	2.40E-01	2.40E-01	2.40E-01	2.40E-01	2.40E-01
Blood 1 to Blood 2	2.70E+01	2.70E+01	2.70E+01	2.70E+01	2.70E+01	2.70E+01
Blood 1 to ST0	1.50E+01	1.50E+01	1.50E+01	1.50E+01	1.50E+01	1.50E+01
Blood 1 to ST1	5.00E+00	5.00E+00	5.00E+00	5.00E+00	5.00E+00	5.00E+00
Blood 1 to ST2	5.00E+00	5.00E+00	5.00E+00	5.00E+00	5.00E+00	5.00E+00
Blood 1 to Cort bone surf	2.00E+00	2.00E+00	2.00E+00	2.00E+00	2.00E+00	2.00E+00
Blood 1 to Trab bone surf	6.00E+00	6.00E+00	6.00E+00	6.00E+00	6.00E+00	6.00E+00
Blood 2 to Blood 1	6.93E-01	6.93E-01	6.93E-01	6.93E-01	6.93E-01	6.93E-01
Liver 1 to Blood 1	9.70E-02	9.70E-02	9.70E-02	9.70E-02	9.70E-02	9.70E-02
Liver 1 to SI contents	3.47E-02	3.47E-02	3.47E-02	3.47E-02	3.47E-02	3.47E-02
Liver 1 to Liver 2	6.93E-03	6.93E-03	6.93E-03	6.93E-03	6.93E-03	6.93E-03
Liver 2 to Blood 1	3.80E-03	3.80E-03	3.80E-03	3.80E-03	3.80E-03	3.80E-03
Urinary path to UB contents	1.39E-01	1.39E-01	1.39E-01	1.39E-01	1.39E-01	1.39E-01
Other kidney tissue to Blood 1	3.80E-03	3.80E-03	3.80E-03	3.80E-03	3.80E-03	3.80E-03
ST0 to Blood 1	9.90E-02	9.90E-02	9.90E-02	9.90E-02	9.90E-02	9.90E-02
ST1 to Blood 1	2.31E-02	2.31E-02	2.31E-02	2.31E-02	2.31E-02	2.31E-02
ST2 to Blood 1	9.50E-04	9.50E-04	9.50E-04	9.50E-04	9.50E-04	9.50E-04
Cort bone surf to Blood 1	7.92E-02	7.92E-02	7.92E-02	7.92E-02	7.92E-02	7.92E-02
Trab bone surf to Blood 1	7.92E-02	7.92E-02	7.92E-02	7.92E-02	7.92E-02	7.92E-02
Cort bone surf to Cort bone vol	1.98E-02	1.98E-02	1.98E-02	1.98E-02	1.98E-02	1.98E-02
Trab bone surf to Trab bone vol	1.98E-02	1.98E-02	1.98E-02	1.98E-02	1.98E-02	1.98E-02
Cort bone vol to Blood 1	8.22E-03	2.88E-03	1.53E-03	9.04E-04	5.21E-04	8.21E-05
Trab bone vol to Blood 1	8.22E-03	2.88E-03	1.81E-03	1.32E-03	9.59E-04	4.93E-04

4324 [a]UB = Urinary bladder, SI= Small intestine, Trab = Trabecular, Cort = Cortical, surf = surface, vol = volume

21.2. Dosimetric data for ruthenium

Table 21.4. Committed effective dose coefficients (Sv Bq^{-1}) for the inhalation or ingestion of ^{106}Ru compounds.

	Effective dose coefficients (Sv Bq^{-1})					
Inhaled gases or vapours	3 mo	1 y	5 y	10 y	15 y	Adult
Ruthenium tetroxide	3.4E-08	2.7E-08	1.6E-08	1.0E-08	7.6E-09	7.0E-09
Inhaled particulate materials (1 µm AMAD aerosols)						
Type F, Chloride, oxalate	4.2E-08	3.5E-08	1.8E-08	1.1E-08	8.1E-09	6.7E-09
Type M, Citrate; all unspecified forms	9.2E-08	8.3E-08	4.9E-08	3.2E-08	2.6E-08	2.6E-08
Type S, Dioxide	2.2E-07	2.1E-07	1.3E-07	8.7E-08	7.2E-08	7.4E-08
Ingested materials						
Adult f_A = 0.05, All forms	2.2E-08	1.2E-08	6.9E-09	4.3E-09	3.0E-09	2.6E-09

22. SILVER (Z = 47)

22.1. Routes of Intake

22.1.1. Inhalation

(398) A few studies give information on absorption of silver from the respiratory tract. For details see Section 25 of *Publication 151* (ICRP, 2022). Absorption parameter values and types, and associated f_A values for inhaled particulate forms of silver are given in Table 22.1.

Table 22.1. Absorption parameter values for inhaled and ingested silver

Inhaled particulate materials		Absorption parameter values* f_r	s_r (d^{-1})	s_s (d^{-1})
Default parameter values†,‡				
Absorption Type	Assigned forms			
F	Nitrate	1	1	–
M§	Iodide	0.2	1	0.005
S	—	0.01	1	$1x10^{-4}$

Ingested materials¶	Age-dependent absorption from the alimentary tract, f_A					
Assigned forms	3 months	1 year	5 years	10 years	15 years	adults
All chemical forms	0.1	0.05	0.05	0.05	0.05	0.05

*It is assumed that for silver the bound state can be neglected *i.e.* $f_b = 0$. The values of s_r for Type F, M and S forms of silver (1 d^{-1}) are element-specific.

†Materials (e.g. Nitrate) are listed here where there is sufficient information to assign to a default absorption type, but not to give specific parameter values (see Section 25 of *Publication 151*, ICRP, 2022).

‡For inhaled material deposited in the respiratory tract and subsequent cleared by particle transport to the alimentary tract, the default f_A values for inhaled materials are applied: *i.e.*, the (rounded) product of f_r for the absorption type and the f_A value for ingested soluble forms of silver applicable to the age-group of interest (*e.g.* 0.05 for adults).

§Default Type M is recommended for use in the absence of specific information on which the exposure material can be assigned to an absorption type, e.g. if the form is unknown, or if the form is known but there is no information available on the absorption of that form from the respiratory tract.

¶Activity transferred from systemic compartments into segments of the alimentary tract is assumed to be subject to reabsorption to blood. The default absorption fraction f_A for the secreted activity is the highest value for ingestion of the radionuclide applicable to the age-group of interest (*e.g.* 0.05 for adults).

22.1.2. Ingestion

22.1.2.1. Adults

(399) There is very little information on the gastrointestinal absorption of silver. For details see Section 25 of *Publication 151* (ICRP, 2022). The value of $f_A = 0.05$ is adopted here for dietary intakes of silver.

22.1.2.2. Children

(400) Inaba et al. (1984) have reported data for rats on the age-dependent biokinetics of $^{110m}AgN0_3$ after oral administration. Their results indicate an enhancement of absorption of

silver in suckling rats compared with adults. Like in *Publication* 67 (ICRP, 1993), an f_A value of 0.1 is adopted here for 3-month-old infants. For children of 1 year and older the f_A value for the adult (0.05) is used.

22.1.3. Systemic Distribution, Retention and Excretion

(401) No information was found on age related changes in the systemic kinetics of silver.

(402) An updated systemic biokinetic model for occupational intake of silver is described in Section 25 of *Publication 151* (ICRP, 2022). That model is applied here to intake of silver at any age.

(403) The structure of the model for systemic silver is shown in Fig. 22.1. Parameter values are listed in Table 22.2.

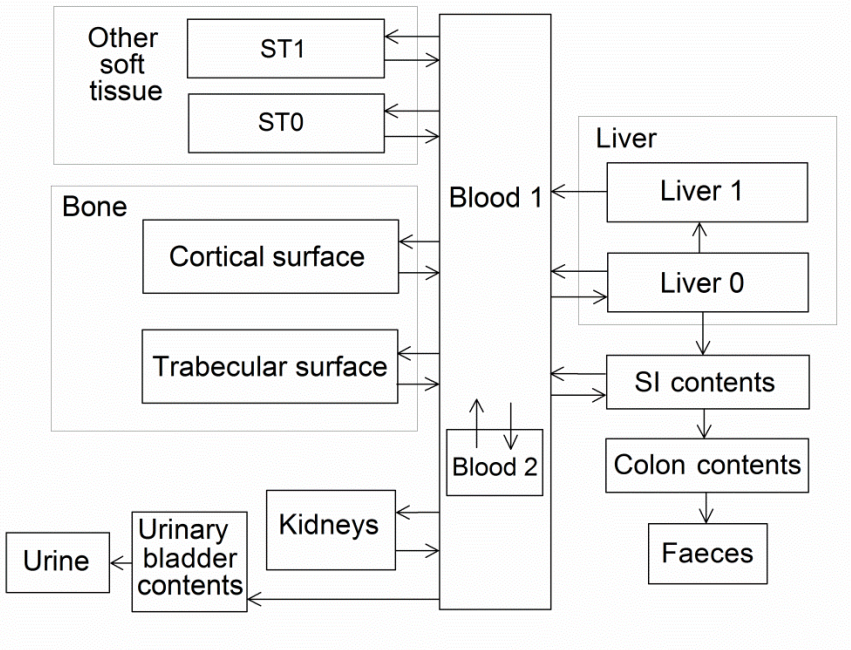

Fig. 22.1. Structure of the biokinetic model for systemic silver. SI = Small intestine.

4373 Table 22.2. Transfer coefficients for the model for systemic silver

Path[a]	Transfer coefficient (d^{-1})					
	Infant	1 y	5 y	10 y	15 y	Adult
Blood 1 to Blood 2	7.20E-01	7.20E-01	7.20E-01	7.20E-01	7.20E-01	7.20E-01
Blood 1 to Kidneys	1.20E+00	1.20E+00	1.20E+00	1.20E+00	1.20E+00	1.20E+00
Blood 1 to Liver 1	3.00E+01	3.00E+01	3.00E+01	3.00E+01	3.00E+01	3.00E+01
Blood 1 to Trab bone surf	1.20E+00	1.20E+00	1.20E+00	1.20E+00	1.20E+00	1.20E+00
Blood 1 to Cort bone surf	1.20E+00	1.20E+00	1.20E+00	1.20E+00	1.20E+00	1.20E+00
Blood 1 to ST0	1.28E+01	1.28E+01	1.28E+01	1.28E+01	1.28E+01	1.28E+01
Blood 1 to ST1	1.28E+01	1.28E+01	1.28E+01	1.28E+01	1.28E+01	1.28E+01
Blood 1 to UB contents	1.30E-01	1.30E-01	1.30E-01	1.30E-01	1.30E-01	1.30E-01
Blood 2 to Blood 1	2.31E-01	2.31E-01	2.31E-01	2.31E-01	2.31E-01	2.31E-01
Kidneys to Blood 1	8.00E-01	8.00E-01	8.00E-01	8.00E-01	8.00E-01	8.00E-01
Liver 1 to SI contents	1.00E+00	1.00E+00	1.00E+00	1.00E+00	1.00E+00	1.00E+00
Liver 1 to Liver 2	9.00E+00	9.00E+00	9.00E+00	9.00E+00	9.00E+00	9.00E+00
Liver 2 to Blood 1	2.00E-01	2.00E-01	2.00E-01	2.00E-01	2.00E-01	2.00E-01
ST0 to Blood 1	8.00E+00	8.00E+00	8.00E+00	8.00E+00	8.00E+00	8.00E+00
ST1 to Blood 1	4.00E-01	4.00E-01	4.00E-01	4.00E-01	4.00E-01	4.00E-01
Trab bone surf to Blood 1	7.00E-02	7.00E-02	7.00E-02	7.00E-02	7.00E-02	7.00E-02
Cort bone surf to Blood 1	7.00E-02	7.00E-02	7.00E-02	7.00E-02	7.00E-02	7.00E-02

4374 [a]Trab = trabecular, Cort = cortical, surf = surface, UB = urinary bladder, SI = small intestine

22.2. Dosimetric data for silver

Table 22.3. Committed effective dose coefficients (Sv Bq^{-1}) for the inhalation or ingestion of ^{110m}Ag compounds.

	Effective dose coefficients (Sv Bq^{-1})					
Inhaled particulate materials (1 μm AMAD aerosols)	3 mo	1 y	5 y	10 y	15 y	Adult
Type F, Nitrate	1.8E-08	1.3E-08	7.5E-09	5.1E-09	3.8E-09	4.2E-09
Type M, Iodide; all unspecified forms	3.0E-08	2.6E-08	1.5E-08	1.0E-08	7.9E-09	9.0E-09
Type S	5.2E-08	4.8E-08	2.9E-08	2.0E-08	1.6E-08	1.8E-08
Ingested materials						
f_A = 0.05, All chemical forms	1.4E-08	7.7E-09	4.5E-09	3.2E-09	2.2E-09	2.3E-09

23. ANTIMONY (Z = 51)

23.1. Routes of Intake

23.1.1. Inhalation

(404) Information on absorption from the respiratory tract is available from experimental studies of antimony inhaled by laboratory animals as chloride, tartrate or oxide. Some information is also available on the behaviour of inhaled ^{125}Sb in man. For details, see Section 3 of *Publication 137* (ICRP, 2017). Absorption parameter values and types, and associated f_A values for particulate forms of antimony are given in Table 23.1 (taken from Section 3 of *Publication 137*).

Table 23.1. Absorption parameter values for inhaled and ingested antimony.

		Absorption parameter values*		
Inhaled particulate materials		f_r	s_r (d^{-1})	s_s (d^{-1})
Default parameter values†,‡				
Absorption Type				
F	Chloride, tartrate	1	30	–
M§	Trioxide	0.2	3	0.005
S	—	0.01	3	1×10^{-4}

Ingested materials¶						
Assigned forms	Age-dependent absorption from the alimentary tract, f_A					
	3 months	1 year	5 years	10 years	15 years	adult
Antimony in food	0.2	0.1	0.1	0.1	0.1	0.1
Other chemical forms	0.1	0.05	0.05	0.05	0.05	0.05

*It is assumed that for antimony the bound state can be neglected, i.e. $f_b = 0.0$. The values of s_r for Type F, M and S forms of antimony (30, 3 and 3 d^{-1}, respectively) are the general default values.

†Materials (e.g. Chloride) are generally listed here where there is sufficient information to assign to a default absorption Type, but not to give specific parameter values (see Section 3 of *Publication 137*, ICRP, 2017).

‡For inhaled material deposited in the respiratory tract and subsequently cleared by particle transport to the alimentary tract, the default f_A values for inhaled materials are applied: i.e. the product of f_r for the absorption type and the f_A value for ingested soluble (excluding dietary) forms of antimony applicable to the age-group of interest (*e.g.* 0.05 for adults).

§Default Type M is recommended for use in the absence of specific information on which the exposure material can be assigned to an absorption type, e.g., if the form is unknown, or if the form is known but there is no information available on the absorption of that form from the respiratory tract.

¶Activity transferred from systemic compartments into segments of the alimentary tract is assumed to be subject to reabsorption to blood. The default absorption fraction f_A for the secreted activity is the highest value for ingestion of the radionuclide applicable to the age-group of interest (*e.g.* 0.1 for adults).

23.1.2. Ingestion

23.1.2.1. Adults

(405) No controlled studies on antimony absorption in humans have been carried out, but bioassay measurements following accidental exposure and animal experiments suggested

variable absorption values, nearly all less than 5% of ingested antimony, except for a somewhat higher absorption of antimonyl potassium tartrate (tartar emetic) (*Publication 137*, ICRP, 2017). For more details, see Section 3 of *Publication 137*. In *Publication 137*, a single f_A value of 0.05 was recommended for all occupational exposures where specific information was not available. Inaba et al. (1984) reported fractional absorption in adult rats as 0.5 of ^{125}Sb biologically incorporated into blood cells. In a further study in which ^{125}Sb was mixed with blood, fractional absorption was only about 0.01; however, hydrolysis may have occurred which would have reduced uptake. Coughtrey and Thorne (1983) have suggested an upper limit for the absorption fraction of about 0.1, based on estimates of the daily dietary intake and the body content of stable antimony. The data indicate there may be considerable differences in absorption for the range of chemical forms of antimony encountered in the environment. Because ingestion of radioantimony by the general public is likely to occur principally in food or drink, *Publication 69* (ICRP, 1995a) assumed a higher value of 0.1 for the fractional absorption of antimony. This value is also adopted here for ingestion by adult of antimony in food. For ingestion of other forms, an f_A of 0.05 is adopted.

23.1.2.2.Children

(406) Few data seem to be available on the absorption of antimony in young animals. Inaba et al. (1984) administered $^{125}SbCl_3$ to 5-d-old suckling rats and to adult rats, and compared their whole body retention of ^{125}Sb. Retention of antimony on the fifth day after administration was about 40% for suckling animals and 0.2% for adults. For 15-d-old suckling animals, retention on the fifth day was 20% and for 25-d-old weanlings it was about the same as for adults (Jiro Inaba et al., 1984). In view of the limited data available, *Publication 69* recommended an absorption fraction for the 3-mo-old infant of 0.2. The same value of $f_A = 0.2$ for 3-mo-old infants is adopted here for antimony in food and an f_A of 0.1 is adopted for all other chemical forms.

23.1.3. Systemic Distribution, Retention and Excretion

(407) Antimony generally occurs in nature either in the trivalent or pentavalent state, with the trivalent state being the more stable state in biological fluids. Trivalent and pentavalent antimony initially show different biokinetics after entering the systemic circulation. For example, Sb(III) is excreted in urine at a lower rate and accumulated by red blood cells at a higher rate than Sb(V) in the first day or two after intravenous or intramuscular injection. There is evidence of some reduction of Sb(V) to Sb(III) *in vivo* and convergence of the systemic biokinetics of these two initial forms over time.

(408) The model for systemic antimony applied in *Publication 137* (ICRP, 2017) to workers is applied here to adult members of the public. That model is based where feasible on results of controlled biokinetic studies of antimony tracers in a few human subjects. Due to the sparsity of such data, however, the model relies heavily on findings for laboratory animals, particularly dogs. The transfer coefficients are based on data for trivalent antimony, which has been studied more than pentavalent antimony and which is expected to be the primary form of antimony in the body except perhaps for a relatively brief period after exposure to Sb(V). For radioisotopes of antimony entering the systemic circulation as pentavalent antimony, the model is expected to underestimate the initial rate of biological removal from the body and overestimate cumulative nuclear transformations in systemic tissues and fluids.

(409) No information was found on age related changes in the systemic behaviour of antimony in human subjects. In rats, total-body retention of ^{125}Sb administered as the chloride appeared to be independent of age (J. Inaba et al., 1984).

(410) The systemic behaviour of antimony is assumed here to be independent of age except that activity is removed from trabecular or cortical bone volume to blood at the age-specific rate of turnover of that bone type.

(411) The structure of the model for antimony is shown in Fig. 23.1. Parameter values are given in Table 23.2.

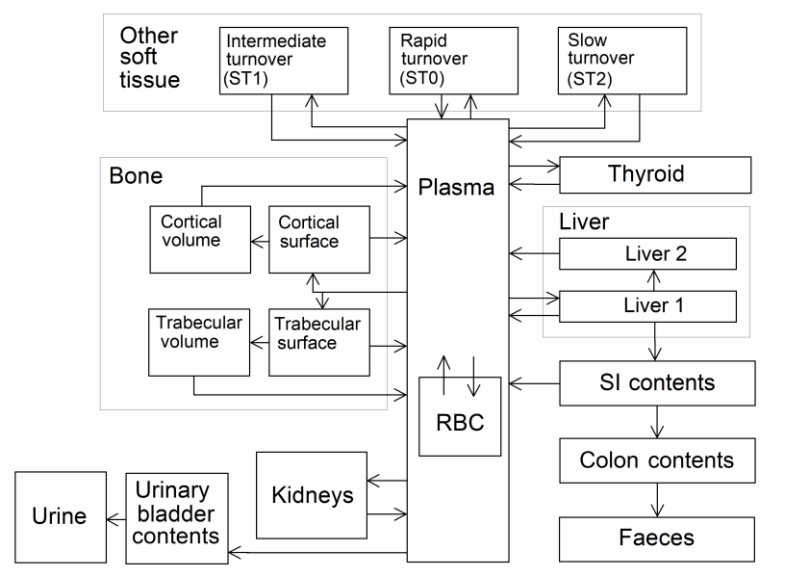

Fig. 23.1. Structure of the biokinetic model for systemic antimony. SI = Small intestine, RBC = Red blood cells.

Table 23.2. Transfer coefficients for the model for antimony

Path[a]	Transfer coefficient (d^{-1})					
	Infant	1 y	5 y	10 y	15 y	Adult
Plasma to UB contents	9.00E+00	9.00E+00	9.00E+00	9.00E+00	9.00E+00	9.00E+00
Plasma to RBC	3.00E+00	3.00E+00	3.00E+00	3.00E+00	3.00E+00	3.00E+00
Plasma to ST0	7.49E+01	7.49E+01	7.49E+01	7.49E+01	7.49E+01	7.49E+01
Plasma to ST1	4.50E+00	4.50E+00	4.50E+00	4.50E+00	4.50E+00	4.50E+00
Plasma to ST2	4.00E-02	4.00E-02	4.00E-02	4.00E-02	4.00E-02	4.00E-02
Plasma to Liver 1	4.00E+00	4.00E+00	4.00E+00	4.00E+00	4.00E+00	4.00E+00
Plasma to Kidneys	2.50E-01	2.50E-01	2.50E-01	2.50E-01	2.50E-01	2.50E-01
Plasma to Cort bone surf	2.00E+00	2.00E+00	2.00E+00	2.00E+00	2.00E+00	2.00E+00
Plasma to Trab bone surf	2.00E+00	2.00E+00	2.00E+00	2.00E+00	2.00E+00	2.00E+00
Plasma to Thyroid	3.00E-01	3.00E-01	3.00E-01	3.00E-01	3.00E-01	3.00E-01
Thyroid to Plasma	1.39E-01	1.39E-01	1.39E-01	1.39E-01	1.39E-01	1.39E-01
RBC to Plasma	6.93E-01	6.93E-01	6.93E-01	6.93E-01	6.93E-01	6.93E-01
ST0 to Plasma	1.39E+00	1.39E+00	1.39E+00	1.39E+00	1.39E+00	1.39E+00
ST1 to Plasma	1.39E-02	1.39E-02	1.39E-02	1.39E-02	1.39E-02	1.39E-02
ST2 to Plasma	6.93E-04	6.93E-04	6.93E-04	6.93E-04	6.93E-04	6.93E-04
Liver 1 to SI contents	2.43E-01	2.43E-01	2.43E-01	2.43E-01	2.43E-01	2.43E-01
Liver 1 to Plasma	4.37E-01	4.37E-01	4.37E-01	4.37E-01	4.37E-01	4.37E-01
Liver 1 to Liver 2	1.39E-02	1.39E-02	1.39E-02	1.39E-02	1.39E-02	1.39E-02
Liver 2 to Plasma	6.93E-04	6.93E-04	6.93E-04	6.93E-04	6.93E-04	6.93E-04

Kidneys to Plasma	2.31E-01	2.31E-01	2.31E-01	2.31E-01	2.31E-01	2.31E-01
Cort bone surf to Plasma	3.43E-01	3.43E-01	3.43E-01	3.43E-01	3.43E-01	3.43E-01
Trab bone surf to Plasma	3.43E-01	3.43E-01	3.43E-01	3.43E-01	3.43E-01	3.43E-01
Cort bone surf to Cort bone vol	3.47E-03	3.47E-03	3.47E-03	3.47E-03	3.47E-03	3.47E-03
Trab bone surf to Trab bone vol	3.47E-03	3.47E-03	3.47E-03	3.47E-03	3.47E-03	3.47E-03
Cort bone vol to Plasma	8.22E-03	2.88E-03	1.53E-03	9.04E-04	5.21E-04	8.21E-05
Trab bone vol to Plasma	8.22E-03	2.88E-03	1.81E-03	1.32E-03	9.59E-04	4.93E-04

4466 [a]UB = Urinary bladder, SI= Small intestine, Trab = Trabecular, Cort = Cortical, surf = surface, vol = volume

23.2. Dosimetric data for antimony

Table 23.3. Committed effective dose coefficients (Sv Bq^{-1}) for the inhalation or ingestion of ^{124}Sb compounds.

	Effective dose coefficients (Sv Bq^{-1})					
Inhaled particulate materials (1 µm AMAD aerosols)	3 mo	1 y	5 y	10 y	15 y	Adult
Type F, Chloride, tartrate	1.1E-08	8.3E-09	4.3E-09	2.5E-09	1.7E-09	1.4E-09
Type M, Trioxide; all unspecified forms	2.1E-08	1.7E-08	9.9E-09	6.6E-09	5.0E-09	5.2E-09
Type S	2.9E-08	2.5E-08	1.5E-08	9.9E-09	7.5E-09	7.9E-09
Ingested materials						
Adult f_A = 0.05, Other chemical forms	7.2E-09	4.7E-09	2.7E-09	1.8E-09	1.2E-09	1.1E-09
Adult f_A = 0.1, Antimony in food	1.1E-08	6.1E-09	3.5E-09	2.2E-09	1.5E-09	1.4E-09

Table 23.4. Committed effective dose coefficients (Sv Bq^{-1}) for the inhalation or ingestion of ^{125}Sb compounds.

	Effective dose coefficients (Sv Bq^{-1})					
Inhaled particulate materials (1 µm AMAD aerosols)	3 mo	1 y	5 y	10 y	15 y	Adult
Type F, Chloride, tartrate	5.6E-09	4.5E-09	2.4E-09	1.4E-09	9.4E-10	8.5E-10
Type M, Trioxide; all unspecified forms	1.4E-08	1.2E-08	6.9E-09	4.5E-09	3.5E-09	3.5E-09
Type S	4.4E-08	4.2E-08	2.7E-08	1.8E-08	1.5E-08	1.6E-08
Ingested materials						
Adult f_A = 0.05, Other chemical forms	3.0E-09	1.6E-09	9.4E-10	6.0E-10	4.1E-10	3.7E-10
Adult f_A = 0.1, Antimony in food	5.2E-09	2.5E-09	1.4E-09	8.8E-10	6.1E-10	5.4E-10

24.TELLURIUM (Z = 52)

24.1.Routes of Intake

24.1.1. Inhalation

(412) A few experimental studies of the behaviour of radio-labelled tellurium (i.e. tracer level) following deposition in the respiratory tract have been identified in the literature. Some information is also available from measurements following inadvertent intakes of irradiated tellurium oxide, from studies of tellurium-132 inhaled by people after the Chernobyl accident, and from toxicology studies of stable tellurium compounds. For details, see Section 4 of *Publication 137* (ICRP, 2017).

(413) Absorption parameter values and types, and associated f_A values for gas and vapour forms of tellurium are given in Table 24.1 and for particulate forms in Table 24.2 (taken from Section 4 of *Publication 137*). Common forms of tellurium (e.g. dioxide) are solids at room temperature. Exposures to gas or vapour forms of tellurium are therefore probably relatively unusual compared to exposures to particulate forms, and it is therefore recommended in this series of documents that particulate form should be assumed in the absence of specific information.

Table 24.1. Deposition and absorption for gas and vapour forms of tellurium.

	Percentage deposited (%)*						Absorption Type†
Chemical form/origin	Total	ET_1	ET_2	BB	bb	AI	
All unspecified compounds	100[b]	0	20	10	20	50	F

	Age-dependent absorption from the alimentary tract, f_A					
Chemical form/origin	3 months	1 year	5 years	10 years	15 years	Adult
All unspecified compounds	0.6	0.3	0.3	0.3	0.3	0.3

ET_1, anterior nasal passage; ET_2, posterior nasal passage, pharynx and larynx; BB, bronchial; bb, bronchiolar; AI, alveolar-interstitial.

**Percentage deposited* refers to how much of the material in the inhaled air remains in the body after exhalation. Almost all inhaled gas molecules contact airway surfaces, but usually return to the air unless they dissolve in, or react with, the surface lining. The default distribution between regions is assumed: 20% ET_2, 10% BB, 20% bb and 50% AI.

†It is assumed that for tellurium the bound state can be neglected i.e. $f_b = 0$.

Table 24.2. Absorption parameter values for inhaled particulate forms of tellurium and for ingested tellurium.

		Absorption parameter values*		
Inhaled particulate materials		f_r	s_r (d^{-1})	s_s (d^{-1})
Default parameter values†,‡				
Absorption Type	Assigned forms			
F	Chloride, Dioxide	1	50	–
M§	Elemental tellurium, cadmium telluride	0.2	3	0.005
S	—	0.01	3	1×10^{-4}

Ingested materials[¶]

Assigned forms	Age-dependent absorption from the alimentary tract, f_A					
	3 months	1 year	5 years	10 years	15 years	adult
All forms	0.6	0.3	0.3	0.3	0.3	0.3

[*]It is assumed that for tellurium the bound state can be neglected i.e. $f_b = 0$. The value of s_r for Type F forms of tellurium is element-specific. The values for Types M and S (3 d^{-1}) are the general default values.
[†]Materials (e.g. Chloride) are listed here where there is sufficient information to assign to a default absorption type, but not to give specific parameter values (see Section 4 of ICRP, 2017).
[‡]For inhaled material deposited in the respiratory tract and subsequently cleared by particle transport to the alimentary tract, the default f_A values for inhaled materials are applied: i.e. the product of f_r for the absorption type and the f_A value for ingested soluble forms of tellurium applicable to the age-group of interest (*e.g.* 0.3 for adults).
[§]Default Type M is recommended for use in the absence of specific information on which the exposure material can be assigned to an absorption type, e.g., if the form is unknown, or if the form is known but there is no information available on the absorption of that form from the respiratory tract.
[¶]Activity transferred from systemic compartments into segments of the alimentary tract is assumed to be subject to reabsorption to blood. The default absorption fraction f_A for the secreted activity is the highest value for ingestion of the radionuclide applicable to the age-group of interest (e.g. 0.3 for adults).

24.1.2. Ingestion

24.1.2.1. Adults

(414) Taking into account experimental data from several animal species *Publication 30* (ICRP, 1979) recommended an absorption fraction of 0.2. Kron et al. (1991) studied the renal excretion of stable tellurium by healthy volunteers after oral administration of Te as sodium tellurate (TeO_3), sodium tellurite (TeO_2) and metallic colloid and proposed that a fractional absorption value of 0.25 should be applied for radiological protection purposes. Based on this study and on recent animal experiments, a value of 0.3 was recommended in *Publication 67* (ICRP, 1993) and in *Publication 137* (ICRP, 2017). The value of $f_A = 0.3$ is adopted here for dietary intakes of tellurium.

24.1.2.2. Children

(415) No information appears to be available from experimental animals or studies in humans for assessing any possible changes with age of tellurium gastrointestinal absorption. Following its general approach, *Publication 67* recommended an absorption fraction for tellurium of 0.6 for the 3-month-old infant. For children of 1 year and older *Publication 67* recommended to use the value for adults (0.3). The same values are adopted here for f_A.

24.1.3. Systemic Distribution, Retention and Excretion

24.1.3.1. Summary of biokinetic data

(416) Kron et al. (1991) studied urinary excretion of tellurium in five healthy volunteers after oral administration of tellurium in different forms: tellurite (Na_2TeO_4), tellurate (Na_2TeO_3), metallic form, and intrinsically bound in cress (*Lepidium sativum*). Cress was consumed both with and without oil and vinegar dressing. The three-day urinary excretion varied between 3 and 25%. Urinary excretion was higher for tellurate (9-25%) than for tellurite (<8%) or metallic tellurium (4-9%). After ingestion of tellurium with cress, the amount excreted over three days was in the range 6-16%, and was reduced to 3% when dressing was

4539 added. For tellurate and metal tellurium most of the excretion occurred in the first 24 h after
4540 administration, whereas for cress and tellurite the excretion curve was delayed.
4541 (417) Schroeder et al. (1967) measured the concentration of tellurium in human tissues and
4542 calculated that a total body content of ~600 mg in a reference adult, approximately 90% of
4543 which was contained in bone
4544 (418) The systemic behaviour of tellurium at early times after intake has been investigated
4545 in laboratory animals including rats (Agnew and Cheng, 1971; Barnes et al., 1955; DeMeio and
4546 Henriques Jr., 1947; Health Council of the Netherlands: Committee on Updating of
4547 Occupational Exposure Limits, 2002; Hollins, 1969; Morgan et al., 1997; Valkonen and
4548 Savolainen, 1985), rabbits (DeMeio and Henriques Jr., 1947), dogs (DeMeio and Henriques Jr.,
4549 1947), guinea pigs, (Barnes et al., 1955), sheep (Casey et al., 1963; Wright and Bell, 1966),
4550 swine (Wright and Bell, 1966), cattle (Mullen and Stanley, 1974). The collective data indicate
4551 that a substantial portion of the administered activity is contained in the liver, kidneys, and
4552 bone during the first few days after administration. A relatively high concentration is also found
4553 in the thyroid gland, but the thyroid content represents only a small percentage of the systemic
4554 content due to its small mass. A substantial portion of the absorbed or injected amount is
4555 removed in urine in the first few days.
4556 (419) Casey et al. (1963) administered a mixture of radionuclides of tellurium and iodine to
4557 lactating sheep and found relatively low transfer of tellurium to milk (two to three orders of
4558 magnitude less than for iodine). Retained tellurium was found mainly in the liver, kidney, lungs.
4559 The highest concentration was found in the thyroid, but the total content of the thyroid was
4560 small due to its small mass.
4561 (420) Wright and Bell (1966) compared the kinetics of ^{127m}Te in sheep and swine following
4562 its intravenous administration as Na_2TeO_3. Activity cleared readily from plasma in both sheep
4563 and swine. Only a small portion of the administered activity was recovered in the cell fraction
4564 in sheep, In swine the corpuscular fraction rose with time to 3% of the injected amount at 5 d.
4565 At 5 d the liver and kidneys contained about 8% and 7%, respectively, in sheep and 7% and
4566 2%, respectively, in swine. No information was given about skeleton or thyroid. Both species
4567 excreted about 11% of the injected ^{127m}Te in the faeces and 34% in the urine over five d. About
4568 two-thirds of the urinary excretion occurred in the first 24 h.
4569 (421) Hollins (1969) studied the metabolism of ^{127m}Te administered orally or
4570 intraperitoneally as tellurous acid to rats. Retention after intraperitoneal injection could be
4571 described as a bi-exponential function with half-times of 0.8 d (49%) and 13 d (51%),
4572 respectively. The highest activity concentrations were observed in the kidneys, blood, liver,
4573 spleen, femur, and lung. Tellurium in blood was almost entirely bound to the protein content
4574 of the red blood cells. The tissues could be divided into three classes according to the retention
4575 half-time: lung, blood, liver and heart with a half-time of approximately 10 d; muscle, spleen,
4576 and kidney with a half-time of approximately 20 d; and femur (skeleton) with a half-time that
4577 was much longer than the duration of the experiment (200 d) and could therefore not be
4578 determined with much confidence. About 27% of the injected tellurium was excreted in urine
4579 during the first 24 h, and 6% was excreted in faeces. Less than 0.25% of the administered dose
4580 was eliminated in the breath in the first 24 h.
4581 (422) Barnes et al. (1955) administered ^{132}Te orally to rats and guinea pigs and determined
4582 the distribution of tellurium in the body at 3-4 d. In guinea pigs the concentration in liver,
4583 kidneys, and bone were substantially higher than in pelt, blood, and carcass. About 5.5% and
4584 6.5% was excreted in the urine over 4 d by the guinea pigs and rats, respectively. Faecal
4585 excretion plus activity present in the gut amounted to about 93% in the guinea pigs and 80% in
4586 the rats.

(423) Morgan et al. (1997) administered cadmium telluride intra-tracheally to rats. After absorption of tellurium into the systemic circulation, relatively high concentrations were found in the spleen (maximum, 82.8±10.2 μg·g^{-1} tissue), kidney (maximum, 8.1±1.3 μg·g^{-1} tissue), liver (maximum, 8.8±0.6 μg·g^{-1} tissue), femur (maximum 3.5±0.5 μg·g^{-1} tissue) and blood (maximum, 5.3±0.2 μg·g^{-1} tissue). The maximum concentration was reached at day 14 after administration in all tissues except liver, where the maximum was reached at day 7.

(424) Mullen and Stanley (1974) studied absorption, distribution and milk secretion of radiotellurium in dairy cows and calves. The transfer of tellurium to milk was low (about 0.25% of the orally administered activity in 13 d). Retained tellurium was found mainly in the liver, bone, and organs of the digestive/ruminal tract. The activity concentration in the thyroid was similar to that in the liver.

(425) No information was found regarding the effect of age on the biokinetics of systemic tellurium.

24.1.3.2. Systemic model

(426) A variation of the generic model structure for bone-surface-seeking radionuclides is applied to tellurium, with the introduction of the thyroid as a separate compartment. The model for the adult member of the public is the same as the model for occupational intake of tellurium used in *Publication 137* (ICRP, 2017). Transfer coefficients for adults are based predominantly on human data with regard to whole body retention and urinary excretion and on data for laboratory animals (particularly swine and guinea pigs) with regard to the system distribution. Due to paucity of age-specific biokinetic data for tellurium the transfer coefficients for adults are applied to all age groups with the exception for the assumption generally made in this report series that activity is removed from trabecular or cortical bone volume to blood at the reference age-specific rate of turnover of that bone type (ICRP, 2002a).

(427) The model structure is shown in Fig. 24.1. Transfer coefficients are listed in Table 24.3.

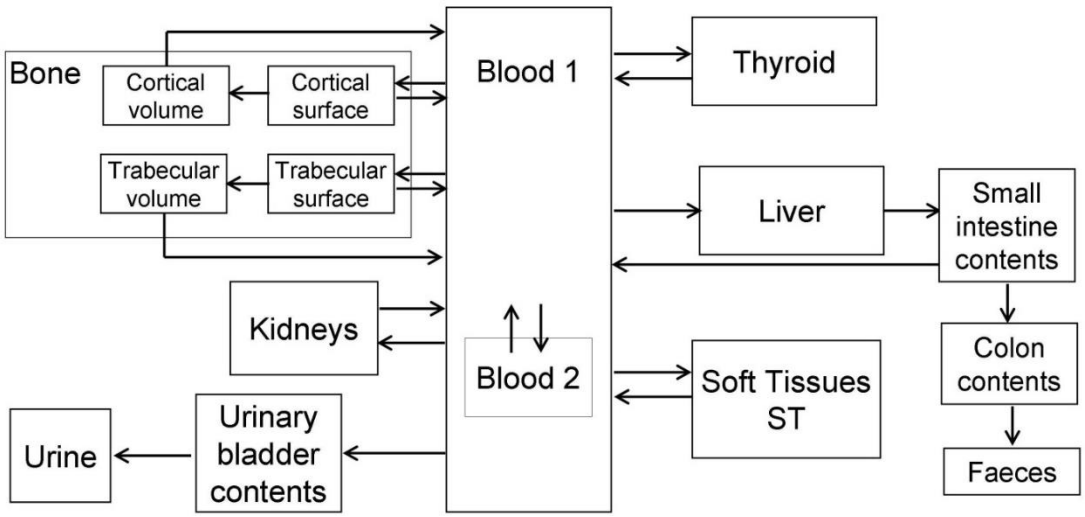

Fig. 24.1. Structure of the biokinetic model for systemic tellurium.

Table 24.3. Age-specific transfer coefficients for tellurium.

	Transfer coefficient (d^{-1})

Pathway[a]	100 d	1 y	5 y	10 y	15 y	Adult
Blood 1 to Urinary bladder contents	7.51E-01	7.51E-01	7.51E-01	7.51E-01	7.51E-01	7.51E-01
Blood 1 to Kidneys	4.04E-02	4.04E-02	4.04E-02	4.04E-02	4.04E-02	4.04E-02
Blood 1 to Liver	1.21E-01	1.21E-01	1.21E-01	1.21E-01	1.21E-01	1.21E-01
Blood 1 to Blood 2	1.01E-01	1.01E-01	1.01E-01	1.01E-01	1.01E-01	1.01E-01
Blood 1 to Other	7.68E-02	7.68E-02	7.68E-02	7.68E-02	7.68E-02	7.68E-02
Blood 1 to Cort bone surface	2.02E-02	2.02E-02	2.02E-02	2.02E-02	2.02E-02	2.02E-02
Blood 1 to Trab bone surface	4.04E-02	4.04E-02	4.04E-02	4.04E-02	4.04E-02	4.04E-02
Blood 1 to Thyroid	4.00E-03	4.00E-03	4.00E-03	4.00E-03	4.00E-03	4.00E-03
Blood 2 to Blood	6.93E-02	6.93E-02	6.93E-02	6.93E-02	6.93E-02	6.93E-02
Liver to Small intestine contents	6.93E-02	6.93E-02	6.93E-02	6.93E-02	6.93E-02	6.93E-02
Thyroid to Blood 1	6.93E-02	6.93E-02	6.93E-02	6.93E-02	6.93E-02	6.93E-02
Kidneys to Blood 1	6.93E-02	6.93E-02	6.93E-02	6.93E-02	6.93E-02	6.93E-02
Other to Blood 1	6.93E-02	6.93E-02	6.93E-02	6.93E-02	6.93E-02	6.93E-02
Cort bone surf to Blood 1	1.16E-02	1.16E-02	1.16E-02	1.16E-02	1.16E-02	1.16E-02
Trab bone surf to Blood 1	1.16E-02	1.16E-02	1.16E-02	1.16E-02	1.16E-02	1.16E-02
Cort bone surf to Cort bone volume	6.93E-04	6.93E-04	6.93E-04	6.93E-04	6.93E-04	6.93E-04
Trab bone surf to Trab bone volume	6.93E-04	6.93E-04	6.93E-04	6.93E-04	6.93E-04	6.93E-04
Cort bone vol to Blood 1	8.22E-03	2.88E-03	1.53E-03	9.04E-04	5.21E-04	8.21E-05
Trab bone vol to Blood 1	8.22E-03	2.88E-03	1.81E-03	1.32E-03	9.59E-04	4.93E-04

[a]Cort = Cortical, Trab = Trabecular

24.1.3.3. Treatment of radioactive progeny

(428) The treatment of radioactive progeny produced in systemic compartments after intake of a radioisotope of tellurium is described in Section 4.2.3.3. of *Publication 137* (ICRP, 2017).

24.2. Dosimetric data for tellurium

Table 24.4. Committed effective dose coefficients (Sv Bq^{-1}) for the inhalation or ingestion of ^{129}Te compounds.

	Effective dose coefficients (Sv Bq^{-1})					
Inhaled gases or vapours	3 mo	1 y	5 y	10 y	15 y	Adult
All unspecified compounds	2.9E-10	2.2E-10	1.3E-10	9.0E-11	6.4E-11	5.8E-11
Inhaled particulate materials (1 µm AMAD aerosols)						
Type F, Chloride, Dioxide	1.4E-10	1.0E-10	4.5E-11	3.3E-11	2.1E-11	1.6E-11
Type M, Elemental tellurium, cadmium telluride; all unspecified forms	1.9E-10	1.4E-10	6.9E-11	5.2E-11	3.7E-11	2.9E-11
Type S	1.9E-10	1.4E-10	6.9E-11	5.2E-11	3.8E-11	2.9E-11
Ingested materials						
Adult f_A = 0.3, All forms	3.3E-10	2.7E-10	1.8E-10	1.3E-10	8.9E-11	6.1E-11

Table 24.5. Committed effective dose coefficients (Sv Bq^{-1}) for the inhalation or ingestion of ^{132}Te compounds.

	Effective dose coefficients (Sv Bq^{-1})					
Inhaled gases or vapours	3 mo	1 y	5 y	10 y	15 y	Adult
All unspecified compounds	3.0E-08	2.5E-08	1.4E-08	6.9E-09	4.7E-09	3.4E-09
Inhaled particulate materials (1 µm AMAD aerosols)						
Type F, Chloride, Dioxide	1.3E-08	1.0E-08	4.9E-09	2.6E-09	1.6E-09	1.2E-09

Type M, Elemental tellurium, cadmium telluride; all unspecified forms	7.5E-09	5.5E-09	2.9E-09	1.9E-09	1.3E-09	1.3E-09
Type S	6.3E-09	4.9E-09	2.6E-09	1.8E-09	1.3E-09	1.3E-09
Ingested materials						
Adult f_A = 0.3, All forms	2.1E-08	1.2E-08	6.6E-09	3.6E-09	2.5E-09	1.9E-09

25. IODINE (Z = 53)

25.1. Routes of Intake

25.1.1. Inhalation

(429) Detailed information on the behaviour of inhaled gases and vapours of iodine is available from studies in human volunteers. Some information on absorption from the respiratory tract is available on inhaled particulate forms of iodine: as iodide from animal experiments; and associated with irradiated fuel fragments from human exposures. For details, see Section 5 of *Publication 137* (ICRP, 2017). Absorption parameter values and types, and associated f_A values for gas and vapour forms of iodine are given in Table 25.1 and for particulate forms in Table 25.2 (taken from Section 5 of *Publication 137*). Exposures to both gas/vapour forms and particulate forms of iodine are common, and it is therefore recommended in this series of documents that in the absence of information 50% particulate; 50% gas/vapour should be assumed.

Table 25.1. Deposition and absorption for gas and vapour forms of iodine[*].

	Fraction deposited (%)[†]						Absorption	
Chemical form/origin	Total	ET_1	ET_2	BB	bb	AI	Type	f_A
Elemental iodine, I_2	100	0	50	50	0	0	F	1.0[¶]
Methyl iodide, CH_3I; ethyl iodide, C_2H_5I	70[‡]	0	14	7	14	35	V	[§]
Unspecified[*]	100	0	50	50	0	0	F	1.0[¶]

ET_1, anterior nasal passage; ET_2, posterior nasal passage, pharynx and larynx; BB, bronchial; bb, bronchiolar; AI, alveolar-interstitial.

[*]For iodine in unspecified gas or vapour form, the behaviour assumed is the same as that for elemental iodine: 100% deposition (50% ET_2 and 50% BB) with Type F absorption. It is assumed that for iodine the bound state can be neglected i.e. $f_b = 0$.

[†]*Fraction deposited* refers to how much of the material in the inhaled air remains in the body after exhalation. Almost all inhaled gas molecules contact airway surfaces, but usually return to the air unless they dissolve in, or react with, the surface lining.

[‡]Since instantaneous absorption to blood (Type V) is assumed, calculations can be performed assuming direct injection into blood, and the regional deposition does not need to be considered. Nevertheless, for completeness, the deposits in each region are assumed to be distributed in the same proportions as in the default distribution for gases and vapours: 20% ET_2, 10% BB, 20% bb and 50% AI.

[§]Not applicable for absorption Type V, because all activity deposited in the respiratory tract is instantaneously absorbed.

[¶]The value of $f_A = 1$ is applicable to all age-groups.

Table 25.2. Absorption parameter values for inhaled particulate forms of iodine and for ingested iodine.

Inhaled particulate materials		Absorption parameter values* f_r	s_r (d^{-1})	s_s (d^{-1})
Default parameter values†,‡				
Absorption Type	Assigned forms			
F§	Sodium iodide; caesium chloride vector, silver iodide	1	100	–
M	—	0.2	3	0.005
S	—	0.01	3	1×10^{-4}

Ingested materials¶	Age-dependent absorption from the alimentary tract, f_A					
Assigned forms	3 months	1 year	5 years	10 years	15 years	adult
All chemical forms	1	1	1	1	1	1

*It is assumed that for iodine the bound state can be neglected i.e. $f_b = 0$. The value of s_r for Type F forms of iodine (100 d^{-1}) is element-specific. The values for Types M and S (3 d^{-1}) are the general default values.

†Materials (e.g. sodium iodide) are generally listed here where there is sufficient information to assign to a default absorption ype, but not to give specific parameter values (see Section 5 of *Publication 137*, ICRP, 2017).

‡For inhaled material deposited in the respiratory tract and subsequently cleared by particle transport to the alimentary tract, the default f_A values for inhaled materials are applied: i.e. the product of f_r for the absorption type and the f_A value for ingested soluble forms of iodine applicable to the age-group of interest (1.0).

§Default Type F is recommended for use in the absence of specific information on which the exposure material can be assigned to an absorption type, e.g. if the form is unknown, or if the form is known but there is no information available on the absorption of that form from the respiratory tract.

¶Activity transferred from systemic compartments into segments of the alimentary tract is assumed to be subject to reabsorption to blood. The default absorption fraction f_A for the secreted activity is the highest value for ingestion of the radionuclide applicable to the age-group of interest (1.0).

25.1.2. Ingestion

25.1.2.1. Adults

(430) The absorption of iodide from the alimentary tract of humans is virtually complete, while subject to changes of the redox conditions in the alimentary tract. For other chemical forms, absorption is less complete but commonly above 70%. (For details see Section 5 of *Publication 137*, ICRP, 2017). Iodine absorption occurs in the stomach as well as the proximal small intestine (Berkovski, 1999). However, assuming half of ingested iodine to be absorbed from the stomach would increase thyroid and effective doses by less than 1% for common isotopes (ICRP, 2006). In *Publication 30* (ICRP, 1979), an absorption fraction of 1 was recommended for all chemical forms of iodine. This value was recommended in *Publication 56* (ICRP, 1990) for dietary intakes and in *Publication 137* (ICRP, 2017) for all forms. A value of $f_A = 1$ is also adopted here for adults and for all chemical forms.

25.1.2.2. Children

(431) Similar results have been obtained in both young children and adolescents (Cuddihy, 1966; van Dilla and Fulwyler, 1963). No differences in uptake between iodine in aqueous media and milk have been found (Comar et al., 1963; Cuddihy, 1966). It is, therefore, assumed that for all ages absorption of iodine is complete when incorporated in foodstuffs (i.e. $f_A = 1$).

25.1.3. Systemic Distribution, Retention and Excretion

25.1.3.1. Age specific data

(a) Thyroidal uptake of iodine

(432) Fractional uptake of ingested iodine by the thyroid is substantially greater in the first few days of life than at higher ages. Twenty-four hour uptake of intramuscularly injected ^{131}I in seven infants of age 2-3 d ranged from 46 to 97% and averaged 70% (Van Middlesworth, 1954). In 25 infants 0.5-2 d of age, uptake of intravenously injected ^{131}I at 24 h ranged from 35 to 88% and averaged 61% (Fisher et al., 1962). In seven premature infants 0.4-3 d old, uptake ranged from 46 to 100% and averaged 73% (Fisher et al., 1962). Thyroidal uptake averaged 70% in 17 infants of age <1.5 d following intramuscular injection and 50% in 8 infants of age <1.5 d following oral administration (Morrison et al., 1963). According to Fisher et al. (1964), "Thyroid function during the first weeks of life is characterized by hyperactivity as measured by increased radioiodine uptake, increased serum hormonal iodine values, and increased erythrocyte triiodothyronine ^{131}I uptake. This neonatal thyroid hyperactivity subsides within one to two weeks, and the elevated test results have returned to normal childhood levels by 8 to 12 weeks of age."

(433) Regional studies of radioiodine uptake by the thyroid in different age groups suggest that there is little if any age dependence in uptake beyond early infancy except perhaps for a modest decline after the fifth or sixth decade (Cuddihy, 1966; Gaffney et al., 1962; Oliner et al., 1957; Quimby et al., 1950; Rosenberg, 1957, 1958; Schober and Hunt, 1976; van Dilla and Fulwyler, 1963). Age-specific uptake values determined in one relatively large set of euthyroid subjects (60 subjects ages 2.5 mo to 18 y and 64 adults) are shown in .

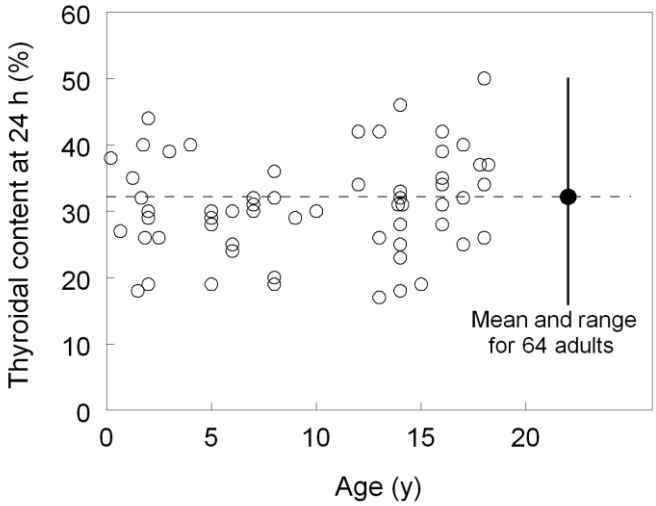

Fig. 25.1. Comparison of thyroidal uptake of ^{131}I at 24 h in euthyroid children and adults from the same region (Oliner et al., 1957).

(b) Biological half-time in the thyroid

(434) In the model for adults (Leggett, 2010) the baseline biological half-time of iodine in the thyroid is 90 d, based on a wide range of reported values. The large variability in the half-

time presumably is related to variation in dietary intake and related thyroid stores of stable iodine.

(435) Observed half-times for pre-adult ages are also highly variable (Fig. 25.2.). For newborn infants, data of Karhausen (1974) for two subjects suggest a half-time of the order of 3 d; Morrison et al. (1963) estimated a half-time of the order of 15-25 d based on "a few" studies; Fisher et al. (1962) determined a mean half-time of approximately 11 d (range 4-40 d) based on "prolonged thyroid ^{131}I decay curves" for 9 premature infants; and Ogborn et al. (1960) and Quimby et al. (1958) estimated half-times of 6 d and 23 d, respectively. Data of Karhausen (1974) indicate a mean half-time of about 9 d (2.5-13 d) in 5 subjects of age 2.5-5 mo; 14 d (4-39 d) for 5 subjects of age 1-2 y; and 64 d (21-142 d) for 12 subjects of age 10-14 y. Data of Cuddihy (1966) indicate mean half-times of 31 d (range, 19-41 d) for four subjects of age 6-9 y and 44 d (39-53 d) for three subjects of age 12-16 y. Longer mean half-times in children and adolescents were determined by Van Dilla and Fulwyler (1963): 85 d (range, 59-163 d) in 7 subjects of age 4-8 y, and 96 d (73-142 d) in 4 subjects of age 10-14 y.

(436) On the basis of a review and analysis of biological half-times reported in the literature, Dunning and Schwarz (1981) estimated means of 16 d (range, 6-23 d) for infants; 13 d (4-39 d) for ages 0.5-2 y; 50 d (19-118 d) for ages 6-16 y; and 85 d (21-372 d) for ages >18 y. Median values determined by Dunning and Schwarz were 13 d for infants, 10 d for ages 0.5-2 y, 44 d for ages 6-16 y, and 72 d for ages >18 y.

(437) Overall, the reported data on biological half-times of iodine in the thyroid suggest a sizable increase between birth and about age 5-6 y and then a more gradual increase to early adulthood. There appears to be little if any change in the half-time from early adulthood until at least the fifth or sixth decade, after which there may be a moderate decline.

(438) Selected baseline biological half-times for use in the iodine model are 10 d in infants (age 100 d), 15 d at age 1 y, 30 d at age 5 y, 50 d at age 10 y, 65 d at age 15 y, and 90 d in young or middle-aged adults. These are the age groups addressed in the ICRP's age-specific biokinetic models for members of the public.

(c) Rate of secretion of organic iodine by the thyroid

(439) Results of clinical and experimental studies indicate that the mass of organic iodine secreted daily by the thyroid increases with age from infancy to early adulthood, remains steady from young adulthood through the fifth or sixth decade of life, and declines thereafter (Fisher et al., 1965; Gregerman et al., 1962; Haddad, 1960; Herrmann et al., 1981; Karhausen, 1974; Mariotti et al., 1995; Oddie et al., 1965, 1966; Sawin, 2005). Representative results from five studies including central estimates based on a review of the literature (Oddie et al., 1966) are shown in Fig. 25.3.

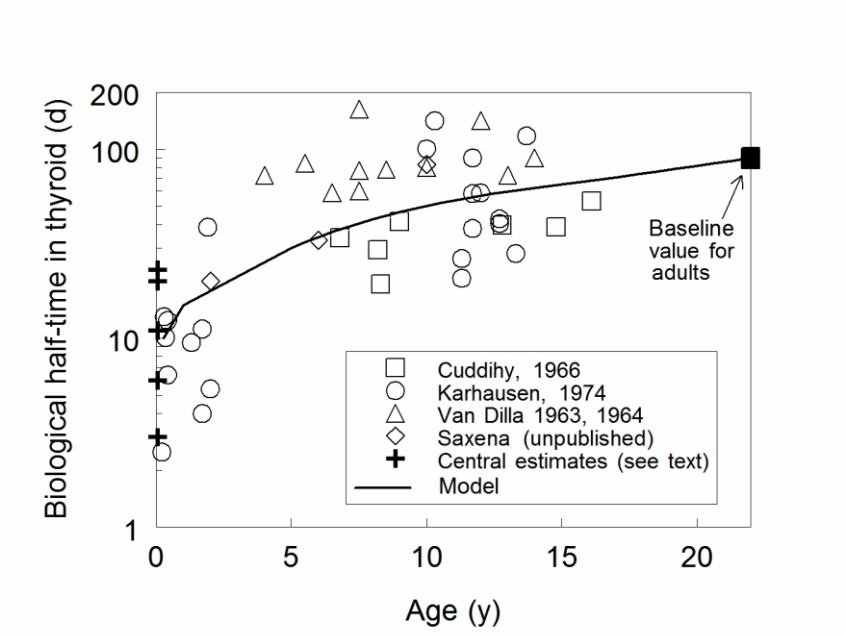

Fig. 25.2. Measured and modeled biological half-time of iodine in the thyroid.

(d) Rate of degradation of extrathyroidal organic iodine

(440) The biological half-time of extrathyroidal T_4 increases with age throughout life (Anbar et al., 1965; Gregerman et al., 1962; Oddie et al., 1966). Central half-times estimated from collected data are 4 days in infants, 5 days in children, 6 days in adolescents, 7 days in young adults, 8 days in middle-aged adults, and 9 days in elderly adults. The half-time of extrathyroidal T_4 essentially determines the half-time of extrathyroidal hormonal iodine. The following reference values are used to develop baseline transfer coefficients describing the behavior of extrathyroidal organic iodine at different ages: 4 d in infants, 4.5 days at age 1 y, 5 d at age 5 y, 5.5 d at age 10 y, 6 d at age 15 y, and 7 d in adults.

25.1.3.2. Systemic model

(441) The structure of the age-specific biokinetic model for iodine, and the transfer coefficients for the adult member of the public are the same as in the model for iodine in the worker adopted in *Publication 137* (ICRP, 2017). The model structure is shown in Fig. 25.4. Transfer coefficients for all six ages at intake are listed in

(442) Table 25.3.

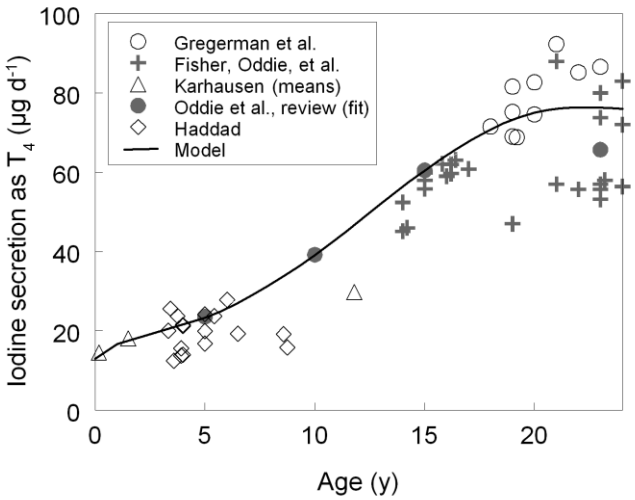

Fig. 25.3. Measured and modeled rate of secretion of T_4 by the thyroid in males from birth to early adulthood. In the model, secretion of iodine as T_4 is assumed to be 93% of total secretion of hormonal iodine by the thyroid.

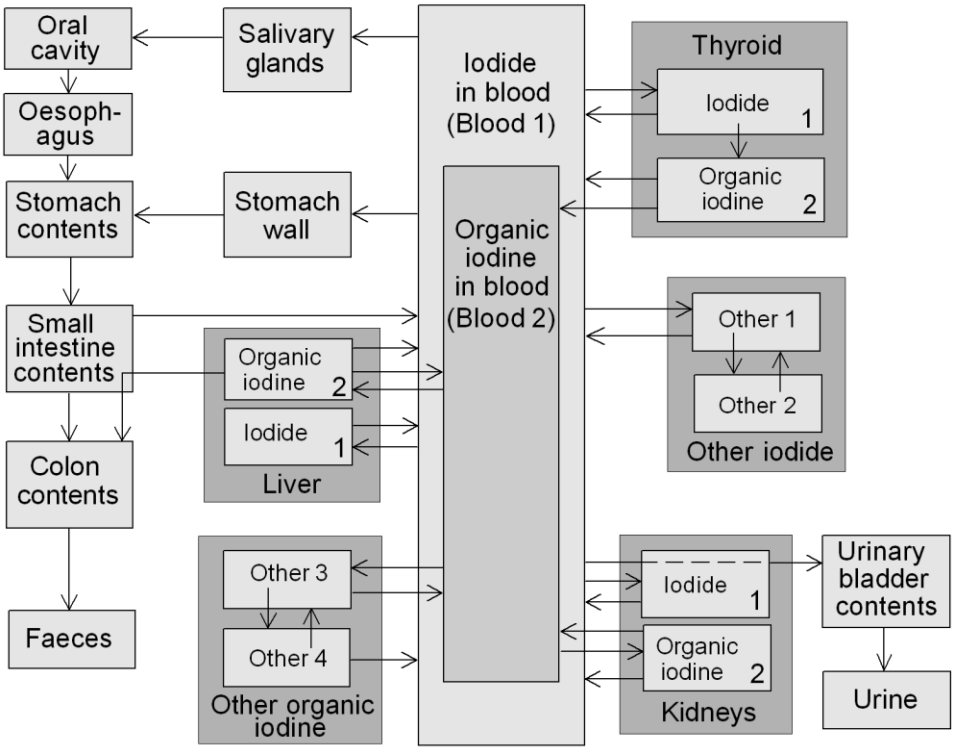

Fig. 25.4. Structure of the biokinetic model for systemic iodine.

(443) The transfer coefficients that vary with age are the coefficient describing transfer of organic iodine from Thyroid 2 to Blood Organic Iodine, and values describing movement of extrathyroidal organic iodine. The transfer coefficients for these paths are calculated as follows: (1) the transfer coefficient from Thyroid 2 to Blood Organic Iodine at a given age is $\ln(2)/T_{1/2}$, where $\ln(2) = 0.69315$ and $T_{1/2}$ refers to the biological half-times of iodine in the thyroid discussed earlier (e.g., 7 d in infants and 50 d at age 10 y); (2) all parameter values

describing the movement of extrathyroidal organic iodine at a given age (the last 12 values in each column in Table 1) are (7/T) times the corresponding value for adults, where T is the age-specific turnover time of extrathyroidal organic iodine discussed earlier, (e.g., 4 d in infants and 5.5 d at age 10 y).

(444) A transfer coefficient developed for adults was applied to children unless there was clear evidence of age dependence. As summarized above, clear evidence of age dependence was found for: (1) the rate of removal of organic iodine from the thyroid to blood, expressed either as a removal half-time or mass of iodine removed per unit time; and (2) the rate of turnover of extrathyroidal organic iodine. It appears that there is little if any age dependence in the rate of transfer of inorganic iodide from blood to the thyroid. Data were insufficient to determine whether other aspects of the kinetics of inorganic iodide changes with age. Hence, the biokinetics of inorganic iodide in the body is assumed to be invariant with age.

4838 Table 25.3. Age-specific transfer coefficients for systemic iodine

	Transfer coefficient (d^{-1})					
Pathway	100 d	1 y	5 y	10 y	15 y	Adult
Blood Iodide to Thyroid 1	7.26E+00	7.26E+00	7.26E+00	7.26E+00	7.26E+00	7.26E+00
Blood Iodide to UB contents	1.18E+01	1.18E+01	1.18E+01	1.18E+01	1.18E+01	1.18E+01
Blood Iodide to Salivary glands	5.16E+00	5.16E+00	5.16E+00	5.16E+00	5.16E+00	5.16E+00
Blood Iodide to St Wall	8.60E+00	8.60E+00	8.60E+00	8.60E+00	8.60E+00	8.60E+00
Blood Iodide to Other 1	6.00E+02	6.00E+02	6.00E+02	6.00E+02	6.00E+02	6.00E+02
Blood Iodide to Kidneys 1	2.50E+01	2.50E+01	2.50E+01	2.50E+01	2.50E+01	2.50E+01
Blood Iodide to Liver 1	1.50E+01	1.50E+01	1.50E+01	1.50E+01	1.50E+01	1.50E+01
Salivary glands to Oral cavity	5.00E+01	5.00E+01	5.00E+01	5.00E+01	5.00E+01	5.00E+01
St Wall to St contents	5.00E+01	5.00E+01	5.00E+01	5.00E+01	5.00E+01	5.00E+01
Thyroid 1 to Thyroid 2	9.50E+01	9.50E+01	9.50E+01	9.50E+01	9.50E+01	9.50E+01
Thyroid 1 to Blood Iodide	3.60E+01	3.60E+01	3.60E+01	3.60E+01	3.60E+01	3.60E+01
Thyroid 2 to Blood Organic	6.93E-02	4.62E-02	2.31E-02	1.39E-02	1.07E-02	7.70E-03
Thyroid 2 to Blood Iodide	0.00E+00	0.00E+00	0.00E+00	0.00E+00	0.00E+00	0.00E+00
Other 1 to Blood Iodide	3.30E+02	3.30E+02	3.30E+02	3.30E+02	3.30E+02	3.30E+02
Other 1 to Other 2	3.50E+01	3.50E+01	3.50E+01	3.50E+01	3.50E+01	3.50E+01
Other 2 to Other 1	5.60E+01	5.60E+01	5.60E+01	5.60E+01	5.60E+01	5.60E+01
Kidneys 1 to Blood Iodide	1.00E+02	1.00E+02	1.00E+02	1.00E+02	1.00E+02	1.00E+02
Liver 1 to Blood Iodide	1.00E+02	1.00E+02	1.00E+02	1.00E+02	1.00E+02	1.00E+02
Blood Organic to Other 3	2.63E+01	2.33E+01	2.10E+01	1.91E+01	1.75E+01	1.50E+01
Other 3 to Blood Organic	3.68E+01	3.27E+01	2.94E+01	2.67E+01	2.45E+01	2.10E+01
Other 3 to Other 4	2.10E+00	1.87E+00	1.68E+00	1.53E+00	1.40E+00	1.20E+00
Other 4 to Other 3	1.09E+00	9.64E-01	8.68E-01	7.89E-01	7.23E-01	6.20E-01
Other 4 to Blood Iodide	2.45E-01	2.18E-01	1.96E-01	1.78E-01	1.63E-01	1.40E-01
Blood Organic to Kidneys 2	6.30E+00	5.60E+00	5.04E+00	4.58E+00	4.20E+00	3.60E+00
Kidneys 2 to Blood Organic	3.68E+01	3.27E+01	2.94E+01	2.67E+01	2.45E+01	2.10E+01
Kidneys 2 to Blood Iodide	2.45E-01	2.18E-01	1.96E-01	1.78E-01	1.63E-01	1.40E-01
Blood Organic to Liver 2	3.68E+01	3.27E+01	2.94E+01	2.67E+01	2.45E+01	2.10E+01
Liver 2 to Blood Organic	3.68E+01	3.27E+01	2.94E+01	2.67E+01	2.45E+01	2.10E+01
Liver 2 to Blood Iodide	2.45E-01	2.18E-01	1.96E-01	1.78E-01	1.63E-01	1.40E-01
Liver 2 to Right colon contents	1.40E-01	1.24E-01	1.12E-01	1.02E-01	9.33E-02	8.00E-02

4839 UB = Urinary bladder, St = Stomach

25.2. Dosimetric data for iodine

Table 25.4. Committed effective dose coefficients (Sv Bq^{-1}) for the inhalation or ingestion of ^{125}I compounds.

	Effective dose coefficients (Sv Bq^{-1})					
Inhaled gases or vapours	3 mo	1 y	5 y	10 y	15 y	Adult
Elemental iodine, I_2; unspecified forms	3.5E-08	4.4E-08	3.6E-08	2.1E-08	1.6E-08	1.3E-08
Methyl iodide, CH_3I; Ethyl iodide, C_2H_5I	2.5E-08	3.1E-08	2.5E-08	1.5E-08	1.2E-08	8.9E-09
Inhaled particulate materials (1 µm AMAD aerosols)						
Type F, Sodium iodide; caesium chloride vector, silver iodide; all unspecified forms	1.8E-08	2.3E-08	1.6E-08	9.7E-09	6.6E-09	5.3E-09
Type M	5.6E-09	6.6E-09	4.7E-09	2.8E-09	2.0E-09	1.7E-09
Type S	2.0E-09	1.8E-09	9.9E-10	6.4E-10	4.5E-10	4.3E-10
Ingested materials						
Adult f_A = 1.0, All chemical forms	3.5E-08	4.3E-08	3.6E-08	2.1E-08	1.6E-08	1.3E-08

Table 25.5. Committed effective dose coefficients (Sv Bq^{-1}) for the inhalation or ingestion of ^{129}I compounds.

	Effective dose coefficients (Sv Bq^{-1})					
Inhaled gases or vapours	3 mo	1 y	5 y	10 y	15 y	Adult
Elemental iodine, I_2; unspecified forms	1.2E-07	1.6E-07	1.7E-07	1.2E-07	1.0E-07	9.4E-08
Methyl iodide, CH_3I; Ethyl iodide, C_2H_5I	8.6E-08	1.1E-07	1.2E-07	8.4E-08	7.2E-08	6.6E-08
Inhaled particulate materials (1 µm AMAD aerosols)						

Type F, Sodium iodide; caesium chloride vector, silver iodide; all unspecified forms	6.2E-08	8.5E-08	7.5E-08	5.4E-08	4.2E-08	4.0E-08
Type M	2.7E-08	3.3E-08	2.9E-08	2.0E-08	1.7E-08	1.7E-08
Type S	4.3E-08	4.4E-08	3.4E-08	2.7E-08	2.6E-08	2.7E-08
Ingested materials						
Adult f_A = 1.0, All chemical forms	1.2E-07	1.6E-07	1.6E-07	1.2E-07	1.0E-07	9.4E-08

Table 25.6. Committed effective dose coefficients (Sv Bq^{-1}) for the inhalation or ingestion of ^{131}I compounds.

	Effective dose coefficients (Sv Bq^{-1})					
Inhaled gases or vapours	3 mo	1 y	5 y	10 y	15 y	Adult
Elemental iodine, I_2; unspecified forms	1.2E-07	1.2E-07	7.5E-08	3.6E-08	2.4E-08	1.7E-08
Methyl iodide, CH_3I; Ethyl iodide, C_2H_5I	8.2E-08	8.6E-08	5.2E-08	2.5E-08	1.7E-08	1.2E-08
Inhaled particulate materials (1 µm AMAD aerosols)						
Type F, Sodium iodide; caesium chloride vector, silver iodide; all unspecified forms	5.9E-08	6.2E-08	3.3E-08	1.6E-08	9.7E-09	6.9E-09
Type M	1.5E-08	1.5E-08	8.3E-09	4.2E-09	2.7E-09	2.1E-09
Type S	3.8E-09	3.1E-09	1.7E-09	1.1E-09	8.3E-10	7.7E-10
Ingested materials						
Adult f_A = 1.0, All chemical forms	1.2E-07	1.2E-07	7.4E-08	3.5E-08	2.4E-08	1.6E-08

26. CAESIUM (Z = 55)

26.1. Routes of Intake

26.1.1. Inhalation

(445) There is some information on the behaviour of inhaled caesium in man following accidental intakes. Information on absorption from the respiratory tract is also available from experimental studies of caesium in ionic forms (chloride, nitrate), in irradiated fuel fragments and other contaminated dusts associated with nuclear facilities, and in fused aluminosilicate particles (FAP). For details, see Section 6 of *Publication 137* (ICRP, 2017). Absorption parameter values and types, and associated f_A values for particulate forms of caesium are given in Table 26.1 (taken from Section 6 of *Publication 137*).

Table 26.1. Absorption parameter values for inhaled and ingested caesium.

		Absorption parameter values*		
Inhaled particulate materials		f_r	s_r (d^{-1})	s_s (d^{-1})
Default parameter values†,‡				
Absorption Type	Assigned forms			
F	Chloride, nitrate, sulphate	1	100	-
M§	Irradiated fuel fragments	0.2	3	0.005
S	—	0.01	3	1×10^{-4}

Ingested materials¶	Age-dependent absorption from the alimentary tract, f_A					
Assigned forms	3 months	1 year	5 years	10 years	15 years	adult
Caesium chloride, nitrate, sulphate; caesium in food, all unspecified compounds	1	1	1	1	1	1
Relatively insoluble forms (irradiated fuel fragments)	0.2	0.1	0.1	0.1	0.1	0.1

*It is assumed that for caesium the bound state can be neglected, i.e. $f_b = 0.0$. The value of s_r for Type F forms of caesium (100 d^{-1}) is element-specific. The values for Types M and S (3 d^{-1}) are the general default values.

†Materials (e.g. chloride) are generally listed here where there is sufficient information to assign to a default absorption ype, but not to give specific parameter values (see Section 6 of *Publication 137*, ICRP 2017).

‡For inhaled material deposited in the respiratory tract and subsequently cleared by particle transport to the alimentary tract, the default f_A values for inhaled materials are applied: i.e. the product of f_r for the absorption type (or specific value where given) and the f_A value for ingested soluble forms of caesium applicable to the age-group of interest (1.0).

§Default Type M is recommended for use in the absence of specific information on which the exposure material can be assigned to an absorption type, e.g. if the form is unknown, or if the form is known but there is no information available on the absorption of that form from the respiratory tract.

¶Activity transferred from systemic compartments into segments of the alimentary tract is assumed to be subject to reabsorption to blood. The default absorption fraction f_A for the secreted activity is the highest value for ingestion of the radionuclide applicable to the age-group of interest (1.0).

26.1.2. Ingestion

(446) Caesium absorption has been shown to occur mainly in the ileum (Majle et al., 1991). Human data and the results of animal experiments indicate that inorganic soluble compounds of caesium are rapidly and almost completely absorbed from the alimentary tract. However ^{134}Cs and ^{137}Cs incorporated into insoluble particles such as inorganic sedimentary material, glass microspheres or irradiated reactor fuel may be less available for absorption. In *Publications 30* (ICRP, 1979) and *137* (ICRP, 2017) complete absorption from the alimentary tract was assumed for all chemical forms of caesium, except in situations where it was considered that the material was insoluble and a lower f_A value of 0.1 was appropriate. (For details, see section 6 of *Publication 137*). Henrichs et al. (1989) measured the uptake of ^{137}Cs in 10 volunteers following the consumption of venison contaminated as a result of the Chernobyl accident. Absorption varied from about 56% to 90% (mean 78%). Hunt (1998) investigated the fractional absorption of ^{137}Cs from cockles (Cerastoderma edule) collected on the Irish Sea coast of the UK. He found that fractional absorption was in the range of 0.08–0.43. Uptake of caesium from food may thus not always be complete. However, since there were insufficient data on the uptake of caesium incorporated in foods, an absorption fraction value of 1 was recommended by *Publication 56* (ICRP, 1990) for caesium in food for all ages. The same value of $f_A = 1$ is adopted here for all ages and for all forms, except insoluble inorganic material for which the value of $f_A = 0.2$ is applied for 3-mo-old and $f_A = 0.1$ is applied to other ages.

26.1.3. Systemic Distribution, Retention and Excretion

26.1.3.1. Age-specific data

(447) The systemic behavior of caesium in humans has been well characterized on the basis of experimental studies involving human volunteers, follow-up of subjects receiving occupational or environmental exposure to ^{137}Cs, and autopsy measurements of the distribution of ^{137}Cs in the body. Whole-body retention of acutely ingested ^{137}Cs has been followed in a number of adult males until little of the intake remained in the body. Results of 14 studies of the long-term half-time in healthy adult males yield mean long-term half-times in the range 79-133 d with an overall mean of about 97 d. Inter-subject variability within a given study generally was small, with a typical coefficient of variation of about 20% and a typical geometric standard deviation of about 1.2 (ICRP, 1989; Leggett, 1986; Leggett et al., 1998, 2003; Lloyd et al., 1973).

(448) In at least eight studies, retention half-times have been measured in adult female as well as adult male subjects. Although there is some overlap in individual half-times for male and female subjects, the mean half-time for the female subjects is 15-35% lower than that for male subjects in each of these studies. The long-term half-time of cesium in the body usually is reduced during pregnancy to about two-thirds of the value when not pregnant, perhaps due to increased aldosterone levels in blood during pregnancy (ICRP, 1989; Leggett, 1986; Lloyd et al., 1966; Melo et al., 1997; Thornberg and Mattsson, 2000; Zundel et al., 1969).

(449) Schwartz and Dunning (1982) collected data from the literature on the equivalent biological half-time of ^{137}Cs in the human body. The equivalent half-time is estimated from simultaneous measurement of the total body content and the excretion rate and assumes that total-body ^{137}Cs is a well-mixed pool. They determined means of 96 ± 23 d (range 47-152 d) from data 116 adult males and 65 ± 29 d (range 30-141 d) for 29 adult females.

(450) Variation with age in the retention time of radiocesium in the human body has been investigated in controlled studies, in subjects exposed to contamination from the Chernobyl accident or other sources of environmental contamination, and in subjects exposed in the accident in Goiania, Brazil. Data from three studies (Lebedev and Yakovlev, 1993; Lloyd et

al., 1973; Melo et al., 1997) are shown in Fig. 26.1. Typical long-term half-times as a function of age and gender are given in Table 26.2 (Lebedev and Yakovlev, 1993; Leggett, 1986; Leggett et al., 1998; Lloyd et al., 1973; McCraw, 1965; Melo et al., 1997).

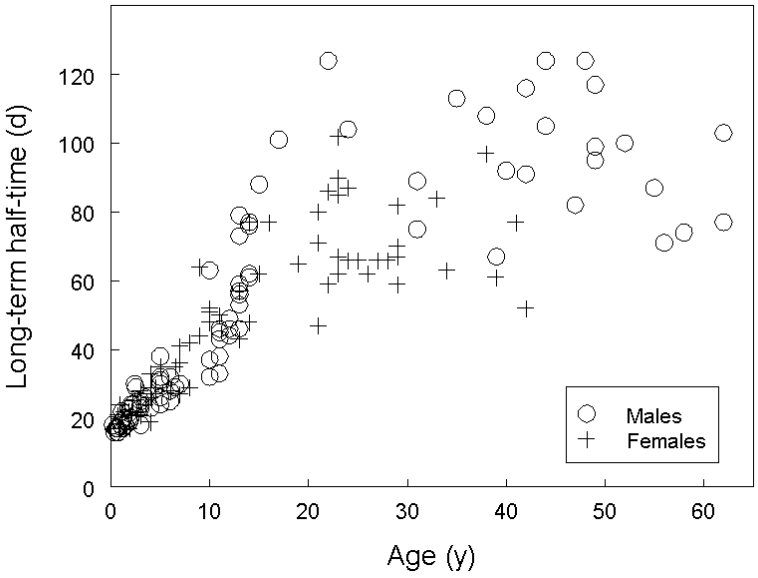

Fig. 26.1. Measured ^{137}Cs whole-body retention half-times at different ages.

Table 26.2. Central estimates for age- and gender-specific long-term retention half-times for cesium in the human body

	Long-term half-time (d)	
Age	Males	Females
Infant (100 d)	17	17
1 y	19	19
2 y	22	22
5 y	32	32
10 y	46	46
15 y	75	65
35 y	97	75
60 y	85	65

26.1.3.2. Systemic model

(451) The systemic model for cesium used in this report is an extension of the model for workers applied in Publication 137 (ICRP, 2017). The model structure is shown in Fig. 26.2. Transfer coefficients are listed in Table 26.3.

(452) Transfer coefficients for pre-adults depict lower residence times of cesium in the total body, a reduced portion of total-body cesium in the relatively smaller mass of skeletal muscle, and higher uptake of cesium by the skeleton at younger age (Leggett et al., 2003). The following approach, modified slightly from a scheme applied to cesium in NCRP Report 161, Part II (2009), was used to extend the parameter values for adults to pre-adult ages:

- The transfer rate from plasma to skeletal muscle at ages 100 d, 1 y, 5 y, and 10 y is assumed to be 0.5, 0.5, 0.7, and 0.85, respectively, times the transfer rate for the adult based on changes with age in muscle mass as a percentage of total-body mass.

- For infants and children through age 10 y, the transfer rated from plasma to bone surface compartments and the compartment representing cartilage is assumed to be twice the value for the adult.
- The transfer rate from plasma to the compartment Other 1 is modified to maintain a constant total outflow rate from plasma at all ages, i.e, to balance the changes in transfer from plasma to skeletal muscle, bone surfaces, and cartilage.
- All flow rates out of tissue compartments are increased by the following factors, chosen to approximate central estimates of the long-term biological half-time in males: 4 at age 100 d, 3.5 at age 1 y, 2.5 at age 5 y, 2.0 at age 10 y, and 1.3 at age 15 y.

(453) The resulting age-specific model predicts the following long-term biological half-times in the total body: 17, 19, 32, 45, 74, and 96 d for intake at ages 100 d, 1 y, 5y, 10 y, 15 y, and adult, respectively. These values are based on the time required for the total-body content to decline from 50% to 25% of an acute input to blood.

26.1.3.3. Treatment of progeny

(454) The model for ^{137m}Ba as ^{137}Cs progeny in the adult is extended to pre-adult age by assuming the ouflow rate from plasma is invariant with age, the age-specific deposition fractions on bone surface are proportional to corresponding values applied in the model for barium as a parent radionuclide, and the deposition fractions in soft tissue and excretion pathways are proportional to values for adults.

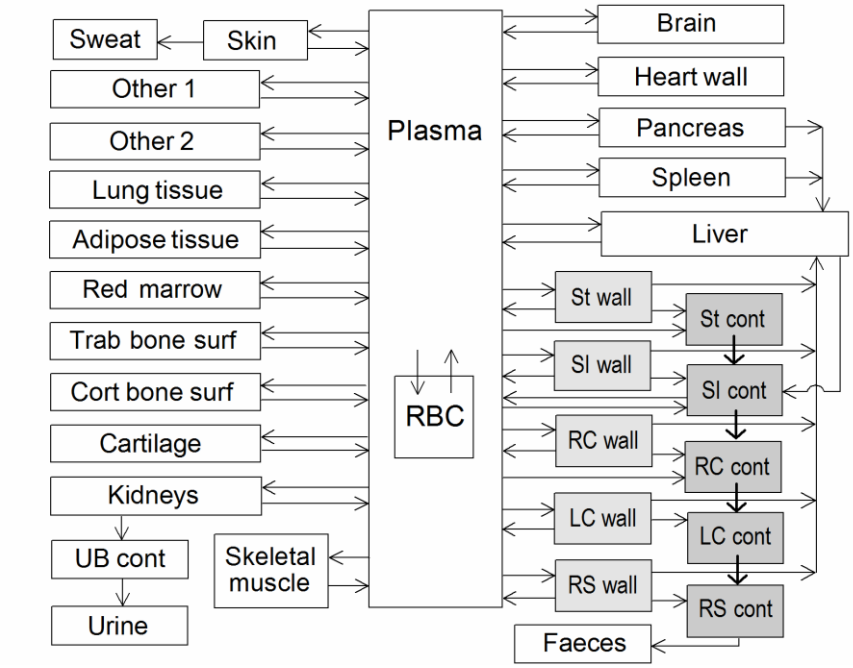

Fig. 26.2. Structure of the model for systemic caesium and its exchange with caesium in the alimentary tract. Abbreviations: Trab = trabecular, Cort = cortical, surf = surface, UB = urinary bladder, cont = content, RBC = red blood cells, St = stomach, SI = small intestine, RC = right colon, LC = left colon, RS = rectosigmoid colon.

Table 26.3. Age-specific transfer coefficients for systemic caesium

	Transfer coefficient (d^{-1})					
Pathway	100 d	1 y	5 y	10 y	15 y	Adult

Blood to heart wall	1.41E+01	1.41E+01	1.41E+01	1.41E+01	1.41E+01	1.41E+01
Blood to Liver	1.95E+01	1.95E+01	1.95E+01	1.95E+01	1.95E+01	1.95E+01
Blood to Kidneys	6.71E+01	6.71E+01	6.71E+01	6.71E+01	6.71E+01	6.71E+01
Blood to Muscle	1.50E+01	1.50E+01	2.10E+01	2.55E+01	3.00E+01	3.00E+01
Blood to Stomach wall	3.53E+00	3.53E+00	3.53E+00	3.53E+00	3.53E+00	3.53E+00
Blood to SI wall	3.53E+01	3.53E+01	3.53E+01	3.53E+01	3.53E+01	3.53E+01
Blood to RC wall	5.65E+00	5.65E+00	5.65E+00	5.65E+00	5.65E+00	5.65E+00
Blood to LC wall	5.65E+00	5.65E+00	5.65E+00	5.65E+00	5.65E+00	5.65E+00
Blood to RS wall	2.83E+00	2.83E+00	2.83E+00	2.83E+00	2.83E+00	2.83E+00
Blood to Stomach contents	4.52E+00	4.52E+00	4.52E+00	4.52E+00	4.52E+00	4.52E+00
Blood to SI contents	1.05E+00	1.05E+00	1.05E+00	1.05E+00	1.05E+00	1.05E+00
Blood to RC contents	2.00E-02	2.00E-02	2.00E-02	2.00E-02	2.00E-02	2.00E-02
Blood to Spleen	5.30E+00	5.30E+00	5.30E+00	5.30E+00	5.30E+00	5.30E+00
Blood to Pancreas	1.77E+00	1.77E+00	1.77E+00	1.77E+00	1.77E+00	1.77E+00
Blood to Brain	4.24E-01	4.24E-01	4.24E-01	4.24E-01	4.24E-01	4.24E-01
Blood to Red marrow	5.30E+00	5.30E+00	5.30E+00	5.30E+00	5.30E+00	5.30E+00
Blood to Trab bone surf	3.18E+00	3.18E+00	3.18E+00	3.18E+00	1.59E+00	1.59E+00
Blood to Cort bone surf	2.12E+00	2.12E+00	2.12E+00	2.12E+00	1.06E+00	1.06E+00
Blood to Cartilage	6.00E+00	6.00E+00	6.00E+00	6.00E+00	3.00E+00	3.00E+00
Blood to Skin	4.42E+00	4.42E+00	4.42E+00	4.42E+00	4.42E+00	4.42E+00
Blood to Lung tissue	4.42E+00	4.42E+00	4.42E+00	4.42E+00	4.42E+00	4.42E+00
Blood to Other 1	1.91E+01	1.91E+01	1.31E+01	8.56E+00	9.71E+00	9.71E+00
Blood to Other 2	3.53E-03	3.53E-03	3.53E-03	3.53E-03	3.53E-03	3.53E-03
Blood to RBC	1.80E+00	1.80E+00	1.80E+00	1.80E+00	1.80E+00	1.80E+00
Blood to Adipose tissue	8.83E+00	8.83E+00	8.83E+00	8.83E+00	8.83E+00	8.83E+00
Heart wall to Blood	3.23E+01	2.82E+01	2.02E+01	1.61E+01	1.05E+01	8.07E+00
Liver to Blood	8.56E+00	7.49E+00	5.35E+00	4.28E+00	2.78E+00	2.14E+00
Liver to SI contents	4.52E-01	3.96E-01	2.83E-01	2.26E-01	1.47E-01	1.13E-01
Kidneys to UB contents	6.72E+00	5.88E+00	4.20E+00	3.36E+00	2.18E+00	1.68E+00
Kidneys to Blood	1.28E+02	1.12E+02	7.98E+01	6.38E+01	4.15E+01	3.19E+01
Muscle to Blood	3.00E-01	2.63E-01	1.88E-01	1.50E-01	9.76E-02	7.51E-02
Stomach wall to Blood	1.66E+01	1.46E+01	1.04E+01	8.32E+00	5.41E+00	4.16E+00
Stomach wall to Liver	8.76E-01	7.67E-01	5.48E-01	4.38E-01	2.85E-01	2.19E-01
Stomach wall to contents	8.40E-01	7.35E-01	5.25E-01	4.20E-01	2.73E-01	2.10E-01
SI wall to Blood	3.95E+01	3.45E+01	2.47E+01	1.97E+01	1.28E+01	9.87E+00
SI wall to Liver	2.08E+00	1.82E+00	1.30E+00	1.04E+00	6.75E-01	5.19E-01
SI wall to contents	8.40E-01	7.35E-01	5.25E-01	4.20E-01	2.73E-01	2.10E-01
RC wall to Blood	2.74E+01	2.40E+01	1.72E+01	1.37E+01	8.92E+00	6.86E+00
RC wall to Liver	1.44E+00	1.26E+00	9.03E-01	7.22E-01	4.69E-01	3.61E-01
RC wall to contents	8.40E-01	7.35E-01	5.25E-01	4.20E-01	2.73E-01	2.10E-01
LC wall to Blood	2.74E+01	2.40E+01	1.72E+01	1.37E+01	8.92E+00	6.86E+00
LC wall to Liver	1.44E+00	1.26E+00	9.03E-01	7.22E-01	4.69E-01	3.61E-01
LC wall to contents	8.40E-01	7.35E-01	5.25E-01	4.20E-01	2.73E-01	2.10E-01
RS wall to Blood	2.74E+01	2.40E+01	1.72E+01	1.37E+01	8.92E+00	6.86E+00
RS wall to Liver	1.44E+00	1.26E+00	9.03E-01	7.22E-01	4.69E-01	3.61E-01

RS wall to contents	8.40E-01	7.35E-01	5.25E-01	4.20E-01	2.73E-01	2.10E-01
Spleen to Blood	2.01E+01	1.76E+01	1.26E+01	1.01E+01	6.54E+00	5.03E+00
Spleen to Liver	1.06E+00	9.28E-01	6.63E-01	5.30E-01	3.45E-01	2.65E-01
Pancreas to Blood	6.72E+00	5.88E+00	4.20E+00	3.36E+00	2.18E+00	1.68E+00
Pancreas to Liver	3.53E-01	3.09E-01	2.21E-01	1.77E-01	1.15E-01	8.83E-02
Skin to Blood	3.47E+00	3.03E+00	2.17E+00	1.73E+00	1.13E+00	8.67E-01
Skin to Excreta	6.36E-02	5.57E-02	3.98E-02	3.18E-02	2.07E-02	1.59E-02
Brain to Blood	3.39E-01	2.97E-01	2.12E-01	1.70E-01	1.10E-01	8.48E-02
Red marrow to Blood	2.82E+00	2.47E+00	1.77E+00	1.41E+00	9.18E-01	7.06E-01
Trab bone surf to Blood	8.48E-01	7.42E-01	5.30E-01	4.24E-01	2.76E-01	2.12E-01
Cort bone surf to Blood	8.48E-01	7.42E-01	5.30E-01	4.24E-01	2.76E-01	2.12E-01
Cartilage to Blood	8.00E-01	7.00E-01	5.00E-01	4.00E-01	2.60E-01	2.00E-01
Lung tissue to Blood	5.88E+00	5.15E+00	3.68E+00	2.94E+00	1.91E+00	1.47E+00
Other 1 to Blood	3.05E+00	2.67E+00	1.91E+00	1.52E+00	9.91E-01	7.62E-01
Other 2 to Blood	5.64E-03	4.94E-03	3.53E-03	2.82E-03	1.83E-03	1.41E-03
Adipose to Blood	7.08E+00	6.20E+00	4.43E+00	3.54E+00	2.30E+00	1.77E+00
RBC to Blood	1.03E+00	9.00E-01	6.43E-01	5.14E-01	3.34E-01	2.57E-01

4972

26.2. Dosimetric data for caesium

Table 26.4. Committed effective dose coefficients (Sv Bq^{-1}) for the inhalation or ingestion of ^{134}Cs compounds.

	Effective dose coefficients (Sv Bq^{-1})					
Inhaled particulate materials (1 μm AMAD aerosols)	3 mo	1 y	5 y	10 y	15 y	Adult
Type F, Chloride, nitrate, sulphate	1.2E-08	9.9E-09	7.0E-09	5.6E-09	5.3E-09	5.9E-09
Type M, Irradiated fuel fragments; all unspecified forms	2.6E-08	2.3E-08	1.4E-08	9.9E-09	8.0E-09	8.8E-09
Type S	7.6E-08	7.2E-08	4.6E-08	3.2E-08	2.7E-08	3.0E-08
Ingested materials						
Adult f_A = 1.0, Chloride, nitrate, sulphate; caesium in food; all unspecified compounds	2.3E-08	1.9E-08	1.5E-08	1.2E-08	1.3E-08	1.4E-08
Adult f_A = 0.1, Relatively insoluble forms (irradiated fuel fragments)	6.6E-09	4.0E-09	2.8E-09	2.1E-09	1.9E-09	2.0E-09

Table 26.5. Committed effective dose coefficients (Sv Bq^{-1}) for the inhalation or ingestion of ^{137}Cs compounds.

	Effective dose coefficients (Sv Bq^{-1})					
Inhaled particulate materials (1 μm AMAD aerosols)	3 mo	1 y	5 y	10 y	15 y	Adult
Type F, Chloride, nitrate, sulphate	1.1E-08	9.1E-09	5.7E-09	4.7E-09	4.6E-09	5.8E-09
Type M, Irradiated fuel fragments; all unspecified forms	2.6E-08	2.3E-08	1.4E-08	9.4E-09	7.8E-09	8.4E-09
Type S	1.6E-07	1.6E-07	1.3E-07	9.9E-08	9.9E-08	1.0E-07
Ingested materials						

Adult f_A = 1.0, Chloride, nitrate, sulphate; caesium in food; all unspecified compounds	2.2E-08	1.7E-08	1.3E-08	1.0E-08	1.1E-08	1.4E-08
Adult f_A = 0.1, Relatively insoluble forms (irradiated fuel fragments)	5.5E-09	2.8E-09	1.9E-09	1.5E-09	1.4E-09	1.6E-09

27.BARIUM (Z = 56)

27.1.Routes of Intake

27.1.1. Inhalation

(455) No information was found on the behaviour of inhaled barium in man. Information on absorption from the respiratory tract is available from experimental studies of barium as chloride, sulphate or in fused aluminosilicate particles (FAP). For details see Section 7 of *Publication 137* (ICRP, 2017). Absorption parameter values and types, and associated f_A values for particulate forms of barium are given in Table 27.1 (taken from Section 7 of *Publication 137*).

Table 27.1. Absorption parameter values for inhaled and ingested barium.

Inhaled particulate materials		Absorption parameter values*		
		f_r	s_r (d^{-1})	s_s (d^{-1})
Default parameter values†,‡				
Absorption Type	Assigned forms			
F	Chloride, carbonate	1	20	
M§	Sulphate	0.2	3	0.005
S	—	0.01	3	1×10^{-4}

Ingested materials¶	Age-dependent absorption from the alimentary tract, f_A					
Assigned forms	3 months	1 year	5 years	10 years	15 years	adult
Soluble forms, including barium in diet	0.6	0.3	0.3	0.3	0.3	0.2
Insoluble forms (sulphate, titanate)	1×10^{-3}	1×10^{-4}	1×10^{-4}	1×10^{-4}	1×10^{-4}	1×10^{-4}

*It is assumed that for barium the bound state can be neglected, i.e. $f_b = 0.0$. The value of s_r for Type F forms of barium (20 d^{-1}) is element-specific. The values for Types M and S (3 d^{-1}) are the general default values.

†Materials (e.g. chloride) are listed here where there is sufficient information to assign to a default absorption type, but not to give specific parameter values (see Section 7 of *Publication 137*, ICRP, 2017).

‡For inhaled material deposited in the respiratory tract and subsequently cleared by particle transport to the alimentary tract, the default f_A values for inhaled materials are applied: i.e. the product of f_r for the absorption type (or specific value where given) and the f_A value for ingested soluble forms of barium applicable to the age-group of interest (*e.g.* 0.2 for adults).

§Default Type M is recommended for use in the absence of specific information on which the exposure material can be assigned to an absorption type, e.g. if the form is unknown, or if the form is known but there is no information available on the absorption of that form from the respiratory tract.

¶Activity transferred from systemic compartments into segments of the alimentary tract is assumed to be subject to reabsorption to blood. The default absorption fraction f_A for the secreted activity is the highest value for ingestion of the radionuclide applicable to the age-group of interest (*e.g.* 0.2 for adults).

27.1.2. Ingestion

27.1.2.1.Adults

(456) Barium absorption, studied in humans and animals, depends on its chemical form. Barium sulfate is poorly absorbed from the gastrointestinal tract of adults while acid-soluble barium salts are readily dissolved in gastric acid and absorbed as a few percents of ingested quantity. Fasting and low calcium concentration in the gut may increase barium absorption by a factor 2 to 3 (*Publication 137*, ICRP, 2017). In *Publication 30* (ICRP, 1979), fractional absorption was taken to be 0.1 for all forms of barium. However, as concluded by Leggett (1992b), absorption for soluble forms of barium may be higher. On the basis of chemical similarity with radium, and similar absorption values reported for the two elements, a value of 0.2 was recommended in *Publication 67* (ICRP, 1993). An f_A of 0.2 for adults was recommended in *Publication 137* for direct ingestion of soluble forms of barium. The value of $f_A = 0.2$ is adopted here for ingestion of barium in food. For insoluble forms such as barium sulfate or titanate, an f_A of 1×10^{-4} is recommended.

27.1.2.2. Children

(457) There appear to be no direct measurements of barium absorption in children. However, data from animals indicate that the gastrointestinal absorption of barium is greater in immature than in mature animals, as is the case for other alkaline earth elements. In rats, there was an inverse relationship of barium absorption with age after administration as the chloride (Taylor et al., 1962). In suckling rats 14-18 days of age, the absorption of both barium and radium was about 80% and in young adult rats (6-8 weeks) about 10%. These results suggest that the high fractional absorption in suckling infants decreases rapidly with increasing age. Della Rosa et al. (1967) reported that following oral administration of ^{133}Ba to beagle dogs of 43, 150 and 250 days of age retention at 30 days after administration was 2.3%, 2.0% and 0.8%, respectively, and 0.4-0.6% in adult dogs. Cuddihy and Griffith (1972) estimated from these data that gastrointestinal absorption may have been 0.7-1.5% in the adult dogs and as high as 7% in the younger animals. In *Publication* 67, based on the consideration that there may be elevated absorption of barium throughout the period of growth, a fractional absorption of barium of 0.6 was recommended for the infant for solubles forms. For ages 1-15 years, a value of 0.3 was recommended. The values are adopted here for children f_A. For insoluble forms, an f_A of 0.001 is adopted in this report for 3 month old infants.

27.1.3. Systemic Distribution, Retention and Excretion

27.1.3.1. Summary of biokinetic data

(458) The alkaline earth element barium is a physiological analogue of the alkaline earths calcium, strontium, and radium but exhibits somewhat different kinetics from those elements in the human body due to discrimination by biological membranes and hydroxyapatite crystals of bone. The biokinetics of barium resembles that of radium more closely than that of calcium or strontium.

(459) The biokinetics of systemic barium has been investigated in a variety of studies involving human subjects or laboratory animals. Reviews and bibliographies can be found in *Publication 20* (ICRP, 1973), *Publication 67* (ICRP, 1993), and *Publication 137* (ICRP, 2017), and in an article by Leggett (1992a). Plasma disappearance curves for barium and other alkaline earth elements indicate an outflow rate of several hundred plasma volumes per day and rapid equilibration with an extravascular pool roughly three times the size of the plasma pool. Based on controlled studies on adult human subjects it is estimated that about a third of barium atoms leaving blood deposit in excretion pathways, predominantly in the colon contents. Observations of retention of injected barium tracers in human soft tissues are largely qualitative but indicate

that little activity remains in soft tissues by a few days after injection. Despite the initially low retention of injected barium in soft tissues, a non-trivial portion of total-body barium has been found in human soft tissues after chronic exposure, presumably representing small, relatively insoluble deposits of barium sulphate. Skeletal retention of barium in mature adults typically decreases from 25% or more of injected activity in the first day or two after injection to roughly 10% after 1 month and 5% after 1 year.

(460) Barium entering bone initially deposits on bone surface, from which activity is largely removed over a few days. Most of the barium atoms leaving bone surface return to blood, but a portion diffuse into a bone volume pool referred to as exchangeable bone volume. Barium atoms entering exchangeable bone volume may return to bone surface or blood over a period of weeks or months or may transfer to nonexchangeable bone volume, meaning that they become firmly fixed in bone crystals. It appears that calcium, strontium, barium, and radium are all about equally likely to transfer from bone surface to exchangeable bone volume but that the likelihood of becoming firmly fixed in bone crystal decreases in the order calcium > strontium > barium > radium. Data from human and animal studies indicate that the rate of loss of alkaline earth tracers from bone over the first few months after acute uptake to blood increases in the order calcium < strontium < barium < radium. Presumably these four elements are removed from trabecular or cortical non-exchangeable bone volume compartments at the rate of bone restructuring of that bone type, so that the rate of transfer from non-exchangeable bone volume is independent of the element.

(461) Age dependence in the biokinetics of barium has been investigated in laboratory animals (Cuddihy and Griffith, 1972; Della Rosa et al., 1967; Domanski et al., 1980; Ellsasser et al., 1969; Farnham and Rowland, 1965; Hardy et al., 1969; Stather, 1974; Wood et al., 1970) and in a study involving administration of a barium trace to human infants, children and adults (Bauer et al., 1957). It has been established from these studies and similar studies of calcium, strontium, and radium kinetics, that fractional deposition of alkaline earth elements in bone is substantially greater, and the turnover rate is substantially higher, for immature bone than for mature bone. Greater deposition of barium in the younger skeleton results in less systemic barium available for excretion and distribution to soft tissues.

27.1.3.2. Systemic model

(462) The age-specific model for systemic barium is taken from *Publication 67* (ICRP, 1993). The same model with parameter values for the adult was adopted in *Publication 137* (ICRP, 2017) for application to workers.

(463) The structure of the model is shown in Fig. 27.1. Transfer coefficients are listed in Table 27.2.

(464) Extension of the barium model to preadult ages is based on results of studies of the age-specific behavior of barium and its physiological analogues in human subjects and laboratory animals, indicating that deposition in bone is higher, and removal from bone is faster, at preadult ages than in adults. The age-specific deposition fraction for bone, and the division of that deposition between trabecular and cortical bone surface, are based on the estimated rates of calcium addition to each of these bone types. For preadult ages the deposition fractions for soft tissues and excretion pathways are reduced uniformly from the values for adults to reflect the elevated competition from bone for circulating barium. The removal half-times from bone surface and exchangeable bone volume compartments are assumed to be independent of age. The removal half-times from bone volume compartments to blood are reference age-specific bone turnover rates (ICRP, 2002a). Removal half-times from soft-tissue compartments are assumed to be independent of age.

(465) The reader is referred to Leggett (1992a) and *Publication 67* for more detailed descriptions of the basis for age-specific parameter values for barium.

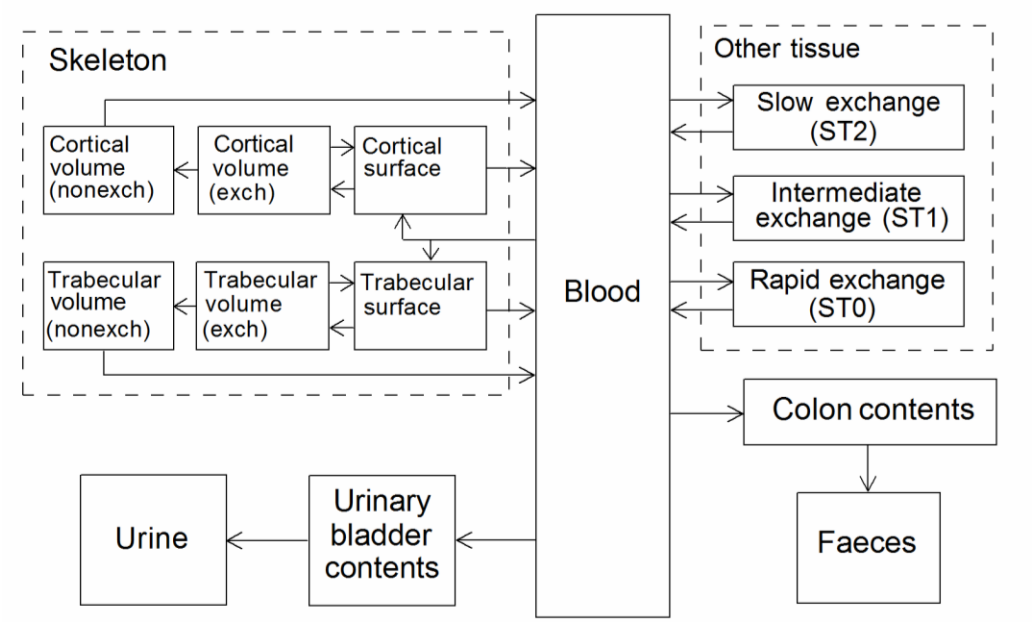

Fig. 27.1. Structure of the model for systemic barium. Abbreviations: exch = exchangeable, nonexch = non-exchangeable. Activity transferred from Blood to Colon contents enters Right colon contents.

Table 27.2. Transfer coefficients for the model for systemic barium

Path[a]	Transfer coefficient (d^{-1})					
	Infant	1 y	5 y	10 y	15 y	Adult
Blood to Urinary bladder contents	7.47E-01	1.64E+00	1.79E+00	1.31E+00	7.77E-01	2.24E+00
Blood to Right colon contents	6.72E+00	1.48E+01	1.61E+01	1.18E+01	6.99E+00	2.02E+01
Blood to Trab bone surface	1.05E+01	6.30E+00	6.22E+00	9.88E+00	1.45E+01	9.72E+00
Blood to Cort bone surface	4.20E+01	2.52E+01	2.18E+01	2.93E+01	3.74E+01	7.78E+00
Blood to ST0	7.67E+00	1.69E+01	1.84E+01	1.35E+01	7.97E+00	2.30E+01
Blood to ST1	2.33E+00	5.13E+00	5.60E+00	4.11E+00	2.43E+00	7.00E+00
Blood to ST2	4.66E-02	1.03E-01	1.12E-01	8.22E-02	4.86E-02	1.40E-01
Trab bone surf to Blood	5.78E-01	5.78E-01	5.78E-01	5.78E-01	5.78E-01	5.78E-01
Trab bone surf to Exch Trab bone vol	1.16E-01	1.16E-01	1.16E-01	1.16E-01	1.16E-01	1.16E-01
Cort bone surf to Blood	5.78E-01	5.78E-01	5.78E-01	5.78E-01	5.78E-01	5.78E-01
Cort bone surf to Exch Cort bone vol	1.16E-01	1.16E-01	1.16E-01	1.16E-01	1.16E-01	1.16E-01
ST0 to Blood	2.56E+00	5.62E+00	6.13E+00	4.50E+00	2.66E+00	7.67E+00
ST1 to Blood	6.93E-01	6.93E-01	6.93E-01	6.93E-01	6.93E-01	6.93E-01
ST2 to Blood	3.80E-04	3.80E-04	3.80E-04	3.80E-04	3.80E-04	3.80E-04
Exch Trab bone vol to Trab bone surface	9.70E-03	9.70E-03	9.70E-03	9.70E-03	9.70E-03	9.70E-03
Exch Trab bone vol to Nonexch Trab vol	4.20E-03	4.20E-03	4.20E-03	4.20E-03	4.20E-03	4.20E-03
Exch Cort bone vol to Cort bone surface	9.70E-03	9.70E-03	9.70E-03	9.70E-03	9.70E-03	9.70E-03
Exch Cort bone vol to Nonexch Cort vol	4.20E-03	4.20E-03	4.20E-03	4.20E-03	4.20E-03	4.20E-03
Nonexch Trab bone vol to Blood	8.22E-03	2.88E-03	1.81E-03	1.32E-03	9.59E-04	4.93E-04
Nonexch Cort bone vol to Blood	8.22E-03	2.88E-03	1.53E-03	9.04E-04	5.21E-04	8.21E-05

[a]Trab = Trabecular, Cort = cortical, vol = volume, Exch = Exchangeable, Nonexch = Nonexchangeable

27.2. Dosimetric data for barium

Table 27.3. Committed effective dose coefficients (Sv Bq^{-1}) for the inhalation or ingestion of ^{133}Ba compounds.

	Effective dose coefficients (Sv Bq^{-1})					
Inhaled particulate materials (1 µm AMAD aerosols)	3 mo	1 y	5 y	10 y	15 y	Adult
Type F, Chloride, carbonate	9.4E-09	3.1E-09	1.8E-09	2.5E-09	4.7E-09	1.0E-09
Type M, Sulphate; all unspecified forms	1.1E-08	8.8E-09	5.1E-09	4.0E-09	4.3E-09	2.9E-09
Type S	4.7E-08	4.6E-08	3.2E-08	2.4E-08	2.4E-08	2.5E-08
Ingested materials						
Adult f_A = 0.2, Soluble forms, including barium in diet	1.5E-08	3.6E-09	2.2E-09	3.0E-09	5.7E-09	1.0E-09
Adult f_A = 0.0001, Insoluble forms (sulphate, titanate)	8.2E-10	7.5E-10	4.2E-10	3.0E-10	2.1E-10	2.0E-10

Table 27.4. Committed effective dose coefficients (Sv Bq^{-1}) for the inhalation or ingestion of ^{140}Ba compounds.

	Effective dose coefficients (Sv Bq^{-1})					
Inhaled particulate materials (1 µm AMAD aerosols)	3 mo	1 y	5 y	10 y	15 y	Adult
Type F, Chloride, carbonate	1.3E-08	4.3E-09	1.7E-09	1.2E-09	1.2E-09	4.8E-10
Type M, Sulphate; all unspecified forms	1.5E-08	1.1E-08	5.8E-09	3.9E-09	3.0E-09	2.9E-09
Type S	1.6E-08	1.3E-08	7.3E-09	4.9E-09	3.7E-09	3.8E-09
Ingested materials						
Adult f_A = 0.2, Soluble forms, including barium in diet	2.0E-08	5.1E-09	2.4E-09	1.7E-09	1.7E-09	7.1E-10
Adult f_A = 0.0001, Insoluble forms (sulphate, titanate)	2.2E-09	2.0E-09	1.2E-09	8.4E-10	5.6E-10	5.3E-10

28. IRIDIUM (Z = 77)

28.1. Routes of Intake

28.1.1. Inhalation

(466) Some information was found on the behaviour of inhaled iridium in man following accidental intakes. Information on absorption from the respiratory tract is available from experimental studies of iridium chloride and elemental iridium. For details see Section 8 of *Publication 137* (ICRP, 2017). Absorption parameter values and types, and associated f_A values for particulate forms of iridium are given in Table 28.1 (taken from Section 8 of *Publication 137*).

Table 28.1. Absorption parameter values for inhaled and ingested iridium.

		Absorption parameter values*		
Inhaled particulate materials		f_r	s_r (d^{-1})	s_s (d^{-1})
Default parameter values†,‡				
Absorption Type	Assigned forms			
F	Chloride	1	30	–
M§	–	0.2	3	0.005
S	Elemental iridium	0.01	3	1×10^{-4}

Ingested materials¶	Age-dependent absorption from the alimentary tract, f_A					
Assigned forms	3 months	1 year	5 years	10 years	15 years	adult
all forms	0.02	0.01	0.01	0.01	0.01	0.01

*It is assumed that for iridium the bound state can be neglected i.e. $f_b = 0$. The values of s_r for Type F, M and S forms of iridium (30, 3 and 3 d^{-1}, respectively) are the general default values.

†Materials (e.g. chloride) are listed here where there is sufficient information to assign to a default absorption type, but not to give specific parameter values (see Section 8 of *Publication 137*, ICRP, 2017).

‡For inhaled material deposited in the respiratory tract and subsequently cleared by particle transport to the alimentary tract, the default f_A values for inhaled materials are applied: i.e. the product of f_r for the absorption type and the f_A value for ingested soluble forms of iridium applicable to the age-group of interest (*e.g.* 0.01 for adults).

§Default Type M is recommended for use in the absence of specific information on which the exposure material can be assigned to an absorption type, e.g. if the form is unknown, or if the form is known but there is no information available on the absorption of that form from the respiratory tract.

¶Activity transferred from systemic compartments into segments of the alimentary tract is assumed to be subject to reabsorption to blood. The default absorption fraction f_A for the secreted activity is the highest value for ingestion of the radionuclide applicable to the age-group of interest (*e.g.* 0.01 for adults).

28.1.2. Ingestion

(467) No human data are available on the absorption of iridium from the gastrointestinal tract. In *Publication 30* (ICRP, 1979) and in *Publication 137* (ICRP, 2017), an absorption fraction of 0.01 was recommended on the basis of animal data. Since no new data on the gastrointestinal absorption seem to be available, an f_A value of 0.01 is adopted here for all chemical forms ingested by adult members of the public. Consistently with the approach of *Publication 56* (ICRP, 1990), an $f_A = 0.02$ is adopted for 3-mo-old infants and $f_A = 0.01$ is adopted for 1-15 y-old children.

28.1.3. Systemic Distribution, Retention and Excretion

(468) The model for systemic iridium applied in *Publication 137* (ICRP, 2017) to workers is applied here to adult members of the public. The model is based on biokinetic studies of iridium in rodents, monkeys, and dogs. Three phases of excretion of absorbed or intravenously injected iridium are indicated: a rapid phase of loss, primarily in urine, with a half-time of a few hours; an intermediate phase of loss with a half-time on the order of 1-2 wk; and a slow phase of loss with a half-time of several months. The fraction of uptake associate with each of these phases depends to some extent on the form of iridium reaching blood. The rate of loss from individual tissues roughly parallels that in the whole body. Concentrations of iridium in the liver and kidneys are much higher than those in most other tissues.

(469) Due to lack of age-specific data for iridium, the transfer coefficients in the model for the adult are applied to all age groups except that iridium is assumed to be removed from trabecular or cortical bone volume to blood at the age-specific turnover rate for that bone type.

(470) The structure of the model for iridium is shown in Fig. 28.1. Parameter values are given in

(471) Table 28.2.

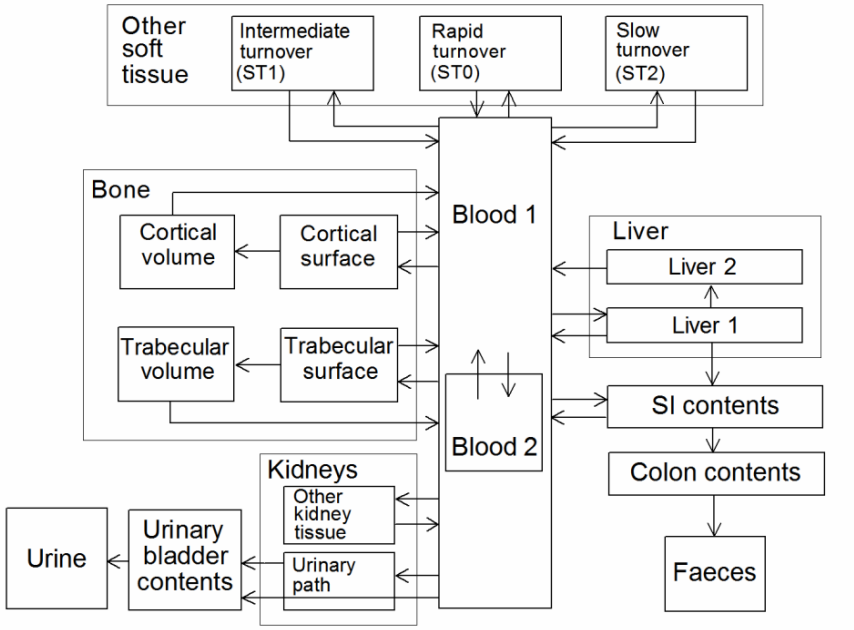

Fig. 28.1. Structure of the biokinetic model for systemic iridium. SI = Small intestine.

Table 28.2. Transfer coefficients for the model for systemic iridium

Path[a]	Transfer coefficient (d^{-1})					
	Infant	1 y	5 y	10 y	15 y	Adult
Blood 1 to SI contents	4.00E+00	4.00E+00	4.00E+00	4.00E+00	4.00E+00	4.00E+00
Blood 1 to UB contents	1.20E+01	1.20E+01	1.20E+01	1.20E+01	1.20E+01	1.20E+01
Blood 1 to Liver 1	1.20E+01	1.20E+01	1.20E+01	1.20E+01	1.20E+01	1.20E+01
Blood 1 to Urinary path	4.00E+00	4.00E+00	4.00E+00	4.00E+00	4.00E+00	4.00E+00
Blood 1 to Other kidney tissue	2.00E+00	2.00E+00	2.00E+00	2.00E+00	2.00E+00	2.00E+00
Blood 1 to Blood 2	2.70E+01	2.70E+01	2.70E+01	2.70E+01	2.70E+01	2.70E+01
Blood 1 to ST0	1.50E+01	1.50E+01	1.50E+01	1.50E+01	1.50E+01	1.50E+01
Blood 1 to ST1	1.50E+01	1.50E+01	1.50E+01	1.50E+01	1.50E+01	1.50E+01

Blood 1 to ST2	1.00E+00	1.00E+00	1.00E+00	1.00E+00	1.00E+00	1.00E+00
Blood 1 to Cortical surf	2.00E+00	2.00E+00	2.00E+00	2.00E+00	2.00E+00	2.00E+00
Blood 1 to Trabecular surf	6.00E+00	6.00E+00	6.00E+00	6.00E+00	6.00E+00	6.00E+00
Blood 2 to Blood 1	6.93E-01	6.93E-01	6.93E-01	6.93E-01	6.93E-01	6.93E-01
Liver 1 to Blood 1	2.31E-02	2.31E-02	2.31E-02	2.31E-02	2.31E-02	2.31E-02
Liver 1 to SI contents	4.62E-02	4.62E-02	4.62E-02	4.62E-02	4.62E-02	4.62E-02
Liver 1 to Liver 2	6.93E-02	6.93E-02	6.93E-02	6.93E-02	6.93E-02	6.93E-02
Liver 2 to Blood 1	6.93E-03	6.93E-03	6.93E-03	6.93E-03	6.93E-03	6.93E-03
Urinary path to UB contents	1.39E-01	1.39E-01	1.39E-01	1.39E-01	1.39E-01	1.39E-01
Other kidney tissue to Blood 1	6.93E-03	6.93E-03	6.93E-03	6.93E-03	6.93E-03	6.93E-03
ST0 to Blood 1	6.93E-02	6.93E-02	6.93E-02	6.93E-02	6.93E-02	6.93E-02
ST1 to Blood 1	6.93E-03	6.93E-03	6.93E-03	6.93E-03	6.93E-03	6.93E-03
ST2 to Blood 1	9.50E-04	9.50E-04	9.50E-04	9.50E-04	9.50E-04	9.50E-04
Cortical surf to Blood 1	1.85E-02	1.85E-02	1.85E-02	1.85E-02	1.85E-02	1.85E-02
Trabecular surf to Blood 1	1.85E-02	1.85E-02	1.85E-02	1.85E-02	1.85E-02	1.85E-02
Cortical surf to Cortical vol	4.62E-03	4.62E-03	4.62E-03	4.62E-03	4.62E-03	4.62E-03
Trabecular surf to Trabecular vol	4.62E-03	4.62E-03	4.62E-03	4.62E-03	4.62E-03	4.62E-03
Cortical vol to Blood 1	8.22E-03	2.88E-03	1.53E-03	9.04E-04	5.21E-04	8.21E-05
Trabecular vol to Blood 1	8.22E-03	2.88E-03	1.81E-03	1.32E-03	9.59E-04	4.93E-04

5169 [a]UB = Urinary bladder, SI= Small intestine, Trab = Trabecular, Cort = Cortical, surf = surface, vol = volume

28.2. Dosimetric data for iridium

Table 28.3. Committed effective dose coefficients (Sv Bq^{-1}) for the inhalation or ingestion of ^{192}Ir compounds.

	Effective dose coefficients (Sv Bq^{-1})					
Inhaled particulate materials (1 µm AMAD aerosols)	3 mo	1 y	5 y	10 y	15 y	Adult
Type F, Chloride	9.5E-09	7.6E-09	3.8E-09	2.4E-09	1.7E-09	1.5E-09
Type M, All unspecified forms	1.3E-08	1.1E-08	6.4E-09	4.2E-09	3.2E-09	3.3E-09
Type S, Elemental iridium	1.9E-08	1.6E-08	9.2E-09	6.2E-09	4.7E-09	4.9E-09
Ingested materials						
Adult f_A = 0.01, All forms	2.4E-09	1.7E-09	1.0E-09	7.0E-10	4.9E-10	4.5E-10

29.LEAD (Z = 82)

29.1.Routes of Intake

29.1.1. Inhalation

(472) Information on absorption from the respiratory tract is available from experimental studies of the behaviour of lead inhaled in a variety of forms by both animals and man. In particular, studies have been conducted to improve assessment of risks from exposure to radioisotopes of lead inhaled as progeny radionuclides of radon, and from exposure to stable lead as an atmospheric pollutant, e.g. from petrol engine exhaust. For details see Section 9 of *Publication 137* (ICRP, 2017). Absorption parameter values and Types, and associated f_A values for particulate forms of lead are given in Table 29.1 (taken from Section 9 of *Publication 137*).

(473) For radiation protection purposes, the most important exposures to radioisotopes of lead are as progeny radionuclides of radon. Dose coefficients for isotopes of lead inhaled as radon progeny are given in the radon section, where factors such as the relevant aerosol size distribution are addressed. Otherwise, exposures to radioisotopes of lead occur most often as progeny radionuclides associated with intakes of uranium, thorium or radium.

Table 29.1. Absorption parameter values for inhaled and ingested lead.

		Absorption parameter values*		
Inhaled particulate materials		f_r	s_r (d^{-1})	s_s (d^{-1})
Specific parameter values‡				
Lead as a progeny of radon		0.1	100	1.7
Default parameter values†,§				
Absorption Type	Assigned forms			
F¶	Dichloride, dibromide, difluoride, hydroxide, nitrate, oxide	1	100	–
M	—	0.2	3	0.005
S	Mineral dusts	0.01	3	0.0001

Ingested material**	Age-dependent absorption from the alimentary tract, f_A					
Assigned forms	3 months	1 year	5 years	10 years	15 years	adult
All forms	0.6	0.3	0.3	0.3	0.3	0.2

*It is assumed that for lead the bound fraction f_b is 0.5 with an uptake rate s_b = 1.7 d^{-1}, and that this applies throughout the respiratory tract (ET_2, BB, bb and AI regions, and associated lymph nodes LN_{ET} and LN_{TH}). The value of s_r for Type F forms of lead (100 d^{-1}) is element-specific. The values for Types M and S (3 d^{-1}) are the general default values.

†For inhaled material deposited in the respiratory tract and subsequently cleared by particle transport to the alimentary tract, the default f_A values for inhaled materials are applied: i.e. the product of f_r for the absorption type (or specific value where given) and the f_A value for ingested soluble forms of lead applicable to the age-group of interest (*e.g.* 0.2 for adults).

‡See Section 9 of *Publication 137* (ICRP, 2017) for summary of information on which parameter values are based, and on ranges of parameter values observed in different studies. For lead as a progeny of radon, specific parameter values are used for dissolution in the lungs, but a default value of f_A (footnote †).

[§]Materials (e.g. dichloride) are listed here where there is sufficient information to assign to a default absorption Type, but not to give specific parameter values (see Section 9 of *Publication 137*).
[¶]Default Type F is recommended for use in the absence of specific information on which the exposure material can be assigned to an absorption type, e.g. if the form is unknown, or if the form is known but there is no information available on the absorption of that form from the respiratory tract.
[**]Activity transferred from systemic compartments into segments of the alimentary tract is assumed to be subject to reabsorption to blood. The default absorption fraction f_A for the secreted activity is the highest value for ingestion of the radionuclide applicable to the age-group of interest (*e.g.* 0.2 for adults).

29.1.2. Ingestion

29.1.2.1. Adults

(474) Lead absorption has been studied extensively in man and animals. (For more details, see reviews by ICRP, 1975, 1993, 2017; Leggett, 1993; Moore, 1986). Factors shown to affect absorption of lead include ingestion of milk, calcium and iron status, protein deficiency, vitamin D, and fasting. In normally fed adults, the absorption fraction ranges from 0.03 to 0.14. Lead is absorbed more readily in fasting subjects than when it is ingested with food (range of absorption fraction 0.1-0.76). Heard and Chamberlain (1982) showed that fasting values of absorption of approximately 0.4–0.5 could be reduced to approximately 0.1–0.2 by giving lead with tea, coffee, or beer rather than water. *Publication 30* (ICRP, 1980) recommended an absorption fraction of 0.2 that was applied in *Publication 67* (ICRP, 1993) for dietary intakes and in *Publication 137* (ICRP, 2017) for direct ingestion of all forms of lead. The same value of $f_A = 0.2$ is adopted here for dietary intakes of lead by adults.

29.1.2.2. Children

(475) Ziegler et al. (1978) reported repeated 3-day balance studies of lead in six normal infants of ages ranging from 14 to 746 days, most being in the range 150 - 300 days. In subjects ingesting more than 5 pg of lead kg^{-1} body weight day^{-1}, the net absorption averaged 42%. In eight children of ages 3 months to 8 years with daily intakes of 5-17 µg kg^{-1} body weight, Alexander et al. (1974) reported absorption of 53% and retention of 18%. There are a number of uncertainties in these estimates and true absorption could have been greater due to endogenous faecal excretion of absorbed lead. However, the results suggest that the fractional absorption of lead in children may remain high for at least the first 8 years of life. Results for non-human primates are qualitatively consistent with these data for humans (Pounds et al., 1978; Willes et al., 1977). Studies in chickens, rats and sheep demonstrate clearly that there is an inverse relationship of age and the capacity to absorb lead (Conrad and Barton, 1978; Gerber and Deroo, 1975; Kostial et al., 1974; Mykkänen and Wasserman, 1981; Quarterman and Morrison, 1978). An absorption fraction of 0.6 was recommended in *Publication 67* for the 3-month-old infant. For ages l - l5 years a value of 0.4 was recommended. Values of $f_A = 0.6$ for 3-mo-old and $f_A = 0.3$ for older children are adopted here for consistency with radium and barium.

29.1.3. Systemic Distribution, Retention and Excretion

29.1.3.1. Summary of biokinetic data

(a) Mature human subjects and laboratory animals

(476) Following intravenous administration of radiolead to adult human subjects, the injected activity initially cleared from blood at a rate of 1 min^{-1} or greater (Chamberlain et al., 1978; Wells et al., 1975). The content of lead in blood declined to about one-third of the injected amount within 2-3 min, at which time roughly three-fourths of activity in blood resided in red blood cells (RBC). Increasing activity in blood was then seen for 24-48 h as the tracer returned from extravascular spaces and accumulated in RBC (Booker et al., 1969; Chamberlain et al., 1978; Wells et al., 1975). Within a few hours after injection, 99% or more of activity in blood was bound to RBC (Booker et al., 1969; Chamberlain et al., 1978; DeSilva, 1981; Everson and Patterson, 1980; Heard and Chamberlain, 1984; Hursh et al., 1969; Manton and Cook, 1984; Wells et al., 1975). At 1-2 d after introduction of radiolead into adult humans by injection or inhalation, the blood contained 40-75% (mean 58 ± 12%) of the amount reaching the circulation (Booker et al., 1969; Chamberlain et al., 1978; Heard and Chamberlain, 1984; Hursh et al., 1969; Hursh and Suomela, 1968; Morrow et al., 1980; Wells et al., 1975). Over the next few weeks, activity was cleared from blood with a biological half-time on the order of 15-20 d (Heard and Chamberlain, 1984; Rabinowitz et al., 1973, 1974, 1976; Wells et al., 1975).

(477) The liver contained about 10-15% of administered radiolead at 1 d after intravenous administration to adult humans (Heard and Chamberlain, 1984), baboons (Cohen et al., 1970), or dogs (Lloyd et al., 1975). Most of the activity deposited in the liver was removed with a biological half-time of a few weeks. Loss of lead from the liver was due in part to its biliary secretion into the contents of the small intestine (Ishihara and Matsushiro, 1986; Rabinowitz et al., 1976). Autopsy measurements on adult humans chronically exposed to environmental lead indicate that the liver typically contains about 2-3% of total-body lead (Barry, 1975, 1981; Gross et al., 1975; Zhu et al., 2010).

(478) In baboons receiving radiolead by intravenous injection, the kidneys contained about 4% of the administered amount after 1 d, 0.6% after 30 d, and 0.1% after 60 d (Cohen et al., 1970). In dogs receiving ^{210}Pb by intravenous injection, the kidneys contained about 0.5% of the administered activity at 1 month (Lloyd et al., 1975).

(479) Gradual loss of lead from RBC, liver, kidneys, and other soft tissues over the first few weeks can be accounted for by a slow loss in urine and faeces and a continual increase in skeletal lead. Typically, 3-5% of injected or absorbed lead is lost in urine during the first day. The urinary to faecal excretion ratio is about 2 during d 3-14 after absorption of lead to blood in humans. About 30% of intravenously injected radiolead is removed in urine and faeces during the first 20 d (Booker et al., 1969; Chamberlain et al., 1978; Heard and Chamberlain, 1984; Hursh et al., 1969; Hursh and Mercer, 1970; Hursh and Suomela, 1968; Wells et al., 1975).

(480) In studies on baboons (Cohen et al., 1970) and human subjects (Heard and Chamberlain, 1984), there was evidence of rapid skeletal uptake of about 10-15% of intravenously administered lead. The skeletal content remained nearly constant over the next 2-3 d and then slowly increased over an extended period as activity returned from RBC and soft tissues to plasma. In human subjects the skeleton contained roughly 20% of the injected amount after 20 d. Autopsy data for persons chronically exposed to environmental lead indicate that the skeletal content of lead increases throughout life and represents 90% or more of systemic lead by the fifth decade (Barry, 1975, 1981; Gross et al., 1975; Leggett, 1993; Tipton and Cook, 1963; Zhu et al., 2010).

(481) Skeletal behaviour of lead appears to be qualitatively similar to that of the alkaline earth elements and quantitatively similar to that of barium or radium, if account is taken of the slower deposition of lead in the skeleton due to competition from RBC (Domanski and Trojanowska, 1980; Heard and Chamberlain, 1984; Hursh, 1973; Lloyd et al., 1975). Lead has been used frequently as a marker of bone growth and osteon formation, and a close resemblance

to calcium has been demonstrated in such studies (Hong et al., 1968; Lacroix, 1960; Scheiman-Tagger and Brodie, 1964; Vincent, 1957; Yen and Shaw, 1977). Lead is incorporated into the crystalline structure of bone, where it replaces calcium ions (MacDonald et al., 1951; Miyake et al., 1986; Verbeeck et al., 1981).

(482) Autoradiographs of bone sections from baboons injected with ^{210}Pb indicate that a portion of skeletal activity remains near bone surfaces at 1 to 2 months after administration, as appears to be the case for radium and barium. Studies on human subjects indicate that the distribution of lead in bone may be skewed toward bone surfaces for at least a few months after exposure, but the subjects generally have been exposed to heavy levels of lead that could affect bone metabolism (Flood et al., 1988; Lindh et al., 1978). Burial of lead beneath the surfaces in regions of bone formation has been observed, and there is evidence that lead is eventually distributed throughout the bone volume (Hong et al., 1968; Hu et al., 1989; Lacroix, 1960; Lindh et al., 1978; Scheiman-Tagger and Brodie, 1964; Vincent, 1957; Yen and Shaw, 1977). In beagles, long-term skeletal retention of lead is similar to that of strontium and radium (Hursh, 1973; Lloyd et al., 1975). Because lead is incorporated into the bone crystal, long-term losses from bone presumably are largely controlled by the rate of bone resorption.

(483) In a study of the comparative behaviour of injected lead, calcium, and barium in bone of rabbits, Domanski and Trojanowska (1980) found that the build-up of lead in bone is similar to that of barium and greater than that of calcium when related to integrated activity in plasma. Similar results for lead and calcium were obtained by Heard and Chamberlain (1984) for humans injected with radioisotopes of these two elements. A relatively low uptake of lead by the skeleton at early times compared with radium, for example, apparently reflects a competition by RBC for lead that does not occur to a significant extent for the alkaline earth elements. The later build-up in the skeleton results from the gradual release of activity from RBC and the relatively longer retention of lead in the skeleton than in RBC.

(b) Immature human subjects and laboratory animals

(484) Autopsy data for persons of all ages exposed only to environmental lead indicate that the content of lead in bone increases gradually from birth to adulthood. The bones of infants may contain roughly one-quarter to one-third of total-body lead and those of young children and teenagers one-half to two-thirds, compared with a value of 90% or more for middle-aged and older persons (Barry, 1973, 1975, 1981; Leggett, 1992a). Data for non-human primates (Kneip et al., 1983; Pounds et al., 1978; Willes et al., 1977) and rodents (Jugo et al., 1975, 1980; Keller and Doherty, 1980; Kello and Kostial, 1978; Kostial et al., 1978; Momčilović and Kostial, 1974) indicate that retention of a lead tracer is greater in growing than in mature animals and that much of the variation with age is due to elevated uptake and/or retention of lead by the immature skeleton. Some differences in uptake and/or retention of lead by the brain, liver and kidneys have been observed between immature and mature rodents (Keller and Doherty, 1980; Momčilović and Kostial, 1974). The combined age-specific data for laboratory animals and environmentally exposed humans are reasonably consistent with assumptions of higher uptake and faster release of lead by the immature than the mature skeleton and substantial retention of lead by blood and soft tissues at all ages.

29.1.3.2. Systemic model

(485) The model for systemic lead applied in *Publication 137* (ICRP, 2017) to workers is applied here to adult members of the public. The systemic behaviour of lead is assumed to be independent of age.

(486) The structure of the model for systemic lead is shown in Fig. 29.1. Transfer coefficients are listed in Table 29.2.

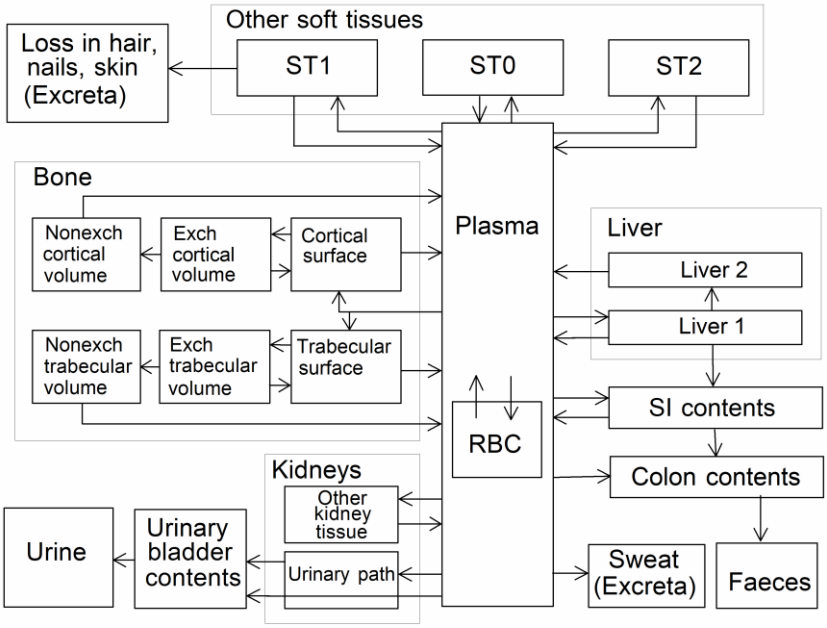

Fig. 29.1. Structure of the model for systemic lead. Activity transferred from Plasma to Colon contents enters Right colon contents. Abbreviations: RBC = Red Blood Cells, SI = Small intestine, Exch = Exchangeable, Nonexch = Non-exchangeable.

Table 29.2. Age-specific transfer coefficients for lead.

Pathway[a]	Transfer coefficient (d^{-1})					
	100 d	1 y	5 y	10 y	15 y	Adult
Blood to Urinary bladder contents	1.25E+00	1.55E+00	1.60E+00	1.44E+00	1.26E+00	1.75E+00
Blood to Right colon contents	5.00E-01	6.20E-01	6.40E-01	5.76E-01	5.04E-01	7.00E-01
Blood to Trab bone surface	5.25E+00	3.15E+00	3.11E+00	4.94E+00	7.23E+00	4.86E+00
Blood to Cort bone surface	2.10E+01	1.26E+01	1.09E+01	1.47E+01	1.87E+01	3.89E+00
Blood to ST0	1.58E+01	1.96E+01	2.03E+01	1.82E+01	1.60E+01	2.22E+01
Blood to ST1	5.00E-01	6.20E-01	6.40E-01	5.76E-01	5.04E-01	7.00E-01
Blood to ST2	1.00E-01	1.24E-01	1.28E-01	1.15E-01	1.01E-01	1.40E-01
Blood to Liver 1	3.50E+00	4.34E+00	4.48E+00	4.03E+00	3.53E+00	4.90E+00
Blood to Kidneys 1	1.75E+00	2.17E+00	2.24E+00	2.02E+00	1.76E+00	2.45E+00
Blood to Kidneys 2	1.75E-02	2.17E-02	2.24E-02	2.02E-02	1.76E-02	2.45E-02
Blood to Blood 1	2.00E+01	2.48E+01	2.56E+01	2.30E+01	2.02E+01	2.80E+01
Blood to Excreta	3.00E-01	3.72E-01	3.84E-01	3.46E-01	3.02E-01	4.20E-01
Blood 1 to Blood	1.39E-01	1.39E-01	1.39E-01	1.39E-01	1.39E-01	1.39E-01
Trab bone surf to Blood	6.50E-01	6.50E-01	6.50E-01	6.50E-01	6.50E-01	5.00E-01
Trab bone surf to Trab bone volume 1	3.50E-01	3.50E-01	3.50E-01	3.50E-01	3.50E-01	5.00E-01
Cort bone surf to Blood	6.50E-01	6.50E-01	6.50E-01	6.50E-01	6.50E-01	5.00E-01
Cort bone surf to Cort bone volume 1	3.50E-01	3.50E-01	3.50E-01	3.50E-01	3.50E-01	5.00E-01

Trab bone vol 1 to Trab bone surface	1.85E-02	1.85E-02	1.85E-02	1.85E-02	1.85E-02	1.85E-02
Trab bone vol 1 to Trab bone volume 2	4.60E-03	4.60E-03	4.60E-03	4.60E-03	4.60E-03	4.60E-03
Cort bone vol 1 to Cort bone surface	1.85E-02	1.85E-02	1.85E-02	1.85E-02	1.85E-02	1.85E-02
Cort bone vol 1 to Cort bone volume 2	4.60E-03	4.60E-03	4.60E-03	4.60E-03	4.60E-03	4.60E-03
Trab bone vol 2 to Blood	8.22E-03	2.88E-03	1.81E-03	1.32E-03	9.59E-04	4.93E-04
Cort bone vol 2 to Blood	8.22E-03	2.88E-03	1.53E-03	9.04E-04	5.21E-04	8.21E-05
Liver 1 to Blood	3.12E-02	3.12E-02	3.12E-02	3.12E-02	3.12E-02	3.12E-02
Liver 1 to SI-contents	3.12E-02	3.12E-02	3.12E-02	3.12E-02	3.12E-02	3.12E-02
Liver 1 to Liver 2	6.93E-03	6.93E-03	6.93E-03	6.93E-03	6.93E-03	6.93E-03
Liver 2 to Blood	6.93E-03	6.93E-03	6.93E-03	1.90E-03	1.90E-03	1.90E-03
Kidneys 1 to Urinary bladder contents	1.39E-01	1.39E-01	1.39E-01	1.39E-01	1.39E-01	1.39E-01
Kidneys 2 to Blood	6.93E-03	6.93E-03	6.93E-03	1.90E-03	1.90E-03	1.90E-03
ST0 to Blood	5.28E+00	6.54E+00	6.75E+00	6.08E+00	5.32E+00	7.39E+00
ST1 to Blood	4.16E-03	4.16E-03	4.16E-03	4.16E-03	4.16E-03	4.16E-03
ST2 to Blood	3.80E-04	3.80E-04	3.80E-04	3.80E-04	3.80E-04	3.80E-04
ST1 to Excreta	2.77E-03	2.77E-03	2.77E-03	2.77E-03	2.77E-03	2.77E-03

[a]Trab = Trabecular, Cort = Cortical

29.1.3.3. Treatment of radioactive progeny

(487) The treatment of radioactive progeny produced in systemic compartments after intake of a radioisotope of lead is described in Section 9.2.3.3. of *Publication 137* (ICRP, 2017).

29.2. Dosimetric data for lead

Table 29.3. Committed effective dose coefficients (Sv Bq^{-1}) for the inhalation or ingestion of ^{210}Pb compounds.

	Effective dose coefficients (Sv Bq^{-1})					
Inhaled particulate materials (1 µm AMAD aerosols)	3 mo	1 y	5 y	10 y	15 y	Adult
Type F, Dichloride, dibromide, difluoride, hydroxide, nitrate, oxide; all unspecified forms	5.7E-06	3.2E-06	1.7E-06	1.4E-06	7.2E-07	4.9E-07
Type M	4.9E-06	4.1E-06	2.4E-06	1.6E-06	1.1E-06	9.8E-07
Type S, Mineral dusts	3.4E-05	3.4E-05	2.4E-05	1.7E-05	1.6E-05	1.6E-05
Ingested materials						
Adult f_A = 0.2, All forms	8.0E-06	2.5E-06	1.5E-06	1.2E-06	6.9E-07	3.2E-07

Table 29.4. Committed effective dose coefficients (Sv Bq^{-1}) for the inhalation or ingestion of ^{212}Pb compounds.

	Effective dose coefficients (Sv Bq^{-1})					
Inhaled particulate materials (1 µm AMAD aerosols)	3 mo	1 y	5 y	10 y	15 y	Adult
Type F, Dichloride, dibromide, difluoride, hydroxide, nitrate, oxide; all unspecified forms	1.0E-06	8.0E-07	3.8E-07	2.7E-07	2.0E-07	1.8E-07
Type M	4.8E-07	3.5E-07	2.2E-07	1.5E-07	1.3E-07	1.2E-07
Type S, Mineral dusts	4.9E-07	3.6E-07	2.3E-07	1.6E-07	1.4E-07	1.2E-07
Ingested materials						
Adult f_A = 0.2, All forms	1.5E-07	5.0E-08	2.5E-08	1.4E-08	8.6E-09	5.6E-09

Table 29.5. Committed effective dose coefficients (Sv Bq^{-1}) for the inhalation or ingestion of ^{214}Pb compounds.

	Effective dose coefficients (Sv Bq^{-1})					
Inhaled particulate materials (1 µm AMAD aerosols)	3 mo	1 y	5 y	10 y	15 y	Adult
Type F, Dichloride, dibromide, difluoride, hydroxide, nitrate, oxide; all unspecified forms	6.5E-08	5.2E-08	2.6E-08	1.9E-08	1.6E-08	1.3E-08
Type M	4.4E-08	3.3E-08	2.0E-08	1.5E-08	1.5E-08	1.2E-08
Type S, Mineral dusts	4.4E-08	3.3E-08	2.0E-08	1.5E-08	1.5E-08	1.2E-08
Ingested materials						
Adult f_A = 0.2, All forms	1.0E-09	4.2E-10	2.5E-10	1.7E-10	1.1E-10	7.7E-11

30. BISMUTH (Z = 83)

30.1. Routes of Intake

30.1.1. Inhalation

(488) Very little information from which parameter values can be assessed is available from experimental studies of the behaviour of bismuth deposited in the respiratory tract. For details see Section 10 of *Publication 137* (ICRP, 2017). Absorption parameter values and types, and associated f_A values for particulate forms of bismuth are given in Table 30.1 (taken from Section 10 of *Publication 137*,).

(489) For radiation protection purposes, the most important exposures to radioisotopes of bismuth are as progeny radionuclides of radon. Dose coefficients for isotopes of bismuth inhaled as radon progeny radionuclides are given in the radon section, where factors such as the relevant aerosol size distribution are addressed. Otherwise, exposures to radioisotopes of bismuth occur most often as progeny radionuclides associated with intakes of uranium, thorium or radium.

Table 30.1. Absorption parameter values for inhaled and ingested bismuth.

Inhaled particulate materials		Absorption parameter values* f_r	s_r (d^{-1})	s_s (d^{-1})
Default parameter values†,‡				
Absorption Type	Assigned forms			
F	Bismuth as a progeny of radon	1	1	–
M§	—	0.2	1	0.005
S	—	0.01	1	1×10^{-4}

Ingested material¶	Age-dependent absorption from the alimentary tract, f_A					
Assigned forms	3 months	1 year	5 years	10 years	15 years	adult
All forms	0.1	0.05	0.05	0.05	0.05	0.05

*It is assumed that for bismuth the bound state can be neglected, i.e. $f_b = 0$. The values of s_r for Type F, M and S forms of bismuth (1 d^{-1}) are element-specific.

†For inhaled material deposited in the respiratory tract and subsequently cleared by particle transport to the alimentary tract, the default f_A values for inhaled materials are applied: i.e. the product of f_r for the absorption type (or specific value where given) and the f_A value for ingested soluble forms of bismuth applicable to the age-group of interest (*e.g.* 0.05 for adults).

‡Materials (e.g. bismuth as a progeny of radon) are listed here where there is sufficient information to assign to a default absorption type, but not to give specific parameter values (see Section 10 of *Publication 137*, ICRP, 2017).

§Default Type M is recommended for use in the absence of specific information on which the exposure material can be assigned to an absorption type, e.g. if the form is unknown, or if the form is known but there is no information available on the absorption of that form from the respiratory tract.

¶Activity transferred from systemic compartments into segments of the alimentary tract is assumed to be subject to reabsorption to blood. The default absorption fraction f_A for the secreted activity is the highest value for ingestion of the radionuclide applicable to the age-group of interest (*e.g.* 0.05 for adults).

30.1.2. Ingestion

(490) There are some available data on bismuth absorption in human and animals. It has been shown that inorganic forms of bismuth are only poorly absorbed (less than 1% of ingested quantity) from the gastrointestinal tract (for more details, see Section 10 of *Publication 137*, ICRP, 2017) and suggested that the fractional absorption of dietary bismuth from the gastrointestinal tract is about 8% (ICRP, 1975). *Publications 30* (ICRP, 1980) and *137* (ICRP, 2017) recommended an absorption fraction of 5% to apply to all chemical forms. The same value $f_A = 0.05$ is adopted here for dietary intakes of bismuth by adult members of the public. Consistently with the approach of *Publication 56* (ICRP, 1990), the value $f_A = 0.1$ is adopted for 3-month-old infants. The adult value of $f_A = 0.05$ is also applied here to 1-15 year-old children.

30.1.3. Systemic Distribution, Retention and Excretion

30.1.3.1. Summary of biokinetic data

(491) Bismuth has been used since the late 1700s as a therapeutic agent for a number of disorders of the human body. The systemic biokinetics of bismuth has been found to vary with the route of administration and the form administered.

(492) Most forms of bismuth show high deposition in the kidneys and subsequent clearance to urine (Durbin, 1959; Eridani et al., 1964; Matthews et al., 1964; Pieri and Wegmann, 1981; Russ et al., 1975; Slikkerveer and de Wolff, 1989). Human subjects injected with bismuth citrate excreted a third or more of the administered bismuth in urine during the first day (Coenegracht and Dorleyn, 1961; Newton, 2001).

(493) Newton et al. (2001) studied the biokinetics of bismuth in a healthy male volunteer after intravenous injection with ^{207}Bi citrate. They estimated that the liver contained 60% of the body content at 3 d. An estimated 55% of the administered amount was lost in excreta, primarily urine, during the first 2 d. The remaining amount was lost more slowly. Approximately 0.6% of the injected amount remained at 924 d. The long-term half-time was estimated as 1.9 y.

(494) Extended retention of a few percent of administered bismuth has been reported for relatively insoluble bismuth compounds used in clinical applications (Sollmann, 1957). Buijs and coworkers (1985) found ^{207}Bi ($T_{1/2}$ = 38 y) remaining in two human subjects treated a quarter century earlier with ^{206}Bi injections contaminated with small amounts of ^{207}Bi. They estimated from measurements of the rate of decline of total-body ^{207}Bi and from assumptions on the early rate of excretion of bismuth that 7% of injected bismuth was retained with a half-time close to 20 y. Autopsy measurements on subjects treated with bismuth compounds indicated that the kidneys and liver each contained nearly 10% of the total found in the body (Sollmann, 1957).

(495) Results of animal studies indicate elevated deposition in the kidneys and in some cases the liver (*Publication 137*, ICRP, 2017). Deposition of bismuth in bone has also been observed in rats, but uptake and retention are highly variable and may depend on the administered form of bismuth (*Publication 137*).

(496) No information was found regarding the effect of age on the biokinetics of systemic bismuth.

30.1.3.2. Systemic model

(497) The model for systemic bismuth applied in *Publication 137* (ICRP, 2017) to workers is applied here to adult members of the public. The systemic behaviour of bismuth is assumed to be independent of age.

(498) The structure of the model for systemic bismuth is shown in Fig. 30.1. Transfer coefficients are listed in Table 30.2.

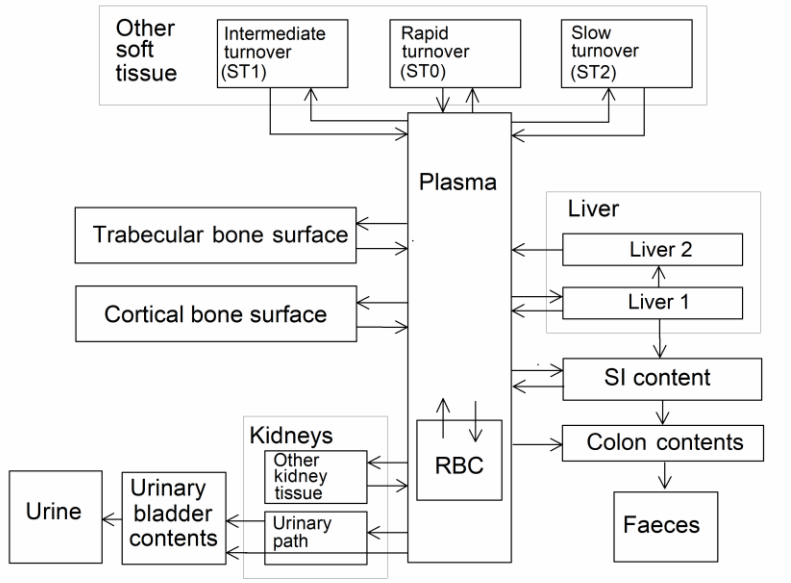

Fig. 30.1. Structure of the model for systemic bismuth. Activity transferring from Plasma to Colon contents enters Right colon contents.

Table 30.2. Age-specific transfer coefficients for bismuth.

Pathway	Transfer coefficient (d^{-1})					
	100 d	1 y	5 y	10 y	15 y	Adult
Blood to Urinary bladder contents	2.00E+01	2.00E+01	2.00E+01	2.00E+01	2.00E+01	2.00E+01
Blood to Right colon contents	4.00E+00	4.00E+00	4.00E+00	4.00E+00	4.00E+00	4.00E+00
Blood to Blood 1	5.00E-01	5.00E-01	5.00E-01	5.00E-01	5.00E-01	5.00E-01
Blood to ST0	3.00E+02	3.00E+02	3.00E+02	3.00E+02	3.00E+02	3.00E+02
Blood to ST1	4.20E+00	4.20E+00	4.20E+00	4.20E+00	4.20E+00	4.20E+00
Blood to ST2	1.30E+00	1.30E+00	1.30E+00	1.30E+00	1.30E+00	1.30E+00
Blood to Liver 1	3.00E+01	3.00E+01	3.00E+01	3.00E+01	3.00E+01	3.00E+01
Blood to Kidneys 1	3.00E+01	3.00E+01	3.00E+01	3.00E+01	3.00E+01	3.00E+01
Blood to Kidneys 2	5.00E+00	5.00E+00	5.00E+00	5.00E+00	5.00E+00	5.00E+00
Blood to Cortical bone surface	2.50E+00	2.50E+00	2.50E+00	2.50E+00	2.50E+00	2.50E+00
Blood to Trabecular bone surface	2.50E+00	2.50E+00	2.50E+00	2.50E+00	2.50E+00	2.50E+00
Blood 1 to Blood	1.73E-01	1.73E-01	1.73E-01	1.73E-01	1.73E-01	1.73E-01
ST0 to Blood	6.65E+01	6.65E+01	6.65E+01	6.65E+01	6.65E+01	6.65E+01
ST1 to Blood	3.47E-02	3.47E-02	3.47E-02	3.47E-02	3.47E-02	3.47E-02
ST2 to Blood	1.16E-03	1.16E-03	1.16E-03	1.16E-03	1.16E-03	1.16E-03
Liver 1 to Small intestine contents	2.08E-01	2.08E-01	2.08E-01	2.08E-01	2.08E-01	2.08E-01
Liver 1 to Liver 2	1.39E-01	1.39E-01	1.39E-01	1.39E-01	1.39E-01	1.39E-01
Liver 2 to Blood	6.93E-02	6.93E-02	6.93E-02	6.93E-02	6.93E-02	6.93E-02

Kidneys 1 to Urinary bladder contents	6.93E-01	6.93E-01	6.93E-01	6.93E-01	6.93E-01	6.93E-01
Kidneys 2 to Blood	1.39E-01	1.39E-01	1.39E-01	1.39E-01	1.39E-01	1.39E-01
Cortical bone surface to Blood	3.47E-02	3.47E-02	3.47E-02	3.47E-02	3.47E-02	3.47E-02
Trabecular bone surface to Blood	3.47E-02	3.47E-02	3.47E-02	3.47E-02	3.47E-02	3.47E-02

5445

5446 30.1.3.3. Treatment of radioactive progeny

5447 (499) The treatment of radioactive progeny produced in systemic compartments after intake
5448 of a radioisotope of bismuth is described in Section 10.2.3.3. of *Publication 137* (ICRP, 2017).

30.2. Dosimetric data for bismuth

Table 30.3. Committed effective dose coefficients (Sv Bq^{-1}) for the inhalation or ingestion of ^{210}Bi compounds.

	Effective dose coefficients (Sv Bq^{-1})					
Inhaled particulate materials (1 µm AMAD aerosols)	3 mo	1 y	5 y	10 y	15 y	Adult
Type F, Bismuth as a decay product of radon	4.7E-08	3.1E-08	1.8E-08	1.2E-08	5.1E-09	3.7E-09
Type M, All unspecified forms	2.3E-07	2.0E-07	1.1E-07	7.4E-08	5.4E-08	4.9E-08
Type S	3.9E-07	3.5E-07	2.0E-07	1.3E-07	9.9E-08	9.4E-08
Ingested materials						
Adult f_A = 0.05, All forms	2.7E-08	1.0E-08	5.9E-09	4.1E-09	1.6E-09	1.1E-09

Table 30.4. Committed effective dose coefficients (Sv Bq^{-1}) for the inhalation or ingestion of ^{214}Bi compounds.

	Effective dose coefficients (Sv Bq^{-1})					
Inhaled particulate materials (1 µm AMAD aerosols)	3 mo	1 y	5 y	10 y	15 y	Adult
Type F, Bismuth as a decay product of radon	4.2E-08	3.3E-08	1.9E-08	1.4E-08	1.3E-08	1.1E-08
Type M, All unspecified forms	4.3E-08	3.3E-08	1.9E-08	1.4E-08	1.3E-08	1.1E-08
Type S	4.3E-08	3.3E-08	1.9E-08	1.4E-08	1.3E-08	1.1E-08
Ingested materials						
Adult f_A = 0.05, All forms	2.7E-10	2.1E-10	1.4E-10	1.0E-10	6.6E-11	4.7E-11

31. POLONIUM (Z = 84)

31.1. Routes of Intake

31.1.1. Inhalation

(500) Information is available on the behaviour of polonium following deposition in the respiratory tract from animal experiments with several chemical forms, and from some accidental human intakes. However, the behaviour of ionic (soluble) Po following deposition in the respiratory tract is difficult to determine because ionic solutions (e.g. chloride) are unstable at neutral pH and in many biological media, resulting in colloid formation. For details, see Section 11 of *Publication 137* (ICRP, 2017). Absorption parameter values and types, and associated f_A values for particulate forms of polonium are given in Table 31.1 (taken from Section 11 of *Publication 137*).

(501) The most important widespread exposures to radioisotopes of polonium are as progeny radionuclides of radon. The alpha-emitting isotopes ^{218}Po (half-life 3 min) and ^{214}Po (half-life 160 μs) give rise to most of the dose from inhalation of the short-lived progeny radionuclides of ^{222}Rn, as do ^{216}Po (half-life 0.15 s) and ^{212}Po (half-life 300 ns) for those of ^{220}Rn (thoron). For the decay schemes see the radon Section of this report. Dose coefficients for isotopes of polonium inhaled as short-lived radon progeny radionuclides are given in the radon section, where factors such as the relevant aerosol size distribution are addressed.

Table 31.1. Absorption parameter values for inhaled and ingested polonium.

Inhaled particulate materials		Absorption parameter values* f_r	s_r (d^{-1})	s_s (d^{-1})
Default parameter values†,‡				
Absorption Type	Assigned forms			
F	—	1	3	–
M§	Chloride, hydroxide, volatilised polonium	0.2	3	0.005
S	—	0.01	3	1×10^{-4}

Ingested material¶	Age-dependent absorption from the alimentary tract, f_A					
Assigned forms	3 months	1 year	5 years	10 years	15 years	adult
polonium in diet	1	0.5	0.5	0.5	0.5	0.5
All other chemical forms	0.2	0.1	0.1	0.1	0.1	0.1

*It is assumed that for polonium the bound state can be neglected, *i.e.* $f_b = 0.0$. The value of s_r for Type F forms of polonium (3 d^{-1}) is element-specific. The values for Types M and S (3 d^{-1}) are the general default values.

†Materials (e.g. polonium chloride) are generally listed here where there is sufficient information to assign to a default absorption type, but not to give specific parameter values (see Section 11 of *Publication 137*, ICRP, 2017).

‡For inhaled material deposited in the respiratory tract and subsequently cleared by particle transport to the alimentary tract, the default f_A values for inhaled materials are applied: i.e. the product of f_r for the absorption type and the f_A value for ingested soluble (excluding dietary) forms of polonium applicable to the age-group of interest (*e.g.* 0.1 for adults).

§Default Type M is recommended for use in the absence of specific information on which the exposure material can be assigned to an absorption type, e.g. if the form is unknown, or if the form is known but there is no information available on the absorption of that form from the respiratory tract.

¶Activity transferred from systemic compartments into segments of the alimentary tract is assumed to be subject to reabsorption to blood. The default absorption fraction f_A for the secreted activity is the highest value for ingestion of the radionuclide applicable to the age-group of interest (*e.g.* 0.5 for adults).

31.1.2. Ingestion

31.1.2.1. Adults

(502) Fractional absorption of ^{210}Po from the alimentary tract has been measured in human subjects and in animals at levels in the order of 1- 15% for inorganic forms (see reviews by Harrison et al., 2007; ICRP, 2017; Scott, 2007). In *Publications 30* (ICRP, 1979) and *137* (ICRP, 2017) an absorption fraction of 0.1 was recommended for all chemical forms in the workplace. Fractional absorption in animals seems to be identical in males and females. Data from humans consuming meat from reindeer exposed to ^{210}Po suggest that polonium incorporated in food may have an absorption fraction of 5-25 times that of inorganic polonium compounds, values of around 0.3 to 0.5 having been estimated (Hill, 1965; Kauranen and Miettinen, 1967; Ladinskaya et al., 1973). Rats absorbed approximately 50% of polonium biologically incorporated into goat's milk. This value is higher than is typically observed for inorganic polonium absorption in rats (McInroy et al., 1972). Similarly, experiments in rats ingesting polonium biologically incorporated into rat liver yielded absorption fractions of 0.10-0.12 which are at least twice those which have been obtained using inorganic polonium compounds (Naylor et al., 1991). In a human volunteer study of the absorption of ^{210}Po from crabmeat, Hunt and Allington (1993) estimated fractional absorption to be about 0.8. In *Publication 67* (ICRP, 1993), an absorption fraction of 0.5 has been recommended for dietary intakes of polonium by adult members of the public. The same value $f_A = 0.5$ is adopted here for polonium in food for adult. f_A for other chemical forms is equal to 0.1.

31.1.2.2. Children

(503) There appear to be no data available for estimating an absorption fraction for polonium in infants and children. Following the approach of *Publication 56* (ICRP, 1990), an absorption fraction of 1 was recommended in *Publication 67* for the 3-month-old infant. For children of 1 year and older the absorption fraction for the adult (0.5) was recommended in *Publication 67*. The same values are adopted here for f_A for polonium in food. When ingested as any other chemical form, an f_A of 0.2 is adopted for 3 month old infants and an f_A of 0.1 is adopted for children of 1 year old and older.

31.1.3. Systemic Distribution, Retention and Excretion

31.1.3.1. Summary of biokinetic data

(504) Leggett and Eckerman (2001) reviewed records of about 1500 former polonium workers and estimated urinary half-times for numerous cases of apparently elevated, acute exposure. Approximately 95% of the derived effective half-times were in the range 8-52 d, corresponding to a range of biological half-times of 8.5-83 d. The mean, median, and mode of the effective half-times were approximately 30 d, 30 d, and 34 d, corresponding to biological half-times of 38 d, 38 d, and 45 d, respectively.

(505) Retention and excretion of ^{210}Po has been studied in workers exposed acutely via wounds or intact skin (Cohen et al., 1989; Sheehan, 1964; Silverman, 1944; Testa, 1972; Wraight and Strong, 1989) or inhalation (Foreman et al., 1958; Jackson and Dolphin, 1966;

Naimark, 1948, 1949; Scott and West, 1975; Sheehan, 1964; Spoerl, 1951). A phase of relatively rapid phase removal of activity from the body generally was observed in cases where measurements were begun soon after exposure. Estimates of the long-term biological half-time were generally in the range 13-42 d for cases of entry through a wound or intact skin and 20-60 d in inhalation cases.

(506) Silberstein et al. (1950) measured ^{210}Po in the urine, faeces, and blood of four lymphosarcoma or leukemia patients who were administered ^{210}Po chloride by intravenous injection and in a leukemia patient administered ^{210}Po chloride by ingestion. Biological half-times fitted to the time-dependent concentration of ^{210}Po in urine, faeces, or blood of these subjects varied with the observation period. Urinary excretion data for the first week after administration yielded biological half-times as short as 3 d. For three subjects followed for several weeks or months, urinary excretion data indicated half-times of 30-50 d for the period starting 1 wk after exposure; faecal excretion data indicated half-times of 33-52 d for this period; and data for red blood cells indicated half-times of 12-48 d for this period.

(507) Measurements on 14 children or adolescents (age range, 6-15 y) exposed to ^{210}Po indicated a retention half-time of about 40 days (Guskova et al., 1964; Kalmykov et al., 1969). This value is near the mean or median value indicated by data on adults summarized above.

31.1.3.2. Systemic model

(508) The model for systemic polonium applied in *Publication 137* (ICRP, 2017) to workers is applied here to adult members of the public. The systemic behaviour of polonium is assumed to be independent of age.

(509) The structure of the model for systemic polonium is shown in Fig. 31.1. Transfer coefficients are listed in Table 31.2.

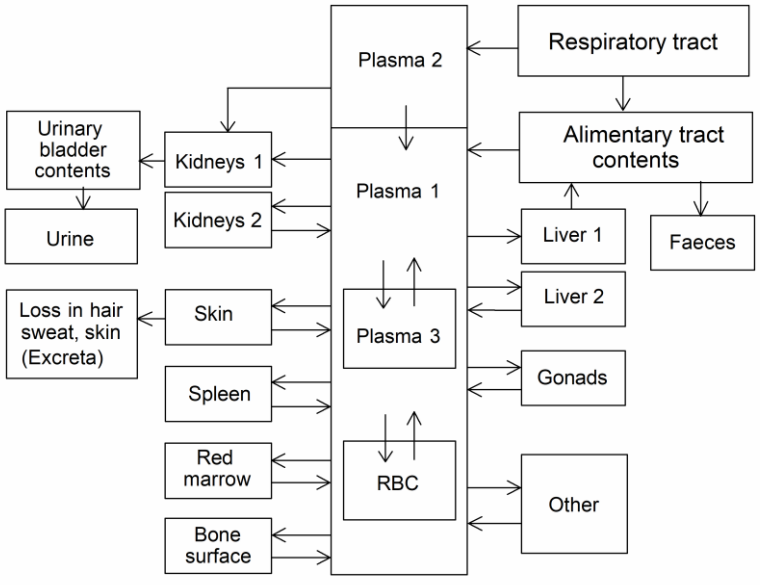

Fig. 31.1. Structure of the model for systemic polonium. Polonium absorbed from the alimentary tract and repiratory tract is assigned to Plasma 1 and Plasma 2, respectively. Polonium transferred from Liver 1 to the alimentary tract contents enters Small intestine contents. RBC = red blood cells.

Table 31.2. Age-specific transfer coefficients for polonium.

Pathway	Transfer coefficient (d^{-1})					
	100 d	1 y	5 y	10 y	15 y	Adult
Plasma 2 to Blood	8.00E+02	8.00E+02	8.00E+02	8.00E+02	8.00E+02	8.00E+02
Plasma 2 to Kidneys 1	2.00E+02	2.00E+02	2.00E+02	2.00E+02	2.00E+02	2.00E+02
Plasma 1 to RBC	6.00E+00	6.00E+00	6.00E+00	6.00E+00	6.00E+00	6.00E+00
Plasma 1 to Plasma 3	4.00E+00	4.00E+00	4.00E+00	4.00E+00	4.00E+00	4.00E+00
Plasma 1 to Other	3.24E+01	3.24E+01	3.24E+01	3.24E+01	3.24E+01	3.24E+01
Plasma 1 to Liver 1	1.75E+01	1.75E+01	1.75E+01	1.75E+01	1.75E+01	1.75E+01
Plasma 1 to Liver 2	1.75E+01	1.75E+01	1.75E+01	1.75E+01	1.75E+01	1.75E+01
Plasma 1 to Kidneys 1	5.00E+00	5.00E+00	5.00E+00	5.00E+00	5.00E+00	5.00E+00
Plasma 1 to Kidneys 2	5.00E+00	5.00E+00	5.00E+00	5.00E+00	5.00E+00	5.00E+00
Plasma 1 to Spleen	2.00E+00	2.00E+00	2.00E+00	2.00E+00	2.00E+00	2.00E+00
Plasma 1 to Red marrow	4.00E+00	4.00E+00	4.00E+00	4.00E+00	4.00E+00	4.00E+00
Plasma 1 to Trab bone surface	7.50E-01	7.50E-01	7.50E-01	7.50E-01	7.50E-01	7.50E-01
Plasma 1 to Cort bone surface	7.50E-01	7.50E-01	7.50E-01	7.50E-01	7.50E-01	7.50E-01
Plasma 1 to Testes	1.00E-01	1.00E-01	1.00E-01	1.00E-01	1.00E-01	1.00E-01
Plasma 1 to Ovaries	5.00E-02	5.00E-02	5.00E-02	5.00E-02	5.00E-02	5.00E-02
Plasma 1 to Skin	5.00E+00	5.00E+00	5.00E+00	5.00E+00	5.00E+00	5.00E+00
RBC to Blood	9.90E-02	9.90E-02	9.90E-02	9.90E-02	9.90E-02	9.90E-02
Plasma 3 to Blood	9.90E-02	9.90E-02	9.90E-02	9.90E-02	9.90E-02	9.90E-02
Other to Plasma 1	9.90E-02	9.90E-02	9.90E-02	9.90E-02	9.90E-02	9.90E-02
Spleen to Plasma 1	9.90E-02	9.90E-02	9.90E-02	9.90E-02	9.90E-02	9.90E-02
Liver 1 to Small intestine contents	1.39E-01	1.39E-01	1.39E-01	1.39E-01	1.39E-01	1.39E-01
Liver 2 to Plasma 1	9.90E-02	9.90E-02	9.90E-02	9.90E-02	9.90E-02	9.90E-02
Kidneys 1 to Urinary bladder contents	1.73E-01	1.73E-01	1.73E-01	1.73E-01	1.73E-01	1.73E-01
Kidneys 2 to Plasma 1	9.90E-02	9.90E-02	9.90E-02	9.90E-02	9.90E-02	9.90E-02
Red marrow to Plasma 1	9.90E-02	9.90E-02	9.90E-02	9.90E-02	9.90E-02	9.90E-02
Trab bone surf to Plasma 1	2.31E-02	2.31E-02	2.31E-02	2.31E-02	2.31E-02	2.31E-02
Cort bone surf to Plasma 1	2.31E-02	2.31E-02	2.31E-02	2.31E-02	2.31E-02	2.31E-02
Skin to Plasma 1	6.93E-03	6.93E-03	6.93E-03	6.93E-03	6.93E-03	6.93E-03
Skin to Excreta	6.93E-03	6.93E-03	6.93E-03	6.93E-03	6.93E-03	6.93E-03
Testes to Plasma 1	1.39E-02	1.39E-02	1.39E-02	1.39E-02	1.39E-02	1.39E-02
Ovaries to Plasma 1	1.39E-02	1.39E-02	1.39E-02	1.39E-02	1.39E-02	1.39E-02

5559

5560 31.1.3.3. Treatment of radioactive progeny

5561 (510) The treatment of radioactive progeny produced in systemic compartments after intake
5562 of a radioisotope of polonium is described in Section 11.2.3.3. of *Publication 137* (ICRP, 2017).

31.2. Dosimetric data for polonium

Table 31.3. Committed effective dose coefficients (Sv Bq^{-1}) for the inhalation or ingestion of ^{210}Po compounds.

	Effective dose coefficients (Sv Bq^{-1})					
Inhaled particulate materials (1 µm AMAD aerosols)	3 mo	1 y	5 y	10 y	15 y	Adult
Type F	5.1E-06	3.1E-06	1.8E-06	1.2E-06	4.5E-07	3.2E-07
Type M, Chloride, hydroxide, volatilised polonium; all unspecified forms	8.5E-06	6.9E-06	4.1E-06	2.7E-06	1.9E-06	1.8E-06
Type S	1.2E-05	1.1E-05	6.3E-06	4.1E-06	3.2E-06	3.0E-06
Ingested materials						
Adult f_A = 0.1, All other chemical forms	5.6E-06	2.1E-06	1.2E-06	8.7E-07	2.8E-07	1.8E-07
Adult f_A = 0.5, Polonium in diet	2.8E-05	1.0E-05	6.1E-06	4.4E-06	1.4E-06	9.2E-07

32. RADON (Z = 86)

32.1. Routes of Intake

32.1.1. Inhalation of short-lived radon and thoron progeny

(511) Absorption parameter values for radon progeny are addressed in the inhalation sections of the elements (lead, bismuth and polonium) of *Publication* 137 (ICRP, 2017). These values are summarised in Annex A of *Publication* 137 and in Table 32.1 below. As described in *Publication* 130, OIR part 1, section 3.2.3 (ICRP, 2015), shared kinetics are assumed in the respiratory tract.

(512) Following deposition in the respiratory tract and subsequent clearance by particle transport to the alimentary tract, the default age-dependent f_A values given in Table 32.1 are applied. These values are taken from the inhalation sections for lead, bismuth and polonium in this report.

Table 32.1. Absorption parameter values for inhaled radon progeny.

Inhaled radon progeny	Dissolution parameter values			Uptake parameter values	
	f_r	s_r (d^{-1})	s_s (d^{-1})	f_b	s_b (d^{-1})
Polonium	1	3	–	0	–
Lead	0.1	100	1.7	0.5	1.7
Bismuth	1	1	–	0	–

	Age-dependent absorption from the alimentary tract, f_A					
	3 months	1 year	5 years	10 years	15 years	Adult
Polonium	0.2	0.1	0.1	0.1	0.1	0.1
Lead	0.6	0.3	0.3	0.3	0.3	0.2
Bismuth	0.1	0.05	0.05	0.05	0.05	0.05

(513) Aerosol characteristics need to be defined in order to calculate doses from inhaled radon or thoron progeny. The activity size distribution of the radon progeny aerosol can be very variable and depends upon the exposure scenario. In *Publication* 137, reference aerosol parameter values were given for indoor workplaces, mines and tourist caves for the purposes of dose calculations for workers (ICRP, 2017). For dose calculations for members of the public, aerosol parameter values are given for home exposures following exposure to radon (^{222}Rn) or thoron (^{220}Rn) progeny (Table 32.2). They are similar to the values assumed for indoor workplaces, because the parameter values for workplaces were based on data for homes as well as for workplaces when available (ICRP, 2017). Any differences are justified below.

Table 32.2. Reference aerosol parameter values for home exposures for radon (^{222}Rn) progeny and thoron (^{220}Rn) progeny.

Nuclides	f_p*	Equilibrium factor, F	Attached aerosol characteristics in the ambient air†				
			Mode, i	f_{pi}	$AMTD_i$ (nm)	σ_{gi}	hgf_i‡
Radon (^{222}Rn) progeny	0.1	0.4	n	0.2	30	2.0	1.75
			a	0.8	200	2.0	1.75
Thoron (^{220}Rn) progeny	0.02	-	n	0.14	40	2.0	1.75
			a	0.86	200	1.8	1.75

f_p = unattached fraction in terms of the potential alpha energy concentration (PAEC); f_{pi} = fraction of attached PAEC for mode *i*; AMTD = activity median thermodynamic diameter; σ_{gi} = geometric standard deviation of mode *i*; hgf_i = hygroscopic growth factor for mode *i*.

*The unattached progeny are assumed to have an AMTD of 1.0 nm with σ_g = 1.3, and unit density and shape factor.

†Indices *i* = 'n' and 'a' represent the nucleation and accumulation modes, respectively.

‡It is assumed that the AMTD increases by *hgf* instantaneously as the particle enters the nose or the mouth. For simplicity, the hygroscopically enlarged particles are assumed to have unit density and shape factor.

32.1.1.1. Radon progeny

(514) The aerosol parameter values for radon progeny are mainly based on the publications of Marsh et al. (2002) and Porstendörfer (2001). They are also consistent with the measurement results from other researchers summarised in *Publication 137* (ICRP, 2017) and in ICRU *Report 88* (ICRU, 2012).

(515) The unattached fraction, f_p depends inversely on the ambient particle concentration. This depends on the ventilation rate and whether additional sources are present. The mean value of f_p measured in dwellings range between 0.04 and 0.2 with some values greater than 0.4 (ICRP, 2017; ICRU, 2012). Compared with indoor workplaces, the air is assumed to be 'cleaner' (i.e. a lower particle concentration), for example in the bedroom while asleep. Thus, a slightly higher f_p value of 0.1 is assumed for homes (Marsh et al., 2002, 2005; Marsh and Bailey, 2013).

(516) The fraction of the attached potential alpha energy concentration (PAEC) of radon progeny in the nucleation mode, f_{pn} is assumed to be 0.2, the same as for indoor workplaces (ICRP, 2017). Measurements have shown that the nucleation mode is present when small aerosols are produced, for example, by cooking, candle burning and gas combustion (ICRP, 2017; ICRU, 2012). However, activity size measurements performed in a house in Germany, without additional aerosols (i.e. for an aged aerosol), also showed a nucleation mode with f_{pn} of about 0.2 (Reineking et al., 1994). In addition, measurements in a dwelling in Okinawa, Japan showed a nucleation mode with an activity fraction of 0.14 (Kranrod et al., 2009). It is acknowledged that for an aged aerosol, the presence of the nucleation mode is not always measured (Huet et al., 2001). Without a nucleation mode the effective dose would decrease by about 20% (Annex C, para. C.20 and Table C.9).

(517) Measurements of the activity median diameter (AMD) of the accumulation mode in dwellings show a wide range of values, typically between 90 nm to 350 nm (El-Hussein et al., 1998; Huet et al., 2001; ICRU, 2012; Kranrod et al., 2009; Mohamed, 2005; Porstendörfer, 2001; Tokonami et al., 1997; Tu et al., 1991; Tu and Knutson, 1988). The mean of the average AMD values in each of these studies is about 190 nm. Porstendörfer (2001) summarised activity size measurements in dwellings and reported activity median diameters (AMD) of 20 to 40 nm for the nucleation mode and 210 nm (120-350 nm) for the accumulation mode. A central value of 200 nm is assumed here for the accumulation mode and 30 nm for the nucleation mode.

(518) Some of the ambient aerosols, to which radon progeny attach, are hygroscopic and are assumed to grow very quickly on inhalation. For modelling purposes and simplicity, it is assumed that the activity median diameter increases by the hygroscopic growth factor (*hgf*) instantaneously as the particle enters the nose or mouth. In *Publication* 137, a *hgf* of 2.0 was assumed based on growth measurements of atmospheric aerosols as the relative humidity (RH) increases from zero to 99% (ICRP, 2017). For example, Li and Hopke (1993) measured average *hgf* between 1.5 and 1.9 for various types of indoor aerosols. Sinclair et al. (1974) showed that atmospheric particles, which originated from an industrial area close to the sea, increase by a factor of 2 due to hygroscopic growth. Because these measurements start with dried aerosols, they represent maximum growth (United Nations Scientific Committee on the

Effects of Atomic Radiation (UNSCEAR), 2020). The data of Sinclair et al. (1974) also showed that the atmospheric particles would increase by factors of 1.5 and 1.8 as the humidity increases from the RH of indoor air (~30-50%) to 99% RH in the respiratory tract. Compared with *Publication* 137, a lower *hgf* of 1.75 is assumed here, recognising that growth starts from the RH of indoor air rather than for the experimentally dried aerosol. Assuming a *hgf* of 1.75 rather than 2.0 only increases the effective dose per unit exposure by a few percent (Marsh and Birchall, 2000).

32.1.1.2. Thoron progeny

(519) In *Publication* 137, the aerosol parameter values assumed for thoron progeny for indoor workplaces are based on the measurements of Reineking et al. (1992) and on the values recommended by Porstendörfer (2001). As these measurements were carried out in houses, the same values are assumed for home exposures.

32.1.1.3. Average breathing rates at home

(520) For a given concentration of radon progeny the intake is directly proportional to the average breathing rate. To a lesser extent, the fraction of the intake deposited in the respiratory tract (i.e. regional depositions) also depends on the breathing rate. At higher respiratory frequencies during increased physical activities, the residence time in the airways decreases, resulting in lower deposition by diffusion.

(521) In *Publication 66* (ICRP, 1994b), the 'time-activity-ventilation' approach was used to calculate mean breathing rates for each reference individual. In this approach, the ventilation rates for the four reference levels of exercise (sleep, sitting, light exercise and heavy exercise) are combined with the time spent in each level of exercise. The daily time budgets at home for the reference individuals are given in Table 2.2, Section 2.2.1. Using these values, the fractions of time spent in each activity at home are given in Table 32.3. The mean breathing rates are also given in Table 32.3, obtained by combing these fractions with the reference ventilation rates for each level of exercise (Table 2.1, Section 2.2.1).

Table 32.3. Mean breathing rates and distribution of time spent in various activities at home for Reference Individuals.

Age	Fraction of time spent in each level of exercise at home			Mean breathing rates (m^3 h^{-1})
	Sleep	Sitting	Light exercise	
3 mo	0.71	-	0.29	0.12
1 y	0.73	0.09	0.18	0.19
5 y	0.67	0.11	0.22	0.32
10 y	0.55	0.15	0.30	0.56
15 y (Male)	0.58	0.21	0.21	0.63
Adult (Male)	0.55	0.15	0.30	0.78

32.1.2. Ingestion

(522) Radon is soluble in water and volunteer experiments have shown that radon is readily absorbed from the alimentary tract into blood. It has not been clearly established whether some absorption takes place in the stomach or not. For details, see section 12 of *Publication* 137 (ICRP, 2017). In the biokinetic model adopted in *Publication* 137 and in this document, it is assumed that radon gas does not diffuse from Stomach contents to Stomach wall, but that radon is absorbed to blood only via the small intestine.

32.1.3. Systemic Distribution, Retention and Excretion

32.1.3.1. Summary of biokinetic data

(523) The noble gases are chemically inert but are absorbed to blood from the lungs or gastrointestinal tract and retained in systemic tissues to some extent, due in part to their solubility in blood and tissues. Radon returns from tissues to blood at tissue-specific rates and is recycled through the lungs and partly removed by exhalation and partly recycled to tissues. It is almost entirely removed from the body over a few hours after intake. Loss of radon by pathways other than inhalation (e.g., via skin, urine, or faeces) appears from experimental studies to be small.

(524) As described in *Publication 137* (ICRP, 2017), the rate of transfer of radon from blood to a tissue can be related to the fraction of cardiac output received by the tissue. The rate of return from a tissue to blood can be estimated from the blood perfusion rate and the relative solubility of the gas in blood and the tissue, represented by a gas-specific tissue-to-blood partition coefficient. The partition coefficient for two compartments is defined as the ratio of the concentrations of the gas in the compartments at equilibrium. Some experimentally determined tissue-to-blood partition coefficients for radon and other noble gases are listed in Table 12.2 of *Publication 137*. Derived half-times for the build-up or washout of radon are a few minutes for tissues with a rich blood supply and relatively low partition coefficients but are much greater for fatty tissues because of their poor blood supply and relatively high tissue-to-blood partition coefficient.

(525) Measurements of ^{222}Rn in breath and external measurements of the short-lived chain member ^{214}Bi have been used to estimate whole-body retention of radon in adult human subjects after ingestion or inhalation of elevated levels (Andersson and Nilsson, 1964; Brown and Hess, 1992; Fernau and Smereker, 1933; Gosink et al., 1990; Harley et al., 1951, 1994; Hursh et al., 1965; Meyer, 1937; Suomela and Kahlos, 1972; Vaternahm, 1922; von Döbeln and Lindell, 1964). The reader is referred to *Publication 137* (ICRP, 2017) for descriptions of several studies. The results of these studies on adult humans have been used as model-free determinations of total-body retention of radon as well as a check on the theoretical method of modeling the kinetics of radon in the body using partition coefficients.

(526) Reported rates of loss of radon from the human body are variable, presumably due in large part to differences in experimental conditions such as the timing of intake of radon relative to meals, the level of physical activity of the subjects after intake of radon, the percentage of body fat, and the length of the observation period. Retention half-times in the range 30-70 min have been reported in several studies involving relatively short observation periods. Multiple retention components with half-times varying from a few minutes to several hours have been determined in some studies with relatively long observation periods.

(527) Age-specific lung “washout” rates have been determined in persons inhaling air mixed with xenon or krypton for several respiratory cycles (Treves et al. 1974; Ciofetta et al. 1980; Treves and Packard 1995; Goo et al. 2013). Those data are assumed to be applicable to radon, because observed washout times for xenon (Susskind et al. 1977) and krypton (Ellis et al. 1977) in adults are consistent with washout times observed for radon in adults (Harley et al. 1994). The removal half-time of xenon or krypton from lung air to the environment appears to increase nearly linearly from about 4-6 s in the first year of life to about 20-30 s in young adults.

32.1.3.2. Biokinetic model for systemic radon

(528) The structure of the radon model applied in this report is shown in Figure 32.1. Age-specific transfer coefficients are listed in Table 32.4 for males and Table 32.5 for females. The basis for the model is discussed in Annex C.

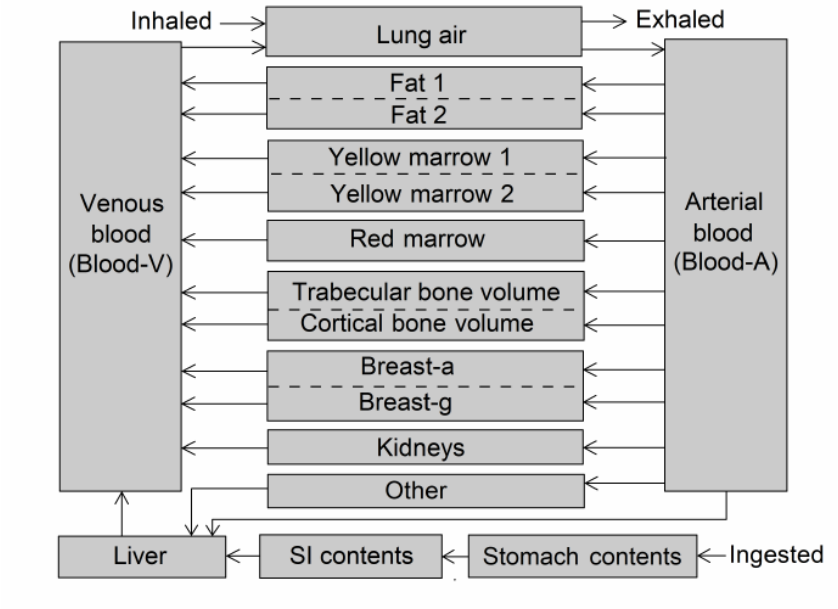

Figure 32.1. Structure of the biokinetic model for systemic radon. Abbreviations: RT-air = respiratory tract air; Blood-A = arterial blood; Blood-V = venous blood; Breast-g = glandular breast tissue; Breast-a = adipose tissue in breast.

5732 Table 32.4. Age-specific transfer coefficients for males (d^{-1}).

From	To	100 d	1 y	5 y	10 y	15 y	Adult
Environment	RT-air	*	*	*	*	*	*
RT-air	Environment	1.33E+04	1.20E+04	7.49E+03	5.44E+03	3.52E+03	2.60E+03
Blood-A	Fat 1	4.91E+02	5.12E+02	5.18E+02	4.44E+02	2.89E+02	2.62E+02
Blood-A	Fat 2	1.23E+02	1.28E+02	1.30E+02	1.11E+02	7.23E+01	6.54E+01
Blood-A	Kidneys	2.33E+03	2.43E+03	2.46E+03	2.11E+03	1.37E+03	1.24E+03
Blood-A	Liver	7.98E+02	8.32E+02	8.42E+02	7.22E+02	4.70E+02	4.25E+02
Blood-A	TB volume	2.21E+02	2.30E+02	2.33E+02	2.00E+02	6.51E+01	5.89E+01
Blood-A	CB volume	1.47E+02	1.54E+02	1.55E+02	1.33E+02	4.34E+01	3.92E+01
Blood-A	Y-Marrow 1	1.52E-01	4.13E-01	3.34E+00	1.13E+01	1.73E+01	2.62E+01
Blood-A	Y-Marrow 2	3.81E-02	1.03E-01	8.36E-01	2.82E+00	4.31E+00	6.54E+00
Blood-A	Red marrow	3.68E+02	3.84E+02	3.89E+02	3.33E+02	2.17E+02	1.96E+02
Blood-A	Breast-g	1.04E-02	2.39E-02	5.33E-02	3.58E-01	2.74E-01	3.11E-01
Blood-A	Breast-a	1.07E-02	2.02E-02	4.41E-02	2.75E-01	5.93E-01	9.97E-01
Blood-A	Other	7.79E+03	8.13E+03	8.22E+03	7.04E+03	4.68E+03	4.22E+03
Fat 1	Blood-V	5.58E+00	5.06E+00	9.44E+00	8.77E+00	7.52E+00	4.96E+00
Fat 2	Blood-V	1.39E+00	1.27E+00	2.36E+00	2.19E+00	1.88E+00	1.24E+00
Kidneys	Blood-V	8.46E+03	7.39E+03	1.33E+04	1.20E+04	1.05E+04	9.04E+03
Liver	Blood-V	2.16E+03	1.96E+03	3.21E+03	3.24E+03	2.52E+03	1.94E+03
TB volume	Blood-V	1.46E+03	1.20E+03	1.66E+03	1.37E+03	4.89E+02	4.03E+02
CB volume	Blood-V	2.50E+02	2.04E+02	2.75E+02	2.28E+02	8.14E+01	6.72E+01
Y-Marrow 1	Blood-V	4.26E-01	6.16E-01	1.74E+00	2.57E+00	3.13E+00	3.34E+00
Y-Marrow 2	Blood-V	1.06E-01	1.54E-01	4.36E-01	6.41E-01	7.82E-01	8.34E-01
Red marrow	Blood-V	1.17E+03	9.98E+02	1.25E+03	9.90E+02	7.05E+02	6.93E+02
Breast-g	Blood-V	8.59E+00	1.37E+01	3.91E+01	5.95E+01	8.54E+01	1.14E+02
Breast-a	Blood-V	1.55E+00	1.51E+00	3.91E+00	5.11E+00	6.76E+00	6.85E+00
Other	Blood-V	4.65E+02	3.86E+02	5.61E+02	4.90E+02	3.34E+02	2.78E+02
Other	Liver	1.99E+02	1.65E+02	2.39E+02	2.10E+02	1.40E+02	1.21E+02
Blood-V	RT-air	4.54E+03	4.73E+03	4.79E+03	4.11E+03	2.67E+03	2.42E+03
RT-air	Blood-A	2.97E+03	2.60E+03	2.35E+03	1.78E+03	1.21E+03	1.04E+03
ST contents	SI contents	1.92E+01	2.06E+01	2.06E+01	2.06E+01	2.06E+01	2.06E+01
SI contents	Liver	5.99E+03	5.99E+03	5.99E+03	5.99E+03	5.99E+03	5.99E+03

* The rate that activity enters the RT air space is assumed to equal $\lambda C_{env} V_{RT-air}$ $[Bq\ d^{-1}]$, where λ is the transfer coefficient from the RT-air space to the environment, C_{env} is the radon concentration in the environment and $V_{RT\text{-}air}$ is the average volume of respiratory tract air space (Table 32.7).
TB = Trabecular bone; CB = cortical bone; Y-Marrow = yellow marrow; ST = stomach; SI = small intestine

5733
5734
5735 Table 32.5. Age-specific transfer coefficients for females (d^{-1})

From	To	100 d	1 y	5 y	10 y	15 y	Adult
Environment	RT-air	*	*	*	*	*	*
RT-air	Environment	1.33E+04	1.20E+04	7.49E+03	5.44E+03	3.52E+03	2.60E+03
Blood-A	Fat 1	4.91E+02	5.12E+02	5.18E+02	4.44E+02	6.70E+02	5.49E+02

Blood-A	Fat 2	1.23E+02	1.28E+02	1.30E+02	1.11E+02	1.68E+02	1.37E+02
Blood-A	Kidneys	2.33E+03	2.43E+03	2.46E+03	2.11E+03	1.68E+03	1.37E+03
Blood-A	Liver	7.98E+02	8.32E+02	8.42E+02	7.22E+02	6.41E+02	5.24E+02
Blood-A	TB volume	2.21E+02	2.30E+02	2.33E+02	2.00E+02	8.87E+01	7.26E+01
Blood-A	CB volume	1.47E+02	1.54E+02	1.55E+02	1.33E+02	5.92E+01	4.84E+01
Blood-A	Y-Marrow 1	1.52E-01	4.13E-01	3.34E+00	1.13E+01	3.02E+01	3.23E+01
Blood-A	Y-Marrow 2	3.81E-02	1.03E-01	8.36E-01	2.82E+00	7.56E+00	8.07E+00
Blood-A	Red marrow	3.68E+02	3.84E+02	3.89E+02	3.33E+02	2.96E+02	2.42E+02
Blood-A	Breast-g	1.04E-02	2.39E-02	5.33E-02	3.58E-01	1.14E+01	2.00E+01
Blood-A	Breast-a	1.07E-02	2.02E-02	4.41E-02	2.75E-01	8.33E+00	1.23E+01
Blood-A	Other	7.79E+03	8.13E+03	8.22E+03	7.04E+03	6.20E+03	5.05E+03
Fat 1	Blood-V	5.58E+00	5.06E+00	9.44E+00	8.77E+00	7.75E+00	5.84E+00
Fat 2	Blood-V	1.39E+00	1.27E+00	2.36E+00	2.19E+00	1.94E+00	1.46E+00
Kidneys	Blood-V	8.46E+03	7.39E+03	1.33E+04	1.20E+04	9.80E+03	8.28E+03
Liver	Blood-V	2.16E+03	1.96E+03	3.21E+03	3.24E+03	2.67E+03	2.40E+03
TB volume	Blood-V	1.46E+03	1.20E+03	1.66E+03	1.37E+03	5.35E+02	5.03E+02
CB volume	Blood-V	2.50E+02	2.04E+02	2.75E+02	2.28E+02	8.91E+01	8.39E+01
Y-Marrow 1	Blood-V	4.26E-01	6.16E-01	1.74E+00	2.57E+00	4.31E+00	4.17E+00
Y-Marrow 2	Blood-V	1.06E-01	1.54E-01	4.36E-01	6.41E-01	1.08E+00	1.04E+00
Red marrow	Blood-V	1.17E+03	9.98E+02	1.25E+03	9.90E+02	7.61E+02	8.18E+02
Breast-g	Blood-V	8.59E+00	1.37E+01	3.91E+01	5.95E+01	7.41E+01	7.69E+01
Breast-a	Blood-V	1.55E+00	1.51E+00	3.91E+00	5.11E+00	5.63E+00	4.58E+00
Other	Blood-V	4.65E+02	3.86E+02	5.61E+02	4.90E+02	4.04E+02	3.69E+02
Other	Liver	1.99E+02	1.65E+02	2.39E+02	2.10E+02	1.87E+02	1.71E+02
Blood-V	RT-air	4.54E+03	4.73E+03	4.79E+03	4.11E+03	3.65E+03	2.98E+03
RT-air	Blood-A	2.97E+03	2.60E+03	2.35E+03	1.78E+03	1.39E+03	1.17E+03
ST contents	SI contents	1.92E+01	2.06E+01	2.06E+01	2.06E+01	1.52E+01	1.52E+01
SI contents	Liver	5.99E+03	5.99E+03	5.99E+03	5.99E+03	5.99E+03	5.99E+03

* The rate that activity enters the RT air space is assumed to equal $\lambda C_{env} V_{RT-air}$ $[Bq\ d^{-1}]$, where λ is the transfer coefficient from the RT-air space to the environment, C_{env} is the radon concentration in the environment and $V_{RT\text{-}air}$ is the average volume of respiratory tract air space (Table 32.7).
TB = Trabecular bone; CB = cortical bone; Y-Marrow = yellow marrow; ST = stomach; SI = small intestine

5736

5737 32.1.3.3. Treatment of radioactive progeny

5738 (529) The treatment of radioactive progeny produced in systemic compartments after intake
5739 of a radioisotope of radon is described in Section 12.3.3.3. of *Publication 137* (ICRP, 2017).

5740 ## 32.2. Dosimetric data for radon

5741 ### 32.2.1. Effective dose coefficient from ingestion of radon gas

5742 (530) The effective dose coefficients for members of the public following ingestion of ^{222}Rn
5743 gas are given in
5744 (531) Table 32.6. Age-dependent effective dose coefficients following ingestion of radon
5745 (^{222Rn}) gas‡ (Sv Bq-1).

Effective dose coefficients following ingestion of ^{222Rn} gas (Sv Bq-1)					
Age					
3 months	1 y	5 y	10 y	15 y	Adult
4.0E-09	2.1E-09	1.2E-09	8.6E-10	7.5E-10	7.7E-10

‡Dose coefficients for ingestion of thoron gas are not given in this report due to its short half-life.

(532) The corresponding equivalent doses to organs per activity of ^{222}Rn ingested are given in the accompanying electronic annex. Dose coefficients for ingestion of ^{220}Rn gas are not given in this report due to its short half-life.

Table 32.6. Age-dependent effective dose coefficients following ingestion of radon (^{222}Rn) gas‡ (Sv Bq^{-1}).

Effective dose coefficients following ingestion of ^{222}Rn gas (Sv Bq^{-1})					
Age					
3 months	1 y	5 y	10 y	15 y	Adult
4.0E-09	2.1E-09	1.2E-09	8.6E-10	7.5E-10	7.7E-10

‡Dose coefficients for ingestion of thoron gas are not given in this report due to its short half-life.

32.2.2. Effective dose coefficients from inhalation of radon gas with its progeny and from inhalation of thoron progeny

(533) **Error! Reference source not found.** provides age-dependent effective doses for the inhalation of radon (^{222}Rn) in the home, expressed in units of mSv per Bq h m^{-3}, mSv per mJ h m-3, and mSv WLM^{-1}. Dose coefficients are given for (i) the inhalation of radon gas alone, (ii) inhalation of the airborne radon progeny and (iii) their sum (gas + progeny). The assumed aerosol parameter values for home exposures are given in Table 32.2. Calculations apply to reference members of the public at home with average breathing rates as given in Table 32.3. Further details of the calculations of doses from radon and radon progeny are given in Annex A of *Publication 137* (ICRP, 2017).

(534) In general, it is the inhalation of the airborne radon progeny rather than the inhalation of the radon gas that dominates the lung dose and the effective dose. The dose from inhaling ^{222}Rn gas is only a small fraction of the total effective dose: about 2% for adults at home assuming F=0.4. (Table 32.7).

(535) The effective dose per unit exposure to radon progeny is relatively insensitive to age (< 15%) because competing effects tend to cancel each other out. For example, children have lower breathing rates, so this decreases the intake and dose for a given activity air concentration. However, this is partly compensated by the smaller target tissue masses, which in turn increases the dose. Children have smaller airways which increase deposition by diffusion, but this is compensated in part by smaller residence times (i.e. higher respiratory frequencies) that decrease deposition by diffusion (Marsh and Birchall, 2000; National Research Council (NRC), 1991; United Nations Scientific Committee on the Effects of Atomic Radiation (UNSCEAR), 2020).

Table 32.7. Age-dependent effective doses per exposure to radon (^{222}Rn) gas, radon progeny and radon gas + progeny for homes.

Age	Effective dose per exposure*

	^{222}Rn gas		^{222}Rn progeny‡		Total (^{222}Rn gas + progeny)		
	mSv per Bq h m^{-3}	mSv per mJ h m^{-3} †	mSv per Bq h m^{-3} †	mSv per mJ h m^{-3}	mSv per Bq h m^{-3}	mSv per mJ h m^{-3}	mSv per WLM
3 mo	9.8E-08	4.4E-02	7.20E-06	3.24	7.3E-06	3.3	12
1 y	1.1E-07	4.9E-02	8.46E-06	3.81	8.6E-06	3.9	14
5 y	1.4E-07	6.3E-02	8.17E-06	3.67	8.3E-06	3.7	13
10 y	1.6E-07	7.3E-02	9.54E-06	4.29	9.7E-06	4.4	15
15 y	1.7E-07	7.7E-02	8.18E-06	3.68	8.4E-06	3.8	13
Adult	1.9E-07	8.5E-02	9.32E-06	4.19	9.5E-06	4.3	15

*For radon (^{222}Rn), 1 mJ h m^{-3} = (1.80 × 10^5/F) Bq h m^{-3} where the equilibrium factor, F=0.4; 1 WLM=3.54 mJ h m^{-3}.

‡The degree of precision of the values given is for computational purposes and does not reflect the certainty with which the central values are known.

† Value calculated assuming F=0.4.

(536) The age-dependent effective doses per exposure to radon (^{222}Rn) progeny as a function of the unattached fraction, f_p and the fraction of the attached PAEC associated with the nucleation mode, f_{pn} are given in the Annex C.

(537) Table 32.8 gives the age-dependent effective dose coefficients following inhalation of thoron (^{220}Rn) progeny in homes. The dose coefficients are expressed in units of mSv per WLM, mSv per mJ h m^{-3}, and mSv per Bq h m^{-3} of equilibrium equivalent concentration (EEC) of ^{220}Rn. The assumed aerosol parameter values for home exposures and the age-dependent breathing rates are given in Tables 32.2 and 32.3 respectively. For thoron, no reference F-value is recommended. This is because thoron gas activity concentrations in air vary significantly with position in a room due to its very short half-life (56 s), leading to a position-dependent relationship between thoron gas and its airborne progeny (ICRU, 2012).

Table 32.8. Age-dependent effective doses per exposure to thoron (^{220}Rn) progeny for homes.

Age	Effective dose per exposure* Thoron (^{220}Rn) progeny		
	nSv per Bq h m^{-3} of EEC	mSv per mJ h m^{-3}	mSv per WLM
3 mo	76	1.0	3.6
1 y	88	1.2	4.1
5 y	81	1.1	3.8
10 y	90	1.2	4.2
15 y	78	1.0	3.6
Adult	86	1.1	4.0

*For thoron (^{220}Rn), 1 WLM=4.68 × 10^4 Bq h m^{-3} of equilibrium equivalent concentration (EEC) of ^{220}Rn; 1 WLM=3.54 mJ h m^{-3}.

32.3. Use of dosimetric data for radon

(538) Protection of the public against radon in homes is based on measurement of radon gas, the application of reference levels and optimisation (ICRP, 2014). Nevertheless, in some circumstances, dose estimates are required in assessing public exposures and are also used in comparisons of sources of public exposure.

(539) The effective dose coefficient per unit exposure to radon gas and progeny can be derived either by dosimetric calculations or by epidemiological comparisons. The epidemiological approach gives values of 3.3 mSv per mJ h m^{-3} (12 mSv per WLM) for workers and 2.5 mSv per mJ h m^{-3} (9 mSv per WLM) for members of the public (ICRP, 2017). In comparison, effective dose coefficients calculated with ICRP reference biokinetic and

dosimetric models gives values of 3 to 4 mSv per mJ h m^{-3} (11 to 14 mSv WLM^{-1}) for workers in mines, sedentary indoor workers and exposures in homes (ICRP, 2017). These values are consistent with the recent review of radon epidemiology and dosimetry conducted by the United Nations Scientific Committee on the Effects of Atomic Radiation (Harrison, 2021; Marsh et al., 2021; United Nations Scientific Committee on the Effects of Atomic Radiation (UNSCEAR), 2020).

(540) The present situation shows good consistency between coefficients obtained by dosimetric calculations and conversion coefficients based on epidemiological comparisons. However, the underlying uncertainties in both approaches should be recognised.

(541) Taking account of both methods, *Publication 137* recommended for workers a single rounded value of 3 mSv per mJ h m^{-3} (approximately 10 mSv WLM^{-1}) to be used in most circumstances of occupational exposure, with no adjustment for aerosol characteristics. A second higher value of 6 mSv per mJ h m^{-3} (approximately 20 mSv per WLM) was referred to in ICRP Publication 137, for specific situations of indoor work involving substantial physical activity and for workers in tourist caves. However, this may be seen as an example of the need to use site-specific data for more realistic dose calculations when warranted. *Publication 137* provides additional dosimetric data for such calculations. ICRP recognises the difficulty in defining substantial physical activity for regulatory purposes and in most cases, it is not practical to distinguish between workers with medium and high physical activities.

(542) The dose coefficients given here for inhalation of radon by members of the public at different ages (Table 32.7) are quite similar to the *Publication 137* reference value (3 mSv per mJ h m^{-3}) for workers, with only small differences according to age at exposure. Taking account of all available data, the Commission recommends the use of the same effective dose coefficient for the inhalation of radon by members of the public in homes as for workers, that is 3 mSv per mJ h m^{-3} (approximately 10 mSv per WLM).

(543) In terms of measurements of ^{222}Rn gas exposure, the dose coefficient of 3 mSv per mJ h m^{-3} corresponds to 6.7×10^{-6} mSv per Bq h m^{-3}, assuming an equilibrium factor, F, of 0.4. With exposure parameters (F=0.4, occupancy of 7000 h y^{-1}), an annual average radon concentration at the upper reference level for homes of 300 Bq m^{-3} (*Publication 126*, ICRP, 2014) corresponds to an effective dose of 14 mSv.

(544) Dose coefficients for the inhalation of thoron progeny in homes also show only small differences according to age at exposure (Table 32.8). Based on these calculations, it is recommended that a rounded value of 1 mSv per mJ h m^{-3} (approximately 4 mSv WLM^{-1} or about 80 nSv per Bq h m^{-3} of EEC of ^{220}Rn) is used for indoor public exposures at all ages.

33. RADIUM (Z = 88)

33.1. Routes of Intake

33.1.1. Inhalation

(545) Several studies have been reported on the behaviour of inhaled radium in man following accidental intakes, especially of the sulphate, which was used in powder form in gamma-ray sources. However, it is difficult to estimate the contribution of absorption to lung clearance in such cases, because the systemic excretion of radium is predominantly by the faecal route. Information on absorption from the respiratory tract is available from experimental studies of radium as nitrate, or in fly ash. For details, see Section 13 of *Publication 137* (ICRP, 2017). Absorption parameter values and types, and associated f_A values for particulate forms of radium are given in Table 33.1. (taken from Section 13 of *Publication 137*).

Table 33.1. Absorption parameter values for inhaled and ingested radium.

		Absorption parameter values*		
Inhaled particulate materials		f_r	s_r (d^{-1})	s_s (d^{-1})
Default parameter values†,‡				
Absorption Type	Assigned forms			
F	Nitrate	1	10	–
M§	—	0.2	3	0.005
S	—	0.01	3	0.0001

Ingested materials¶	Age-dependent absorption from the alimentary tract, f_A					
Assigned forms	3 months	1 year	5 years	10 years	15 years	adult
All chemical forms	0.6	0.3	0.3	0.3	0.3	0.2

*It is assumed that for radium the bound state can be neglected, i.e. $f_b = 0.0$. The value of s_r for Type F forms of radium (10 d^{-1}) is element-specific. The values for Types M and S (3 d^{-1}) are the general default values.

†Materials (e.g. nitrate) are generally listed here where there is sufficient information to assign to a default absorption ype, but not to give specific parameter values (see Section 13 of *Publication 137*, ICRP, 2017).

‡For inhaled material deposited in the respiratory tract and subsequently cleared by particle transport to the alimentary tract, the default f_A values for inhaled materials are applied: i.e. the (rounded) product of f_r for the absorption type and the f_A value for ingested soluble forms of radium applicable to the age-group of interest (*e.g.* 0.2 for adults).

§Default Type M is recommended for use in the absence of specific information on which the exposure material can be assigned to an absorption type, e.g. if the form is unknown, or if the form is known but there is no information available on the absorption of that form from the respiratory tract.

¶Activity transferred from systemic compartments into segments of the alimentary tract is assumed to be subject to reabsorption to blood. The default absorption fraction f_A for the secreted activity is the highest value for ingestion of the radionuclide applicable to the age-group of interest (*e.g.* 0.2 for adults).

33.1.2. Ingestion

33.1.2.1. Adults

(546) Radium is a good chemical analogue of barium and calcium, Fasting and low calcium intake increase its absorption. Results from human ingestion studies of radium soluble salt or $^{224}RaSO_4$ in mock dial paint suggested fractional absorption in the order of 0.2-0.3 (For more

details, see Section 13 of *Publication 137*, ICRP, 2017). Data from balance studies reviewed by the ICRP Task Group on Alkaline Earth Metabolism in Adult Man (ICRP, 1973) indicated the fraction of radium absorbed from food or drinking water to be between 0.15 and 0.21 (Stehney and Lucas Jr, 1956). In *Publications 30* (ICRP, 1979), *67* (ICRP, 1993) and *137* (ICRP, 2017) an absorption fraction of 0.2 was recommended for all forms of radium. The same value of $f_A = 0.2$ is adopted here for adults.

33.1.2.2. Children

(547) There is considerable evidence of elevated gastrointestinal absorption of the alkaline earth elements by both laboratory animals and humans during periods of rapid growth, but there is relatively little radium-specific information. Results reported by Muth and Glöbe1 (1983) for ^{226}Ra in food, water and human bone suggest a much higher rate of transfer of ^{226}Ra from diet to bone during periods of rapid growth than during adulthood or periods of relatively slow growth during childhood. In a study of variation with age in absorption of alkaline earths from the gastrointestinal tract of the rat, Taylor et al. (1962) determined that absorption of radium averaged 79% in suckling rats, 11% in young adult rats and 3% in old rats. Similarly, data of Della Rosa et al. (1967) suggest considerably greater gastrointestinal absorption of radium in immature than in mature beagles. The available data for radium and other alkaline earth elements, mainly strontium, suggest that two controlling factors may be variation with age in gastrointestinal absorption and corresponding changes in deposition and retention in the skeleton. In the absence of more specific information, fractional absorptions of radium of 0.6 for the infant and 0.3 for ages 1-15 years were recommended *in Publication 67*. The same values are adopted here for f_A during childhood.

33.1.3. Systemic Distribution, Retention and Excretion

33.1.3.1. Summary of biokinetic data

(548) The alkaline earth element radium is a physiological analogue of the alkaline earths calcium, strontium, and barium but has somewhat different biokinetics from those elements due to discrimination by biological membranes and hydroxyapatite crystals of bone (ICRP, 1973; Leggett, 1992a). The biokinetics of radium resembles that of barium more closely than that of calcium or strontium.

(549) Data on the systemic behaviour of radium in adults are reviewed in *Publication 137* (ICRP, 2017). Briefly, the biokinetics of radium and its physiological analogues barium, strontium, and calcium has been studied extensively in adult human subjects with elevated intakes of radioisotopes of radium and in more detailed investigations involving laboratory animals, particularly dogs. Plasma disappearance curves indicate an outflow rate of several hundred plasma volumes per day and rapid equilibration with an extravascular pool roughly three times the size of the plasma pool. Based on controlled studies on adult human subjects it is estimated that about a third of radium atoms leaving blood deposit in excretion pathways, predominantly in the colon. Soft tissues initially accumulate a substantial portion of retained systemic radium but lose most of the accumulated activity within a few days. After intravenous administration of radium isotopes to adult dogs, soft tissues contained roughly 60% of retained activity at one hour, 30% at 1 d, and 12% at 7 d. In adult dogs, the liver and kidneys contained roughly one-third of soft-tissue radium from 7 to 1200 d after intravenous administration. Bone typically becomes the primary systemic repository of radium within the first day or two after acute uptake to blood. Skeletal retention of radium in mature adult humans is estimated to

decrease from about 25-30% of injected activity in the first day or two after injection to roughly 8% after 1 month and 3% after 1 year.

(550) Radium entering bone initially deposits on bone surface, from which activity is removed over a period of hours or days back to blood and to a lesser extent to a trabecular or cortical bone volume pool referred to as exchangeable bone volume. Activity entering this pool may return to bone surface or blood over a period of weeks or months or they may enter a non-exchangeable bone volume pool, i.e., they may become firmly fixed in bone crystals and retained there until removed by relatively slow bone restructuring processes. It appears that calcium, strontium, barium, and radium are all about equally likely to transfer from bone surface to exchangeable bone volume but that the likelihood of becoming firmly fixed in bone crystal decreases in the order calcium > strontium > barium > radium. Data from human and animal studies indicate that the rate of loss of alkaline earth tracers from bone over the first few months after acute uptake to blood increases in the order calcium < strontium < barium < radium. Presumably these four elements are removed from trabecular or cortical non-exchangeable bone volume compartments at the rate of bone restructuring of that bone type, so that the rate of transfer from non-exchangeable bone volume is independent of the element.

(551) Information is available on the systemic behaviour of radium in immature humans (ICRP, 1973; Keane and Schlenker, 1987; Muth and Glōbel, 1983; Parks et al., 1978; Parks and Keane, 1983). More detailed data on the age-specific behaviour of systemic radium are available for laboratory animals, particularly beagle dogs (Bruenger et al., 1983, 1989; Lloyd, Bruenger, Jones, et al., 1983; Lloyd, Bruenger, Mays, et al., 1983; Lloyd, C.W. Jones, Bruenger, Atherton, et al., 1983; Lloyd et al., 1982; Lloyd, G.N. Taylor, Jones and Mays, 1983; Lloyd, Mays and Atherton, 1976; Lloyd, Mays, Atherton, et al., 1976). Differences with age in the systemic behaviour of radium are consistent with findings for other alkaline earth elements. That is, retention of radium is greater in growing bone than in mature bone. Changes with age in uptake of radium by the skeleton are roughly proportional to the age-specific rate of calcium addition to bone from bone growth plus bone remodelling (Fig. 33.1). At times remote from exposure, skeletal burdens acquired during periods of growth tend to remain higher than those acquired by mature skeletons except for skeletal burdens acquired during or soon after infancy, when bone shows a particularly high rate of turnover. Both deposition and removal of radium appear to be greater in areas of bone undergoing rapid remodelling than in areas of relatively slow remodelling. Greater deposition of radium in the younger skeleton results in less systemic radium available for excretion and distribution to soft tissues.

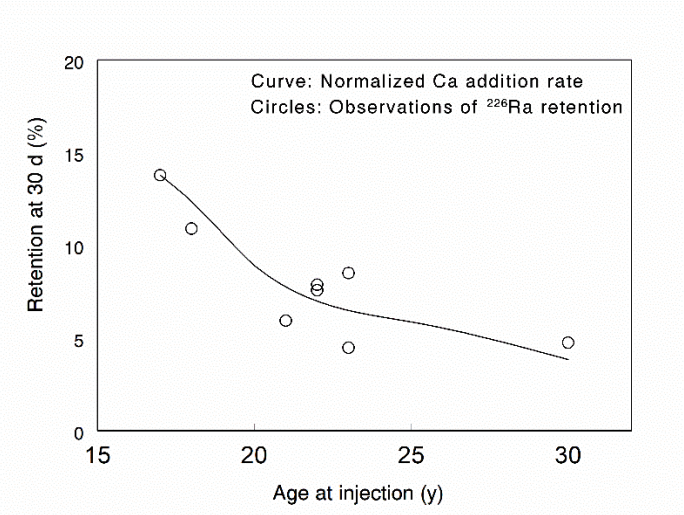

Fig. 33.1. Comparison of the rate of calcium addition to bone with observations of total-body retention of ^{226}Ra at 30 d after injection for different ages at injection. The calcium addition

rate is normalized to observed retention in a 17-year-old subject.

33.1.3.2. Systemic model

(552) The model for systemic radium applied in this report is a modification of the model adopted in *Publication 67* (ICRP, 1993). In the earlier version of the model the liver was represented as a single compartment, and the kidneys were not depicted explicitly but were included as part of Other soft tissues. In the present version of the model the kidneys are also depicted explicitly, and both the liver and kidneys are modelled as two compartments representing relatively fast and relatively slow loss of radium.

(553) The structure of the model for systemic radium is shown in Fig. 33.2. Transfer coefficients are listed in Table 33.2.

(554) Transfer coefficients for adults are the same as those applied to workers in *Publication 137* (ICRP, 2017). Extension of the model to preadult ages is based on results of studies of the age-specific behavior of radium in humans and laboratory animals, indicating that deposition of radium in bone is higher, and removal of radium from bone is faster, at preadult ages than in adults. The age-specific deposition fraction for bone, and the division of that deposition between trabecular and cortical bone surface, are based on the estimated rates of calcium addition to each of these bone types. For preadult ages the deposition fractions for soft tissues and excretion pathways are reduced uniformly from the values for adults to reflect the elevated competition from bone for circulating radium. The removal half-times from bone surface and exchangeable bone volume compartments are assumed to be independent of age. The removal half-times from bone volume compartments to blood are reference age-specific bone turnover rates (ICRP, 2002a). Removal half-times from soft-tissue compartments are assumed to be independent of age.

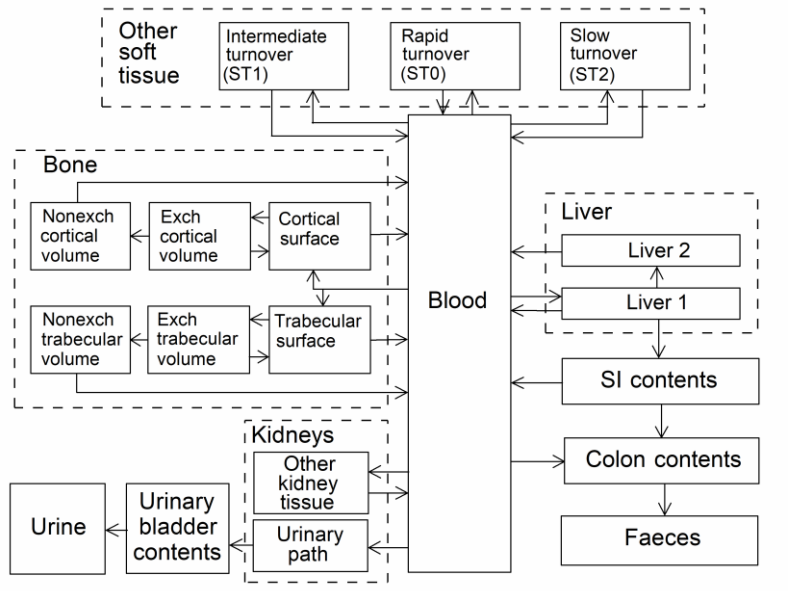

Fig. 33.2. Model for systemic radium used in this report. Activity transferred from Blood to Colon contents enters Right colon contents. SI = Small intestine.

5993 Table 33.2. Age-specific transfer coefficients for radium.

Path[a]	Transfer coefficient (d^{-1})					
	100 d	1 y	5 y	10 y	15 y	Adult
Blood to Urinary bladder contents	2.02E-01	4.44E-01	4.85E-01	3.56E-01	2.10E-01	6.06E-01
Blood to Right colon contents	7.26E+00	1.60E+01	1.74E+01	1.28E+01	7.55E+00	2.18E+01
Blood to Trab bone surface	1.05E+01	6.30E+00	6.23E+00	9.87E+00	1.44E+01	9.72E+00
Blood to Cort bone surface	4.20E+01	2.52E+01	2.18E+01	2.93E+01	3.74E+01	7.78E+00
Blood to ST0	6.98E+00	1.53E+01	1.67E+01	1.23E+01	7.26E+00	2.09E+01
Blood to ST1	1.17E+00	2.57E+00	2.80E+00	2.05E+00	1.21E+00	3.50E+00
Blood to ST2	2.33E-02	5.13E-02	5.60E-02	4.11E-02	2.43E-02	7.00E-02
Blood to Liver 1	1.40E+00	3.08E+00	3.36E+00	2.46E+00	1.46E+00	4.20E+00
Blood to Kidneys 1	4.67E-01	1.03E+00	1.12E+00	8.21E-01	4.85E-01	1.40E+00
Trab bone surf to Blood	5.78E-01	5.78E-01	5.78E-01	5.78E-01	5.78E-01	5.78E-01
Trab bone surf to Exch trab bone vol	1.16E-01	1.16E-01	1.16E-01	1.16E-01	1.16E-01	1.16E-01
Cort bone surf to Blood	5.78E-01	5.78E-01	5.78E-01	5.78E-01	5.78E-01	5.78E-01
Cort bone surf to Exch trab bone vol	1.16E-01	1.16E-01	1.16E-01	1.16E-01	1.16E-01	1.16E-01
ST0 to Blood	6.98E+00	6.98E+00	6.98E+00	6.98E+00	6.98E+00	6.98E+00
ST1 to Blood	6.93E-*01	6.93E-01	6.93E-01	6.93E-01	6.93E-01	6.93E-01
ST2 to Blood	3.80E-04	3.80E-04	3.80E-04	3.80E-04	3.80E-04	3.80E-04
Liver 1 to Blood	6.91E-01	6.91E-01	6.91E-01	6.91E-01	6.91E-01	6.91E-01
Liver 1 to Liver 2	2.08E-03	2.08E-03	2.08E-03	2.08E-03	2.08E-03	2.08E-03
Liver 2 to Blood	1.90E-03	1.90E-03	1.90E-03	1.90E-03	1.90E-03	1.90E-03
Kidneys 1 to Blood	2.07E+00	2.07E+00	2.07E+00	2.07E+00	2.07E+00	2.07E+00
Kidneys 1 to Kidneys 2	6.24E-03	6.24E-03	6.24E-03	6.24E-03	6.24E-03	6.24E-03
Kidneys 2 to Blood	1.90E-03	1.90E-03	1.90E-03	1.90E-03	1.90E-03	1.90E-03
Exch trab bone vol to Trab bone surface	1.85E-02	1.85E-02	1.85E-02	1.85E-02	1.85E-02	1.85E-02
Exch to Nonexch trab bone vol	4.60E-03	4.60E-03	4.60E-03	4.60E-03	4.60E-03	4.60E-03
Exch cort bone vol to Cort bone surface	1.85E-02	1.85E-02	1.85E-02	1.85E-02	1.85E-02	1.85E-02
Exch to Nonexch cort bone vol	4.60E-03	4.60E-03	4.60E-03	4.60E-03	4.60E-03	4.60E-03
Nonexch cort bone vol to Blood	8.22E-03	2.88E-03	1.53E-03	9.04E-04	5.21E-04	8.21E-05
Nonexch trab bone vol to Blood	8.22E-03	2.88E-03	1.81E-03	1.32E-03	9.59E-04	4.93E-04

5994 [a]Trab = Trabecular, Cort = cortical, vol = volume, Exch = Exchangeable, Nonexch = Nonexchangeable

33.2. Dosimetric data for radium

Table 33.3. Committed effective dose coefficients (Sv Bq^{-1}) for the inhalation or ingestion of ^{226}Ra compounds.

	Effective dose coefficients (Sv Bq^{-1})					
Inhaled particulate materials (1 µm AMAD aerosols)	3 mo	1 y	5 y	10 y	15 y	Adult
Type F, Nitrate	2.9E-06	8.8E-07	4.2E-07	4.2E-07	5.2E-07	1.5E-07
Type M, All unspecified forms	1.0E-05	8.3E-06	4.9E-06	3.2E-06	2.6E-06	2.3E-06
Type S	5.0E-05	4.9E-05	3.5E-05	2.6E-05	2.4E-05	2.4E-05
Ingested materials						
Adult f_A = 0.2, All forms	4.7E-06	9.5E-07	4.9E-07	5.0E-07	6.5E-07	1.3E-07

Table 33.4. Committed effective dose coefficients (Sv Bq^{-1}) for the inhalation or ingestion of ^{228}Ra compounds.

	Effective dose coefficients (Sv Bq^{-1})					
Inhaled particulate materials (1 µm AMAD aerosols)	3 mo	1 y	5 y	10 y	15 y	Adult
Type F, Nitrate	2.3E-05	5.5E-06	2.0E-06	2.0E-06	2.2E-06	3.7E-07
Type M, all unspecified forms	1.6E-05	1.1E-05	5.5E-06	3.6E-06	3.0E-06	2.0E-06
Type S	8.8E-05	8.8E-05	5.9E-05	4.1E-05	3.8E-05	4.0E-05
Ingested materials						
Adult f_A = 0.2, All forms	3.8E-05	6.2E-06	2.5E-06	2.5E-06	2.8E-06	3.4E-07

REFERENCES

Aarkrog, A., 1971. Prediction models for strontium-90 and caesium-137 levels in the human food chain. Health Phys. 20(3), 297–311.

Agnew, W.F., Cheng, J.T., 1971. Protein binding of tellurium-127m by maternal and fetal tissues of the rat. Toxicol. Appl. Pharmacol. 20(3), 346–356.

Alexander, F.W., Clayton, B.E., Delves, H.T., 1974. Mineral and trace-metal balances in children receiving normal and synthetic diets. QJM 43(1), 89–111.

Altman, P.L., Katz, D.D., 1961. Blood and other body fluids. In: Federation of American Societies for Experimental Biology, Washington, DC, .

Anbar, M., Guttmann, S., Rodan, G., et al., 1965. The determination of the rate of deiodination of thyroxine in human subjects. J. Clin. Invest. 44(12), 1986–1991.

Anderson, J.B., Comar, C.L., 1968. Strontium retention as a function of age in the dog. Radiat. Res. 34(1), 153–169.

Andersson, I., Nilsson, I., 1964. Exposure following ingestion of water containing radon-222. In: Assessment of Radioactivity in Man. Vol. II. Proceedings of the Symposium on the Assessment of Radioactive Body Burdens, IAEA, Vienna, Austria, pp. 317–326.

Apostoaei, A.I., Miller, L.F., 2004. Uncertainties in dose coefficients from ingestion of 131I, 137Cs, and 90Sr. Health Phys. 86(5), 460–482.

Apostoaei, A.I., Lewis, C.J., Hammonds, J.H., et al., 1998. Uncertainties in doses from ingestion of Cs-137, Sr-90, Co-60, Ru-106, and I-131. Health Phys. 74, S14.

Atherton, D.R., Stover, B.J., Mays, C.W., 1965. Soft tissue retention of 226Ra in the beagle. Health Phys. 11(2), 101–108.

Bahadori, A.A., Johnson, P., Jokisch, D.W., et al., 2011. Response functions for computing absorbed dose to skeletal tissues from neutron irradiation. Phys. Med. Biol. 56(21), 6873–6897.

Ballou, J.E., Thompson, R.C., 1961. Metabolism of zinc-65 in the rat consideration of permissible exposure limits. Health Phys. 6(1), 6–18.

Barnes, D.W.H., Cook, G.B., Harrison, G.E., et al., 1955. The metabolism of 132tellurium-iodine mixture in mammals. J. Nucl. Energy (1954) 1(2–4), 218–230.

Barry, P.S.I., 1973. A comparison of lead concentrations in human bones and in soft tissues. In: International Symposium on Environmental Health Aspects of Lead, Commission of the European Communities, Luxembourg, pp. 415–426.

Barry, P.S.I., 1975. A comparison of concentrations of lead in human tissues. Br. J. Ind. Med. 32(2). 119–139.

Barry, P.S.I., 1981. Concentrations of lead in the tissues of children. Br. J. Ind. Med. 38(1). 61–71.

Barton, J.C., Edwards, C.Q., 2000. Hemochromatosis: Genetics, Pathophysiology, Diagnosis and Treatment. Cambridge University Press, New York, USA.

Bauer, G.C., Carlsson, A. 1955. Metabolism of bone salt investigated by simultaneous administration of 45Ca and 32P to rats. J. Bone Joint Surg. Br. 37 B(4), 658–662.

Bauer, G.C., Carlsson, A., Lindquist, B., 1957. Metabolism of Ba140 in man. Acta. Orthop. Scand. 26(4), 241–254.

Bawden, J.W., Hammarström, L.E., 1977. Autoradiography of 65zinc in developing rat teeth and bones. Arch. Oral Biol. 22(7), 449-451,453-454.

Bedford, J., Harrison, G.E., Raymond, W.H.A., et al., 1960. The metabolism of strontium in children. Br. Med. J. 1(5173), 589–592.

Bennett, B.G., 1975. Strontium-90 in human bone - 1974 results for New York City and San Francisco. In: Health and Safety Laboratory, Environmental Quarterly, pp. I21–I23.

Bergman, B., Friberg, U., Lohmander, S., et al., 1972. The importance of zinc to cell proliferation in endochondral growth sites in the white rat. Eur. J. Oral Sci. 80(6), 486–492.

6048 Berkovski, V. 1999. Radioiodine biokinetics in the mother and the fetus. Part 1. Pregnant women. In:
6049 Radiation and Thyroid Cancer. Publication No. EUR 18552 EN. World Scientific Publishing,
6050 London, UK, pp. 319–325.
6051 Berkovski, V., Eckerman, K.F., Phipps, A.W., et al., 2003. Dosimetry of radioiodine for embryo and
6052 fetus. Radiat. Prot. Dosimetry 105(1–4), 265–268.
6053 Bhattacharyya, M.H., Breitenstein, B.D., Metivier, H., et al., 1992. Guidebook for the treatment of
6054 accidental internal radionuclide contamination of workers. Radiat. Prot. Dosimetry 41(1). 1–49.
6055 Bjorn-Rasmussen, E., Hallberg, L., Isaksson, B., et al., 1974. Food iron absorption in man. Applications
6056 of the two pool extrinsic tag method to measure heme and nonheme iron absorption from the whole
6057 diet. J. Clin. Invest. 53(1), 247–255.
6058 Blake, H.H., Henning, S.J., 1988. Absorption and transport of milk calcium by infant rats. Am. J.
6059 Physiol. Gastrointest. Liver Physiol. 254(1).
6060 Bolch, W.E., Farfan, E.B., Huh, C., et al., 2001. Influences of parameter uncertainties within the ICRP
6061 66 respiratory tract model: particle deposition. Health Phys. 81(4), 378–394.
6062 Bolch, W.E., Huston, T.E., Farfan, E.B., et al., 2003. Influences of parameter uncertainties within the
6063 ICRP-66 respiratory tract model: particle clearance. Health Phys. 4(4), 421–435.
6064 Bonner, J.F., 1948. The Influence of Age on the Uptake of Radioactive Phosphorus by the Skeleton.
6065 University of Rochester, Rochester, NY.
6066 Booker, D.V., Chamberlain, A.C., Newton, D., et al., 1969, Uptake of radioactive lead following
6067 inhalation and injection. Br. J. Radiol. 42(498), 457–466.
6068 Bothwell, T.H., Charlton, R.W., Cook, J.D., et al., 1979. Iron Metabolism in Man. Blackwell Scientific
6069 Publications, Oxford.
6070 Bronner, F., Harris, R.S., Maletskos, C.J., et al., 1956. Studies in calcium metabolism; the fate of
6071 intravenously injected radiocalcium in human beings. J. Clin. Invest. 35(1), 78–88.
6072 Brown, W.L., Hess, C.T., 1992. Measurement of the biotransfer and time constant of radon from
6073 ingested water by human breath analysis. Health Phys. 62(2), 162–170.
6074 Brozovic, B. 1975. Absorption of iron. In: McColl I and Sladen G (eds) Intestinal Absorption in Man.
6075 Academic Press, pp. 263–314.
6076 Bruenger, F.W., Smith, J.M., Atherton, D.R., et al., 1983. Skeletal retention and distribution of 226Ra
6077 and 239Pu in beagles injected at ages ranging from 2 days to 5 years. Health Phys. 44, 513–527.
6078 Bruenger, F.W., Lloyd, R.D., Miller, S.C., 1989. The influence of age at time of exposure on the
6079 distribution and retention of Ra-226 or Pu-239 in beagle dogs. Inhalation Toxicology Research
6080 Institute Annual Report 1988-1989, Inhalation Toxicology Research Institute, Albuquerque, New
6081 Mexico.
6082 Buijs, W.C., Corstens, F.H., Beentjes, L.B., 1985. Long-term retention of 207Bi in the human body
6083 after injection of 206Bi. Health Phys. 49(6), 1267–1269.
6084 Calhoun, N.R., Campbell, S.Jr., Smith, J.C.Jr., 1970. Accumulation of Labeled Zinc, Strontium, and
6085 Calcium in Bone Injuries. J. Dent. Res. 49(5), 1083–1085.
6086 Cantone, M.C., De Bartolo, D., Gambarini, G., et al., 1995. Proton activation analysis of stable isotopes
6087 for a molybdenum biokinetics study in humans. Med. Phys. 22(8), 1293–1298.
6088 Cantone, M.C., De Bartolo, D., Giussani, A., et al. 1997. A methodology for biokinetic studies using
6089 stable isotopes: Results of repeated molybdenum investigations on a healthy volunteer. Appl. Radiat.
6090 Isot. 48(3), 333–338.
6091 Cantone, M.C., Bartolo, D., Giussani, A., et al., 1997. Stable tracers for tracer kinetic investigations of
6092 molybdenum: intrinsic and extrinsic tagging. In: Fisher PWF, L'Abbé MR, Cockell KA, et al. (eds)
6093 Trace Elements in Man and Animals 9. NRC Research Press, Ottawa, pp. 267–269.
6094 Casey, H.W., Case, A.C., McClellan, R.O., et al., 1963. Metabolism of te132-I132 in lactating sheep.
6095 Health Phys. 9(12), 1223–1226.
6096 Chamberlain, A.C., Heard, M.J., Little, P., et al., 1978. Investigations into lead from motor vehicles.
6097 UK Atomic Energy Authority Report AERE-R 9198. HMSO, London, UK.
6098 Christensen, J.M., Poulsen, O.M., Thomsen, M., 1993. A short-term cross-over study on oral
6099 administration of soluble and insoluble cobalt compounds: sex differences in biological levels. Int.
6100 Arch. Occup. Environ. Health 65(4), 233–240.

6101 Ciofetta, G., Silverman, M., Hughes, J.M.B., 1980. Quantitative approach to the study of regional lung
6102 function in children using krypton 81m. Br. J. Radiol. 53(634), 950–959.
6103 Coenegracht, J.M., Dorleyn, M., 1961. The distribution of intravenously administered tracer doses of
6104 Bi-206 compounds in the human body. J. Belge. Radiol. 44, 485–504.
6105 Cohen, N., Eisenbud, M., Wrenn, M.E., 1970. The retention and distribution of lead-210 in the adult
6106 baboon. Progress report, Radioactivity studies. New York University Medical Center, New York,
6107 USA.
6108 Cohen, N., Fellman, A.L., Hickman, D.P., et al., 1989. Primate polonium metabolic models and their
6109 use in estimation of systemic radiation doses from bioassay data. Final report. EG and G Mound
6110 Applied Technologies, Miamisburg, OH (United States).
6111 Comar, C.L., Wentworth, R.A., Georgi, J.R., 1963. Thyroidal deposition in man, rat and dog of
6112 radioiodine from milk and non-milk sources. Health Phys. 9(12), 1249–1252.
6113 Conrad, M.E., Barton, J.C., 1978. Factors affecting the absorption and excretion of lead in the rat.
6114 Gastroenterology 74(4), 731–740.
6115 Coughtrey, P.J., Thorne, M.C., 1983. Radionuclide Distribution and Transport in Terrestrial and
6116 Aquatic Ecosystems: A Critical Review of Data. Volume 2. A. A. Balkema. Rotterdam.
6117 Cristy, M., 1980. Mathematical phantoms representing children of various ages for use in estimates of
6118 internal dose. Report ORNL/NUREG/TM-367. Oak Ridge National Laboratory.
6119 Cristy, M., Eckerman, K.F., 1987. Specific absorbed fractions of energy at various ages from internal
6120 photon sources. Report No. ORNL/TM-8381:Vol 1-7. Oak Ridge National Laboratory.
6121 Cristy, M., Leggett, R.W., 1986., Determination of metabolic data appropriate for HLW dosimetry.
6122 Volume II. Gastrointestinal absorption. Oak Ridge National Lab.
6123 Cuddihy, R.G., 1966. Thyroidal iodine-131 uptake, turnover and blocking in adults and adolescents.
6124 Health Phys. 12(8), 1021–1025.
6125 Cuddihy, R.G., Griffith, W.C., 1972. A biological model describing tissue distribution and whole-body
6126 retention of barium and lanthanum in beagle dogs after inhalation and Gavage. Health Phys. 23(5),
6127 621–633.
6128 Darby, W.J., Hahn, P.F., Kaser, M.M., et al., 1947. The absorption of radioactive iron by children 7-10
6129 years of age. J. Nutr. 33(1), 107–119.
6130 Decker, C.F., Kaspar, L.V., Norris, W.P., 1964. The variation of strontium metabolism with age in the
6131 dog. Radiat. Res. 23, 475–490.
6132 DellaRosa, R.J., Goldman, M., Andersen, A.C., et al., 1965. Absorption and retention of ingested
6133 strontium and calcium in beagles as a function of age. Nature 205(4967), 197–198.
6134 DellaRosa, R.J., Goldman, M., Wolf, H.G., 1967. Uptake and retention of orally administered Ra-226
6135 and Ba-133: A preliminary report. Report 472-114. University of California, Davis, California.
6136 DeMeio, R.H., Henriques Jr., F.C., 1947. Tellurium; excretion and distribution in tissues studied with
6137 a radioactive isotope. J. Biol. Chem. 169(3), 609–623.
6138 DeSilva, P.E., 1981. Determination of lead in plasma and studies on its relationship to lead in
6139 erythrocytes. Br. J. Ind. Med. 38(3), 209–217.
6140 Domanski, T., Trojanowska, B., 1980. Studies on metabolic kinetics of lead and alkaline earth elements
6141 (Ca, Ba). Acta Physiol. Pol. 31(4), 439–447.
6142 Domanski, T., Witkowska, D., Garlicka, I., 1980. Influence of age on the discrimination of barium in
6143 comparison with strontium during their incorporation into compact bone. Acta Physiol. Pol. 31(3),
6144 289–296.
6145 Dorrian, M-D., 1997. Particle size distributions of radioactive aerosols in the environment. Radiat. Prot.
6146 Dosim. 69(2), 117–132.
6147 Dorrian, M-D., Bailey, M.R., 1996. Particle size distributions of radioactive aerosols measured in the
6148 workplace and the environment. J. Aerosol Sci. 27(SUPPL.1), S439–S440.
6149 Dostal, L.A., Toverud, S.U., 1984. Effect of vitamin D3 on duodenal calcium absorption in vivo during
6150 early development. Am. J. Physiol. 246(5 Pt 1), G528-534.
6151 Dunning, D.E.Jr., Schwarz, G., 1981. Variability of human thyroid characteristics and estimates of dose
6152 from ingested 131I. Health Phys. 40(5), 661–675.
6153 Durbin, P.W., 1959. Metabolic characteristics within a chemical family. Health Phys. 2(3), 225–238.

6154 Dziewiatkowski, D.D., 1954. Effect of age on some aspects of sulfate metabolism in the rat. J. Exp.
6155 Med. 99(3), 283–298.
6156 Dziewiatkowski, D.I., 1952. Radioautographic studies of sulfate-sulfur (S35) metabolism in the
6157 articular cartilage and bone of suckling rats. J. Exp. Med. 95, 489–496.
6158 Eckerman, K.F., Westfall, R.J., Ryman, J.C., et al., 1994. Availability of nuclear decay data in electronic
6159 form, including beta spectra not previously published. Health Phys. 67(4), 338–345.
6160 Ehrenkranz, R.A., Ackerman, B.A., Nelli, C.M., et al., 1985. Absorption of calcium in premature infants
6161 as measured with a Stable isotope 46Ca extrinsic tag. Pediatr. Res. 19(2), 178–184.
6162 El-Hussein, A., Ahmed, A.A., Mohammed, A. 1998. Radiation dose to the human respiratory tract from
6163 inhalation of radon- 222 and its progeny. Appl. Radiat. Isot. 49(7), 783–790.
6164 Elian, E., Bar-Shani, S., Liberman, A., et al., 1966. Intestinal blood loss: A factor in calculations of
6165 body iron in late infancy. J. Pediatr. 69(2), 215–219.
6166 Ellis, K.J., Cohn, S.H., Susskind, H., et al., 1977. Kinetics of inhaled krypton in man. Health Phys 33(6),
6167 515–522.
6168 Ellsasser, J.C., Farnham, J.E., Marshall, J.H., 1969. Comparative kinetics and autoradiography of 45Ca
6169 and 133Ba in ten-year-old beagle dogs. The diffuse component distribution throughout the skeleton.
6170 J Bone Joint Surg Am 51(7), 1397–1412.
6171 Endo, A., Yamaguchi, Y., Eckerman, K.F., 2003. Development and assessment of a new radioactive
6172 decay database used for dosimetry calculation. Radiat. Prot. Dosim. 105(1–4), 565–569.
6173 Endo, A., Yamaguchi, Y., Eckerman, K.F., 2005. Nuclear Decay for Dosimetry Calculations: Revised
6174 Data of ICRP Publication 38. JAERI 1347. Japan Atomic Energy Research Institute. Available at:
6175 http://jolissrch-inter.tokai-sc.jaea.go.jp/pdfdata/JAERI-1347.pdf.
6176 Engel, R.W., Price, N.O., Miller, R.F., 1967. Copper, manganese, cobalt, and molybdenum balance in
6177 pre-adolescent girls. J. Nutr. 92(2), 197–204.
6178 Eridani, S., Balzarini, M., Taglioretti, D., et al., 1964. The distribution of radiobismuth in the rat. Brit.
6179 J. Radiol. 37, 311–314.
6180 Erlandson, M.E., Walden, B., Stern, G., et al., 1962. Studies on congenital hemolytic syndromes, IV.
6181 Gastrointestinal absorption of iron. Blood 19, 359–378.
6182 Evans, G.W., Johnson, P.E., 1980. Characterization and quantitation of a zinc- binding ligand in human
6183 milk. Pediatr. Res. 14(7), 876–880.
6184 Everson, J., Patterson, C.C., 1980. 'Ultra-clean' isotope dilution/mass spectrometric analyses for lead
6185 in human blood plasma indicate that most reported values are artificially high. Clin. Chem. 26(11),
6186 1603–1607.
6187 Farnham, J.E., Rowland, R.E., 1965. The retention of Ba-133 in beagles. ANL-7060, Radiological
6188 Physics Division Annual Report. Argonne National Laboratory, Argonne, IL.
6189 Fernau, A., Smereker, H., 1933. Concerning the remaining radioactive substance in organisms due to
6190 radon emanation. Strahlentherapie 46, 365–373.
6191 Fisher, D.A., Oddie, T.H., Burroughs, J.C., 1962. Thyroidal Radioiodine Uptake Rate Measurement in
6192 Infants. Am. J. Dis. Child. 103(6), 738–749.
6193 Fisher, D.A., Oddie, T.H., Wait, J.C., 1964. Thyroid Function Tests: Findings in Arkansas Children and
6194 Young Adults. Am. J. Dis. Child. 107(3), 282–287.
6195 Fisher, D.A., Oddie, T.H., Epperson, D. 1965. Effect of increased dietary iodide on thyroid
6196 accumulation and secretion in euthyroid Arkansas subjects. J. Clin. Endocrinol. Metab. 25(12),
6197 1580–1590.
6198 Fletcher, C.V., Acosta, E.P., Strykowski, J.M., 1994. Gender differences in human pharmacokinetics
6199 and pharmacodynamics. J. Adolesc. Health 15(8), 619–629.
6200 Flood, P.R., Schmidt, P.F., Wesenberg, G.R., et al., 1988. The distribution of lead in human hemopoietic
6201 tissue and spongy bone after lead poisoning and Ca-EDTA chelation therapy - Observations made
6202 by atomic absorption spectroscopy, laser microbeam mass analysis and electron microbeam X-ray
6203 analysis. Arch. Toxicol. 62(4), 295–300.
6204 Foreman, H., Moss, W., Eustler, B.C., 1958. Clinical experiences with radioactive materials. Am. J.
6205 Roentgenol. Radium Ther. Nucl. Med. 79(6), 1071–1079.
6206 Freiman, H.D., Tauber, S.A., Tulsky, E.G., 1963. Iron absorption in the healthy aged. Geriatrics 18,
6207 716–720.

6208 Fritsch, P., Moutairou, K., Lataillade, G., et al., 1988. Localization of Plutonium Retention in the Small
6209 Intestine of the Neonatal Rat, Guinea Pig, Baboon and Macaca after Pu-citrate Ingestion. Int. J.
6210 Radiat. Biol. 54(4), 537–543.
6211 Gaffney, G.W., Regerman, R.I., Shock, N.W., 1962. Relationship of age to the thyroidal accumulation,
6212 renal excretion and distribution of radioiodide in euthyroid man. J. Clin. Endocrinol. Metab. 22,
6213 784–794.
6214 Garby, L., Sjolin, S., 1959. Absorption of labelled iron in infants less than three months old. Acta
6215 Paediatr. Suppl. 48(Supp 117), 24–28.
6216 Garby, L., Sjoelin, S., Vuille, J.C., 1964. Studies on erythro-kinetics in infancy. IV. The long-term
6217 behaviour of radioiron in circulating foetal and adult haemoglobin, and its faecal exertion. Acta
6218 Paediatr. 53, 33–41.
6219 Gerber, G.B., Deroo, J. 1975. Absorption of radioactive lead (210Pb) by different parts of the intestine
6220 in young and adult rats. Environ Physiol Biochem. 5(5), 314–318.
6221 Gerber, G.B., VanHees, M., Garten, C.T., et al., 1989. Technetium absorption and turnover in
6222 monogastric and polygastric animals. Health Phys. 57(2), 315–319.
6223 Ghishan, F.K., Jenkins, J.T., Younoszai, M.K., 1980. Maturation of calcium transport in the rat small
6224 and large intestine. J. Nutr. 110(8), 1622–1628.
6225 Ghishan, F.K., Stroop, S., Meneely, R. 1982. The effect of lactose on the intestinal absorption of
6226 calcium and zinc in the rat during maturation. Pediatr. Res. 16(7), 566–568.
6227 Giussani, A., 2008. A recycling systemic model for the biokinetics of molybdenum radionuclides. Sci.
6228 Total Environ. 404(1), 44–55.
6229 Giussani, A., Roth, P., Werner, E., et al., 1998. A biokinetic model for molybdenum radionuclides: New
6230 experimental results. Radiat. Prot. Dosim. 79(1–4), 367–370.
6231 Giussani, A., Heinrichs, U., Roth, P., et al., 1998. Biokinetic studies in humans with stable isotopes as
6232 tracers. Part 1: A methodology for incorporation of trace metals into vegetables. Isot. Environ.
6233 Health Stud. 34(3), 291–296.
6234 Giussani, A., Arogunjo, A.M., Cantone, M.C., et al., 2006. Rates of intestinal absorption of
6235 molybdenum in humans. Appl. Radiat. Isot 64(6), 639–644.
6236 Giussani, A., Cantone, M.C., Höllriegl, V., et al., 2007. Modelling urinary excretion of molybdenum
6237 after oral and intravenous administration of stable tracers. Radiat. Prot. Dosim. 127(1–4), 136–139.
6238 Glad, B.W., Mays, C.W., Fisher, W., 1960. Strontium studies in beagles. Radiat. Res. 12, 672–681.
6239 Goo, H.W., 2013. Dual-energy lung perfusion and ventilation in children. Pediatr. Radiol 43: 298–307.
6240 Goodman, J.E., Prueitt, R.L., Thakali, S., et al., 2011. The nickel ion bioavailability model of the
6241 carcinogenic potential of nickel-containing substances in the lung. Crit. Rev. Toxicol. 41(2), 142–
6242 174.
6243 Gorten, M.K., Hepner, R., Workman, J.B., 1963. Iron metabolism in premature infants. I. Absorption
6244 and utilization of iron as measured by isotope studies. J. Pediatr. 63(6): 1063–1071.
6245 Gosink, T.A., Baskaran, M., Holleman, D.F., 1990. Radon in the human body from drinking water.
6246 Health Phys. 59(6), 919–924.
6247 Gran, F.C., 1960. Studies on calcium and strontium-90 metabolism in rats. Acta Physiol. Scand. Suppl.
6248 48(167): 1–109.
6249 Green, R., Charlton, R., Seftel, H., et al., 1968. Body iron excretion in man. A collaborative study. Am.
6250 J. Med. 45(3): 336–353.
6251 Gregerman, R.I., Gaffney, G.W., Shock, N.W., et al., 1962. Thyroxine turnover in euthyroid man with
6252 special reference to changes with age. J. Clin. Investig. 41: 2065–2074.
6253 Griffin, I.J., King, J.C., Abrams, S.A., 2000. Body weight-specific zinc compartmental masses in girls
6254 significantly exceed those reported in adults: A stable isotope study using a kinetic model. J Nutr
6255 130(10): 2607–2612.
6256 Gross, S.B., Pfitzer, E.A., Yeager, D.W., et al., 1975. Lead in human tissues. Toxicol. Appl. Pharmacol.
6257 32(3): 638–651.
6258 Guskova, A.K., Drutman, R.D., Malysheva, M.S., et al., 1964. The assessment of doses and the
6259 possibility of clinical recognition of the disease associated with 210Po affection. Med. Radiol. 9(8).
6260 Inst. of Industrial Sanitation and Occupational Diseases, Academy of Medical, USSR, 51–60.

6261 Haddad, H.M., 1960. Rates of 131I-labeled thyroxine metabolism in euthyroid children. J. Clin. Investig.
6262 39, 1590–1594.
6263 Halloran, B.P., DeLuca, H.F., 1980. Calcium transport in small intestine during early development:
6264 Role of vitamin D. Am. J. Physiol. Gastrointest. Liver Physiol. 2(6), G473–G479.
6265 Hardy, E., Rivera, J., Fisenne, I., et al., 1969. Comparative utilization of dietary radium-226 and other
6266 alkaline earths by pigs and sheep. In: Radiation biology of the fetal and juvenile mammal. Proc. (eds
6267 MR Sikov and DD Mahlam), US AEC, Division of Technical Information, Richland, Washington.
6268 Harley, J.H., 1966. Fallout Strontium 90 as a Metabolic Tracer. Arch. Environ. Health 12(5), 578–582.
6269 Harley, J.H., Jetter, E.S., Nelson, N., 1951. Elimination of radon from the body. Report No. 3. Reissued
6270 as Health and Safety Report, HASL-32 1958., U.S. Atomic Energy Commission, New York, USA.
6271 Harley, J.H., Jetter, E.S., Nelson, N., 1994. Elimination of radon from the body. Environ. Int. 20(5),
6272 573–584.
6273 Harrison, H.N., 1979. Pharmacology of sulfadiazine silver. Its attachment to burned human and rat skin
6274 and studies of gastrointestinal absorption and extension. Arch. Surg. 114, 281–285.
6275 Harrison, J., Leggett, R., Lloyd, D., et al., 2007, Polonium-210 as a poison. J. Radiol. Prot. 27(1), 17–
6276 40.
6277 Harrison, J.D., 2021. Lung cancer risk and effective dose coefficients for radon: UNSCEAR review and
6278 ICRP conclusions. J. Radiol. Prot. 41(2), 433–441.
6279 Harrison, J.D., Phipps, A., 2001. Invited editorial: Gut transfer and doses from environmental
6280 technetium. J. Radiol. Prot. 21(1), 9–11.
6281 Harrison, J.D., Haines, J.W., Popplewell, D.S., 1990. The gastrointestinal absorption and retention of
6282 niobium in adult and newborn Guinea pigs. Int. J. Radiat. Biol. 58(1), 177–186.
6283 Harrison, J.D., Leggett, R.W., Nosske, D., et al., 2001. Reliability of the ICRP's dose coefficients for
6284 members of the public, II. Uncertainties in the absorption of ingested radionuclides and the effect
6285 on dose estimates. Radiat. Prot. Dosim. 95(4), 295–308.
6286 Harrison, J.D., Khursheed, A., Lambert, B.E., 2002. Uncertainties in dose coefficients for intakes of
6287 tritiated water and organically bound forms of tritium by members of the public. Radiat. Prot. Dosim.
6288 98(3): 299–311.
6289 Haumont, S., 1961. Distribution of zinc in bone tissue. J. Histochem. Cytochem. 9, 141–145.
6290 Health Council of the Netherlands: Committee on Updating of Occupational Exposure Limits (2002)
6291 Tellurium and tellurium compounds (excluding TeF6). Health-based Reassessment of
6292 Administrative Occupational Exposure Limits 2000/15OSH/055. Health Council of the Netherlands,
6293 The Hague, Nederlands.
6294 Heard, M.J., Chamberlain, A.C., 1982. Effect of Minerals and Food on Uptake of Lead from the
6295 Gastrointestinal Tract in Humans. Hum. Exp. Toxicol. 1(4), 411–415.
6296 Heard, M.J., Chamberlain, A.C., 1984. Uptake of Pb by human skeleton and comparative metabolism
6297 of Pb and alkaline earth elements. Health Phys. 47(6), 857–865.
6298 Henrichs, K., Werner, E., Schmitt, A., 1984. Re-evaluation of radiation exposure due to administration
6299 of radioactive calcium-47. In: Proc. 6th Int. Congr. IRPA, pp. 458–461.
6300 Henrichs, K., Paretzke, H.G., Voigt, G., et al., 1989. Measurements of Cs absorption and retention in
6301 man. Health Phys. 57(4), 571–578.
6302 Herrmann, J., Heinen, E., Kröll, H.J., et al., 1981. Thyroid function and thyroid hormone metabolism
6303 in elderly people low T3-syndrome in old age? Klin. Wochenschr. 59(7), 315–323.
6304 Hill, C.R., 1965. Polonium-210 in man. Nature 208(5009), 423–428.
6305 Hillman, L.S., Tack, E., Covell, D.G., et al., 1988. Measurement of true calcium absorption in premature
6306 infants using intravenous 46Ca and oral 44Ca. Pediatr. Res. 23(6), 589–594.
6307 Hoag, M.S., Wallerstein, R.O., Pollycove, M., 1961. Occult blood loss in iron deficiency anemia of
6308 infancy. Pediatrics 27, 199–203.
6309 Hollins, J.G., 1969. The metabolism of tellurium in rats. Health Phys. 17(3), 497–505.
6310 Hong, Y.C., Yen, P.K-J., Shaw, J.H., 1968. An analysis of the growth of the cranial vault in rabbits by
6311 vital staining with lead acetate. Calcif. Tissue Int. 2(1), 271–285.
6312 Honstead, J.F., Brady, D.N., 1967. The uptake and retention of 32P and 65Zn from the consumption of
6313 columbia river fish. Health Phys. 13(5), 455–463.

6314 Hough, M., Johnson, P., Rajon, D., et al., 2011. An image-based skeletal dosimetry model for the ICRP
6315 reference adult male - Internal electron sources. Phys. Med. Biol. 56(8), 2309–2346.
6316 Hu, H., Milder, F.L., Burger, D.E., 1989. X-ray fluorescence: Issues surrounding the application of a
6317 new tool for measuring burden of lead. Environ. Res. 49(2), 295–317.
6318 Huet, C., Tymen, G., Boulaud, D., 2001. Size distribution, equilibrium ratio and unattached fraction of
6319 radon decay products under typical indoor domestic conditions. Sci. Total Environ. 272(1–3), 97–
6320 103.
6321 Hunt, G.J., 1998. Transfer across the human gut of environmental plutonium, americium, cobalt,
6322 caesium and technetium: Studies with cockles (Cerastoderma edule) from the Irish Sea. J. Radiol.
6323 Prot. 18(2), 101–109.
6324 Hunt, G.J., Allington, D.J., 1993. Absorption of environmental polonium-210 by the human gut. J.
6325 Radiol. Prot. 13(2), 119–126.
6326 Hursh, J.B., 1973. Retention of 210Pb in beagle dogs. Health Phys. 25(1), 29–35.
6327 Hursh, J.B., Mercer, T.T., 1970. Measurement of 212Pb loss rate from human lungs. J. Appl. Physiol.
6328 28(3), 268–274.
6329 Hursh, J.B., Suomela, J., 1968. Absorption of 212Pb from the gastrointestinal tract of man. Acta Oncol.
6330 7(2), 108–120.
6331 Hursh, J.B., Morken, D.A., Davis, T.P., et al., 1965. The fate of radon ingested by man. Health Phys.
6332 11(6), 465–476.
6333 Hursh, J.B., Schraub, A., Sattler, E.L., et al., 1969. Fate of 212Pb inhaled by human subjects. Health
6334 Phys. 16(3), 257–267.
6335 IAEA, 1996. Direct Methods for Measuring Radionuclides in the Human Body. Safety Series 114.
6336 International Atomic Energy Agency. Vienna.
6337 ICRP, 1973. Alkaline Earth Metabolism in Adult Man. ICRP Publication 20. Pergamon Press, Oxford.
6338 ICRP, 1975. Report of the Task Group on Reference Man. ICRP Publication 23. Pergamon Press,
6339 Oxford.
6340 ICRP, 1977. Recommendations of the ICRP. ICRP Publication 26. Ann. ICRP 1(3).
6341 ICRP, 1979. Limits for intakes of radionuclides by workers, ICRP Publication 30, Part 1. Ann. ICRP
6342 2(3/4).
6343 ICRP, 1980. Limits for intakes of radionuclides by workers. ICRP Publication 30, Part 2. Ann. ICRP
6344 4(3/4).
6345 ICRP, 1981. Limits for intakes of radionuclides by workers. ICRP Publication 30, Part 3. Ann. ICRP
6346 6(2/3).
6347 ICRP, 1983. Radionuclide Transformations - Energy and Intensity of Emissions. ICRP Publication 38.
6348 Ann. ICRP 11–13.
6349 ICRP, 1987. Radiation Dose to Patients from Radiopharmaceuticals. ICRP Publication 53. Ann. ICRP
6350 18(1–4).
6351 ICRP, 1988. Limits for intakes of radionuclides by workers: an addendum. ICRP Publication 30, Part
6352 4. Ann. ICRP 19(4).
6353 ICRP, 1989. Individual Monitoring for Intakes of Radionuclides by Workers. ICRP Publication 54. Ann.
6354 ICRP 19(1–3).
6355 ICRP, 1990. Age-dependent Doses to Members of the Public from Intake of Radionuclides - Part 1.
6356 ICRP Publication 56. Ann. ICRP 20(2).
6357 ICRP, 1991. 1990 Recommendations of the International Commission on Radiological Protection.
6358 ICRP Publication 60. Ann. ICRP 21(1–3).
6359 ICRP, 1993. Age dependent doses to members of the public from intake of radionuclides: Part 2,
6360 Ingestion dose coefficients. ICRP Publication 67. Ann. ICRP 23(3/4).
6361 ICRP, 1994a. Dose coefficients for intake of radionuclides by workers. ICRP Publication 68. Ann.
6362 ICRP 24(4).
6363 ICRP, 1994b. Human respiratory tract model for radiological protection. ICRP Publication 66. Ann.
6364 ICRP 24(1–3).
6365 ICRP, 1995a. Age-dependent Doses to Members of the Public from Intake of Radionuclides: Part 3.
6366 Ingestion Dose Coefficients, ICRP Publication 69. Ann. ICRP 25(1).

ICRP, 1995b. Age-dependent Doses to Members of the Public from Intake of Radionuclides: Part 4. Inhalation Dose Coefficients, ICRP Publication 71. Ann. ICRP 25(3/4).
ICRP, 1995c. Age-dependent Doses to the Members of the Public from Intake of Radionuclides - Part 5 Compilation of Ingestion and Inhalation Coefficients. ICRP Publication 72. Ann. ICRP 26(1).
ICRP, 1995d. Basic anatomical and physiological data: The skeleton. ICRP Publication 70. Ann. ICRP 25.
ICRP, 1996. Conversion Coefficients for use in Radiological Protection against External Radiation. ICRP Publication 74. Ann. ICRP 26(3–4).
ICRP, 1997. Individual monitoring for internal exposure of workers. ICRP Publication 78. Ann. ICRP 27(3/4).
ICRP, 2001. Doses to the Embryo and Fetus from Intakes of Radionuclides by the Mother. ICRP Publication 88. Ann. ICRP 31(1–3).
ICRP, 2002a. Basic anatomical and physiological data for use in radiological protection: reference values. ICRP Publication 89. Ann. ICRP 32(3–4).
ICRP, 2002b. Guide for the practical application of the ICRP Human Respiratory Tract Model. Supporting Guidance 3. Ann. ICRP 32(1/2).
ICRP, 2004. Doses to Infants from Ingestion of Radionuclides in Mothers' Milk. ICRP Publication 95. Ann. ICRP 34(3–4).
ICRP, 2006. Human alimentary tract model for radiological protection. ICRP Publication 100. Ann. ICRP 36(1–2). Pergamon Press, Oxford.
ICRP, 2007. The 2007 Recommendations of the International Commission on Radiological Protection. ICRP Publication 103. Ann. ICRP 37(2–4).
ICRP, 2008. Nuclear Decay Data for Dosimetric Calculations. ICRP Publication 107. Ann. ICRP 38(3).
ICRP, 2009. Adult reference computational phantoms. ICRP Publication 110. Ann. ICRP 39(2).
ICRP, 2010a. Conversion Coefficients for Radiological Protection Quantities for External Radiation Exposures. ICRP Publication 116. Ann. ICRP 40(2–5).
ICRP, 2010b. Lung Cancer Risk from Radon and Progeny and Statement on Radon. ICRP Publication 115. Ann. ICRP 40(1).
ICRP, 2014. Radiological Protection against Radon Exposure. ICRP Publication 126. Ann. ICRP 43(3).
ICRP, 2015. Occupational Intakes of Radionuclides: Part 1. ICRP Publication 130. Ann. ICRP 44(2).
ICRP, 2016a. Occupational intakes of radionuclides: Part 2. ICRP Publication 134. Ann. ICRP 45(3/4).
ICRP, 2016b. The ICRP computational framework for internal dose assessment for reference adults: specific absorbed fractions. ICRP Publication 133. Ann. ICRP 45(2).
ICRP, 2017. Occupational intakes of radionuclides: Part 3. ICRP Publication 137. Ann. ICRP 46(3/4).
ICRP, 2019. Occupational Intakes of Radionuclides: Part 4. ICRP Publication 141. Ann. ICRP 48(2/3).
ICRP, 2020. Paediatric Computational Reference Phantoms. ICRP Publication 143. Ann. ICRP 49(1).
ICRP, 2022. Occupational Intakes of Radionuclides: Part 5. ICRP Publication 151. Ann. ICRP 51(1-2).
ICRU, 2012. Measurement and reporting of radon exposures. J. ICRU 12(2): 1–191.
Inaba, J., Nishimura, Y., Kimura, K-I., et al., 1982. Whole-body retention and tissue distribution of 60Co in rats after oral administration of freshwater fish contaminated with 60Co. Health Phys. 43(2), 247–250.
Inaba, J., Nishimura, Y., Ichikawa, R., 1984. Effect of age on the metabolism of some important radionuclides in the rat. In: Radiation Risk Protection (eds A Kaul, R Neider, J Pensko, et al.), Fachverband fur Strahlenschutz e V, Berlin pp. 481–484.
Inaba, J., Nishimura, Y., Ichikawa, R., 1984. Studies on the metabolism of antimony-125 in the rat. NIRS-N-49. National Institute of Radiological Sciences, Chiba, Japan.
Institute of Medicine, 1997. Dietary Reference Intakes for Calcium, Phosphorus, Magnesium, Vitamin D, and Fluoride. The National Academies Press, Washington, DC.
Ishihara, N., Matsushiro, T., 1986. Biliary and urinary excretion of metals in humans. Arch. Environ. Health 41(5), 324–330.
Jackson, S., Dolphin, G.W., 1966. The estimation of internal radiation dose from metabolic and urinary excretion data for a number of important radionuclides. Health Phys. 12(4), 481–500.

6419 Johnson, P.B., Bahadori, A.A., Eckerman, K.F., et al., 2011. Response functions for computing
6420 absorbed dose to skeletal tissues from photon irradiation - An update. Phys. Med. Biol. 56(8), 2347–
6421 2365.
6422 Jokisch, D.W., Rajon, D.A., Bahadori, A.A., et al., 2011. An image-based skeletal model for the ICRP
6423 reference adult male - Specific absorbed fractions for neutron-generated recoil protons. Phys. Med.
6424 Biol. 56(21), 6857–6872.
6425 Jokisch, D.W., Rajon, D.A., Patton, P.W., et al., 2011. Methods for the inclusion of shallow marrow
6426 and adipose tissue in pathlength-based skeletal dosimetry. Phys. Med. Biol. 56(9), 2699–2713.
6427 Jugo, S., Maljković, T., Kostial, K., 1975. Influence of chelating agents on the gastrointestinal
6428 absorption of lead. Toxicol. Appl. Pharmacol. 34(2), 259–263.
6429 Jugo, S., Markovic, Z., Padovan, I., 1980. Wound-healing in lead-poisoned rats. Periodicum
6430 biologorum 82(3). HRVATSKO PRIRODOSLOVNO DRUSTVO ILICA 16/111, ZAGREB,
6431 CROATIA, 303–305.
6432 Kallfelz, F.A., Wentworth, R.A., 1969. Evaluation of bone calcium accretion rate as a function of age
6433 in beagle dogs. J. Nutr. 99(4), 459–464.
6434 Kalmykov, L.Z., Kruichitskaia, K.I., Stratienko, V.V., et al., 1969. Regularities of Po-310 elimination
6435 from the human organism. Med. Radiol. 14(12), 26–30.
6436 Karhausen, L., 1974. Iodine metabolism in children and adolescents in an area of the community. CEA-
6437 tr-7481. CEA Centre d'Etudes Nucleaires de Grenoble, Grenoble, France.
6438 Kauranen, P., Miettinen, J.K., 1967. 210Po and 210Pb in environmental samples in Finland. In:
6439 Radioecological concentration processes (eds B Aberg and FP Hungate), Pergamon Press, Oxford,
6440 pp. 275–280.
6441 Kawrakow, I., Mainegra-Hing, E., Rogers, D.W.O., et al., 2006. The EGSnrc code system: Monte Carlo
6442 simulation of electron and photon transport. NRCC Report PIRS-701. National Research Council of
6443 Canada, Ottawa (ON).
6444 Keane, A.T., Schlenker, R.A., 1987. Long-term loss of radium in 63 subjects first exposed at ages 6 to
6445 46. In: Age-related Factors in Radionuclide Metabolism and Dosimetry, Martinus Nijhoff Publishers,
6446 Dordrecht, pp. 127–135.
6447 Keller, C.A., Doherty, R.A., 1980. Distribution and excretion of lead in young and adult female mice.
6448 Environ. Res. 21(1), 217–228.
6449 Kello, D., Kostial, K., 1978. Lead and cadmium in hair as an indicator of body burden in rats of different
6450 age. Bull. Environ. Contam. Toxicol. 20(1), 618–623.
6451 Kereiakes, J.G., Wellman, H.N., Saenger, E.L., 1968. Radiation exposure from radiopharmaceuticals
6452 in children. In: Proceedings of the First International Congress of Radiation Protection, Elsevier, pp.
6453 775–781.
6454 Kneip, T.J., Mallon, R.P., Harley, N.H., 1983. Biokinetic modelling for mammalian lead metabolism.
6455 Neurotoxicology 4(3), 189–192.
6456 Kostial, K., Maljković, T., Jugo, S., 1974. Lead acetate toxicity in rats in relation to age and sex. Arch.
6457 Toxicol. 31(3), 265–269.
6458 Kostial, K., Kello, D., Jugo, S., et al., 1978. Influence of age on metal metabolism and toxicity. Environ.
6459 Health Perspect 25, 81–86.
6460 Kramer, R., Zankl, M., Williams, G., et al., 1982. The Calculation of Dose from External Photon
6461 Exposures using Reference Human Phantoms and Monte Carlo Methods: Part I. The Male (Adam)
6462 and Female (Eva) Adult Mathematical Phantoms. GSF Report S-885. GSF-National Research for
6463 Environment and Health, Neuherberg, Germany.
6464 Kranrod, C., Tokonami, S., Ishikawa, T., et al., 2009. Mitigation of the effective dose of radon decay
6465 products through the use of an air cleaner in a dwelling in Okinawa, Japan. Appl. Radiat. Isot 67(6),
6466 1127–1132.
6467 Kron, T., Hansen, C., Werner, E., 1991. Renal excretion of tellurium after peroral administration of
6468 tellurium in different forms to healthy human volunteers. J. Trace Elem. Med. Biol. 5(4), 239–244.
6469 Kulp, J.L., Schulert, A.R., 1962. Strontium-90 in man V. Science 136(3516), 619–632.
6470 Kyere, K., Oldroyd, B., Oxby, C.B., et al., 1982. The feasibility of measuring total body carbon by
6471 counting neutron inelastic scatter gamma rays. Phys. Med. Biol. 27(6), 805–817.

6472 Lacroix, P., 1960. Ca-45 autoradiography in the study of bone tissue. In: Rodahl K, Nicolson JT, and
6473 Brown EM (eds) Bone as a Tissue. McGraw-Hill. New York, USA, pp. 262–79.
6474 Ladinskaya, L.A., Parfenov, Y.D., Popov, D.K., et al., 1973. 210Pb and 210Po content in air, water,
6475 foodstuffs, and the human body. Arch. Environ. Health 27(4). 254–258.
6476 Layrisse, M., Martinez-Torres, C., 1971. Food iron absorption: iron supplementation of food. Prog.
6477 Hematol. 7, 137.
6478 Layrisse, M., Martínez-Torres, C., 1972. Model for measuring dietary absorption of heme iron: test with
6479 a complete meal. Am. J. Clin. Nutr. 25(4), 401–411.
6480 Lebedev, O.V., Yakovlev, V.A., 1993. The correlation between 137 Cs half-time and age, body mass
6481 and height in individuals contaminated from the Chernobyl accident. In: Merwin SE and Balonov
6482 MI (eds) The Chernobyl Papers. Volume 1. Doses to the Soviet Population and Early Health Effects
6483 Studies, pp. 219–243.
6484 Lee, C., Lodwick, D., Hasenauer, D., et al., 2007. Hybrid computational phantoms of the male and
6485 female newborn patient: NURBS-based whole-body models. Phys. Med. Biol. 52(12), 3309–3333.
6486 Lee, C., Lodwick, D., Hurtado, J., et al., 2010. The UF family of reference hybrid phantoms for
6487 computational radiation dosimetry. Phys. Med. Biol. 55(2), 339–363.
6488 Lee, W.R., Marshall, J.H., Sissons, H.A., 1965. Calcium accretion and bone formation in dogs: an
6489 experimental. J. Bone Joint Surg. Br. 47, 157–180.
6490 Leggett, R., Harrison, J., Phipps, A., 2007. Reliability of the ICRP'S dose coefficients for members of
6491 the public: IV. basis of the human alimentary tract model and uncertainties in model predictions.
6492 Radiat. Prot. Dosim. 123(2): 156–170.
6493 Leggett, R.W., 1986. Predicting the retention of Cs in individuals. Health Phys. 50(6), 747–759.
6494 Leggett, R.W., 1992a. A generic age-specific biokinetic model for calcium-like elements. Radiat. Prot.
6495 Dosim. 41(2–4), 183–198.
6496 Leggett, R.W., 1992b. Fractional absorption of ingested barium in adult humans. Health Phys. 62(6),
6497 556–561.
6498 Leggett, R.W., 1993. Research advances: An age-specific kinetic model of lead metabolism in humans.
6499 Environ. Health Perspect. 101(7), 598–616.
6500 Leggett, R.W., 2001. Reliability of the ICRP's dose coefficients for members of the public. 1. Sources
6501 of uncertainty in the biokinetic models. Radiat. Prot. Dosim. 95(3), 199–213.
6502 Leggett, R.W., 2010. A physiological systems model for iodine for use in radiation protection. Radiat.
6503 Res. 174(4), 496–516.
6504 Leggett, R.W., Eckerman, K.F., 2001. A systemic biokinetic model for polonium. Sci. Total Environ.
6505 275(1–3), 109–125.
6506 Leggett, R.W., Eckerman, K.F., Williams, L.R., 1982. Strontium-90 in bone: A case study in age
6507 dependent dosimetric modeling. Health Phys. 43(3), 307–322.
6508 Leggett, R.W., Dunning, D.E., Eckerman, K.F., 1984. Modelling the behaviour of chains of
6509 radionuclides inside the body. Radiat. Prot. Dosim. 9(2), 77–91.
6510 Leggett, R.W., Bouville, A., Eckerman, K.F., 1998. Reliability of the ICRP's systemic biokinetic
6511 models. Radiat. Prot. Dosim. 79(1–4), 335–342.
6512 Leggett, R.W., Barton, J.C., Eckerman, K.F., 2000. Mathematical models of metal metabolism in
6513 hemochromatosis. In: Edwards CQ (ed.) Hemochromatosis: Genetics, Pathophysiology, Diagnosis
6514 and Treatment. Cambridge University Press, New York, USA.
6515 Leggett, R.W., Williams, L.R., Melo, D.R., et al., 2003. A physiologically based biokinetic model for
6516 cesium in the human body. Sci. Total Environ. 317, 235–255.
6517 Leggett, R.W., Eckerman, K.F., Meck, R.A., 2008. Reliability of current biokinetic and dosimetric
6518 models for radionuclides: a pilot study. ORNL/TM-2008/131. Oak Ridge National Laboratory, Oak
6519 Ridge, TN.
6520 Leide-Svegborn, S., Stenström, K., Olofsson, M., et al., 1999. Biokinetics and radiation doses for
6521 carbon-14 urea in adults and children undergoing the Helicobacter pylori breath test. Eur. J. Nucl.
6522 26(6), 573–580.
6523 Li, W., Hopke, P.K., 1993. Initial size distributions and hygroscopicity of indoor combustion aerosol
6524 particles. Aerosol. Sci. Technol. 19(3), 305–316.

Li, W.B., Klein, W., Blanchardon, E., et al., 2014. Parameter uncertaintyanalysis of a biokinetic model of caesium. Radiat. Prot. Dosim. 163(1), 37–57.
Likhtarev, I., Minenko, V., Khrouch, V., et al., 2003. Uncertainties in thyroid dose reconstruction after Chernobyl. Radiat. Prot. Dosim. 105(1–4), 601–608.
Likhtarev, I.A., Dobroskok, I.A., Ilyin, L.A., et al., 1975. A study of certain characteristics of strontium metabolism in a homogeneous group of human subjects. Health Phys. 28(1), 49–60.
Lindh, U., Brune, D., Nordberg, G., 1978. Microprobe analysis of lead in human femur by proton induced X-ray emission (PIXE). Sci. Total Environ. The 10(1), 31–37.
Liu, Y-M., Neal, P., Ernst, J., et al., 1989. Absorption of calcium and magnesium from fortified human milk by very low birth weight infants. Pediatr. Res. 25(5), 496–502.
Liu-Sheng, H., Xiao-Shan, Y., De-Chang, W., 1991. Age-dependent variation of zinc-65 metabolism in LACA mice. Int. J. Radiat. Biol. 60(6), 907–916.
Lloyd, R.D., Zundel, W.S., Mays, C.W., et al., 1966. Enhanced Cs-137 elimination in pregnant and dystrophic humans. Radiat. Res. 27(548).
Lloyd, R.D., Mays, C.W., McFarland, S.S., et al., 1973. Metabolism of Rb-83 and Cs-137 in persons with muscle disease. Radiat. Res. 54(3), 463–478.
Lloyd, R.D., Mays, C.W., Atherton, D.R., et al., 1975. 210Pb studies in beagles. Health Phys. 28(5), 575–583.
Lloyd, R.D., Mays, C.W., Atherton, D.R., 1976. Distribution of injected 226Ra and 90Sr in the beagle skeleton. Health Phys. 30(2), 183–189.
Lloyd, R.D., Mays, C.W., Atherton, D.R., et al., 1976. Retention and skeletal dosimetry of injected 226Ra, 228Ra, and 90Sr in beagles. Radiat. Res. 66(2), 274–287.
Lloyd, R.D., Mays, C.W., Taylor, G.N., et al., 1982. Radium-224 retention, distribution, and dosimetry in beagles. Radiat. Res. 92(2), 280–295.
Lloyd, R.D., Jones, C.W., Bruenger, F.W., et al., 1983. Radium retention and dosimetry in juvenile beagles. Radiat. Res. 94(2), 295–304.
Lloyd, R.D., Taylor, G.N., Jones, C.W., et al., 1983 Radium retention and dosimetry in the St. Bernard. Radiat. Res. 95(1), 150–157.
Lloyd, R.D., Bruenger, F.W., Jones, C.W., et al., 1983. Radium retention in mature beagles injected at 5 years of age. Radiat. Res. 94(1), 210–216.
Lloyd, R.D., Bruenger, F.W., Mays, C.W., et al., 1983 Skeletal radon-to-radium ratios in neonatal, juvenile and mature beagles and in adult St. Bernards. Health Phys. 44(1), 61–63.
Lowe, N.M., Shames, D.M., Woodhouse, L.R., et al., 1997. A compartmental model of zinc metabolism in healthy women using oral and intravenous stable isotope tracers. Am. J. Clin. Nutr. 65(6), 1810–1819.
MacDonald, N.S., Ezmirlian, F., Spain, P., et al., 1951. The ultimate site of skeletal deposition of strontium and lead. J. Biol. Chem. 189(1), 387–399.
MacDonald, N.S., Nusbaum, R.E., Alexander, G.V., et al., 1952. The skeletal deposition of yttrium. J. Biol. Chem. 195(2), 837–841.
Macdonald, N.S., Figueroa, W.G., Urist, M.R., 1965. Short-term retention of strontium-85 and estimation of initial strontium-90 burdens in humans. Health Phys. 11(11), 1187–1194.
Majle, T., Gorzkowski, B., Sobociński, L., 1991. The role of individual segments of the gastrointestinal tract in the elimination of cesium radioisotopes. Rocz. Panstw. Zakl. Hig. 42(1), 51–54.
Manton, W.I., Cook, J.D., 1984. High accuracy (stable isotope dilution) measurements of lead in serum and cerebrospinal fluid. Br. J. Ind. Med. 41(3), 313–319.
Mariotti, S., Franceschi, C., Cossarizza, A., et al., 1995. The aging thyroid. Endocr. Rev. 16(6), 686–715.
Marsh, J.W., Bailey, M.R., 2013. A review of lung-to-blood absorption rates for radon progeny. Radiat. Prot. Dosim. 157(4), 499–514.
Marsh, J.W., Birchall, A., 2000. Sensitivity analysis of the weighted equivalent lung dose per unit exposure from radon progeny. Radiat. Prot. Dosim. 87(3), 167–178.
Marsh, J.W., Birchallt, A., Butterweck, G., et al., 2002. Uncertainty analysis of the weighted equivalent lung dose per unit exposure to radon progeny in the home. Radiat. Prot. Dosim. 102(3), 229–248.

6578 Marsh, J.W., Birchall, A., Davis, K., 2005. Comparative dosimetry in homes and mines: estimation of
6579 K-factors. Radioactivity in the Environment 7(C), 290–298.
6580 Marsh, J.W., Tomášek, L., Laurier, D., et al., 2021. Effective dose coefficients for radon and progeny:
6581 A review of ICRP and UNSCEAR values. Radiat. Prot. Dosim. 195(1), 1–20.
6582 Martinez-Torres, C., Layrisse, M., 1973. Nutritional factors in iron deficiency: food iron absorption. In:
6583 Callender ST (ed.) Clinics in Haematology. 2nd ed., WB Saunders and Co., London, pp. 339–352.
6584 Marx, J.J.M., 1979. Normal iron absorption and decreased red cell iron uptake in the aged. Blood 53(2),
6585 204–211.
6586 Matsusaka, N., Inaba, J., Ichikawa, R., et al., 1969. Some special features of nuclide metabolism in
6587 juvenile mammals. In: Sikov MR and Mahlam DD (eds) Radiobiology of the Fetal and Juvenile
6588 Mammal. Oak Ridge, USAEC, Division of Technical Information Extension, TN, USA, pp. 217–
6589 226.
6590 Matthews, C.M., Dempster, W.J., Kapros, C., et al., 1964. The effect of bismuth 206 irradiation on
6591 survival of skin homografts. Brit. J. Radiol. 37, 306–310.
6592 McCraw, T.F., 1965. The half-time of cesium 137 in man. Radiol. Health Data Rep. 6(12), 711–718.
6593 McElligott, T.F., Collins, D.H., 1960. Chondrocyte function of human articular and costal cartilage
6594 compared by measuring the in vitro uptake of labelled (35S) sulphate. Ann. Rheum. Dis. 19(1). 31.
6595 McInroy, J.F., Watters, R.L., Johnson, J.E., 1972. Polonium-210 absorption in rats: Effects of biological
6596 modification. Nature New Biol. 236(65), 118–120.
6597 Medovar, B., 1976. Characteristics of the label incorporation from 2-14C-glycine into the tissues of
6598 animals of differing ages. Ukr Biokhim Zh 48(5), 572.
6599 Melo, D.R., Lipsztein, J.L., Oliveira, C.A., et al., 1997. A biokinetic model for 137Cs. Health Phys.
6600 73(2), 320–332.
6601 Meyer, S., 1937. Physical foundations of radon cures. Strahlentherapie 58, 656–663.
6602 Miller, J.Z., Smith, D.L., Flora, L., et al., 1989. Calcium absorption in children estimated from single
6603 and double stable calcium isotope techniques. Clin. Chim. Acta 183(2), 107–113.
6604 Minski, M., Vennart, J., 1971. Maximum permissible intakes of 35S-l-methionine and 35S-sodium
6605 sulphate deduced from experiments on rats. Health Phys. 20(1), 1–9.
6606 Miyake, M., Ishigaki, K., Suzuki, T., 1986. Structure refinements of Pb2+ ion-exchanged apatites by x-
6607 ray powder pattern-fitting. J. Solid State Chem. 61(2), 230–235.
6608 Mohamed, A., 2005. Study on radon and radon progeny in some living rooms. Radiat. Prot. Dosim.
6609 117(4), 402–407.
6610 Momčilović, B., Kostial, K., 1974. Kinetics of lead retention and distribution in suckling and adult rats.
6611 Environ. Res. 8(2), 214–220.
6612 Moore, M.R., 1986. Lead in humans. In: Lansdown R and Yule W (eds) Lead Toxicity. History and
6613 Environmental Impact. The Johns Hopkins University Press. Baltimore, pp. 54–95.
6614 Morgan, D.L., Shines, C.J., Jeter, S.P., et al., 1997. Comparative pulmonary absorption, distribution,
6615 and toxicity of copper gallium diselenide, copper indium diselenide, and cadmium telluride in
6616 Sprague-Dawley rats. Toxicol. Appl. Pharmacol. 147(2), 399–410.
6617 Morrison, R.T., Birkbeck, J.A., Evans, T.C., et al., 1963. Radioiodine uptake studies in newborn infants.
6618 J. Nucl. Med. 4, 162–166.
6619 Morrow, P.E., Beiter, H., Amato, F., et al., 1980. Pulmonary retention of lead: An experimental study
6620 in man. Environ. Res. 21(2), 373–384.
6621 Mraz, F.R., Eisele, G.R., 1977a. Gastrointestinal absorption of 95Nb by rats of different ages. Radiat.
6622 Res. 69(3), 591–593.
6623 Mraz, F.R., Eisele, G.R., 1977b. Gastrointestinal absorption, tissue distribution, and excretion of 95Nb
6624 in newborn and weanling swine and sheep. Radiat. Res. 72(3), 533–536.
6625 Mullen, A.A., Stanley, R.E., 1974. Absorption, distribution and milk secretion of radionuclides by the
6626 dairy cow III. Radiotellurium. Health Phys. 27(3), 279–284.
6627 Munro, H.N., Linder, M.C., 1978. Ferritin: Structure, biosynthesis, and role in iron metabolism. Physiol.
6628 Rev. 58(2), 317–396.
6629 Murray, E.J., Messer, H.H., 1981. Turnover of bone zinc during normal and accelerated bone loss in
6630 rats. J. Nutr. 111(9), 1641–1647.

6631 Muth, H., Glōbel, B., 1983. Age dependent concentration of 226Ra in human bone and some transfer
6632 factors from diet to human tissues. Health Phys. 44, 113–121.
6633 Mykkänen, H.M., Wasserman, R.H., 1981. Gastrointestinal absorption of lead (203Pb) in chicks:
6634 Influence of lead, calcium, and age. J. Nutr. 111(10), 1757–1765.
6635 Naimark, D.H., 1948. Acute exposure to polonium (medical study of three human cases). Report MLM-
6636 67. Ohio: Mound Laboratory, Miamisburg.
6637 Naimark, D.H., 1949. Effective half-life of polonium in the human. Report MLM-272. OH: Mound
6638 Lab., Miamisburg.
6639 NCRP, 2009. Uncertainties in internal radiation dose assessment. NCRP Report 164. National Council
6640 on Radiation Protection and Measurements, Bethesda.
6641 National Research Council (NRC), 1991. Comparative Dosimetry of Radon in Mines and Homes.
6642 National Academy Press, Washington, DC.
6643 National Research Council (NRC), Committee on Medical and Biological Effects of Environmental
6644 Pollutants, 1975. Nickel. National Academy of Sciences, Washington.
6645 Naylor, G.P.L., Harrison, J.D., Haines, J.W., 1989. The absorption and intestinal retention of ingested
6646 radionuclides in neonatal mammals. In: Radiation Protection–Theory and Practice (ed. EP
6647 Goldfinch), Institute of Physics, Bristol, pp. 451–454.
6648 Naylor, G.P.L., Bonas, H.E., Haines, J.W., et al., 1991. The gastrointestinal absorption and tissue
6649 distribution of apha-emitting actinide isotopes and polonium-210. In: The British Nuclear Energy
6650 Society Conference: Occupational Radiation Protection, Thomas Telford Publishing, Guernsey, h,
6651 pp. 291–297.
6652 NCRP, 1980. Management of Persons Accidentally Contaminated with Radionuclides. NCRP Report
6653 No 65. National Council on Radiation Protection and Measurements, Washington, DC.
6654 NCRP, 2006. Development of a biokinetic model for radionuclide-contaminated wounds and
6655 procedures for their assessment, dosimetry and treatment. NCRP Report No. 156. National Council
6656 on Radiation Protection and Measurements, Bethesda.
6657 NCRP, 2009, Management of Persons Contaminated with Radionuclides: Handbook:
6658 Recommendations of the National Council on Radiation Protection and Measurements. National
6659 Council on Radiation Protection and Measurements, Bethesda.
6660 Neuman, W.F., Neuman, M.W., 1958. The Chemical Dynamics of Bone Mineral. University of Chicago
6661 Press, Chicago.
6662 Newton, D., 2001. Human biokinetics of injected bismuth-207. Hum. Exp. Toxicol. 20(12), 601–609.
6663 Niita, K., Matsuda, N., Iwamoto, Y., et al., 2010. PHITS: Particle and heavy ion transport code system,
6664 version 2.23. JAEA-Data/code 22(8).
6665 Nipper, J.C., Williams, J.L., Bolch, W.E., 2002. Creation of two tomographic voxel models of
6666 paediatric patients in the first year of life. Phys. Med. Biol. 47(17), 3143–3164.
6667 Nishimura, Y., Inaba, J., Ichikawa, R., 1976. Whole-Body Retention of 60CoCl2 and 58Co-
6668 Cyanocobalamin in Young and Adult Rats. J. Radiat. Res. 17(4), 240–246.
6669 Nishimura, Y., Inaba, J., Matusaka, N., et al., 1991. Biokinetics of selenium in rats of various ages. Biol.
6670 Trace Elem. Res. 2, 11–19.
6671 NEA, 1988, Committee on Radiation Protection and Public Health. Report of an Expert Group on Gut
6672 Transfer Factors. NEA/OECD. Paris, France.
6673 Oddie, T.H., Fisher, D.A., Epperson, D., 1965. Effect of exogenous thyroxine on thyroid accumulation
6674 and secretion in euthyroid subjects. J. Clin. Endocrinol. Metab. 25(9), 1196–1206.
6675 Oddie, T.H., Meade, Jr. J.H., Fisher, D.A., 1966. An analysis of published data on thyroxine turnover
6676 in human subjects. J. Clin. Endocrinol. Metab. 26(4), 425–436.
6677 Ogborn, R.E., Waggener, R.E., Vanhove, E., 1960. Radioactive-iodine concentration in thyroid glands
6678 of newborn infants. Pediatrics 26, 771–776.
6679 Oliner, L., Kohlenbrener, R.M., Fields, T., et al., 1957. Thyroid function studies in children: Normal
6680 values for thyroidal I-131 uptake and PBI-131 levels up to the age of 18. J. Clin. Endocrinol. Metab.
6681 17(1), 61–75.
6682 O'Reilly, S.E., Deweese, L.S., Maynard, M.R., et al., 2016. An image-based skeletal dosimetry model
6683 for the ICRP reference adult female - Internal electron sources. Phys. Med. Biol. 61(24), 8794–8824.

6684 Osanov, D.P., Panova, V.P., Arefieva, S.S., 1971. Evaluation of age influence on accumulation and
6685 elimination rate of radioactive strontium. Health Phys. 21(2), 205–210.
6686 Osipov, V.A., 1983. Biological effects of radioactive carbon. Kinetics of carbon-14 (14C-stearic acid)
6687 metabolism in animals of various ages. Radiobiologia 23(6), 774.
6688 Pafundi, D., Rajon, D., Jokisch, D., et al., 2010. An image-based skeletal dosimetry model for the ICRP
6689 reference newborn - Internal electron sources. Phys. Med. Biol. 55(7), 1785–1814.
6690 Paley, K.R., Sussman, E.S., 1963. Absorption of radioactive cobaltous chloride in human subjects.
6691 Metab. Clin. Exp. 12, 975–982.
6692 Pansu, D., Bellaton, C., Bronner, F., 1983. Developmental changes in the mechanisms of duodenal
6693 calcium transport in the rat. Am. J. Physiol. Gastrointest. Liver Physiol. 7(1), G20–G26.
6694 Papworth, D.G., Vennart, J., 1984. The uptake and turnover of 90Sr in the human skeleton. Phys. Med.
6695 Biol. 29(9), 1045–1061.
6696 Paquet, F., Houpert, P., Verry, M., et al., 1998. The gastrointestinal absorption of 63Ni and 95Nb in
6697 adult and neonatal rats: effect of the chemical form administered. Radiat. Prot. Dosim. 79, 191–195.
6698 Parfitt, A.M., Kleerekoper, M., 1980. The divalent ion homeostatic system: physiology and metabolism
6699 of calcium, phosphorus, magnesium and bone. In: Maxwell MH and Kleeman CR (eds) Clinical
6700 Disorders of Fluid and Electrolyte Metabolism, 3rd Edition. McGraw-Hill, New York, pp. 269–398.
6701 Parks, N.J., Keane, A.T., 1983. Consideration of age-dependent radium retention in people on the basis
6702 of the beagle model. Health Phys. 44, 103–112.
6703 Parks, N.J., Pool, R.R., Williams, J.R., et al., 1978. Age and dosage-level dependence of radium
6704 retention in beagles. Radiat. Res. 75(3), 617–632.
6705 Pawel, D.J., Leggett, R.W., Eckerman, K.F., et al., 2007. Uncertainties in cancer risk coefficients for
6706 environmental exposure to radionuclides. ORNL/TM-2006/583. Oak Ridge National Laboratory,
6707 Oak Ridge, TN.
6708 Pearson, H.A., 1967. Life-span of the fetal red blood cell. J. Pediatr. 70(2), 166–171.
6709 Pelowitz, D.B., 2008. MCNPX—User's Manual version 2.6. 0: A technical document. LA-CP-07-1473.
6710 Los Alamos National Laboratory, New Mexico.
6711 Phipps, A.W., Smith, T.J., Fell, T.P., et al., 2001. Doses to the embryo/foetus and neonate from intakes
6712 of radionuclides by the mother. Contract Research Report to the Health and Safety Executive.
6713 Caerphilly: HSE Information Services, CRR 397.
6714 Pieri, F., Wegmann, R., 1981. Pharmacokinetic study of 205-206Bi-citrate in the rat. Compartmental
6715 repartition. Cell. Mol. Biol. 27(1), 57–60.
6716 Pietrzak-Flis, Z., Radwan, I., Indeka, L., 1978. Tritium in rabbits after ingestion of freeze-dried tritiated
6717 food and tritiated water. Radiat. Res. 76(2), 420–428.
6718 Pollack, S., George, J.N., Reba, R.C., et al., 1965. The absorption of nonferrous metals in iron
6719 deficiency. J. Clin. Investig. 44, 1470–1473.
6720 Porstendörfer, J., 2001. Physical parameters and dose factors of the radon and thoron decay products.
6721 Radiat. Prot. Dosim. 94(4), 365–373.
6722 Pounds, J.G., Marlar, R.J., Allen, J.R., 1978. Metabolism of lead-210 in juvenile and adult rhesus
6723 monkeys (Macaca mulatta). Bull. Environ. Contam. Toxicol. 19(1), 684–691.
6724 Quarterman, J., Morrison, E., 1978. The effect of age on the absorption and excretion of lead.
6725 Environ. Res. 17(1), 78–83.
6726 Quimby, E.H., Werner, S.C., Schmidt, C., 1950. Influence of Age, Sex, and Season upon Radioiodine
6727 Uptake by the Human Thyroid. Proc. Soc. Exp. Biol. Med. 75(2), 537–540.
6728 Quimby, E.H., Feitelberg, S., Silver, S., 1958. Radioactive Isotopes in Clinical Practice. Lea and
6729 Febiger. Pergamon, Philadelphia.
6730 Rabinowitz, M., Wetherill, G.W., Kopple, J.D., 1974. Studies of human lead metabolism by use of
6731 stable isotope tracers. Environ. Health Perspect No. 7, 145–153.
6732 Rabinowitz, M.B., Wetherill, G.W., Kopple, J.D., 1973. Lead metabolism in the normal human: Stable
6733 isotope studies. Science 182(4113), 725–727.
6734 Rabinowitz, M.B., Wetherill, G.W., Kopple, J.D., 1976. Kinetic analysis of lead metabolism in healthy
6735 humans. J. Clin. Investig. 58(2), 260–270.
6736 Reineking, A., Butterweck, G., Kesten, J., et al., 1992. Thoron gas concentration and aerosol
6737 characteristics of thoron decay products. Radiat. Prot. Dosim. 45(1-4 SUPPL.), 353–356.

6738 Reineking, A., Knutson, E.A., George, A.C., et al., 1994. Size distribution of unattached and aerosol
6739 attached short-lived radon decay products: Some results of intercomparison measurements.
6740 Radiat. Prot. Dosim. 56(1–4), 113–118.
6741 Rios, E., Hunter, R.E., Cook, J.D., 1975. The absorption of iron as supplements in infant cereal and
6742 infant formulas. Pediatrics 55(5), 686–693.
6743 Rivera, J., 1967. Predicting strontium-90 concentrations in human bone. In: Strontium metabolism,
6744 Proceedings of the international symposium on some aspects of strontium metabolism held at
6745 Chapelcross, Glasgow and Strontian, 5-7 May 1966 (eds JMA Lenihan, JF Loutit, and JH Martin),
6746 Academic Press, London, pp. 47–55.
6747 Robinson, M.F., McKenzie, J.M., Thomson, C.D., et al., 1973. Metabolic balance of zinc, copper,
6748 cadmium, iron, molybdenum and selenium in young New Zealand women. Br. J. Nutr. 30(2), 195–
6749 205.
6750 Rosenberg, G., 1957. Effect of age on 24 hour iodine 131 uptake in healthy males. Can. Serv. Med. J.
6751 13(9), 565–569.
6752 Rosenberg, G., 1958. Biologic half-life of I 131 in the thyroid of healthy males. J. Clin. Endocrinol.
6753 Metab. 18(5), 516–521.
6754 Russ, G.A., Bigler, R.E., Tilbury, R.S., et al., 1975. Metabolic studies with radiobismuth. I. Retention
6755 and distribution of 206Bi in the normal rat. Radiat. Res. 63(3), 443–454.
6756 Saarinen, U.M., Siimes, M.A., 1977. Iron absorption from infant milk formula and the optimal level of
6757 iron supplementation. Acta Paediatr 66(6), 719–722.
6758 Saarinen, U.M., Siimes, M.A., Dallman, P.R., 1977. Iron absorption in infants: High bioavailability of
6759 breast milk iron as indicated by the extrinsic tag method of iron absorption and by the concentration
6760 of serum ferritin. J. Pediatr. 91(1), 36–39.
6761 Saito, H., Sargent 3rd. T., Parker, H.G., et al., 1964. Whole-body iron loss in normal man measured
6762 with a gamma spectrometer. J. Nucl. Med. 5, 571–580.
6763 Sanchez, G., 2007. Fitting bioassay data and performing uncertainty analysis with BIOKMOD. Health
6764 Phys. 92(1), 64–72.
6765 Sandstrom, B., Cederblad, A., 1980. Zinc absorption from composite meals. II. Influence of the main
6766 protein source. Am. J. Clin. Nutr. 33(8), 1778–1783.
6767 Sandström, B., Davidsson, L., Kivistö, B., et al., 1987. The effect of vegetables and beet fibre on the
6768 absorption of zinc in humans from composite meals. Br. J. Nutr. 58(1), 49–57.
6769 Sandstrom, B., Almgren, A., Kivisto, B., et al., 1989. Effect of protein level and protein source on zinc
6770 absorption in humans. J. Nutr. 119(1), 48–53.
6771 Sawin, C.T., 2005. Age-related changes in thyroid secretion. In: Werner SC, Ingbar SH, Braverman LE,
6772 et al. (eds) Werner & Ingbar's The Thyroid: A Fundamental and Clinical Text, 9th Edition.
6773 Lippincott Wikkiams & Wilkins, New York, USA, pp. 214–219.
6774 Schade, S.G., Felsher, B.F., Bernier, G.M., et al., 1970. Interrelationship of cobalt and iron absorption.
6775 J. lab. clin. med. 75(3), 435–441.
6776 Scheiman-Tagger, E., Brodie, A.G., 1964. Lead acetate as a marker of growing calcified tissues a
6777 modified method. Anat. Rec. 150(4), 435–439.
6778 Schober, B., Hunt, J.A., 1976. Evaluation of the normal range of values for uptake of radioactive iodine
6779 by the thyroid gland. Can. Med. Assoc. J. 115(1), 29–35.
6780 Schroeder, H.A., Buckman, J., Balassa, J.J., 1967. Abnormal trace elements in man: Tellurium. J.
6781 Chronic Dis. 20(3), 147–161.
6782 Schubert, J., Armstrong, W.D., 1949. Rate of elimination of radioactive carbon administered as
6783 carbonate from the tissues and tissue components of mature and growing rats. J. Biol. Chem. 177(2),
6784 521–527.
6785 Schulz, J., Smith, N.J., 1958. A Quantitative Study of the Absorption of Food Iron in Infants and
6786 Children. A.M.A. j. dis. child. 95(2), 109–119.
6787 Schwarz, B.C., Godwin, W.J., Wayson, M.B., et al., 2021a. Specific absorbed fractions for a revised
6788 series of the UF/NCI pediatric reference phantoms: internal electron sources. Phys. Med. Biol. 66(3).
6789 Schwarz, B.C., Godwin, W.J., Wayson, M.B., et al., 2021b. Specific absorbed fractions for a revised
6790 series of the UF/NCI pediatric reference phantoms: internal photon sources. Phys. Med. Biol. 66(3).

6791 Schwarz, G., Dunning, D.E. Jr., 1982. Imprecision in estimates of dose from ingested 137Cs due to
6792 variability in human biological characteristics. Health Phys. 43(5), 631–645.
6793 Scott, B.R., 2007. Health risk evaluations for ingestion exposure of humans to polonium-210. Dose-
6794 Response 5(2). SAGE Publications Sage CA: Los Angeles, CA, 94–122.
6795 Scott, L.M., West, C.M., 1975. Excretion of 210-Po oxide following accidental inhalation. Health Phys.
6796 28(5), 563–565.
6797 Shagina, N.B., Tolstykh, E.I., Zalyapin, V.I., et al., 2003. Evaluation of age and gender dependences of
6798 the rate of strontium elimination 25-45 years after intake: Analysis of data from residents living
6799 along the Techa River. Radiat. Res. 159(2), 239–246.
6800 Shagina, N.B., Tolstykh, E.I., Degteva, M.O., et al., 2015. Age and gender specific biokinetic model
6801 for strontium in humans. J Radiol Prot. 35(1), 87–127.
6802 Shah, A.P., Bolch, W.E., Rajon, D.A., et al., 2005. A paired-image radiation transport model for skeletal
6803 dosimetry. J. Nucl. Med. 46(2), 344–353.
6804 Sheehan, W.E., 1964. Effective half-life of polonium. In: Proc. 10th Annual Bioassay and Analytical
6805 Chemistry Meeting Conf, pp. 32–8.
6806 Sherif, Y.S., Schwarz, F.J., Kirchgessner, M., 1981. Influence of age and sex on in vitro intestinal
6807 absorption of zinc and manganese. Arch. Tierernahr. 31(9), 597–607.
6808 Shiraishi, Y., Ichikawa, R., 1972. Absorption and retention of144Ce and95Zr-95Nb in newborn,
6809 juvenile and adult rats. Health Phys. 22(4), 373–378.
6810 Shohl, A.T., Sato, A., 1923. Acid-base metabolism II. Mineral metabolism. J. Biol. Chem. 58(1), 257–
6811 266.
6812 Sievers, E., Oldigs, H-D., Dörner, K., et al., 2001. Molybdenum balance studies in premature male
6813 infants. Eur. J. Pediatr. 160(2), 109–113.
6814 Sievers, E., Dörner, K., Garbe-Schönberg, D., et al., 2001. Molybdenum metabolism: Stable isotope
6815 studies in infancy. J. Trace Elem. Med. Biol. 15(2–3), 185–191.
6816 Silberstein, H.E., Valentine, W.N., Minto, W.L., et al., 1950. Studies of Polonium Metabolism in
6817 Human Subjects, Intravenous Studies, Comparison of Intravenous Studies, Oral Administration. In:
6818 Biological Studies with Polonium, Radium, and Plutonium. McGraw-Hill, New York, USA. pp.
6819 122–148.
6820 Silverman, L.B., 1944. Excretion activity analyses as a monitor for postum exposures. Final Report No.
6821 10.
6822 Sinclair, D., Countess, R.J., Hoopes, G.S., 1974. Effect of relative humidity on the size of atmospheric
6823 aerosol particles. Atmos. Environ. (1967) 8(11), 1111–1117.
6824 Sivulka, D.J., 2005. Assessment of respiratory carcinogenicity associated with exposure to metallic
6825 nickel: A review. Regul. Toxicol. Pharmacol. 43, 117–133.
6826 Skrable, K.W., French, C.S., Chabot, G.E., et al., 2002. Variance models for estimating intakes from
6827 repetitive bioassay measurements. In: Practical Applications of Internal Dosimetry. Medical Physics
6828 Publishing. Madison, WI, pp. 257–305.
6829 Slikkerveer, A., de Wolff, F.A., 1989. Pharmacokinetics and Toxicity of Bismuth Compounds. Med.
6830 Toxicol. Adverse Drug Exp. 4(5), 303–323.
6831 Snyder, W.S., FisherJr., H.L., Ford, M.R., et al., 1969. Estimates of absorbed fractions for
6832 monoenergetic photon sources uniformly distributed in various organs of a heterogeneous phantom.
6833 J. Nucl. Med. Suppl 3, 7-52.
6834 Sollmann, T., 1957. A Manual of Pharmacology and Its Applications to Therapeutics and Toxicology.
6835 WB Saunders Company, Philadelphia, P.
6836 Solomons, N.W., Cousins, R.J., 1984. Zinc. In: Absorption and Malabsorption of Mineral Nutrients.
6837 Alan R Liss, New York, pp. 125–97.
6838 Solomons, N.W., Janghorbani, M., Ting, B.T.G., et al., 1982. Bioavailability of zinc from a diet based
6839 on isolated soy protein: Application in young men of the stable isotope tracer, 70Zn. J. Nutr. 112(10),
6840 1809–1821.
6841 Spoerl, E.S., 1951. A derived biological half-life of polonium in humans. MLM–626, Report for
6842 biological research. Mound Laboratory, Miamisburg, Ohio.
6843 Stather, J.W., 1974. Distribution of 32P, 45Ca, 85Sr and 133Ba as a function of age in the mouse
6844 skeleton. Health Phys. 26(1), 71–79.

Stather, J.W., Phipps, A.W., Harrison, J.D., et al., 2003. Dose coefficients for the embryo and fetus following intakes of radionuclides by the mother. Radiat. Prot. Dosim. 105(1–4), 257–264.

Stehney, A.F., LucasJr, H.F., 1956. Studies on the radium content of humans arising from the natural radium of their environment. In: Peaceful Uses of Atomic Energy, United Nations, New York, USA, pp. 49–54.

Stevenson, A.F., 1975. The influence of age and sex on the activity ratio of yttrium-90 to strontium-90 in the rat skeleton after incorporation of strontium-90. Health Phys. 29(2), 285–290.

Sullivan, M.F., Graham, T.M., Cataldo, D.A., et al., 1978. Absorption and retention of inorganic and organically incorporated technetium-95 by rats and guinea pigs. Pacific Northwest Laboratory Annual Report for 1977, Part I. Biomedical Sciences PNL-2500. Pacific Northwest National Laboratory, Richland, Washington.

Sullivan, M.F., Hardy, J.T., Miller, B.M., et al., 1984. Absorption and distribution of cadmium in mice fed diets containing either inorganic or oyster-incorporated cadmium. Toxicol. Appl. Pharmacol. 72(2), 210–217.

Sullivan, M.F., Ruemmler, P.S., Ryan, J.L., 1984. Effects of fasting and/or oxidizing and reducing agents on absorption of neptunium from the gastrointestinal tract of mice and adult or neonatal rats. Radiat. Res. 100(3), 519–526.

Sullivan, M.F., Miller, B.M., Goebel, J.C., 1984. Gastrointestinal absorption of metals (51Cr, 65Zn, 95mTc, 109Cd, 113Sn, 147Pm, and 238Pu) by rats and swine. Environ. Res. 35(2), 439–453.

Suomela, M., Kahlos, H., 1972. Studies on the elimination rate and the radiation exposure following ingestion of 222Rn rich water. Health Phys. 23(5), 641–652.

Susskind, H., Atkins, H.L., Cohn, S.H., et al., 1977. Whole body retention of radioxenon. J. Nucl. Med. 18(5), 462–471.

Taylor, D.M., 1959. The Metabolism of Some Trace Metals in Animals and Man. PhD Thesis. University of London (Institute of Cancer Research).

Taylor, D.M., 1962. The absorption of cobalt from the gastro-intestinal tract of the rat. Phys. Med. Biol. 6(3), 445–451.

Taylor, D.M., Bligh, P.H., Duggan, M.H., 1962. The absorption of calcium, strontium, barium and radium from the gastrointestinal tract of the rat. Biochem. J. 83, 25–29.

Testa, C., 1972. Indirect methods used at CNEN for the evaluation of internal contamination. Assessment of radioactive contamination in man IAEA-SM-150/18. IAEA, Vienna, Austria.

Thornberg, C., Mattsson, S., 2000. Increased 137Cs metabolism during pregnancy. Health Phys. 78(5), 502–506.

Till, J.E., Hoffman, F.O., Dunning, D.E.Jr, 1979. A new look at 99Tc releases to the atmosphere. Health Phys. 36(1), 21–30.

Tipton, I., Stewart, P., Martin, P., 1966. Trace elements in diet and excreta. Health Phys. 12, 1683–1689.

Tipton, I.H., Cook, M.J., 1963. Trace elements in human tissue: Part II. Adult subjects from the united states. Health Phys. 9(2), 103–145.

Tipton, I.H., Stewart, P.L., Dickson, J., 1969. Patterns of elemental excretion in long term balance studies. Health Phys. 16(4), 455–462.

Tokonami, S., Takahashi, F., Iimoto, T., et al., 1997. A new device to measure the activity size distribution of radon progeny in a low level environment. Health Phys. 73(3), 494–497.

Treves, S., Ahnberg, D.S., Laguarda, R., et al., 1974. Radionuclide evaluation of regional lung function in children. J. Nucl. Med. 15(7), 582–587.

Treves, S.T., Packard, A.B., 1995. Lungs, Chapter 11. In: Treves ST (ed.) Pediatric nuclear medicine. Springer Nature, pp. 159–197.

Trubowitz, S., Davis, S., 1982. The Human Bone Marrow: Anatomy, Physiology, and Pathophysiology. CRC PressI, Boca Raton, Florida.

Tu, K.W., Knutson, E.O., 1988. Indoor radon progeny particle size distribution measurements made with two different methods. Radiat. Prot. Dosim. 24(1–4), 251–255.

Tu, K.W., Knutson, E.O., George, A.C., 1991. Indoor radon progeny aerosol size measurements in urban, suburban, and rural regions. Aerosol Sci. Technol. 15(3), 170–178.

Turnlund, J.R., King, J.C., Keyes, W.R., et al., 1984. A stable isotope study of zinc absorption in young men: Effects of phytate and α-cellulose. Am. J. Clin. Nutr. 40(5), 1071–1077.

Turnlund, J.R., Keyes, W.R., Peiffer, G.L., 1995. Molybdenum absorption, excretion, and retention studied with stable isotopes in young men at five intakes of dietary molybdenum. Am. J. Clin. Nutr. 62(4), 790–796.

Turnlund, J.R., Keyes, W.R., Peiffer, G.L., et al., 1995. Molybdenum absorption, excretion, and retention studied with stable isotopes in young men during depletion and repletion. Am. J. Clin. Nutr. 61(5), 1102–1109.

Turnlund, J.R., Weaver, C.M., Kim, S.K., et al., 1999. Molybdenum absorption and utilization in humans from soy and kale intrinsically labeled with stable isotopes of molybdenum. Am. J. Clin. Nutr. 69(6), 1217–1223.

UNSCEAR, 2020. Report of the United Nations Scientific Committee on the Effects of Atomic Radiation. UNSCEAR 2019 Report, Annex B, Lung Cancer from Exposure to Radon. United Nations Scientific Committee on the Effects of Atomic Radiation, New-York.

Valberg, L.S., Ludwig, J., Olatunbosun, D., 1969. Alteration in Cobalt Absorption in Patients with Disorders of Iron Metabolism. Gastroenterology 56(2), 241–251.

Valkonen, S., Savolainen, H., 1985. Tellurium burden and neurochemical effects in moderate peroral exposure. Bull. Environ. Contam. Toxicol. 34(1), 170–174.

van Dilla, M.A., Fulwyler, M.J., 1963. Thyroid metabolism in children and adults using very small (nanocurie) doses of iodine125 and iodine131. Health Phys. 9(12), 1325–1331.

Van, M.L., 1954. Radioactive iodide uptake of normal newborn infants. American Journal of Diseases of Children 88(4). American Medical Association, 439–442.

Vaternahm, T., 1922. Comparative investigation of the radon capacity of exhaled breath after drinking of radon ladened water and oil. Zschr. Phys. Diätet. Therap 26, 361–364.

Verbeeck, R.M.H., Lassuyt, C.J., Heijligers, H.J.M., et al., 1981. Lattice parameters and cation distribution of solid solutions of calcium and lead hydroxyapatite. Calcif. Tissue Int. 33(1), 243–247.

Vincent, J., 1957. Changes of compact bone labeled with lead. Revue belge de pathologie et de médecine expérimentale 26(3), 161–168.

Volwiler, W., Goldworthy, P.D., MacMartin, M.P., et al., 1955. Biosynthetic determination with radioactive sulphur of turnover rates of various plasma proteins in normal and cirrhotic men. J. Clin. Invest 34, 1126–1146.

von Döbeln, W., Lindell, B., 1964. Some aspects of radon contamination following ingestion. Ark. Fys. 27, 531–572.

Wellman, H.N., Branson, B.M., Kereiakes, J.G., 1970. Total- and partial-body counting of children for radiopharmaceutical dosimetry data. In: Proceedings of a symposium held at Oak Ridge Associated Universities, December 8 11, 1969 (eds RJ Cloutier, CL Edwards, and WS Snyder), U.S. Atomic Energy Commission, Oak Ridge, TN, pp. 133–156.

Wells, A.C., Venn, J.B., Heard, M.J., 1975. Deposition in the lung and uptake to blood of motor exhaust labelled with 203Pb. In: Inhaled particles IV (eds WH Walton and B McGovern), Edinburgh, 1975, pp. 175–189.

Werner, E., Giussani, A., Heinrichs, U., et al., 1998. Biokinetic studies in humans with stable isotopes as tracers. Part 2: Uptake of molybdenum from aqueous solutions and labelled foodstuffs. Isot. Environ. Health Stud. 34(3), 297–301.

Werner, E., Roth, P., Heinrichs, U., et al., 2000. Internal biokinetic behaviour of molybdenum in humans studied with stable isotopes as tracers. Isot. Environ. Health Stud. 36(2), 123–132.

Widdowson, E.M., Slater, J.E., Harrison, G.E., et al., 1960. Absorption, excretion and retention of strontium by breast-fed and bottle-fed babies. Lancet 276(7157), 941–944.

Willes, R.F., Lok, E., Truelove, J.F., et al., 1977. Retention and tissue distribution of 210Pb(NO3)2 administered orally to infant and adult monkeys. J. Toxicol. Environ. Health 3(3), 395–406.

Wood, S.K., Farnham, J.E., Marshall, J.H., 1970. Ca-45, Ba-133, and Ra-226 in 6-to 10-year-old beagle dogs: a 100-day study. ANL-7760, Part II, Biology and Medicine, Radiological Physics Division annual report, Argonne National Laboratory. Center for Human Radiobiology, Argonne, IL.

6951 Woodard, H.Q., Dwyer, A.J., 1972. Whole-body retention of Sr-85 in three children. In: Second
6952 International Conference on Strontium Metabolism, Glasgow and Strontian, pp. 91–109.
6953 Woodhead, J.C., Drulis, J.M., Nelson, S.E., et al., 1991. Gender-related differences in iron absorption
6954 by preadolescent children. Pediatr. Res. 29(5), 435–439.
6955 Wraight, J.C., Strong, R., 1989. A case study on the retention and excretion of internally deposited
6956 polonium. In: Radiation protection-theory and practice, pp. 227–230.
6957 Wright, J.B., Martin, P.G., Skellenger, M.L., et al., 1960. Metabolic patterns in preadolescent children.
6958 III. Sulfur balance on three levels of nitrogen intake. J. Nutr. 72, 314.
6959 Wright, P.L., Bell, M.C., 1966. Comparative metabolism of selenium and tellurium in sheep and swine.
6960 Am. J. Physiol. 211, 6–10.
6961 Yen, PK-J., Shaw, J.H., 1977. Basic biological sciences: Remodeling of Compact Bone Studied with
6962 Lead Acetate as an Intravital Stain. J. Dent. Res. 56(8), 961–966.
6963 Zankl, M., Fill, U., Petoussi-Henss, N., et al., 2002. Organ dose conversion coefficients for external
6964 photon irradiation of male and female voxel models. Phys. Med. Biol. 47(14), 2367–2385.
6965 Zankl, M., Petoussi-Henss, N., Fill, U., et al., 2003. The application of voxel phantoms to the internal
6966 dosimetry of radionuclides. Radiat. Prot. Dosim. 105(1–4), 539–548.
6967 Zankl, M., Eckerman, K.F., Bolch, W.E., 2007. Voxel-based models representing the male and female
6968 ICRP reference adult - The skeleton. Radiat. Prot. Dosim. 127(1–4), 174–186.
6969 Zhu, H., Wang, N., Zhang, Y., et al., 2010. Element contents in organs and tissues of Chinese adult
6970 men. Health Phys. 98: 61–71.
6971 Ziegler, E.E., Edwards, B.B., Jensen, R.L., et al., 1978. Absorption and retention of lead by infants.
6972 Pediatr. Res. 12(1), 29–34.
6973 Zundel, W.S., Tyler, F.H., Mays, C.W., et al., 1969. Short half-times of caesium-137 in pregnant women.
6974 Nature 221(5175), 89–90.
6975

ANNEX A. SUPPLEMENTARY INFORMATION RELATING TO APPLICATION OF THE HRTM TO ENVIRONMENTAL EXPOSURE

A.1. Deposition in respiratory tract regions for Reference Individuals as a function of aerosol size

(A 1) In the original HRTM, it was assumed that particles deposited in the nasal passages during inhalation are partitioned equally between ET_1 and the posterior nasal passage, which is part of ET_2. [However, because of the way the deposition efficiencies were calculated for polydispersed aerosols during inhalation and exhalation, for most aerosol sizes of interest in radiation protection the deposition fractions given in *Publication 66* (ICRP, 1994) are somewhat higher for ET_2 than for ET_1]. In the revised HRTM, it is assumed that for nose breathing, the deposit in the ET airways is distributed 65% to ET_1 and 35% to ET_2. To calculate the fractions of inhaled material deposited in ET_1 and ET_2 in the revised HRTM, the fractions deposited in ET_1 and ET_2 (calculated using the original HRTM) were summed to give the total deposit in the ET airways, and then re-partitioned 65% to ET_1 and 35% to ET_2.For mouth breathing, there is no deposition in ET_1 and the fraction deposited in ET_2 remains as calculated using the original HRTM.

(A 2) Table A.1 gives values of fractional deposition in each region of the respiratory tract as a function of aerosol size, for each Reference Individual and for the time budget and ventilation parameter values used in this series of reports for environmental exposure (Main Text, Table 2.3). Values for the Reference Individuals for aerosols of 1 μm AMAD inhaled for environmental exposure are given in the Main Text (Table 2.4). Tables of fractional deposition for each Reference Individual at each exercise level are provided in a supplementary file.

Table A.1. Fractional deposition in regions of the respiratory tract for environmental exposure as a function of aerosol size[*,†,‡].

(a) Infant 3 mo old (breathing rate = 0.12 $m^3\ h^{-1}$)

μm	ET_1	ET_2	BB	bb	AI	Total
AMTD						
0.001	5.520×10^{-1}	2.972×10^{-1}	1.187×10^{-1}	2.124×10^{-2}	3.060×10^{-5}	9.892×10^{-1}
0.003	3.519×10^{-1}	1.895×10^{-1}	1.827×10^{-1}	1.989×10^{-1}	1.687×10^{-2}	9.398×10^{-1}
0.01	1.383×10^{-1}	7.446×10^{-2}	8.727×10^{-2}	2.707×10^{-1}	2.365×10^{-1}	8.072×10^{-1}
0.03	5.918×10^{-2}	3.187×10^{-2}	3.742×10^{-2}	1.530×10^{-1}	3.500×10^{-1}	6.314×10^{-1}
0.1	5.480×10^{-2}	2.951×10^{-2}	1.970×10^{-2}	7.764×10^{-2}	2.126×10^{-1}	3.942×10^{-1}
AMAD						
0.3	1.038×10^{-1}	5.588×10^{-2}	1.432×10^{-2}	5.144×10^{-2}	1.541×10^{-1}	3.795×10^{-1}
1	3.131×10^{-1}	1.686×10^{-1}	1.042×10^{-2}	2.045×10^{-2}	8.562×10^{-2}	5.981×10^{-1}
3	4.908×10^{-1}	2.643×10^{-1}	1.021×10^{-2}	9.462×10^{-3}	4.645×10^{-2}	8.212×10^{-1}
5	5.177×10^{-1}	2.788×10^{-1}	8.978×10^{-3}	6.335×10^{-3}	2.910×10^{-2}	8.408×10^{-1}
10	4.931×10^{-1}	2.655×10^{-1}	6.050×10^{-3}	3.057×10^{-3}	1.169×10^{-2}	7.795×10^{-1}
20	4.311×10^{-1}	2.321×10^{-1}	3.066×10^{-3}	1.085×10^{-3}	3.274×10^{-3}	6.707×10^{-1}

(b) Infant 1 y old (breathing rate = 0.22 $m^3\ h^{-1}$)

μm	ET1	ET2	BB	bb	AI	Total

AMTD						
0.001	5.434×10^{-1}	2.926×10^{-1}	1.124×10^{-1}	3.911×10^{-2}	2.319×10^{-4}	9.878×10^{-1}
0.003	3.406×10^{-1}	1.834×10^{-1}	1.460×10^{-1}	2.318×10^{-1}	3.787×10^{-2}	9.396×10^{-1}
0.01	1.322×10^{-1}	7.121×10^{-2}	6.436×10^{-2}	2.439×10^{-1}	3.215×10^{-1}	8.332×10^{-1}
0.03	5.746×10^{-2}	3.094×10^{-2}	2.758×10^{-2}	1.304×10^{-1}	4.105×10^{-1}	6.569×10^{-1}
0.1	5.479×10^{-2}	2.950×10^{-2}	1.459×10^{-2}	6.476×10^{-2}	2.377×10^{-1}	4.013×10^{-1}
AMAD						
0.3	1.047×10^{-1}	5.638×10^{-2}	1.109×10^{-2}	4.250×10^{-2}	1.708×10^{-1}	3.854×10^{-1}
1	3.144×10^{-1}	1.693×10^{-1}	1.041×10^{-2}	1.707×10^{-2}	9.636×10^{-2}	6.075×10^{-1}
3	4.910×10^{-1}	2.644×10^{-1}	1.147×10^{-2}	8.506×10^{-3}	5.314×10^{-2}	8.286×10^{-1}
5	5.176×10^{-1}	2.787×10^{-1}	1.014×10^{-2}	5.898×10^{-3}	3.329×10^{-2}	8.457×10^{-1}
10	4.930×10^{-1}	2.655×10^{-1}	6.757×10^{-3}	2.936×10^{-3}	1.329×10^{-2}	7.815×10^{-1}
20	4.311×10^{-1}	2.321×10^{-1}	3.355×10^{-3}	1.056×10^{-3}	3.673×10^{-3}	6.713×10^{-1}

(c) Child 5y old (breathing rate = 0.36 m^3 h^{-1})

µm	ET1	ET2	BB	bb	AI	Total
AMTD						
0.001	5.395×10^{-1}	2.905×10^{-1}	9.893×10^{-2}	5.396×10^{-2}	6.077×10^{-4}	9.835×10^{-1}
0.003	3.356×10^{-1}	1.807×10^{-1}	1.161×10^{-1}	2.434×10^{-1}	5.398×10^{-2}	9.296×10^{-1}
0.01	1.304×10^{-1}	7.021×10^{-2}	4.931×10^{-2}	2.261×10^{-1}	3.514×10^{-1}	8.273×10^{-1}
0.03	5.973×10^{-2}	3.216×10^{-2}	2.212×10^{-2}	1.240×10^{-1}	3.679×10^{-1}	6.060×10^{-1}
0.1	4.551×10^{-2}	2.451×10^{-2}	1.164×10^{-2}	6.050×10^{-2}	1.958×10^{-1}	3.380×10^{-1}
AMAD						
0.3	7.864×10^{-2}	4.235×10^{-2}	9.022×10^{-3}	3.977×10^{-2}	1.420×10^{-1}	3.118×10^{-1}
1	2.581×10^{-1}	1.390×10^{-1}	1.035×10^{-2}	1.851×10^{-2}	9.855×10^{-2}	5.245×10^{-1}
3	4.468×10^{-1}	2.406×10^{-1}	1.372×10^{-2}	1.253×10^{-2}	6.861×10^{-2}	7.822×10^{-1}
5	4.874×10^{-1}	2.624×10^{-1}	1.294×10^{-2}	9.703×10^{-3}	4.684×10^{-2}	8.193×10^{-1}
10	4.791×10^{-1}	2.580×10^{-1}	9.292×10^{-3}	5.389×10^{-3}	2.068×10^{-2}	7.724×10^{-1}
20	4.262×10^{-1}	2.295×10^{-1}	4.926×10^{-3}	2.107×10^{-3}	6.249×10^{-3}	6.690×10^{-1}

(d) Child 10 y old (breathing rate = 0.64 m^3 h^{-1})

µm	ET1	ET2	BB	bb	AI	Total
AMTD						
0.001	5.293×10^{-1}	2.850×10^{-1}	8.804×10^{-2}	7.860×10^{-2}	2.590×10^{-3}	9.835×10^{-1}
0.003	3.233×10^{-1}	1.741×10^{-1}	9.244×10^{-2}	2.523×10^{-1}	9.347×10^{-2}	9.355×10^{-1}
0.01	1.249×10^{-1}	6.723×10^{-2}	3.782×10^{-2}	2.016×10^{-1}	4.169×10^{-1}	8.483×10^{-1}
0.03	5.863×10^{-2}	3.157×10^{-2}	1.722×10^{-2}	1.090×10^{-1}	3.789×10^{-1}	5.954×10^{-1}
0.1	4.658×10^{-2}	2.508×10^{-2}	9.166×10^{-3}	5.219×10^{-2}	1.918×10^{-1}	3.248×10^{-1}
AMAD						
0.3	8.224×10^{-2}	4.428×10^{-2}	7.774×10^{-3}	3.418×10^{-2}	1.371×10^{-1}	3.056×10^{-1}
1	2.640×10^{-1}	1.421×10^{-1}	1.167×10^{-2}	1.702×10^{-2}	9.513×10^{-2}	5.300×10^{-1}
3	4.483×10^{-1}	2.414×10^{-1}	1.595×10^{-2}	1.299×10^{-2}	6.757×10^{-2}	7.862×10^{-1}
5	4.871×10^{-1}	2.623×10^{-1}	1.484×10^{-2}	1.041×10^{-2}	4.667×10^{-2}	8.213×10^{-1}
10	4.781×10^{-1}	2.574×10^{-1}	1.042×10^{-2}	5.957×10^{-3}	2.099×10^{-2}	7.729×10^{-1}
20	4.256×10^{-1}	2.292×10^{-1}	5.419×10^{-3}	2.381×10^{-3}	6.478×10^{-3}	6.690×10^{-1}

(e) 15 y male (breathing rate = 0.84 m^3 h^{-1})

µm	ET1	ET2	BB	bb	AI	Total
AMTD						
0.001	4.911×10^{-1}	3.017×10^{-1}	8.757×10^{-2}	9.531×10^{-2}	5.717×10^{-3}	9.814×10^{-1}
0.003	3.000×10^{-1}	1.792×10^{-1}	8.582×10^{-2}	2.561×10^{-1}	1.124×10^{-1}	9.334×10^{-1}

0.01	1.161×10^{-1}	6.872×10^{-2}	3.443×10^{-2}	1.948×10^{-1}	4.331×10^{-1}	8.472×10^{-1}
0.03	5.471×10^{-2}	3.252×10^{-2}	1.571×10^{-2}	1.048×10^{-1}	3.772×10^{-1}	5.848×10^{-1}
0.1	3.770×10^{-2}	2.182×10^{-2}	8.451×10^{-3}	5.002×10^{-2}	1.889×10^{-1}	3.069×10^{-1}
AMAD						
0.3	6.037×10^{-2}	3.381×10^{-2}	7.770×10^{-3}	3.320×10^{-2}	1.367×10^{-1}	2.718×10^{-1}
1	2.049×10^{-1}	1.155×10^{-1}	1.689×10^{-2}	1.995×10^{-2}	1.065×10^{-1}	4.638×10^{-1}
3	3.792×10^{-1}	2.233×10^{-1}	2.965×10^{-2}	1.938×10^{-2}	8.596×10^{-2}	7.376×10^{-1}
5	4.250×10^{-1}	2.569×10^{-1}	2.991×10^{-2}	1.658×10^{-2}	6.236×10^{-2}	7.907×10^{-1}
10	4.298×10^{-1}	2.689×10^{-1}	2.254×10^{-2}	1.002×10^{-2}	2.968×10^{-2}	7.609×10^{-1}
20	3.896×10^{-1}	2.505×10^{-1}	1.201×10^{-2}	4.127×10^{-3}	9.589×10^{-3}	6.657×10^{-1}

(f) 20 y (male) (breathing rate = 0.93 $m^3\ h^{-1}$)

µm	ET1	ET2	BB	bb	AI	Total
AMTD						
0.001	5.182×10^{-1}	2.877×10^{-1}	8.460×10^{-2}	9.028×10^{-2}	3.595×10^{-3}	9.844×10^{-1}
0.003	3.152×10^{-1}	1.738×10^{-1}	8.430×10^{-2}	2.633×10^{-1}	1.056×10^{-1}	9.422×10^{-1}
0.01	1.212×10^{-1}	6.668×10^{-2}	3.369×10^{-2}	2.002×10^{-1}	4.459×10^{-1}	8.676×10^{-1}
0.03	5.669×10^{-2}	3.121×10^{-2}	1.524×10^{-2}	1.066×10^{-1}	4.051×10^{-1}	6.148×10^{-1}
0.1	3.953×10^{-2}	2.163×10^{-2}	8.126×10^{-3}	5.105×10^{-2}	2.062×10^{-1}	3.265×10^{-1}
AMAD						
0.3	6.421×10^{-2}	3.486×10^{-2}	7.082×10^{-3}	3.387×10^{-2}	1.498×10^{-1}	2.898×10^{-1}
1	2.194×10^{-1}	1.192×10^{-1}	1.286×10^{-2}	1.951×10^{-2}	1.148×10^{-1}	4.858×10^{-1}
3	4.049×10^{-1}	2.222×10^{-1}	2.071×10^{-2}	1.766×10^{-2}	9.004×10^{-2}	7.554×10^{-1}
5	4.529×10^{-1}	2.501×10^{-1}	2.049×10^{-2}	1.483×10^{-2}	6.456×10^{-2}	8.028×10^{-1}
10	4.571×10^{-1}	2.545×10^{-1}	1.536×10^{-2}	8.872×10^{-3}	3.035×10^{-2}	7.662×10^{-1}
20	4.136×10^{-1}	2.320×10^{-1}	8.328×10^{-3}	3.669×10^{-3}	9.724×10^{-3}	6.673×10^{-1}

*Reference values are given to a greater degree of precision than would be chosen to reflect the certainty with which the average value of each parameter is known.

†The particles are assumed to have density 3.00 g cm^{-3}, and shape factor 1.5 (typical of compact, irregular, i.e. non-spherical particles). The particle diameters are assumed to be log-normally distributed with geometric standard deviation, σ_g increasing from a value of 1.0 at 0.6 nm to a value of 2.5 above approximately 1 µm [*Publication 66* (ICRP, 1994), Paragraph 170]. The value of σ_g is not a reference value, but is derived from the corresponding AMTD (ICRP, 1994).

‡ The distribution of time spent at each of the four reference exercise levels are as given in Table 2.3. The deposition fractions are volume-weighted average values for deposition at the four exercise levels.

(A 3) For aerosols with an AMAD below approximately 0.3 µm, deposition in the respiratory tract is dominated by thermodynamic mechanisms (i.e. diffusion) and as a result, deposition fractions are mainly dependent on the AMTD. Table A.1 therefore tabulates deposition fractions against the AMTD in this size range. For aerosols with an AMAD above approximately 0.3 µm, deposition in the respiratory tract is dominated by impaction and sedimentation, and so deposition fractions are mainly dependent on the AMAD. Therefore, in this size range, Table A.1 tabulates deposition fractions against AMAD.

A.2. Reference values for regional deposition

(A 4) Tables A.2-A.5 provide fractional deposition in each region of the respiratory tract for each Reference Individual at each exercise level (sleep, rest, light exercise and heavy exercise) as a function of aerosol size.

Fractional depositions for environmental exposure (Table A.1) are calculated as volume-weighted average values for deposition at the four exercise levels (Tables A.2-A.5). For each regional deposition *DE*:

$$DE = \sum_{i=1}^{4} w_i \, DE_i$$

where DE_i is the fractional deposition at exercise level i and the volume-weight is

$$w_j = \frac{B_j t_j}{\sum_{i=1}^{4} B_i t_i}$$

where B_i and t_i are the breathing rate and the time spent at the exercise level i. The breathing rate (m^3 h^{-1}) and the distribution of time spent (h) at each of the four reference exercise levels are given in Table 2.3 for each Reference Individual.

Deposition data contained in Tables A.1-A.5 may also be accessed by the user by using the Data Viewer.

Table A.2. Fractional deposition in regions of the respiratory tract for sleeping subjects (normal nose breathers) as a function of aerosol size[*,†].

(a) Infant 3 mo old (breathing rate = 0.09 m^3 h^{-1})

µm	ET_1	ET_2	BB	bb	AI	Total
AMTD						
0.001	5.592E-01	3.011E-01	1.168E-01	1.156E-02	1.224E-06	9.887E-01
0.003	3.616E-01	1.947E-01	2.016E-01	1.708E-01	6.617E-03	9.354E-01
0.01	1.436E-01	7.734E-02	1.012E-01	2.841E-01	1.779E-01	7.841E-01
0.03	6.122E-02	3.297E-02	4.365E-02	1.678E-01	2.972E-01	6.029E-01
0.1	4.695E-02	2.528E-02	2.299E-02	8.667E-02	1.871E-01	3.690E-01
AMAD						
0.3	8.272E-02	4.454E-02	1.636E-02	5.821E-02	1.394E-01	3.412E-01
1	2.718E-01	1.464E-01	1.040E-02	2.464E-02	8.720E-02	5.404E-01
3	4.621E-01	2.488E-01	1.002E-02	1.242E-02	5.332E-02	7.867E-01
5	4.993E-01	2.688E-01	9.121E-03	8.574E-03	3.490E-02	8.207E-01
10	4.854E-01	2.613E-01	6.523E-03	4.276E-03	1.475E-02	7.723E-01
20	4.286E-01	2.308E-01	3.511E-03	1.563E-03	4.318E-03	6.688E-01

(b) Infant 1 y old (breathing rate = 0.15 m^3 h^{-1})

µm	ET1	ET2	BB	bb	AI	Total
AMTD						
0.001	5.528E-01	2.977E-01	1.139E-01	2.268E-02	1.479E-05	9.871E-01
0.003	3.527E-01	1.900E-01	1.676E-01	2.065E-01	1.658E-02	9.334E-01
0.01	1.387E-01	7.470E-02	7.788E-02	2.657E-01	2.491E-01	8.061E-01
0.03	5.973E-02	3.216E-02	3.345E-02	1.480E-01	3.604E-01	6.337E-01
0.1	4.511E-02	2.429E-02	1.761E-02	7.484E-02	2.179E-01	3.797E-01
AMAD						
0.3	7.864E-02	4.234E-02	1.277E-02	4.989E-02	1.619E-01	3.455E-01
1	2.622E-01	1.412E-01	9.810E-03	2.153E-02	1.052E-01	5.399E-01
3	4.537E-01	2.443E-01	1.103E-02	1.181E-02	6.665E-02	7.875E-01
5	4.934E-01	2.657E-01	1.030E-02	8.493E-03	4.397E-02	8.219E-01
10	4.827E-01	2.599E-01	7.442E-03	4.414E-03	1.866E-02	7.731E-01
20	4.277E-01	2.304E-01	3.999E-03	1.657E-03	5.448E-03	6.692E-01

7056
7057 (c) Child 5 y old (breathing rate = 0.12 m^3 h^{-1})

µm	ET1	ET2	BB	bb	AI	Total
AMTD						
0.001	5.503E-01	2.963E-01	1.045E-01	3.271E-02	4.233E-05	9.838E-01
0.003	3.493E-01	1.881E-01	1.395E-01	2.254E-01	2.418E-02	9.264E-01
0.01	1.371E-01	7.383E-02	6.226E-02	2.560E-01	2.817E-01	8.109E-01
0.03	6.120E-02	3.296E-02	2.758E-02	1.443E-01	3.505E-01	6.165E-01
0.1	3.869E-02	2.083E-02	1.448E-02	7.211E-02	1.984E-01	3.445E-01
AMAD						
0.3	5.667E-02	3.051E-02	1.051E-02	4.826E-02	1.498E-01	2.957E-01
1	2.001E-01	1.077E-01	9.099E-03	2.426E-02	1.199E-01	4.611E-01
3	3.942E-01	2.122E-01	1.248E-02	1.795E-02	9.449E-02	7.313E-01
5	4.497E-01	2.422E-01	1.261E-02	1.439E-02	6.765E-02	7.865E-01
10	4.609E-01	2.482E-01	1.001E-02	8.373E-03	3.168E-02	7.592E-01
20	4.198E-01	2.261E-01	5.849E-03	3.446E-03	1.011E-02	6.653E-01

7058
7059 (d) Child 10 y old (breathing rate = 0.31 m^3 h^{-1})

µm	ET1	ET2	BB	bb	AI	Total
AMTD						
0.001	5.493E-01	2.958E-01	1.004E-01	3.685E-02	5.550E-05	9.824E-01
0.003	3.481E-01	1.874E-01	1.295E-01	2.321E-01	2.668E-02	9.237E-01
0.01	1.366E-01	7.355E-02	5.704E-02	2.545E-01	2.906E-01	8.123E-01
0.03	6.169E-02	3.322E-02	2.551E-02	1.442E-01	3.449E-01	6.095E-01
0.1	3.593E-02	1.935E-02	1.336E-02	7.177E-02	1.919E-01	3.323E-01
AMAD						
0.3	4.609E-02	2.482E-02	9.649E-03	4.841E-02	1.466E-01	2.756E-01
1	1.630E-01	8.775E-02	8.594E-03	2.758E-02	1.309E-01	4.178E-01
3	3.508E-01	1.889E-01	1.312E-02	2.436E-02	1.156E-01	6.928E-01
5	4.149E-01	2.234E-01	1.395E-02	2.065E-02	8.679E-02	7.597E-01
10	4.417E-01	2.379E-01	1.181E-02	1.276E-02	4.318E-02	7.473E-01
20	4.121E-01	2.218E-01	7.334E-03	5.529E-03	1.459E-02	6.614E-01

7060
7061 (e) 15 y male (breathing rate = 0.42 m^3 h^{-1})

µm	ET1	ET2	BB	bb	AI	Total
AMTD						
0.001	5.470E-01	2.945E-01	9.608E-02	4.267E-02	9.551E-05	9.803E-01
0.003	3.449E-01	1.857E-01	1.182E-01	2.376E-01	3.199E-02	9.184E-01
0.01	1.351E-01	7.275E-02	5.110E-02	2.450E-01	3.030E-01	8.069E-01
0.03	6.179E-02	3.328E-02	2.307E-02	1.383E-01	3.379E-01	5.943E-01
0.1	3.444E-02	1.855E-02	1.203E-02	6.836E-02	1.836E-01	3.170E-01
AMAD						
0.3	4.027E-02	2.168E-02	8.691E-03	4.644E-02	1.401E-01	2.572E-01
1	1.398E-01	7.528E-02	8.216E-03	2.983E-02	1.319E-01	3.850E-01
3	3.202E-01	1.724E-01	1.382E-02	3.019E-02	1.255E-01	6.622E-01
5	3.888E-01	2.093E-01	1.525E-02	2.659E-02	9.751E-02	7.375E-01
10	4.260E-01	2.294E-01	1.352E-02	1.708E-02	5.075E-02	7.367E-01
20	4.053E-01	2.182E-01	8.732E-03	7.658E-03	1.790E-02	6.578E-01

7062
7063 (f) 20 y (male) (breathing rate = 0.45 m^3 h^{-1})

µm	ET1	ET2	BB	bb	AI	Total

AMTD						
0.001	5.463E-01	2.942E-01	9.632E-02	4.523E-02	9.859E-05	9.821E-01
0.003	3.441E-01	1.853E-01	1.172E-01	2.468E-01	3.317E-02	9.266E-01
0.01	1.345E-01	7.241E-02	5.036E-02	2.525E-01	3.164E-01	8.262E-01
0.03	6.099E-02	3.285E-02	2.252E-02	1.411E-01	3.621E-01	6.195E-01
0.1	3.385E-02	1.823E-02	1.176E-02	6.997E-02	1.994E-01	3.332E-01
AMAD						
0.3	3.903E-02	2.102E-02	8.516E-03	4.780E-02	1.529E-01	2.693E-01
1	1.350E-01	7.269E-02	8.189E-03	3.163E-02	1.448E-01	3.923E-01
3	3.133E-01	1.686E-01	1.405E-02	3.257E-02	1.381E-01	6.667E-01
5	3.828E-01	2.061E-01	1.562E-02	2.877E-02	1.073E-01	7.406E-01
10	4.224E-01	2.275E-01	1.398E-02	1.853E-02	5.592E-02	7.383E-01
20	4.038E-01	2.174E-01	9.102E-03	8.329E-03	1.975E-02	6.584E-01

*Reference values are given to a greater degree of precision than would be chosen to reflect the certainty with which the average value of each parameter is known.

†The particles are assumed to have density 3.00 g cm^{-3}, and shape factor 1.5 (typical of compact, irregular, i.e. non-spherical particles). The particle diameters are assumed to be log-normally distributed with geometric standard deviation, σ_g increasing from a value of 1.0 at 0.6 nm to a value of 2.5 above approximately 1 μm [*Publication 66* (ICRP, 1994), Paragraph 170]. The value of σ_g is not a reference value, but is derived from the corresponding AMTD (ICRP, 1994).

Table A.3. Fractional deposition in regions of the respiratory tract for resting (sitting) subjects (normal nose breathers) as a function of aerosol size.*

(a) Infant 1 y old (breathing rate = 0.22 m^3 h^{-1})

μm	ET1	ET2	BB	bb	AI	Total
AMTD						
0.001	5.448E-01	2.934E-01	1.147E-01	3.566E-02	8.444E-05	9.887E-01
0.003	3.420E-01	1.842E-01	1.494E-01	2.353E-01	3.193E-02	9.428E-01
0.01	1.329E-01	7.155E-02	6.556E-02	2.515E-01	3.196E-01	8.411E-01
0.03	5.717E-02	3.078E-02	2.783E-02	1.329E-01	4.269E-01	6.755E-01
0.1	5.153E-02	2.775E-02	1.467E-02	6.600E-02	2.532E-01	4.131E-01
AMAD						
0.3	9.833E-02	5.295E-02	1.102E-02	4.338E-02	1.842E-01	3.899E-01
1	3.065E-01	1.650E-01	1.019E-02	1.731E-02	1.065E-01	6.055E-01
3	4.881E-01	2.628E-01	1.150E-02	8.392E-03	5.858E-02	8.294E-01
5	5.165E-01	2.782E-01	1.028E-02	5.737E-03	3.638E-02	8.471E-01
10	4.930E-01	2.654E-01	6.913E-03	2.807E-03	1.428E-02	7.824E-01
20	4.312E-01	2.322E-01	3.440E-03	9.896E-04	3.861E-03	6.717E-01

(b) Child 5 y old (breathing rate = 0.32 m^3 h^{-1})

μm	ET1	ET2	BB	bb	AI	Total
AMTD						
0.001	5.442E-01	2.930E-01	1.033E-01	4.426E-02	1.465E-04	9.849E-01
0.003	3.413E-01	1.838E-01	1.265E-01	2.439E-01	3.834E-02	9.337E-01
0.01	1.328E-01	7.152E-02	5.426E-02	2.428E-01	3.331E-01	8.345E-01
0.03	5.961E-02	3.209E-02	2.399E-02	1.326E-01	3.864E-01	6.347E-01
0.1	4.118E-02	2.217E-02	1.261E-02	6.541E-02	2.141E-01	3.555E-01
AMAD						
0.3	6.676E-02	3.594E-02	9.420E-03	4.332E-02	1.589E-01	3.143E-01
1	2.313E-01	1.245E-01	9.661E-03	2.050E-02	1.172E-01	5.032E-01

3	4.258E-01	2.293E-01	1.331E-02	1.397E-02	8.445E-02	7.668E-01
5	4.734E-01	2.549E-01	1.297E-02	1.085E-02	5.814E-02	8.103E-01
10	4.731E-01	2.547E-01	9.724E-03	6.063E-03	2.584E-02	7.694E-01
20	4.243E-01	2.285E-01	5.349E-03	2.386E-03	7.826E-03	6.683E-01

(c) Child 10 y old (breathing rate = 0.38 m^3 h^{-1})

µm	ET1	ET2	BB	bb	AI	Total
AMTD						
0.001	5.450E-01	2.935E-01	9.875E-02	4.511E-02	1.341E-04	9.825E-01
0.003	3.424E-01	1.844E-01	1.198E-01	2.429E-01	3.663E-02	9.261E-01
0.01	1.337E-01	7.198E-02	5.142E-02	2.429E-01	3.215E-01	8.215E-01
0.03	6.099E-02	3.285E-02	2.313E-02	1.355E-01	3.563E-01	6.087E-01
0.1	3.707E-02	1.996E-02	1.208E-02	6.666E-02	1.934E-01	3.292E-01
0.3	5.147E-02	2.772E-02	8.890E-03	4.454E-02	1.456E-01	2.782E-01
1	1.835E-01	9.881E-02	9.030E-03	2.413E-02	1.234E-01	4.389E-01
3	3.758E-01	2.023E-01	1.392E-02	2.018E-02	1.036E-01	7.158E-01
5	4.352E-01	2.344E-01	1.442E-02	1.677E-02	7.601E-02	7.768E-01
10	4.530E-01	2.440E-01	1.171E-02	1.008E-02	3.667E-02	7.555E-01
20	4.166E-01	2.243E-01	6.952E-03	4.236E-03	1.201E-02	6.641E-01

(d) 15 y male (breathing rate = 0.48 m^3 h^{-1})

µm	ET1	ET2	BB	bb	AI	Total
AMTD						
0.001	5.441E-01	2.930E-01	9.487E-02	4.837E-02	1.662E-04	9.805E-01
0.003	3.412E-01	1.837E-01	1.122E-01	2.442E-01	3.912E-02	9.204E-01
0.01	1.332E-01	7.174E-02	4.778E-02	2.377E-01	3.236E-01	8.140E-01
0.03	6.131E-02	3.302E-02	2.163E-02	1.328E-01	3.461E-01	5.948E-01
0.1	3.489E-02	1.879E-02	1.127E-02	6.516E-02	1.853E-01	3.154E-01
AMAD						
0.3	4.298E-02	2.315E-02	8.237E-03	4.396E-02	1.402E-01	2.585E-01
1	1.519E-01	8.180E-02	8.542E-03	2.718E-02	1.281E-01	3.975E-01
3	3.368E-01	1.814E-01	1.446E-02	2.658E-02	1.183E-01	6.775E-01
5	4.031E-01	2.170E-01	1.569E-02	2.314E-02	9.060E-02	7.496E-01
10	4.346E-01	2.340E-01	1.353E-02	1.461E-02	4.626E-02	7.430E-01
20	4.090E-01	2.202E-01	8.481E-03	6.423E-03	1.600E-02	6.601E-01

(e) 20 y (male) (breathing rate = 0.54 m^3 h^{-1})

µm	ET1	ET2	BB	bb	AI	Total
AMTD						
0.001	5.424E-01	2.921E-01	9.541E-02	5.381E-02	2.054E-04	9.839E-01
0.003	3.390E-01	1.826E-01	1.104E-01	2.591E-01	4.395E-02	9.351E-01
0.01	1.317E-01	7.093E-02	4.638E-02	2.454E-01	3.541E-01	8.485E-01
0.03	5.963E-02	3.210E-02	2.060E-02	1.338E-01	3.953E-01	6.414E-01
0.1	3.411E-02	1.837E-02	1.077E-02	6.594E-02	2.170E-01	3.462E-01
AMAD						
0.3	4.231E-02	2.279E-02	7.949E-03	4.469E-02	1.656E-01	2.833E-01
1	1.502E-01	8.088E-02	8.673E-03	2.800E-02	1.509E-01	4.187E-01
3	3.343E-01	1.801E-01	1.497E-02	2.734E-02	1.369E-01	6.936E-01
5	4.011E-01	2.159E-01	1.626E-02	2.373E-02	1.040E-01	7.610E-01
10	4.336E-01	2.335E-01	1.402E-02	1.493E-02	5.244E-02	7.485E-01

20	4.087E-01	2.200E-01	8.780E-03	6.540E-03	1.793E-02	6.620E-01

*See notes of Table A.2.

Table A.4. Fractional deposition in regions of the respiratory tract for subjects (normal nose breathers) engaged in light exercise as a function of aerosol size.*

(a) Infant 3 mo old (breathing rate = 0.19 $m^3 h^{-1}$)

µm	ET_1	ET_2	BB	bb	AI	Total
AMTD						
0.001	5.437E-01	2.928E-01	1.209E-01	3.236E-02	6.438E-05	9.899E-01
0.003	3.406E-01	1.835E-01	1.609E-01	2.312E-01	2.867E-02	9.448E-01
0.01	1.321E-01	7.115E-02	7.123E-02	2.553E-01	3.039E-01	8.337E-01
0.03	5.685E-02	3.061E-02	3.025E-02	1.358E-01	4.107E-01	6.642E-01
0.1	6.384E-02	3.437E-02	1.592E-02	6.724E-02	2.419E-01	4.233E-01
AMAD						
0.3	1.280E-01	6.893E-02	1.196E-02	4.366E-02	1.710E-01	4.235E-01
1	3.605E-01	1.941E-01	1.043E-02	1.563E-02	8.380E-02	6.645E-01
3	5.239E-01	2.821E-01	1.044E-02	6.057E-03	3.853E-02	8.610E-01
5	5.388E-01	2.901E-01	8.813E-03	3.759E-03	2.242E-02	8.639E-01
10	5.020E-01	2.703E-01	5.507E-03	1.656E-03	8.170E-03	7.877E-01
20	4.340E-01	2.337E-01	2.554E-03	5.350E-04	2.072E-03	6.728E-01

(b) Infant 1 y old (breathing rate = 0.35 $m^3 h^{-1}$)

µm	ET1	ET2	BB	bb	AI	Total
AMTD						
0.001	5.346E-01	2.879E-01	1.103E-01	5.497E-02	4.734E-04	9.882E-01
0.003	3.292E-01	1.773E-01	1.255E-01	2.534E-01	5.889E-02	9.442E-01
0.01	1.262E-01	6.796E-02	5.181E-02	2.218E-01	3.872E-01	8.550E-01
0.03	5.550E-02	2.988E-02	2.223E-02	1.138E-01	4.504E-01	6.718E-01
0.1	6.452E-02	3.474E-02	1.185E-02	5.530E-02	2.506E-01	4.170E-01
AMAD						
0.3	1.301E-01	7.007E-02	9.604E-03	3.558E-02	1.746E-01	4.200E-01
1	3.638E-01	1.959E-01	1.102E-02	1.297E-02	8.521E-02	6.689E-01
3	5.256E-01	2.830E-01	1.184E-02	5.564E-03	3.927E-02	8.652E-01
5	5.397E-01	2.906E-01	9.950E-03	3.613E-03	2.271E-02	8.666E-01
10	5.024E-01	2.705E-01	6.093E-03	1.647E-03	8.149E-03	7.888E-01
20	4.341E-01	2.338E-01	2.749E-03	5.348E-04	2.018E-03	6.732E-01

(c) Child 5 y old (breathing rate = 0.57 $m^3 h^{-1}$)

µm	ET1	ET2	BB	bb	AI	Total
AMTD						
0.001	5.314E-01	2.862E-01	9.418E-02	7.011E-02	1.094E-03	9.830E-01
0.003	3.253E-01	1.752E-01	9.832E-02	2.546E-01	7.718E-02	9.306E-01
0.01	1.254E-01	6.755E-02	3.974E-02	2.025E-01	4.005E-01	8.357E-01
0.03	5.884E-02	3.168E-02	1.816E-02	1.087E-01	3.738E-01	5.912E-01
0.1	5.104E-02	2.748E-02	9.586E-03	5.177E-02	1.890E-01	3.289E-01
AMAD						
0.3	9.586E-02	5.161E-02	7.970E-03	3.342E-02	1.324E-01	3.213E-01
1	3.023E-01	1.628E-01	1.133E-02	1.432E-02	7.981E-02	5.706E-01
3	4.859E-01	2.616E-01	1.462E-02	8.696E-03	4.782E-02	8.187E-01

5	5.151E-01	2.774E-01	1.314E-02	6.420E-03	3.052E-02	8.425E-01
10	4.922E-01	2.650E-01	8.718E-03	3.315E-03	1.229E-02	7.816E-01
20	4.308E-01	2.320E-01	4.225E-03	1.184E-03	3.367E-03	6.715E-01

(d) Child 10 y old (breathing rate = 1.12 m^3 h^{-1})

µm	ET1	ET2	BB	bb	AI	Total
AMTD						
0.001	5.207E-01	2.804E-01	8.256E-02	9.667E-02	3.759E-03	9.840E-01
0.003	3.126E-01	1.683E-01	7.680E-02	2.598E-01	1.229E-01	9.405E-01
0.01	1.199E-01	6.455E-02	2.981E-02	1.789E-01	4.705E-01	8.636E-01
0.03	5.732E-02	3.086E-02	1.376E-02	9.407E-02	3.929E-01	5.889E-01
0.1	5.136E-02	2.766E-02	7.428E-03	4.392E-02	1.915E-01	3.219E-01
AMAD						
0.3	9.819E-02	5.288E-02	7.028E-03	2.820E-02	1.328E-01	3.191E-01
1	3.076E-01	1.656E-01	1.304E-02	1.269E-02	7.971E-02	5.787E-01
3	4.895E-01	2.636E-01	1.712E-02	8.401E-03	4.720E-02	8.259E-01
5	5.174E-01	2.786E-01	1.517E-02	6.297E-03	2.978E-02	8.472E-01
10	4.931E-01	2.655E-01	9.793E-03	3.240E-03	1.174E-02	7.834E-01
20	4.311E-01	2.322E-01	4.590E-03	1.132E-03	3.132E-03	6.721E-01

(e) 15 y male (breathing rate = 1.38 m^3 h^{-1})

µm	ET1	ET2	BB	bb	AI	Total
AMTD						
0.001	5.203E-01	2.802E-01	7.953E-02	9.987E-02	4.032E-03	9.839E-01
0.003	3.122E-01	1.681E-01	7.319E-02	2.615E-01	1.266E-01	9.416E-01
0.01	1.196E-01	6.439E-02	2.827E-02	1.780E-01	4.783E-01	8.685E-01
0.03	5.707E-02	3.073E-02	1.303E-02	9.329E-02	4.002E-01	5.943E-01
0.1	4.387E-02	2.363E-02	6.966E-03	4.369E-02	1.962E-01	3.144E-01
AMAD						
0.3	7.840E-02	4.221E-02	6.487E-03	2.838E-02	1.387E-01	2.942E-01
1	2.644E-01	1.424E-01	1.287E-02	1.437E-02	9.368E-02	5.277E-01
3	4.560E-01	2.456E-01	1.883E-02	1.111E-02	6.304E-02	7.946E-01
5	4.949E-01	2.665E-01	1.751E-02	8.740E-03	4.191E-02	8.296E-01
10	4.831E-01	2.601E-01	1.201E-02	4.750E-03	1.766E-02	7.776E-01
20	4.277E-01	2.304E-01	5.967E-03	1.749E-03	5.019E-03	6.708E-01

(f) 20 y (male) (breathing rate = 1.50 m^3 h^{-1})

µm	ET1	ET2	BB	bb	AI	Total
AMTD						
0.001	5.192E-01	2.796E-01	7.855E-02	1.037E-01	4.225E-03	9.852E-01
0.003	3.110E-01	1.674E-01	7.156E-02	2.670E-01	1.302E-01	9.472E-01
0.01	1.187E-01	6.393E-02	2.745E-02	1.799E-01	4.909E-01	8.808E-01
0.03	5.638E-02	3.036E-02	1.258E-02	9.370E-02	4.167E-01	6.097E-01
0.1	4.302E-02	2.317E-02	6.758E-03	4.399E-02	2.057E-01	3.226E-01
AMAD						
0.3	7.657E-02	4.123E-02	6.378E-03	2.864E-02	1.458E-01	2.986E-01
1	2.601E-01	1.401E-01	1.304E-02	1.465E-02	9.938E-02	5.272E-01
3	4.523E-01	2.435E-01	1.930E-02	1.138E-02	6.733E-02	7.938E-01
5	4.923E-01	2.650E-01	1.801E-02	8.949E-03	4.488E-02	8.292E-01
10	4.819E-01	2.595E-01	1.241E-02	4.858E-03	1.897E-02	7.777E-01
20	4.273E-01	2.301E-01	6.185E-03	1.789E-03	5.411E-03	6.707E-01

*See notes of Table A.2.

Table A.5. Fractional deposition in regions of the respiratory tract for subjects (normal nose augmenters) engaged in heavy exercise as a function of aerosol size.*

(a) 15 y male (breathing rate = 2.92 m^3 h^{-1})

µm	ET1	ET2	BB	bb	AI	Total
AMTD						
0.001	2.595E-01	3.966E-01	9.724E-02	1.973E-01	2.480E-02	9.754E-01
0.003	1.553E-01	2.048E-01	6.013E-02	2.737E-01	2.438E-01	9.378E-01
0.01	6.096E-02	7.557E-02	2.024E-02	1.434E-01	5.593E-01	8.595E-01
0.03	3.016E-02	3.733E-02	9.265E-03	7.183E-02	3.800E-01	5.286E-01
0.1	2.305E-02	2.285E-02	6.018E-03	3.240E-02	1.738E-01	2.581E-01
AMAD						
0.3	4.110E-02	3.111E-02	1.057E-02	2.148E-02	1.216E-01	2.259E-01
1	1.357E-01	1.084E-01	5.116E-02	1.902E-02	9.600E-02	4.103E-01
3	2.303E-01	2.558E-01	1.045E-01	2.661E-02	8.106E-02	6.983E-01
5	2.488E-01	3.270E-01	1.078E-01	2.405E-02	5.873E-02	7.663E-01
10	2.421E-01	3.883E-01	8.098E-02	1.439E-02	2.697E-02	7.527E-01
20	2.140E-01	3.954E-01	4.131E-02	5.398E-03	8.026E-03	6.641E-01

(b) 20 y (male) (breathing rate = 3.0 m^3 h^{-1})

µm	ET1	ET2	BB	bb	AI	Total
AMTD						
0.001	2.596E-01	3.970E-01	9.953E-02	2.016E-01	2.274E-02	9.805E-01
0.003	1.555E-01	2.050E-01	6.173E-02	2.867E-01	2.409E-01	9.498E-01
0.01	6.013E-02	7.447E-02	2.043E-02	1.488E-01	5.862E-01	8.900E-01
0.03	2.927E-02	3.621E-02	9.213E-03	7.383E-02	4.276E-01	5.761E-01
0.1	2.194E-02	2.200E-02	5.938E-03	3.375E-02	2.012E-01	2.848E-01
AMAD						
0.3	3.855E-02	2.930E-02	1.018E-02	2.243E-02	1.428E-01	2.433E-01
1	1.297E-01	1.017E-01	4.985E-02	1.925E-02	1.158E-01	4.163E-01
3	2.251E-01	2.442E-01	1.052E-01	2.658E-02	9.953E-02	7.006E-01
5	2.452E-01	3.152E-01	1.104E-01	2.414E-02	7.279E-02	7.678E-01
10	2.405E-01	3.793E-01	8.502E-02	1.463E-02	3.393E-02	7.533E-01
20	2.135E-01	3.906E-01	4.444E-02	5.586E-03	1.028E-02	6.644E-01

*See notes of Table A.2.

A.3. Progeny radionuclides formed in the respiratory tract

(A 5) As noted in Section 3.3.1 of the Main Text, many issues relating to the behaviour of progeny in the respiratory tract arise in connection with the natural decay series, which are therefore shown in Figs. A.1 (uranium-238 series), A.2 (uranium-235 series) and A.3 (thorium-232 series).

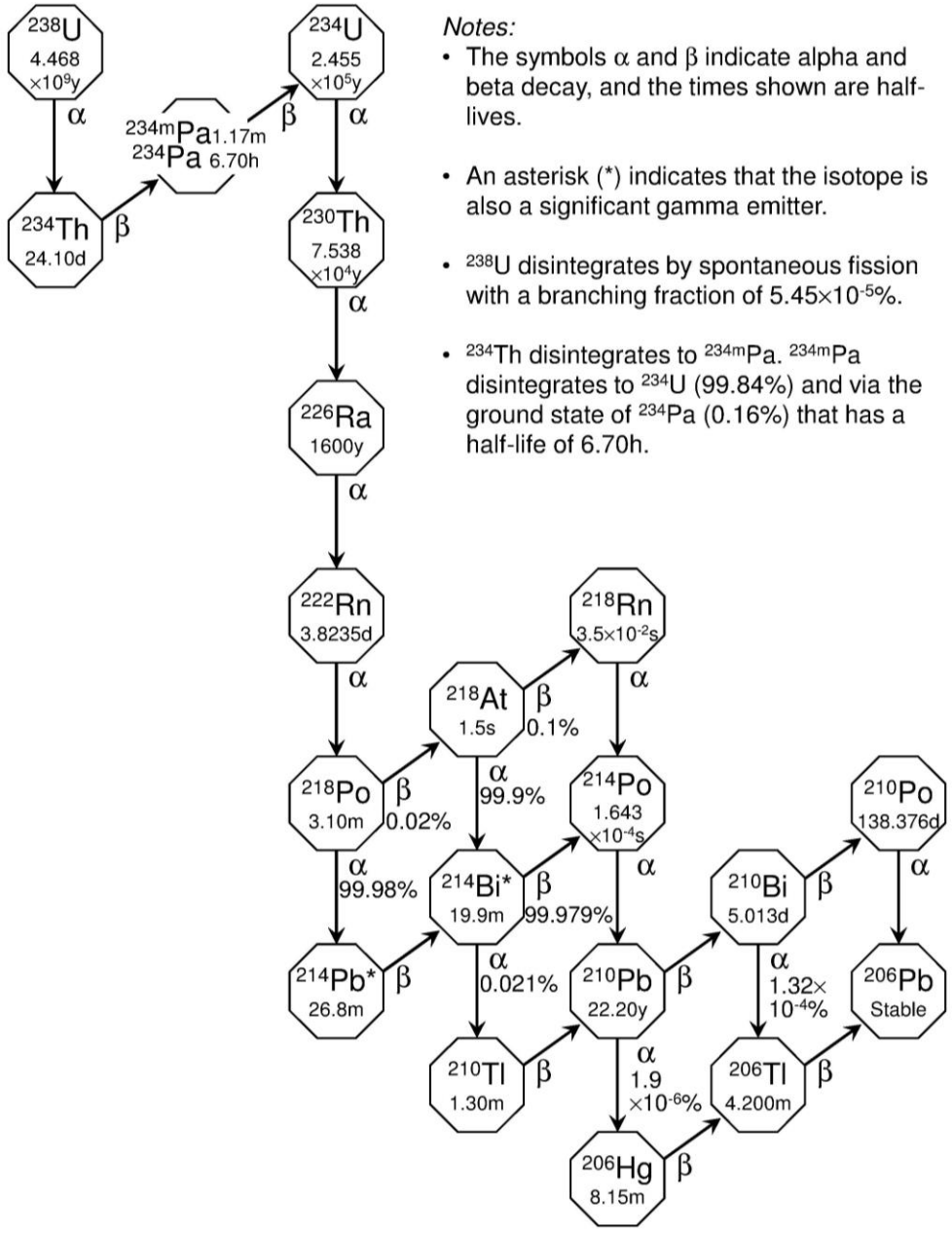

Fig. A.1. Natural decay series: Uranium-238 (ICRP, 2008).

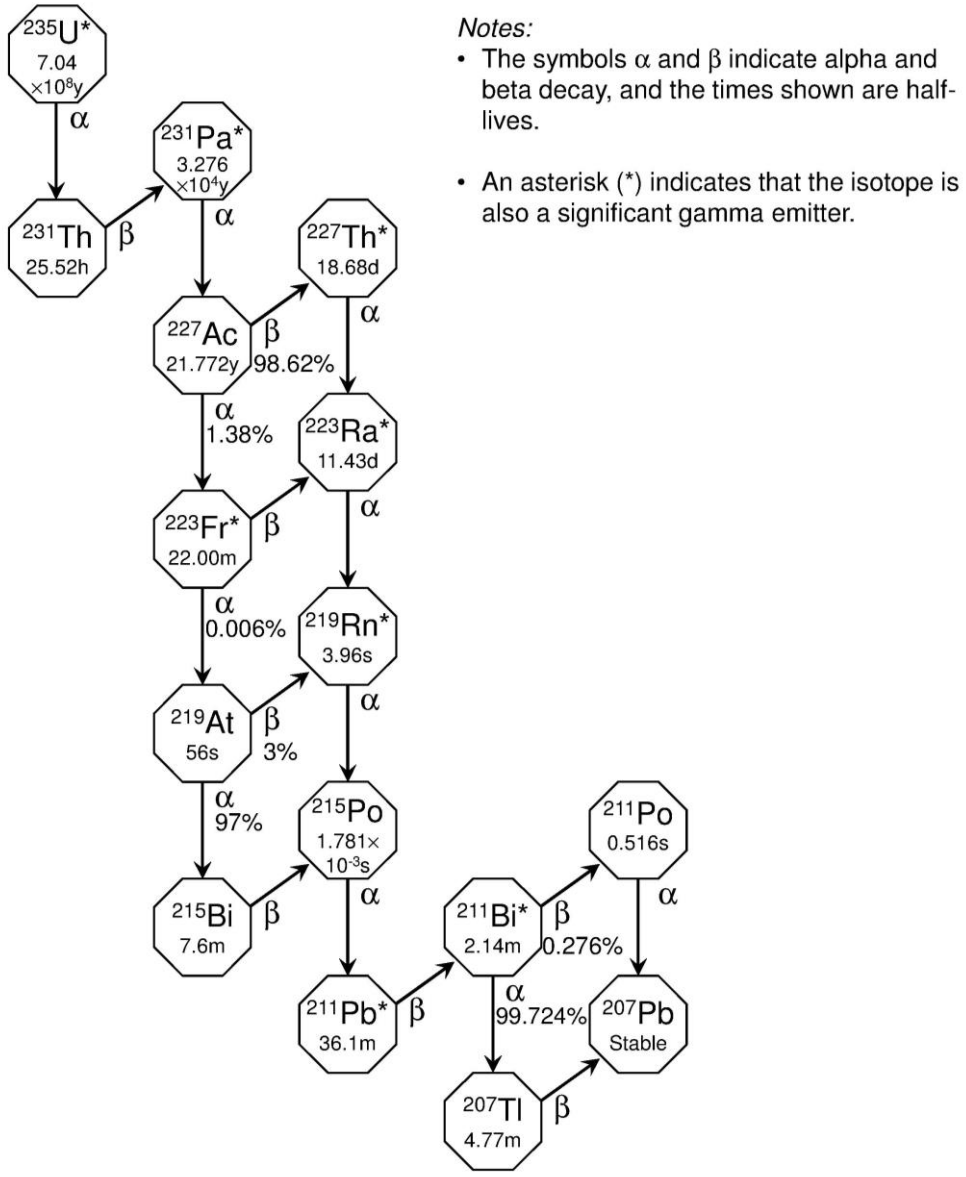

Fig. A.2. Natural decay series: Uranium-235 (ICRP, 2008).

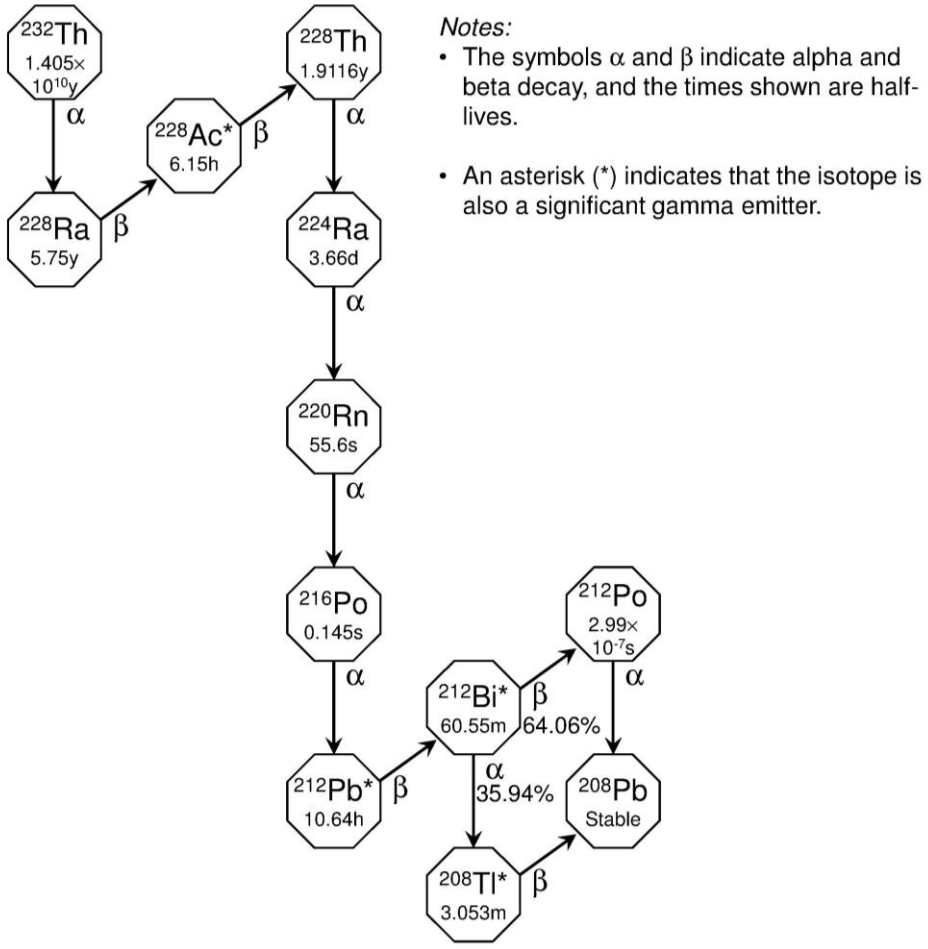

Fig. A.3. Natural decay series: Thorium-232 (ICRP, 2008).

A.4. References

ICRP, 1994. Human respiratory tract model for radiological protection. ICRP Publication 66. Ann. ICRP 24(1–3).

ICRP, 2008. Nuclear Decay Data for Dosimetric Calculations. ICRP Publication 107. Ann. ICRP 38(3).

ANNEX B. EVOLUTION OF ICRP'S SYSTEMIC BIOKINETIC MODELS

B.1. Formulation of systemic models in modern ICRP reports

(B 1) *Publication 30* (ICRP, 1979, 1980, 1981, 1988) provided a comprehensive set of systemic biokinetic models for radionuclides commonly encountered in occupational settings. The models were generally in the form of retention functions (e.g. sums of exponential terms) that may be interpreted as first-order compartmental models with one-directional flow. These models were designed mainly to estimate the cumulative activities of each radionuclide in its main repositories in the body. They do not depict realistic paths of movement of radionuclides in the body, but describe only the initial distribution of elements after uptake to blood and the net biological half-times of elements in source organs. Activity absorbed from the gastrointestinal or respiratory tract or through wounds is assumed to enter a transfer compartment, from which it transfers to source organs with a specified half-time, typically 0.25 d or longer. Retention in a source organ is usually described in terms of one to three first-order retention components, with multiple biological half-times representing retention in multiple hypothetical compartments within a source organ. Feedback of activity from tissues to blood is not treated explicitly in *Publication 30* with the exception of the model for iodine (ICRP, 1979). It is generally assumed that activity leaving an organ moves directly to a collective excretion compartment, i.e. radioactive decay along actual routes of excretion is not assessed. Relatively short-lived radionuclides (half-lives up to 15 d) depositing in bone are generally assigned to bone surface, and longer-lived radionuclides are assigned either to bone surface or bone volume, depending on their main sites of retention in bone as indicated by available data.

(B 2) The systemic biokinetic models of the *Publication 30* series (ICRP, 1979, 1980, 1981, 1988) were intended primarily for calculation of dose per intake coefficients for planning purposes rather than for retrospective evaluation of doses. For some elements, these systemic biokinetic models were developed separately from ICRP's concurrent bioassay models. For example, urinary and faecal excretion models for plutonium, americium, and curium recommended in *Publication 54* (ICRP, 1989) were derived independently of the concurrent systemic biokinetic model for these elements, shown in Fig. B.1.

(B 3) A series of ICRP reports on doses to members of the public from intake of radionuclides (ICRP, 1990, 1993, 1995a,b,c, 2001, 2004) provide age-specific systemic biokinetic models for selected radioisotopes of 31 elements: hydrogen, carbon, sulphur, calcium, iron, cobalt, nickel, zinc, selenium, strontium, zirconium, niobium, molybdenum, technetium, ruthenium, silver, antimony, tellurium, iodine, caesium, barium, cerium, lead, polonium, radium, thorium, uranium, neptunium, plutonium, americium and curium. Those reports are referred to here as the *Publication 56* series, after the first document in the series (ICRP, 1990). Most of the systemic biokinetic models in the *Publication 56* series (ICRP, 1990, 1993, 1995a,b,c) follow the same modelling scheme as applied in the *Publication 30* series (ICRP, 1979, 1980, 1981, 1988) and illustrated in Fig. B.1, except that explicit excretion pathways are included in reports completed after the issue of *Publication 60* (ICRP 1991). These pathways are included to allow the assessment of doses to the urinary bladder and colon, both of which are assigned tissue weighting factors in *Publication 60* (ICRP, 1991). A different modelling scheme involving more realistic paths of movement of systemic radionuclides is applied in the *Publication 56* series (ICRP, 1990, 1993, 1995a,b,c, 2001, 2004) to iron and the following 'bone-seeking' elements: calcium, strontium, barium, lead, radium, thorium,

uranium, neptunium, plutonium, americium and curium. The model structures for these elements and the structure for iodine, carried over from *Publication 30*, depict feedback of material from organs to blood and, where feasible, physiological processes that determine the biokinetics of radionuclides. Examples of such physiological processes are bone remodelling, which results in removal of plutonium or americium from bone surface, and phagocytosis of aging erythrocytes by reticuloendothelial cells, which results in transfer of iron from blood to iron storage sites.

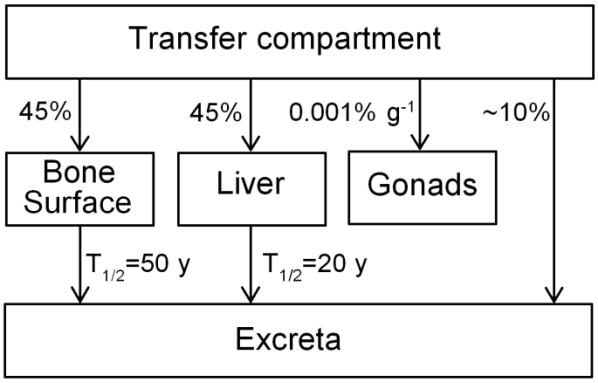

Fig. B.1. Systemic biokinetic model for plutonium, americium, and curium recommended in *Publication 30*, Part 4 (ICRP, 1988). This illustrates the one-directional flow of systemic activity depicted in models of *Publication 30* series (ICRP, 1979, 1980, 1981, 1988) and, for many radionuclides, in later ICRP documents on occupational or environmental exposure to radionuclides.

(B 4) The physiologically based modelling scheme applied in the *Publication 56* series is illustrated in Fig. B.2, which shows the generic model structure used for the actinide elements thorium, neptunium, plutonium, americium and curium. The systemic tissues and fluids are divided into five main components: blood, skeleton, liver, kidneys, and other soft tissues. Blood is treated as a uniformly mixed pool. Each of the other main components is further divided into a minimal number of compartments needed to model the available biokinetic data on these five elements or, more generally, 'bone-surface-seeking' elements. The liver is divided into compartments representing short- and long-term retention. Activity entering the liver is assigned to the short-term compartment (Liver 1), from which it may transfer back to blood, to the intestines via biliary secretion, or to the long-term compartment from which activity slowly returns to blood. The kidneys are divided into two compartments, one that loses activity to urine over a period of hours or days (Urinary path) and another that slowly returns activity to blood (other kidney tissue). The remaining soft tissue other than bone marrow is divided into compartments ST0, ST1, and ST2 representing rapid, intermediate, and slow return of activity to blood, respectively. ST0 is used to account for a rapid build-up of activity in soft tissues and rapid feedback to blood after acute input of activity to blood and is regarded as part of the activity circulating in blood. The skeleton is divided into cortical and trabecular fractions, and each of these fractions is subdivided into bone surface, bone volume, and bone marrow. Activity entering the skeleton is assigned to bone surface, from which it is transferred gradually to bone marrow and bone volume by bone remodelling processes. Activity in bone volume is transferred gradually to bone marrow by bone remodelling. Activity is lost from bone marrow to blood over a period of months and is subsequently redistributed in the same pattern as the original input to blood. The rates of transfer from cortical and trabecular bone compartments to all destinations are functions of the turnover rate of cortical and trabecular bone, assumed to

be 3% and 18% per year, respectively. Other parameter values in the model are element-specific.

(B 5) A variation of the model structure shown in Fig. B.2 was applied in the *Publication 56* series to calcium, strontium, barium, radium, lead and uranium (Fig. B.3). These elements behave differently from the bone-surface seekers addressed above in that they diffuse throughout bone volume within hours or days after depositing in bone. After reaching bone volume, these elements may migrate back to plasma (via bone surface in the model) or they may become fixed in bone volume and then gradually transfer to blood at the rate of bone remodelling. The compartments in Fig. B.2 representing bone-marrow and gonads are omitted from the model for bone-volume seekers because generally these are not sites of elevated accumulation of these elements. Some of the compartments shown in Fig. B.3 are not applicable to all bone-volume seekers. For example, the liver, kidneys and red blood cells are not important sites of accumulation of calcium and strontium but are important repositories for lead. If a particular compartment or pathway shown in Fig. B.3 is not important for a given element, it is not considered separately in the model for that element. For example, in the model for calcium, blood is treated as a single well-mixed pool, and the liver and kidneys are assumed to be part of 'Other soft tissues'.

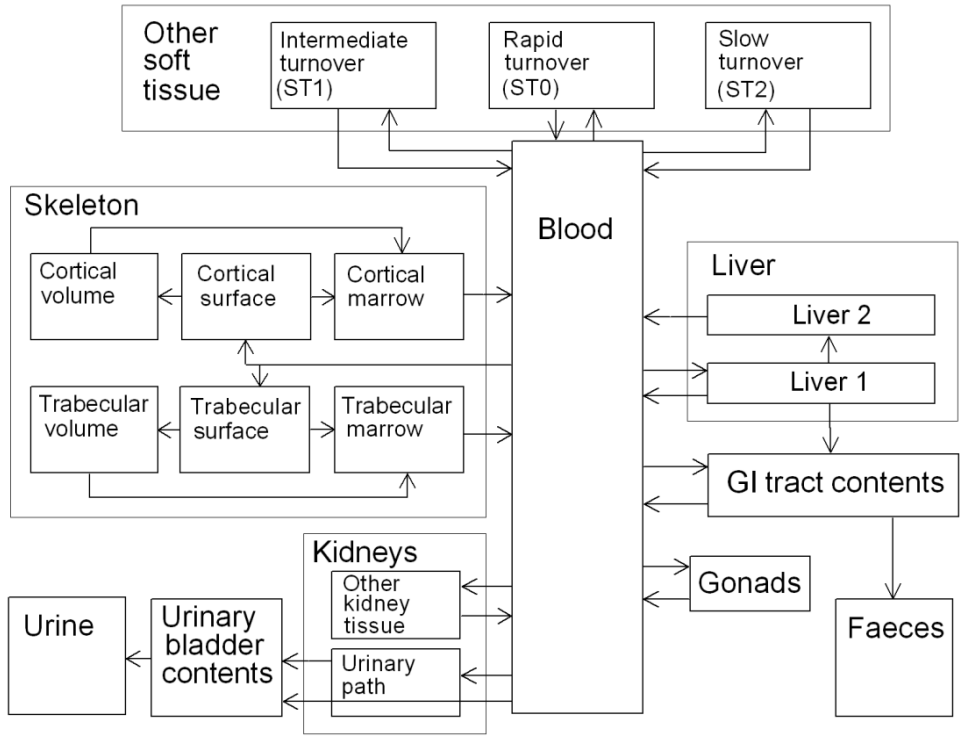

Fig. B.2. Model structure applied in the *Publication 56* series to the bone-surface seekers thorium, neptunium, plutonium, americium and curium. This structure (or its modest variations) is applied to a number of elements in this series of reports, including elements not regarded as bone-seekers. GI, gastrointestinal.

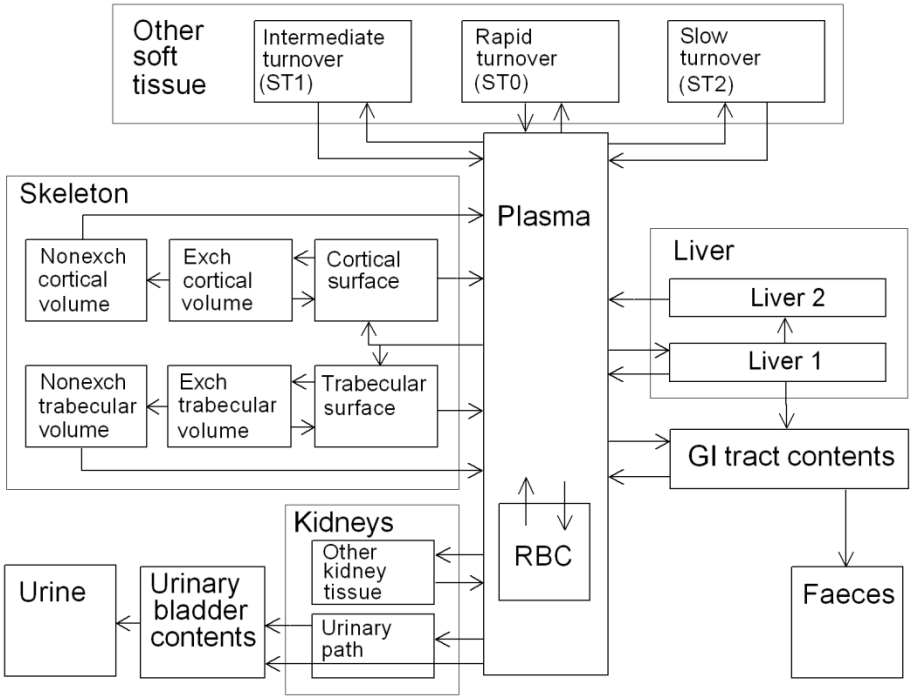

Fig. B.3. Model structure applied in the *Publication 56* series (ICRP, 1990, 1993, 1995a,b,c, 1996) to calcium, strontium, barium, lead, radium and uranium.
This structure (or modest variations of it) is applied to a number of elements in this series of reports, including elements not regarded as bone-seekers. Exch, exchangeable; Nonexch, nonexchangeable; RBC, red blood cells; GI, gastrointestinal.

(B 6) The systemic models used in Parts 2–4 of the *Publication 56* series (ICRP 1993, 1995a,b) were applied in *Publication 68* (ICRP, 1994a), along with ICRP's HRTM (ICRP, 1994b), to update dose coefficients for occupational intake of radionuclides based on recommendations in *Publication 60* (ICRP, 1991). For elements not addressed in Parts 2–4 of the *Publication 56* series (ICRP 1993, 1995a,b), the systemic biokinetic models applied in *Publication 68* (ICRP, 1994a) were taken from *Publication 30* series (ICRP, 1979, 1980, 1981, 1988) and modified to include specific excretion pathways to address doses to the urinary bladder and colon.

(B 7) The biokinetic models applied in *Publication 68* (ICRP, 1994a) were used in *Publication 78* (ICRP, 1997) to update recommendations concerning interpretation of bioassay data for workers for selected radioisotopes of 15 elements. The systemic models for nine of the 15 elements addressed in *Publication 78* (ICRP, 1997) were physiologically based models adopted in the *Publication 56* series (ICRP 1993, 1995a,b,c, 2001, 2004).

B.2. Systemic model structures used in this report series

(B 8) It is now generally recognised that the physiologically descriptive model structures introduced for selected elements in the *Publication 56* series (ICRP 1990, 1993, 1995a,b,c, 2001, 2004) have a number of potential advantages over the retention-function models traditionally used in radiation protection. For example, a physiological descriptive model structure:

- facilitates the use of physiological information and physiologically reasonable assumptions as a supplement to radiobiological data in the development of model parameter values;
- provides a basis for extrapolating beyond the radiobiological database to different subgroups of the population and to times outside the period of observation: for example, a parameter value found to depend on the rate of bone remodelling can be varied with age on the basis of age-specific data on bone remodelling rates;
- facilitates the extrapolation of biokinetic data from laboratory animals to man, in that it helps to focus interspecies comparisons on specific physiological processes and specific subsystems of the body for which extrapolation may be valid, even if whole-body extrapolations are not;
- facilitates the extrapolation of biokinetic data from an element to its chemical analogues, in that the degree of physiological similarity of chemical analogues may vary from one physiological process to another: for example, the alkaline earth elements show similar rates of transfer from blood to bone but much different rates of transfer to non-exchangeable sites in bone;
- links excretion with exchanges of activity among body tissues and fluids, so that the same model can be used for dose calculation and bioassay interpretation;
- allows modelling of the differential biokinetics of parent radionuclides and their radioactive progeny produced in the body; and
- allows the addition of compartments and pathways to the model for purposes of extending the model to new applications, as was demonstrated in the ICRP documents on doses to the embryo and fetus (ICRP, 2001) and to the nursing infant (ICRP, 2004) from intakes of radionuclides by the mother.

(B 9) On the other hand, the level of physiological realism in the systemic biokinetic models currently used in radiation protection, including those recommended in the present report, should not be overstated. Even the most sophisticated models represent a compromise between biological realism and practical considerations regarding the quantity and quality of information available to determine parameter values. For example, the recycling models applied to bone-seeking radionuclides in the *Publication 56* series all include soft-tissue compartments representing fast, intermediate, and slow exchange with blood for all soft tissues not explicitly identified in the models. These soft tissue compartments are typically defined on a kinetic basis rather than a physiological basis: i.e. the compartment sizes and turnover rates are set for reasonable consistency with data on accumulation and loss of elements by soft tissues. For some elements, these soft tissue compartments appear to be associated with specific sites or processes, but the associations are not generally confirmed by available information. For example, biokinetic studies of calcium suggest, but do not establish that: the rapid-turnover pool in soft tissues may correspond roughly to interstitial fluids plus some rapidly exchangeable cellular calcium (Harrison et al., 1968; Hart and Spencer, 1976; Heaney, 1964); the intermediate turnover rate may stem from a composite of several pools with slower exchange rates, including mitochondrial calcium, cartilage calcium and exchangeable dystrophic calcium (e.g. arterial plaque and calcified nodes) (Borle, 1981; Heaney, 1964); and long-term retention in soft tissues may be associated with relatively nonexchangeable dystrophic calcium that gradually accumulates in the human body (Heaney, 1964).

(B 10) For many elements, it is not feasible to develop genuine physiological system models due to inadequate information on the processes that determine the systemic behaviour of these elements. Even for relatively well understood elements, the model components are

7311 often intended only to represent the net result of multiple processes. For example, in the model
7312 for bone-surface-seeking radionuclides shown in Fig. B.2 and its precursors (Leggett, 1985,
7313 1992), the depiction of burial of activity in bone volume is intended to approximate the net
7314 result over time of a number of known or suspected burial processes occurring at different rates.
7315 Activity depositing in bone remodelling units, either in the formation period or in the
7316 transitional period between resorption and formation, may be buried relatively quickly.
7317 Delayed burial of surface activity may result from 'local recycling' during bone restructuring
7318 processes: that is, some of the surface activity removed by osteoclasts during bone remodelling
7319 may be redeposited almost immediately at closely adjacent sites of new bone formation that
7320 are supplied by the same blood vessels. Such local redeposition of mineral ions is thought to
7321 occur, particularly in cortical bone (Parfitt and Kleerekoper, 1980). Burial of surface deposits
7322 may also occur as a result of 'bone drift', a phenomenon in which new bone is deposited on
7323 previously formed bone without any prior resorption process. Bone drift occurs on a larger
7324 scale in immature bone than in mature bone, but drift within bones and expansion of bone
7325 volume via periostial-endosteal drift continues throughout life in humans (Epker and Frost,
7326 1965a,b; Frost 1986; Priest et al., 1992). 'Drifting osteons' are observed at all ages within
7327 human cortical bone, and their count is used in forensics for age-at-death estimation.

7328 B.3. References

7329 Borle, A.B., 1981. Control, Modulation, and regulation of cell calcium.
7330 Rev. Physiol. Biochem. Pharmacol. 90, 13–153.
7331 Epker, B.N., Frost, H.M., 1965a. Correlation of Bone Resorption and Formation with the Physical
7332 Behavior of Loaded Bone. J. Dent. Res. 44(1), 33–41.
7333 Epker, B.N., Frost, H.M., 1965b. The direction of transverse drift of actively forming osteons in human
7334 rib cortex. J. Bone Jt. Surg. 47, 1211–1215.
7335 Frost, H.M., 1986. Intermediary Organization of the Skeleton. Volumes I & II. Boca Raton, CRC Press,
7336 FL, USA.
7337 Harrison, G.E., Carr, T.E.F., Sutton, A., 1968. Distribution of radioactive calcium, strontium, barium
7338 and radium following intravenous injection into a healthy man. Int. J. Radiat. Biol. 13(3), 235–247.
7339 Hart, H.E., Spencer, H., 1976. Vascular and extravascular calcium interchange in man determined with
7340 radioactive calcium. Radiat. Res. 67(1), 149–161.
7341 Heaney, R.P., 1964. Interpretation of calcium kinetic data. In: Pearson OH and Joplin GF (eds) Dynamic
7342 Studies of Metabolic Bone Disease. Oxford, Blackwell, pp. 11–23.
7343 ICRP, 1979. Limits for intakes of radionuclides by workers, ICRP Publication 30, Part 1. Ann. ICRP
7344 2(3/4).
7345 ICRP, 1980. Limits for intakes of radionuclides by workers. ICRP Publication 30, Part 2. Ann. ICRP
7346 4(3/4).
7347 ICRP, 1981. Limits for intakes of radionuclides by workers. ICRP Publication 30, Part 3. Ann. ICRP
7348 6(2/3).
7349 ICRP, 1988. Limits for intakes of radionuclides by workers: an addendum. ICRP Publication 30, Part
7350 4. Ann. ICRP 19(4).
7351 ICRP, 1989. Individual Monitoring for Intakes of Radionuclides by Workers. ICRP Publication 54. Ann.
7352 ICRP 19(1–3).
7353 ICRP, 1990. Age-dependent Doses to Members of the Public from Intake of Radionuclides - Part 1.
7354 ICRP Publication 56. Ann. ICRP 20(2).
7355 ICRP, 1991. 1990 Recommendations of the International Commission on Radiological Protection.
7356 ICRP Publication 60. Ann. ICRP 21(1–3).
7357 ICRP, 1993. Age Dependent Doses to Members of the Public from Intake of Radionuclides: Part 2,
7358 Ingestion Dose Coefficients. ICRP Publication 67. Ann. ICRP 23(3/4).

ICRP, 1994a. Dose coefficients for intake of radionuclides by workers. ICRP Publication 68. Ann. ICRP 24(4).

ICRP, 1994b. Human respiratory tract model for radiological protection. ICRP Publication 66. Ann. ICRP 24(1–3).

ICRP, 1995a. Age-Dependent Doses to Members of the Public from Intake of Radionuclides: Part 3. Ingestion Dose Coefficients, ICRP Publication 69. Ann. ICRP 25(1).

ICRP, 1995b. Age-Dependent Doses to Members of the Public from Intake of Radionuclides: Part 4. Inhalation Dose Coefficients, ICRP Publication 71. Ann. ICRP 25(3/4).

ICRP, 1995c. Age-Dependent Doses to the Members of the Public from Intake of Radionuclides - Part 5 Compilation of Ingestion and Inhalation Coefficients. ICRP Publication 72. Ann. ICRP 26(1).

ICRP, 1997. Individual monitoring for internal exposure of workers. ICRP Publication 78. Ann. ICRP 27(3/4).

ICRP, 2001. Doses to the Embryo and Fetus from Intakes of Radionuclides by the Mother. ICRP Publication 88. Ann. ICRP 31(1-3).

ICRP, 2004. Doses to Infants from Ingestion of Radionuclides in Mothers' Milk. ICRP Publication 95. Ann ICRP 34(3-4).

Leggett, R.W., 1985. A model of the retention, translocation and excretion of systemic Pu. Health Phys. 49(6), 1115–1138.

Leggett, R.W., 1992. A generic age-specific biokinetic model for calcium-like elements. Radiat. Prot. Dosim. 41(2–4), 183–198.

Parfitt, A.M., Kleerekoper, M., 1980. The divalent ion homeostatic system: physiology and metabolism of calcium, phosphorus, magnesium and bone. In: Maxwell MH and Kleeman CR (eds) Clinical Disorders of Fluid and Electrolyte Metabolism, 3rd Edition. McGraw-Hill, New York, pp. 269–398.

Priest, N.D., Haines, J.W., Humphreys, J.A.M., et al., 1992. The bone volume effect on the dosimetry of plutonium-239 and americium-241 in the skeleton of man and baboon. J. Radioanal. Nucl. Chem. 156(1), 33–53.

ANNEX C. SUPPLEMENTARY INFORMATION RELATING TO RADON

C.1. Fractional deposition of radon and thoron progeny in the respiratory tract

(C 1) Table C.1. gives values of fractional deposition for each Reference Individual and in each region of the respiratory tract as a function of aerosol size for home exposures for radon (^{222}Rn) and thoron (^{220}Rn) progeny. The AMTD values given in Table C.1 are the reference aerosol sizes in the ambient air (Table 32.2). For the attached modes, it is assumed that the AMTD increases by the hygroscopic growth factor instantaneously as the particle enters the nose or mouth.

Table C.1. Fractional deposition in regions of the respiratory tract for inhalation of radon progeny as a function of aerosol size[*,†]

a) Infant 3 mo old (breathing rate = 0.12 $m^3\ h^{-1}$)

µm	ET_1	ET_2	BB	bb	AI	Total
AMTD						
1	5.484×10^{-1}	2.953×10^{-1}	1.184×10^{-1}	2.594×10^{-2}	1.370×10^{-4}	9.882×10^{-1}
30	4.442×10^{-2}	2.392×10^{-2}	2.818×10^{-2}	1.140×10^{-1}	2.856×10^{-1}	4.961×10^{-1}
40	3.792×10^{-2}	2.042×10^{-2}	2.344×10^{-2}	9.516×10^{-2}	2.542×10^{-1}	4.311×10^{-1}
200	9.182×10^{-2}	4.944×10^{-2}	9.035×10^{-3}	2.899×10^{-2}	9.420×10^{-2}	2.735×10^{-1}

b) Infant 1 y old (breathing rate = 0.19 $m^3\ h^{-1}$)

µm	ET_1	ET_2	BB	bb	AI	Total
AMTD						
1	5.426×10^{-1}	2.922×10^{-1}	1.117×10^{-1}	3.957×10^{-2}	4.709×10^{-4}	9.865×10^{-1}
30	4.359×10^{-2}	2.347×10^{-2}	2.203×10^{-2}	1.002×10^{-1}	3.161×10^{-1}	5.054×10^{-1}
40	3.710×10^{-2}	1.998×10^{-2}	1.832×10^{-2}	8.316×10^{-2}	2.782×10^{-1}	4.368×10^{-1}
200	8.454×10^{-2}	4.552×10^{-2}	7.318×10^{-3}	2.483×10^{-2}	1.022×10^{-1}	2.644×10^{-1}

c) Child 5 y old (breathing rate = 0.32 $m^3\ h^{-1}$)

µm	ET_1	ET_2	BB	bb	AI	Total
AMTD						
1	5.387×10^{-1}	2.901×10^{-1}	9.890×10^{-2}	5.385×10^{-2}	1.035×10^{-3}	9.826×10^{-1}
30	4.462×10^{-2}	2.403×10^{-2}	1.763×10^{-2}	9.468×10^{-2}	2.764×10^{-1}	4.574×10^{-1}
40	3.730×10^{-2}	2.009×10^{-2}	1.464×10^{-2}	7.813×10^{-2}	2.368×10^{-1}	3.870×10^{-1}
200	5.797×10^{-2}	3.121×10^{-2}	5.803×10^{-3}	2.280×10^{-2}	8.626×10^{-2}	2.040×10^{-1}

d) Child 10 y old (breathing rate = 0.56 $m^3\ h^{-1}$)

µm	ET_1	ET_2	BB	bb	AI	Total
AMTD						
1	5.285×10^{-1}	2.846×10^{-1}	8.812×10^{-2}	7.748×10^{-2}	3.719×10^{-3}	9.824×10^{-1}
30	4.380×10^{-2}	2.359×10^{-2}	1.369×10^{-2}	8.264×10^{-2}	2.768×10^{-1}	4.405×10^{-1}
40	3.676×10^{-2}	1.979×10^{-2}	1.135×10^{-2}	6.777×10^{-2}	2.330×10^{-1}	3.687×10^{-1}
200	6.311×10^{-2}	3.398×10^{-2}	5.085×10^{-3}	1.931×10^{-2}	8.137×10^{-2}	2.029×10^{-1}

e) 15 y male (breathing rate = 0.63 $m^3\ h^{-1}$)

µm	ET_1	ET_2	BB	bb	AI	Total

AMTD						
1	5.310×10^{-1}	2.860×10^{-1}	8.690×10^{-2}	7.389×10^{-2}	3.128×10^{-3}	9.809×10^{-1}
30	4.398×10^{-2}	2.368×10^{-2}	1.370×10^{-2}	8.528×10^{-2}	2.720×10^{-1}	4.386×10^{-1}
40	3.647×10^{-2}	1.964×10^{-2}	1.136×10^{-2}	6.999×10^{-2}	2.293×10^{-1}	3.668×10^{-1}
200	4.299×10^{-2}	2.315×10^{-2}	4.693×10^{-3}	2.044×10^{-2}	8.251×10^{-2}	1.738×10^{-1}

f) 20 y (male) (breathing rate = 0.78 m^3 h^{-1})

µm	ET_1	ET_2	BB	bb	AI	Total
AMTD						
1	5.268×10^{-1}	2.837×10^{-1}	8.436×10^{-2}	8.438×10^{-2}	4.072×10^{-3}	9.833×10^{-1}
30	4.297×10^{-2}	2.314×10^{-2}	1.237×10^{-2}	8.207×10^{-2}	2.942×10^{-1}	4.548×10^{-1}
40	3.570×10^{-2}	1.922×10^{-2}	1.026×10^{-2}	6.726×10^{-2}	2.480×10^{-1}	3.804×10^{-1}
200	4.629×10^{-2}	2.493×10^{-2}	4.489×10^{-3}	1.961×10^{-2}	8.883×10^{-2}	1.841×10^{-1}

*Reference values are given to a greater degree of precision than would be chosen to reflect the certainty with which the average value of each parameter is known.

†Aerosol parameter values used in the calculations are given in Table 32.2, Section 32.1.1.

C.2. Biokinetic model for radon gas

(C 2) Several compartmental biokinetic models including the model for radon adopted in *Publication 137* (2017) have been developed for inert gases on the basis of physical laws governing transfer of a non-reactive and soluble gas between materials. In these models the kinetics of an inert gas is assumed to be determined by the blood-to-air partition coefficient (ratio of concentrations of the gas in blood and air) and the blood perfusion rates, tissue-to-blood partition coefficients, and volumes of the tissues represented by the compartments of the model. It is assumed that gas entering respiratory air (RT-air) after inhalation, or pulmonary blood after ingestion, equilibrates rapidly between RT-air and pulmonary blood with relative concentrations determined by the blood-to-air partition coefficient. Part of the gas in pulmonary blood is assumed to be removed from the body in expired air and the remainder is assumed to transfer to arterial blood and distribute to tissues in proportion to the percentage of cardiac output received by each tissue. It is assumed that the perfusion of the gas in tissues is instantaneous, allowing equilibrium to be achieved between venous blood and tissue. The gas is carried in the venous blood to the pulmonary blood, and the cycle is repeated. In the case of acute intake of radon, virtually all of the inhaled or ingested radon is removed from the body within a few hours.

(C 3) The age-specific biokinetic model for radon used in this report is based on the idealized system described above, together with empirical age-specific removal half-times of radon from lung air to the environment. The structure of the model and age- and sex-specific transfer coefficients can be found in the main text (Figure 32.1, Table 32.4, and Table 32.5). The reader is referred to the radon section in *Publication 137* (ICRP, 2017) for a more detailed discussion of the rationale for the modelling approach and the methods for deriving the transfer coefficients from physical principles.

(C 4) The partition coefficients used in the derivation of age-specific transfer coefficients for the radon model used in this report are listed in Table C.2. These values are taken from Table 12.2 of *Publication 137* (ICRP, 2017) or derived from values listed in that table in the case of model compartments representing a mixture of tissues addressed in that table. The partition coefficients are assumed to be independent of age with one exception: the partition coefficient for adipose breast tissue (Breast-a in Figure 32.1) increases with age up to adulthood because its fractional content of fat is assumed to increase with age. The age-specific tissue volumes (Table C.3) are based on age-specific tissues masses given in *Publication 89* (2002)

(Table C.4) and tissue densities (Table C.5) given in *Publication 23* (1975) and *Publication 89* (2002). It is assumed that bone is 80% cortical bone and 20% trabecular bone by mass for all ages. A density of 1.04 g/cc is applied to soft tissues other than fat and adipose tissue. The age-specific density of trabecular bone is assumed to be the same as that of cortical bone, which has been studied more extensively. Age-specific blood flow rates are listed in Table C.6.

Table C.2. Reference partition coefficients (tissue/blood) *

Tissues	100 d	1 y	5-y	10-y	15-y		Adult	
					Male	Female	Male	Female
Fat	11	11	11	11	11	11	11	11
Fat 1	11	11	11	11	11	11	11	11
Fat 2	11	11	11	11	11	11	11	11
Yellow marrow	8.9	8.9	8.9	8.9	8.9	8.9	8.9	8.9
Yellow marrow 1	8.9	8.9	8.9	8.9	8.9	8.9	8.9	8.9
Yellow marrow 2	8.9	8.9	8.9	8.9	8.9	8.9	8.9	8.9
Kidneys	0.66	0.66	0.66	0.66	0.66	0.66	0.66	0.66
Liver	0.71	0.71	0.71	0.71	0.71	0.71	0.71	0.71
Trabecular volume	0.36	0.36	0.36	0.36	0.36	0.36	0.36	0.36
Cortical volume	0.36	0.36	0.36	0.36	0.36	0.36	0.36	0.36
R-marrow	0.36	0.36	0.36	0.36	0.36	0.36	0.36	0.36
Breast								
Breast-g	1.4	1.4	1.4	1.4	1.4	1.4	1.4	1.4
Breast-a	5.1	6.7	7.3	7.8	8.3	8.3	8.9	8.9
Other	0.36	0.36	0.36	0.36	0.36	0.36	0.36	0.36
Blood/Air	0.43	0.43	0.43	0.43	0.43	0.43	0.43	0.43

*Values taken from Table 12.2 of Publication 137 (2017) and see discussions in text of partition coefficients for yellow marrow and breast.

Table C.3. Reference tissue volumes* (L)

	100 d	1 y	5 y	10 y	15 y		Adult	
					Male	Female	Male	Female
Fat	1.6E+00	2.5E+00	3.8E+00	6.0E+00	8.5E+00	1.4E+01	1.4E+01	1.8E+01
Fat 1	7.8E-01	1.2E+00	1.9E+00	3.0E+00	4.2E+00	7.0E+00	6.9E+00	9.0E+00
Fat 2	7.8E-01	1.2E+00	1.9E+00	3.0E+00	4.2E+00	7.0E+00	6.9E+00	9.0E+00
Yellow marrow	7.8E-03	2.0E-02	1.6E-01	6.4E-01	1.5E+00	1.4E+00	2.5E+00	1.8E+00
Yellow marrow 1	3.9E-03	1.0E-02	8.2E-02	3.2E-01	7.6E-01	7.0E-01	1.3E+00	9.2E-01
Yellow marrow 2	3.9E-03	1.0E-02	8.2E-02	3.2E-01	7.6E-01	7.0E-01	1.3E+00	9.2E-01
Kidneys	4.1E-02	6.7E-02	1.1E-01	1.7E-01	2.4E-01	2.3E-01	3.0E-01	2.6E-01
Liver	2.0E-01	3.2E-01	5.5E-01	8.0E-01	1.3E+00	1.3E+00	1.7E+00	1.3E+00
Trabecular volume	4.1E-02	7.2E-02	1.5E-01	2.6E-01	4.5E-01	4.1E-01	5.8E-01	4.2E-01
Cortical volume	1.6E-01	2.8E-01	5.9E-01	1.1E+00	1.8E+00	1.6E+00	2.3E+00	1.7E+00
Red marrow	8.5E-02	1.4E-01	3.3E-01	6.1E-01	1.0E+00	9.6E-01	1.1E+00	8.7E-01
Breast	2.1E-04	4.3E-04	9.5E-04	7.2E-03	1.6E-02	2.5E-01	2.6E-02	5.1E-01
Breast-g	8.3E-05	1.7E-04	3.6E-04	2.7E-03	2.7E-03	9.6E-02	2.7E-03	1.9E-01
Breast-a	1.3E-04	2.7E-04	5.9E-04	4.5E-03	1.3E-02	1.6E-01	2.3E-02	3.2E-01
Other	3.2E+00	5.5E+00	1.1E+01	1.8E+01	3.3E+01	2.7E+01	4.1E+01	2.8E+01
Blood†	3.6E-01	5.0E-01	1.4E+00	2.4E+00	4.5E+00	3.3E+00	5.3E+00	3.9E+00
Blood-A	9.7E-02	1.4E-01	3.8E-01	6.5E-01	1.2E+00	8.9E-01	1.4E+00	1.1E+00
Blood-V	2.6E-01	3.7E-01	1.0E+00	1.8E+00	3.3E+00	2.4E+00	3.9E+00	2.8E+00
Lung-air vol‡	1.7E-01	2.9E-01	9.0E-01	1.7E+00	3.1E+00	2.7E+00	3.9E+00	3.1E+00

* Based on reference tissue masses and specific gravities listed in Tables C.4 and C.5, respectively.
† Blood volumes given in ICRP Publication 89 for ages 1 year old to adult. Value for infant based on mass and density listed in Tables C.4 and C.5 respectively.
‡ Adult value based on value given in ICRP Publication 68 (1994a) and other ages scaled by age-specific functional residual capacity (ICRP Publication 66, 1994b).

Table C.4. Reference tissue masses* (g)

	100 d	1 y	5 y	10 y	15 y		Adult	
					Male	Female	Male	Female
Fat†	1.4E+03	2.3E+03	3.5E+03	5.5E+03	7.8E+03	1.3E+04	1.3E+04	1.7E+04
Fat 1	7.2E+02	1.1E+03	1.7E+03	2.7E+03	3.9E+03	6.4E+03	6.3E+03	8.3E+03
Fat 2	7.2E+02	1.1E+03	1.7E+03	2.7E+03	3.9E+03	6.4E+03	6.3E+03	8.3E+03
Yellow marrow	7.7E+00	2.0E+01	1.6E+02	6.3E+02	1.5E+03	1.4E+03	2.5E+03	1.8E+03
Yellow marrow 1	3.8E+00	1.0E+01	8.0E+01	3.2E+02	7.4E+02	6.9E+02	1.2E+03	9.0E+02
Yellow marrow 2	3.8E+00	1.0E+01	8.0E+01	3.2E+02	7.4E+02	6.9E+02	1.2E+03	9.0E+02
Kidneys	4.2E+01	7.0E+01	1.1E+02	1.8E+02	2.5E+02	2.4E+02	3.1E+02	2.8E+02
Liver	2.1E+02	3.3E+02	5.7E+02	8.3E+02	1.3E+03	1.3E+03	1.8E+03	1.4E+03
Trabecular volume	6.8E+01	1.2E+02	2.5E+02	4.6E+02	8.1E+02	7.4E+02	1.1E+03	8.0E+02
Cortical volume	2.6E+02	4.7E+02	1.0E+03	1.8E+03	3.2E+03	3.0E+03	4.4E+03	3.2E+03
Red marrow	8.8E+01	1.5E+02	3.4E+02	6.3E+02	1.1E+03	1.0E+03	1.2E+03	9.0E+02
Breast‡	2.1E-01	4.3E-01	9.4E-01	7.1E+00	1.5E+01	2.5E+02	2.5E+01	5.0E+02
Breast-g§	8.6E-02	1.7E-01	3.8E-01	2.8E+00	2.8E+00	1.0E+02	2.8E+00	2.0E+02
Breast-a	1.3E-01	2.6E-01	5.6E-01	4.3E+00	1.2E+01	1.5E+02	2.2E+01	3.0E+02

Other[¶]	3.3E+03	5.8E+03	1.1E+04	1.9E+04	3.4E+04	2.8E+04	4.2E+04	2.9E+04
Total Body	6.0E+03	1.0E+04	1.9E+04	3.2E+04	5.6E+04	5.3E+04	7.3E+04	6.0E+04
Blood	3.8E+02	5.3E+02	1.5E+03	2.5E+03	4.8E+03	3.5E+03	5.6E+03	4.1E+03

[*] Based on reference values ICRP Publication 89 for ages 1 through adult. For age 100 d, masses are based on growth trends indicated in Publication 89 for total body and, where available, individual tissues.
[†] Mass of fat taken as mass of storage fat minus mass of fat assigned to yellow marrow compartments. See text on the assumptions of the % of fat in yellow marrow.
[ǂ] The reference breast masses for infant to 10 year old are extrapolated from data given in Publication 89.
[§] Assumes mass of glandular breast is 40% of total breast apart from ages after 10 years old for males where the glandular breast stops growing.
[¶] Mass of "other" calculated as mass of total body minus masses of tissues and fluids explicitly identified in systemic model and contents of stomach, intestines, gallbladder, and urinary bladder.

Table C.5. Reference tissue densities[*]

	100 d	1 y	5 y	10 y	15 y		Adult	
					Male	Female	Male	Female
Fat	0.92	0.92	0.92	0.92	0.92	0.92	0.92	0.92
Fat 1	0.92	0.92	0.92	0.92	0.92	0.92	0.92	0.92
Fat 2	0.92	0.92	0.92	0.92	0.92	0.92	0.92	0.92
Yellow marrow	0.98	0.98	0.98	0.98	0.98	0.98	0.98	0.98
Yellow marrow 1	0.98	0.98	0.98	0.98	0.98	0.98	0.98	0.98
Yellow marrow 2	0.98	0.98	0.98	0.98	0.98	0.98	0.98	0.98
Kidneys[†]	1.04	1.04	1.04	1.04	1.04	1.04	1.04	1.04
Liver[†]	1.04	1.04	1.04	1.04	1.04	1.04	1.04	1.04
Trabecular volume[ǂ]	1.65	1.66	1.70	1.75	1.80	1.80	1.90	1.90
Cortical volume	1.65	1.66	1.70	1.75	1.80	1.80	1.90	1.90
Red marrow[†]	1.04	1.04	1.04	1.04	1.04	1.04	1.04	1.04
Breast								
Breast-g[†]	1.04	1.04	1.04	1.04	1.04	1.04	1.04	1.04
Breast-a[§]	0.99	0.97	0.96	0.96	0.95	0.95	0.94	0.94
Other	1.04	1.04	1.04	1.04	1.04	1.04	1.04	1.04
Blood	1.06	1.06	1.06	1.06	1.06	1.06	1.06	1.06

[*] Based on data in ICRP Publication 23 (1975) and Publication 89 (2002).
[†] The reference soft tissue density of 1.04 g/cc was applied to kidneys, liver, red marrow, glandular breast and 'other'.
[ǂ] The age-specific density of trabecular bone was assumed to be the same as that of cortical bone.
[§] The age-specific density of adipose breast takes account of the change in fat content with age.

Table C.6. Reference blood flow rates to tissues (% of cardiac output)[*]

	100 d	1 y	5 y	10 y	15 y		Adult	
Tissue					Male	Female	Male	Female
Fat	5.0E+00	5.0E+00	5.0E+00	5.0E+00	5.0E+00	8.5E+00	5.0E+00	8.5E+00
Fat 1	4.0E+00	4.0E+00	4.0E+00	4.0E+00	4.0E+00	6.8E+00	4.0E+00	6.8E+00
Fat 2	1.0E+00	1.0E+00	1.0E+00	1.0E+00	1.0E+00	1.7E+00	1.0E+00	1.7E+00
Yellow marrow[†]	1.6E-03	4.0E-03	3.2E-02	1.3E-01	3.0E-01	3.8E-01	5.0E-01	5.0E-01
Yellow marrow 1	1.2E-03	3.2E-03	2.6E-02	1.0E-01	2.4E-01	3.1E-01	4.0E-01	4.0E-01
Yellow marrow 2	3.1E-04	8.1E-04	6.5E-03	2.5E-02	6.0E-02	7.7E-02	1.0E-01	1.0E-01
Kidneys	1.9E+01	1.9E+01	1.9E+01	1.9E+01	1.9E+01	1.7E+01	1.9E+01	1.7E+01

Liver								
Arterial	6.5E+00	6.5E+00	6.5E+00	6.5E+00	6.5E+00	6.5E+00	6.5E+00	6.5E+00
Total	2.6E+01	2.6E+01	2.6E+01	2.6E+01	2.6E+01	2.7E+01	2.6E+01	2.7E+01
Trabecular volume[‡]	1.8E+00	1.8E+00	1.8E+00	1.8E+00	9.0E-01	9.0E-01	9.0E-01	9.0E-01
Cortical volume[‡]	1.2E+00	1.2E+00	1.2E+00	1.2E+00	6.0E-01	6.0E-01	6.0E-01	6.0E-01
Red marrow	3.0E+00	3.0E+00	3.0E+00	3.0E+00	3.0E+00	3.0E+00	3.0E+00	3.0E+00
Breast[§]	1.7E-04	3.4E-04	7.5E-04	5.7E-03	1.2E-02	2.0E-01	2.0E-02	4.0E-01
Breast-g	8.5E-05	1.9E-04	4.1E-04	3.2E-03	3.8E-03	1.2E-01	4.8E-03	2.5E-01
Breast-a	8.7E-05	1.6E-04	3.4E-04	2.5E-03	8.2E-03	8.4E-02	1.5E-02	1.5E-01
Other[¶]	6.3E+01	6.3E+01	6.3E+01	6.3E+01	6.5E+01	6.3E+01	6.4E+01	6.3E+01
Cardiac output (L/min)	0.83	1.2	3.4	5.0	6.1	6.1	6.5	5.9

[*] Blood flow rates for adults taken from ICRP Publication 89 (2002).
[†] The total blood flow rate to yellow marrow at different ages was scaled by mass from the reference value for adult given in ICRP Publication 89 (2002).
[‡] The percentage of cardiac output received by bone in infants and children through age 10 y is assumed to be twice the percentage received by bone in adults.
[§] The blood flow rate (i.e. % of cardiac output) to breast at different ages and for males were scaled from the value for the adult non-pregnant female breast based on mass. The fraction of this blood flow rate to 'breast-a' reflects the varying percentages of fat in adipose breast with age.
[¶] The percentage of cardiac output to "other" is calculated as 100% minus the % of cardiac output to the tissues explicitly identified in systemic model (i.e. fat, yellow marrow, kidneys, liver (arterial), trabecular and cortical volume, red marrow and breast).

(C 5) The model structure shown in Figure 32.1 differs from the structure applied to workers in *Publication 137* (2017). The modification was made for greater consistency between the source regions depicted in the biokinetic model for radon and the target regions addressed in the ICRP's current dosimetry system. With the model structure applied to workers in *Publication 137*, the dose estimates for red marrow were imprecise because the compartment named "Red marrow" in that model included some non-hematopoietic tissue. In the modified structure used in this report, the compartment named "Red marrow" includes only hematopoietic tissue. Two compartments representing two phases of retention of radon in yellow marrow have been added to the model used in *Publication 137*. These two phases of retention are based on the division and half-times of the two compartments of the model representing fat.

(C 6) Some modifications of the parameter values for adult males used in *Publication 137* (2017) resulted from modifications in this report regarding the mass, density, or composition of tissues. Assumptions used to develop the parameter values in the present model are summarized below.

(C 7) The flow rates between blood and breast are assumed to be the same for males and females through age 10 y. For assignment of transfer coefficients to breast at higher ages it is taken into account that, beginning at puberty, the increased testosterone levels cause involution of the glandular tissue in the male breast (Chen et al. 2006). Data for U.S. subjects indicate that the onset of puberty for boys may be around age 10 y (Herman-Giddens et al. 2012). It is assumed in the model that growth of the male breast after age 10 y results only from an increase in the mass of adipose tissue.

(C 8) For all age groups, the total mass of the compartments labelled Fat 1 and Fat 2 in Figure 32.1 was calculated from reference values for storage fat given in *Publication 89* (2002) minus the mass of fat in bone marrow. For age 100 d, total fat including breast and marrow fat

is assumed to be 24% of the total body weight (Fomon et al. 1982, Fomon and Nelson 2002). For other ages the mass of Fat 1 + Fat 2 is based on reference masses of storage fat given in *Publication 89*.

(C 9) For each age the compartment named "Breast-a" representing adipose tissue in the breast is assumed to contain the same percentage of fat as total adipose tissue for that age. Adipose tissue excluding yellow marrow is assumed to be 45% fat for age 100 d (Fomon and Nelson, 2002). For ages 1 y and greater the percentage of fat in adipose tissue other than yellow marrow were taken from *Publication 89* (60% at 1 y, 65% at 5 y, 70% at 10, 75% at 15 y, and 80% in adults). It is assumed that fat represents 80% of the mass of yellow marrow at all ages based on the lipid content of yellow marrow estimated for adults (*Publication 23*, Guillerman 2013, Chan 2016, Karampinos 2018) and the lack of clear evidence of an age dependence of the lipid content of yellow marrow. The age-specific masses of red marrow (active marrow) were taken from *Publications 70* and *89* (1995, 2002). The compartment named "Breast-g" representing glandular breast is assumed to contain 10% intraglandular fat for each age (ICRP, 2017).

(C 10) The blood flow rates to individual tissues expressed as a percentage of cardiac output were modified from reference values for adult given in *Publication 89* (2002). As in the age-specific model for systemic caesium described in this report, the percentage of cardiac output received by bone in infants and children through age 10 y is assumed to be twice the percentage received by bone in adults. Blood flow rates were also adjusted for a given age to reflect the age-specific composition and masses of some tissues, e.g., for the varying percentages of fat and other soft tissue in adipose tissue.

(C 11) For example, the blood flow rate to breast was scaled from the reference value for non-pregnant adult female breast based on mass. Thus, the age- and sex-specific percentage of cardiac output received by breast is given by:

$$0.4 \times \frac{m_{\text{breast}}}{500} \qquad \text{(C.1)}$$

where 0.4 is the % of cardiac output to non-pregnant adult female breast with a reference mass of 500 g (ICRP, 2002), and m_{breast} is the reference age- and sex-specific mass of the breast given in Table C.3.

(C 12) The distribution of blood flow to breast between adipose breast (breast-a) and glandular breast (breast-g), was based on the relative blood perfusion rates of fat and 'other' and the age-specific fat content of breast-a and breast-g. Thus, the fraction of the % of cardiac output to breast that goes to 'breast-a' is calculated as follows:

$$\frac{m_{\text{breast-a}} \times \left(\frac{f_{\text{fat}} \times \%CO_{\text{storage fat}}}{m_{\text{storage fat}}} + \frac{(1-f_{\text{fat}}) \times \%CO_{\text{other}}}{m_{\text{other}}} \right)}{\frac{\left(f_{\text{fat}} \times m_{\text{breast-a}} + 0.1 \times m_{\text{breast-g}}\right) \times \%CO_{\text{storage fat}}}{m_{\text{storage fat}}} + \frac{\left((1-f_{\text{fat}}) \times m_{\text{breast-a}} + 0.9 \times m_{\text{breast-g}}\right) \times \%CO_{\text{other}}}{m_{\text{other}}}} \qquad \text{(C.2)}$$

where

$m_{\text{breast-a}}$, $m_{\text{breast-g}}$, $m_{\text{storage fat}}$, and m_{other} are the masses of adipose breast, glandular breast, storage fat and other, respectively (Table C.3).

f_{fat} is the age-specific fraction of fat in adipose tissue.

$\%CO_{\text{storage fat}}$ is the reference blood flow rate to storage fat for adult (5% for males and 8.5% for females).

$\%CO_{other}$ is the % of cardiac output to Other (Table C.5)

The remaining fraction of the % of cardiac output to breast goes to breast-g.

(C 13) For pre-adults the partition coefficients for individual tissues are consistent with values for adult and, where applicable, reflect the relative amounts of different tissues that make up a compartment of the model. The partition coefficients for yellow marrow are based on a composition of 80% fat and 20% other soft tissue; for the compartment named Breast-g (glandular breast tissue) are based on an assumed composition of 10% fat and 90% other soft tissue; and for the compartment named Breast-a (adipose tissue of breast) are based on the assumed age-specific percentage of fat in adipose tissue.

(C 14) Age-specific removal half-times of radon from lung air to the environment are based on measured washout rates of xenon and krypton in infants and children (Treves et al. 1974, Ciofetta et al. 1980). The following reference half-times were selected: 4.5 s for infants, 5 s for age 1 y, 8 s for 5 y, 11 s for 10 y, 17 s for 15 y, and 23 s for adults. The half-time assigned to the adult male is the same as in the Rn model for workers used in *Publication 137* (ICRP, 2017).

(C 15) The average volume of the RT-air space for an adult male is 3.858 l (Bailey, et al., 1996; ICRP, 1994b). This was scaled downward to other ages using the age-specific functional residual capacity (FRC) values from Table 15 of *Publication 66* (ICRP, 1994a). In other words, the age-specific FRC values are multiplied by (3.858/3.30).

(C 16) The revised model described here for the adult male replaces the model given in *Publication 137* (ICRP, 2017).

C.3. Dosimetric data for radon and thoron

C.3.1. **Inhalation of radon or thoron gas**

(C 17) The age-dependent equilibrium effective dose rates for continuous chronic exposure to unit concentration of ^{222}Rn (or ^{220}Rn) are given in Table C.7. In other words, these are the effective dose rates following chronic exposure to unit concentration of radon (or thoron) after the radon (or thoron) concentration in organs and tissues have reached saturation (i.e. equilibrium).

(C 18) The effective dose coefficients in terms of Sv Bq^{-1} intake of radon gas are also given in Table C.7. and the corresponding equivalent doses to organs are given in the accompanying electronic annex. These values can be converted to the effective dose per exposure (Sv per Bq h m^{-3}) by multiplying the Sv Bq^{-1} value by $(\lambda \times \bar{V}_{RT-air} \times 1/24)$, where λ is the transfer coefficient (d^{-1}) from the the RT-air space to the environment in the radon gas biokinetic model (Table 32.4 or 32.5), and $\bar{V}_{RT-air}$ (m^3) is the sex-average volume of RT-air space for the reference age group (Table C.3). It is noteworthy that unlike the inhalation of radon progeny, the dose per exposure (Sv per Bq h m^{-3}) from inhaling ^{222}Rn gas is approximately independent of the breathing rate.

Table C.7. Age-dependent effective dose coefficients following inhalation of radon (^{222}Rn) or thoron (^{220}Rn) gas alone.

Age	Effective dose coefficients			
	Radon (^{222}Rn) gas		Thoron (^{220}Rn) gas	
	Sv Bq^{-1}	mSv per Bq h m^{-3} *	Sv Bq^{-1}	mSv per Bq h m^{-3} *
3 mo	1.0E-09	9.8E-08	3.5E-10	3.4E-08
1 y	7.6E-10	1.1E-07	2.6E-10	3.8E-08
5 y	5.0E-10	1.4E-07	2.0E-10	5.7E-08

10 y	4.1E-10	1.6E-07	1.7E-10	6.6E-08
15 y	4.0E-10	1.7E-07	1.6E-10	6.8E-08
Adult	5.0E-10	1.9E-07	1.8E-10	6.7E-08

* This is the effective dose rate following chronic exposure to unit concentration of radon (or thoron) after the radon (or thoron) concentration in organs and tissues have reached saturation (i.e. equilibrium).

C.3.2. **Inhalation of radon or thoron progeny**

(C 19) Table C.8. lists effective dose coefficients (Sv Bq^{-1}) for inhalation of individual short-lived radon (^{222}Rn or ^{220}Rn) progeny. Values are calculated for each mode of the assumed aerosol distribution for homes (Table 32.2). The progeny addressed in Table C.8. are those that generally dominate the estimated lung dose and effective dose from exposure to radon and accompanying progeny. The tabulated values can be used to calculate values of effective dose per potential alpha energy exposure (ICRP, 2017).

Table C.8. Effective dose coefficients (in Sv Bq^{-1}) for inhaled radon (^{222}Rn) or thoron (^{220}Rn) progeny. Values are given for each mode of the assumed aerosol distribution for homes*

		Effective dose coefficients (Sv Bq^{-1})					
		Age					
Mode	Nuclide	3 mo	1 y	5 y	10 y	15 y	Adult
Radon (^{222}Rn) progeny							
unattached	Po-218	3.9E-08	3.2E-08	2.0E-08	1.5E-08	1.1E-08	1.1E-08
	Pb-214	2.2E-07	1.8E-07	1.1E-07	8.3E-08	6.3E-08	6.1E-08
	Bi-214	2.1E-07	1.7E-07	1.0E-07	7.5E-08	5.7E-08	5.5E-08
nucleation	Po-218	2.8E-08	2.0E-08	1.1E-08	7.1E-09	5.5E-09	4.9E-09
	Pb-214	1.3E-07	9.5E-08	5.4E-08	3.4E-08	2.6E-08	2.3E-08
	Bi-214	1.1E-07	7.9E-08	4.5E-08	2.8E-08	2.2E-08	1.9E-08
accumulation	Po-218	8.4E-09	5.9E-09	3.2E-09	2.1E-09	1.6E-09	1.4E-09
	Pb-214	4.3E-08	3.0E-08	1.6E-08	1.0E-08	7.8E-09	7.1E-09
	Bi-214	3.7E-08	2.6E-08	1.4E-08	8.9E-09	6.6E-09	6.0E-09
Thoron (^{220}Rn) progeny							
unattached	Pb-212	1.4E-06	1.2E-06	7.7E-07	6.2E-07	4.6E-07	4.6E-07
	Bi-212	4.5E-07	3.6E-07	2.3E-07	1.7E-07	1.3E-07	1.2E-07
nucleation	Pb-212	1.2E-06	9.0E-07	5.1E-07	3.2E-07	2.5E-07	2.2E-07
	Bi-212	2.4E-07	1.7E-07	9.8E-08	6.1E-08	4.7E-08	4.2E-08
accumulation	Pb-212	4.4E-07	3.1E-07	1.7E-07	1.0E-07	7.9E-08	7.1E-08
	Bi-212	8.7E-08	6.1E-08	3.3E-08	2.1E-08	1.6E-08	1.4E-08

* Assumed aerosol distributions are given in Table 32.2.

(C 20) The age-dependent effective doses per exposure to radon (^{222}Rn) progeny as a function of the unattached fraction, f_p and the fraction of the attached PAEC associated with the nucleation mode, f_{pn} are given in Table C.9. Values of effective dose coefficients with f_p=0.1 and f_{pn} = 0.2 are also shown. Here, the doses from inhaling ^{222}Rn gas are excluded. If there is no nucleation mode present (i.e. f_{pn} =0) then the dose reduces by about 20% for exposures at home.

Table C.9. Age-dependent effective doses per exposure to radon (^{222}Rn) progeny as a function of the unattached fraction, f_p and the fraction of the attached potential alpha energy concentration (PAEC) associated with the nucleation mode, f_{pn}.

Age	Effective dose per exposure to radon (^{222}Rn) progeny*	
	mSv per mJ h m^{-3}	nSv per Bq h m^{-3} of EEC† of ^{222}Rn

	$a f_p + (1- f_p)[b f_{pn} + c(1- f_{pn})]$			Calculated value‡	$a f_p + (1- f_p)[b f_{pn} + c(1- f_{pn})]$			Calculated value‡
	a	b	c		a	b	c	
3 mo	8.4	5.8	1.9	3.2	47	32	10	18
1 y	11	6.6	2.1	3.8	61	37	12	21
5 y	12	6.3	1.9	3.7	64	35	11	20
10 y	15	6.8	2.1	4.3	84	38	12	24
15 y	13	6.0	1.8	3.7	72	33	10	20
Adult	16	6.6	2.0	4.2	86	36	11	23

*Doses from inhaling ^{222}Rn gas are excluded.

† EEC = equilibrium equivalent concentration; 1 h Bq m^{-3} of EEC exposure of ^{222}Rn = 1.57 × 10^{-6} WLM = 5.56 × 10^{-6} mJ h m^{-3}. EEC of ^{222}Rn = F × Radon gas activity concentration (Bq m^{-3}), where F is the equilibrium factor.

‡ Effective dose per unit exposure to radon progeny calculated with f_p=0.1 and f_{pn} = 0.2.

C.4. References

Bailey, M. R., Birchall, A., Marsh, J.W., et al., 1996. Application of the new ICRP Respiratory Tract Model to gases and vapours in ICRP Publication 68. NRPB Memorandum, NRPB-M688. Public Health England, Chiltoin, Didcot.

Chan, B.Y., Gill, K.G., Rebsamen, S.L., et al., 2016. MR imaging of pediatric bone marrow. Radiographics 36(6), 1911–1930.

Chen, L., Chantra, P.K., Larsen, L.H., et al., 2006. Imaging characteristics of malignant lesions of the male breast. Radiographics 26(4), 993–1006.

Ciofetta, G., Silverman, M., Hughes, J.M.B., 1980. Quantitative approach to the study of regional lung function in children using krypton 81m. Brit. J. Radiol. 53(634), 950–959.

Fomon, S.J., Nelson, S.E., 2002. Body composition of the male and female reference infants. Annu. Rev. Nutr. 22, 1–17.

Fomon, S.J., Haschke, F., Ziegler, E.E., et al., 1982. Body composition of reference children from birth to age 10 years. Am. J. Clin. Nutr. 35(5 Suppl.), 1169–1175.

Guillerman, R.P., 2013. Marrow: Red, yellow and bad. Pediatr. Radiol. 43(SUPPL. 1), S181–S192.

Herman-Giddens, M.E., Steffes, J., Harris, D., et al., 2012. Secondary sexual characteristics in boys: Data from the pediatric research in office settings network. Pediatrics 130(5), e1058–e1068.

ICRP, 1975. Report of the Task Group on Reference Man. ICRP Publication 23. Pergamon Press, Oxford.

ICRP, 1994a. Dose coefficients for intake of radionuclides by workers. ICRP Publication 68. Ann. ICRP 24(4).

ICRP, 1994b. Human respiratory tract model for radiological protection. ICRP Publication 66. Ann. ICRP 24(1–3).

ICRP, 2002a. Basic anatomical and physiological data for use in radiological protection: reference values. ICRP Publication 89. Ann. ICRP 32(3–4).

ICRP, 2017. Occupational intakes of radionuclides: Part 3. ICRP Publication 137. Ann. ICRP 46(3/4).

Karampinos, D.C., Ruschke, S., Dieckmeyer, M., et al., 2018. Quantitative MRI and spectroscopy of bone marrow. J. Magn. Reson. Imaging 47(2), 332–353.

Treves, S., Ahnberg, D.S., Laguarda, R., et al., 1974. Radionuclide evaluation of regional lung function in children. J. Nucl. Med. 15(7), 582–587.

GLOSSARY

Active (bone) marrow

Active marrow is haematopoietically active and gets its red colour from the large numbers of erythrocytes (red blood cells) being produced. Active bone marrow serves as a target region for radiogenic risk of leukaemia.

Blood

Corresponds to the transfer compartment in the biokinetic models. Also called 'transfer compartment' or 'body fluids' in previous ICRP publications.

Bone marrow. See also 'Active (bone) marrow' and 'Inactive (bone) marrow'

Bone marrow is a soft, highly cellular tissue that occupies the cylindrical cavities of long bones and the cavities defined by the bone trabeculae of the axial and appendicular skeleton. Total bone marrow consists of a sponge-like, reticular, connective tissue framework called stroma, myeloid (blood-cell-forming) tissue, fat cells (adipocytes), small accumulations of lymphatic tissue, and numerous blood vessels and sinusoids. There are two types of bone marrow: active (red) and inactive (yellow) where these adjectives refer to the marrow's potential for blood cell element production (haematopoiesis).

Clearance

The removal of material from the respiratory tract by particle transport and by absorption into blood.

Committed effective dose, $E(\tau)$. See also 'Effective dose'.

In this series of reports, the integration time τ following the intake is taken to be 50 y for adults and from intake to age 70 y for children. The committed effective dose $E(\tau)$ is calculated with the use of male and female committed equivalent doses to individual target organs or tissues, T according to the expression:

$$E(\tau) = \sum_T w_T \left[\frac{H_T^M(\tau) + H_T^F(\tau)}{2}\right]$$

The SI unit for committed effective dose is the same as for absorbed dose, J kg^{-1}, and its special name is sievert (Sv).

Committed equivalent dose $H_T(\tau)$. See also 'Equivalent dose'.

In this series of reports, the equivalent dose to an organ or tissue region is the time integral of the equivalent dose rate in a target organ or tissue T of the Reference Individual. This is calculated using reference biokinetic and dosimetric models following the intake of radioactive material into the body of the Reference Individual. The integration period τ following the intake is taken to be 50 y for adults and from intake to age 70 y for children:

$$H_T(\tau) = \int_0^\tau \dot{H}(r_T, t)dt$$

For both sexes, the equivalent dose rate $\dot{H}(r_T, t)$ in target region r_T at time t after an acute intake is expressed as:

$$\dot{H}(r_T, t) = \sum_{r_S} A(r_S, t) \cdot S_w(r_T \leftarrow r_S, t)$$

where:

$A(r_S,t)$ is the activity of the radionuclide in source region r_S at time t after intake, in Bq, as predicted by the reference biokinetic models for the Reference Individual,

$S_w(r_S \leftarrow r_T)$ is the radiation weighted S coefficient; i.e. the equivalent dose to target region r_T per nuclear transformation in source region r_S, in Sv (Bq s)$^{-1}$, for the Reference Individual.

The SI unit for committed equivalent dose is the same as for absorbed dose, J kg^{-1}, and its special name is sievert (Sv).

Compartment

In this series of reports: mathematical pool of radioactive materials in the body which can be characterised by first order kinetics. Activity is considered to be uniformly distributed in a compartment. One or more compartments can be associated with an organ (e.g. the liver), a part of an organ (e.g. the bronchial region of the lungs), a tissue (e.g. the bone), a part of a tissue (e.g. the bone surface) or another substance of the body (e.g. the blood).

Dose coefficient

In this series of reports, a dose coefficient is defined as either the committed equivalent dose in organ or tissue T per intake, $h_T(\tau)$, or the committed effective dose per intake, $e(\tau)$, where τ is the dose-commitment period in years over which the dose is calculated. Note that elsewhere the term 'dose per intake coefficient' is sometimes used for dose coefficient.

Dose per intake coefficient. See also 'Dose coefficient'

In this series of reports: the committed effective dose per radionuclide intake, $e(\tau)$, or committed equivalent dose to the tissue or organ r_T per radionuclide intake, $h_T(r_T,\tau)$, where τ is the dose-commitment period over which the dose is calculated.

Endogenous excretion

Term used to specify the excretion of materials from blood to the alimentary tract, applying to biliary excretion and passage of materials through the alimentary tract wall.

Extrathoracic (ET) airways

Part of the respiratory tract, consisting of the anterior nose (the ET_1 region) and the posterior nasal passages, pharynx and larynx (the ET_2 region). Note that the oral part of the pharynx is no longer part of ET_2 because it is included in the HATM.

Inactive (bone) marrow

In contrast to the active marrow, the inactive marrow is haematopoietically inactive (i.e. does not directly support haematopoiesis). It gets its yellow colour from fat cells (adipocytes) which occupy most of the space of the bone marrow framework.

Nasal augmenter

A person who breathes entirely through the nose at the exercise levels of 'sleep', 'sitting' and 'light exercise', but oro-nasally (partly through the nose and partly through the mouth) during 'heavy exercise'. Also known as a 'normal nose breather', because most people breathe according to this pattern. All Reference Individuals defined in this series of reports are assumed to be Nasal Augmenters.

Normal nose breather See 'Nasal Augmenter'

Reference Man

An individual with the anatomical and physiological characteristics previously defined in the report of the ICRP Task Group on Reference Man (ICRP, 1975) and now given in *Publication 89* (ICRP, 2002a). *Publication 89* gives reference anatomical and physiological values for male and female individuals of six age groups: newborn, 1 y, 5 y, 10 y, 15 y, and adults.

Reference Member of the Public

A newborn, 1 y, 5 y, 10 y, 15 y old or adult Reference Person combined with the reference biokinetic and dosimetric models and their parameter values, as defined in this report series systemic biokinetic models (HRTM, HATM, and dosimetric models). The structure and parameter values of biokinetic models of the Reference Member of the Public are invariant on the sex, race and other individual-specific characteristics, but depend on its age group and are based on reference male parameter values where sex-specific models are available.

S-coefficient (radiation-weighted) $S_w(r_T \leftarrow r_S, t)$

The equivalent dose to target region r_T per nuclear transformation of a given radionuclide in source region r_S, Sv (Bq s)$^{-1}$, for the Reference Individual of age t.

$$S_w(r_T \leftarrow r_S, t) = \sum_R w_R \sum_i E_{R,i}\ Y_{R,i}\ \Phi(r_T \leftarrow r_S,\ E_{R,i}, t)$$

where:

$E_{R,i}$ is the energy, in joules, of the i^{th} radiation of type R emitted in nuclear transformations of the radionuclide;

$Y_{R,i}$ is the yield of the i^{th} radiation of type R per nuclear transformation, (Bq s)$^{-1}$,

w_R is the radiation weighting factor for radiation type R (Table 1.2),

$\Phi(r_T \leftarrow r_S, E_{R,i})$ $\Phi(r_T \leftarrow r_S, E_{R,i}, t)$ is the specific absorbed fraction (SAF), defined as the fraction of energy $E_{R,i}$ $E_{R,i}$of radiation type R emitted within the source region r_S that is absorbed per mass in the target region r_T for the reference individual of age t, kg^{-1}.

Note that anatomical parameters depend on the age-group. In case of intake of long-lived radionuclides during childhood, S_w will vary with respect to time. S-coefficients for times in between the 6 reference individual ages are obtained via interpolation. Its value represents either the equivalent dose rate (Sv s^{-1}) per activity (Bq), or the equivalent dose (Sv) per nuclear transformation (Bq s) in the target region.

Specific absorbed fraction (SAF), $\Phi(r_T \leftarrow r_S, E_{R,i}, t)$

Fraction of radiation R of energy $E_{R,i}$ emitted within the source region r_S that is absorbed per mass in the target region r_T for the reference individual of age t .

Spongiosa

Term referring to the combined tissues of the bone trabeculae and marrow tissues (both active and inactive) located beneath cortical bone cortices across regions of the axial and appendicular skeleton. Spongiosa is one of three bone regions defined in the *Publication 110* (ICRP, 2009) reference phantoms, the other two being cortical bone and medullary marrow of the long bone shafts. As the relative proportions of trabecular bone, active marrow, and inactive marrow vary with skeletal site, the homogeneous elemental composition and mass density of spongiosa are not constant but vary with skeletal site (see *Publication 110 and Publication 143* (ICRP, 2020)).
.

ACKNOWLEDGEMENTS

This report is the first in a series of documents replacing the *Publication 56* series (ICRP, 1989, 1993, 1995b,c, 1996a, 2001, 2004) to provide revised age-dependent dose coefficients for members of the public for environmental intakes of radionuclides by inhalation and ingestion. The revised dose coefficients have been calculated using the *Publication 100* (ICRP, 2006) Human Alimentary Tract Model (HATM) and the revision of the *Publication 66* (ICRP, 1994a) Human Respiratory Tract Model (HRTM) described in *Publication 130* (ICRP, 2015). Revisions have been made to many of the models that describe the systemic biokinetics of radionuclides absorbed to blood, making them more physiologically realistic representations of uptake and retention in organs and tissues and of excretion.

This first report in the series provides an introduction to the report series and includes Sections on biokinetic and dosimetric models plus data on individual elements and their radioisotopes, including biokinetic data and models, and dose coefficients. Additional data accompanying this series are available on the ICRP website and give extensive additional information. This current report provides the above data for the elements already described in OIR Parts 2–5 (*Publications 134, 137, 141, 151)* i.e.: Hydrogen (H), Carbon (C), Phosphorus (P), Sulphur (S), Calcium (Ca), Iron (Fe), Cobalt (Co), Zinc (Zn), Strontium (Sr), Yttrium (Y), Zirconium (Zr), Niobium (Nb), Molybdenum (Mo), Technetium (Tc), Ruthenium (Ru), Antimony (Sb), Tellurium (Te), Iodine (I), Caesium (Cs), Barium (Ba), Iridium (Ir), Lead (Pb), Bismuth (Bi), Polonium (Po), Radon, (Rn), and Radium (Ra).

Subsequent reports will provide data for most of the remaining elements.

ICRP thanks all those involved in the development of this publication for their hard work and dedication over many years.

Task Group 95 members *(*2014-present*)*

F. Paquet (Chair)	J.W. Marsh	D. Melo
M. R. Bailey	T. Fell	D. Noβke
V. Berkovski	A. Giussani	G. Ratia
L. Bertelli	D. Gregoratto	
E. Blanchardon	D. Jokisch	
S. Lamart	T. Smith	
E. Davesne	M.A. Lopez	
G. Etherington	R. W. Leggett	

Main Commission critical reviewers

M. Kai S. Romanov

Editorial members

C.H. Clement (Scientific Secretary and *Annals of the ICRP* Editor-in-Chief)
H. Yu (Assistant Scientific Secretary and *Annals of the ICRP* Associate Editor)
T. Yasumune (Assistant Scientific Secretary and *Annals of the ICRP* Associate Editor)

Committee 2 members during preparation of this publication

(2017-2021)

J.D. Harrison (Chair)	A. Giussani	T. Sato
F. Paquet (Vice-Chair)	D. Jokisch	T. Smith
W.E. Bolch (Secretary)	C.H. Kim	A. Ulanowski
M. Antonia Lopez	R. Leggett	F. Wissmann
V. Berkovski	J. Li	
E. Blanchardon	N. Petoussi-Henss	

(2021-2025)

F. Bochud (Chair)	A. Giussani	J. Li
F. Paquet (Vice-chair)	D. Jokisch	J.W. Marsh
M.A. Lopez (Secretary)	C.H. Kim	N. Petoussi-Henss
M. Andersson	M.S. Kulkarni	T. Sato
V. Berkovskyy	S. Lamart	T. Smith
D. de Souza Santos	C. Lee	A. Ulanowski

Committee 2 emeritus members

K. Eckerman

Main Commission members at the time of approval of this publication

Chair: W. Rühm, *Germany*
Vice-Chair: D.A. Cool, *USA*
Scientific Secretary: C.H. Clement, *Canada*; *sci.sec@icrp.org*[*]

K.E. Applegate, *USA*	S. Liu, *China*	**Emeritus members**
F. Bochud, *Switzerland*	S. Romanov, *Russia*	R.H. Clarke, *UK*
S. Bouffler, *UK*	T. Schneider, *France*	F.A. Mettler Jr, *USA*
K.W. Cho, *Korea*	A. Wojcik, *Sweden*	R.J. Pentreath, *UK*
G. Hirth, *Australia*		R.J. Preston, *USA*
M. Kai, *Japan*		C. Streffer, *Germany*
D. Laurier, *France*		E. Vañó, *Spain*

[*]Although formally not a Main Commission member since 1988, the Scientific Secretary is an integral part of the Main Commission.